AD-A193 177 ION-EXCHANGED WAVEGUIDES FOR SIGNAL PROCESSING APPLICATIONS - A NOVEL ELE (U) FLORIDA UNIV GAINESVILLE DEPT OF ELECTRICAL ENGINEERING 1/4

UNCLASSIFIED R V RAMASWAMY 07 MAR 87 AFOSR-TR-88-0279 F/G 20/6.1 NL

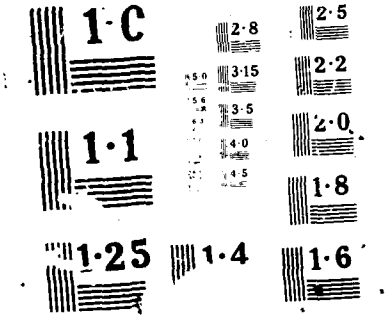
1·C
2·8
2·5
3·15
2·2
1·1
3·5
2·0
4·0
1·8
4·5
1·25
1·4
1·6

(2)

AFOSR-TR- 88-0279

ION-EXCHANGED WAVEGUIDES FOR SIGNAL PROCESSING APPLICATIONS—A NOVEL ELECTOLYTIC PROCESS

FINAL REPORT

AIR FORCE OFFICE OF SCIENTIFIC RESEARCH
BOLLING AIR FORCE BASE, DC 20332

CONTRACT NO. 84-0369

PERIOD COVERED: Oct. 1984-Nov. 1987

Submitted by:

R.V. Ramaswamy
Department of Electrical Engineering
University of Florida
Gainesville, FL 32611

March, 1988

College of Engineering

University of Florida

Gainesville, Florida

(2)

ION-EXCHANGED WAVEGUIDES FOR SIGNAL PROCESSING APPLICATIONS—A NOVEL ELECTOLYTIC PROCESS

FINAL REPORT

AIR FORCE OFFICE OF SCIENTIFIC RESEARCH
BOLLING AIR FORCE BASE, DC 20332

CONTRACT NO. 84-0369

PERIOD COVERED: Oct. 1984-Nov. 1987

Submitted by:

R.V. Ramaswamy
Department of Electrical Engineering
University of Florida
Gainesville, FL 32611

March, 1988

SECURITY CLASSIFICATION OF THIS PAGE

REPORT DOCUMENTATION PAGE

1a. REPORT SECURITY CLASSIFICATION Unclassified	1b RESTRICTIVE MARKINGS
2a. SECURITY CLASSIFICATION AUTHORITY	3 DISTRIBUTION / AVAILABILITY OF REPORT Approved for public release: Distribution unlimited
2b. DECLASSIFICATION / DOWNGRADING SCHEDULE	
4. PERFORMING ORGANIZATION REPORT NUMBER(S)	5. MONITORING ORGANIZATION REPORT NUMBER(S) AFOSR-TR- 88-[illegible]
6a. NAME OF PERFORMING ORGANIZATION University of Florida 6b OFFICE SYMBOL (If applicable)	7a. NAME OF MONITORING ORGANIZATION Air Force Office of Scientific Research AFOSR/NC
6c. ADDRESS (City, State, and ZIP Code) Department of Electrical Engineering Gainesville, FL 32611	7b. ADDRESS (City, State, and ZIP Code) Bolling Air Force Base, DC 20332
8a. NAME OF FUNDING / SPONSORING ORGANIZATION AFOSR 8b. OFFICE SYMBOL (If applicable) NC	9. PROCUREMENT INSTRUMENT IDENTIFICATION NUMBER AFOSR- 84-0369
8c. ADDRESS (City, State, and ZIP Code) Bldg. 410 Bolling AFB, DC 20332-6448	10 SOURCE OF FUNDING NUMBERS PROGRAM ELEMENT NO. 61102F; PROJECT NO. 2303; TASK NO. A3; WORK UNIT ACCESSION NO.
11. TITLE (Include Security Classification) ION-EXCHANGED WAVEGUIDES FOR SIGNAL PROCESSING APPLICATIONS--A NOVEL ELECTOLYTIC PROCESS	
12. PERSONAL AUTHOR(S) R. V. Ramaswamy	
13a. TYPE OF REPORT Final 13b. TIME COVERED FROM 10/1/84 TO 11/30/87	14. DATE OF REPORT (Year, Month, Day) 880307 15. PAGE COUNT 310
16. SUPPLEMENTARY NOTATION	
17. COSATI CODES FIELD / GROUP / SUB-GROUP	18. SUBJECT TERMS (Continue on reverse if necessary and identify by block number) attenuation, bistability, borosilicate, concentration cell, concentration profile, diffusion, electrolytic release, electromigration, fiber optics, galvanic cell, glasses,

19. ABSTRACT (Continue on reverse if necessary and identify by block number)

Ion exchange process and technology for fabrication of optical waveguides has been studied systematically to improve the reproducibility and establish the correlation between the process parameters and the component characteristics. Two-step process has been studied extensively and used for fabrication of low-loss fiber-compatible single-mode buried channel waveguides using the Na^+ - Ag^+ cation pair. Nonlinear waveguides have been studied theoretically and some of the predictions have been verified experimentally in K^+ - Na^+ ion-exchanged waveguides in semiconductor-doped glasses.

20 DISTRIBUTION / AVAILABILITY OF ABSTRACT ☒ UNCLASSIFIED/UNLIMITED ☐ SAME AS RPT ☐ DTIC USERS	21 ABSTRACT SECURITY CLASSIFICATION Unclassified
22a NAME OF RESPONSIBLE INDIVIDUAL Donald F. Ulrich	22b TELEPHONE (Include Area Code) 202-767-4963 22c OFFICE SYMBOL NC

DD FORM 1473, 84 MAR 83 APR edition may be used until exhausted
All other editions are obsolete.

SECURITY CLASSIFICATION OF THIS PAGE

18. Subject Terms (Continued)

guided waves, insertion loss, integrated optics, interconnects, ion-exchange, mode cutoffs, mode mismatch, near field profile, nonlinear guided waves, nonlinear index, nonlinear optics, optical characterization, optical communications, optical signal processing, optical switching, passive components, power limiting, prism coupling, semiconductor glasses, soda-lime silicate, thermal nonlinearity

TABLE OF CONTENTS

FINAL REPORT OF AFOSR CONTRACT NO. 84-0369

"ION-EXCHANGED WAVEGUIDES FOR SIGNAL PROCESSING APPLICATIONS—A NOVEL ELECTOLYTIC PROCESS"

I. Introduction

A. Overview of Program

The primary objective of the project is to investigate theoretically as well as experimentally the ion-exchange process and technology for fabrication of passive waveguide components in commercial glasses. The application areas of such components include optical communications, sensors, integrated optics and optical signal processing. The study was initiated in an Air Force contract (No. F08635-83-K-0263) in 1983 and has been funded almost exclusively by the AFOSR since 1984. At the beginning of the study, the effort in glass-waveguide-based I-O components was sporadic inspite of the fact that the first glass waveguide using an ion-exchange process was reported in 1972 and since then several laboratories around the world have been involved in investigations. It was not evident whether the technology had the potential to permit fabrication of devices with reproducible characteristics. In fact, so few single-mode waveguides had been fabricated and characterized that any significant evaluation of their performance in integrated optical systems was not feasible. The progress was hindered by the fact that several different cations were used in various glass substrates and melt compositions without any systematic approach to the problem.

In this report, we summarize the results of a systematic study of the ion-exchange process, the optical characterization of the waveguides fabricated using this process and the guided wave nonlinear optical work carried out under the program. All of the publications presented have resulted from this contract. Copies of the publications are attached with

this report and the readers are referred to these papers for further details. Also listed are the patents generated under this program.

B. Ag^+-Na^+ Cation Pair

Cognizant of the above considerations, we soon recognized the importance of choosing a cation pair, a specific glass system and a suitable melt composition to fabricate single-mode waveguides. Since passive components require extremely high reproducibility, this factor was given utmost attention in our approach. A careful evaluation of the status of the technology by us revealed that of all the monovalent cations which were being studied, Ag^+ was the most versatile due to the following reasons:

(1) The refractive index change caused by incorporation of silver ions in glass can be varied over a wide range (0 - 0.1). This flexibility is important in fabricating fiber-compatible waveguides [1].

(2) Silver films can be easily fabricated and diffused in a clean atmosphere at relatively low temperatures to fabricate waveguides which can be buried in a single-step process, thus minimizing the process time [2].

(3) Silver can be electrolytically released in melt at a controlled rate [3-6]. Furthermore, an on-line measurement of silver concentration can be performed to monitor any fluctuations [7]. A feedback system can thus be implemented for electronic control of the processing conditions which would provide the desired reproducibility.

(4) Silver is a heavy atom and its concentration in glass can be analyzed using conventional SEM and microprobe techniques even at low concentrations. This permits a direct measurement of a diffusion (index) profile with high accuracy [8-10].

In spite of the above distinct advantages, there were reports of silver being responsible for large scattering and absorption losses. However, it was

soon recognized that these losses were characteristic of only those waveguides where a relatively large fraction of sodium ions in the substrate glass had been exchanged for silver. In such cases, silver was not only reduced to metallic form, aggregates were formed that scatterd light abundantly. Fortunately, for single-mode fiber-compatible waveguides, less than 10% of sodium ions are replaced by silver and such detrimental effects have not been noted [3].

C. Nonlinear Waveguides

Optical nonlinearity, caused by the intensity dependent refractive index of the guiding or the surrounding medium, has generated a great deal of interest due to its potential for applications in all optical signal processing systems. The guided wave approach is attractive for nonlinear optical applications because of several reasons: interaction geometry involved allows larger power densities propagating over relatively large distances thereby causing a significant reduction in the threshold power requirements as compared to the nonguided configurations such as Fabry-Perot interferometers. Secondly, the waveguides are compatible with optical fibers and integrated optical systems. We have studied theoretically and experimentally the propagation characteristics of these waveguides.

II. Summary of Results

The systematic study of ion-exchanged waveguides performed in this project under AFOSR contract (No. 84-0369), involved several steps:

(1) Ion-exchange equilibrium at the $NaNO_3$+$AgNO_3$ melt-glass interface was studied as a function of melt composition and stirring conditions. The results provided a relationship between silver concentration in the melt and at the glass surface [11-14].

(2) An electrolytic release technique was developed to control silver concentration in the melt [3-6]. An insitu measurement method was developed to monitor the silver concentration on-line, thus paving the way for automation of the process with better control and reproducibility [7].

(3) The process of fabrication from melts was automated. This implied setting up the predetermined values for diffusion time, the magnitude of the electric field, the stirring conditions, monitoring the current and temperature with feedback mechanisms for automatic control of these parameters. A unique ceramic sample holder was designed to allow application of an external field with a cathode, which is a molten salt mixture. This technique eliminates the use of gold films as cathodes which in turn eliminates the deterioration of the films [10]. Consequently, this technique is time and cost efficient. Similarly, a unique pump design prevents bubble formation at the melt-glass interface, assuring the uniformity of the waveguides.

(4) Besides the use of molten baths, waveguides were also fabricated from evaporated silver films by electric field induced migration [2]. The technique allows significant flexibility and simplicity. Tapered waveguide sections can be fabricated. Steps are currently underway to fabricate buried single-mode channel waveguides using only one step.

(5) A complete characterization of the diffusion profile was performed by using conventional analytical tools such as electron-microprobe and atomic absorption spectroscopy [15]. A new method was developed in which back scattered electrons were analyzed in a scanning electron microscope [8]. These tools are now routinely used for characterization of the waveguides.

(6) The diffusion process was modelled [16-18] by solving the diffusion equation and correlating the results with the experimental data in both the planar and channel surface waveguides [10, 16-19]. The calculation is based on a finite-difference method. Processes such as side diffusion and concentration dependence of the interdiffusion coefficient are taken into account [18].

(7) Once the diffusion profile was measured, the wave equation was solved to predict the propagation properties of the waveguide. Both, the planar and channel waveguides can thus be analyzed theoretically [16-21]. The numerical technique involves a solution using a finite difference method.

(8) Optical characterization techniques were developed. These include measurements of attenuation [3], mode indices [3], near field distribution [15], and cutoff wavelengths [22] of the waveguide modes. All the experiments were automated such that the measurements are rendered more accurate and the data processing is faster.

(9) The results of the systematic study have provided the guidelines for fabrication of buried single-mode channel waveguides with desired mode field distribution. The two-step ion-exchange involves diffusion of silver ions in the glass matrix in the first-step [8, 10, 15-17, 23]. No application of electric field is necessary during this step [16, 17]. When a second-step ion-exchange is performed with an external field and no silver in the melt, a symmetric buried profile is obtained. Using this process, low-loss (< 0.2db/km) fiber-compatible waveguides have been fabricated [18, 24].

(10) We have studied theoretically the effect of a nonlinear cover medium on the propagation of guided waves in a graded index planar waveguide [25]. The results show that the threshold power requirements are reduced as compared to the step-index case. The calculations predict transfer of power from the film region to the cover medium, indicating occurance of optical switching [25, 26].

(11) We have fabricated planar as well as channel waveguides in semiconductor-doped colored glass using the K^+-Na^+ ion-exchange process. Nonlinear prism coupling, power limiting, and mode field variations were observed in planar guides with the threshold for power limiting as low as 20 mW using a cw Ar^+ laser [27]. The effect was identified as thermal in origin. In channel waveguides, the nonlinear saturation was also observed [27]. Experiments are underway to isolate the thermal component from the fast electronic contribution.

III References

[1a] R. V. Ramaswamy and R. Srivastava, "Ion-Exchanged Glass Waveguides: A Review," **INVITED PAPER**, Special Joint Issue of IEEE J. Quantum Electron. and J. Lightwave Technology, May 1988.

[1b] R. V. Ramaswamy and R. Srivastava, "Recent Advances in Ion-Exchanged Optical Waveguides and Components," **INVITED PAPER**, Journal of Modern Optics. (In Press).

[2] S. I. Najafi, P. G. Suchoski, Jr., and R. V. Ramaswamy, "Silver-Diffused Glass Waveguides: Diffusion Process and Optical Properties," IEEE J. Quantum Electron., QE-22, pp. 2213-2218, 1986.

[3] R. K. Lagu and V. Ramaswamy, "Fabrication of Single Mode Glass Waveguide by Electrolytic Release of Silver Ions," Appl. Phys. Lett., 45, pp. 117-118, 1984.

[4] R. K. Lagu and V. Ramaswamy, "Fabrication of Ion-Exchanged Glass Waveguides by Electrolytic Release of Silver Ions," Seventh Topical Meetings on Integrated and Guided-Wave Optics, Post Deadline Paper PD-8, April 24-26, 1984.

[5] R. V. Ramaswamy, R. K. Lagu, and S. I. Najafi, "Fabrication of Ion-Exchanged Glass Waveguides through Electrolytic Release of Silver Ions," SPIE PROCEEDINGS 1st International Conference on Integrated Optical Circuit Engineering, Cambridge, MA, Oct. 21-26, 1984.

[6] S. I. Najafi, R. V. Ramaswamy, and R. K. Lagu, "An Improved Method for Fabricating Ion-Exchanged Waveguides Through Electrolytic Release of Silver Ions," IEEE J. Lightwave Tech., LT-3, pp. 763-766, 1985.

[7] R. K. Lagu, S. I. Najafi and V. Ramaswamy, "In Situ Measurement of Ionic Concentration During Fabrication of Ion-Exchanged Waveguides," Appl. Opt., 23, pp 3925-3930, 1984.

[8] R. K. Lagu, R. V. Ramaswamy, and S. I. Najafi, "Fabrication and Characterization of Buried Glass Waveguides with Symmetric Index Profiles," Digest of 3rd European Conference on Integrated Optics (ECIO), Paper II-R, pp. 75-80, Berlin, May 1985.

[9] S. I. Najafi and R. V. Ramaswamy, "Ag^{+}-Diffused Graded-Index Waveguides: Diffusion and Modal Characterization," Conference Digest-Gradient-Index Optical Imaging Systems Conference, Palermo, pp. 142-145, Sept. 26-27, 1985.

[10] R. V Ramaswamy and S. I. Najafi, "Planar, Buried, Ion-Exchanged Glass Waveguides: Diffusion Characteristics," IEEE J. Quantum Electron., QE-22, pp. 883-891, 1986.

[11] P. Chludzinski, R. V. Ramaswamy, and T. J. Anderson, "Ion-Fxchange Between Sode-Lime Silicate Glass and Sodium Nitrate-Silver Nitrate Molten Salts," Phys. Chem. Glasses, 28, pp. 169-173, 1987.

[12] R. V. Ramaswamy, R. Srivastava and Chludzinski, "Influence of Ag^+ - Na^+ Ion-Exchange Equilibrium on the Index Profile of Single-Mode Glass Waveguides," **GRIN** '87, Paper ThB2-1, Reno, NV, Jan. 1987.

[13] P. Chludzinski, R. V. Ramaswamy, and T. J. Anderson, "Microstructural Definition of Ion-Exchanged Glass Optical Waveguides," Proceedings of the Third International Conference on Ultrastructure Processing of Ceramics, Glasses and Composites, Vacation Village, San Diego, CA, Feb. 23-27, 1987. (In Press).

[14] R. V. Ramaswamy, R. Srivastava, P. Chludzinski and T. J. Anderson, "Influence of Ag^+-Na^+ Ion-Exchange Equilibrium on Waveguide Index Profile," IEEE J. Quantum Electron. (In Press).

[15] R. Srivastava, R. V. Ramaswamy, H. C. Cheng and H. Zhenguang. "Fabrication and Characterization of Single-Mode Glass Waveguide Components," **SPIE**'s 31st Annual International Symposium on Optical and Optoelectronic Applied Science and Engineering, San Diego, CA, Aug. 1987.

[16] H. C. Cheng, R. V. Ramaswamy and R. Srivastava, "Buried Na^+ - Ag^+ Ion-Exchanged Waveguides: Theory and Experiment," Seventh Topical Meeting on Gradient-Index Optical Imaging Systems (**GRIN** '87), Paper TuC2-1, Reno, NV, Jan. 1987.

[17] R. V. Ramaswamy, H. C. Cheng and R. Srivastava, "Process Optimization of Buried Ag^+ - Na^+ Ion-Exchanged Waveguides: Theory and Experiment," Appl. Opt. (In Press).

[18] H. C. Cheng, H. Zhenguang, A. Miliou, R. Srivastava and R. V. Ramaswamy, "Buried Low-Loss Fiber Compatible Single-Mode Ion-Exchanged Channel Waveguides," To be presented at Integrated and Guided Wave Optics Conference (IGWO'88), Santa Fe, NM, March 1988.

[19] R. K. Lagu and R. V. Ramaswamy, "Process and Waveguide Parameter Relationships for the Design of Planar, Silver Ion-Exchanged Glass Waveguide," IEEE J. Lightwave Tech., LT-4, pp. 176-181, 1986.

[20] R. K. Lagu and R. V. Ramaswamy, "A Variational Finite-Difference Method for Analyzing Channel Waveguides with Arbitrary Index Profiles," IEEE J. Quantum Electron., QE-22, pp. 968-976, 1986.

[21] R. Srivastava, C. K. Kao and R. V. Ramaswamy, "WKB Analysis of Planar Surface Waveguides with Truncated Index Profiles," IEEE J. Lightwave Tech., LT-5, pp. 1605-1609, 1987.

[22] S. I. Najafi, R. Srivastava and R. V. Ramaswamy, "Wavelength Dependent Propagation Characteristics and Mode Cutoffs in Ag^{+}-Na^{+} Exchanged Planar Glass Waveguides," App. Opt., 25, pp. 1840-1843, 1986.

[23] R. K. Lagu and R. V. Ramaswamy, "Silver Ion-Exchanged, Buried Glass Optical Waveguides with Symmetric Index Profiles," Appl. Phys. Lett., 48, pp. 19-20, 1986.

[24] S. I. Najafi and R. V. Ramaswamy, "Diffusion and Modal Characterization of Ag^{+}-Na^{+} Exchanged Channel Waveguides," Conference on Integrated and Guided Wave Optics (IGWO'86), Atlanta, GA, pp. 60-61, February 26-28, 1986.

[25] R. K. Varshney, M. A. Nehme, R. Srivastava and R. V. Ramaswamy, "Guided Waves in Graded-Index Planar Waveguides with Nonlinear Cover Medium," NSF Workshop on Optical Nonlinearities, Fast Phenomena and Signal Processing, Tucson, AZ, pp. 185-199, May 1986.

[26] R. K. Varshney, M. A. Nehme, R. Srivastava and R. V. Ramaswamy, "Guided Waves in Graded-Index Planar Waveguides with Nonlinear Cover Medium," Appl. Opt. 25, pp. 3899-3902, 1986.

[27] H. Zhenguang, R. Srivastava and R. V. Ramaswamy, "Nonlinear Prism Coupling and Power Limiting in Ion-Exchanged Waveguides," To be presented at Integrated and Guided Wave Optics Conference (IGWO'88), Santa Fe, NM, March 28-30, 1988.

IV. Patents Filed

1. Dry Silver-Diffusion Technique for Fabrication of Multimode and Variable Index Waveguide Devices in Glass: S. I Najafi, R. V. Ramaswamy and P. G. Suchoski, Jr.
2. Buried, Three-Dimensional Tapered Coupler in Glass Utilizing Field-Assisted Ag^{+}-Na^{+} Exchange: R. V. Ramaswamy, P. G. Suchoski, and S. I. Najafi.
3. Electrolytic Release Technique for Fabrication of Low-Loss Optical Waveguides and Devices: R. K. Lagu and R. V. Ramaswamy.
4. Fabrication of Nonlinear Waveguide Devices in Glass: R. V. Ramaswamy, L. Ross and R. Srivastava.

APPENDIX

REFERENCE [1a]

Ion-Exchanged Glass Waveguides: A Review
(Invited Paper)

R.V. Ramaswamy and R. Srivastava
Department of Electrical Engineering
University of Florida
Gainesville, Fl 32611

Abstract

Passive glass waveguides made by ion-exchange technique are potential candidates for integrated optics [I-O] applications. In this paper, we review the advances in the technology as applied to fabrication of useful single-mode structures. Progress in process, fabrication, modeling and waveguide performance using different monovalent cation systems and glass compositions is described with emphasis on fiber-compatible single-mode structures prepared from molten baths. It is shown how a systematic study allows a correlation between the process parameters and the waveguide characteristics so desirable in assuring reproducible characteristics of the devices.

I. Introduction

Ion-exchange technique, which has been used for more than a century to produce tinted glass, has received increased attention in recent years as it improves surface-mechanical properties of glass and, more importantly, creates a waveguiding region in the glass. Today, glass waveguides are considered to be prime candidates for optical signal processing applications in optical communications, sensors and other related areas. The importance of the glass waveguide components is borne out by their compatibility with optical fibers, potentially low cost, low propagation losses and the ease of their integration into the system. However, the index of the glass substrate cannot be changed by application of an electric field. Therefore, fabrication of glass devices with assured reproducibility within specified tolerances is a must.

Since 1972 when Izawa and Nakagome [1] reported the first ion-exchanged waveguides by exchange of Tl^+ ions in a silicate glass containing oxides of sodium and potassium, significant progress has been made towards understanding the ion-exchange process and the role of the processing conditions on the propagation characteristics of the resulting waveguides. Various cation pairs and several different glass compositions and cation sources have been studied in the past dozen years with considerable attention given to fabrication of useful devices. Published reports of these advances abound in almost all the related journals at an increasing rate. Findakly [2] summarized most of the developments which occured till 1983. Since then, there has been rapid growth in the literature leading to a better understanding of the ion-exchange process in general and to the process optimization for reproducible waveguide performance in particular. The objective of this paper is to describe recent developments which have permitted establishment of the necessary correlation between the ion-exchange process parameters and the waveguide

characteristics. Emphasis is placed on single-mode structures and effort is made to point out similarities as well as dissimilarities observed or expected in the exchange process for different cation pairs and glass compositions. Because of the multidisciplinary nature of the field, it is not possible to give an exhaustive bibliography. For example, ion-exchange process and ionic diffusion in glasses have been discussed in many excellent reviews [3,4] and we will confine our attention to only those topics in the area which are of direct relevance to the waveguide work.

This paper is structured in the following format. In Section II we briefly describe the results of ion-exchanged waveguides for each cation pair. Both of the methods, molten salt bath as well as film-diffusion, are considered. The process parameters are identified and a procedure outlining the various steps for a systematic correlation between theory and experiment is presented. Section III describes how the ion-exchange equilibrium at the glass-melt interface influences the boundary conditions for the cation diffusion in the glass. Surface-index change depends on this equilibrium. Section IV presents theoretical considerations to model the modification of the glass refractive index as a result of the ion-exchange. Surface deformation, stress and the birefringence resulting from the cation substitution are also considered. In Section V, a general formulation of the two-dimensional diffusion equation is given from which the refractive index distribution is obtained in special cases of interest for planar as well as channel waveguides. Both surface and buried guides obtained by electric field induced migration are considered. Issues such as side diffusion under the masks in the case of channel waveguides, space-charge effects and the double alkali effect are also addressed in this section. The next section describes some fabrication and characterization procedures with particular emphasis on

single-mode waveguides. Finally, we present the recent developments and state-of-the-art in waveguide and device fabrication and speculate into the future of the field.

II. Ion-Exchange Process

II A. Exchange from Molten Bath

Since Izawa and Nakagome [1] reported the first ion-exchanged waveguide made by Tl^+ - Na^+ exchange from a mixture of molten nitrate salts, molten bath has almost invariably been used as the source of exchanging ions for fabrication of glass waveguides. Several cation pairs have been studied. In most cases [1,5-9] sodium ions in the substrate glass are exchanged for one of the alkali cations, namely Cs^+, Rb^+, Li^+, K^+, Ag^+ or Tl^+. Recently Cs^+ - K^+ exchange [9] has also been reported for waveguide fabrication. Table I lists the first published reports for each cation pair along with the ion-exchange conditions, the salt bath, the substrate glass and the accompanying surface-index change (Δn). The electronic polarizability and ionic radii of each ion are also listed.

Of the various monovalent ions, each one has its advantages and drawbacks. For example, Tl^+ is known to be toxic but gives rise to relatively large index change ($\Delta n \sim 0.1$) and is therefore more suitable for multimode waveguides. The losses are also reasonably low ($\sim$ 0.1 dB/cm). Ag^+ is susceptible to being reduced to metallic form and thereby may introduce losses if incorporated in the glass in large concentrations [10]. Surface index changes as large as 0.13 have been reported [5]. In both the above cases (Tl^+ and Ag^+), dilute melts [1,11,12] can be used to reduce Δn and thereby fabricate single-mode waveguides. K^+ can be easily incorporated in glass [5,13,14] but the accompanying index change is substantially

smaller ($\Delta n \lesssim 0.01$) along with smaller diffusion rates. Thus large diffusion times are required for suitable waveguiding to occur, limiting its use for single-mode guides. The resulting waveguides are birefringent [13] although they exhibit negligible depolarization [15] and small propagation losses. Li^+ is very mobile in glasses and highly multimode guides with index profiles compatible with optical fibers can be produced in few minutes [7]. The maximum index change of the order of 0.015 is achievable, but so far no low-loss guides have been demonstrated. Moreover, because of large mismatch in the ionic radii of the two ions [Table I], large stress is introduced in the glass network causing surface damage. In the case of Cs^+, an index change of the order of 0.04 has been achieved [9] in a special potassium-rich BGG21 glass with very low losses (< 0.2 dB/cm). However, one disadvantage of using Cs^+ is that cesium salts react with most materials and diffusion must be carried out in crucibles made of special materials such as platinum, thereby adding to the cost.

For I-O applications, it is desirable to fabricate waveguides with low propagation loss and desired refractive index profile. Both depend upon the substrate glass (The relatively slow progress in ion-exchange technology can be attributed to this dependence. No standard glass compositions have been targeted so far. The requirements for an ideal substrate glass material have been listed in [16].) The losses are dominated by absorption, primarily due to presence of foreign impurities, and scattering contributions caused by glass inhomogeneity and surface or geometric imperfections. By careful choice of the host glass, waveguide losses below 0.1 dB/cm can be obtained [10,12,16]. Scattering losses, on the other hand, are generally introduced in the processing steps. Dopants introduce additional Rayleigh scattering to the background losses caused by the multicomponent nature of the glass. Reduction

of cations to metallic form, such as in the case of silver pointed out earlier, can give rise to additional absorption and scattering losses. Surface irregularities invariably interact with the propagating field and contribute to losses via scattering. This can be minimized by burying the waveguide below the glass surface by carrying out a two-step ion-exchange process (see Section V E). In channel waveguides, the imperfect wall boundaries caused during the photolithography may introduce additional loss. This loss contribution is less serious, however, since the diffusion process smooths out such irregularities. Finally, in devices, the waveguides invariably undergo bending, bifurcations or tapered transitions. These transitions have to be designed carefully to limit the radiation losses.

The refractive index profile, on the other hand, depends on various process parameters in an intricate manner. The composition of the host glass, the nature of the incoming ion and its concentration in the source, the temperature, the diffusion time, and the magnitude of the externally applied field, all affect the index profile. Since the waveguide characteristics are determined by the index profile, it is necessary to establish a correlation between the process parameters and the index distribution before the process can be tailored to produce waveguides of desired characteristics through a judicious choice and control of the process parameters. For a given substrate glass, such a systematic study entails the following distinct steps:

(1) Study of ion-exchange equilibrium to determine the relationship between the melt composition and the glass-surface-ion concentration.

(2) Analysis of the diffusion equation with appropriate boundary conditions to predict the concentration profile.

(3) Fabrication of the waveguide with a set of process parameters.

(4) Measurement of the diffusion profile and correlation with the theoretical analysis. It is generally assumed that the diffusion (concentration) profile is a replica of the index profile. This assumption has been experimentally verified and is valid as long as the concentration of the dopant in the glass is small [17,18,19].

(5) Calculations of the waveguide propagation characteristics by solving the Helmholtz equation for the given index profile.

(6) Optical characterization of the waveguide and correlation between the measured characteristics and the process parameters. This involves measurement of mode indices (where applicable), mode cutoff wavelengths [20], mode field profiles and attenuation.

II B. Film-Diffused Ion-Exchange

An alternative method for fabricating glass waveguides utilizes diffusion of ions from a solid metallic film, first presented by Chartier et al [21]. In this method, a thin film is deposited on a glass substrate and diffusion is carried out at an elevated temperature with the aid of an electric field applied across the sample. Since no other alkali metal films can be deposited and maintained in a stable form, this technique is used only for silver ion exchange.

Since the first report of film-diffused process [21] where single - mode as well multimode guides were fabricated and the diffusion coefficient and the activation energy measured, several workers [22-25] have utilized the process using somewhat different geometries and electrode structures. After the initial conflicting results and discrepancies [25] it appears that the process is better understood today and can be summarized as follows.

Initially, a several thousand angstrom thick silver film is deposited. To prevent oxidation and flaking of the film during diffusion, it is necessary to deposit a cover layer such as a gold [25] or an aluminum film [21]. This structure serves as the anode. The cathode can be either a metallic flim or a molten salt bath. The latter has the advantage that it does not deteriorate due to accumulation of sodium metal which diffuse out of the glass as a result of the ionic current under the applied field. The current is monitored during the entire process and the voltage is switched off well before the depletion of the silver film. Otherwise, depletion of cations from the waveguide surface results in surface defects (bubbles). Moreover, for reproducible waveguides, it is desirable to apply the voltage only when thermal equilibrium has been reached. In this regime, a constant current flow can be maintained during diffusion as the mobility of silver is not very different from that of sodium in the glass and the material resistance does not change significantly [25]. It must be emphasized that in the absence of an applied voltage, ion-exchange is negligible [24,25] since the silver atoms cannot be ionized in sufficient number and those which may be ionized due to thermal energy distribution, cannot enter the glass as the presence of an electrochemical potential between the silver film and the glass substrate blocks their movement. This potential barrier is overcome when a voltage is applied. Fields as low as 1V/mm can give rise to waveguides showing that the potential barrier is not very large [25].

Figure 1 shows the variation of diffusion depth W and surface index change Δn as a function of the applied voltage V [25]. The diffusion depth varies linearly with the applied field as is expected when the diffusion term is negligible (Section **V C**). If the ionic current is integrated over the total diffusion time needed to deplete the silver film, it is found to be

proportional to the thickness of the film. This suggests that by controlling the diffusion time, temperature, and the current flow precisely, the index profile and the waveguide characteristics can be controlled.

The index change varies very strongly with the applied field and the reason for this appears to be in the energy distribution of the cations. Higher the voltage, larger the number of cations capable of overcoming the energy barrier at the interface. The saturation of Δn at higher fields is a result of limited sodium sites available for ionic exchange.

The silver-film techniques has some distinct advantages over the molten bath technique:

(1) The process is relatively clean as pure silver film is deposited on a clean substrate and diffusion is carried out in a closed atmosphere.

(2) Relatively low temperatures are involved which facilitates design of sample holder and other components.

(3) Index change is field dependent. This may allow fabrication of tapered transitions by varying the electric field along the waveguide length.

(4) Buried waveguide may be obtainable in a single-step process. Bubble formation due to silver depletion can be prevented by surrounding the silver film by a pure $NaNO_3$ melt, for example.

In conclusion, substantial progress has been made in understanding the relationship between the diffusion depth, surface-index change and applied field. However, index profiling has not been modeled well and no satisfactory correlation with the experimental data is available. Most of the work has been done in multimode guides and much remains to be studied for making the process viable for practical applications.

III. Ion-Exchange Equilibrium at the Melt-Substrate Interface

When the glass containing a monovalent cation B is introduced into a molten salt solution containing the diffusing monovalent cation A, ion A is driven into the glass by an interphase chemical potential gradient and, in order to maintain charge neutrality, ion B is released into the melt. This ion exchange process can be represented by an overall chemical reaction as follows [26]:

$$A + \bar{B} = \bar{A} + B , \qquad (1)$$

where the bar denotes the cations in the glass phase.

The rate of ion exchange may be limited by the following processes:

(1) Mass transfer of reactants to and removal of products from the reaction interface in the melt.

(2) Kinetics of the reaction at the interface.

(3) Transport of cations in the glass phase.

Transfer of cations in the melt takes place via diffusion and convection. Convection can be enhanced by stirring the melt. However, even in the forced convection case, a region may exist near the glass-melt interface where no convective mixing occurs because of fluid friction at the interface. Across this stagnant boundary, all the mass transfer of the cations (in the melt) to and from the reaction interface occurs through diffusion. If the liquid-phase diffusion can supply ample reactants and remove enough products to and from the interface, the process is not melt mass transfer limited i.e., source depletion does not occur at the interface. For diffusion to be a limiting process in the melt, the important parameters is $(\bar{N}_A/N_A)\,(\bar{D}_A/D_A)^{1/2}$ where N_A denotes the molar concentration of cation A and

D_A its self diffusion coefficient. It has been shown that if this parameter $\gtrsim 10$, the rate is not mass transfer limited due to diffusion in the melt [27]. Although in the early reports [5] of ion-exchange waveguides using pure $AgNO_3$ melts such a depletion was believed to occur, more recent results [28] indicate that in the case of Ag^+ - Na^+ exchange from dilute melts, the melt mass transfer is not a limiting process.

At the interface, the surface kinetics are not likely to be a rate-limiting factor and are thus assured to be much faster than the transport processes in the melt and glass phases.

In the glass phase, mass transport is carried out entirely by diffusion of the cations which is a relatively slow process. The equilibrium state of (1) specifies the surface boundary condition for the diffusion process and the accompanying surface index change. Thus the control of the cation diffusion profile in glass is subject to manipulation of this boundary condition and the cation transport (diffusion) properties in the glass. The equilibrium state is governed by an equilibrium constant K defined as

$$K = \frac{\bar{a}_A \, a_B}{\bar{a}_B \, a_A}$$

where a's represent thermodynamic activities of the cations in the respective phases. Using the Regular Solution Theory [29] for the ratio of the activity coefficients in the melt and the n-type behavior [30] in the glass phase, the relationship between the melt concentration (N_A) and the surface concentration in the glass ($\bar{N}_A$) can be written [26] as follows:

$$\ell n\left(\frac{N_A}{1 - N_A}\right) + \frac{A}{RT}\,(1 - 2N_A) = n\ \ell n\ \left(\frac{\bar{N}_A}{1 - \bar{N}_A}\right) - \ell nK \qquad (2)$$

where n is given by

$$n = \partial \ln \bar{a}_A / \partial \ln \bar{C}_A$$

A is the interaction energy of the two cations in the melt, R is the gas constant, T is the temperature in Kelvin, and $\bar{C}_A$ is the absolute concentration of cation A in the glass.

The linear relationship between $\ln \{N_A/(1 - N_A)\}$ and the $\ln (\bar{N}_A/1 - \bar{N}_A)$ given by (2) yields a straight line from which the values of n and K can be derived. When n is unity the glass is said to have ideal behavior. A large value of K on the other hand would indicate a large uptake of the cation A by the glass for the given melt composition.

Studies of ion-exchange equilibrium in glasses include the early work of Schulze [31] and later, the pioneering work of Garfinkel [26] involving various cation pairs and glass compositions. Houde-Walter and Moore [32] have listed the values of n and K for Ag^+ - Na^+ exchange from several melt compositions. Of all the cases studied in [26], only K^+ - Na^+ binary system gives a linear relation between $\bar{N}_k$ and N_k. In the case of Ag^+ - Na^+ in soda lime silicate glasses, recent studies [11,19,28] carried out up to very low melt concentrations ($N_{Ag} \sim 10^{-4}$) indicate that K is very large (75-120 range). Figure 2 shows the relationship between $\bar{N}_{Ag}$ and N_{Ag} as obtained in [19]. Similar nonlinearity has recently been reported for the Cs^+ - K^+ system [33]. This highly nonlinear behaviour suggests that for single-mode fiber compatible glass waveguides fabricated by Ag^+ - Na^+ ion-exchange, it is necessary to keep melt concentrations very low ($N_{Ag} \sim 10^{-4}$). Since in this region the slope of $\bar{N}_{Ag}$ vs N_{Ag} curve is very large, a rigid control of N_{Ag} is a must for fabrication of single-mode guides of reproducible characteristics. The other important characteristic of the curve in Fig. 1 is

observation of the plateau when nearly half the Na^+ sites in the glass are occupied by Ag^+. In this region, fluctuations in the melt concentrations do not influence the surface silver uptake to any significant degree. Ideally one would like to use this region for waveguide fabrication if the corresponding index change could be made compatible with the single mode fibers ($\Delta n \sim 5 \times 10^{-3}$). However, this would required special low sodium content glass as the commercially available soda-lime or boro- and alumino-silicate glasses contain $\gtrsim$ 10% Na_2O by weight which gives $\Delta n \sim 0.05$ for $\bar{N}_{Ag} = 0.5$ [34].

IV. Index Change by Ion Substitution

IV A. Polarizability and Volume Changes

In the binary ion-exchange process, both the cations which exchange with each other are network modifiers. As a result, the basic structure of the glass is left unchanged and only the refractive index of the glass is modified. The net index variation depends on three major physical changes; namely, ionic polarizability, molar volume (related to ionic size) and the stress state created by the substitution. Besides these three factors, secondary influence on the index is caused by the accompanying effect on the electronic polarizability of the neighboring (oxygen) ions. In order to estimate the refractive index of glass as a function of its composition, the Gladstone-Dale equation and the Lorentz-Lorentz relation have been most widely used [34,35,36]. Based on Gladstone-Dale relation, Huggins and Sun [34] provided a recipe for the calculation of the density, refractive index and dispersion of a glass from its composition, expressed in terms of the weight precent of its oxide constituents. The basic model predicts that the value of the index change resulting from the ionic substitution is given by

$$\Delta n \simeq \frac{\chi}{V_o} \left(\Delta R - R_o \frac{\Delta V}{V_o} \right) \qquad (3)$$

where χ is the fraction of cations replaced by the incoming ion, V_o is the volume per mole of oxygen atoms, R_o is the refraction per mole of oxygen atoms, and ΔR and ΔV are the changes in these quantities as a result of cation exchange. In this simple model, the index change represented by (3) is caused by two factors: the first term arises as a result of the difference in the ionic polarizability of the exchanging ions and the second term represents the contribution due to the change in the molar volume of the glass caused by the difference in ionic radii of the two ions [Table I]. The simplicity of (3) is very instructive. Consider the case of Li^+ - Na^+ exchange in soda-lime glass [7]. The first term of is negative and the second term is also negative. However, the an ontribution in this case comes from a local contraction of the sample and consequent increase in the density which increases the total polarizability per unit volume and the refractive index increases. On the other hand, in the case of Ag^+ - Na^+ exchange the first term of (3) contributes dominantly as the polarizability of silver ion is much larger than that of sodium ion in the glass. The difference in the two ionic radii is not very large. $\Delta V > 0$ and the second term subtracts from the first. Between the two extreme examples given above lies the intermediate case of K^+ - Na^+ exchange. In this case the net index change as predicted by (3) has been found to be two orders of magnitude smaller than the measured values [37]. This discrepancy arises from the simplicity of the above model in which the contribution caused by the large stresses induced by ion-exchange is ignored.

IV B. Stress-Induced Index Change

Ion-exchange process involves exchange of two cations of different ionic radii at temperatures well below the stress relaxation temperature of the glass [38]. As a result, the accompanying volume changes have to be accommodated only in the direction normal to the substrate since the surface is prevented from expanding (or contracting) laterally due to resistance to bending of the glass substrate. This constriction gives rise to swelling of the surface in the case of K^+ - Na^+ exchange [39] and causes residual compressive stresses in the exchanged layer which are balanced by tensile stresses in the substrate. The stress-optic effect contributes to the index change by increasing the compressive layer index and decreasing the index of the tensile region [38]. The stress profile generally follows the concentration profiles. Moreover, since the residual stresses are anisotropic, the index change depends on the state of polarization of the optical electric field, i.e., the resulting waveguides are birefringent [13,38].

Analysis of stress in planar and channel ion-exchanged waveguides has been investigated and the resulting birefringence [38], surface damage (cracks, elevations and dips) and swelling [38,39] have been observed as well as explained [36,37,38,39]. Typical values of birefringence in K^+ - Na^+ exchange, carried out in 350-400°C range are $\sim 1 \times 10^{-3}$ whereas in the case of Ag^+ - Na^+ exchange no birefringence has been detected when low melt concentrations are used. Moreover, as pointed out earlier, the dominant effect which contributes to index change in K^+ - Na^+ case arises from the compressive stress [37].

Another factor which causes stress in ion-exchanged waveguides is the mismatch between the thermal expansion coefficients of the waveguide and the substrate materials. However, this effect is very small [36,38] and can be neglected in comparison to the compositional stresses unless the exchange is carried out above the stress relaxation temperature as in the case of Li^+ - Na^+ exchange in aluminosilicate glass [40].

V. Diffusion Kinetics and Index Profile

As was pointed out earlier, the index profile in ion-exchanged waveguides is a replica of the diffusion (concentration) profile which can be calculated by solving the diffusion equation with appropriate boundary conditions.

V A. Diffusion Equation

In silicate glasses, only small monovalent cations diffuse readily whereas the oxygen anions remain fixed in the silicon-oxygen network. The diffusion is characterized by the self-diffusion coefficient D_i. In the binary ion-exchange process the cation A is transported via diffusion process within the glass where it exchanges with the other alkali cation B which has to diffuse out. The flux of each cation species is given by [41]

$$\vec{\bar{\phi}}_i = - \bar{D}_i \nabla \bar{C}_i \frac{\partial \ell n \, \bar{a}_i}{\partial \ell n \, \bar{C}_i} + \bar{\mu}_i \bar{C}_i \vec{E} \qquad (4)$$

where $\vec{\bar{\phi}}_i$ = molar flux of cation i (moles/m^2-s)

$\bar{\mu}_i$ = electrochemical mobility (m^2/V-s)

$\bar{C}_i$ = concentration of cation i in glass (moles/m^3)

and $\vec{E}$ = electric field (V/m).

The tracer (self) diffusion coefficient $\bar{D}_i$ depends on temperature and glass composition. The temperature dependence of $\bar{D}_i$ below the glass transition temperature can be fit to the Arrhenius equation [3]

$$D_i = D_o \exp(-Q_i/RT) \tag{5}$$

where Q is called the activation energy (J/mole). It is believed the Q is made up of two contributions: the Coulombic energy required for separation of positive and negative charges, and the energy required to squeeze an ion through a restricted opening in the network.

As regards the diffusion mechanism in glasses, various theories have been proposed and to date no unified picture has emerged. In the simplest picture leading to (5) it is assumed that the transport of the alkali ion takes place via tunneling from one vacant site in the glass network to another adjacent site if it acquires the necessary energy to surmount the energy barrier. If the ionic transport (conduction) mechanism is also assumed to be the same under an applied field, then Nernst-Einstein relation results:

$$\bar{D}_i = \frac{kT}{\bar{N}_i e^2}\sigma_i = \frac{kT}{e}\bar{\mu}_i \tag{6}$$

where k is Boltzmann constant, $\bar{N}_i$ is the total number of cations of the kind under consideration σ_i is the ionic conductivity, and e is the electronic charge.

In most glasses, however, the thermal cation migration process is slightly different from the electric field induced transport and (6) is not obeyed. The relation between the self diffusion coefficient and mobility is instead written as

$$\bar{D}_i = f_i \frac{KT}{e} \bar{\mu}_i \qquad (7)$$

Where f_i is a correlation factor whose value depends on glass composition and varies from 0.2 to 1. The factors leading to deviation from (6) in glasses are summarized in [4] and references therein.

Another important characteristic of the self-diffusion coefficient which is of interest in ion exchange is the mixed alkali or double alkali effect [42]. When a second alkali is added to a glass, a significant reduction in the self-diffusion coefficient of the original alkali ion occurs. While this reduction occurs whether the second alkali ion is smaller or larger than the original one, the magnitude of the change varies directly with the concentration and the size mismatch of the second alkali. In fact, the self-diffusion coefficient of an alkali ion is always considerably higher than that of the impurity alkali ion and the diffusion curves of the two alkalis intersect at a certain concentration ratio, suggesting the alternation of the principal current carrying species. As a result, the electrical conductivity passes through a minimum where the two diffusion curves intersect. Although such a concentration dependence of the self-diffusion coefficients has been measured in several glasses [42], the data for most glasses of practical interest for ion-exchanged glass waveguide applications are almost nonexistent. This is specially true for the Ag^+ - Na^+ case as silver-rich glasses have not been fabricated and studied. The mixed alkali effect has considerable influence on the diffusion profile [8].

Returning to the flux equation (4), $\vec{E}$ includes any externally applied field as well as the component arising from a local space-charge distribution near the diffusion boundary which moves deeper into the substrate as time

evolves. The space-charge region is caused by the lower mobility of the incoming ion ($\bar{\mu}_A < \bar{\mu}_B$) and is governed by the following relation:

$$\nabla \cdot (\varepsilon \vec{E}) = \rho \tag{8}$$

where the local space-charge density ρ is given by

$$\rho = e(\bar{C}_A + \bar{C}_B - \bar{C}_B^{\,o}) \tag{9}$$

In the above equation $C_B^{\,o}$ is the absolute concentration of the cation B in the glass before the ion-exchange. For weakly guiding case, the change in the dielectric constant due to ion substitution is very small and (8) can be replaced by

$$\nabla \cdot \vec{E} = \rho/\varepsilon \tag{10}$$

In some cases of interest the space-charge effects can be neglected and the condition of charge neutrality

$$\bar{C}_A + \bar{C}_B = \bar{C}_B^{\,o} \tag{11}$$

is found to be very nearly valid during diffusion [43]. The diffusion equation can be derived by combining (4), (11) and the continuity equations for the two cations. It can be written in the following form [44]:

$$\frac{\partial \bar{C}_A}{\partial t} = \bar{\mu}_A \vec{E} \cdot \nabla \bar{C}_A \left[\frac{1}{1 - \alpha \bar{C}_A}\right] + \frac{n}{1 - \alpha \bar{C}_A} \bar{D}_A \nabla^2 \bar{C}_A \tag{12}$$

where $\alpha = \left(1 - \frac{\bar{\mu}_A}{\bar{\mu}_B}\right)$ and n was defined in Section III. In (12) it has been assumed that the Nernst-Einstein relation is satisfied.

V B. Diffusion without external field

In this case it can be shown [43] that the two-dimensional diffusion equation becomes

$$\frac{\partial \bar{N}_A}{\partial t} = \frac{\partial}{\partial x}\left(\frac{n\bar{D}_A}{1 - \alpha\bar{N}_A}\frac{\partial \bar{N}_A}{\partial x}\right) + \frac{\partial}{\partial y}\left(\frac{n\bar{D}_A}{1 - \alpha\bar{N}_A}\left(\frac{\partial \bar{N}_A}{\partial y}\right)\right) \qquad (13)$$

Further simplifications occur in the following cases:

(i) $\alpha = 0$, i.e.; the two cations are equally mobile. In this case

$$\frac{\partial \bar{N}_A}{\partial t} = nD_A\left(\frac{\partial^2 \bar{N}_A}{\partial x^2} + \frac{\partial^2 \bar{N}_A}{\partial y^2}\right) \qquad (14)$$

(ii) $\bar{N}_A \ll 1$, i.e., the concentration of the incoming ion is much smaller than the host alkali ion in the glass. In this case also the diffusion equation reduces to (14). This approximation is not valid when diffusion is carried out from concentrated melts (e.g. $K^+ - Na^+$ process from pure KNO_3 melts), but is reasonably valid for dilute silver melt concentrations in $NaNO_3$ used for single-mode waveguide fabrication (see Fig. 1).

(iii) In the case of planar waveguides (13) reduces to

$$\frac{\partial \bar{N}_A}{\partial t} = \frac{\partial}{\partial x}\left(\tilde{D}\frac{\partial \bar{N}_A}{\partial x}\right) \qquad (15)$$

where $\tilde{D}$ is called the concentration dependent interdiffusion coefficient given by

$$\tilde{D} = n\bar{D}_A/(1 - \alpha\bar{N}_A) \tag{16}$$

which can be written as

$$\tilde{D} = \frac{n\,\bar{D}_A\,\bar{D}_B}{\bar{D}_A\,\bar{N}_A + \bar{D}_B\,\bar{N}_B} \tag{17}$$

Note that the concentration dependence in $\tilde{D}$ above comes explicitly from the term $\bar{N}_A$ in the denominator. It does not account for the concentration dependence of individual self-diffusion coefficients mentioned earlier. For the two cases (i) and (ii) pointed out above, $\tilde{D} = n\bar{D}_A$ and the diffusion equation takes the simplest form

$$\frac{\alpha\bar{N}_A}{\alpha t} = n\bar{D}_A \frac{\alpha^2\bar{N}_A}{\alpha x^2} \tag{18}$$

A complete solution of (18) requires knowledge of the initial and two boundary conditions. For

$$\bar{N}_A(x,o) = 0 \quad \text{for } x > 0$$

$$\left.\begin{aligned} \bar{N}_A(\infty,t) &= 0 \\ \text{and } \bar{N}_A(0,t) &= \bar{N}_o \end{aligned}\right\} \quad \text{for all } t \geq 0,$$

the solution is [27]:

$$\bar{N}_A(x,t) = \bar{N}_o \text{erfc}(x/W_o) \tag{19}$$

where $W_o = 2\sqrt{n\bar{D}_A t}$ is called the effective depth of diffusion and corresponds to that distance from the waveguide surface ($x = 0$) where $(\bar{N}_A/\bar{N}_o) = \text{erfc}(1) = 0.157$. The 1/e width $W_e = 0.64W_o$. Such index profiles have been observed in dilute Ag^+ - Na^+ exchange [19,45], Cs^+-K^+ exchange [9], and K^+ - Na^+ process in BK-7 glass [14].

In general, ion-exchange is carried out from concentrated melt solutions and ion-exchange equilibrium results discussed in Section III show that near the glass surface, $\bar{N}_A \to 1$. Moreover, in most cases of interest, $\alpha \to 1$. Crank [27] has given the solutions for various values of α. Step-like profiles are obtained when α approaches unity (e.g. Cs^+ - Na^+ [8]) and Gaussian-like diffusion profiles are obtained for intermediate values of α (e.g. K^+ - Na^+ [46] or Ag^+ - Na^+ when $\bar{N}_{Ag} \to 1$ [41,43]). In all these cases, numerical techniques [18,43,46] have been used to solve the nonlinear differential equation (15).

V C. Ion-Exchange with External Field

The migration of incoming ion can be enhanced by applying an electric field across the substrate. In this case one has to solve the combined system of equations (12) and (10). This has to be done numerically. In the planar case, however, approximate analytical solutions are obtained for the following specific cases:

(i) For the special boundary conditions

$$\bar{N}_A = \bar{N}_o, \frac{\partial \bar{N}_A}{\partial x} = 0 \quad \text{for } x = 0$$

and

$$\bar{N}_A = 0, \frac{\partial N_A}{\partial x} = 0 \quad \text{for } x \to \infty$$

the solution of (12) for one-dimensional case is [47]:

$$\bar{N}_A(x) = \bar{N}_o \{1 + \exp [v\bar{N}_o \frac{\alpha}{n\bar{D}_A} (x - vt)]\}^{-1} \tag{20}$$

with a concentration-dependent diffusion front velocity

$$v = v_o(1 - \alpha)/(1 - \alpha\bar{N}_o) \tag{21}$$

where $v_o = i_o/e\bar{C}_B^o$ depends on the ionic current density i_o caused by the applied field.

(ii) For low concentrations ($\bar{N}_A << 1$) , (12) in planar case reduces to

$$\frac{\partial \bar{N}_A}{\partial t} = n\bar{D}_A \frac{\partial^2 \bar{N}_A}{\partial x^2} - \mu E \frac{\partial \bar{N}_A}{\partial x} \tag{22}$$

and $\bar{N}_A(x,t)$is calculated by a Laplace-transform technique [48].

$$\bar{N}_A = \tfrac{1}{2} \bar{N}_o\{\text{erfc}(x' - r) + \exp(4rx')\text{erfc}(x' + r)\} \tag{23}$$

where $x' = x/W_o = x/2\sqrt{n\bar{D}_A t}$ is the normalized effective depth of diffusion without external field and $r = \mu Et/W_o$.

It has been shown that in practical cases, even for $\bar{N}_A$ as small as 0.2 such as in the case of single-mode $Ag^+ - Na^+$ waveguides [44,49], the space

charge leads to steeper diffusion fronts when compared to the solution (23). For large electric fields such that r > 2.5, it can be shown [49] that the contribution of the second term in (23) can be neglected and diffusion does not play significant role in the index profile. Index profile is step-like with the diffusion depth given by $v_0 t$ [47].

Abou-el-Leil and Cooper [47] have analyzed the problem of electric field induced ion-exchange in detail and compared their results with the data from the viewpoint of strengthening of glass. Not much consideration was given to the conditions characteristic of waveguide formation. Recently numerical solutions of (22) have been obtained [18,50] and compared with the experimental results in the case of Ag^+ - Na^+ waveguides [18]. Figure 3 shows these results for surface waveguides [18].

V D. *Two-dimensional Waveguides*

The case of channel waveguides is more complex due to the lack of knowledge of boundary conditions when masks are present. In the absence of external field, the two-dimensional equation (12) has been solved numerically [43] but the accuracy of such calculations is limited by the simplifying approximations involved in deriving (12) which is valid whenever the only electric field present is that directly due to the imbalance of the Fickian flux components (caused by the nonequality of the two cationic mobilities). The presence of the masks is expected to introduce an electric field generated by the electrochemical bias [51] between the melt and the mask. Presence of such a bias results in side-diffusion of incoming ions under the masks giving rise to wider index profiles than the mask opening. [52]. A qualitative comparision of the diffusion modeling with the experimental mode field data in

single-mode surface channel waveguides has recently been performed [53] and the results show reasonable agreement in the case of Ag^+-Na^+ process.

When an external field is applied to accelerate the transport of cations in the glass, the complexity increases. Assuming that the interdiffusion coefficient and mobility are concentration independent (a very severe approximation in cases where $\alpha \to 1$ and double alkali effect is prominent), and neglecting the diffusion term ($r \gg 1$), Lilienhof et al [44] calculated index profiles of highly multimode waveguides and observed a qualititative agreement with the experimental results in Ag^+ - Na^+ waveguides. A constant index change with step-like distribution was observed, as predicted by the simplified approximations. These simplifications, however, are not expected to give accurate results in the single-mode case as the diffusion term and space charge effects may play significant role in practical cases of interest. For example, in the case of single-mode Ag^+-Na^+ waveguides, we have observed that for reproducible characteristics, $t > 30$ min. At 330° C (fabrication temperature), $\mu \sim 5.0\ \mu m^2/V$ - min , $D \sim 0.05\ \mu m^2/V$ and $E_{max} \sim 30$ V/mm. This gives $r \simeq 2$ showing that diffusion effects must be considered to give accurate profile. Moreover, when electric field is applied in the presence of masks, severe side diffusion occurs due to depletion of sodium ions under the masked region. To date, only one report of fabrication of surface channel waveguides under these conditions has been published [54], but no mention of a side diffusion was made.

V E. Buried Waveguides

In order to increase the symmetry of the index profile (thereby improve fiber-waveguide coupling) and reduce the scattering losses caused by the proximity of the glass surface to the waveguiding region, a second-step ion-

exchange is necessary in absence of cations A in the melt. The diffusion equation is solved numerically in this case with the first-step index profile as the initial condition [18]. In the case of planar guides, results show [18,49] that the width of the diffused guides varies as the square root of the second-step diffusion time t_2 and the depth x_{peak} to which the guide is buried is proportional to the product of the applied field E_2 and the time t_2. Moreover, it is desirable that no field be applied in the first-step, otherwise scewed nonsymmetric index profiles are obtained [55]. Figure 4 shows the comparison of the experimental results with those predicted theoretically assuming concentration independent mobility, diffusion coefficient and electric field. While these assumptions are reasonable in the case of Ag^+ - Na^+ process used in [18,49] where dilute melt concentration were used, the same does not hold for K^+ - Na^+ or Cs^+ - K^+ processes where $\bar{N}_A \rightarrow 1$ and the space charge effects play an important role. While one-step electric field induced ion-exchange has been performed in the above two systems, [56,9], no buried waveguides have been investigated to date. It has been pointed out that the K^+ ions in the glass do not diffuse out in the second step [56].

Two-dimensional, buried channel waveguides have been fabricated by several workers [44,51,53]. However, only one report of theoretical modeling of Ag^+ - Na^+ process in buried waveguides under electric field has been published thus far and that too was related to multimode guides [44]. A detailed modeling of the two-step process in single-mode channel waveguides still remains a challenge. In the following we point out some of the issues which have to be addressed in order to achieve the desired correlation between the theoretical analysis and experimental data.

V F. Side- Diffusion

As mentioned earlier, side diffusion of cations A under the mask increases the guide width and influences the index profile. Several authors have paid attention to this problem [44,51]. Chartier et al [51] claim its origin in the electrochemical potential between the mask and the melt. They showed a qualititative agreement with the experimental profiles with numerical discrepancies in the case of their multimode waveguides fabricated without any externally applied field. Lilienhof et al [44] contended this hypothesis, however, as the side diffusion in their multimode waveguides fabricated under an electric field did not show any dependence on the mask material. The origin of side diffusion in the later case may be attributed to the depletion of cations A under the mask when a voltage is applied across the substrate. Such a depletion is likely to distort the field lines and transport the cations towards the region under the masks. This argument is supported by lack of side diffusion observed in multimode waveguides when guard rings were deposited in the proximity of the mask openings [57] and in the case of buried waveguides where no additional side diffusion is observed when electric field is applied in the second step with no mask present [53]. Although a quantitative measurement of the large side diffusion in single-mode guides made by Ag^+ - Na^+ exchange has been reported [52], no theoretical analysis has been performed to account for its magnitude. Nevertheless, two-dimensional fiber-like index profiles can be produced by the two-step process by choosing proper mask openings [53] as we will describe later in Section VII.

V G. Space Charge Effect

Space charge is created by the unequal ionic mobilities ($\bar{\mu}_A/\bar{\mu}_B \neq 1$). Since the substrate glass is rich in cations B, $\bar{\mu}_A < \bar{\mu}_B$ when glass is immersed in the melt. Cation B migrates faster than A, causing space-charge region. However, as ion-exchange proceeds, the depth of the cation A rich region increases and in this region $\bar{\mu}_A > \bar{\mu}_B$ provided sufficient cations of species B have been replaced by A. As a result of this interplay, the ionic conductivity of the glass varies across the substrate, being the lowest in the space-charge region. This variation is time-dependent and the ionic current is not constant [25]. The extent to which space-charge effects modify the index profile depends upon the range of variation of $\bar{\mu}_A$ and $\bar{\mu}_B$ in the two extreme concentrations. In the case of Ag^+ - Na^+ exchange, the effects are not severe and the ionic current is time-independent during the process [53]. However, in the cases such as K^+ - Na^+ it may be an important factor and therefore must be considered in the analysis.

VI Fabrication and Characterization

VI A. Fabrication

The schematics of the ion-exchange technique from molten salts is shown in Fig. 5. The melt is held in a crucible or beaker which is kept at a constant temperature by enclosing it in a furnace. The melt consists of the appropriate salt as the source for the diffusing ions. The desirable characteristics which influence the choice of the salt for a given ion are its melting point and the dissociation temperature. Nitrate salts have been used extensively as they have some of the lowest melting temperatures and exhibit reasonable stability. The diffusion temperature is adjusted to control the rate of diffusion. In some cases, melting temperatures can be lowered by

using a mixture of two nitrate salts [58]. For example, pure KNO_3 melts at 334°C and pure $NaNO_3$ at 307°C; however, a mixture of 10wt% KNO_3 and 90wt% $NaNO_3$ melts at 290°C. In the schematics of Fig. 5, silver ions are released electrolytically [12] and their concentration measured during diffusion [59].

For planar waveguide fabrication, polished glass substrates are immersed in the molten bath by using an aluminum sample holder. Strip waveguides are prepared by first carrying out photolithography to create masked regions of aluminum or some other material such as Al_2O_3, SiO_2, etc. In order to apply the electric field during the ion exchange process, two approaches have been implemented. In one case, the negative electrode consists of a platinum wire pressing against a gold film evaporated on a thin chromium film on the back surface of the glass sample [49]. Chromium is helpful in making a good contact with the gold film. An alternative to the gold film is to use a molten salt mixture. This eliminates the step of evaporating gold and therefore, is the less expensive method. The melt has to be kept bubble-free to assure uniform field across the substrate. In either case, the anode consists of a platinum wire immersed in the molten salt as shown in Fig. 5. The resistivity of the melt depends on its composition and temperature and there is a potential drop across the melt which may be of the order of 10% of the total applied voltage for 1mm thick soda-lime glass substrates with 4-5 cm^2 area [49].

VI B. Characterization

The important characterization of passive waveguides includes measurement of index (dopant) profile, propagation constants of the guided modes, attenuation and mode field pattern.

There are two different approaches for measurement of the refractive index profile in a glass waveguide fabricated by ion-exchange process. One of these involves measuring the dopant profile using analytical tools such as electron or ion microprobe [5], analysis of back-scattered electrons in a scanning electron microscope [55], or atomic absorption spectrophotometry [28]. The other alternative is to carry out optical measurements of parameters such as surface reflectivity or mode indices of the guided modes. The latter data are then used to derive the index profile by using inverse WKB approximation [60].

Concentration Profile

Electron microprobe has been used to measure the profile of the diffusing ion [5]. In this technique, the high-energy electrons are collected and analyzed for the concentration of the ion of interest. The results have to be analyzed carefully as the presence of other ions e.g. Ca^{++}, Al^{+++}, Mg^{++} etc. in the glass may give rise to spurious effects [5]. Electron microprobe is universal in the sense that any ion can be analyzed. However, sensitivity depends strongly on the ion and the data can be very noisy to draw useful or definite conclusion, particularly if the concentration of the ion is extremely low, such as the case of Ag^{+} - Na^{+} exchanged single mode waveguides [12].

Scanning electron microscope can be used for determination of the profile in two ways. One either analyzes the x-rays (energy dispersive spectrometry, EDS) characteristic of the ion in question [17] or, alternatively, analyze the back-scattered electrons originating from the ion [55]. Both have been successfully used to measure Ag^{+} concentration in soda-lime glass waveguides. The resolution is of the order of 1 μm and since the scattering efficiency is higher for ions of larger atomic numbers, only heavier ions such

as Cs^+, Rb^+ and Ag^+ may be amenable for this analysis. High mobility of ions such as sodium under the beam precludes their measurement using this method.

Atomic absorption spectrophotometry is an analytical tool for concentration measurement of any element. Here a thin layer of the sample surface is etched using HF and the solution is analyzed for the ionic concentration. Subsequent etching is performed and the analysis repeatedly carried out until the concentration profile is determined [28]. Depending on the diffusion depth, and the spatial resolution desired, the number of steps may be anywhere between 10 and 20. The technique is destructive but is capable of giving absolute concentrations without a great deal of effort.

Refractive-Index Profile

Although for low concentration of the diffusing ions generally encountered in ion-exchange problems the concentration profile gives the refractive index profile, there are cases where this is not true. In fact, it has been shown recently that Huggin's relation [34] widely used for predicting the index change upon substitution of the host ion by the diffusing ion, does not hold in certain cases such as in K^+ - Na^+ case [37] or when Ag^+ - Na^+ exchange occurs from pure $AgNO_3$ melt in high-content sodium glasses [32]. Thus, it is of great importance to know the index profile and surface index change directly.

There are several techniques for measurement of the index profile in waveguides. These include interferometry, reflectivity measurement and the inverse WKB method which relies on the mode indices data.

Interferometry is by far the most accurate and direct technique [11]. However, the sample preparation is time consuming and laborious and the technique is destructive. The two-dimensional index profile can also be determined by measuring reflectivity from polished faces with the aid of an

optical multi-channel detection system [44]. The surface of the sample is first beveled to a small angle (few degrees) and then illuminated at normal incidence in an optical microscope. The two-dimensional reflectivity is measured by a vidicon tube attached to the microscope. The index distribution is calculated from Fresnel's formula. High spatial resolution can be easily achieved because of the beveling. The system can be calibrated by measuring the reflectivity of a known sample. It is necessary that the vidicon response be linear for the intensity levels involved and sample surface be very clean. The system should be capable of accounting for the stray light. Requirement of absolute measurements of power levels make this technique subject to error. The resolution of index change measured is limited to 10^{-3}, making this method suitable only for multimode guides.

Although both the methods described above yield the index distribution in two dimensions, they require absolute measurements of illumination. Another method which yields the index profile of the waveguide relies on the measurement of mode indices. This can be easily accomplished by the prism coupler technique [61] with accuracies approaching 1×10^{-4}. From the mode-index data, the index profile is derived using the inverse WKB method [60]. While this method gives reasonably good results in multimode guides in the case of ERFC and exponential profiles, there are serious problems in determining the refractive index near the glass surface [60] as well as at the profile tails (where it approaches the substrate value and mode index values are inaccurate). Thus, care should be taken in the case of Gaussian or step-like transitions such as the case of electric-field induced ion-exchange or the Cs^+ - Na^+ ion-exchange (where the double alkali effect gives a sharp, step-like profile [8]). Moreover, the WKB approximation is known to be erroneous near the mode cutoffs [62]. The method may thus give reliable

results for diffusion depths but the value of surface-index change is always subject to error. In case of surface waveguides (such that prism coupling can be employed for measurement of mode indices) with the large number of guided modes, WKB method has been used extensively for characterization of waveguides. In the Ag^+ - Na^+ exchanged single-mode guides the index profile is ERFC ($N_{Ag} \sim 10^{-4}$). W_o and Δn thus are determined by fitting the measured mode indices to those calculated by solving the Helmholtz equation and treating W_o and Δn as adjustible parameters [45]. Alternatively, an effective interdiffusion coefficient D_e can be defined via the diffusion depth $W_e = \sqrt{D_e t}$ [46] . Table II lists values of $\tilde{D}$ and activation energy Q for various ions.

Attenuation and Mode Field Profile

The techniques for measurement of attenuation and mode field profile in ion-exchanged waveguides are similar to those used in integrated optics with $Ti:LiNbO_3$ waveguides. For planar guides, attenuation can be measured by the three-prism method [63]. This method measures total attenuation, i.e., contribution from scattering as well as absorption. Alternatively, scattering contribution to attenuation can be measured independently by probing a fiber tip along the waveguide and capturing the scattered signal. The variation of this signal as a function of propagation distance along the waveguide is plotted to determine the scattering loss. If the attenuation is below 0.1 dB/cm, neither the three-prism nor the fiber probe method is adequate and one resorts to resonant structures such as Fabry-Perot ring resonator [64,65]. In this case light is coupled into a ring waveguide from a straight waveguide by distributed directional coupling mechanism and the output from the ring is extracted in a similar fashion. By measuring the transmission of the Frabry-Parot as a function of temperature, both the finesse and the contrast can be

determined and from these parameters the loss per unit pass can be extracted [65]. Another method of estimating propagation losses in single-mode channel waveguides is described in the following section.

Mode field profile measurement is of paramount importance in waveguide characterization. Fiber-waveguide coupling, performance of the directional coupler, curvature-induced losses, all depend on the mode field. Near field method shown schematically in Fig. 6 is the most convenient and direct way to measure the field pattern. In fact, beside the waveguide mode field, the method shown here allows determination of various other parameters with very little additional effort. These are: the fiber mode field, the fiber-waveguide coupling loss and the propagation loss in the waveguide. The measurement procedure is as follows [66]:

Light from either a He - Ne laser or a 1.3 μm semiconductor laser is coupled into a short piece of a single-mode fiber. The fiber is either birefringent type so that it maintains the linear polarization or in the case of conventional fiber, the fiber is kept as steady as possible to prevent polarization fluctuations and linear output polarization is achieved by adjusting the compensator at the input end. Linear polarization allows excitation of either TE or TM like modes in the guide. The waveguide output is collected by a high-quality planar objective by imaging the waveguide end on a phodetector/amplifier with a pinhole mounted at the front end of the detector. The two-dimensional nearfield intensity pattern is measured by scanning the detector horizontally and vertically. The Fabry-Perot effect caused by the Fresnel reflections at the fiber-waveguide gap can be eliminated by adjusting the spacing for maximum transmission [66]. Fiber-near field can also be measured using the same procedure after removing the waveguide. The

magnification of the system is determined by imaging a known mask pattern at the detector face and scanning the detector.

In order to determine the fiber-waveguide throughtput efficiency, the output from the fiber is first measured. Then the waveguide is adjusted for maximum transmission and the output once again measured. Accuracies of the order of 0.01dB can be achieved using this procedure [66].

In order to derive the propagation losses from the measurement of fiber-waveguide throughput loss and the fiber and waveguide mode profiles, the following procedures can be used. The total throughtput loss is made of three components: 1) Fresnel loss due to reflections of the optical field at the waveguide input and output interfaces, 2) the propagation loss, and 3) mode mismatch loss due to different field distributions of the single-mode fiber and channel waveguide. Since the refractive indices of the fiber and glass substrate are very nearly equal (1.46 and 1.51 respectively), the Fresnel loss is small. Nevertheless, it can be made negligible if the fiber-waveguide spacing is adjusted for maximum transmission. The mode mismatch loss is calculated by evaluating the normalized overlap integral [67].

$$\eta = \frac{\left[\int_{-\infty}^{\infty}\int_{-\infty}^{\infty} E_f(x,y)\, E_g(x,y)\,dxdy\right]^2}{\left[\int_{-\infty}^{\infty}\int_{-\infty}^{\infty} E^2_f(x,y)\,dxdy\right]\left[\int_{-\infty}^{\infty}\int_{-\infty}^{\infty} E^2_g(x,y)\,dxdy\right]} \qquad (24)$$

where $E_f(x,y)$ and $E_g(x,y)$ are the mode field profiles of the fiber and waveguide respectively. The mode-mismatch loss is given by $-10 \log_{10} \eta$. If it is assumed that the two mode profiles are Gaussian along both the x and y axes, then

$$\eta = \frac{4}{\left(\frac{w_x}{d} + \frac{d}{w_x}\right)\left(\frac{w_y}{d} + \frac{d}{w_y}\right)} \qquad (25)$$

where w_x and w_y are the 1/e intensity full width and depth of the waveguide mode and d is the 1/e intensity diameter of the fiber mode. Although the Gaussian mode approximation may be reasonable for well-guided modes in buried channel waveguides where the field distribution tends to be symmetric, surface waveguides with not-so-well guided modes deviate from the Gaussian case and a numerical evaluation of integral (24) is necessary to determine the mode-mismatch loss accurately.

Once the mode mismatch losses have been determined, the propagation loss in the waveguide is obtained by subtracting is from the overall fiber-waveguide throughoutput loss.

VII Results

VII A. Single-mode Waveguides

Most of the progress is the area of single-mode guides in the past few years has occurred in three basic cation pair systems, namely Ag^+ - Na^+, K^+ - Na^+ and Cs^+ - K^+ exchange. In the following, we summarize these results.

Ag^+ - Na^+ Exchange

This is by far the most studied system. There are several advantages of choosing this cation pair:

(i) Index change can be varied diluting the $AgNO_3$ melt with $NaNO_3$. Dilute concentrations also help reduce reduction of Ag^+ to metallic silver [43]. No birefringence or depolarization is observed. Losses are also kept low.

(ii) Diffusion temperatures are the lowest and diffusion times are also reasonable as silver has high mobility.

(iii) Precise control of N_{Ag} can be maintained using electrolylic release method [12]. This allows reproducibility in propagation constant of 1×10^{-4}.

(iv) Buried waveguides are easy to fabricate by thermal diffusion as Ag^+ near the glass surface duffuses out in the second step ion exchange.

(v) Film diffusion technique can be adopted for dry diffusion.

(vi) Low concentrations of silver in the glass allow modeling without the complications involved in concentration dependence. Moreover, the space-charge effects have minimum significance since $\bar{\mu}_{Ag}$ and $\bar{\mu}_{Na}$ are of the same order.

(vii) Concentration profile can be measured non destructively using the SEM technique [55].

An extensive study of Ag^+ - Na^+ planar guides has been performed at the University of Florida over the years with a view to fabricate single-mode waveguides optimized for operation at 1.3 μm. The results can be summarized as follows:

(i) The surface-index change Δn is given by Fig. 2 and fiber-compatible guides can be prepared with $N_{Ag} \sim 10^{-4}$.

(ii) The index profile has been determined using several different techniques. Figure 7 shows the planar waveguide index profile as measured by these methods.

(iii) Planar waveguides fabricated under the influence of applied field show step-like profiles. Using $W = \bar{\mu}_A Et$, the mobility $\bar{\mu}_A$ of silver ions in glass is determined to be 5.0 $\mu m^2/min$ V at 330° C.

(iv) Channel surface waveguides prepared by thermal diffusion using Al masks were compared to planar guides. Figure 8 shows the typical

index profile [52]. The values of Δn and diffusion depth and width depend on the mask width as shown in Figs. 9,10 and 11 respectively. For mask width $W_c > 5\mu m$, the values of Δn and the width approach the respective planar values. Because of the side diffusion the waveguide width for $W_c \sim 5\ \mu m$ can be made fiber compatible for 1.3 μm operation provided the aspect ratio be kept close to unity, i.e. the waveguide depth be increased without affecting the width significantly. This was achieved when waveguides were buried by applying electric field in the second step [53]. The ratio of the additional depth to the side diffusion is given by $r = \frac{\mu E t}{2\sqrt{\tilde{D}t}}$. The magnitude of the field was kept sufficiently high and the exchange time small so that the thermal diffusion is low. It is necessary to remove the metallic mask in the second step so that Na^+ ions can enter the glass through the previously masked regions. Otherwise, their depletion would cause side diffusion of silver.

A study of the effect of mask material on the side diffusion has been performed [68] and preliminary results obtained indirectly from the mode field measurements show that the mode width is somewhat reduced if Al_2O_3 mask is used in the first step. Because of low concentration of silver involved in these buried guides, SEM technique is inadequate for profile determination.

Figure 12 shows the intensity profiles of typical surface waveguides as obtained by scanning the near field along the depth (vertical - V, normal to the substrate plane) and width (horizontal - H, in the substrate plane) directions. Notice the asymmetry along the depth direction caused by the air interface. The dotted curves show the fitted Gaussian using the maximization criteria of the launching efficiency given by (24). The mode field asymmetry

of the surface guides causes fiber-waveguide mismatch loss and additional scattering losses. When the guides are buried, the mode symmetry is improved and circular fiber-like distribution is produced [53]. The mismatch loss of 0.2dB, obtained in the optimized case of mask widths W_c in the 5-6 μm range is relatively insensitive to the exact value of the mask width. This relative insensitivity of the total loss to the exact channel width is very encouraging. The propagation losses of 0.4dB/cm at 1.3 μm in commercial sodalime microscope slide have been achieved in these buried waveguides. The measured mode intensity distribution is in qualitative agreement with the solution of the Helmholtz equation [69]. However, a quantitative comparison cannot be made lest the index profile be modeled more realistically. Efforts are presently underway to obtain a correlation in channel waveguides to the same level of satisfaction as is obtainable in planar guides [18].

While the attempts to optimize the single-mode guides for low losses and fiber compatibility have given favorable results, the progress on the device end using Ag^+ - Na^+ exchange has been tardy. Part of this can be attributed to the lack of enthusiam owing to the general belief that silver glasses are lossy and prone to deterioration in their optical transmission. While this is true if pure $AgNO_3$ melts are used, single-mode structures with low silver contents are not likely to suffer from these drawbacks. The early efforts of Walker and Wilkinson [64,70] in Ag^+ - Na^+ devices using pure $AgNO_3$ melts included fabrication of directional couplers and ring resonators which showed high losses. Working on similar lines substantial progress has been reported in ring structures by Mahapatra and co-workers [65,71,72] with losses of the order of ~ 0.8 dB/cm at 0.63 μm and a finesse of 55 for the ring. Recently, buried directional couplers for wavelength multiplexing at 0.85 μm and 1.30 μm

in a borosilicate glass has been reported using dilute melts [56]. However, the losses are still high (~ 1 dB/cm) and the waveguides support two transverse modes at 0.85 μm. In none of the above studies reproducibility factor has been adquently discussed and at present it is not clear what the limitations will be.

K^+ - Na^+ Exchange

This system has by far been the most used for single-mode device fabrications. This preference may be attributed to two principal factors:

(i) The index change with pure KNO_3 melt is highly compatible with single-mode fibers.

(ii) Unlike Ag^+ - Na^+ process, no conentration control of the melt is required.

Yip et al [13,46] have reported an extensive study of K^+ - Na^+ planar guides in soda-lime glass. It includes determination of the index profile, measurement of the interdiffusion coefficient and its temperature dependence, Δn, and birefringence. Similar studies have been extended to BK - 7 [14], Pyrex glass [14], and semiconductor-doped colored glasses [73]. Index profile and stress-induced index change and birefringence have been calculated and correlated with the experimental data [36,38,46,73].

Single-mode devices have been observed to preserve the polarization [15,74] with cross coupling of 25 dB. Both, Y-type and directional coupler type 1 x 3 star couplers have been fabricated [74,75], analyzed [74] and characterized [74] with losses as low as 0.5 dB/cm at 0.63 μm. Directional couplers using one-step [56] as well as two-step [76] process have been fabricated and characterized. The attenuation of 2.1 dB in the former case (66 mm long waveguides) is caused by the surface scattering. However, the

authors claim that their attempts to bury the K^+ - Na^+ waveguides were unsuccessful and they attribute this to a strong affinity of K^+ to the glass.

Symmetric and asymmetric couplers consisting of two circular guides or a pair of a straight and a circular waveguide have been fabricated using K^+ - Na^+ process in BK - 7 glass [77]. The coupling ratio varies exponentially with the separation and the results are in good agreement with the calculations performed using coupled mode theory [77] as well as Beam Propagation Method [54]. In the latter work, an electric field was applied across the substrate and identical mode fields at 0.63 μm were obtained for 2 μm and 4 μm wide windows. It is not obvious whether this was a result of the two waveguides having same index profile (caused by different side diffusion in the two cases) or it was due to the weaker guidance in the 2 μm channel.

Cs^+ - K^+ Exchange

This cation pair system has recently been adopted by several workers in West Germany [9,16,78]. They use a special glass BGG21 made by Schott Glassworke. The composition of the glass [9,16] is such that it allows optimization of the process parameters for single-mode waveguide fabrication. The waveguides are nearly stress-free [16], low-loss (<0.1 dB/cm) and reproducible [33] and can be buried using a two-step process [78]. Diffusion is performed from a molten mixture of $CsNO_3$ and $CsC\ell$ which gives $\Delta n = 0.04$. Dilution with KNO_3 gives smaller Δn and can be controlled to the desired value [78]. Characterization of the ion-exchange process using planar waveguides appears to be complete, paving the way to useful device fabrication.

VIII Conclusion

Recent developments in the study of ion-exchange process have permitted a better understanding of the role of the processing conditions and the substrate glass in influencing the index profile of planar, surface and buried single-mode waveguides. While such detailed correlations in the case of Ag^+-Na^+ exchange have allowed fabrication of low-loss, fiber compatible, reproducible, buried channel waveguides whose characteristics are in qualitative agreement with those predicted by solutions of the two-dimensional diffusion equation with simplified approximations, difficulties remain in obtaining quantitative agreement with the theory under realistic processing conditions. Buried waveguide fabrication using K^+-Na^+ process still remains to be demonstrated and optimized for losses and mode symmetry. The subject of the tolerance of processing parameters required for a specified degree of *assured reproducibility* is an open question as is the concern with the prevalence of myrads of non-standard glass compositions. Finally, the issues of the possible degradation and other ultimate limitations of ion-exchanged waveguide components have to be resolved. Nevertheless, significant developments in fabrication of devices such as multiplexers, star couplers, and ring resonators using Ag^+-Na^+ as well as K^+-Na^+ process have stimulated renewed interest in other cation pair systems for fabrication of single-mode devices and in spite of the belated entry into the arena of integrated optics, glass waveguides appear to be more viable candidates for applications as passive I-O components than ever before.

Acknowledgement: The authors acknowledge valuable discussions with H.C. Cheng, H. Zhenguang, A. Miliou, and T.J. Anderson. This work was supported by AFOSR Contract No. 84-0369.

References

1. T. Izawa and H. Nakagome, 'Optical waveguide formed by electrically induced migration of ions in glass plates,' Appl. Phys. Lett. 21, 584 (1972).

2. T. Findakly, 'Glass waveguides by ion-exchange: A Review,' Opt. Engg. 24, 244 (1985).

3. R.H. Doremus, 'Ion Exchange in Glass,' Chapter 1 in Ion Exchange-A Series of Advances, Vol. 2. Ed. J.A. Marinsky, Marcel Dekker, New York (1969).

4 R. Terai and R. Hayami, 'Ionic diffusion in glasses,' J. Non-cryst solids, 18, 217 (1975).

5. T.G. Giallorenzi, E.J. West, R. Kirk, R. Ginther, and R.A. Andrews, 'Optical waveguides formed by thermal migration of ions in glass,' Appl. Opt. 12, 1240 (1973).

6. G. Stewart, C.A. Millar, P.J.R. Laybourn, C.D.W. Wilkinson, and R.M. de la Rue, 'Planar optical waveguides formed by silver-ion migration in glass,' IEEE J. Quantum Electron. QE-13, 192 (1977).

7. G.H. Chartier, P. Jaussaud, A.D. de Oliveira and O. Parriaux, "Fast fabrication method for thick and highly multimode optical waveguides," Electron. Lett. 13, 763 (1977).

8. V. Neuman, O. Parriaux and L.M. Walpita, 'Double-alkali effect: Influence on index profile of ion-exchanged waveguides,' Electron. Lett. 15, 704 (1979).

9. L. Ross, H.J. Lilienhof, H. Holscher, H.F. Schlaak and A. Brandenburg, 'Improved substrate glass for planar waveguides by Cs-ion exchange,' Tech. Digest, Topical Meeting on Integrated and Guided-Wave Optics, 26-28 Feb. 1986, Atlanta, Ga. Paper ThBB2, pp. 25-26.

10. R.G. Eguchi, E.A. Maunders and I.K. Naik, 'Fabrication of Low-loss waveguides in BK-7 by ion-exchange,' Proc. SPIE 408, 21 (1983).

11. G. Stewart and P.J.R. Laybourn, 'Fabrication of ion-exchanged optical waveguides from dilute silver nitrate melts,' IEEE J. Quantum Electron. QE-14, 930 (1978).

12. R.K. Lagu and V. Ramaswamy, 'Fabrication of single-mode glass waveguides by electrolytic release of silver ions,' App. Phys. Lett. 45, 117 (1984).

13. G.L. Yip and J. Albert, 'Characterization of planar optical waveguides by K^+-ion exchange in glass,' Opt. Lett. 10, 151 (1985).

14. J.E. Gortych and D.G. Hall, 'Fabrication of planar optical waveguides by K^+-ion exchange in BK7 and pyrex glass,' IEEE J. Quantum Electron. QE-22, 892 (1986).

15. J.L. Jackel, K.Y. Lee, and F.J. Favire, 'Do glass waveguides depolarize?' IEEE J. Lightwave Tech. LT-3, 818 (1985).

16. L. Ross, N. Fabricius, and H. Oeste, 'Single mode integrated optical waveguides by ion-exchange in glass,' European Fiber Optic Conference, LAN 87, Basel, Switzerland.

17. I. Fainaro, M. Ish Shalom, M. Ron and S. Lipson, 'Interdiffusion of silver in glasses and the related variations in electronic polarizability,' Phys. Chem. Glasses 25, 16 (1984).

18. H.C. Cheng, R.V. Ramaswamy and R. Srivastava, 'Buried Na^+-Ag^+ ion-exchanged glass waveguides: Theory and experiment,' Tech. Dig. 7th Topical Meeting on Gradient-Index Optical Imaging Systems, Jan. 15-16, 1987, Reno (Nevada), Paper ThC2-1.

19. R.V. Ramaswamy, R. Srivastava, and P. Chludzinski, 'Influence of Ag^+-Na^+ ion-exchange equilibrium on the index profile of single-mode glass waveguides,' Tech. Dig. Gradient-Index Optical Imaging Systems, GRIN '87, Reno, Nev., Paper ThB4-1, Jan. 1987.

20. S.I. Najafi, R. Srivastava and R.V. Ramaswamy, 'Wavelength-dependent propagation characteristics and mode cutoffs in Ag^+-Na^+ exchanged planar glass waveguides,' Appl. Opt. 25, 1840 (1986).

21. G.H. Chartier, P. Jaussaud, A.D. de Oliveira, and O. Parriaux, 'Optical waveguides fabricated by electric-field controlled ion exchange in glass,' Electron. Lett. 14, 132 (1978).

22. J. Viljanen and M. Leppihalme, 'Fabrication of optical strip waveguides with nearly circular cross section by silver ion migration technique,' J. Appl. Phys. 51, 3563 (1980).

23. C.W. Pitt, A.A. Stride and R.I. Trigle, 'Low temperature diffusion process for fabricating optical waveguides in glass,' Electron. Lett. 16, 701 (1980).

24. T. Findakly and E. Garmire, 'Reduction and control of optical waveguide losses in glass,' Appl. Phys. Lett. 37, 855 (1980).

25. S.I. Najafi, P.G. Suchoski, Jr., and R.V. Ramaswamy, 'Silver film-diffused glass waveguides: Diffusion process and optical properties,' IEEE J. Quantum Electron. QE-22, 2213 (1986).

26. H.M. Garfinkel, 'Ion-exchange equilibria between glass and molten salts,' J. Phys Chem. 72, 4175 (1968).

27. J. Crank: The Mathematics of Diffusion--Oxford at the Clarendon Press, 1956.

28. P. Chludzinski, R.V. Ramaswamy and T.J. Anderson, 'Silver-sodium ion-exchange in soda-lime silicate glass,' Phys. Chem. Glasses. To be published in Nov. 1987.

29. J.G. Kirkwood and J. Oppenheim, Chemical Thermodynamics--McGraw Hill, New York, 1961.

30. V. Rothmund and G. Kornfeld, 'Der basenaustausch im permutit. I.,' Z. Anorg, Allg. Chem. 103, 129 (1918).

31. G. Schulze, 'Versuche uber die diffusion von silber in glas,' Ann. Physik, 40, 335 (1913).

32. S.N. Houde-Walter and D.T. Moore, 'Delta-n control in GRIN glass by additives in AgCl diffusion baths,' Appl. Opt. 25, 3373 (1986).

33. N. Fabricius, H. Oeste and L. Ross, 'Reproducibility of the thermal ion exchange process in substrate glass BGG 21.' Unpublished.

34. M.L. Huggins and K.H. Sun, 'Calculation of density and optical constants of a glass from its composition in weight percentage,' J. Am. Ceram. Soc., 26, 4 (1943).

35. S.D. Fantone, 'Refractive index and spectral models for gradient-index materials,' Appl. Opt. 22, 432 (1983).

36. M. Abou-el-Leil and F. Leonberger, 'A model for ion exchanged waveguides in glass,' 86th Annual Meeting of American Ceramic Society, Paper 105-G-86, Chicago, Ill. April, 1986.

37. J. Albert and G.L. Yip, 'Stress-induced index change for K^+-Na^+ ion exchange in glass,' Electron. Lett. 23, 737 (1987).

38. A. Brandenburg, 'Stress in ion-exchanged glass waveguides,' J. Lightwave Tech. LT-4, 1580 (1986).

39. K. Tsutsumi, H. Hirai and Y. Yuba, 'Characteristics of swelling of sodium-potassium ion-exchanged glass waveguides,' Electron. Lett. 22, 1299 (1986).

40. W.G. French and A.D. Pearson, 'Refractive index changes produced in glass by ion-exchange,' Ceram. Bull. 49[11], 474 (1970).

41. R.H. Doremus, 'Exchange and diffusion of ions in glass,' J. Phys Chem. 68, 2212 (1964).

42. D.E. Day, 'Mixed alkali glasses--their properties and uses,' J-Non-cryst solids, 21, 343 (1976).

43. R.G. Walker, C.D.W. Wilkinson and J.A.H. Wilkinson, 'Integrated optical waveguiding structures made by silver ion exchange in glass: 1. The propagation characteristics of stripe ion-exchanged waveguides; a theoretical and experimental investigation,' Appl. Opt. 22, 1923 (1983).

44. H.J. Lilienhof, E. Voges, D. Ritter, and B. Pantschew, 'Field-induced index profiles of multimode ion-exchanged strip waveguides,' IEEE J. Quantum Electron., QE-18, 1877 (1982).

45. R.K. Lagu and R.V. Ramaswamy, 'Process and waveguide parameter relationships for the design of planar silver ion-exchanged glass waveguides,' J. Lightwave Tech. LT-4, 176 (1986).

46. J. Albert and G.L. Yip, 'Refractive-index profiles of planar waveguides made by ion-exchange in glass,' Appl. Opt. 24, 3692 (1985).

47. M. Abou-el-Leil and A.R. Cooper, 'Analysis of field-assisted binary ion exchange,' J. Am. Ceram. Soc. 62, 390 (1979).

48. T. Kaneko, and H. Yamamoto, 'On the ionic penetration of silver film into glasses under the electric field,' Proc. 10th Int. Congr. Glass, Kyoto, Japan, 1974, pp. 8, 79-8-86.

49. R.V. Ramaswamy and S.I. Najafi, 'Planar, buried, ion-exchanged glass waveguides: Diffusion characteristics,' IEEE J. Quantum Electron. QE-22, 883 (1986).

50. H. Yoshida and T. Kataoka, 'Migration of two ions during electrolysis of glass waveguide,' J. Appl. Phys. 58, 1739 (1985).

51. G. Chartier, P. Collier, A. Guez, P. Jaussaud, and Y. Won, 'Graded-index surfade or buried waveguides by ion-exchange in glass,' Appl. Opt. 19, 1092 (1980).

52. S.I. Najafi and R.V. Ramaswamy, 'Diffusion and modal characterization of Ag^+-Na^+ exchanged channel waveguides,' Tech. Digest, Topical Meeting in Integrated and Guided-Wave Optics, 26-28, Feb. 1986, Atlanta, Ga., paper FDD2, pp. 60-61.

53. H.C. Cheng, R.V. Ramaswamy and R. Srivastava, 'Modeling and Fabrication of buried, fiber-compatible single-mode channel waveguides by Ag^+-Na^+ ion exchange, unpublished.

54. H.W. Melcher, H.J. Lilienhof and H.F. Schlaak, 'Fabrication of monomode ring coupler by field enhanced K^+ ion-exchange in BK-7 glass,' Third Int. Symp. Optical and Optoelectronic Appl. Sci. and Engg., Innsbruck, Austria, paper 651-09, April 13-23 (1986).

55. R.K. Lagu, R.V. Ramaswamy, and S.I. Najafi, 'Fabrication and characterization of buried glass waveguides with symmetric index profiles,' Tech. Dig. Third European Conf. Int. Optics (ECIO), Berlin, paper II-R, pp 75-80, May 1985.

56. M. McCourt, R. Rimet and C. Nissim, 'Multiplexing characteristics of K^+ and Ag^+ ion-exchanged directional couplers,' European Fiber Optic Conference LAN 87, Basel, Switzerland.

57. T.W. Cline, 'Diffused channel glass waveguide optical splitters'; Tech. Digest, Topical Meeting on Integrated and Guided Wave Optics, IGFO '86, Feb. 1986, Atlanta, Ga., Paper FDD4.

58. J.L. Jackel, 'Glass waveguides made using ion exchange in a KNO_3: $AgNO_3$ equimolar melt,' Tech. Dig. Gradient-Index Optical Imaging Systems, (GRIN), Reno, Nev. Paper Th B3-1, Jan. 1987.

59. R.K. Lagu, S.I. Najafi and V. Ramaswamy, 'In situ measurement of ionic concentration during fabrication of ion-exchanged waveguides,' Appl. Opt. 23, 3925 (1984).

60. J.M. White and P.F. Heidrich, 'Optical waveguide refractive index profiles determined from measurement of mode indices: A simple analysis,' Appl. Opt. 15, 151 (1976).

61. P.K. Tien, R. Ulrich and R.J. Martin, 'Modes of propagating light waves in thin deposited semiconductor films', Appl. Phys. Lett. 14, 291 (1969).

62. R. Srivastava, C.K. Kao and R.V. Ramaswamy, 'WKB analysis of planar surface waveguides with truncated index profiles,' IEEE J. Lightwave Tech. To be published in Nov., 1987.

63. Y.H. Won, P.C. Jaussaud, and G.H. Chartier, 'Three-prism loss measurements of optical waveguides,' Appl. Phys. Lett. 37, 269 (1980).

64. R.G. Walker and C.D.W. Wilkinson, 'Integrated optical ring resonators made by silver ion-exchange in glass,' Appl. Opt. 22, 1029 (1983).

65. A. Mahapatra and J.M. Connors, 'Double Tapped Ring Resonators Fabricated in Glass,' Topical Meeting on Optical Fiber Communications and International Conference on Integrated Optics and Optical Communications, Jan. 1987, Reno, Nev. Paper TuK3.

66. P.G. Suchoski, Jr. and R.V. Ramaswamy, 'Minimum mode-size low-loss Ti: $LiNbO_3$ channel waveguides for efficient modulator operation at 1.3 μm,' IEEE J. Quantum Electron. To be published.

67. W.K. Burns and G.B. Hocker, 'End fire coupling between optical fibers and diffused channel waveguides,' Appl. Opt. 16, 2048 (1977).

68. H. Zhenguang, A. Miliou, H.C. Cheng, R. Srivastava, and R.V. Ramaswamy, 'Fiber compatible buried low-loss single-mode K^+-Na^+ ion exchanged waveguides.' Unpublished.

69. R.K. Lagu and R.V. Ramaswamy, 'A variational finite-difference method for analyzing channel waveguides with arbitrary index profiles,' IEEE J. Quantum Electron., QE-22, 968 (1986).

70. R.G. Walker and C.D.W. Wilkinson, 'Integrated optical waveguiding structures made by silver ion-exchange in glass 2: Directional coupler and bends,' Appl. Opt. 22, 1929 (1983).

71. A. Mahapatra and J.M. Connors, 'High finesse ring resonators-fabrication and analysis,' SPIE Integrated Optical Circuit Engineering III, 651, 272 (1986).

72. A. Mahapatra and J.M. Connors, 'Tapped ring resonators fabricated in glass,' SPIE Integrated Optical Circuit Engineering IV, 704, 168 (1986).

73. T.J. Cullen, C.N. Ironside, C.T. Seaton, and G.I. Stegeman, 'Semiconductor-doped glass ion-exchanged waveguides,' Appl. Phys. Lett. 49, 1403 (1986).

74. T. Findakly and B. Chen, 'Single-mode integrated optical 1xN star coupler,' Appl. Phys. Lett. 40, 549 (1982).

75. M. Haruna, M. Belanger, and G.L. Yip, 'Passive 3-branch optical power divider by K^+-ion exchange in glass,' Electron, Lett. 21, 535 (1985).

76. G.L. Yip and J. Finak, 'Directional-coupler power divider by two-step K^+-ion exchange,' Opt. Lett. 9, 423 (1984).

77. H.F. Schlaak, A. Brandenburg, and G. Sulz, 'Integrated optical couplers with circular waveguides,' Tech. Dig. Topical Meeting in Integrated and Guided Wave Optics, Atlanta, Ga., Paper FDD2, Feb. 1986.

78. L. Ross and H.J. Lilienhof, 'Buried waveguides for passive integrated optics by Cs^+ ion-exchange,' SPIE 3rd International Symposium on Optical and Optoelectronic Appl. Sci. and Engg. Innsbruck, Austria, April 13-23, 1986.

Table I. Easiest Results of Ion-Exchanged Waveguides for Various Ions. The host ion is Na^+.

Ion	Radius A°	Polarizability $A°^3$	Glass	Melt	Temperature (°C)	∇n	Reference
Tl^+	1.49	5.2	Boro-silicate	$TlNO_3$ +KNO_3 +$NaNO_3$	530	0.001 -0.1	1
K^+	1.33	1.33	Soda-lime and	KNO_3	365	0.003	5
Ag^+	1.26	2.4	Alumino-silicate	$AgNO_3$	225-270	0.13	5
Li^+	0.65	0.03	Soda-lime	Li_2SO_4 +K_2SO_4	520-620	0.012	7
Rb^+	1.49	1.98	Soda-lime	$RbNO_3$	520	0.015	8
Cs^+	1.65	3.34	Soda-lime	$CsNO_3$	520	0.03	8
Cs^+	1.65	3.34	BGG21	$CsNO_3$ +$CsCl$	435	0.043	9*

*Cs^+-K^+ ion exchange. For Na^+ ions, ionic radius is 0.95 A and its polarizability is 0.43 $A°^3$.

Table II. Diffusion Coefficients of Various Cations in Glasses used for Waveguides.

Cations	Glass	Temperature (°C)	$\tilde{D}$ (10^{-14} m^2/s)	Q (10^4 J/mole)	Reference
Tl^+	Borosilicate	530	20	--	1
Li^+	Soda-lime	575	64	14.2	7
Ag^+	Soda-lime	374	0.7	9.1	11
Ag^+	Borosilicate	615	0.26	9.1	44
Ag^+	Soda-lime	215	0.010	--	43
Ag^+	BK-7	320	0.025	9.8	10
Ag^+	Soda-lime	330	0.01-0.03	8.9	49
K^+	Soda-lime	385	0.11	12.5	13
K^+	BK-7	385	0.14	--	14
K^+	Pyrex	385	0.06	--	14
Cs^+	BGG21	407	0.32	20	9
Na^+	Soda-lime	371	12	16	41

Figure Captions

Fig. 1. Variation of Δn and W (measured at 1/e point) of silver film diffused guides at 275°C with applied voltage (1mm thick substrate). [25].

Fig. 2. Variation of Δn and the glass surface-silver concentration $\bar{N}_{Ag}$ with the melt concentration N_{Ag}. [19].

Fig. 3. Refractive index profile of planar surface Ag^+ - Na^+ waveguides using WKB method (0) with electric field and (x) without applied field. Solid curves are the best fit to data using theoretical calculations [18]. Curve 1 is ERFC and 2 is the fit to Eq (23).

Fig. 4. Calculated variation of the index peak position x_{peak} and the 1/e index width W with the second-step parameters [18]. Curves 1,2, and 3 correspond to E_2 = 10, 40, and 70 V/mm respectively. The data points (x) are from [49].

Fig. 5. Schematics of Ag^+ - Na^+ exchange using electrolytic release [12] and on-line concentration control [59].

Fig. 6. Experimental arrangement for measuring near-field profile and waveguide losses [66].

Fig. 7. A comparison of the index profile results using various techniques. +AAS [28], x SEM [49], 0 Inv. WKB, * Electron microprobe, - fitted ERFC to the measured mode indices using finite-difference method. $W_o = 2\sqrt{\tilde{D}t}$.

Fig. 8. Silver concentration profile in channel waveguides measured by SEM. $N_{Ag} = 2 \times 10^{-4}$, T = 330°C and t = 60 min. Mask opening width = 10 μm. Insets represent the 1-D scans along the dotted lines. [52].

Fig. 9. Comparison of surface-index change of channel waveguides with planar guides as a function of mask width. [52].

Fig. 10. Diffusion depth of surface channel waveguides as a function of mask width. The horizontal lines represent planar guide widths under identical diffusion conditions. [52].

Fig. 11. Variation of aspect ratio (width/depth) and total side diffusion (guide width-mask width) as a function of mask width for surface channel waveguides. [52].

Fig. 12. Typical mode intensity profiles of single-mode surface channel waveguides at 1.3 μm x horizontal, 0 vertical. The curves represent the best Gaussion fit using (24). [53]. $\eta = 0.933$ for fiber with 1/e intensity width of 6.83 μm, showing 0.30 dB coupling loss.

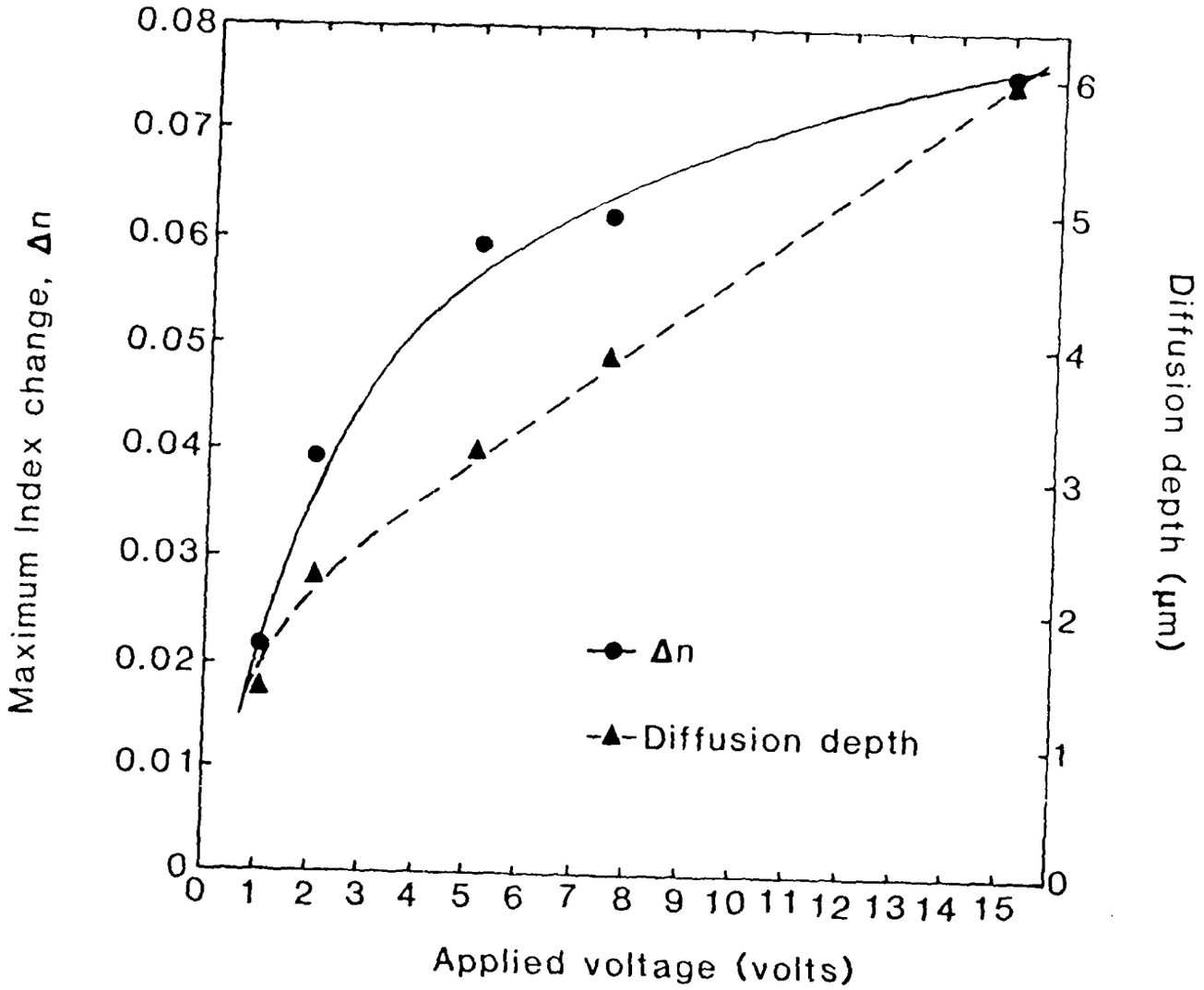

64

RVR & RS

Fig. 1

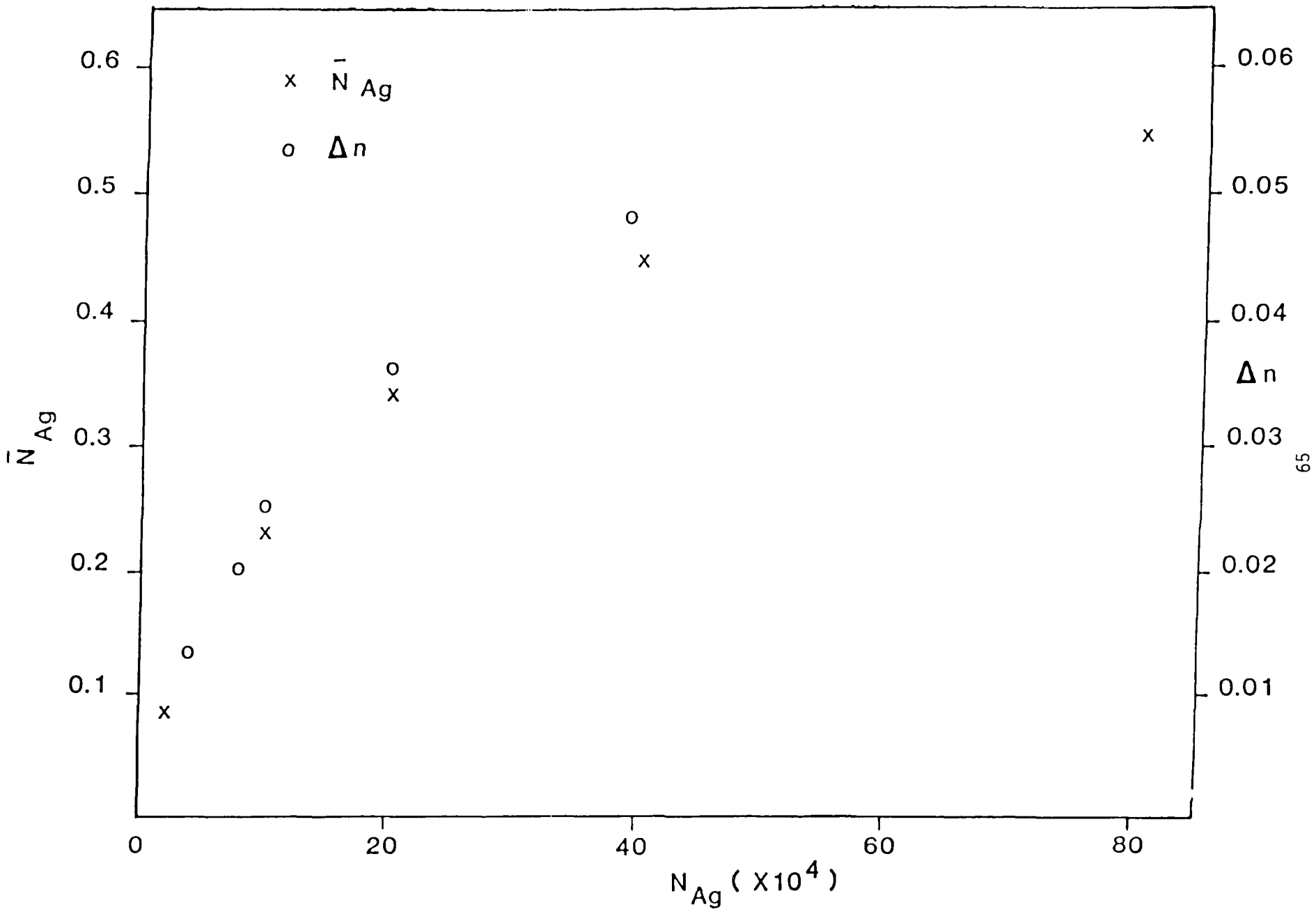
0.6
0.5
0.4
0.3
0.2
0.1
$\bar{N}_{Ag}$
x $\bar{N}_{Ag}$
o Δn
0.06
0.05
0.04
0.03
0.02
0.01
Δn
0
20
40
60
80
N_{Ag} (X10^4)

RVR & RS

Fig. 2

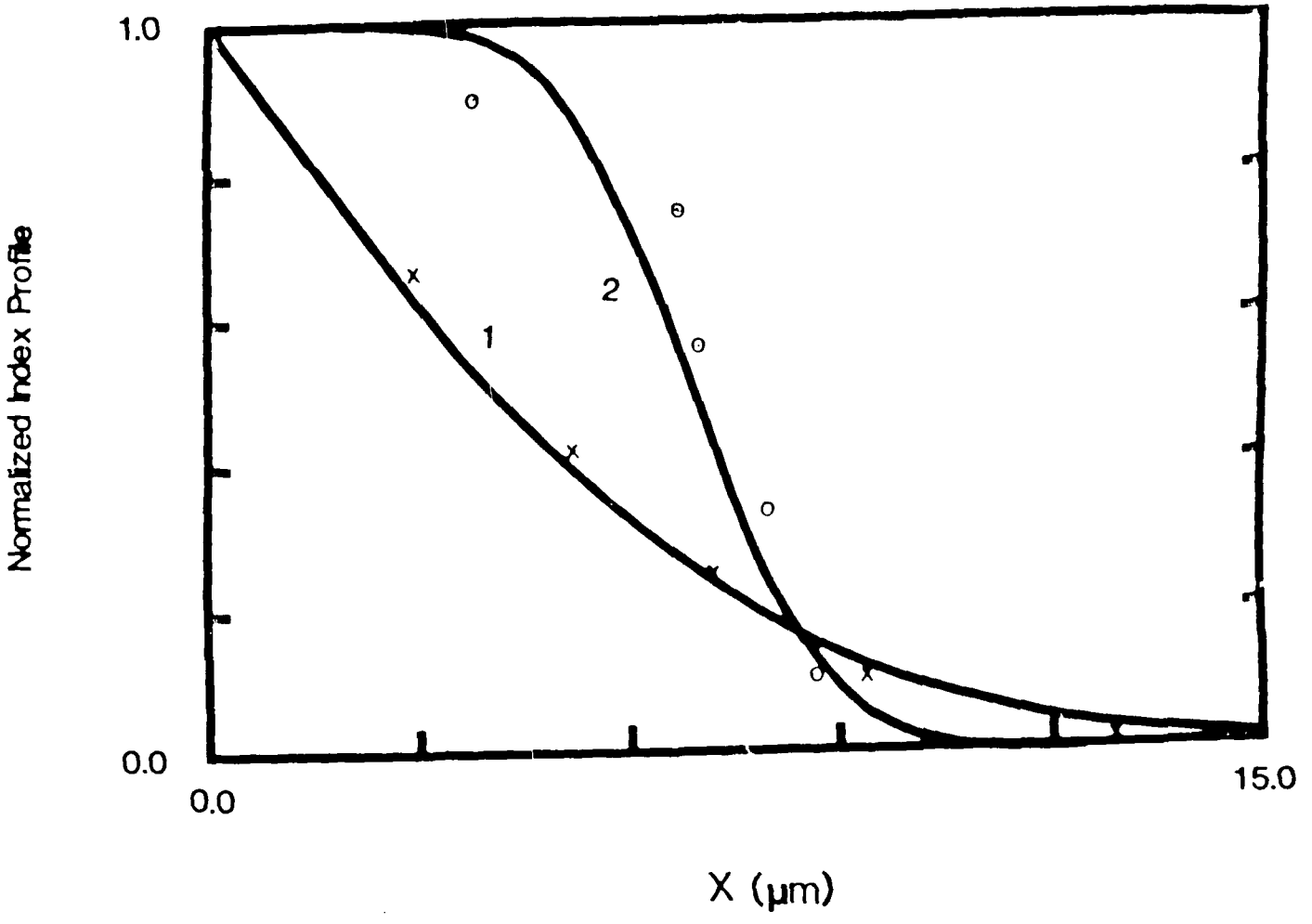

RVR & RS
Fig. 3

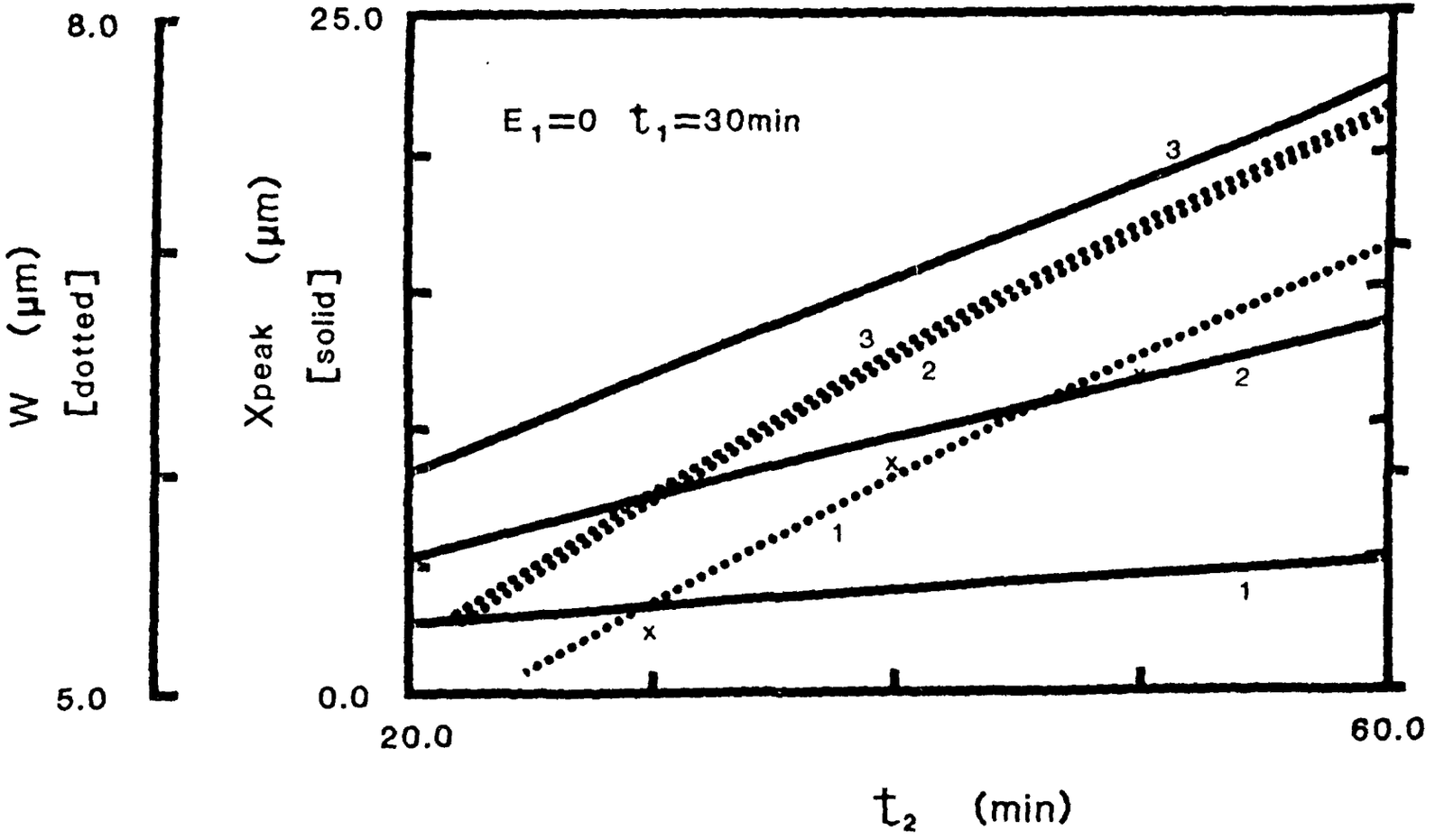
8.0
5.0
W (μm)
[dotted]
25.0
0.0
Xpeak (μm)
[solid]
$E_1=0$ $t_1=30$min
3
3
2
2
1
1
20.0
60.0
t_2 (min)

RVR & R.S.
Fig. 4

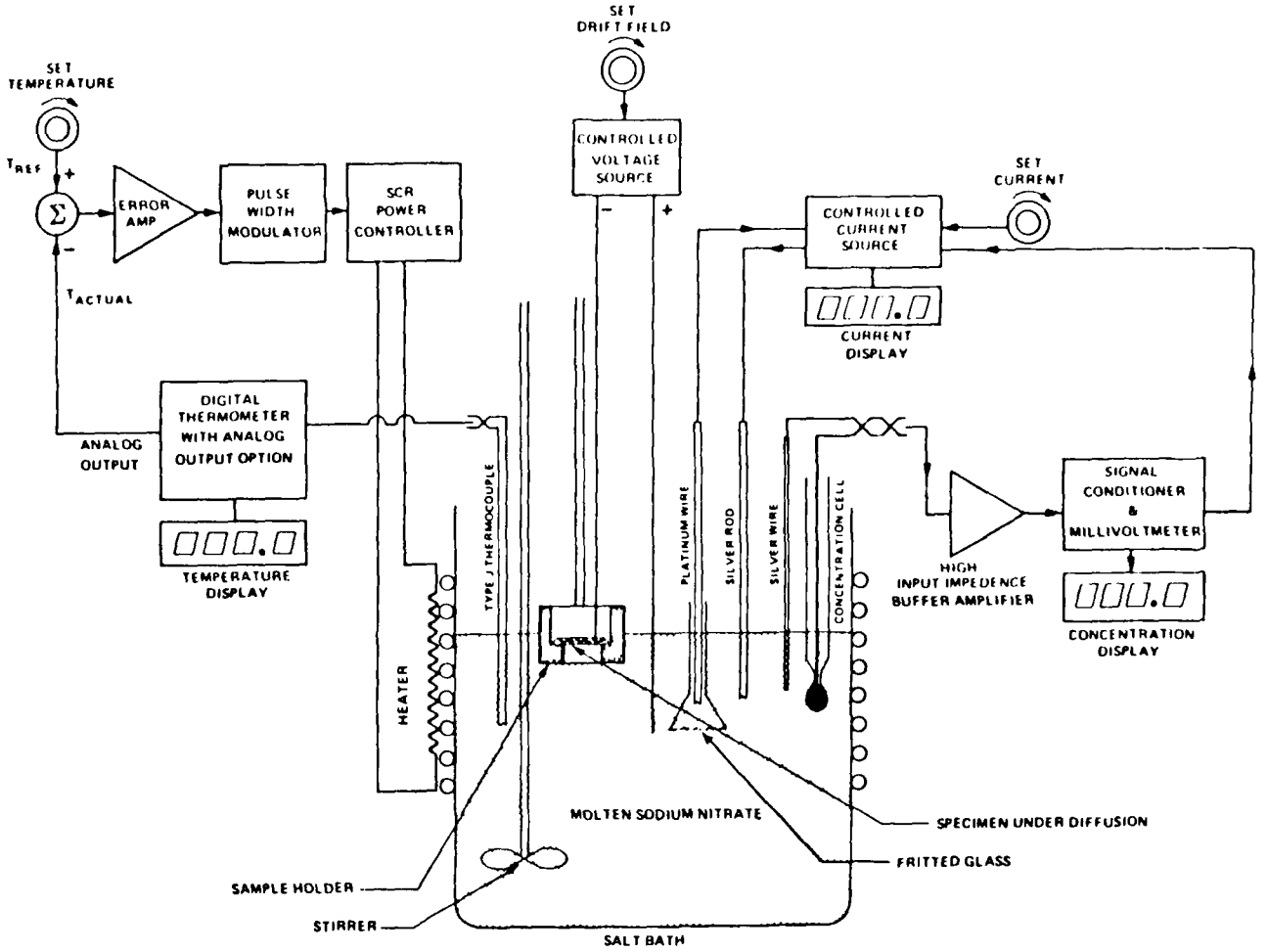
SET TEMPERATURE
T_{REF}
+
Σ
−
ERROR AMP
PULSE WIDTH MODULATOR
SCR POWER CONTROLLER
T_{ACTUAL}
ANALOG OUTPUT
DIGITAL THERMOMETER WITH ANALOG OUTPUT OPTION
000.0
TEMPERATURE DISPLAY
SET DRIFT FIELD
CONTROLLED VOLTAGE SOURCE
− +
SET CURRENT
CONTROLLED CURRENT SOURCE
000.0
CURRENT DISPLAY
SIGNAL CONDITIONER & MILLIVOLTMETER
HIGH INPUT IMPEDENCE BUFFER AMPLIFIER
000.0
CONCENTRATION DISPLAY
TYPE J THERMOCOUPLE
PLATINUM WIRE
SILVER ROD
SILVER WIRE
CONCENTRATION CELL
HEATER
MOLTEN SODIUM NITRATE
SPECIMEN UNDER DIFFUSION
FRITTED GLASS
SAMPLE HOLDER
STIRRER
SALT BATH

R V R & R S

Fig. 5

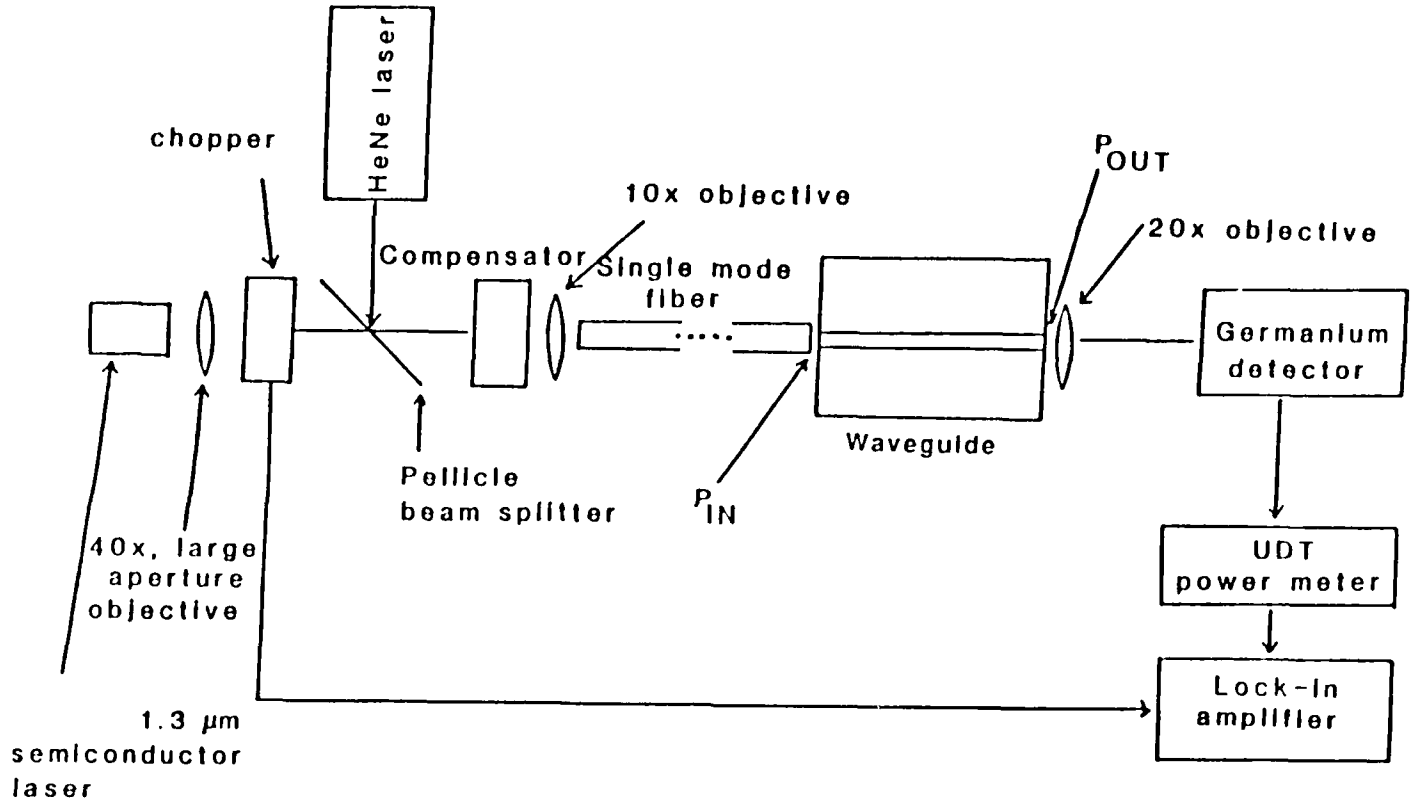
HeNe laser
chopper
10x objective
P_{OUT}
20x objective
Compensator
Single mode fiber
Germanium detector
Waveguide
Pellicle beam splitter
P_{IN}
40x, large aperture objective
UDT power meter
Lock-in amplifier
1.3 μm semiconductor laser

RVR & RS
Fig. 6

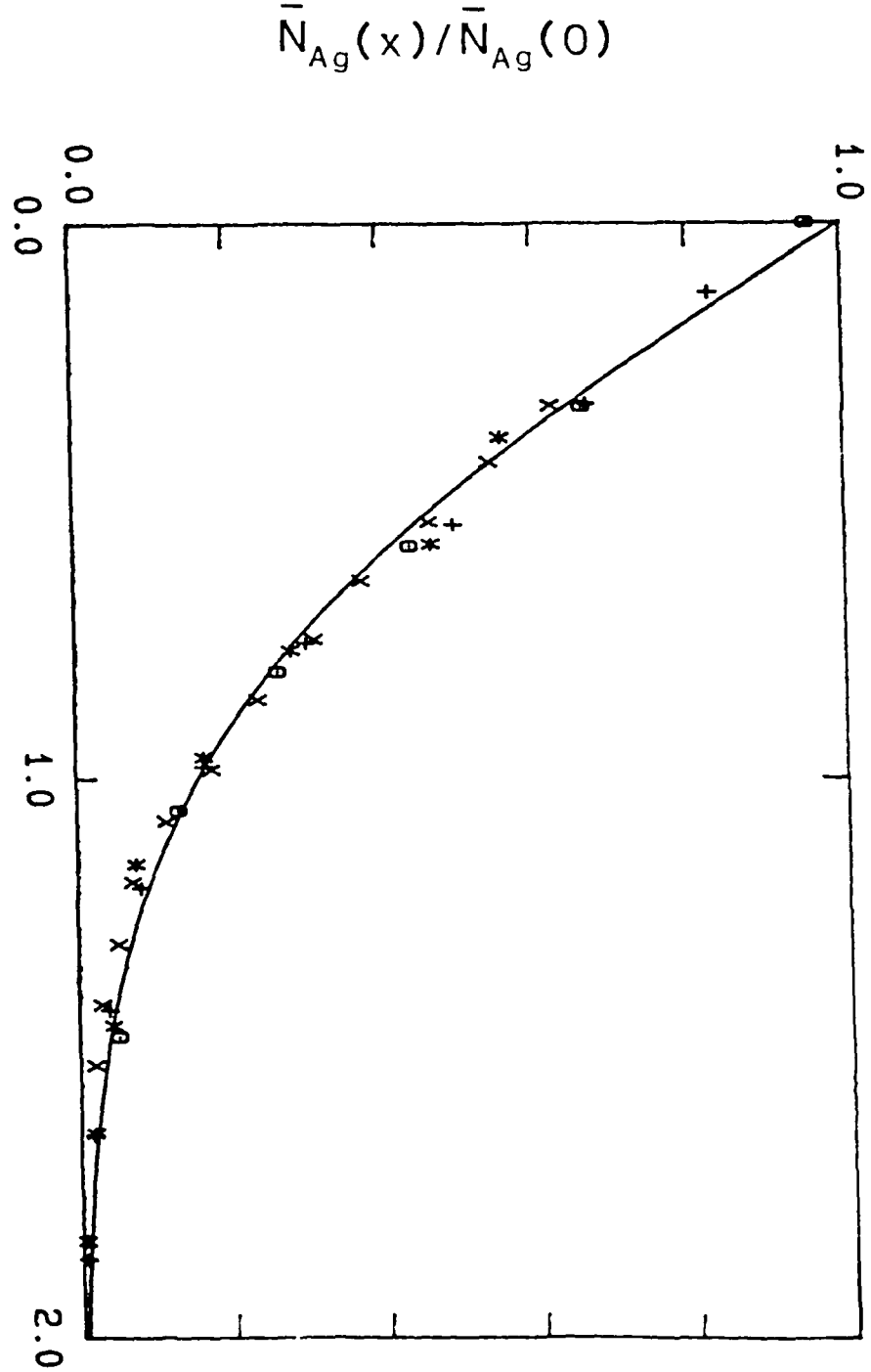

R vs R & RS
Fig. 7

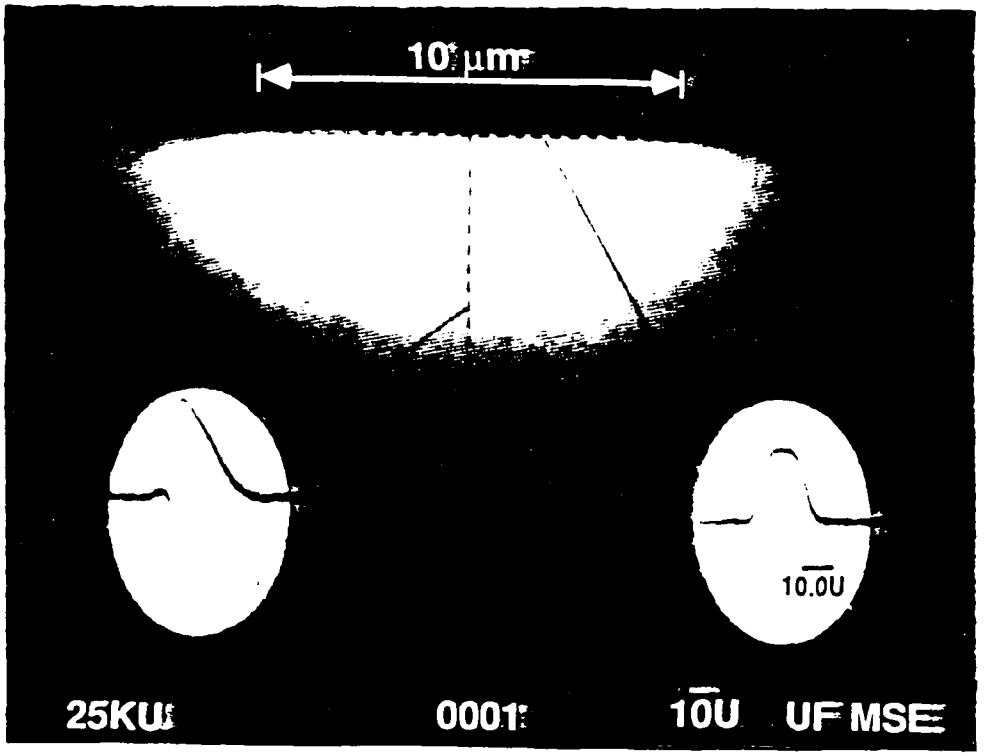

RVR & RS
Fig. 8

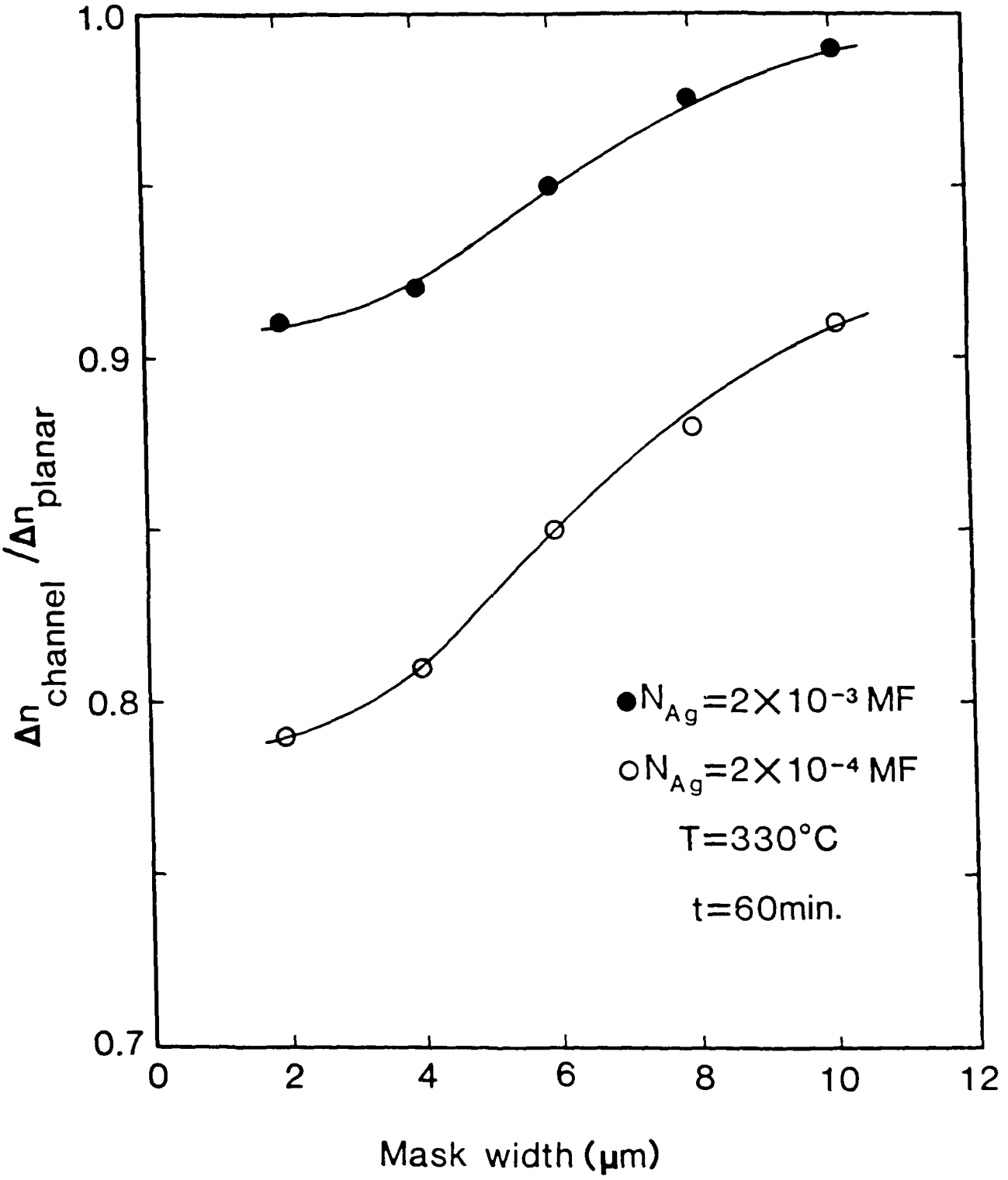
1.0
0.9
0.8
0.7
0
2
4
6
8
10
12
$\Delta n_{channel} / \Delta n_{planar}$
Mask width (μm)
●N_{Ag}=2X10^{-3} MF
○N_{Ag}=2X10^{-4} MF
T=330°C
t=60min.

RVR & FS
Fig 9

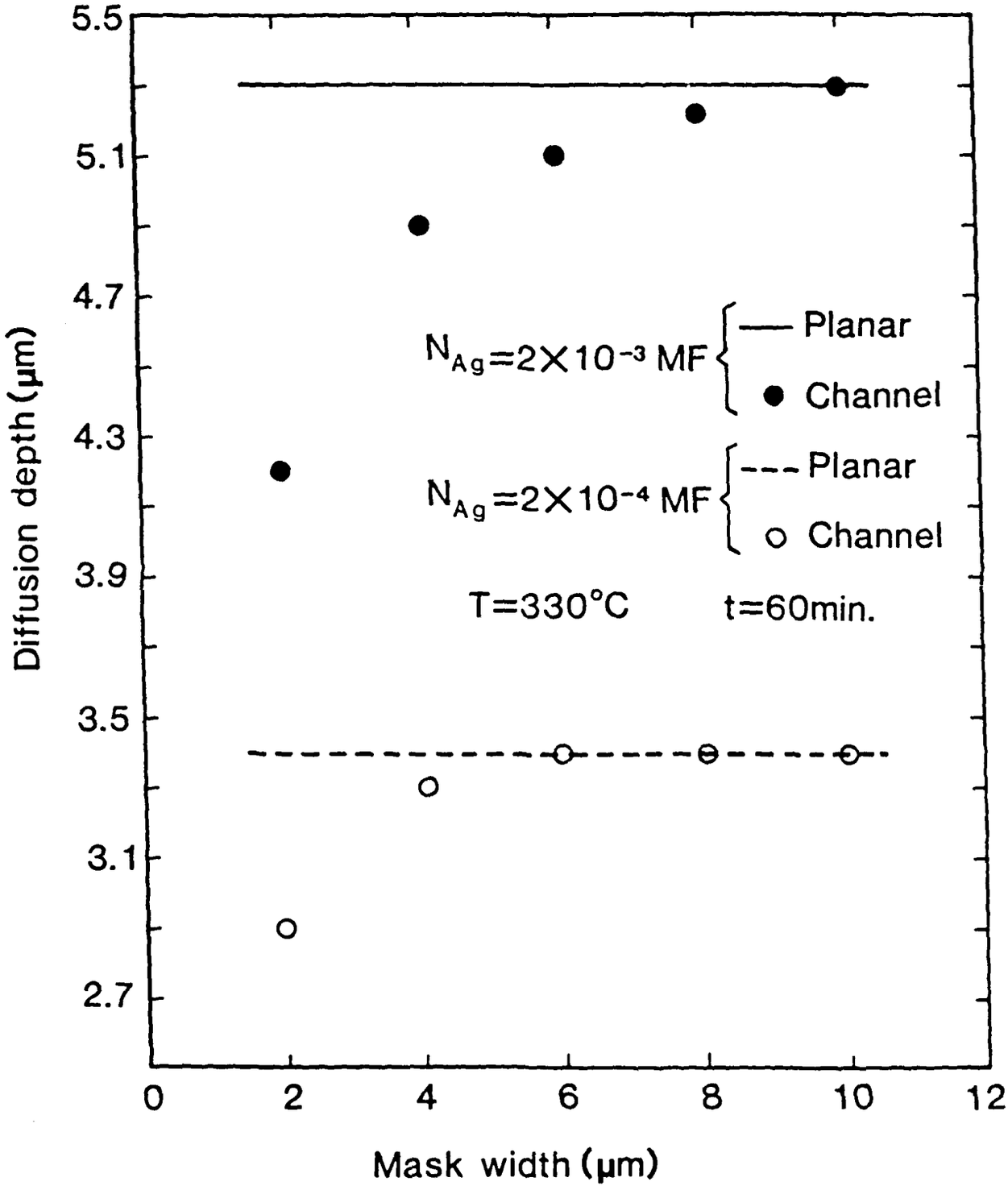
5.5
5.1
4.7
4.3
3.9
3.5
3.1
2.7
Diffusion depth (μm)
0
2
4
6
8
10
12
Mask width (μm)
$N_{Ag}=2\times10^{-3}$ MF
Planar
Channel
$N_{Ag}=2\times10^{-4}$ MF
Planar
Channel
T=330°C
t=60min.

KVR & RS
Fig. 1.2

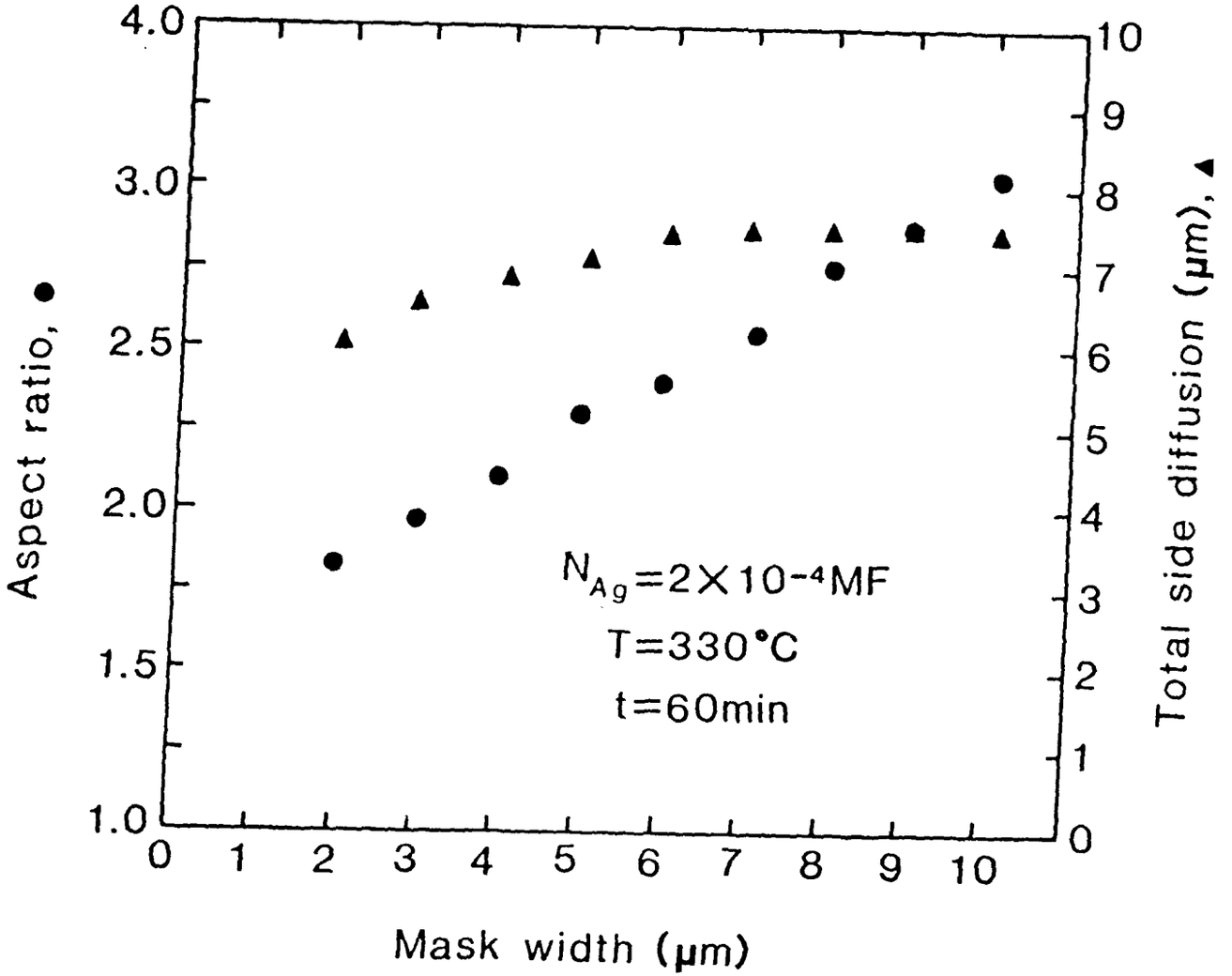
4.0
3.0
2.5
2.0
1.5
1.0
Aspect ratio, ●
10
9
8
7
6
5
4
3
2
1
0
Total side diffusion (μm), ▲
0 1 2 3 4 5 6 7 8 9 10
Mask width (μm)
$N_{Ag}=2\times10^{-4}$MF
T=330°C
t=60min

RVR & RS
Fig. 11

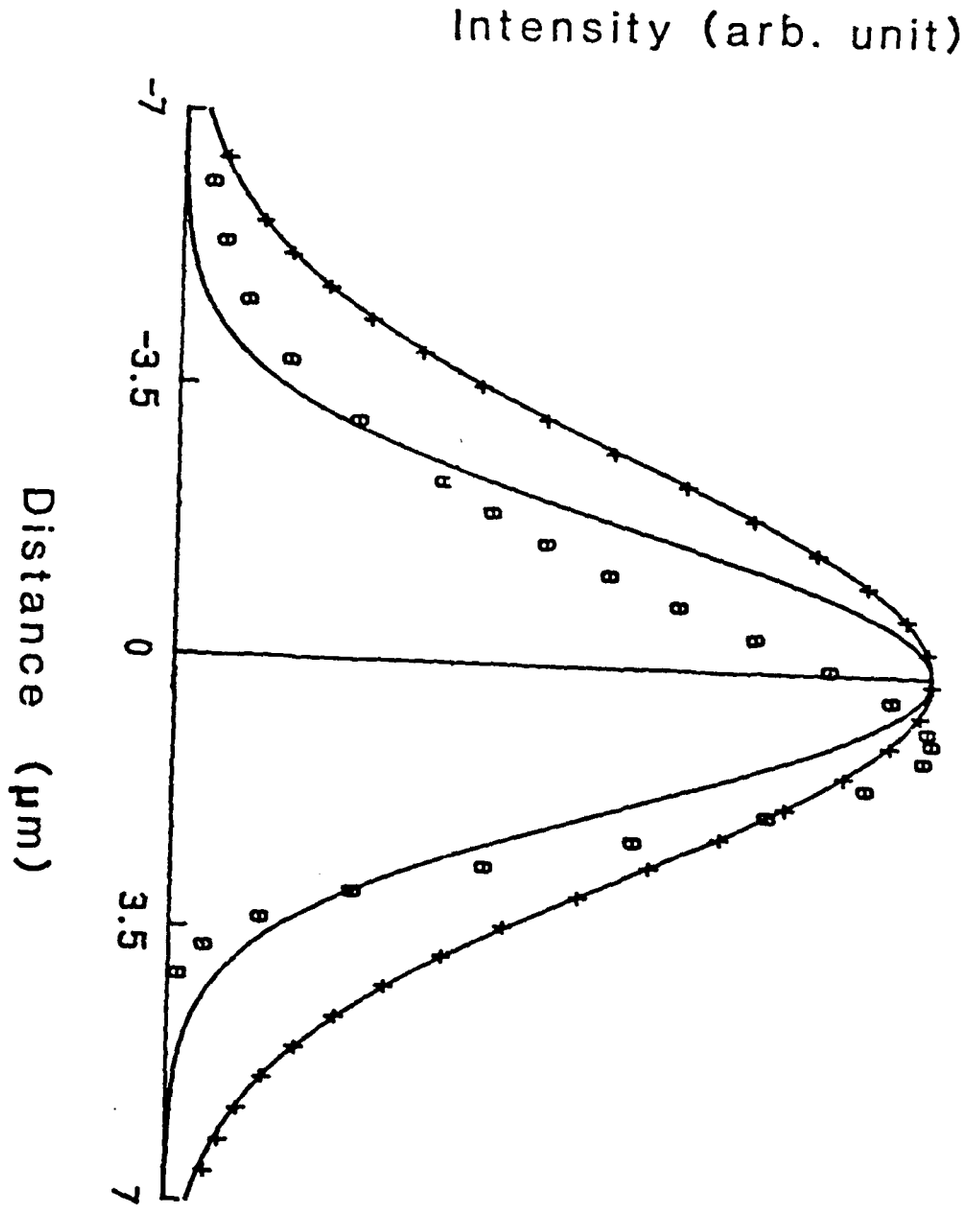

R.V.R. & R.S

REFERENCE [1b]

INVITED PAPER

Recent Advances In Ion-Exchanged Optical Waveguides and Components

R. V. Ramaswamy and R. Srivastava
Department of Electrical Engineering
University of Florida
Gainesville, FL 32611 USA

Abstract

There has been considerable interest in recent years in the technology for fabrication of glass waveguide components for integrated optics and sensor applications. This paper reviews the recent developments in the ion-exchange technology of single-mode glass waveguides and components. Fabrication, characterization and modelling of both surface and buried, planar as well as channel waveguides involving a two-step ion-exchange process are described. It is shown how a systematic study allows a correlation between the process parameters: namely, composition and temperature of the molten salts, diffusion time and applied field at each step, and the waveguide performance. We present the results on low-loss single-mode waveguides with mode field distribution compatible with single-mode fibers at 1.3 μm with a view towards optimization of passive devices at this wavelength.

Recent Advances In Ion-Exchanged Optical Waveguides and Components

R. V. Ramaswamy and R. Srivastava
Department of Electrical Engineering
University of Florida
Gainesville, FL 32611 USA

Introduction

The ion-exchange technique has received increased attention in recent years because it has been found to improve the surface-mechanical properties of glass [1] and, more importantly, to introduce a gradient index in the glass. The technique has been successfully used in the manufacture of low-loss optical fibers, gradient-index optical components for imaging applications, and, more recently, in the fabrication of planar and channel waveguides in glass substrates. In fact, glass waveguides are considered to be prime candidates for integrated optic (I-O) device applications such as star couplers, access couplers, wavefront sensors, multiplexers, demultiplexers, and in sensors such as gyroscopes. The importance of the glass waveguide-based I-O components is borne out by their compatibility with optical fibers and potentially low cost. In addition, they have low propagation loss and can be fabricated and integrated into the system with relative ease. However, unlike its electro-optic and semiconducting counterpart substrate materials (e.g., $LiNbO_3$, GaAs, etc.), index of the glass substrate cannot be tuned by application of an external electric field, and therefore glass devices must be fabricated with assured reproducibility within specified tolerances.

For I-O applications, one of the most important criteria in the selection of the host glass and the species of the exchanging ions is the simultaneous achievement of low propagation losses and the desired refractive index pro-

diffusion process be studied in detail to understand the role of the processing parameters. Only through a careful correlation of these parameters with the waveguide performance, it would be possible to establish guidelines for fabrication of devices with the desired characteristics.

Ion-Exchange Process

Since Izawa and Nakagome [3] reported the first ion-exchanged waveguide by Tl^+-Na^+ exchange, optical waveguides in glass substrates have invariably been fabricated by the ion-exchange process which creates a thin layer of higher refractive index beneath the surface of the substrates. This is normally accomplished by the diffusion of monovalent atoms of higher polarizability, e.g., Cs^+, Rb^+, K^+, Ag^+, and Tl^+ into the glass matrix where they exchange with Na^+ or K^+ ions. Besides the polarizability of the cations, the net index change also depends on the difference in the sizes of the two exchanging ions (formation of elastic stress in the glass) and the change in the polarizability of the oxygen ions. For example, when K^+ replaces Na^+, the exchange causes the glass to swell and undergo stress-induced birefringence [4]. On the other hand, when Li^+ exchanges with Na^+ in soda-lime glass, the glass index increases due to the collapse of the network near the smaller Li^+ ion [5].

In practice, there are two approaches to waveguide formation by ion exchange. In the most popular and widely studied approach [2-25], the glass substrate is immersed in a molten salt bath at an elevated temperature. In an alternative approach [26-31], a metallic film is deposited on the glass surface, and diffusion is carried out by applying an external field to incorporate the ions into the glass structure where they exchange with the alkali ion. This method has been used only for the Ag^+-Na^+ process because, silver, compared to other metals of the alkali group, does not suffer oxidation

easily. In this paper, we will be concerned with ion exchange from molten salt mixtures only with emphasis on single-mode waveguide structures.

Of the various monovalent ions exchanged in glass by diffusion, each one has its advantages and drawbacks. For example, Tl^+ is known to be somewhat toxic but gives rise to a relatively large index change (~0.1) and is therefore more suitable for multimode waveguides [3,9]. The losses are also reasonably low (~0.1 dB/cm). Ag^+ is susceptible to being reduced (becoming metallic) and thereby may introduce losses if diffused in large concentrations [2,15,32]. K^+ can be easily incorporated in soda lime [19], borosilicate or pyrex glasses [20], but the accompanying index change is substantially smaller (~0.01) along with smaller diffusion rates. Thus large diffusion times (a few hours) are required for suitable waveguiding to occur, limiting its use for single-mode guides. On the other hand, the diffusion coefficient of Li^+ is much larger, and highly multimode guides with index profiles compatible with optical fibers can be produced in a few minutes [5]. The maximum index change of the order of 0.015 can be achieved easily, but so far no low-loss guides have been demonstrated. In the case of Cs^+, the index change of the order of 0.043 has been achieved [21], but sufficient data are not yet available regarding loss, etc. One disadvantage in using Cs^+ is that it reacts with most materials, and therefore diffusion has to be carried out in a platinum crucible, thereby adding to the cost.

The K^+-Na^+ and Ag^+-Na^+ exchange processes have been used by several workers for fabricating single-mde devices such as star couplers, directional couplers, filters and ring resonators [33-42]. While single-mode optimization studies in Ag^+-Na^+ case have been reported [45], no systematic study of the fabrication parameters in the case of K^+-Na^+ exchange has been reported so far, with the result that the structures have not been optimized for loss and

file. The propagation losses are dominated by absorption primarily due to the presence of foreign impurities in the glass and the scattering contributions caused by the glass inhomogeneity and surface or geometric imperfections. By careful choice of the host glass, absorption losses as low as 0.07 dB/cm have been obtained [2]. Scattering losses, on the other hand, are generally introduced in the processing steps. Dopants introduce additional Rayleigh scattering to the background losses caused by the multicomponent nature of the glass. Reduction of the incoming ion in the glass matrix can give rise to additional losses. Surface irregularities invariably interact with the propagating field and contribute to losses by scattering. However, this can be minimized by burying the waveguides under the glass surface by carrying out a two-step diffusion process. Finally, even in straight channel waveguides the imperfect boundaries present in the mask and reproduced during the photolithographic process may introduce additional loss. This loss component is less serious, however, since the diffusion process smooths out such irregularities.

The refractive index profile, on the other hand, depends on various parameters in an intricate manner. The composition of the host glass, the nature of the incoming ion and its concentration in the source, the diffusion temperature, the diffusion time, and the magnitude of the externally applied field, all affect the index profile. While most of the research to date has been concerned with the creation of multimode waveguide regions, for I-O applications it is mandatory that single-mode structures be reliably fabricated and characterized. Fabrication of devices such as multiplexers calls for reproducibility in the propagation constant of the guided mode to an accuracy of better than 10^{-4}. In order to fabricate glass waveguide devices of such reproducible characteristics, it is necessary that the exchange and

mode field distribution. For example the 2.5 μm deep surface waveguide with ~10μm channel width used for making directional couplers [42] are likely to give highly elliptical mode field profiles with large surface scatter losses. If these waveguides were buried by applying an electric field in a second-step diffusion, the resultant guides are expected to be compatible with fibers and exhibit lower attenuation.

Ag^+-Na^+ Exchange

The binary exchange of Ag^+-Na^+ is by far the most researched technique and in the following we will confine our attention to this binary system only. Readers are referred to a review by Findakly [43] describing the developments in other binary systems as of 1983. When pure $AgNO_3$ melt is used for the exchange process, large Δn(~0.1) waveguides are obtained which have some disadvantages: a large silver concentration causes coloring due to silver reduction [2]; secondly, single-mode waveguides are shallow and thus incompatible with fibers[15]. Moreover, the time of diffusion involved is rather short, thereby causing uncertainty and lack of reproducibility in the waveguide characteristics. Dilute solutions of $AgNO_3$ and $NaNO_3$ allow achievement of lower Δn and more controllable diffusion times [10,23]. This is generally achieved by adding a known amount of $AgNO_3$ in $NaNO_3$, and the diffusion is carried out near the melting point of the mixture ($> 330^0$c). However, such a process is not applicable to batch processing as silver concentrations will change during the process, causing alterations in the waveguide characteristics. This problem can, however, be overcome by the electrolytic release technique [18]. The process allows generation of a very small concentration of silver ions precisely. Since a metallic silver electrode rather than a salt mixture is used, the impurities can be kept minimal as ultrapure silver rods are commercially available. The process of

electrolytic release can be controlled electronically allowing a high degree of accuracy in the concentration of Ag^+ ions in the bath. Using a concentration cell [44] for the in situ measurement of Ag^+ ion concentration, high-measurement accuracy and assured reproducibility have been demonstrated to facilitate on-line concentration control (to better than 1 μg) by periodic pumping of the silver ions into the molten bath.

The Ag^+-Na^+ ion-exchange process is fairly versatile, and both planar [2,6-8,12,14-16,18,23,25] and channel [7,14,15,22,41] waveguides have been fabricated. The surface waveguides made in the first-step diffusion have been buried under the glass surface by carrying out diffusion in a second step with or without an externally applied electric field across the glass substrate when no silver ions are present in the melt [12,14,15,25,45]. Thus the index profile can be tailored to the desired characteristics by a judicious choice of the process parameters (melt composition, temperature and applied field) in each step for a given glass and a given ion. Concentration of the incoming ion in the melt determines the net index change.

Process and Performance--A Necessary Link

In order to establish a correlation between the process parameters and the waveguide performance, it is necessary to investigate the various steps involved. These studies can be categorized in the following distinct areas:

1) Ion-exchange equilibrium to determine the relationship between the melt ion concentration and the glass-surface ion concentration.
2) Analysis of the diffusion equation with appropriate boundary conditions to predict the concentration profile.
3) Fabrication of the waveguides.
4) Experimental determination of the diffusion profile and correlation with the theoretical analysis. It is generally assumed that the

concentration profile is a replica of the index profile. This assumption has been experimentally verified and is valid as long as the concentration is small [46,47].

5) Calculation of the waveguide propagation characteristics by solving the Helmholtz equation for the given index profile.

6) Optical characterization of the waveguide and the correlation between the measured parameters and the process parameters. This involves measurement of mode indices (in the case of surface waveguides where prism coupling technique can be used), the cutoffs of the modes [48] and their field profiles and, of course, the attenuation. In most of the work reported in the literature [2,10,12,16], the mode indices data have been used to determine the index profile by using the inverse WKB approach [49]. In this case step 4) is a part of 6). However, this method is not suitable for analyzing single-mode guides or steep profiles.

II Theory

A. Ion-Exchange Equilibrium

When the glass containing a monovalent cation B is introduced into a molten salt solution containing the diffusing monovalent cation A, ion A is driven into the glass by an interphase chemical potential gradient and in order to maintain charge neutrality, ion B is released into the melt. This ion exchange process can be represented by an overall chemical reaction as follows [50]:

$$A + \bar{B} = \bar{A} + B \quad , \qquad (1)$$

where the bar denotes the cations in the glass phase.

In the study of chemical reactions, one is concerned about the rate of reaction and the equilibrium characteristics. The rate of ion exchange may be

limited by the following processes:

(i) Mass transfer of reactants and removal of products from the reaction interface in the melt.

(ii) Kinetics of the reaction at the interface.

(iii) Transport of ions in the glass.

Transfer of cations in the melt takes place via diffusion and convection. Convection in the melt can be altered by stirring the melt. However, near the glass-melt interface, a region may exist where no convective mixing occurs because of fluid friction at the interface. Across this stagnant boundary all the mass transfer of the cations to and from the reaction interface occurs through diffusion [51]. If the liquid-phase diffusion can supply ample reactants and remove enough products to and from the interface, the process is not mass transfer limited. For diffusion to be a limiting process in the melt, the important parameter is $(\bar{N}_A/N_A)\ (\bar{D}_A/D_A)^{1/2}$, where N_A denotes the molar concentration of cation A and D_A its self-diffusion coefficient. It has been shown [51] that if this parameter is greater than about 10, the rate is not mass transfer limited due to diffusion in the melt.

At the interface, the overall rate of the reaction is affected by kinetics of the ion-exchange reaction. It is highly unlikely that surface kinetics are a rate-limiting step and are thus assumed to be much faster than the transport processes in the melt and glass phase. In the glass phase, mass transport is carried out entirely by diffusion of the cations. The equilibrium state of reaction (1) specifies the surface boundary condition for the diffusion process and the accompanying surface-index change. Thus the control of the cation diffusion profile in glass is subject to manipulation of this boundary condition and the cation transport (diffusion) properties in the glass.

A convenient method of notation in a binary problem is the definition of the cation fractions:

$$N_A = \frac{C_A}{C_A + C_B},$$

and

$$N_B = \frac{C_B}{C_A + C_B},$$

where N_i is the cation fraction and C_i is the absolute concentration of the cation i in the salt phase. It can be seen from the above relations that

$$N_A + N_B = 1 \tag{2}$$

Similarly in the glass phase, we have

$$\bar{N}_A + \bar{N}_B = 1 \tag{3}$$

Garfinkel [50] proposed a model to describe ion-exchange equilibrium between glass and molten salts successfully. For the overall raction (1), an equilibrium constant is defined as

$$K = \frac{\bar{a}_A \; a_B}{\bar{a}_B \; a_A} \tag{4}$$

The thermodynamic activities of the cations in the salt can be expressed as

$$a_i = \gamma_i N_i$$

where γ_i is the activity coefficient of the respective ion. The ratio of the activity coefficient in the molten salt can be represented by the Regular Solution Theory [52]:

$$\ln \frac{\gamma_B}{\gamma_A} = \frac{A}{RT} (1-2 N_B) \tag{5}$$

where R is the gas constant, T is the temperature of the melt in Kelvin and A is the interaction energy of the two cations in the melt. In this model, the reference state for the activity of each ion is chosen as

$$\lim_{N_i \to 1} \gamma_i = 1$$

In the glass phase, the ratio of the activities of the two cations is represented by the n-type behaviour first suggested by Rothmund and Kornfeld [53] which states:

2

$$\frac{\bar{a}_A}{\bar{a}_B} = \left(\frac{\bar{N}_A}{\bar{N}_B} \right)^n \qquad (6)$$

Here the reference state is defined as:

$$\lim_{\bar{N}_i \to 1} \bar{a}_i = \bar{N}_i$$

Substituting Eqns. (2), (3), (5) and (6) into (4), the following equation is obtained.

$$\ln \left(\frac{N_A}{1-N_A} \right) + \frac{A}{RT} \left(1 - 2 N_A \right) = n \ln \left(\frac{\bar{N}_A}{1 - \bar{N}_A} \right) - \ln K \qquad (7)$$

If the models for the activity coefficients in the two phases are valid, a plot of the left-hand-side of (7) versus $\ln \{ \bar{N}_A / (1 - \bar{N}_A) \}$ should yield a straight line with slope equal to n and intercept equal to ln (1/K). When the parameter n is unity, the glass is said to be ideal. A large value of K on the other hand would indicate a large intake of the cation A by the glass for a given melt composition. Once the paramters n and K are determined, Eq. (7) provides a relation between $\bar{N}_A$ and N_A at the glass surface from which accurate boundary conditions for solution of the diffusion equation can be obtained.

Studies of ion-exchange equilibrium in glasses include the early work of Schulze [54] and later, the pioneering work of Garfinkel [50] involving many

different cation pairs. In both these studies, the silver cation concentrations were relatively large ($N_{Ag} > 0.1$). More recently, Stewart and Laybourn [10] reported a study of Ag^+-Na^+ exchange at very low concentrations ($N_{Ag} \sim 10^{-4}$) required for fabrication of single-mode waveguides. However, the information on the surface concentration of Ag^+ in glass was obtained indirectly by optical measurements on the waveguides. There are two drawbacks in such a method; first, the WKB method employed to determine the mode indices is subject to error in cases where waveguide supports only one or two modes [55], and second, the assumption that in the case of pure $AgNO_3$ melt, all the surface Na^+ ions in glass are substituted for Ag^+ ions, may not necessarily be valid [56]. It is therefore desirable to measure absolute concentration profile of Ag^+ ions in the glass. Recent results [57] of Ag^+-Na^+ ion-exchange equilibrium using atomic absorption spectrometry for the measurement of absolute concentration of Ag^+ ions in glass indicate that at the processing temperature and under variable mixing conditions, neither mass transfer in the melt nor the reaction kinetics at the melt-glass interface influence the exchange process. The dopant profile is observed to be primarily determined by the diffusion of silver ions in the glass matrix. The diffusion profile at low melt concentrations (N_{Ag}-10^{-4}) is found to be erfc which is not only in excellent agreement with that obtained by the SEM analysis [25], it also correlates well with the index profile derived from the measured mode indices [23,45]. This correlation allows determination of an empirical relation for the surface-index change from the known melt concentration (see Fig. 1). The results also show that the assumption of a concentration independent interdiffusion coefficient in solving the diffusion equation [12,15,23] is valid in the case of low silver melt concentration ($\sim 10^{-4}$MF) employed for single-mode waveguide fabrication. The subject of the index profile will be further discussed in the following when we describe

the diffusion process.

B. **Diffusion Equation**

The Fickian diffusion molar flux components of the two cations in the glass phase are given by [58]

$$\vec{\phi}_i = - \bar{D}_i \nabla \bar{C}_i \frac{\partial \ln \bar{a}_i}{\partial \ln \bar{C}_i} + \mu_i \bar{C}_i \vec{E} \quad , \tag{8}$$

where ϕ_i= molar flux of cation i (moles/m^2-s) ,

$\bar{D}_i$ = self-diffusion coefficient of the cation i ,

μ_i = electrochemical mobility (m^2/V-s) ,

$\bar{a}_i$ = thermodynamic activity (mole/m^3) ,

and $\vec{E}$ = electric field (V/m).

It must be pointed out that in glasses, Einstein relation between the self-diffusion coefficient and mobility, i.e.,

$$\bar{D}_i = \frac{kT}{e} \bar{\mu}_i \tag{9}$$

is generally not valid. Instead, equation (9) is written in a modified form given by

$$\bar{D}_i = f \frac{kT}{e} \bar{\mu}_i \quad , \tag{10}$$

where the correlation factor f depends on the glass composition and has been found [59] to be in the range $0.1 < f < 1$.

A few words about the electric field $\vec{E}$ are in order here. $\vec{E}$, as it appears in equation (8), includes any external applied field as well as the component arising from a local space-charge distribution near the diffusion boundary which moves deeper into the substrate as time evolves. The space charge region is caused by the lower mobility of the incoming ion ($\mu_A < \mu_B$) and is governed by the following relation

$$\nabla \cdot (\varepsilon \vec{E}) = \rho \tag{11}$$

where the local space-charge density

$$\rho = e\ (\ \bar{C}_A + \bar{C}_B - \bar{C}_B^{\,o}) \tag{12}$$

In the above equation $\bar{C}_B^{\,o}$ is the absolute concentrations of cation B in the glass before the ion exchange. For weakly guiding case, (11) can be replaced by $\nabla\cdot\vec{E} = \rho/\varepsilon$. The fact that $\nabla\cdot\vec{E} \neq 0$ shows that in the presence of the space charge, the Eq. (13).

$$\bar{C}_A + \bar{C}_B = \bar{C}_B^{\,o} \tag{13}$$

is not strictly valid but during diffusion it is found to be very nearly so [15].

Using the continuity equations

$$\nabla \cdot \vec{\$}_i = - \frac{\partial \bar{C}_i}{\partial t} ,$$

(13) gives

$$\nabla \cdot (\vec{\$}_A + \vec{\$}_B) = 0 \tag{14}$$

Using the Eq. (14) in (8) and assuming that the self-diffusion coeffieients $\bar{D}_i$ are not concentration dependent, the diffusion equation can be derived in the following form

$$\frac{\partial \bar{C}_A}{\partial t} = \mu_A \vec{E}\cdot\nabla\bar{C}_A \left[\frac{1}{1 - \alpha\, \bar{C}_A} \right] + \frac{n}{1 - \alpha\, \bar{C}_A} \bar{D}_A\, \nabla^2\, \bar{C}_A \tag{15}$$

where $$\alpha = 1 - \frac{\mu_A}{\mu_B} \tag{16}$$

and $$n = \frac{\partial \ln\, \bar{a}_A}{\partial \ln\, \bar{C}_A} \tag{17}$$

Eq. (15) can be solved to obtain the concentration profile provided the initial condition and the boundary conditions are known. One of the boundary conditions involves knowledge of the concentration of cation A at the glass surface which is a function of the melt concentration via the equilibrium condition of reaction (1). Eq. (7) provides such relationship.

The Mixed Alkali Effect

Although it is generally assumed that the self-diffusion coefficient of each ion is concentration independent, it is known that when two alkali ions are present in the glass, some properties directly related to alkali ion movement show large departures form additivity [60]. A general consequence of adding a second alkali is signficant reduction in the diffusion coefficient of the original alkali ion. While this reduction in diffusion coefficient occurs whether the second alkali is larger or smaller than the original one, the magnitude of the change varies directly with the concentration and the size mis-match of the second alkali. Moreover, the self-diffusion coefficient of an alkali ion is always considerably higher than the impurity alkali diffusion coefficient. This implies that

$$D_A \ll D_B \text{ for } N_A \ll 1$$

and furthermore suggests that D_A and D_B vary with the concentration of the diffusing species A and hence are position dependent.

The ratio of the two self-diffusion coefficients (D_A/D_B) thus varies drastically in the glass during the diffusion process and this concentration dependence of the self-diffusion constants should be considered explicitely in deriving the diffusion equation. To the best of our knowledge, this has not been done, obviously due to the complications involved not only in the

analysis, but in some cases such as Ag^+ - Na^+ exchange, sufficient experimental data is not available to include the dependence of $\bar{D}_{Ag}$ on $\bar{N}_{Ag}$ in the analysis. However, for large silver concentrations such as involved in fabrication of gradient index components for imaging applications, an exponential dependence of $\bar{D}_{Ag}$ has been assumed [61]. One consequence of the mixed alkali effect is that step-like diffusion profiles are obtained when there is considerably large concentration dependence of the two diffusion coefficients [11].

C. Solution of the Diffusion Equation

a) Diffusion without external field

Eq. (15) can be further simplified if there is no external field present and $\nabla \cdot \vec{E}$ is set equal to zero. In other words, the local space charge is neglected. In this case it can be shown [15] that the two-dimensional diffusion equation becomes

$$\frac{\partial \bar{N}_A}{\partial t} = \frac{\partial}{\partial x}\left(\frac{n\bar{D}_A}{1-\alpha \bar{N}_A}\frac{\partial \bar{N}_A}{\partial x}\right) + \frac{\partial}{\partial y}\left(\frac{n\bar{D}_A}{1-\alpha \bar{N}_A}\frac{\partial \bar{N}_A}{\partial y}\right) \tag{18}$$

Further simplifications occur in the following cases:

(i) $\alpha = 0$, i.e., the two cations are equally mobile. In this case

$$\frac{\partial \bar{N}_A}{\partial t} = n\bar{D}_A\left(\frac{\partial^2 \bar{N}_A}{\partial x^2} + \frac{\partial^2 \bar{N}_A}{\partial y^2}\right) \tag{19}$$

(ii) $\bar{N}_A \ll 1$, i.e., concentration of the incoming ion is much smaller than that of the outgoing ion in the glass. In this case also the diffusion equation reduces to (19). This approximation is reasonably valid for single-mode waveguide fabrication conditions [25,57].

(iii) In the case of planar waveguides (18) reduces to the one dimensional

AD-A193 177 ION-EXCHANGED WAVEGUIDES FOR SIGNAL PROCESSING APPLICATIONS - A NOVEL ELE (U) FLORIDA UNIV GAINESVILLE DEPT OF ELECTRICAL ENGINEERING 2/4

UNCLASSIFIED R V RAMASWAMY 07 MAR 87 AFOSR-TR-88-0279 F/G 20/6.1 NL

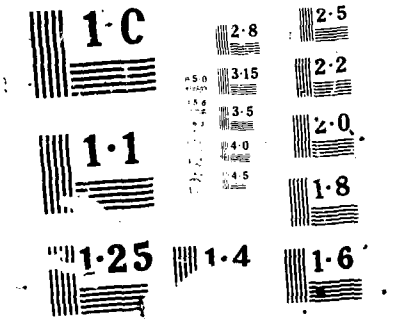
1·C
1·1
1·25
1·4
2·8
3·15
3·5
4·0
4·5
2·5
2·2
2·0
1·8
1·6

diffusion equation which is normally written as

$$\frac{\partial \bar{N}_A}{\partial t} = \frac{\partial}{\partial x} \left(\tilde{D} \frac{\partial \bar{N}_A}{\partial x} \right) \tag{20}$$

where $\tilde{D}$ is called the interdiffusion coefficient given by

$$\tilde{D} = \frac{n\bar{D}_A}{1 - \alpha \bar{N}_A} \tag{21}$$

If it is further assumed that in the glass, the Einstein relation (9) is valid, and if not, at least the correlation factors f_i [Eq. (10)] for the two cations are the same, then

$$\tilde{D} = \frac{n \bar{D}_A \bar{D}_B}{\bar{D}_A \bar{N}_A + \bar{D}_B \bar{N}_B} \tag{22}$$

For the two cases (i) and (ii) pointed out above, $\tilde{D} = n\bar{D}_A$. In this case the diffusion equation has the simplest form:

$$\frac{\partial \bar{N}_A}{\partial t} = n\bar{D}_A \frac{\partial^2 \bar{N}_A}{\partial x^2} \tag{23}$$

and with the initial and boundary conditions given respectively by

$$\bar{N}_A (x,0) = 0 \text{ at } x > 0 \tag{24}$$

$$\bar{N}_A (\infty,t) = 0$$

and $$\bar{N}_A (0,t) = \bar{N}_o \text{ for all } t > 0,$$

the solution [51] of (23) is,

$$\bar{N}_A (x,t) = \bar{N}_o \operatorname{erfc} (x/W_o) \tag{25}$$

where $$W_o = 2\sqrt{n\bar{D}_A t} \tag{26}$$

and $$\text{erfc}\ (z) = \frac{2}{\sqrt{\pi}} \int_z^\infty \bar{e}^{\alpha^2} d\alpha \tag{27}$$

W_o is called the effective depth of diffusion and corresponds to that distance from the waveguide surface where $(\bar{N}_A / \bar{N}_o) = \text{erfc}\ (1) = 0.157$.

When $\alpha \to 1$ such as the case of $C_s^+ - Na^+$ exchange [11], the interdiffusion coefficient is highly concentration dependent and the solution of the diffusion equation

$$\frac{\partial \bar{N}_A}{\partial t} = n \frac{\partial}{\partial x} \left(\frac{\bar{D}_A}{1-\alpha \bar{N}_A} \frac{\partial \bar{N}_A}{\partial x} \right) \tag{28}$$

for various values of α is obtained by numerical solution. The results have been given by Crank [51]. Step-like profiles are obtained when α approaches unity. For intermediate values of α, Gaussian-like diffusion profiles are obtained [62]. Finite-difference method has been used by several workers to solve one-dimensional as well as two-dimensional equations successfully [15].

b). **Diffusion With External Electric Field**

The diffusion of incoming ion can be enhanced by applying an electric field across the substrate. In this case, one has to solve the combined equations (15) and (11) which is a difficult task at best in the two-dimensional case. However, in the case of one-dimensional (planar) waveguides, approximate solutions can be obtained under certain conditions.

(i) For the special boundary conditions

$$\left.\begin{aligned} \bar{N}_A &= \bar{N}_o \\ \frac{\partial \bar{N}_A}{\partial x} &= 0 \end{aligned}\right\} \text{ for } x = 0$$

and $$\begin{matrix} \bar{N}_A = 0, \\ \frac{\partial \bar{N}_A}{\partial x} = 0 \end{matrix} \quad \text{for} \quad x \to \infty \ ,$$

the solution of (15) in one-dimensional case is [63]

$$\bar{N}_A (x) = \bar{N}_0 \{ 1 + \exp [v \bar{N}_0 \frac{\alpha}{n\bar{D}_A} (x - vt) \approx \}^{-1} \qquad (29)$$

with a concentration-dependent diffusion front velocity

$v = v_0 (1 - \alpha) / (1 - \alpha \bar{N}_0)$

The velocity $v_0 = i_0/e \bar{C}^0_B$ depends on the current density i_0 in the presence of the applied field.

(ii) For low concentrations ($\bar{N}_A << 1$), space-charge effects can be neglected and for planar waveguides Eq. (18) reduces to

$$\frac{\partial \bar{N}_A}{\partial t} = n\bar{D}_A \frac{\partial^2 \bar{N}_A}{\partial x^2} - \mu E \frac{\partial \bar{N}_A}{\partial x} \qquad (30)$$

and $\bar{N}_A (x,t)$ is calculated by a Laplace-transform techniques [64]

$$\bar{N}_A = \frac{1}{2} \bar{N}_0 \{ \text{erfc} (x' - r) + \exp (4rx') \text{ erfc} (x' + r) \} \qquad (31)$$

where $x' = x/W_0 = x /2\sqrt{n\bar{D}_A t}$ is the normalized effective depth of diffusion without external field and $r = \mu Et/W_0$.

It has been shown [14,45] that the influence of the space charge [Equation (11)] leads to steeper diffusion fronts when compared to the solution (31). For large values of r, the contribution by the second term in (31) is negligible and the diffusion profile can be approximated as [25]:

and $$\left.\begin{matrix} \bar{N}_A = 0, \\ \frac{\partial \bar{N}_A}{\partial x} = 0 \end{matrix}\right\} \text{ for } x \to \infty ,$$

the solution of (15) in one-dimensional case is [63]

$$\bar{N}_A(x) = \bar{N}_0 \{ 1 + \exp [v \bar{N}_0 \frac{\alpha}{n\bar{D}_A} (x - vt) \approx \}^{-1} \qquad (29)$$

with a concentration-dependent diffusion front velocity

$$v = v_0 (1 - \alpha) / (1 - \alpha \bar{N}_0)$$

The velocity $v_0 = i_0/e \bar{C}^o_B$ depends on the current density i_0 in the presence of the applied field.

(ii) For low concentrations ($\bar{N}_A << 1$), space-charge effects can be neglected and for planar waveguides Eq. (18) reduces to

$$\frac{\partial \bar{N}_A}{\partial t} = n\bar{D}_A \frac{\partial^2 \bar{N}_A}{\partial x^2} - \mu E \frac{\partial \bar{N}_A}{\partial x} \qquad (30)$$

and $\bar{N}_A(x,t)$ is calculated by a Laplace-transform techniques [64]

$$\bar{N}_A = \frac{1}{2} \bar{N}_0 \{ \text{erfc} (x' - r) + \exp (4rx') \text{ erfc} (x' + r) \} \qquad (31)$$

where $x' = x/W_0 = x/2\sqrt{n\bar{D}_A t}$ is the normalized effective depth of diffusion without external field and $r = \mu Et/W_0$.

It has been shown [14,45] that the influence of the space charge [Equation (11)] leads to steeper diffusion fronts when compared to the solution (31). For large values of r, the contribution by the second term in (31) is negligible and the diffusion profile can be approximated as [25]:

$$\bar{N}_A(x', r) \simeq \frac{\bar{N}_o}{2}\{\text{erfc}(x' - r)\}, \quad r > 2.5 \tag{32}$$

In the two-dimensional case, Eq. (15) has been solved [14] neglecting the concentration dependence of the interdiffusion coefficient and assuming that the diffusion term in (15) is small. While such solutions are valid for very large applied fields such as involved in multimode waveguides, the case of single-mode guides does not fall in this category. In such situations equation (15) can be solved only by numerical methods [15].

c). **Two-Step Ion Exchange (Buried Waveguides)**

Surface waveguides obtained by ion-exchange are characterized by higher loss caused by surface scattering. Furthermore, the intensity profile of the guided mode is not circularly symmetric and compatible with optical fiber. These drawbacks can be overcome by burying the waveguides in a second ion exchange in a melt free of the cation A. An external field may be applied during this step to control the buried depth and the index profile. Since the initial conditions in this case are determined by the first-step diffusion profile, analytical solutions to Eq. (15) cannot be obtained and one has to resort to numerical techniques once again and has been attempted by several workers in the past [15,45,65]. While in the case of planar waveguides the correlation between theory and experiment has been successfully achieved [45], there is not sufficient evidence whether the results and the approximations made predict satisfactory results in the case of channel waveguides.

III. Results

A. Planar Waveguides

Modelling of the diffusion (index) profile in the case of planar waveguides has been reported by many workers [15,45,65]. At low melt

concentrations used for fabrication of single-mode guides, it has been shown [45] that interdiffusion coefficient is only weakly dependent on the silver concentration. Assuming that electrical mobility μ and the electric field $\vec{E}$ do not depend on position, the one-dimensional diffusion equation is given by (30). The waveguide index profile for the two-step process for given fabrication parameters can be predicted reasonably well [45,65] provided $\tilde{D}$, μ and the surface index change Δn in the first step (without applied field) have been previously determined. Fig.2 shows the schematics used by the authors for the fabrication, modelling, characterization and correlation of the experimental and theoretical results.

The value of $\tilde{D}$ is obtained by measuring the width W of the index profile and using the relation $W = 2\sqrt{\tilde{D}t}$. The surface-index change is determined by measuring the mode indices of the guided modes using a prism coupler. In the case of waveguides which support one or two modes, the mode index data can be correlated with the theory as follows: The one-dimensional normalized Holmholtz equation is solved for the index profile by a finite-difference method to obtain the mode indices of the TE modes. The two variables Δn and W_0 are adjusted to give the best fit to the measured indices. In the case of multimode waveguides (> 6 modes), the inverse WKB method [49] may be employed to give the index profile and the surface-index change. Ionic mobility μ can be determined by fabricating a surface waveguide in presence of an external field and using the mode-indices data to determine the index profile. A subsequent fit to the calculated profile with the predicted result of Eq. (31) then yields the values of $\tilde{D}$ and μ [25]. The surface-index change Δn has been observed to be independent of the applied field [25].

Once all the necessary parameters are determined from single-step ion exchange, buried symmetric index profiles can be obtained by carrying out ion-

exchange in a second step by applying an external field in a $NaNO_3$ molten bath free of silver. The resulting index profile can be measured by SEM analysis [25]. Alternatively, it can be predicted by solving the diffusion equation with the use of appropriately known boundary and initial conditions. Fig. 3 shows the evolution of the index profile with the second-step diffusion time as calculated by using a simple numerical method [45].

The variation of index profile width W and the index-peak position X_{peak} below the waveguide surface with the diffusion time and the field during the second-step are shown in Fig.4. It is observed that $W \sim \sqrt{t_2}$, a result in agreement with the experimental data [25] shown by the crosses (x) in the curve 1. The index-peak position (x_{peak}) depends linearly on time as well as on the field. This result suggests that the whole profile is translated by the applied field and the net translation is governed by the product μEt.

B. Channel Waveguides

Although planar waveguides form the basis for study of the basic ion-exchange process, they cannot be used in real system applications because of geometrical incompatibility with fibers. For practical applications, therefore two-dimensional channel waveguides are fabricated. This is achieved by delineating open channel patterns of varying widths on glass substrates by photolithographic techniques and then carrying out ion exchange process creating a waveguiding region via the mask openings. Although channel waveguides using the ion-exchange techniques have been around for quite a while (in fact, the first glass waveguides were of stripe geometry [3]), not until recently adequate attention was given to optimization of singe-mode structures in terms of the mode symmetry, attenuation, and fiber-compatibility. Modelling of surface channel waveguides has enjoyed partial success as the two-dimensional diffusion equation (15) has been solved numerically in special

cases [14,15]. The two-step process still remains to be modelled. Part of the problem in modelling has been the presence of significant side diffusion of silver under the metallic (mostly aluminum) masks [22]. A systematic study of single-mode channel surface waveguides prepared from dilute $AgNO_3$-$NaNO_3$ melts was carried out recently with mask widths ranging from 2 to 10 μm [22]. Their diffusion profiles were determined along the widths as well as along the depth direction. Fig. 5 shows the profile for a mask opening of 10μm width as obtained by SEM. A comparison of these waveguides with the planar structure fabricated under identical conditions shows:

a) Decreasing N_{Ag} decreases diffusion depth in channels, a result similar to that observed in planar guides [25].

b) Increasing channel width increases the diffusion depth approaching that of the planar guides for large widths. However, for lower N_{Ag}, planar values are achieved at lower guide widths.

c) Channels have smaller Δn as compared to their planar counterparts, approaching their value for mask widths of the order of 10 μm.

d) There is substantial side diffusion under the masks. The aspect ratio of the index profile varies between 1.5 and 3.0 as the mask width increases from 2 to 10 μm. However, the surface guides are single-moded at 1.3 μm wavelength up to mask widths of ~ 6 μm when $N_{Ag} = 2 \times 10^{-4}$MF and diffusion is carried out at 330° for 60 min.

e) In single-mode regions the channel waveguides have negligible deplarization whereas multimode guides exhibit measurable depolarization due to mode connversion. Moreover, no deposition of silver under the edges of metallic aluminum masks was observed, contrary to what has been reported in the literature [15] when diffusion was carried out from pure $AgNO_3$ melts. The lack of

depolarization and the high quality of the waveguides free from scattering centers and birefringence can be attributed to the low level of silver concentration ($N_{Ag} \sim 10^{-4}MF$).

Following this study and availability of the relevant parameters from two-step process in planar waveguides, low-loss single-mode buried channel waveguides have been successfully fabricated by a two-step process with a view towards process optimization for 1.3 μm operation [66]. Measurements of the mode field distribution have been carried out by using an experimental arrangement shown schematically in Fig. 6. A conventional Corning single-mode fiber with 1/e mode-field diameter of 10 μm was employed to couple light into a photodetector covered with a 10 μm pinhole and the near field intensity distribution was scanned parallel and perpendicular to the channel width.

Typical results are shown in Fig. 7. It is obvious that in absence of an external field in the second step, the mode field is elliptical for any mask width. This is attributed to significant side diffusion under the masks [22]. Applied field is essential to improve the symmetry of the index profile by reducing the diffusion time in the second step and a consequent reduction in side diffusion. Nearly circular mode fields with mode-field diameter in the 9-10 μm range can be obtained from mask widths in the range of 4.5 - 6.5 μm. For these optimum buried waveguides, the fiber-waveguide total throughput loss (including the coupling loss, Fresnel loss and propagation loss) on the order of 1dB have been achieved [66] for 15 mm long channel using commercial slides as the soda-lime glass substrates. It is expected that lower losses can be achieved by using better quality glass. The experimental arrangement of Fig. 7 allows evalution of the coupling efficiency via the mode overlap integral [67] and Fresnel loss is estimated by knowing the refractive indices of the fiber and the waveguide. The technique thus allows

determination of the propagation loss.

Theoretical analysis of channel waveguides of arbitrary refractive index profiles is carried out using one of the several techniques. Effecive index approach [68,69], variational methods [70,71] and a host of other numerical methods [72-74] have been used over the years to predict the propagation characteristics with reasonable accuracy. The theoretical results, however, have not been compared to experimental values due to lack of accurate knowledge of index profiles in practical waveguides. This challenge is one of the subjects under study. This lack of correlation between theoretical and experimental work does not present any significant obstacles as far as the prediction of mode-field profile is concerned since the field profile is not very sensitive to the index distribution [75]. However, parameters such as the propagation constant and coupling coefficient between two adjacent waveguides (such as in a directional coupler) cannot be calculated with reasonable accuracy to design useful devices.

CONCLUSION

Ion-exchange technology for fabrication of passive waveguide components in glasses has made significant progress in the past few years. Improved fabrication and characterization techniques and modelling of the ion-exchange process have allowed a deeper understanding of the processes and the role played by the fabrication parameters in determining the waveguide characteristics. Although low-loss fiber compatible single-mode waveguides can be fabricated with reproducible mode field profile and low loss, the repeatability of the process for useful I-O devices is yet to be demonstrated. A vigorous activity to respond to this challenge is leading to renewed enthusiasm in the field. We expect to see major thrust in this area in the coming years as the economic viability of massive employment of fibers in such

applications as local area networks depends to a great deal on potentially inexpensive glass waveguide devices.

Acknowledgement

The authors would like to acknowledge many helpful discussions with Mr. H. C. Cheng and Dr. Don Ulrich and the support of AFOSR under grant No. 84-3069.

References

1. A. J. Burggraaf, "Phillips Research Reports," Suppl. No. 3, 1 (1966).

2. R. G. Eguchi, E. A. Maunders and I. K. Naik, "Fabrication of Low-loss waveguides in BK-7 by ion-exchange," Proc. SPIE 408, 21 (1983).

3. T. Izawa and H. Nakagome, "Optical waveguide formed by electrically induced migration of ions in glass plates," Appl. Phys. Lett. 21, 584 (1972).

4. A. Brandenburg, "Stress in ion-exchanged glass waveguides," J. Lightwave Tech. LT-4, 1583 (1986).

5. G. H. Chartier, P. Jaussaud, A. D. de Oliveira and O. Parriaux, "Fast fabrication method for thick and highly multimode optical waveguides," Electron. Lett. 13, 763 (1977).

6. T. G. Giallorenzi, E. J. West, R. Kirk, R. Ginther, and R. A. Andrews, 'Optical waveguides formed by thermal migration of ions in glass,' Appl. Opt. 12, 1240 (1973).

7. J. G. Gallagher and R. M. de la Rue, 'Single-mode stripe optical waveguides formed by silver ion exchange,' Electron. Lett. 12, 397 (1976).

8. G. Stewart, C. A. Millar, P. J. R. Laybourn, C. D. W. Wilkinson, and R. M. de la Rue, 'Planar optical waveguides formed by silver-ion migration in glass,' IEEE J. Quantum Electron. QE-13, 192 (1977).

9. M. Hafisch, D. Chen, and J. Huber, 'Properties of optical waveguides formed by thermal migration of thallium ions in glass,' Appl. Phys. Lett. 33, 997 (1978).

10. G. Stewart and P. J. R. Laybourn, "Fabrication of ion-exchanged optical waveguides from dilute silver nitrate melts," IEEE J. Quantum Electron. QE-14, 930 (1978).

11. V. Neuman, O. Parriaux and L. M. Walpita, 'Double-alkali effect: Influence on index profile of ion-exchanged waveguides,' Electron. Lett. 15, 704 (1979).

12. G. Chartier, P. Collier, A. Guez, P. Jaussaud, and Y. Won, 'Graded-index surface or buried waveguides by ion-exchange in glass,' Appl. Opt 19, 1092 (1980).

13. J. L. Coutaz and P. C. Jaussaud, 'High index gradient in glass by ion exchange,' Appl. Opt. 21, 1063 (1982).

14. H. J. Lilienhof, E. Voges, D. Ritter, and B. Pantschew, 'Field-induced index profiles of multimode ion-exchanged strip waveguides,' IEEE J. Quantum Electron., QE-18, 1877 (1982).

15. R. G. Walker, C. D. W. Wilkinson and J. A. H. Wilkinson, "Integrated optical waveguiding structures made by silver ion exchange in glass: 1. The propagation characteristics of stripe ion-exchanged waveguides; a theoretical and experimental investigation," Appl. Opt. 22, 1923 (1983).

16. M. Imai, N. Haneda and Y. Ohtsuka, 'Losses in optical waveguides formed by silver-sodium ion exchange,' IEEE J. Lightwave Tech. LT-1, 611 (1983).

17. J. L. Jackel, K. Y. Lee, and F. J. Favire, 'Do glass waveguides depolarize?' IEEE J. Lightwave Tech. LT-3, 818 (1985).

18. R. K. Lagu and V. Ramaswamy, "Fabrication of single-mode glass waveguides by electrolytic release of silver ions," App. Phys. Lett. 45, 117 (1984).

19. G. L. Yip and J. Albert, "Characterization of planar optical waveguides by K^+-ion exchange in glass," Opt. Lett. 10, 151 (1985).

20. J. E. Gortych and D. G. Hall, ""Fabrication of planar optical waveguides by K^+-ion exchange in BK7 and pyrex glass,: IEEE J. Quantum Electron. QE-22, 892 (1986).

21. L. Ross, H. J. Lilienhof, H. Holscher, H. F. Schlaak and A. Brandenburg, "Improved substrate glass for planar wavaeguides by Cs-ion exchange," Tech. Digest, Topical Meeting on Integrated and Guided-Wave Optics, 26-28 Feb. 1986, Atlanta, Ga. Paper ThBB2, pp. 25-26.

22. S. I. Najafi and R. V. Ramaswamy, "Diffusion and modal characterization of Ag^+-Na^+ exchanged channel waveguides," Tech. Digest, Topical Meeting in Integrated and Guided-Wave Optics, 26-28 Feb. 1986, Atlanta, Ga., paper FDD2, pp. 60-61.

23. R. K. Lagu and R. V. Ramaswamy, "Process and waveguide parameter relationships for the design of planar silver ion-exchanged glass waveguides," J. Lightwave Tech. LT-4, 176 (1986).

24. E. M. Garmire and K. Honda, 'Depolarization in channel glass waveguides,' IEEE, J. Lightwave Tech. LT-4, 220 (1986).

25. R. V. Ramaswamy and S. I. Najafi, "Planar, buried, ion-exchanged glass waveguides: Diffusion characheristics," IEEE J. Quantum Electron. QE-22, 883 (1986).

26. G. H. Chartier, P. Jaussaud, A. D. de Oliveira and O. Parriaux, 'Optical wavaeguides fabricated by electric-field controlled ion exchange in glass,' Electron,. Lett. 14, 132 (1978).

27. J. Viljanen and M. Leppihalme, 'Fabrication of optical strip wavaeguides with nearly circular cross section by silver ion migration technique,' J. Appl. Phys. 51, 3563 (1980).

28. C. W. Pitt, A. A. Stride and R. I. Trigle, 'Low temperature diffusion process for fabricating optical waveguides in glass,' Electron. Lett. 16, 701 (1980).

29. T. Findakly and E. Garmire, 'Reduction and control of optical waveguide losses in glass,' Appl. Phys. Lett. 37, 855 (1980).

30. K. Forrest, S. Pagano, W. Viehmann, 'Channel waveguides in glass via silver-sodium field-assisted ion-exchange,' IEEE J. Lightwave Tech. LT-4, 140 (1986).

31. S. I. Najafi, P. G. Suchoski, Jr., and R. V. Ramaswamy, 'Silver film-diffused glass waveguides: Diffusion process and optical properties,' IEEE J. Quantum Eelctron. QE-22, 2213 (1986).

32. R. H. Doremus, 'Optical properties of small silver particles,' J. Chem. Phys. 42, 414 (1965).

33. A. D. de Oliveira, M. G. F. Wilson, and O. Parriaux, 'Stripe waveguide Y-intersection as efficient coupler for multimode optical communication systems,' Electron. Lett. 17, 100 (1981).

34. T. Findakly and B. Chen, 'Single-mode integrated optical 1xN star coupler,' Appl. Phys. Lett. 40, 549 (1982).

35. T. W. Cline, 'Diffused channel glass waveguide optical splitters,; Tech. Digest, Topical Meeting on Integrated and Guided Wave Optics, IGFO'86, Feb. 1986, Atlanta, Ga., Paper FDD4.

36. A. Yi-Yan and C. D. W. Wilkinson, 'Optical frequency-selective filters in ion-exchanged waveguides,' Electron. Lett. 15, 240 (1979).

37. E. Y. B. Pun and A. Yi-Yan, 'Fabrication of periodic waveguides by ion exchange,' Appl. Phys. Lett. 38, 673 (1981).

38. T. Suhara, J. Viljanen, and M. Leppihalme, Integrated-Optic wavelength multi-and demultiplexers using a chirped, grating on an ion-exchanged waveguide,' Appl. Opt. 21, 2195 (1982).

39. R. G. Walker and C. D. W. Wilkinson, 'Integrated optical waveguiding structures made by silver ion-exchange in glass 2: Directional coupler and bends,' Appl. Opt. 22, 1929 (1983).

40. K. Honda, E. Garmire, and K. Wilson, 'Characteristics of an integrated optics ring resonator fabricated in glass,' IEEE J. Lightwave Tech. LT-2, 714 (1984).

41. A. Mahapatra and J.M. Connors, 'Double Tapped Ring Resonators Fabricated in Glass,' Topical Meeting on Optical fiber Communications and International Conference on Integrated Optic and Optical Communications, Jan. 1987, Reno, Nev. Paper TuK3.

42. G. L. Yip and J. Finak, 'Directional-coupler, power divider by two-step K^+-ion exchange,' Opt. Lett. 9, 423 (1984).

43. T. Findakly, "Glass waveguides by iion-exchange: A review," Opt. Engg. 24, 244 (1985).

44. R. K. Lagu, S. I. Najafi and V. Ramaswamy, "In situ measurement of ionic concentration during fabrication of ion-exchanged waveguides,' Appl. Opt. 23, 3925 (1984).

45. H. C. Cheng, R. V. Ramaswamy and R. Srivastava, "Buried Na^+-Ag^+ ion-exchanged glass waveguides: Theory and experiment," Tech. Dig. 7th Topical Meeting on Gradient-Index Optical Imaging Systems, Jan. 15-16, 1987, Reno (Nevada), Paper ThC2-1.

46. I. Fainaro, M. Ish Shalom, M. Ron and S. Lipson, 'Interdiffusion of silver in glasses and the related variations in electronic polarizability," Phys. Chem. Glasses 25, 16 (1984).

47. R. V. Ramaswamy, R. Srivastava, P. Chludzinski and T. J. Anderson, 'Influence of Ag^+-Na^+ ion-exchange equilibrium on waveguide index profile,' IEEE J. Quantum Electron., Submitted for publication.

48. S.I. Najafi, R. Srivastava and R.V. Ramaswamy, 'Wavelength-dependent propagation characteristics and mode cutoffs in Ag^+-Na^+ exchanged planar glass waveguides,' Appl. Opt. 25, 1840 (1986).

49. J. M. White and P. F. Heidrich, "Optical waveguide refractive index profiles determined from measurement of mode indices: A simple analysis," Appl. Opt. 15, 151 (1976).

50. H. M. Garfinkel, 'Ion-exchange equilibria between glass and molten salts,' J. Phys Chem. 72, 4175 (1968).

51. J. Crank; The Mathematics of Diffusion-Oxford at the Clarendon Press, 1956.

52. J. G. Kirkwood and J. Oppenheim; Chemical Thermodynamics - McGraw Hill New York, 1961.

53. V. Rothmund and G. Kornfeld, 'Der basenaustausch im permutit. I.,' Z. Anorg, Allg. Chem. 103, 129 (1918).

54. G. Schulze, 'Versuche uber die diffusion von silber in glas,' Ann. Physik, 40, 335 (1913).

55. R. Srivastava, C. K. Kao and R. V. Ramaswamy, 'WKB analysis of planar surface waveguides with truncated index profiles,' IEEE J. Lightwave Tech. To be published.

56. T. J. Cullen, C. N. Ironside, C. T. Seaton, and G. I. Stegeman, 'Semiconductor-doped glass ion-exchanged waveguides,' Appl. Phys. Lett. 49, 1403 (1986).

57. P. Chludzinski, R. V. Ramaswamy and T. J. Anderson, "Silver-sodium ion-exchange in soda-lime silicate glass," Phys. Chem. Glasses. To be published.

58. R. H. Doremus, 'Exchange and diffusion of ions in glass,' J. Phys Chem. 68, 2212 (1964).

59. R. Terai and R. Hayami, 'Ionic diffusion in glasses,' J. Non-cryst solids, 18, 217 (1975).

60. D. E. Day, 'Mixed alkali glasses-their properties and uses,' J-Non-cryst solids, 21, 343 (1976).

61. X. F. Zhu and K. Iga, 'Characterization of planar microlenses made by ion-exchange diffusion,' Tech. Digest, 7th Topical Meeting on Gradient-Index optical Imaging systems, Jan. 1987, Reno, Nev. Paper ThB1-1.

62. J. Albert and G. L. Yip, 'Refractive-index profiles of planar waveguides made by ion-exchange in glass,' Appl. Opt. 24, 3692 (1985).

63. A. R. Cooper and M. Abou-el-Leil, 'Index variation from field-assisted ion exchange,' Appl. Opt. 19, 1087 (1980).

64. T. Kaneko, and H. Yamamoto, 'On the ionic penetration of silver film into glasses under the electric field, Proc. 10th Int. Congr. Glass, Kyoto, Japan, 1974, pp. 8, 79-8-86.

65. H. Yoshida and T. Kataoka, 'Migration of two ions during electrolysis of glass waveguide,' J. Appl. Phys. 58, 1739 (1985).

66. H. C. Cheng, R. V. Ramaswamy and R. Srivastava, 'Modeling and Fabrication of buried, fiber-compatible singe-mode channel waveguides by Ag^+-Na^+ ion exchange, unpublished.

67. W.K. Burns and G.B. Hocker, 'End fire coupling between optical

fibers and diffused channel waveguides,' Appl. Opt. 16, 2048 (1977).

68. R. M. Knox and P. P. Toulios, 'Integrated circuits for the millimeter through optical frequency range,' Proc. MRI Symposium on submillimeter waves,' J. Fox Ed. (Polytechnic Press, Brooklyn, 1970).

69. G. B. Hocker and W. K. Burns, 'Mode dispersion in diffused channel waveguides by the effective index method,' Appl. Opt. 16, 113 (1977).

70. H. Matsuhara, 'Analysis of TEM modes in dielectric waveguides by a variational method,' J. Opt. Soc. Am. 63, 1514 (1973).

71. R. K. Lagu and R. V. Ramaswamy, 'A variational finite-difference method for analyzing channel waveguides with arbitrary index profiles,' IEEE J. Quantum Electron., QE-22, 968 (1986).

72. E. Schweig and W.B. Bridges, 'Computer analysis of dielectric waveguides: A finite-difference method,' Trans. Microwave Th. Tech., MTT-32, 531 (1984).

73. C. Yeh, S. B. Dong, and W. Oliver, 'Arbitrarily shaped inhomogeneous optical fiber or interated optical waveguides,' J. Appl. Phys. 46, 2125 (1975).

74. K. Yawuura, K. Shimohara and T. Miyamoto, 'Numerical analysis of a thin film waveguide by mode-matching method,' J. Opt. Soc. Am. 70, 183 (1980).

75. V. Ramaswamy and R. K. Lagu, 'Numerical field solution for an arbitrary asymmetrical graded index planar waveguide,' IEEE J. Lightwave Tech., LT-1, 408 (1983).

FIGURE CAPTIONS

Fig. 1. Variation of surface-silver concentration N_{Ag} and index change Δn with melt silver concentration N_{Ag} at 330°C in a soda-lime glass. [Ref. 57]

Fig. 2. Schematics for study of two-step ion exchanged waveguides.

Fig. 3. Evolution of index profile with second-step diffusion time. [Ref. 45]

Fig. 4. Variation of the index peak position x_{peak} below the glass surface and the 1/e index width W with the second-step parameters. The data points are from Ref. [25] and the theoretical curves from [45].

Fig. 5. Silver concentration profile in channel waveguide as measured by SEM. [Ref. 22]

Fig.6. Mode-field measurement schematics.

Fig.7. Variation of measured 1/e intensity width in (1) surface and (2) buried waveguide with mask width. H denotes horizontal scan (paralled to the substrate surface) and V denotes vertical scan [Ref. 66].

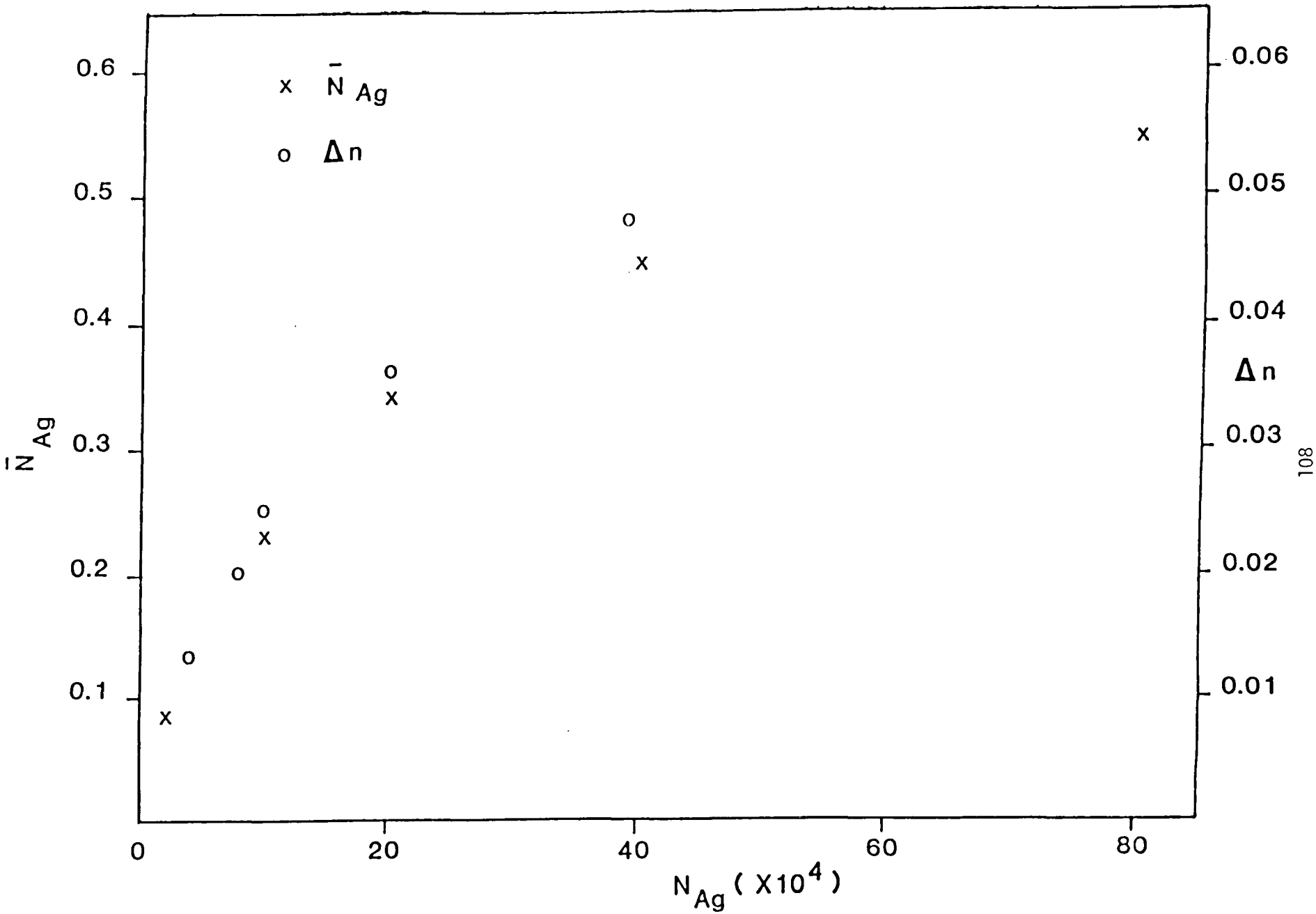
x $\bar{N}_{Ag}$
o Δn
0.6
0.5
0.4
0.3
0.2
0.1
$\bar{N}_{Ag}$
0.06
0.05
0.04
0.03
0.02
0.01
Δn
0
20
40
60
80
N_{Ag} (X10^4)

Two - Step Ion - Exchange

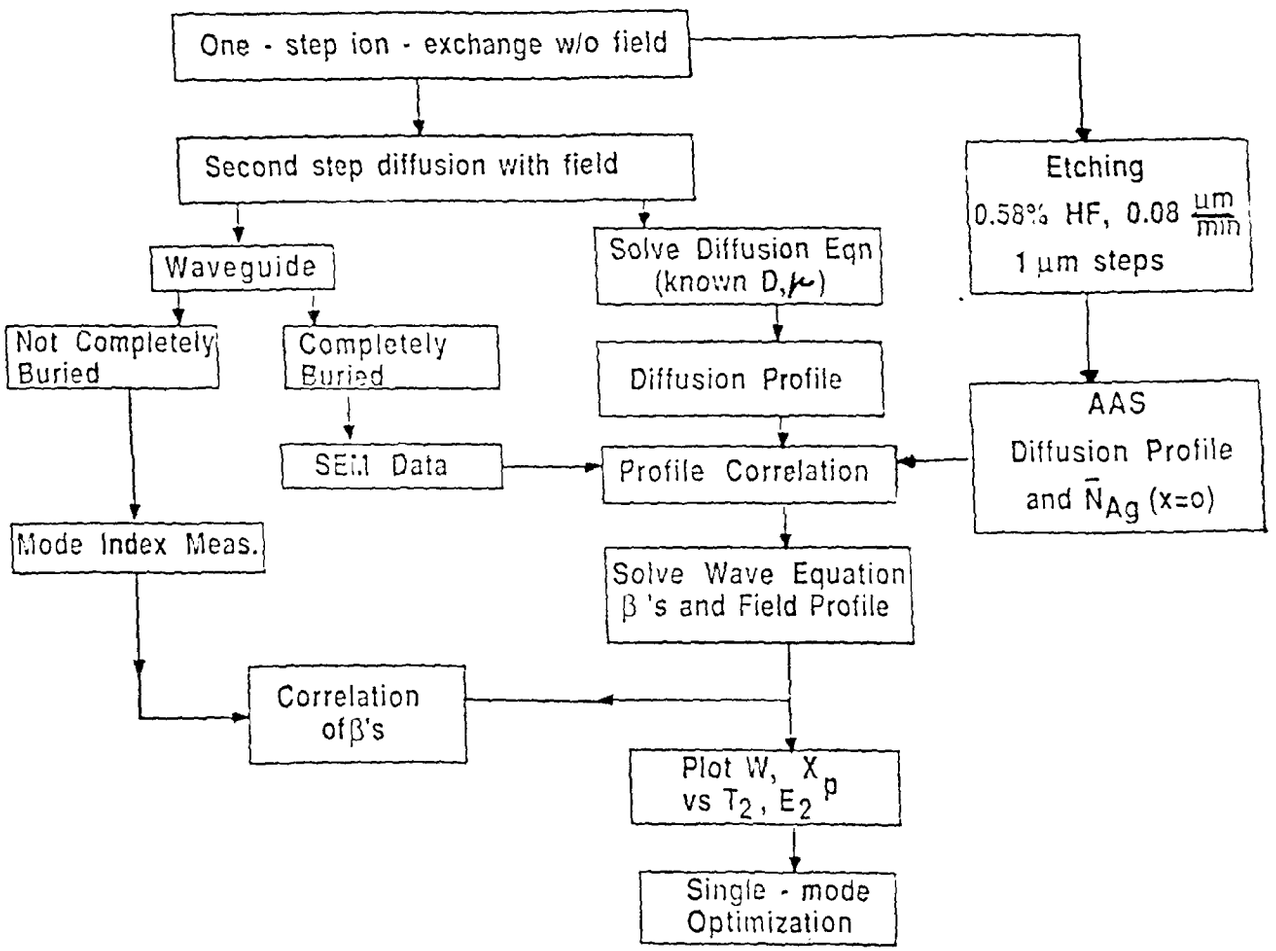

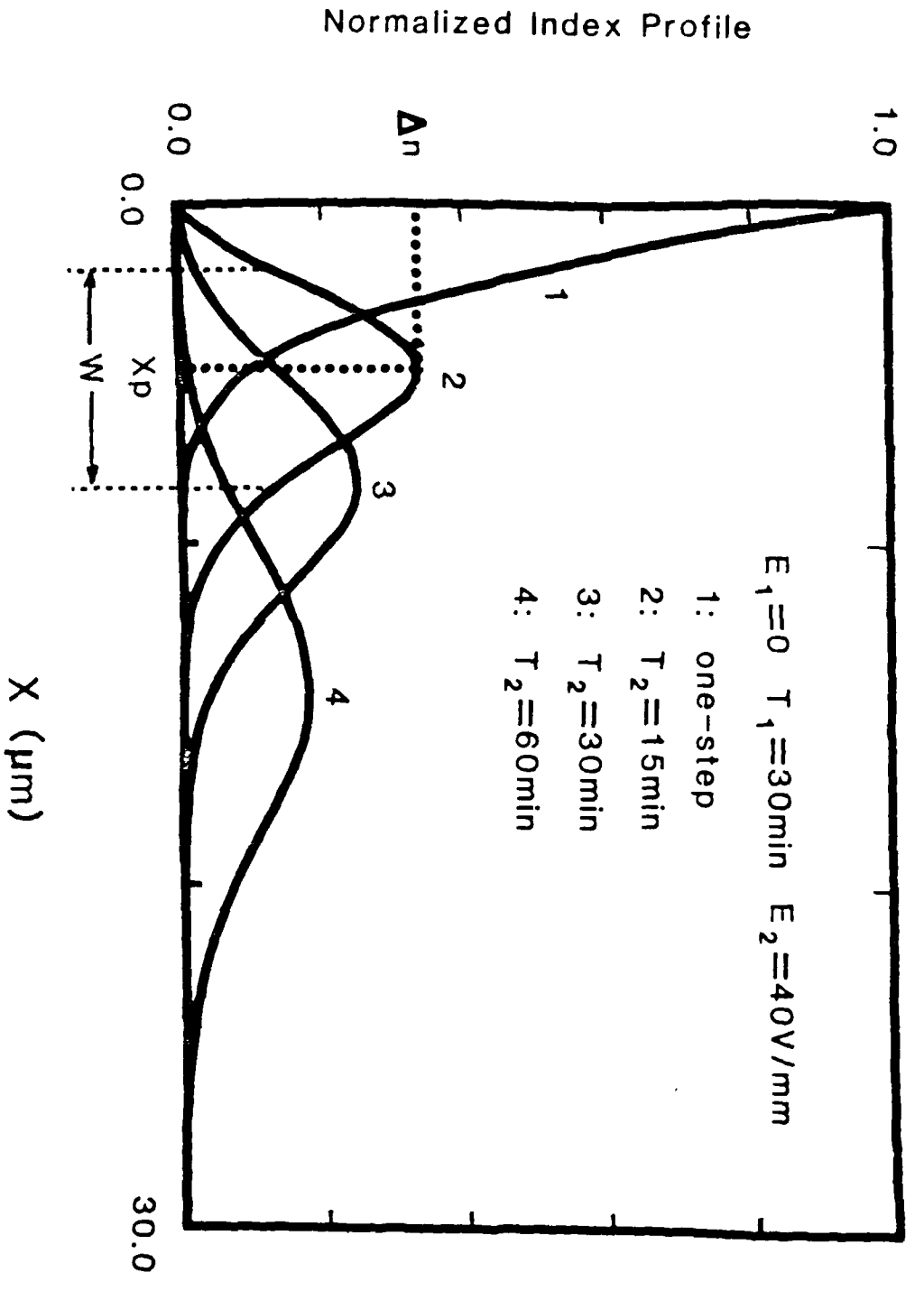
Normalized Index Profile
Δn
1.0
0.0
0.0
30.0
X (μm)
W
Xp
1
2
3
4
E1=0 T1=30min E2=40V/mm
1: one-step
2: T2=15min
3: T2=30min
4: T2=60min

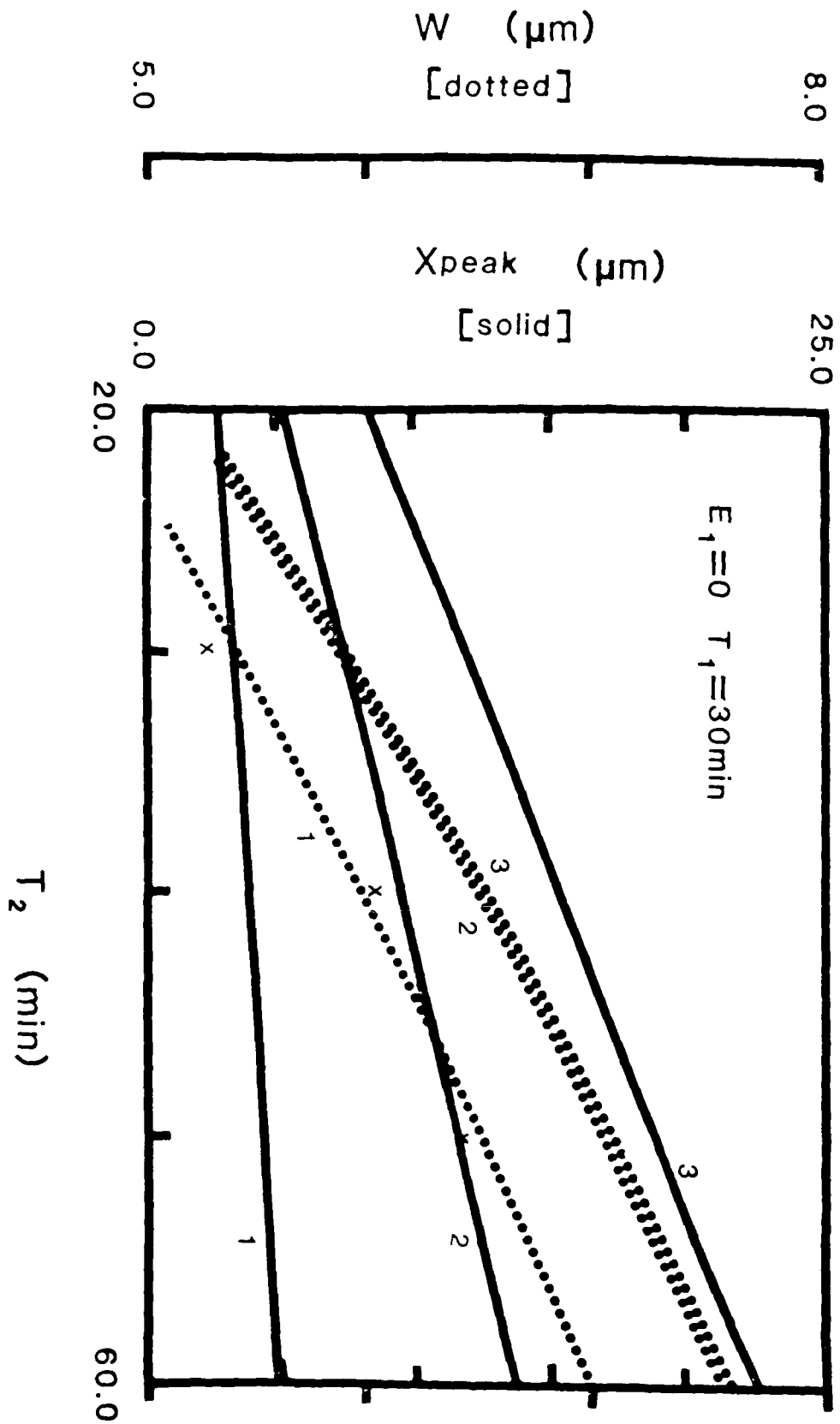
W (μm)
[dotted]
5.0
8.0
Xpeak (μm)
[solid]
0.0
25.0
20.0
60.0
T_2 (min)
E_1=0 T_1=30min
1
2
3
x

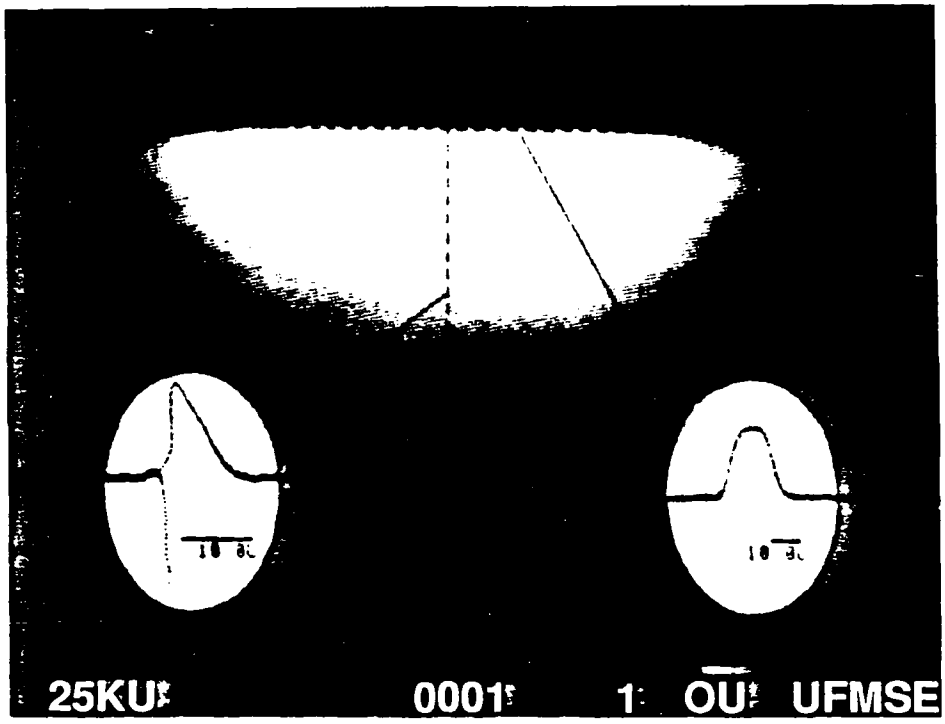
25KU
0001
1
OU
UFMSE

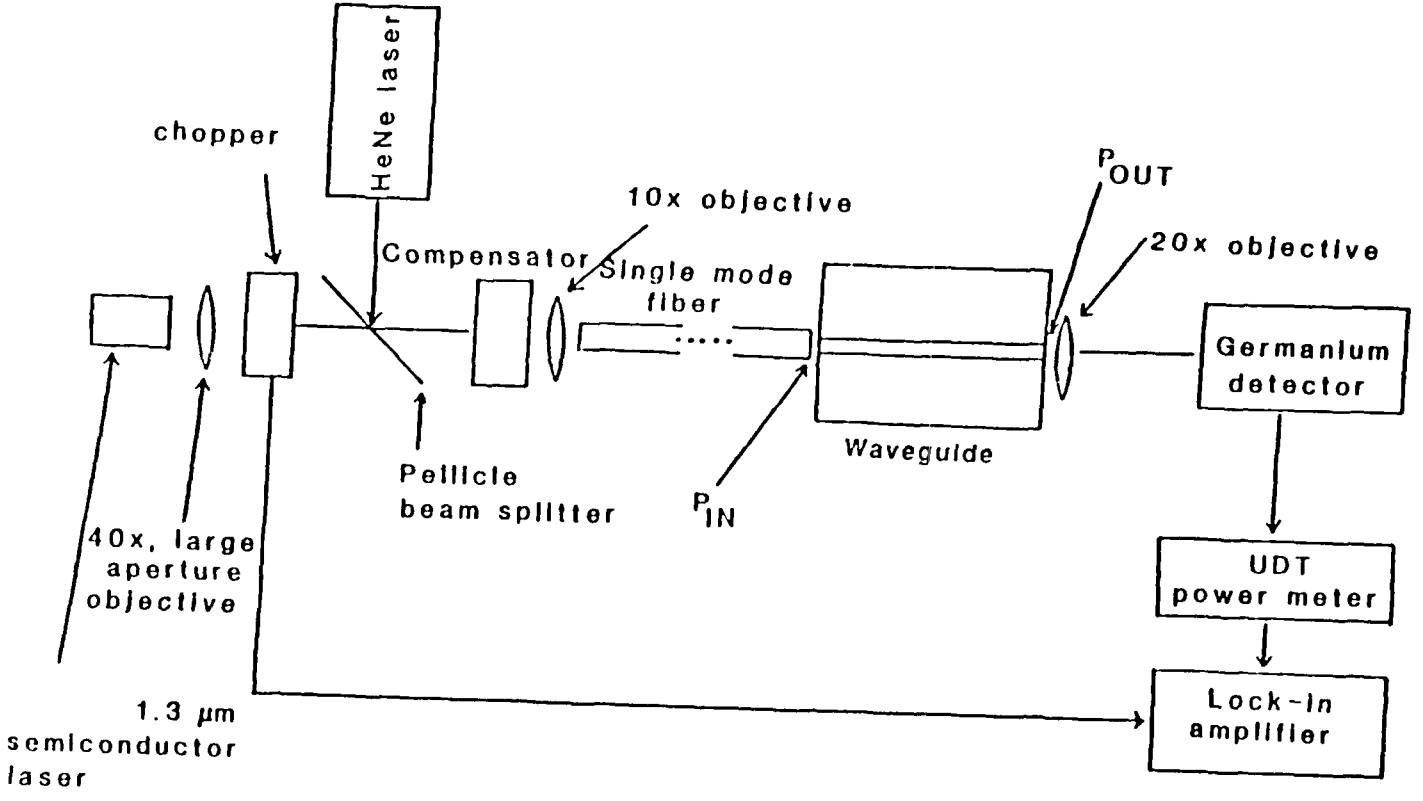
HeNe laser
chopper
10x objective
P_{OUT}
20x objective
Compensator
Single mode fiber
Germanium detector
Waveguide
Pellicle beam splitter
P_{IN}
40x, large aperture objective
UDT power meter
1.3 μm semiconductor laser
Lock-in amplifier

1: FIRST STEP W/O FIELD

2: TWO-STEP W/ FIELD

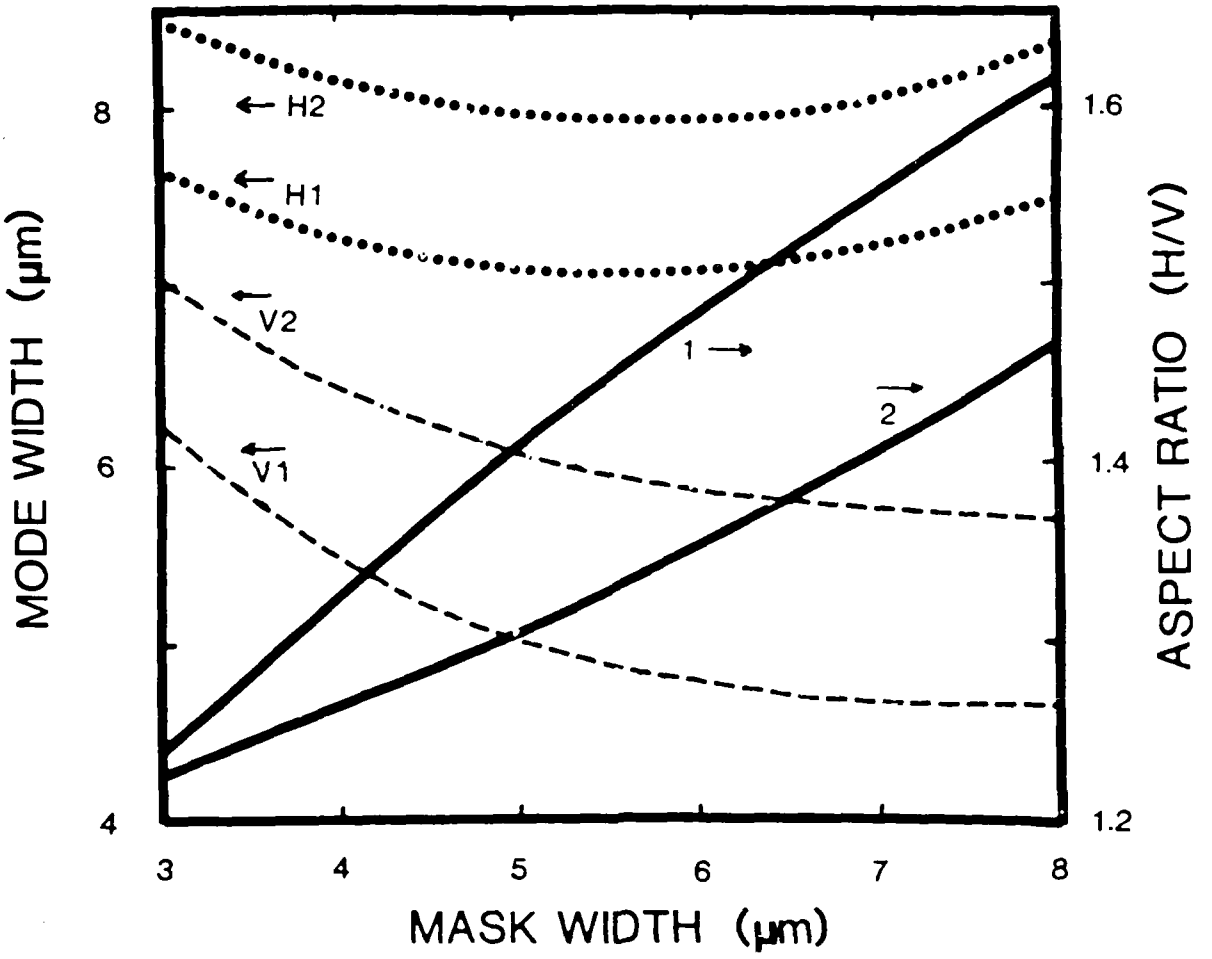

IEEE JOURNAL OF QUANTUM ELECTRONICS, VOL. QE-22, NO. 12, DECEMBER 1986

Silver Film-Diffused Glass Waveguides: Diffusion Process and Optical Properties

S. IRAJ NAJAFI, MEMBER, IEEE, PAUL G. SUCHOSKI, JR., AND RAMU V. RAMASWAMY, SENIOR MEMBER, IEEE

Abstract—Diffusion of a silver film into a glass substrate in the presence of an electric field is used to fabricate a series of planar waveguides in an effort to better understand the diffusion process and to relate the process parameters to the device parameters. The results indicate that it is possible to fabricate highly multimode waveguides which exhibit no fabrication-induced surface defects and no coloration due to silver reduction provided the silver film is not depleted during the diffusion process and the diffusion temperature is low (275°C or less). In addition, scanning electron microscope (SEM) analysis and optical characterization indicate that the maximum index change in the waveguide is strongly dependent on the applied field. We demonstrate that Δn varies from approximately 0 to 0.075 for fields ranging from 0 to 15 V/mm, making this technique specially attractive for the fabrication of waveguide structures requiring a large, variable change in refractive index.

I. Introduction

GLASS waveguides have recently received considerable attention since they appear to be suitable candidates for the fabrication of low-cost, low-loss integrated optical devices. To date, the majority of the waveguides studied have been fabricated by placing a glass substrate in a molten salt bath at an elevated temperature and exchanging the constituent sodium ions with various monovalent ions [1]. At the University of Florida, we have investigated extensively the Ag^+-Na^+ exchange in glass [2] and have been able to fabricate reproducible, low-loss single-mode and multimode planar and channel waveguides. Although Ag^+-Na^+ exchange seems to be an extremely promising technique for fabricating single-mode passive devices, it appears that it may not be quite suitable for certain device applications, e.g., highly multimode waveguides with numerical apertures comparable to that of multimode fibers and nonuniform waveguide structures.

An alternative method for fabricating glass waveguides utilizes diffusion of silver films into glass [3]–[5]. In this process, a silver film is deposited directly on a glass substrate and then diffused at an elevated temperature. An electric field can be applied across the sample to aid the diffusion process. We find that this technique offers several advantages over ion-exchange: 1) the process is relatively clean since pure (99.999 percent) silver is deposited directly on a clean substrate and the subsequent diffusion is performed in a closed chamber; 2) the temperature and concentration gradients across the width of the sample are negligible compared to the ion-exchange technique resulting in uniform waveguides; 3) the waveguides can be fabricated at relatively low temperatures; and 4) it is possible to fabricate low-loss waveguides with large Δn whereas similar waveguides fabricated using ion-exchange tend to be colored due to silver reduction. The major disadvantage of this technique is that it is difficult to make deep (10 μm) single-mode waveguides whereas this can be easily achieved using the ion-exchange technique.

In the earlier work on silver-diffused glass waveguides first presented by Chartier *et al.* [3], a thin layer of silver (used as both the dopant and the anode) was deposited on the top surface of a glass substrate while a layer of aluminum, deposited on the back of the sample, served as the cathode. The diffusion was carried out at temperatures ranging from 170 to 300°C with applied fields from 0 to 500 V/mm. Chartier *et al.* obtained single-mode waveguides after 35 min of diffusion at 180°C using an electric field of 50 V/mm. The maximum index change of their silver-diffused waveguides was approximately the same (0.09) as their Ag^+-Na^+ exchanged waveguides made using pure molten $AgNO_3$. In addition, they reported fabricating waveguides with seven guided modes at 250°C without an applied field (diffusion time of 2 h).

Findakly and Garmire [4] used an almost similar technique where a few hundred angstrom thick silver film served as both the dopant and the anode. For the cathode, they utilized a gold film for the fabrication of single-mode guides and molten sodium nitrate for highly multimode guides. The waveguides ranged in width from a few microns to a few tens of microns depending on the applied field (up to 100 V/mm) and the diffusion temperature (250–500°C). The authors estimated a Δn of 0.001 for guides fabricated with no applied field and a Δn of up to 0.025 with an applied field. As they mentioned, these results did not agree with the results presented in [3]. In

Manuscript received February 13, 1986, revised July 22, 1986. This work was supported by the Air Force Office of Scientific Research under Contract 84-0369.

S. I. Najafi was with the Department of Electrical Engineering, University of Florida, Gainesville, FL 32611. He is now with the Departement de Genie Physique, Ecole Polytechnique, Campus de l'Universite de Montreal, Montreal, P.Q. H3C 3A7, Canada.

P. G. Suchoski, Jr. and R. V. Ramaswamy are with the Department of Electrical Engineering, University of Florida, Gainesville, FL 32611.

IEEE Log Number 8610823

0018-9197/86/1200-2213$01.00

addition, they were unable to make a single-mode waveguide even after 4 h of diffusion at 250°C ($E = 0$) which again was in contrast with [3]. Our own experience confirms the results of Findakly and Garmire [4].

Pitt *et al.* [5] developed a slightly different set-up for the diffusion process which made use of a separate anode and dopant source. The aluminum anode also acted as a pattern-delineation mask for defining the desired device geometry. The solid dopant source was replaced by a silver vapor stream continuously supplied during the diffusion, so that there was no limit to the guide depth imposed by the silver film thickness. As in the previous experiments, a metallic film was used as the back electrode. Pitt *et al.* fabricated waveguides with a maximum Δn of 0.08 using diffusion temperatures ranging from 100 to 300°C and applied fields from 0 to 100 V/mm. During the diffusion process, the authors monitored current flow through the glass and observed that after a certain period of time, the current flow began to decrease. They attributed this reduction to sodium depletion from the surface of the sample.

In this paper, we report on a series of planar, silver-diffused waveguides fabricated with various silver thicknesses, diffusion times, and applied fields in an effort to better understand the physics of the diffusion process. The setup is similar to that reported in [4], except we deposit a gold film over the silver film to prevent oxidation of the silver during the diffusion process. SEM (scanning electron microscope) analysis and the prism coupling method are used to determine how the various process parameters affect waveguide performance. Included in this discussion is a demonstration of how Δn varies with applied field. Finally, we compare the optical properties of the silver-diffused waveguides to Ag^+-Na^+ exchanged waveguides fabricated in our laboratory.

II. Waveguide Fabrication

We utilized the set-up depicted in Fig. 1 for fabricating the silver-diffused waveguides. Initially, a several thousand angstrom thick silver film was deposited on the soda-lime-glass, Fisher Brand Premium substrate (composition (wt percent): SiO_2—72.25 percent, Na_2O—14.31 percent, CaO—6.4 percent, Al_2O_3—1–1.2 percent, K_2O—1.2 percent, MgO—4.3 percent, Fe_2O_3—0.03 percent, and SO_3—0.3 percent) using an electron beam evaporation system. To prevent oxidation and flaking of the silver film during the diffusion process, a 2000 angstrom gold film was deposited on top of the silver. This structure served as the anode. We chose to use a molten salt for the cathode since metallic back electrodes tend to deteriorate with time due to an accumulation of sodium metal [4]. A small amount of powdered silver nitrate was placed on top of the glass sample and melted to form the cathode. Molten silver nitrate was chosen for this purpose because it has a considerably lower melting point than sodium nitrate. Connection to the molten silver nitrate electrode was accomplished using a large loop of copper wire. Due to the finite resistivity of the molten silver nitrate, care must be taken to locate the copper wire at least 0.5 cm from the back surface of the glass or else the applied voltage will vary across the sample, resulting in a nonuniform diffusion.

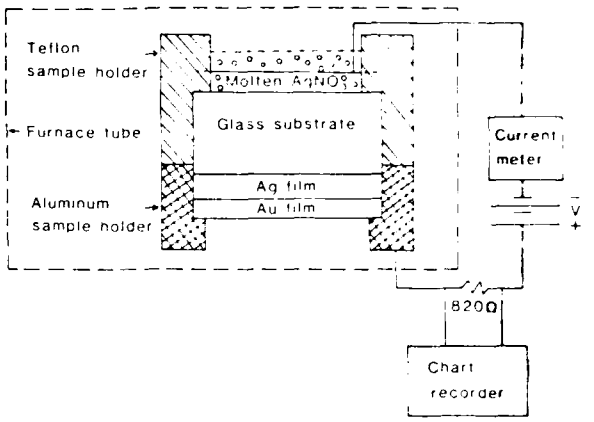

Fig. 1. Experimental set-up used for fabricating silver-diffused waveguides.

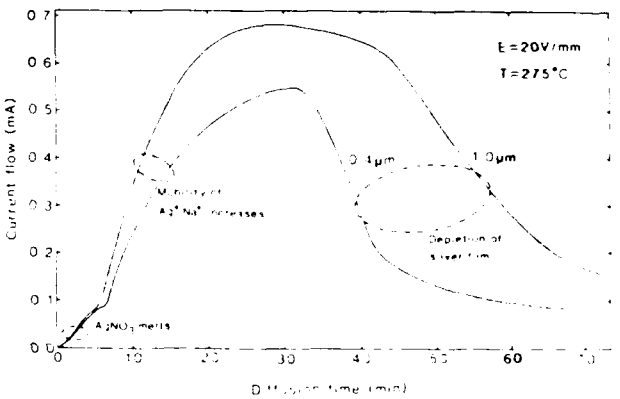

Fig. 2. Current flow versus time for waveguides fabricated with two different silver thicknesses (0.4 and 1.0 μm). $T = 275$ °C, $E = 20$ V/mm.

The diffusion was carried out at 275°C in a quartz furnace tube. The current flow was monitored during the diffusion process by measuring the voltage drop across an 820 Ω series resistor (see Fig. 1) and was plotted using a chart recorder. In Fig. 2, we present plots of current flow versus time for waveguides fabricated with an applied field of 20 V/mm and silver thicknesses of 0.4 and 1.0 μm. In both plots, the current initially rises slowly for the first 5–7 min of diffusion as the $AgNO_3$ powder begins to melt, making electrical contact with the back surface of the glass. As the sample warms (we estimate that it takes approximately 20 min for the sample to reach equilibrium from the time the $AgNO_3$ powder melts and current flow begins), the current flow increases rapidly due to the fact that the mobilities of the silver and sodium ions in glass increase exponentially with temperature. After a length of time, the current flow reaches a maximum value as the sample reaches thermal equilibrium (275°C). The current then begins to decrease and goes to zero after very long diffusion times. This behavior is similar to that reported

by Pitt *et al.* [5]; however, we do not believe that it is due to depletion of sodium from the anode as previously predicted [5], but instead is due to depletion of the silver dopant source. To ascertain this fact, we determined the total current flow through the glass by integrating the current flow plots for the two samples. The total current flow through the 1.0 μm Ag film sample is approximately 2.5 times the total current flow through the 0.4 μm sample. Thus, it appears that the total current flow is directly proportional to the deposited silver film thickness, leading us to believe that the only factor limiting the dry diffusion process is the finite silver thickness. We believe that the reduction in current observed in [5] is not due to depletion of the anode since the authors have essentially an infinite supply of dopant, but instead is due to deterioration of the aluminum electrode as has been reported elsewhere in literature [41].

We fabricated a set of waveguides with 1.0 μm of silver, diffusion temperature of 275°C, and electric fields ranging from 0 to 20 V/mm. In fabricating waveguides using the silver film diffusion process, it is important to stop the process well before depleting the silver source. Otherwise, there is a depletion of cations from the waveguide surface resulting in surface defects (bubbles). For this reason, we stopped the diffusion process 30 min after the current had reached its maximum (steady-state) value.

In Fig. 3, we present the current flow plots for the various samples. The magnitude and shape of the current flow plots is determined by the applied electric field and the thickness of the silver film. For a given applied electric field, it is possible for the system to reach a quasi-steady state provided there is sufficient silver dopant on the surface of the sample. In this case, the current flow increases rapidly until it saturates at a steady-state value. From examining Fig. 3, it appears that 1.0 μm of silver is sufficient for the 1, 2, 5, 7.5, and 15 V/mm samples to reach steady state. On the other hand, since the current flow begins to decrease almost immediately after reaching its peak value (Fig. 2), it appears that 1.0 μm of silver is not sufficient for the 20 V/mm sample to reach steady state. For this reason, we diffused an additional sample using an applied field of 20 V/mm and a 1.5 micron thick silver film.

We should state that the current flow never reaches a true steady state as described above but instead decreases slightly with time. (See Fig. 3.) This effect can be attributed to the fact that the silver ions have a lower mobility in glass than the constituent sodium ions (the ionic radii of Ag^+ and Na^+ are 1.26 and 0.97 Å, respectively [6]). Thus, as more of the silver ions diffuse into the glass, the overall conductivity of the sample decreases slightly, resulting in a small decrease in current flow. This phenomenon should not be confused with the sharp decrease in current flow due to depletion of the silver dopant.

In Fig. 4, we plot maximum (steady-state) current flow versus the applied electric field for the above mentioned samples. Note that there is essentially a linear relationship between these two parameters provided there is sufficient

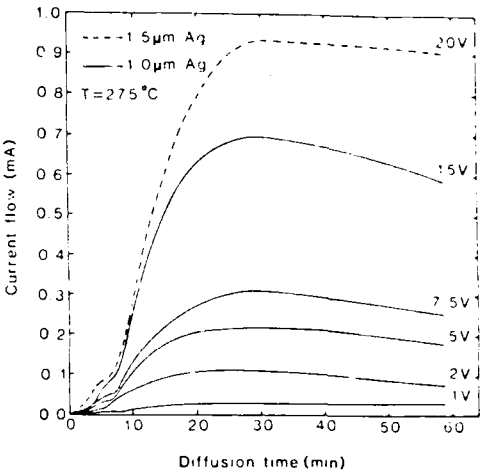

Fig. 3. Current flow versus time for samples fabricated at 275°C with various applied fields. A 1.0 μm silver film is used for the 1, 2, 5, 7.5, and 15 V/mm samples while a 1.5 μm film is used for the 20 V/mm sample.

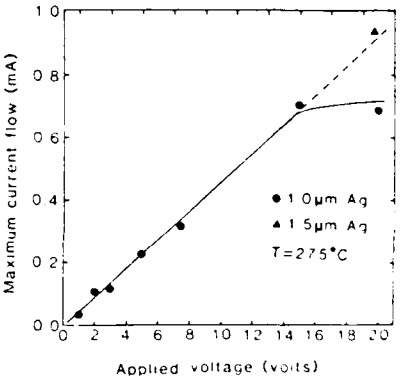

Fig. 4. Maximum (steady state) current versus applied voltage for the samples depicted in Fig. 3.

silver dopant for the sample to reach steady state. This is demonstrated by the fact that the 1.5 μm-20 V/mm data point lies on the I-V curve (Fig. 4) whereas the 1.0 μm-20 V/mm data point lies well below this curve due to depletion of silver prior to reaching steady state. In addition, it appears that the chemical potential between the silver film and the glass substrate at this temperature (275°C) is extremely small since the 1 V data point lies on the applied field-current flow line.

In order to better understand the physical phenomena influencing the current flow plots depicted in Figs. 2 and 3, we performed the following experiment. Initially, we placed the glass sample in the diffusion tube and let it reach thermal equilibrium (approximately 30 min after the $AgNO_3$ melts). We then applied 15 V/mm across the sample and observed that the current flow increased immediately to its steady-state value. This indicates that the rise in current in our previous samples (Figs. 2 and 3) is due to thermal effects. Since the resistivity of the molten $AgNO_3$ back electrode actually increases with temperature (see Fig. 5), it is obvious that the second stage increase in current, which occurs after the initial 5-7 min

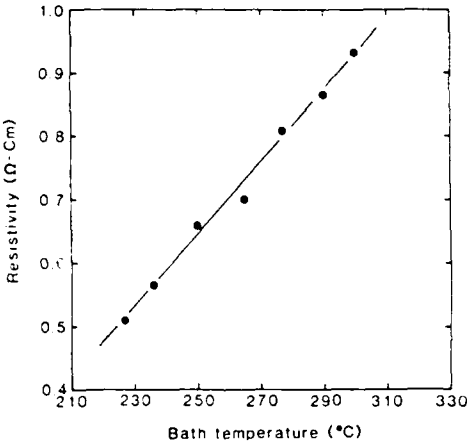

Fig. 5. Resistivity of molten silver nitrate as a function of bath temperature.

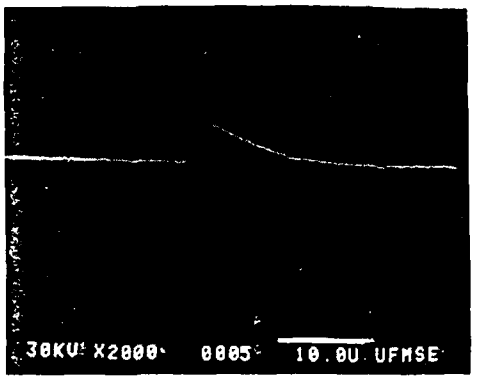

Fig. 6. SEM photograph used to determine Δn in the silver-diffused guide. The sample on the left was fabricated using Ag^+-exchange with an Ag^+ concentration of 2×10^{-4} MF and bath temperature of 330°C. The sample on the right was fabricated using silver-diffusion with an applied field of 1 V/mm and an oven temperature of 275°C.

related to the melting of $AgNO_3$, is not just due to thermal effects at the back electrode; instead, it must be due to a combination of thermal effects at the silver-glass interface, within the bulk glass, and at the molten back electrode. Although it is difficult to experimentally determine which of these effects more strongly influences current flow, we suspect that the sudden change in rate of current flow (5–8 min after melting of the $AgNO_3$) is due to the fact that the mobilities of the silver and sodium ions in the bulk glass increase exponentially with temperature and can overcome significantly the other two thermal effects. We have noticed similar behavior in ion-exchange where a 4 or 5°C change in bath temperature causes as much as a 25 percent change in current flow.

III. SEM Analysis

In order to investigate the effect of silver thickness and applied electric field on Δn and diffusion depth, we epoxied several waveguides together, polished them, and then analyzed them using the scanning electron microscope (SEM) [7]. Our analysis indicates that the thickness of the silver dopant layer does not significantly affect the maximum index change in the waveguide, however, Δn does vary strongly with applied field. To determine the magnitude of Δn as a function of the applied field, we compared the silver-diffused samples to an Ag^+–Na^+ exchanged sample fabricated at 330°C in a $NaNO_3$ bath with an Ag^+ concentration of 2×10^{-4} MF (See Fig. 6). The Ag^+–Na^+ exchanged guide presented on the left-hand-side of Fig. 7 has an index change of 0.005 [2c]. Thus, assuming that Δn varies linearly with Ag^+ concentration, the silver-diffused sample (right-hand side of Fig. 6) which was fabricated with an applied field of 1 V/mm has a maximum index change of 0.021. In a similar fashion, we determined Δn for other values of applied field. These values of Δn along with the diffusion depths are plotted in Fig. 7 as a function of applied field.

As indicated in Fig. 7, the maximum index change we obtained using the dry diffusion method is approximately 0.075. This value is in close agreement with the values

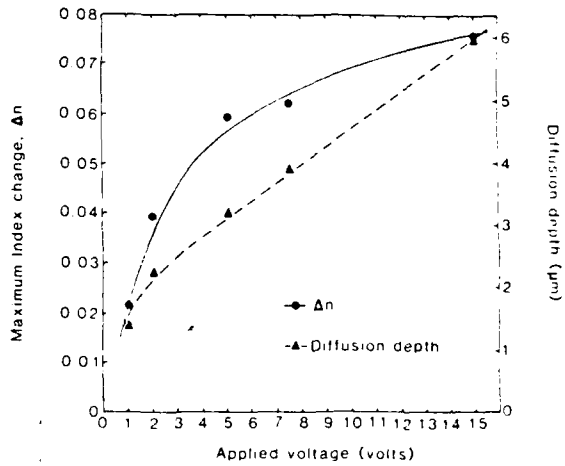

Fig. 7. Variation of Δn and diffusion depth (measured at 1/e point) with applied field.

of Δn presented in [3] and [5] but differs from that presented in [4]. One reason for this discrepancy may be due to the fact that different brands of soda-lime-glass, possibly with different percentages of compositional constituents (Na, Ca, and K), are being used by each of the groups. We have recently observed [8] that the maximum index change of a waveguide obtained using one brand of soda-lime-glass may be several times smaller or larger than the Δn value obtained using another brand of soda-lime-glass under the same fabrication conditions. Another possible reason for the discrepancy may be that Findakly *et al.* [4] has used relatively thin silver films and long diffusion times, thus resulting in lower Δn due to depletion of the silver dopant.

It is interesting to note the strong variation of Δn with applied field. This behavior can be explained by realizing that the silver ions in the film have a certain energy distribution which depends essentially on applied field and temperature. The only ions which leave the film and enter the glass are those which have energy larger than the chemical potential which exists between the silver film

TABLE I
EFFECTIVE MODE INDEXES OF Ag^+-DIFFUSED AND Ag^+-Na^+ EXCHANGED GLASS WAVEGUIDES. SILVER DIFFUSED WAVEGUIDES ARE THOSE REPRESENTED IN FIG. 3. SILVER EXCHANGE DATA IS FROM [2a, TABLE I]. REFRACTIVE INDEX OF SUBSTRATE IS 1.512 AT 0.6338 μm.

Silver Diffused Waveguides					Silver Exchanged Waveguides				
Diffusion Time (min)	Applied Field (V/mm)	No. of TE Modes	Mode Order	Effective Index	Diffusion Time (min)	Applied Field (V/mm)	No. of TE Modes	Mode Order	Effective Index
30	1	1	0	1.51830	30	0	1	0	1.51465
30	2	2	0	1.53800	60	0	2	0	1.51640
			1	1.52200				1	1.51293
30	3	3	0	1.54535	90	0	2	0	1.51706
			1	1.52880				1	1.51408
			2	1.51356	120	0	3	0	1.51716
30	5	4	0	1.55724				1	1.51465
			1	1.54402				2	1.51313
			2	1.53046	150	0	3	0	1.51798
			3	1.51673				1	1.51511
30	7.5	6	0	1.56874				2	1.51363
			1	1.55784	30	30	4	0	1.51822
			2	1.54674				1	1.51605
			3	1.53530				2	1.51496
			4	1.52244				3	1.51295
			5	1.51211					

and the glass surface. As long as the silver film is not depleted during the diffusion process, the index change (Δn) is determined strictly by the number of ions which enter the glass per unit time. This number obviously increases with both the applied field and temperature. This effect has not been noticed in Ag^+-Na^+ exchanged guides where to the first-order, Δn is determined entirely by the silver ion concentration (C_o) in the salt bath [2]. Because of the strong variation of Δn with E, it should be possible to use the silver-diffusion technique to make novel waveguide structures. As expected, for relatively large fields and a constant diffusion time (30 min), the diffusion depth varies linearly with applied field.

As indicated in Fig. 7, the deepest waveguides that we have fabricated are 6 μm. However, as mentioned earlier, it appears that there is no fundamental limitation on the amount of silver which can be introduced into the glass using the silver film diffusion method. Thus, a 50 μm deep waveguide, compatible with multimode fibers, can be fabricated by simply increasing the silver film thickness and diffusing for 4 h rather than 30 min.

IV. OPTICAL CHARACTERIZATION

We initially used a HeNe laser and the prism coupling method to characterize silver-diffused waveguides fabricated at 275°C with no applied field. Even after several hours of diffusion, the structure supports only a single guided mode. This result is in agreement with that of [4] but again is in contrast to the results presented in [3]. We suspect that this temperature is too low to transport many of the silver ions from the silver film into the surface of the glass without an applied field. Therefore, there is only a very small Ag^+ concentration (small Δn) inside the glass surface and a very limited diffusion unless an electric field is applied across the sample.

We used the prism coupling technique to determine the number of TE modes and the effective indexes of the modes at the HeNe wavelength for waveguides fabricated with applied fields ranging from 1 to 15 V/mm. Using the silver-diffusion technique, it is possible to fabricate highly multimode waveguides using relatively small fields and short diffusion times. This is demonstrated by the fact that a 15 V/mm sample diffused for 30 min supports 10 guided modes.

The number of guided TE modes along with the effective mode indexes for waveguides fabricated with applied fields less than 15 V/mm are presented in Table I and compared to Ag^+-Na^+ exchanged waveguide results. As indicated in this table, it is possible to fabricate single mode waveguides using the Ag^+-diffused technique provided the applied electric field is relatively small (1 V/mm) and the diffusion time is short (30 min). Also, we note that the difference in the effective indexes of the fundamental and the fifth order modes for the 7.5 V/mm sample is 0.057. This value is in close agreement with the predicted Δn value of 0.061 obtained using the scanning electron microscope.

It is important to note that no yellow coloring of the

glass waveguides was observed, even in the samples with large Δn. In addition, loss measurements using the three prism technique yielded average loss values of 0.5 dB/cm for multimode guides and 1.0 dB/cm for single-mode guides fabricated on Fisher brand substrates. We did not expect this result since highly multimode (large Δn) waveguides previously fabricated in our laboratory using the ion-exchange technique with the same brand of glass substrate tended to be highly colored due to reduction of silver ions. We suspect that the silver-diffused multimode waveguides do not exhibit this coloration since the diffusion is performed at a considerably lower temperature (275°C) than has previously been used. (Typical temperatures for Ag^+-Na^+ exchange are 330°C or higher.)

V. Conclusions

We fabricated a series of planar glass waveguides using the Ag^+ film-diffusion technique in an effort to better understand the diffusion process and to determine the effect of the process parameters (diffusion time, silver thickness, and electric field) on the waveguide parameters (number of guided modes, effective mode index, and maximum index change). It appears that low loss, high Δn waveguides can be easily fabricated using this technique provided the deposited silver film is sufficiently thick and the diffusion temperature is low (275°C or less). Single-mode waveguides using Fisher Brand substrates exhibit losses on the order of 1 dB/cm, which is comparable to the loss values obtained with ion-exchange techniques using similar substrates. The multimode guides provide losses better than 0.5 dB/cm and are comparable to those of Findakly and Garmire [4]. We expect both the single-mode and multimode guides to exhibit substantially lower losses if a better substrate with minimal transition metal impurities is used and the guiding layers are buried.

In addition, we demonstrated that the maximum index change (Δn) obtained using this technique is strongly dependent on the applied field. Therefore, we believe that the silver film-diffusion technique will be extremely useful for fabricating highly multimode waveguide devices as well as other novel waveguide structures. The technique should be especially attractive for mass production due to its simplicity, low risk of contamination, and reduced raw material consumption.

References

[1] T. Findakly, "Glass waveguides by ion exchange: A review," *Opt. Eng.*, vol. 24, pp. 244-250, 1985.

[2] For example: (a) S. I. Najafi, R. V. Ramaswamy, and R. K. Lagu, "An improved method for fabricating ion-exchanged waveguides through electrolytic release of silver ions," *J. Lightwave Technol.*, vol. LT-3, pp. 763-766, 1985; (b) R. V. Ramaswamy and S. I. Najafi, "Planar, buried, ion-exchanged glass waveguides: Diffusion characteristics," *J. Lightwave Technol.*, Special Issue on Integrated Optics, accepted for publication; (c) R. K. Lagu and R. V. Ramaswamy, "Process and waveguide parameter relationships for the design of planar, silver ion-exchanged glass waveguides," *J. Lightwave Technol.*, accepted for publication.

[3] G. H. Chartier, P. Jaussaud, A. D. de Oliveira, and O. Parriaux, "Optical waveguides fabricated by electric-field controlled ion exchange in glass," *Electron. Lett.*, vol. 14, pp. 132-134, 1978.

[4] T. Findakly and E. Garmire, "Reduction and control of optical waveguide losses in glass," *Appl. Phys. Lett.*, vol. 37, pp. 855-856, 1980.

[5] C. W. Pitt, A. A. Stride, and T. I. Trigle, "Low temperature diffusion process for fabricating optical waveguides in glass," *Electron. Lett.*, vol. 16, pp. 701-703, 1980.

[6] R. H. Doremus, *Glass Science*. New York: Wiley, 1973.

[7] R. K. Lagu and R. V. Ramaswamy, "Silver ion-exchanged, buried, glass waveguides with symmetric index profile," *Appl. Phys. Lett.*, accepted for publication.

[8] S. I. Najafi, R. Srivastava, and R. V. Ramaswamy, "Wavelength dependent propagation characteristics of Ag^+-Na^+ exchange planar glass waveguides," *Appl. Opt.*, submitted for publication.

S. [illegible] **Najafi** (M'85), for a photograph and biography, see p. 891 of the June 1986 issue of this JOURNAL.

Paul G. Suchoski, Jr., was born in Gainesville, FL, on September 3, 1960. He received the B.S.E.E. and M.E. degrees, and the Ph.D. degree in electrical engineering in 1982, 1985, and 1986, respectively, from the University of Florida, Gainesville.

Since 1982, he has been a Graduate Research Assistant in the Department of Electrical Engineering, University of Florida, Gainesville, where he has analyzed, designed, and fabricated tapered transitions for various integrated optic applications. In addition, he has held temporary positions at the Laboratory for Physical Sciences, College Park, MD, and TRW Electro-Optic Research Center, El Segundo, CA. His current research interests include integrated-optical and optoelectronic devices.

Ramu V. Ramaswamy (M'62-SM'80), for a photograph and biography, see p. 891 of the June 1986 issue of this JOURNAL.

REFERENCE [3]

Fabrication of single mode glass waveguides by electrolytic release of silver ions

R. K. Lagu and V. Ramaswamy
Department of Electrical Engineering, University of Florida, Gainesville, Florida 32611

(Received 22 March 1984; accepted for publication 25 April 1984)

We report a novel electrolytic process that is used to fabricate reproducible, low loss, single mode waveguides. By precisely controlling the current pumped through high purity Ag and Pt electrodes in molten $NaNO_3$, as well as its duration, a high degree of accuracy over the release and hence the control of Ag^+ concentration is achieved. The inherent capability of the process to generate very low level of silver ion concentration with high precision implies much higher time of diffusion, thus removing the time criticality factor faced by the existing processes while fabricating single mode waveguides.

The need for optical components using ion-exchanged glass waveguides has continued to remain strong primarily because of their compatibility with optical fibers, cost effectiveness, and potential for integration. Since there is no need to modulate any information at the receiving end of an optical communication system, passive components on glass substrates would be an ideal choice. These devices, on the other hand, cannot be tuned electro-optically and hence need to be fabricated to strict specification with assured repeatability. This in turn demands good process control.

We report a novel technique to fabricate reproducible single mode waveguides by accurate control of Ag^+ concentration. Ion exchange is a well-known technique for fabricating optical components in glasses. Both thallium[1] and silver[2-4] ions are used to create high index surface layers on glass substrates. The existing processes take either pure $AgNo_3$ or a mixture of $AgNO_3$ and $NaNO_3$ (silver nitrate about 10% by weight) for carrying out diffusion, resulting in multimode waveguides. With such high concentration of silver ions, their reduction to metallic state is highly likely causing excessive absorption and scattering losses. The time of diffusion to produce a single mode waveguide is about 2–3 min. This makes the timing very critical, thus making the reproducibility a serious problem. A single mode waveguide fabricated under such conditions is usually shallow and hence couples poorly to an optical fiber which can be thought of as a buried structure of a reasonably large cross-sectional dimension (8–10 μm).

The proposed process[5] overcomes the existing problems by generating very small concentration of silver ions precisely. The idea is based on the well-known Faraday's law of electrolysis:

When 96500 coulombs of charge are passed through a metallic electrode, 1 g equivalent of the metal is released into the solution as metal ions.

Thus, generation of silver ions can be accomplished by using a metallic silver electrode rather than a salt mixture of $AgNO_3$ and $NaNO_3$. Furthermore, melt impurities can be kept minimal as ultrapure (99.999%) silver rods are commercially available. The process of releasing silver ions can now be electronically controlled through the realization of an accurate, variable current source using off-the-shelf operational amplifiers. In addition, the Ag^+ concentration in the bath can be changed with time so that the diffusion can be carried out with a variety of boundary conditions, thus providing a larger control of the refractive index profile.

The process as shown in Fig. 1 is described briefly as follows. The setup consists of a salt bath heated by a band heater coiled around it. The temperature of the bath is sensed by a thermocouple and controlled with a closed-loop controller to an accuracy of $\pm$ 0.5 °C. Initially 400 g of pure sodium nitrate (A.C.S. grade, Fisher) are weighed and heated to 330 °C. Then a pure silver rod and a platinum reference electrode are introduced into the salt bath and 0.2 g of silver is released into the molten salt as ions by electrolysis. Then precleaned soda-lime-silicate glass slides are placed in the bath and the diffusion is carried for periods ranging from 20 to 120 min. The slides are then taken out of the bath, cooled for about 5 min and the residual salt is rinsed off with warm water.

The prism coupling technique is used to measure the mode indices. Table I shows the propagation characteristics of the various waveguides. It is seen that the first four waveguides are single mode. An iterative program is written to estimate the maximum refractive index change (Δn) from the measured values of the mode indices. For this set of waveguides, Δn is found to be 0.005. Preliminary results indicate that it is possible to find relations between process parameters and the mode index so that single mode waveguides

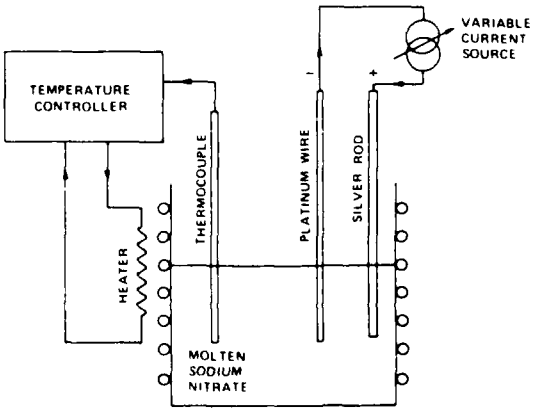

FIG. 1. Process schematic diagram.

 0003-6951/84/140117-02$01.00

TABLE I. Diffusion times and mode indices for TE modes. Substrate refractive index = 1.512 at 0.6328 μm.

Time of diffusion (min)	No. of modes	Mode order	Mode index
20	1	0	1.51245
40	1	0	1.51301
60	1	0	1.51337
80	1	0	1.51357
100	2	0	1.51407
		1	1.51232
120	2	0	1.51425
		1	1.51245

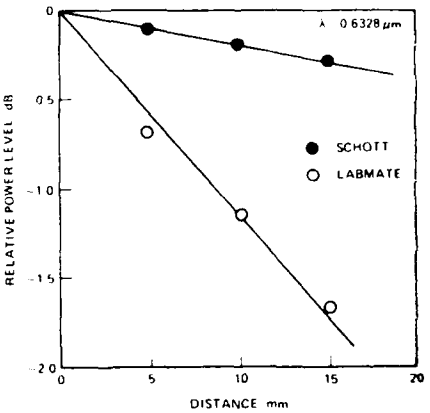

FIG. 2. Loss measurement at 0.6328 μm.

with known propagation constants can be fabricated. The waveguides show no signs of yellow stain due to silver ion reduction. To measure the loss, initially an output prism was used to tap off the transmitted power. To have a reliable loss measurement, however, it seemed necessary to take care not to disturb the input coupling and not to spoil the guide surface at the contact point. These conditions seemed rather restrictive and hence an improved three-prism loss measurement technique[6] was used.

It is reported[7] that waveguides fabricated on optical quality glass sometimes have much higher losses due to the presence of reducing agents in the substrate material. To select the best material, microscope slides from various glass manufacturers, viz., Labmate (Fisher), Corning, Scientific Glass Apparatus, and Schott were used as substrates. The lowest losses are exhibited by Labmate and Schott as shown in Fig. 2. The least square error fit to the measured points gives a loss of 1.0 dB/cm for Labmate and 0.2 dB/cm for the Schott glass. The losses are measured at 0.6328 μm. Operation in the infrared at 1.3 μm will further reduce the losses.

The process thus looks promising for making low loss, single mode components. It also lends itself to computerized automation. Since the silver ion generation and temperature can be adjusted electronically, an on-line computer can be used to supervise the process operation. The parameters which are set manually now, can then be entered in the operating software of a microcomputer which will execute the programmed sequence of operations to control the diffusion process. Efforts are under way to measure the concentration of silver ions *in situ* and to study the electrochemical aspects of the process.

The possibilities of applying a drift electric field to enhance the diffusion and burying the waveguides are also under investigation.

This work was supported in part by a grant from U.S. Air Force, contract No. F08635-83-K-0263.

[1]T. Izawa and H. Nakagome, Appl. Phys. Lett. **21**, 584 (1972).
[2]G. Stewart, C. A. Miller, P. J. R. Laybourn, C. D. W. Wilkinson, and R. M. De Larue, IEEE J. Quantum Electron. **QE-13**, 192 (1977).
[3]G. Chartier, P. Collier, A. Guez, P. Jaussaud, and Y. Won, Appl. Opt. **19**, 1092 (1980).
[4]H. J. Lilienhof, E. Voges, D. Ritter, and P. Pantschew, IEEE J. Quantum Electron. **QE-18**, 1857 (1982).
[5]Patent application under consideration.
[6]Y. H. Won, P. C. Jaussaud, and G. H. Chartier, Appl. Phys. Lett. **37**, 269 (1980).
[7]T. Findakly and E. Garmire, Appl. Phys. Lett. **37**, 855 (1980).

REFERENCE [4]

FABRICATION OF ION-EXCHANGED GLASS WAVEGUIDES BY ELECTROLYTIC RELEASE OF SILVER IONS

R. K. Lagu and V. Ramaswamy

Department of Electrical Engineering

University of Florida

Gainesville, FL 32611

ABSTRACT

We report a novel electrolytic process that is used to fabricate reproducible, low loss, single mode glass waveguides.

FABRICATION OF ION-EXCHANGED GLASS WAVEGUIDES BY ELECTROLYTIC RELEASE OF SILVER IONS

R. K. Lagu and V. Ramaswamy

Department of Electrical Engineering

University of Florida

Gainesville, FL 32611

Growing interest in single mode fiber optic communication system because of its high bandwidth and hence the large information carrying capacity, as well as the prospect of making efficient, inexpensive optical components have continued to stimulate activity in Integrated Optics. For the most part, integrated optical devices such as high speed switches [1], interferometers [2,3], fast A/D converters [4,5] and etc have been fabricated using Ti diffused $LiNbO_3$ guides. However, since $LiNbO_3$ is an electro-optic material, electro-optic tuning has been extremely useful in meeting the design criteria.

The need for optical components using glass waveguides has continued to remain strong primarily because of their compatibility with optical fibers and their cost effectiveness. Such devices fabricated using glass waveguides are expected to find applications at the receiving end of an optical communication system. However, these 'passive' components on glass substrates cannot be tuned electro-optically to compensate for fabrication errors and hence need to be fabricated to strict specification with assured repeatability. This in turn demands good process control.

Ion-exchange has been most extensively used for fabricating optical waveguides on glass substrates. Both thallium [6] and silver [7-9] ions have been used to exchange

sodium ions in glass thus forming high index surface guiding layers on glass substrates. The existing process involves the use of either pure $AgNO_3$ or a mixture of $AgNO_3$ and $NaNO_3$ (usually, silver nitrate 10% by weight) for carrying out the diffusion and the resulting guides are usually multimode. Moreover with such high concentration of silver ions, reduction to metallic state is highly likely causing excessive absorption as well as scattering loss. The time of diffusion to produce single mode guide with such heavy concentration of silver ions is about two to three minutes. This makes timing very critical, thus making the reproducibilty a serious problem. A single mode waveguide fabricated under such conditions is usually shallow and therefore, couples poorly to an optical fiber which can be thought of as a buried structure of a relatively large cross section (8 - 10 μm).

We propose and present results of a novel process [10] that overcomes the existing problems by generating precisely very small concentration silver ions. Generation of silver ions is accomplished by using a silver electrode as anode and a platinum electrode as cathode rather than a salt mixture of $AgNO_3$ and $NaNO_3$. When a known amount of current is passed for known time through the electrodes dipped in molten sodium nitrate [Fig. 1], the half-reaction at the anode accounts for the oxidation of silver and hence the release of precise quantity of Ag^+ ions. Melt impurities are kept minimal by using ultra pure (99.999%) silver rods. In addition, in this process, release of silver ions is electronically controlled through the realization of an accurate, variable current source using off the shelf operational amplifiers. Moreover, the silver ion concentration in the bath can be changed with time so that diffusion can be carried out using a variety of boundary conditions, thus providing excellent control over the refractive index profile.

The set-up consists of a salt bath heated by a band heater coiled around it. The temperature of the bath is sensed by a th rmocouple and controlled with a closed-loop controller to an accuracy of $\pm 0.5°C$. Initially 100 grams of pure sodium nitrate(

A.C.S. grade, Fisher) are weighed and heated to 330°C. Then a pure silver rod and a platinum reference electrode is introduced into the salt bath and 0.2 grams of silver is released into the molten salt as ions by electrolysis. Then pre-cleaned soda-lime-silicate glass slides are placed in the bath and the diffusion is carried for periods ranging from 20 to 120 minutes. The slides are then taken out of the bath, cooled for about 5 minutes and the residual salt is rinsed off with warm water.

The prism coupling technique is used to measure the mode indices. Table I shows the propagation characteristics of the various waveguides. It is seen that the first four waveguides are single mode. An iterative program is written to estimate the maximum refractive index change (Δn) from the measured values of the mode indices. For this set of waveguides, Δn is found to be 0.005. Priliminary results indicate that it is possible to find relations between process parameters and the mode index so that single mode waveguides with known propagation constants can be fabricated. The waveguides show no signs of yellow stain due to silver ion reduction. To measure the loss, initially an output prism was used to tap off the transmitted power. To have a reliable loss measurement, however, it seemed necessary to take care not to disturb the input coupling and not to spoil the guide surface at the contact point. These conditions seemed rather restrictive and hence an improved three prism loss measurement technique [11] was used.

It is reported [12] that waveguides fabricated on optical quality glass sometimes have much higher losses due to the presence of reducing agents in the substrate material. To select the best material, microscope slides from various glass manufacturers, viz. Labmate(Fisher), Corning, Scientific Glass Apparatus and Schott were used as substrates. The lowest losses are exhibited by Labmate and Schott as shown in figure 2. The least square error fit to the measured points gives a loss of 1.0 dB/cm. for Labmate and 0.2 dB/cm. for the Schott glass. The losses are measured at 0.6328μm. Operation in the infrared at 1.3μm will further reduce the losses.

The process thus looks promising for making low loss single mode components. It also lends itself to computerized automation. Since the silver ion generation and temperature can be adjusted electronically, an on-line computer can be used to supervise the process operation. The parameters which are set manually now, can then be entered in the operating software of a microcomputer which will execute the programmed sequence of operations to control the diffusion process. Efforts are underway to measure the concentration of silver ions *in situ* and to study the electrochemical aspects of the process.

The possibilities of applying a drift electric field to enhance the diffusion and burying the waveguides are also under investigation.

REFERENCES

1. R. C. Alferness, IEEE J. Quantum Electron., QE-17, 946 (1981)

2. W. E. Martin, Appl. Phys. Lett., 26, 562 (1975)

3. V. Ramaswamy, M. D. Divino and R. D. Standley, Appl. Phys. Lett., 32, 644 (1978)

4. H. F. Taylor, IEEE J. Quantum Electron., QE-15, 210 (1979)

5. P. J. Leonberger, C. R. Woodward and R. A. Becker, Appl. Phys. Lett., 40, 565 (1982)

6. T. Izawa and H. Nakagome, Appl. Phy. Lett., 21, 584 (1972)

7. G. Stewart, C. A. Miller, P. J. R. Laybourn, C. D. S. Wilkinson and R. M. De Larue, IEEE J. Quantum Electron., QE-13, 192 (1977)

8. G. Chartier, P. Collier, A. Guez, P. Jaussaud and Y. Won, Appl. Opt., 19, 1092 (1980)

9. E. J. Lilienhof, E. Voges, D. Ritter and P. Pantschew, IEEE J. Quantum Electron., QE-18, 1857 (1982)

10. Patent Application under consideration

11. Y. E. Won, P. C. Jaussaud and G. E. Chartier, Appl. Phy. Lett., 37, 269 (1980)

12. T. Findakly and E. Garmire, Appl. Phy. Lett., 37, 855 (1980)

TABLE-I

Substrate refractive index = 1.512 at 0.6328 μm

Time of diffusion (minutes)	No. of modes	Mode order	Mode index
20	1	0	1.512452
40	1	0	1.513014
60	1	0	1 .513365
80	1	0	1.513565
100	2	0 1	1.514071 1.512327
120	2	0 1	1.514250 1.512452

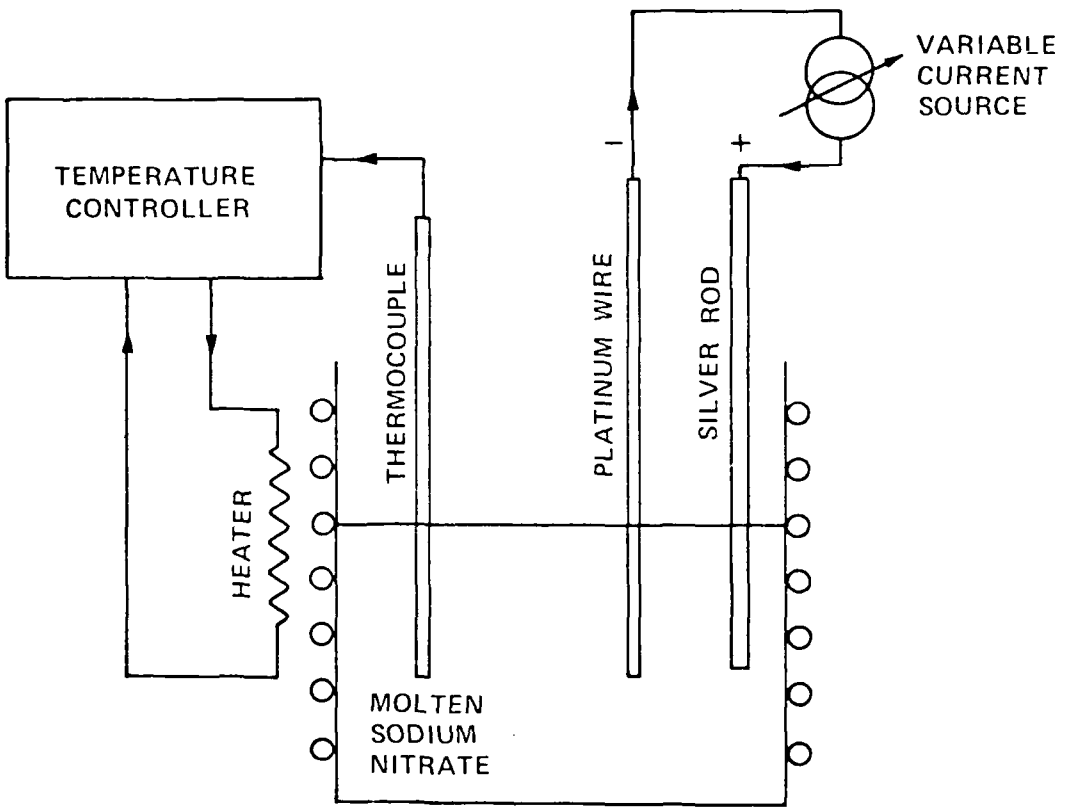
TEMPERATURE CONTROLLER
HEATER
THERMOCOUPLE
PLATINUM WIRE
SILVER ROD
VARIABLE CURRENT SOURCE
MOLTEN SODIUM NITRATE

Figure 1

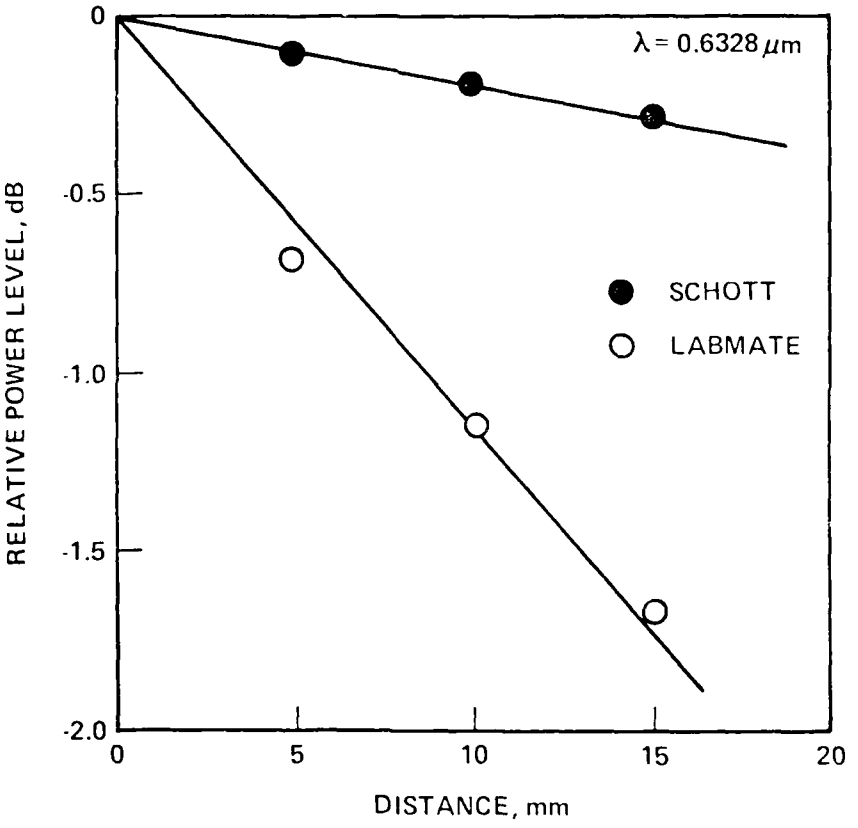
λ = 0.6328 μm
SCHOTT
LABMATE
RELATIVE POWER LEVEL, dB
0
-0.5
-1.0
-1.5
-2.0
0
5
10
15
20
DISTANCE, mm

Figure 2

REFERENCE [5]

Fabrication of ion-exchanged glass waveguides through electrolytic release of silver ions

R. V. Ramaswamy, R. K. Lagu and S. I. Najafi

Department of Electrical Engineering, University of Florida
Gainesville, Florida 32611

Abstract

We describe the fabrication of low loss (≈ 0.2 dB) Ag^+-Na^+ exchanged glass optical waveguides using the novel electrolytic release technique. Development of a concentration cell that can be used to measure the Ag^+ ionic concentration in situ provides opportunities for on-line concentration control. Since the silver ion generation and control as well as the temperature can be adjusted electronically, the process may be computer controlled.

Introduction

Glass waveguides have formed the basis for the development of passive integrated optical components, e.g., star and access couplers, channel dropping filters at the receiving end of an optical communication system, and in certain specific applications wavefront sensors and interferometric couplers, because of their low optical propagation loss, compatibility with optical fibers (both single and multimode), immunity to optical damage, and potential cost-effectiveness under mass production.

The ion-exchange technique is becoming increasingly popular for fabricating glass waveguides. The technique involves the exchange of monovalent ions of large electronic polarizability such as potassium K^+,[1-3] rubidium Rb^+,[4] cesium Cs^+,[4] silver Ag^+,[1,5-10] or thallium Tl^+,[11,12] with an ion of smaller polarizability such as sodium Na^+ which usually is a component of the glass matrix of soda-lime silicate (or borosilicate) glass.

The existing processes take either pure $AgNO_3$ or a mixture of $AgNO_3$ and $NaNO_3$ (silver nitrate about 10% by weight) for carrying out diffusion, resulting in multimode waveguides. With such high concentration of silver ions, their reduction to metallic state is highly likely causing excessive absorption and scattering losses. The time of diffusion to produce a single mode waveguide is about 2-3 min. This makes the timing very critical, thus making the reproducibility a serious problem. A single mode waveguide fabricated under such conditions is usually shallow and hence couples poorly to an optical fiber which can be thought of as buried structure of a reasonably large cross-sectional dimension (8-10 μm).

Novel Electrolytic Release Technique

Recently, we reported a novel technique[10] capable of fabricating reproducible single mode waveguides by accurate control of Ag^+ concentration. This process overcomes the existing problems by generating very small concentration of silver ions precisely. The idea is based on the well known Faraday's Law of Electrolysis:

When 96500 coulombs of charge are passed through a metallic electrode, 1 g equivalent of the metal is released into the solution as metal ions.

Thus, generation of silver ions can be accomplished by using a metallic silver electrode rather than a salt mixture of $AgNO_3$ and $NaNO_3$. Furthermore, melt impurities can be kept minimal as ultrapure (99.999%) silver rods are commercially available. The process of releasing silver ions can now be electronically controlled through the realization of an accurate, variable current source using off-the-shelf operational amplifiers. In addition, the Ag^+ concentration in the bath can be changed with time so that the diffusion can be carried out with a variety of boundary conditions, thus providing large control of the refractive index profile.

The process as shown in Fig. 1 is described briefly as follows. The setup consists of a salt bath heated by a band heater coiled around it. The temperature of the bath is sensed by a thermocouple and controlled with a closed-loop controller to an accuracy of ±0.5°C. Initially 400 g of pure sodium nitrate (A.C.S. grade, Fisher) are weighed and heated to

330°C. Then a pure silver rod and a platinum reference electrode are introduced into the salt bath and 0.2 g of silver is released into the molten salt as ions by electrolysis. Then precleaned soda-lime-silicate glass slides are placed in the bath and the diffusion is carried for periods ranging from 20 to 120 min. The slides are then taken out of the bath, cooled for about 5 min and the residual salt is rinsed off with warm water.

Mode Indices and Loss Measurements

The prism coupling technique is used to measure the mode indices. Table 1 shows the propagation characteristic of the various waveguides. The waveguides show no signs of yellow stain due to silver ions reduction. To measure the loss, initially an output prism was used to tap off the transmitted power. To have a reliable loss measurement, however, it seemed necessary to take care not to disturb the input coupling and not to spoil the guide surface at the contact point. These conditions seemed rather restrictive and hence an improved three-prism loss measurement technique was used. Substrates from various glass manufacturers, viz., Labmate (Fisher), Corning, Scientific Glass Apparatus, and Schott were used for fabricating Ag^+-Na^+ exchanged waveguides. The lowest losses are exhibited by Labmate and Schott as shown in Fig. 2. The least square error fit to the measured points gives a loss of 1.0 dB/cm for Labmate and 0.2 dB/cm for the Schott glass. The losses are measured at 0.6328 μm. Operation in the infrared at 1.3 μm will further reduce the losses.

Table 1. Diffusion times and mode indices for TE modes.
Substrate refractive index = 1.512 at 0.6328 μm.

Time of diffusion (min)	Number of modes	Mode order	Mode index
20	1	0	1.51245
40	1	0	1.51301
60	1	0	1.51337
80	1	0	1.51357
100	2	0	1.51407
		1	1.51232
120	2	0	1.51425
		1	1.51245

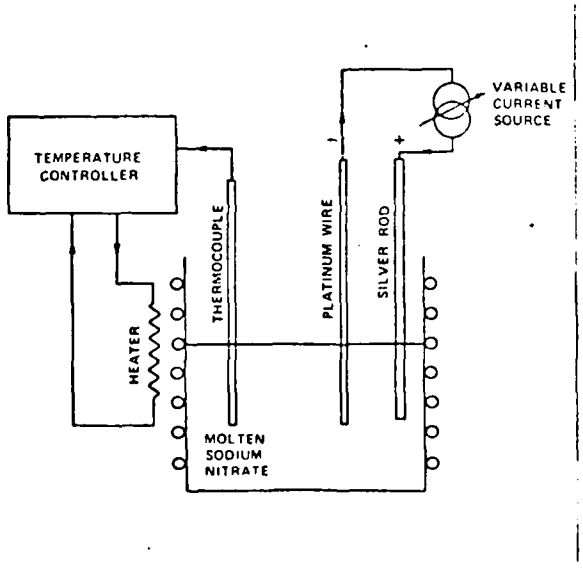

Fig. 1. Process schematic diagram.

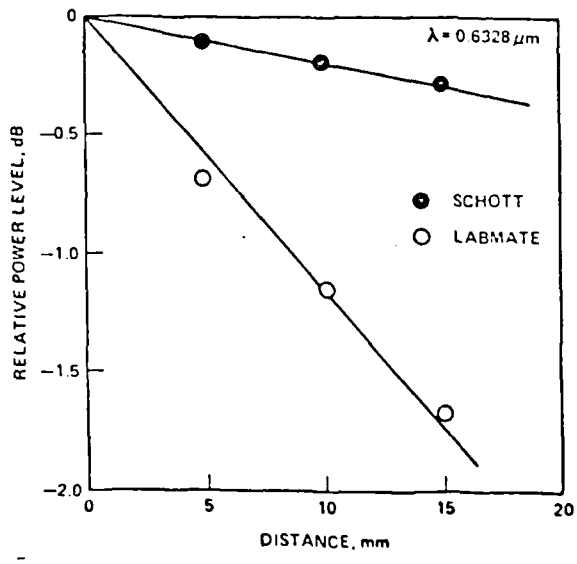

Fig. 2. Loss measurement at 0.6328 μm.

Concentration Measurement and Control

One of the process parameters, the temperature, can be easily controlled to within ±0.2°C using a *feedback control system*[10] even at elevated temperatures (300-600°C). To maintain the concentration of the diffusing ion, first, it is necessary to measure its concentration in the melt. The conventional methods to measure concentration, e.g., mass spectrometry, atomic absorption, emission, and fluorescent spectrometry or nuclear activation, are not suitable for application of feedback control of the concentration. On-line measurement of the concentration is essential for making reproducible glass waveguides. Furthermore, since the guides are fabricated by diffusion at elevated temperatures, it appears that use of a concentration cell is an ideal way to measure the concentration. In situ measurement of the concentration would make the compensation and control of the ionic content of the melt much easier especially if the ions were released by electrolytic means[10].

We experimented with different types of concentration cell and reported the results and the final design of the cell[13] which is suitable for the glass waveguide ion-exchange process application. Measurements of Ag^+ ion concentration, released electrolytically, in a molten $NaNO_3$ bath are illustrated using the cell.

Commercially available electrodes which are sensitive for selective ions unfortunately operate at relatively low temperatures, typically in the 0-80°C range, and therefore are not suitable for our applications. For molten salt applications, the emf generated by a voltaic cell can be used to measure concentration. In principle, any spontaneous reduction-oxidation (redox) reaction can be used to generate a cell potential and since this cell potential depends on the substance that makes up the cell and their concentrations, the measured voltage may be used to represent their concentration as long as the same substances are present in both the anode and cathode compartments but at different concentrations.

The resultant voltaic cell illustrated in Fig. 3, which supports the reactions

$$\begin{aligned} &\text{anode:} && Ag(s) \rightarrow Ag^+(c_2) + e^-, \\ &\text{cathode:} && Ag^+(c_1) + e^- \rightarrow Ag(s) \\ &\text{———————} && \text{———————} \\ & && Ag^+(c_1) \rightarrow Ag^+(c_2) \end{aligned} \tag{1}$$

will generate a potential difference V, that depends on the ratio of the Ag^+ concentrations (c_1/c_2) and the temperature T. The Nernst potential difference of the cell[13] is given by

$$V = 1.98 \times 10^{-4} T \log(c_1/c_2) \tag{2}$$

If one of the concentrations, say c_1 (reference concentration), is known, the unknown salt bath concentration c_2 can be determined by measuring the cell emf V with a high impedance voltmeter.

Although the above argument seems reasonable, the electron released at the anode when a Ag atom disassociates into solution as an Ag^+ ion can move through the external circuit to the cathode where it reduces another Ag^+ ion; such a movement in reality indeed cannot occur. The reasons this concentration cell is an incomplete voltaic cell is because, when a Ag^+ ion is released into the solution at the anode with a simultaneous reduction at the cathode, both of the half-cell become charged, immediately blocking any further movement of the electron.

Therefore, we need a means that would allow the migration of the Ag^+ ions from the bath to the cathode region in the bulb. In other words, we need to physically distinguish the two regions of different concentrations and yet simultaneously permit the diffusion of Ag^+ ion to facilitate current flow and, hence, the redox reaction. Fortunately, in our case, the glass bulb itself acts as a good membrane. Inman[14] has reported the use of such a glass bulb containing the reference electrode to form part of a concentration cell. The underlying idea is that Pyrex glass at elevated temperatures (330-370°C) can act as a resistive ion bridge between the solutions because the sodium ions with a thin membrane (walls of the glass bulb) have rather high mobility at these temperatures. Since there are no pores present within the membrane, the two solutions are physically isolated.

Glass Bulbs for Reference Electrodes

A Pyrex glass test tube ~6 mm i.d. with ~0.5 mm wall thickness is heated with a torch and blown at one end to form a glass bulb with a tubular stem. The glass bulb is nearly spherical in shape with ~12 mm in diameter and ~0.1 mm wall thickness as shown in Fig. 4(a).

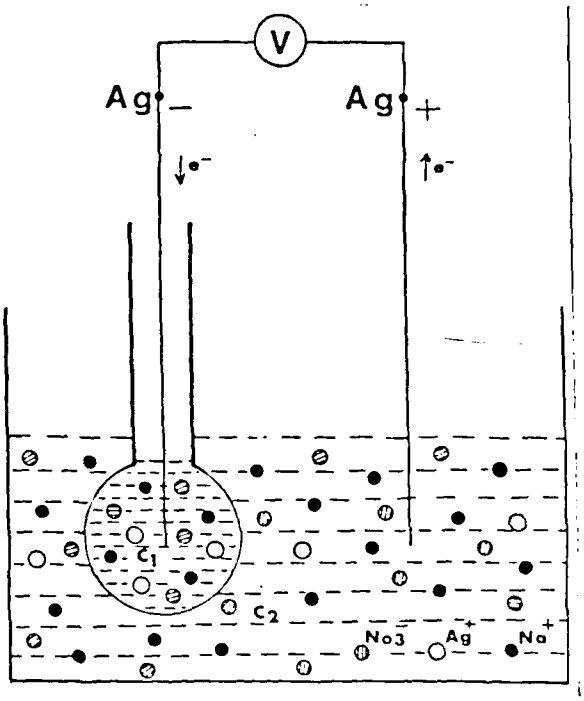

Fig. 3. $Ag||Ag^+(NaNO_3)||Ag$ concentration cell.

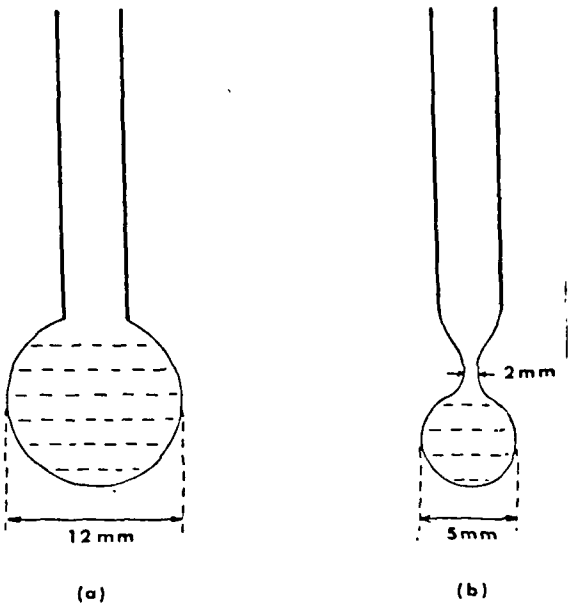

Fig. 4. Large and small reference electrode glass bulb.

A reference melt is produced by releasing 2.0 g of silver from a high purity (99.999%) rod into a melt of 400 g $NaNO_3$ by electrolysis[10]; the reference melt concentration c_1 approximately equals 3.94×10^{-3} mole fraction (MF). The glass bulb is then filled to its neck with ~3-4 g of the reference melt. High purity silver wires are also used as the cathode within the glass bulb as well as the anode immersed in the bath. The cell is then used to measure the silver-ion concentration in the salt bath (Fig. 1). The Nernst potential difference is measured with a 10 MΩ input impedance, digital voltmeter.

By electrolytically releasing known quantities of Ag^+ ions in 400 g of $NaNO_3$, different known concentration of Ag^+ in $NaNO_3$ in the bath are prepared. By measuring the cell potential each time, we obtain the plot of cell emf V vs $\log(c_1/c_2)$ as shown in Fig. 5. The solid line represents the theoretical cell potential as given by Eq. (2). As expected, both curves V vs $\log(c_1/c_2)$ exhibit linear behavior. Both the experimental and theoretical lines have nearly the same slope with the slope of experimental line slightly lower. The temperature gradient in the bath in the vertical direction amounts to almost 20°C. The estimation of the bath temperature from the measured value near the reference bulb is susceptable to an error of a few degrees and may be responsible for the difference in the slope. Moreover, when the two concentrations are equal, we measure an asymmetry potential of ~14 mV rather than 0 as predicted by Eq. (2).

Although temperature of the salt bath was maintained at a constant set temperature using a feedback control arrangment[10], the temperature of the reference melt was considerably lower (310°) due its large thermal capacity. In fact, the temperature of the bath had to be ~340°C before the salt in the reference bulb would completely melt implying a temperature

difference of ~30°C between the bath and reference cell. However, Eq. (2) assumes the same temperature for both the electrodes. Now then, if $c_1 = c_2 = c$, with both reference and bath electrodes at different temperatures, namely, T_1 and T_2, yields an assymmetry potential:

$$\Delta V = 1.98 \times 10^{-4} \Delta T \log c, \tag{3}$$

where $\Delta T = T_1 - T_2$. Since T_2 is always larger than T_1, ΔT is negative. In our case, we have $\Delta T \approx -30°C$ and $c = 3.94 \times 10^{-3}$ and obtain $\Delta V = 14.28$ mV which agrees very well with our measured asymmetry potential when $c_1 = c_2$.

The basic problem of asymmetry potential and the temperature restriction primarily due to temperature difference between the electrodes was solved by using a small reference cell (Fig. 4(b)), which eliminates the requirement of large quantities of $NaNO_3$ and a separate temperature controller. The cell can easily be fabricated as before but now using a Pasteur pipette.

The solid circles in Fig. 6 represent the measured concentration cell potential at 350°C and shows excellent agreement with Nernst Eq. (2). Typically <5 mV changes in the measured value occur depending upon the volume difference of the salt inside the reference cell or the vertical positioning of either the silver wire within the cell or the entire cell itself. In addition, it is extremely important to ensure that there are no air bubbles within the reference bulb. When necessary precautions are taken, the experimental curve is repeatable when using the same cell after repeated cleaning and filling with the same standard solution. However, it seems that small variations in the absolute value of the cell potential do take place depending upon the position of the reference bulb in the bath. But once this is standardized, the measurements are repeatable within ±2 mV.

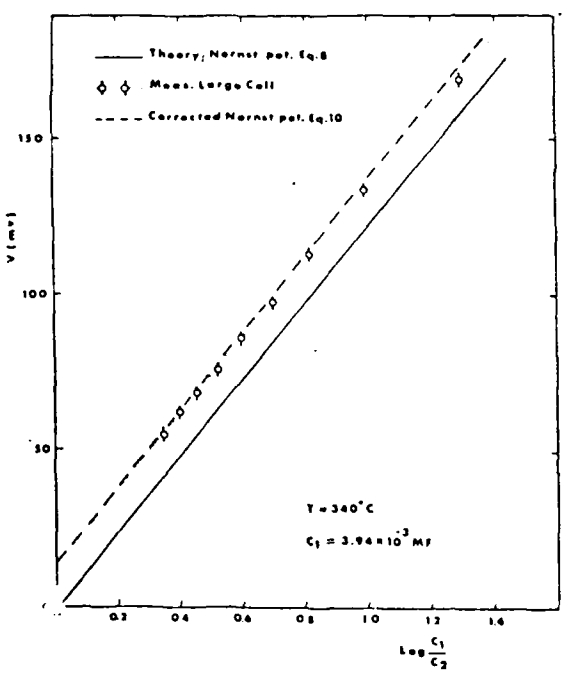

Fig. 5. Measured and calculated Nernst potential for large reference electrode glass bulb at T = 340°C.

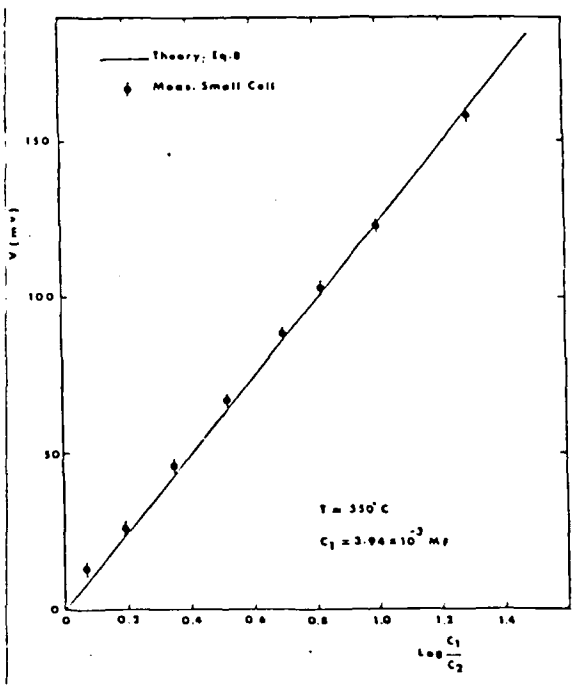

Fig. 6. Measured and calculated Nernst potential for small reference electrode glass bulb at T = 350°C.

To avoid the errors due to the sources mentioned above, it is necessary to use a given calibrated concentration cell for the measurement, keeping the experimental conditions the same. In these conditions, such a cell can be used for in situ concentration measurement during the fabrication of ion-exchanged waveguides.

Conclusions

We have described a novel electrolytic release technique for fabricating Ag^+-Na^+ ion-exchanged optical waveguides and a $Ag||Ag^+(NaNO_3)||Ag$ concentration cell that can be used to measure concentration of Ag^+ ions in a molten $NaNO_3$ bath during fabrication of the ion-exchanged waveguides. The process looks promising for making low loss, single mode components. It also lends itself to computerized automation. Since the silver ion generation and the temperature can be controlled electronically during the fabrication process, an on-line computer can be used to supervise the process operation. The parameters which are set manually now, can then be entered in the operating software of a microcomputer which will execute the programmed sequence of operations to control the diffusion process.

The possibilities of applying a drift electric field to enhance the diffusion and burying the waveguides are also under investigation.

This work was supported in part by a grant from AFOSR 84-0369.

References

1. T.G. Giallorenzi, E.J. West, R. Kirk, R. Ginther, and ..... Andrews, "Optical waveguides formed by thermal migration of ions in glass," Appl. Opt. 12, 1240 (1973).

2. Y.H. Won, P.C. Jaussaud, and G.H. Chartier, "Three-prism loss measurements of optical waveguides," Appl. Phys. Lett. 37, 269 (1980).

3. T. Findakly and B. Chen, "Single-mode integrated optical 1xN star coupler," Appl. Phys. Lett. 40, 549 (1982).

4. V. Neuman, O. Parriaux and L.M. Walpita, "Double-alkali effect: Influence on index profile of ion-exchanged waveguides," Electron. Lett. 15, 704 (1979).

5. G. Stewart, C.A. Miller, P.J.R. Laybourn, C.D.W. Wilkinson, and R.M. De LaRue, "Planar optical waveguides formed by silver-ion migration in glass," IEEE J. Quantum Electron. QE-13, 192 (1971).

6. G. Stewart and P.J.R. Laybourn, "Fabrication of ion-exchanged optical waveguides from dilute silver nitrate melts," IEEE J. Quantum Electron. QE-14, 930 (1978).

7. G.H. Chartier, P. Jaussaud, A.D. DeOliveira, O. Parriaux, "Optical waveguides fabricated by electric-field controlled ion exchange in glass," Electron. Lett. 14, 132 (1978).

8. G.H. Chartier, P. Collier, A. Guez, P. Jaussaud, and Y. Won, "Graded-index surface or buried waveguides by ion exchange in glass," Appl. Opt., 19, 1092 (1980).

9. M. Imai, N. Haneda and Y. Ohtsuka, "Losses in optical waveguides formed by silver-sodium ion exchange," IEEE/OSA J. Lightwave Technol. LT-1, 611 (1983).

10. R.K. Lagu and V. Ramaswamy, "Fabrication of single-mode glass waveguides by electrolytic release of silver ions," Appl. Phys. Lett. 45, 117 (1984).

11. T. Izawa and H. Nakagome, "Optical waveguides formed by electrically induced migration of ions in glass plates," Appl. Phys. Lett. 21, 584 (1972).

12. E. Okuda, H. Wada and T. Yamasaki, in Technical Digest of Topical Meeting on Integrated and Guided-Wave Optics (Optical Society of America, Washington, D.C., 1984). paper ThB6.

13. R.K. Lagu, S.I. Najafi and V. Ramaswamy, "In situ measurement of ionic concentration during fabrication of ion-exchanged waveguide," Appl. Opt. 23, 3925 (1984).

14. D. Inman, "A glass contained reference electrode for molten nitrate solvents," J. Sci. Instrum. 39, 391 (1962).

JOURNAL OF LIGHTWAVE TECHNOLOGY, VOL. LT-3, NO. 4, AUGUST 1985

An Improved Method for Fabricating Ion-Exchanged Waveguides Through Electrolytic Release of Silver Ions

S. IRAJ NAJAFI, RAMU V. RAMASWAMY, SENIOR MEMBER, IEEE, AND RAJENDRA K. LAGU

Abstract—**In this paper, an improved technique for electrolytic release of silver ions while fabricating Na^+–Ag^+ exchanged glass waveguides is reported. In this method, a porous glass shell such as fritted glass is used around the cathode to prevent the reduction of the released silver ions. The result of quantitative estimation of silver ion concentration using atomic fluorescence spectroscopy, and sodium ion concentration using atomic emission spectroscopy are also reported.**

I. Introduction

GLASS WAVEGUIDES are prime candidates for the development of passive integrated optical components such as access and star couplers, wavelength mutliplexers, demultiplexers, interferometric couplers, and wavefront sensors. Passive glass waveguide components are attractive because they are compatible with optical fibers and potentially inexpensive. Since the passive glass components cannot be tuned electrooptically, they must be fabricated with assured reproducibility within specified tolerances.

Ion-exchange has proven to be the most popular technique used in the fabrication of glass waveguides. The process involves the exchange of monovalent Na^+ in the glass with another ion of larger polarizability, e.g., Ag^+ [1], Tl^+ [2], and Cs^+ [3]. We have recently described a novel electrolytic release technique [4], [5] which has been used to fabricate low-loss single-mode glass waveguides. We have also reported use of a thin-walled glass bulb galvanic concentration cell [6] for *in situ* measurement of Ag^+ concentration in the molten salt bath.

In order to ensure reproducibility of the waveguide devices, it is necessary to relate the device parameters to process parameters and then to control the process parameters accurately. By precisely controlling the current pumped through high-purity Ag and Pt electrodes, a high degree of accuracy over the release of Ag^+ is achieved. However, Ag^+ concentration analysis performed on the contents of the molten salt ($Ag^+/NaNO_3$) indicates that due to the reduction of some of the silver at the cathode, the silver ion concentration is smaller than that predicted by Faraday's Law. Before the concentration control can effectively be implemented, it is necessary that the silver ion concentration in the bath exhibit a direct correlatin with the current during release. This means the reduction of silver ions at the cathode should be avoided at all cost. In this paper, we report an improved technique using a fritted glass shell to surround the cathode which avoids the reduction of silver ions. The results of the analysis indicate that the fritted glass does indeed prevent silver ions from reaching the Pt-cathode. The content of the fritted glass and the Pt-cathode deposits as well as the molten salt bath is analyzed using atomic fluorescence spectroscopy (AFS) and atomic emission spectroscopy (AES). Possible reaction mechanisms that explain the results of the concentration analysis are outlined. Through this work, it is shown that use of a porous glass shell such as a fritted glass bulb prevents the reduction of Ag^+, and is therefore necessary for on-line concentration control during the fabrication of ion-exchanged glass waveguides.

Manuscript received November 23, 1984, revised January 22, 1985. This work was supported in part by AFOSR under Contract 84-0369.

S. I. Najafi and R. V. Ramaswamy are with the Department of Electical Engineering, University of Florida, Gainesville, FL 32611.

R. K. Lagu was with the University of Florida, Gainesville, FL 32611. He is now with the University of Iowa, Iowa City, Iowa 52242.

II. Electrolytic Release Technique

Fabrication of ion-exchanged waveguides using the electrolytic release technique [4], [5] accomplishes the precise generation of very small quantities of the diffusing ions into a molten salt bath with careful control of both the duration and the magnitude of the current pumped through high-purity electrodes immersed in molten salt bath. The idea is based on the well-known Faraday's Law of Electrolysis: When 96500 C of charge are passed through a metallic electrode, 1 gm equivalent of the metal is released into the solution as metal ions. The number of grams of the metal atoms (ions) released at the anode or collected at the cathode can be expressed as

$$W = \frac{ItA}{FZ}$$

where

- I current through the circuit in amperes,
- t time of release in seconds,
- A atomic weight of the released atom,
- F Faraday's constant equal to 96 500 J/V mole e^-,
- Z valence of the atom.

The technique involves (Fig. 1) the fabrication of Ag^+–Na^+ exchanged glass waveguides in which the electrolytic generation of the monovalent silver ions into a molten $NaNO_3$ bath is accomplished using 99.999-percent pure silver rod as the anode and a platinum wire as the cathode.

0733-8724/85/0800-0763$01.00

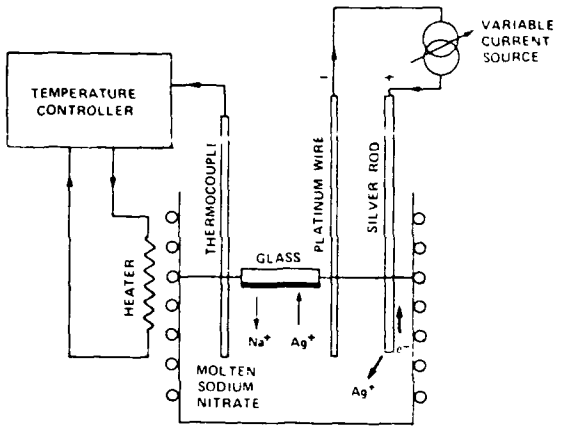

Fig. 1. Process schematic diagram (without fritted glass).

Flow of 100 mA of current for 15 min releases 0.1 gm of silver ion in the salt bath.

The possible electrode reactions in this process are:

anode:

$$Ag \rightarrow Ag^+ + e^- \quad (1a)$$

$$4NO_3^- \rightarrow 2N_2O_5 + O_2 + 4e^- \quad (1b)$$

cathode:

$$Ag^+ + e^- \rightarrow Ag \quad (2a)$$

$$Na^+ + e^- \rightarrow Na. \quad (2b)$$

At the anode, due to the fact the silver atom has higher tendency to lose an electron than NO_3^-, the likely reaction is the oxidation of silver as given by (1a). Since Ag^+ is a stronger reducing agent than Na^+, the reaction given by (2a) is more likely to take place at the cathode. However, since the Na^+ also reduces at the cathode, it appears that some of the silver ions do remain in the salt bath. The procedure previously described [4], [5] utilizes only these remaining silver ions for the Ag^+-Na^+ exchange to form optical waveguides in glass. Since we want a uniform Ag^+ concentration throughout the bath, we must stir the solution when on-line control is needed. Therefore, in order to obtain a correlation between the Ag^+ concentration in the bath and the magnitude and time of current flow, it is necessary to develop some means of preventing the reduction of silver ions at the cathode.

III. Fritted Glass Bulb Around the Cathode

A solution to this problem is to surround the cathode (Pt-wire) with a porous glass shell such as the fritted glass bulb shown in Fig. 2. The fritted glass bulb is similar to the immersion tubes fitted with porous discs used to draw off (or filter) supernatant from precipitates. Based on our experience, the pore size must be 4–5.5 μm to prevent any significant amount of Ag^+ from reaching the Pt wire. During the release, a small deposit seems to collect on the Pt-wire near the liquid surface. Na^+ and Ag^+ concentration analyses have been performed on the contents of the fritted glass bulb, on the deposits of the Pt-wire, and on the contents of the molten salt bath. The concentration analysis described below indicates that the above mentioned pore size is sufficient to prevent any noticable amount of Ag^+ reaching the Pt-wire, thus, avoiding the reduction of the released silver ions available for Ag^+–Na^+ exchange.

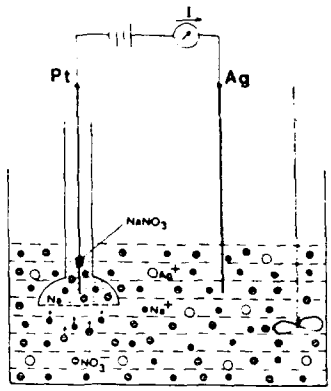

Fig. 2. Electrolytic release of silver ions using fritted glass.

A number of experiments using the improved technique with fritted glass around the Pt-wire were performed in which different quantities of Ag^+ were released into 400 gm of molten $NaNO_3$ by circulating 100 mA of current for different periods of time. The concentation of Ag^+ was measured with the use of a concentration cell [6]. During the release the bath was not stirred. Before each release, the silver electrode was weighed to an accuracy of ± 1 mg. After the release, the electrode was weighed again and the weight loss was recorded. Also,in each case, a number of samples were taken from the bath and were analyzed by AFS [7]. The technique involves photon excitation of atoms in the sample to produce excited atoms which undergo radiation de-excitation and subsequent comparison with a known reference. To prepare the reference, 1.575 gm of $AgNO_3$ corresponding to 1.0 gm of Ag was mixed into 400 gm of $NaNO_3$ at 330 C. An aluminum rod was dipped into the liquid coating the rod. After cooling, the rod was scraped and the scrapings were weighed. Using water as the solvent, several reference solutions were prepared with concentration ranging from 1 to 10 ppm volume. About 10–20 cc of each was used for the flame absorption analysis and a calibration curve was obtained. A sample of about 5-ppm volume of the bath was prepared in each case and both were analyzed using the atomic absorption method. By comparing the power output of the sample in relation to that of the reference at a given wavelength, concentration of the Ag^+ in the bath was evaluated. The results are summarized in Table I. The measured value of Ag^+ concentation from both the AFS and the concentration cell measurement agree well with the estimated value according to Faraday's Law. However, there is some discrepancy between these results and the measured weight loss. For small release time, this discrepancy is small but with an increase in time, the difference in weight Δm between the estimated weight loss and the measured weight loss of the Ag-rod before and after the release (Fig. 3) seems to increase rapidly at first, but begins to taper off indicating an oxidation process on the rod which slows down with time.

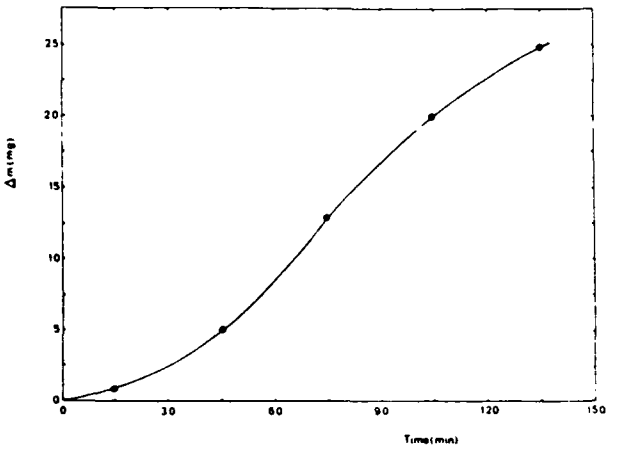

Fig. 3. Difference in the predicted and measured weight of silver rod Δm after release. Δm = predicted weight—measured weight.

TABLE I
THE QUANTITY OF SILVER PRESENT IN THE MOLTEN BATH

Silver Release (I = 100 mA)	Ag^+ in the bath (gm)			
time (min)	Released Ag(gm) calculated	Ag-rod weight difference	Concentration cell	AFS
15	0.1	0.103	0.11	0.103
45	0.3	0.296	0.32	0.330
75	0.5	0.488	0.53	0.503
105	0.7	0.677	0.71	0.704
135	0.9	0.876	0.91	0.917

Note: T = 330°C, without stirring. (AFS refers to the atomic fluorescence spectroscopy method.)

TABLE II
THE QUANTITY OF SILVER PRESENT IN THE MOLTEN BATH

Silver Release (I = 100 mA)	Ag^+ in the bath (gm)			
time (min)	Released Ag(gm) calculated	Ag-rod weight difference	Concentration cell	AFS
15	0.100	0.099	0.11	0.099
45	0.300	0.295	0.31	0.296
75	0.500	0.487	0.52	0.506
105	0.700	0.680	0.71	0.695
135	0.900	0.875	0.89	0.912

Note: T = 330°C, with stirring. (AFS refers to atomic fluorescence spectroscopy.)

The above experiments are repeated; this time with the bath being stirred while releasing silver ions. The results are tabulated in Table II. The measured Ag^+ concentration in the bath is again in excellent agreement with the quantity of silver actually released, indicating that with the presence of the fritted glass, reduction of Ag^+ at the cathode has been avoided.

In order to compare this result and to further understand the mechanisms of the process, samples were taken from the contents of the fritted glass as well as the deposits on the Pt-wire. The samples were prepared in the following manner. The contents of the fritted glass and Pt-wire deposits were dissolved separately in dilute HNO_3 and samples of less than 10-ppm volume were prepared for analysis. These samples were analyzed by two chemical methods, depending on the elements to be measured: AFS for silver and AES for sodium [7]. The results, which are tabulated in Table III indicate that in both cases (content of fritted glass and Pt-wire deposits) the quantity of silver is extremely small and the element which is reduced at the Pt-wire is indeed sodium. Therefore, it is clear that the current in this electrolytic process with fritted glass is maintained by the oxidation of silver at the anode and the reduction of sodium at the cathode. As seen from Table III, the ratio of the total weight (added to the content of the fritted glass or deposited on the Pt-wire) to the weight of sodium (added or deposited) is close to the ratio of the molecular weight of $NaNO_3$ to the atomic weight of Na, namely 3.7, which leads us to the conclusion that both Na^+ and NO_3^- penetrate inside the porous tube and the silver ions remain in the bath. It seems that this phenomenon is possible due to the larger size and lower concentration of the silver ions present in the bath compared to that of sodium ions. It should be pointed out that when larger size porous glass (10 μm) was tried, the contents of fritted glass turned black, indicating that Ag^+ penetrated and reduced at the cathode.

Since all of the Ag^+ ions released into the molten salt bath with the use of fritted glass now remain in the bath, it is expected that the fabricating single-mode planar waveguides will now require less time.

To determine the effect of the fritted glass on the waveguide parameters, a known amount of silver is released by pumping a current of 100 mA through molten $NaNO_3$ at 330°C using the improved fritted glass scheme (Fig. 2)

TABLE IIIa
ANALYSIS OF FRITTED GLASS CONTENTS

Exp.	Before Release		After Release			Total Wt. Added / Na Added
	$NaNO_3$	Ag	$NaNO_3$ + Ag	Ag (AFS)	Na (AES)	
I	4.76 g	1.29 g	6.30 g	1.15 mg	1.79 g	$\frac{1.54}{0.50} = 3.08$
II	5.24 g	1.42 g	6.75 g	2.00 mg	1.95 g	$\frac{1.51}{0.53} = 2.85$

(AFS refers to atomic fluorescence spectroscopy and AES to atomic emission spectroscopy.

TABLE IIIb
ANALYSIS OF PT-WIRE DEPOSITS (AFTER RELEASE)

Exp.	Ag (AFS)	Na (AES)	Total Wt.	Total Wt. Deposited / Na Deposited
I	0.012 mg	9.68 mg	34.0 mg	$\frac{34.0}{9.68} = 3.51$
II	0.003 mg	5.63 mg	18.0 mg	$\frac{18.0}{5.63} = 3.21$

Note: AFS and AES refer to atomic fluorescence and emission spectroscopy, respectively.

TABLE IV
DIFFUSION TIME, APPLIED FIELD, AND MODE INDEXES.

Diffusion time (min)	Drift field (volts aa)	No. of modes (TE or TM)	Mode order	TE Mode Index
30	0	1	0	1.51465
60	0	2	0	1.51640
			1	1.51293
90	0	2	0	1.51706
			1	1.51408
120	0	3	0	1.51716
			1	1.51465
			2	1.51313
150	0	3	0	1.51798
			1	1.51511
			2	1.51363
30	30	4	0	1.51822
			1	1.51605
			2	1.51496
			3	1.51295

Note: Substrate refractive index is 1.512 at 0.6328 μm. Salt bath is 0.1-gm Ag^+/400-gm $NaNO_3$ at 330°C.

for known periods of time. The precleaned glass slides are then placed in the bath and field-assisted or nonfield-assisted diffusion is carried out for given periods of time. Field-assisted waveguides are fabricated by depositing a metallic electrode on the glass sample during the diffusion process. We have prepared the electrode by a two-layer evaporation of Cr (50 Å) and Au (1000 Å) on the samples. Table IV summarizes the number of TE (or TM) modes and the TE mode indexes of the waveguides fabricated using a concentration of 0.1-gm Ag/400-gm $NaNO_3$. Comparison with the results obtained without using fritted glass [4], [5] shows that as expected, the mode indexes are higher and the time required to stay within the single-mode regime is not as high as before for the same magnitude of electrolytic release. Obviously, by decreasing either the current or the time, the situation can be improved.

In conclusion, we have presented an improved technique for a precise control of silver ion concentration while fabricating Ag^+–Na^+ exchanged glass waveguides. The modified technique ensures that the released Ag^+ concentration is the same as that in the bath. This is essential for monitoring and controlling the Ag^+ concentration in the bath by pumping appropriate amount of current in the external electrolytic circuit as needed. For a given glass substrate of known composition, process control (Ag^+ concentration, diffusion time, and temperature) facilitates the fabrication of reproducible single and multimode waveguides.

REFERENCES

[1] T. G. Giallorenzi, E. J. West, R. Kirk, R. Ginther, and R. A. Andrews, "Optical waveguides formed by thermal migration of ions in glass," *Appl. Opt.*, vol. 12, p. 1240, 1973.

[2] T. Izawa and H. Nakagome, "Optical waveguides formed by electrically induced migration of ions in glass plates," *Appl. Phys. Lett.*, vol. 21, p. 584, 1972.

[3] V. Neuman, O. Parriaux, and I. M. Walpita, "Double alkali effect influence on index profile of ion-exchanged waveguides," *Electron. Lett.*, vol. 15, p. 704, 1979.

[4] R. K. Lagu and V. Ramaswamy, "Fabrication of single mode glass waveguides by electrolytic release of silver ions," *Appl. Phys. Lett.*, vol. 45, p. 117, 1984.

[5] R. V. Ramaswamy, R. K. Lagu, and S. I. Najafi, "Fabrication of ion-exchanged glass waveguides through electrolytic release of silver ions," *SPIE Proc. 1st Int. Conf. Integrated Opt. Circuit Eng.* (Cambridge, MA), Oct. 21–26, 1984.

[6] R. K. Lagu, S. I. Najafi, and V. Ramaswamy, "In situ measurement of ionic concentration during fabrication of ion-exchange waveguides," *Appl. Opt.*, vol. 23, p. 3925, 1984.

[7] J. D. Winefordner, "Principle methodologies and applications of atomic fluorescence spectrometry," *J. Chem. Educ.*, vol. 55, p. 72, 1978.

*

S. Iraj Najafi was born in Tabrize, Iran, on March 2, 1953. He received the B.Sc. and M.Sc. degrees in physics from Pahlavi University of Shiraz and Docteur-Ingenieur (Ph.D.) degree from Ecole Centrale des Arts et Manufactures of Paris.

From 1976 to 1979, he was a graduate student at Pahlavi University where he worked on light-curve measurement of binary stars, neutron-induced fission and statistical analysis of particle-induced reactions. In 1983, he received his Ph.D. from Ecole Centrale. His thesis was in the area of activation analysis and gamma ray spectrometry. He joined the optical communication group, Department of Electrical Engineering, University of Florida in June 1984 as a postdoctoral research associate. His present research interests include fabrication and characterization of integrated-optical and optoelectronic devices.

*

Ramu V. Ramaswamy (M'62–SM'80) was born in Madras, India, in June 1938. He received the B.S. degree in physics from Madras University, Madras, India, in 1957, and the Diploma D.M.I.T. in electronics engineering from Madras Institute of Technology, Chromepet, Madras, India, in 1960. He received the M.S. and Ph.D. degrees in electrical engineering from Northwestern University, Evanston, IL, in 1962 and 1969, respectively. His doctoral work consisted of wave-propagation studies in semiconductor plasmas.

From 1962 and 1965, he served as a member of the research department at Zenith Radio Corporation, Chicago, IL, working on solid-state parametric amplifiers, and microwave components. In 1969, he joined Bell Laboratories, Crawford Hill Laboratory, Holmdel, NJ, where he was engaged in research on thin-film optical device, polarization effects in single-mode fibers and fiber-waveguide couplers. Since 1981, he has been a Professor in the Department of Electrical Engineering, University of Florida, Gainesville, where his current interests include passive integrated-optical devices, fiber-optic sensors, and optoelectronic devices.

Dr. Ramaswamy is a member of Sigma Xi.

*

Rajendra K. Lagu was born in Poona, India, on June 7, 1956. He received his B.Tech. and M.Tech. in electrical engineering from the Indian Institute of Technology, Bombay, India, in May 1978 and December 1981, respectively. He received his Ph.D. in electrical engineering from the University of Florida, Gainesville, in December 1984.

He worked as a Development Engineer in Peico Electronics and Electricals Limited, India, from June 1978 to May 1979. He was a Research Fellow in the Department of Electrical Engineering, I.I.T., Bombay, from June 1979 to December 1981. He worked as a Graduate Research Assistant in the Department of Electrical Engineering, University of Florida, Gainesville, from January 1982 to December 1984. Currently he is working as an Assistant Professor in the Department of Electrical and Computer Engineering, University of Iowa, Iowa City. His current research interests include fiber and integrated optics.

Dr. Lagu is a member of Eta Kappa Nu, Tau Beta Pi, and Phi Kappa Phi.

Reprinted from Applied Optics, Vol. 23, page 3925, November 1, 1984

in situ measurement of ionic concentration during fabrication of ion-exchanged waveguides

R. K. Lagu, S. I. Najafi, and V. Ramaswamy

In this paper we describe a concentration cell for the measurement of Ag^+ ion concentration useful for fabrication of $Ag^+ - Na^+$ exchanged waveguides in glass. The scheme is adaptable to other ion exchanges as well. High measurement accuracy (±2 mV) and assured repeatability are possible by standardizing the reference electrode and experimental conditions. Use of such a cell with appropriate analog signal processing should facilitate on-line concentration control by periodic pumping of the exchanging ion into the molten salt bath.

I. Introduction

Recently, glass waveguides have received considerable attention in the development of passive integrated optical components such as star and access couplers, channel dropping filters at the receiving end of an optical communication system, and in certain specific applications such as wave front sensors and interferometric couplers. Glass waveguides have formed the basis for such components because of their low optical propagation loss, compatibility with optical fibers (both single and multimode), immunity to optical damage, and potential cost-effectiveness under mass production.

The ion-exchange technique has so far been the most popular approach for fabricating glass waveguides. The technique involves the exchange of monovalent ions of larger electronic polarizability such as potassium K^+,[1-3] rubidium Rb^+,[4] cesium Cs^+,[4] silver Ag^+,[1,5-10] or thallium Tl^+,[11,12] with an ion of smaller polarizability such as sodium Na^+ which usually is a component of the glass matrix of soda-lime silicate (or borosilicate) glass. The ion exchange creates an increase in the refractive index thus forming a guiding layer at the surface of the glass substrates. The guiding characteristics are determined by the process parameters such as self- and interdiffusion coefficients of these ions, temperature and concentration of the diffusing ions in the melt as well as concentration of Na^+ in the substrate. As the passive devices fabricated using these waveguides on glass substrates cannot be tuned electrooptically to compensate for fabrication errors, precise fabrication to strict specifications is necessary for assured repeatability. In addition, an electric field is often applied to enhance the thermal diffusion, primarily because the binary exchange of Na^+ ion with a heavier ion such as Ag^+ or Tl^+ is relatively slow compared to the alkali ion due to their lower mobility. However, the self-diffusion coefficient of Na^+ is rather large compared with that of the heavier ion and the application of an electric field therefore depletes the Na^+ ions at the surface which need to be compensated in order to control the index profile. To ensure repeatability of the waveguide devices, it is necessary to relate the device parameters to process parameters and then control the process parameters accurately.

One of the process parameters, the temperature, can be easily controlled to within ±0.2°C using a feedback control system,[10] even at elevated temperatures (300–600°C). To maintain the concentration of the diffusing ion, first it is necessary to measure its concentration in the melt. The conventional methods to measure concentration, e.g., mass spectrometry, atomic absorption, emission, and fluorescent spectrometry or nuclear activation, are not suitable for application of feedback control of the concentration. On-line measurement of the concentration is essential for making reproducible glass waveguides. Furthermore, since the guides are fabricated by diffusion at elevated temperatures, it appears that use of a concentration cell is an ideal way to measure the concentration. *In situ* measurement of the concentration would make the compensation and control of the ionic content of the melt much easier especially if the ions were released by electrolytic means.[10]

In this paper we report the results of our experiments with different types of concentration cell and the final

The authors are with University of Florida, Department of Electrical Engineering, Gainesville, Florida 32611.

Received 23 July 1984.
0003-6935/84/213925-06$02.00/0.

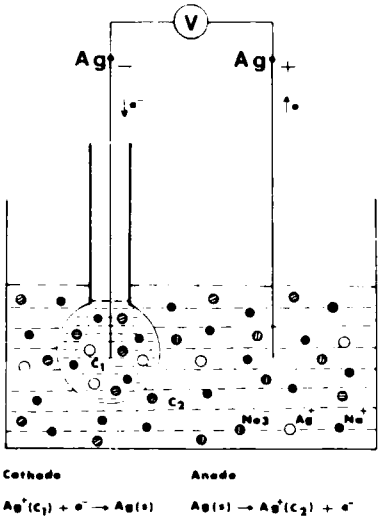

Fig. 1. $Ag||Ag^+(NaNO_3)||Ag$ concentration cell

design of the cell which is suitable for the glass waveguide ion-exchange process application. Measurements of Ag^+ ion concentration, released electrolytically, in a molten $NaNO_3$ bath are illustrated using the cell.

II. Voltaic Cell as a Concentration Cell

Commercially available electrodes which are sensitive for selective ions unfortunately operate at relatively low temperatures, typically in the 0–80°C range, and therefore are not suitable for our applications. For molten salt applications, the emf generated by a voltaic cell can be used to measure concentration. In principle, any spontaneous reduction–oxidation (redox) reaction can be used to generate a cell potential and since this cell potential depends on the substance that makes up the cell and their concentrations, the measured voltage may be used to represent their concentration as long as the same substances are present in both the anode and cathode compartments but at different concentrations.

For illustrative purposes, let us consider a cathode compartment consisting of a silver wire electrode and a concentration c_1 of Ag^+ ions in molten $NaNO_3$ and a similar anode compartment, however, consisting of lower concentration c_2 of Ag^+ ions in $NaNO_3$. Figure 1 shows such a concentration cell where the anode region is represented by the entire bath with the cathode enclosed in a glass bulb.[13]

At the anode where oxidation occurs

$$Ag(s) \rightarrow Ag^+(c_2) + e^-. \tag{1}$$

If the cathode had been a hydrogen electrode H_2 (1 atm) and the cathode $Ag||Ag^+$ (1 M) in standard state conditions in an aqueous solution, the standard potential would have been $E^\circ_{ox} = -0.8$ V. However, since the oxidation process at the anode is not occurring in standard state conditions (solutions at 1-M concentration at $T = 298$ K) and the oxidation takes place in molten $NaNO_3$, the electrode potential can be represented by the Nernst equation[14]

$$E_2 = E_{ox} - \frac{RT}{F} \ln(c_2), \tag{2a}$$

$$E_2 = E_{ox} - \frac{2.30RT}{F} \log(c_2), \tag{2b}$$

where E_{ox} is the assumed electrode potential in molten $NaNO_3$, R is the gas constant (8.317 J/K mole), T is temperature in kelvin, and F is the Faraday constant (96,500 J/V mole e^-). Concentration of the bath c_2 appears as $\log c_2$ because when the concentration of the Ag^+ ion (the product of the reaction) increases, the electrode potential becomes less positive. Equation (2b) can therefore be rewritten as

$$E_2 = E_{ox} - 1.98 \times 10^{-4} T \log(c_2). \tag{3}$$

Similarly at the cathode where the reduction of Ag^+ occurs,

$$Ag^+(c_1) + e^- \rightarrow Ag(s). \tag{4}$$

The standard potential in an aqueous solution now is $E^\circ_{red} = -E^\circ_{ox} \approx +0.8$ V. As before, for Ag^+ ions in our case in nonstandard conditions in molten $NaNO_3$,

$$E_1 = -E_{red} - \frac{2.30RT}{F} \log(1/c_1), \tag{5}$$

where E_{red} is the assumed electrode potential and is equal in magnitude to E_{ox}.

As the concentration c_1 of Ag^+ ions is increased, the electrode becomes more positive and therefore c_1 appears in the denominator of the logarithmic function. Thus, Eq. (5) with values of R and F substituted becomes

$$E_1 = -E_{red} + 1.98 \times 10^{-4} T \log(c_1). \tag{6}$$

The resultant voltaic cell illustrated in Fig. 1, which supports the reactions

$$\begin{array}{ll} \text{anode:} & Ag(s) \rightarrow Ag^+(c_2) + e^-, \\ \text{cathode:} & Ag^+(c_1) + e^- \rightarrow Ag(s) \\ \hline & Ag^+(c_1) \rightarrow Ag^+(c_2) \end{array} \tag{7}$$

will generate a potential difference V, that depends on the ratio of the Ag^+ concentrations (c_1/c_2) and the temperature T, and equals the sum of Eqs. (3) and (6). Therefore, the Nernst potential difference of the cell is given by

$$V = 1.98 \times 10^{-4} T \log(c_1/c_2). \tag{8}$$

If one of the concentrations, say c_1 (reference concentration), is known, the unknown salt bath concentration c_2 can be determined by measuring the cell emf V with a high impedance voltmeter.

Although the above argument seems reasonable, the electron released at the anode when a Ag atom disassociates into solution as an Ag^+ ion can move through the external circuit to the cathode where it reduces another Ag^+ ion; such a movement in reality indeed cannot occur. The reason this concentration cell is an incomplete voltaic cell is becuase, when a Ag^+ ion is released into the solution at the anode with a simultaneous reduction at the cathode, both of the half-cells become

charged, immediately blocking any further movement of the electron.

Therefore, we need a means that would allow the migration of the Ag^+ ions from the bath to the cathode region in the bulb. In other words, we need to physically distinguish the two regions of different concentrations and yet simultaneously permit the diffusion of Ag^+ ion to facilitate current flow and, hence, the redox reaction. Concentration cells using fritted glass[15] in place of the glass bulb or glass tubes with asbestos fibers[16] as well as tubes with loosely plugged glass wool have been reported. Our experience with such schemes similar to the conventional salt bridge using porous or semipermeable membranes is that, within a reasonable time period (of the order of an hour or so), complete mixing between the separated solutions occurs. In addition, an unpredictable liquid junction with an unknown potential exists across the membrane. Furthermore, the cell potential, while the solutions tend toward dynamics equilibrium, continues to decrease with time and, therefore, the measurements are not reliable.

Fortunately, in our case, the glass bulb itself acts as a good membrane. Inman[13] has reported the use of such a glass bulb containing the reference electrode to form part of a concentration cell. The underlying idea is that Pyrex glass at elevated temperatures (330–370°C) can act as a resistive ion bridge between the solutions because the sodium ions with a thin membrane (walls of the glass bulb) have rather high mobility at these temperatures. Since there are no pores present within the membrane, the two solutions are physically isolated.

III. Reference Electrode in a Large Glass Cell

A Pyrex glass test tube ~6-mm i.d. with ~0.5-mm wall thickness is heated with a torch and blown at one end to form a glass bulb with a tubular stem. The glass bulb is nearly spherical in shape with ~12 mm in diameter and ~0.1-mm wall thickness as shown in Fig. 2(a).

A reference melt is produced by releasing 2.0 g of silver from a high purity (99.999%) rod into a melt of 400-g $NaNO_3$ by electrolysis[10]; the reference melt concentration c_1 approximately equals 3.94×10^{-3} mole fraction (MF). The glass bulb is then filled to its neck with ~3–4 g of the reference melt. High purity silver wires are also used as the cathode within the glass bulb as well as the anode immersed in the bath. The cell is then used to measure the silver-ion concentration in the salt bath (Fig. 1). The Nernst potential difference is measured with a 10-MΩ input impedance, digital voltmeter.

By electrolytically releasing known quantities of Ag^+ ions in 400 g of $NaNO_3$, different known concentrations of Ag^+ in $NaNO_3$ in the bath are prepared. By measuring the cell potential each time, we obtain the plot of cell emf V vs $\log(c_1/c_2)$ as shown in Fig. 3. The solid line represents the theoretical cell potential as given by Eq. (8). As expected, both curves V vs $\log(c_1/c_2)$ exhibit linear behavior. Both the experimental and theoretical lines have nearly the same slope with the slope of the experimental line slightly lower. The temperature gradient in the bath in the vertical direction amounts to almost 20°C. The estimation of the bath temperature from the measured value near the reference bulb is susceptible to an error of a few degrees and may be responsible for the difference in the slope. Moreover, when the two concentrations are equal, we measure an asymmetry potential of ~14 mV rather than 0 as predicted by Eq. (8).

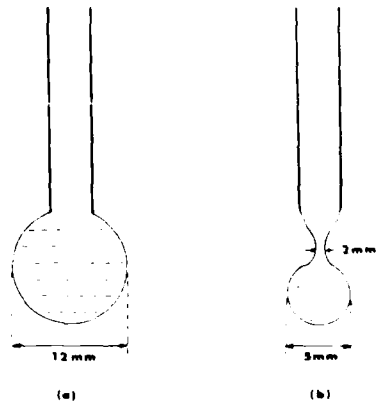

Fig. 2. Large and small reference electrode glass bulbs.

Inman[13] attributes the asymmetry potential to a difference of sodium-ion concentration in the glass between the inside and outside of the bulb which occurs during the blowing. Although this may occur, we believe it is highly unlikely; our careful experimentation has led us to a different conclusion. Note the temperature at which the measurements in this experiment were made, namely, 340°. However, $NaNO_3$ melts at 308°C. Although temperature of the salt bath was maintained at a constant set temperature using a feedback control arrangement,[10] the temperature of the reference melt was considerably lower (310°) due to its large thermal capacity. In fact, the temperature of the bath had to be ~340°C before the salt in the reference bulb would completely melt implying a temperature difference of ~30°C between the bath and reference cell. However, Eq. (8) assumes the same temperature for both the electrodes. Now then, if $c_1 = c_2 = c$, with both reference and bath electrodes at different temperatures, namely, T_1 and T_2, respectively, use of Eqs. (3) and (6) yields an asymmetry potential:

$$\Delta V = 1.98 \times 10^{-4} \Delta T \log c, \tag{9}$$

where $\Delta T = T_1 - T_2$. Since T_2 is always larger than T_1, ΔT is negative. In our case, we have $\Delta T \approx -30$°C and $c = 3.94 \times 10^{-3}$ and obtain $\Delta V = 14.28$ mV which agrees very well with our measured asymmetry potential when $c_1 = c_2$.

The corrected Nernst equation, when $c_1 \neq c_2$, is therefore

$$\Delta V = 1.98 \times 10^{-4} (T_1 \log c_1 - T_2 \log c_2). \tag{10}$$

which is plotted as a dashed line in Fig. 3. The excellent

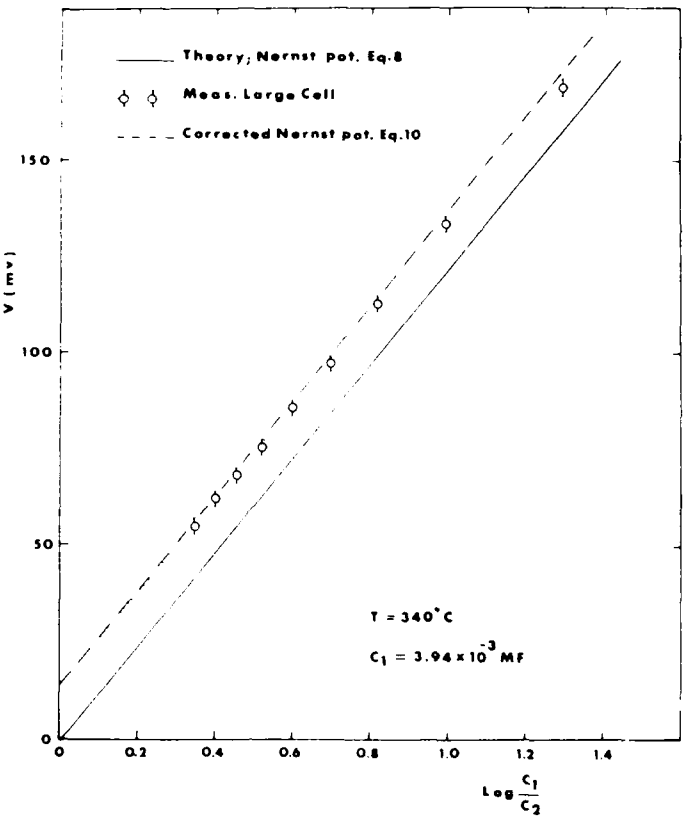

Fig. 3. Measured and calculated Nernst potential for large reference electrode glass bulb at $T = 340°C$.

agreement indicates the asymmetry is indeed due to temperature difference between the electrodes.

From the above discussion it is clear that, at temperatures below ~350°C, measurements are not meaningful as the salt inside the reference cell freezes around the Ag electrode. Thus, this type of cell would not permit fabrication of our ion-exchanged waveguides at lower temperatures. The asymmetric potential, because of its temperature dependence, would require temperature-dependent compensation of the analog signal when using signal processing means to maintain the concentration.

IV. Modified Reference Electrode Cell

The basic problem of asymmetry potential and the temperature restriction primarily due to temperature difference between the electrodes can be solved, for example, by heating the upper part of the reference cell independently to compensate for the heat loss. This would require two temperature controllers and *a priori* knowledge of ΔT for each concentration cell. Another possibility is to increase the thermal mass, i.e., the amount of $NaNO_3$ in the salt bath, and immerse the cell deeper to ensure that the reference electrode temperature approaches that of the bath. This would require large amounts of $NaNO_3$, which becomes expensive, plus a more elaborate high powered temperature controller to maintain the bath temperature would be required.

An alternative arrangement is to use a smaller reference bulb as shown in Fig. 2(b). Use of such a small reference cell eliminates the requirement of large quantities of $NaNO_3$ and a separate temperature controller. The cell can easily be fabricated as before but now using a Pasteur pipette.

The solid circles in Figs. 4(a) and (b) and 5 represent the measured concentration cell potential at the three different temperatures, namely, 325°C, 350°C, and 360°C, respectively. The small amount of asymmetry potential at all the above temperatures can be due to a difference in temperatures of only a few degrees centigrade between the bath and the reference cell. In fact, the discrepancy of a few millivolts is within the measurement error. Typically <5 mV changes in the measured value happen depending on the volume difference of the salt inside the reference cell or the vertical positioning of either the silver wire within the cell or the entire cell itself.

Figure 5 shows the results for various types of cell measured at 360°C. As before, the large cell exhibited the highest asymmetry potential. Three different types of smaller version cell were also used. The ⊗ marked data point indicates that the concentration c_1 of Ag^+ ions in the reference cell is less than that of the bath

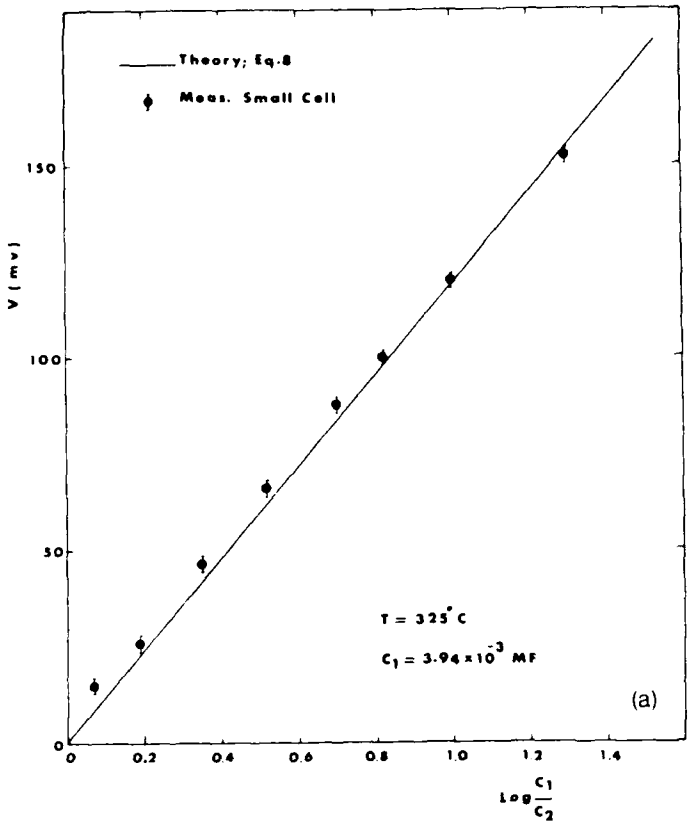

The authors would like to thank T. Anderson and H. A. Laitinen for helpful discussions. This work was supported in part by a grant from the U.S. Air Force, contract FO 8635-83-K-0263, AFOSR contract 84-0369 and Engineering and Industrial Experiment Station at University of Florida.

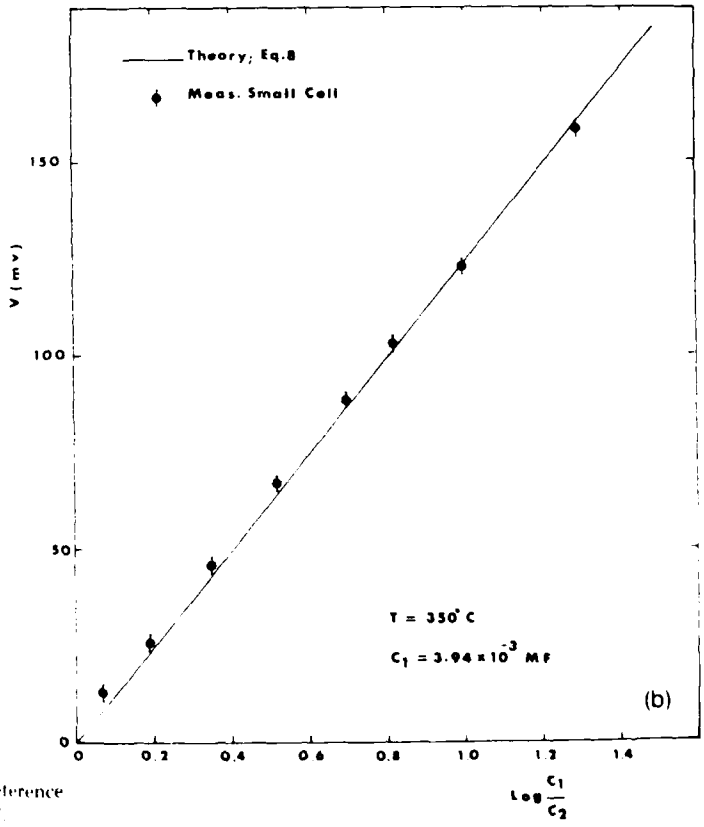

Fig. 4. Measured and calculated Nernst potential for small reference electrode glass bulb at (a) $T = 325°C$, (b) $T = 350°C$.

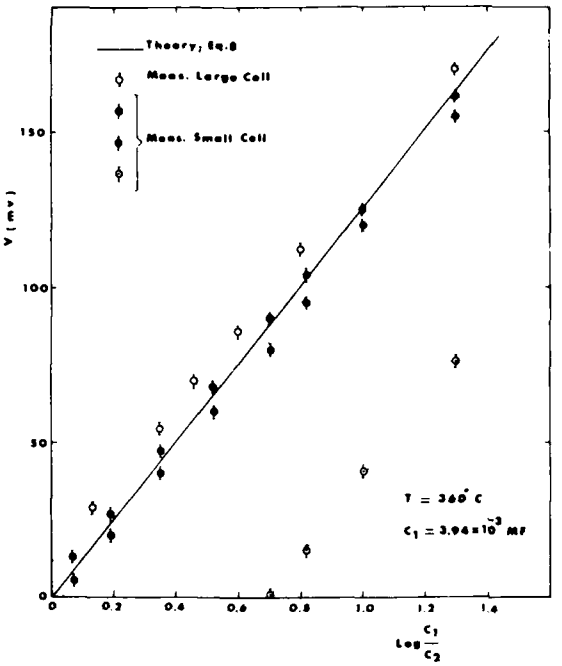

Fig. 5. Concentration cell performance between large and small reference electrode bulbs at 360°C. ⊙ points indicate small bulb potential measurements; but a fairly large air bubble present within the neck at the small reference bulb gives a large zero crossover point ($c_1/c_2 = 0.7$).

since at the origin, the y intercept is negative. A very small air bubble in the reference cell can cause this. A very large air bubble trapped within the constriction of a small bulb results (⊙ points) in zero cell potential for $\log(c_1/c_2) = 0.7$.

Therefore, it is extremely important to ensure that there are no air bubbles within the reference bulb. When necessary precautions are taken, the experimental curve is repeatable when using the same cell after repeated cleaning and filling with the same standard solution. However, it seems that small variations in the absolute value of the cell potential do take place depending on the position of the reference bulb in the bath. But once again when this is standardized, the measurements are repeatable within ±2 mV.

To avoid the errors due to the sources mentioned above it is necessary to use a given calibrated concentration cell for the measurement, keeping the experimental conditions the same. In these conditions, such a cell can be used for *in situ* concentration measurement during the fabrication of ion-exchanged waveguides.

V. Conclusions

We have described a $Ag||Ag^+(NaNO_3)||Ag$ concentration cell that can be used to measure concentration of Ag^+ ions in a molten $NaNO_3$ bath during fabrication of $Ag^+ - Na^+$ ion-exchanged waveguides. By suitable selection of the electrodes, the diffusant ion, and the electrolyte, the scheme can be adapted to other ion exchanges used in optical waveguide fabrications. The measurements are quite repeatable as long as a small reference electrode glass bulb is used and experimental conditions are standardized. The error in our experiments is ±2 mV. Thus, it will help to have a large c_1/c_2 ratio by choosing a relatively large reference-ion concentration compared to that of the bath. In these conditions we can maintain the bath-ion concentration by use of appropriate analog antilog amplifiers and other necessary process controls. On-line concentration control should be possible by periodic pumping of ions into the bath. This would permit fabrication of ion-exchanged glass waveguides repeatedly with the same characteristics. We are presently working toward meeting this objective.

References

1. T. G. Giallorenzi, E. J. West, R. Kirk, R. Ginther, and R. A. Andrews, "Optical Waveguides Formed by Thermal Migration of Ions in Glass," Appl. Opt. **12**, 1240 (1973).
2. Y. H. Won, P. C. Jaussaud, and G. H. Chartier, "Three-Prism Loss Measurements of Optical Waveguides," Appl. Phys. Lett. **37**, 269 (1980).
3. T. Findakly and B. Chen, "Single-Mode Integrated Optical 1 × N Star Coupler," Appl. Phys. Lett. **40**, 549 (1982).
4. V. Neuman, O. Parriaux, and L. M. Walpita, "Double-Alkali Effect: Influence on Index Profile of Ion-Exchanged Waveguides," Electron. Lett. **15**, 704 (1979).
5. G. Stewart, C. A. Miller, P. J. R. Laybourn, C. D. W. Wilkinson, and R. M. De LaRue, "Planar Optical Waveguides Formed by Silver-Ion Migration in Glass," IEEE J. Quantum Electron. **QE-13**, 192 (1971).
6. G. Stewart and P. J. R. Laybourn, "Fabrication of Ion-Exchanged Optical Waveguides from Dilute Silver Nitrate Melts," IEEE J. Quantum Electron. **QE-14**, 930 (1978).
7. G. H. Chartier, P. Jaussaud, A. D. DeOliveira, and O. Parriaux, "Optical Waveguides Fabricated by Electric-Field Controlled Ion Exchange in Glass," Electron. Lett. **14**, 132 (1978).
8. G. H. Chartier, P. Collier, A. Guez, P. Jaussaud, and Y. Won, "Graded-Index Surface or Buried Waveguides by Ion Exchange in Glass," Appl. Opt. **19**, 1092 (1980).
9. M. Imai, N. Haneda, and Y. Ohtsuka, "Losses in Optical Waveguides Formed by Silver-Sodium Ion Exchange," IEEE/OSA J. Lightwave Technol. **LT-1**, 611 (1983).
10. R. K. Lagu and V. Ramaswamy, "Fabrication of Single-Mode Glass Waveguides by Electrolyte Release of Silver Ions," Appl. Phys. Lett. **45**, 117 (1984).
11. T. Izawa and H. Nakagome, "Optical Waveguides Formed by Electrically Induced Migration of Ions in Glass Plates," Appl. Phys. Lett. **21**, 584 (1972).
12. E. Okuda, H. Wada, and T. Yamasaki, in *Technical Digest of Topical Meeting on Integrated and Guided-Wave Optics* (Optical Society of America, Washington, D.C., 1984), paper ThB6.
13. D. Inman, "A Glass Contained Reference Electrode for Molten Nitrate Solvents," J. Sci. Instrum. **39**, 391 (1962).
14. T. L. Brown and H. E. LeMay, Jr., *Chemistry—General Science* (Prentice-Hall, Englewood Cliffs, N.J., 1977).
15. F. R. Duke and H. M. Garfinkel, "Complex Ions in Fused Salts. Cadmium and Lead Bromides," J. Phys. Chem. **65**, 1627 (1961).
16. S. N. Flengas and Sir E. Rideal, "On Electrometric Titration in Fused Salts," Proc. R. Soc. London Ser. A **233**, 443 (1956).

REFERENCE [8]

Fabrication and Characterization of Buried Glass Waveguides with Symmetric Index Profile

R.K. Lagu, V. Ramaswamy, and S.I. Najafi

Department of Electrical Engineering, University of Florida
Gainesville, FL 32611, USA

Diffusion studies and modal behavior of Ag^+-Na^+ exchanged planar waveguides in glass substrate are presented. In addition, a simple SEM technique to determine the refractive index profile and the realization of symmetrical buried waveguides with fiber-like refractive index profile are also reported.

1. Introduction

Ion-exchanged glass waveguides have received considerable attention recently and they are expected to form the basis for passive integrated optical components. Significant progress has been made in the fabrication of ion-exchanged waveguides. Recent electrolytic release technique [1] and the improved method [2] using fritted glass bulb around the cathode provide opportunities for fabrication of passive waveguide devices with repeatable characteristics. This is quite important because glass waveguide devices being passive, cannot be tuned electro-optically to compensate for fabrication errors.

The guiding characteristic of a planar waveguide depends on the device parameters such as maximum index change, index profile, effective guide depth, which in turn depend on the process parameters like the diffusion temperature, time and silver ion concentration in the bath. To design a waveguide supporting specific number of modes with desired propagation constants, it is necessary to determine relations between process and device parameters. In this paper, we present an empirical relation between process and device parameters. We also present a procedure for fabricating symmetrical buried waveguides which are comparable in shape and size to the core of single mode fibers. A precise technique to characterize these waveguides using back-scattered electrons in SEM is also reported.

2. Planar Surface Waveguide Diffusion Characteristics

The Ag^+-Na^+ ion-exchanged waveguides are fabricated in a molten $NaNO_3$ bath with small concentration of silver ions. The bath can be considered to

be an infinite source of silver ions as the number of ions diffusing into the glass sample is very small compared to that of the ions present in the bath. Under these conditions, the diffusion equation has a closed form analytical solution, namely the complementary error function. Planar waveguides fabricated in this manner, therefore, exhibit a complementary error function index profile. The D-V characteristics for this highly asymmetric profile have been determined by solving the normalized mode dispersion equation [3] and the cut-off values for the V parameter for the first three modes are found to be 2.7, 6.3 and 9.9.

The V parameter is defined as

$$V = \frac{2\pi}{\lambda} d \sqrt{2n_b \Delta n}$$

where λ is the wavelength of operation, d is the effective waveguide depth measured between values at 0.158 of peak refractive index at the surface, and is given by $d = 2\sqrt{Dt}$ where t is the time of diffusion and D is the diffusion coefficient, n_b is bulk refractive index, and Δn is the maximum refractive index change which depends on the concentration of silver ions C_0.

We fabricated several sets of single and multimode waveguides using Labmate microscope slides for different value of C_0 and measured the propagation constants of the modes they suported. Using an iterative computer program, the data was fitted into the D-V characteristics of the erfc profile to estimate Δn and d. Using these results, the value of D was estimated and the relation between Δn and C_0 plotted as shown in figure 1. It was noted the diffusion coefficient D did not vary much with different brands (e.g., Corning, Schott and Labmate) of glass substrates.

For small C_0, Δn versus C_0 is essentially linear. For guides with small number of modes, the relationship between Δn and C_0 can therefore be approxi-

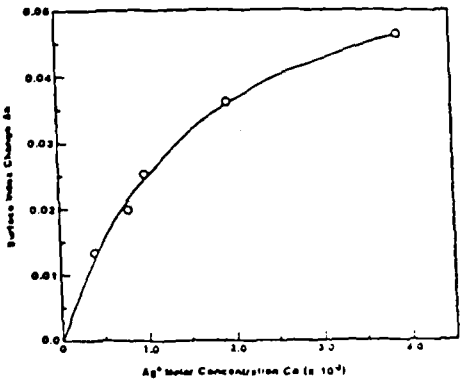

Figure 1. Relation between surface index change Δn and Ag^+ concentration

mated as

$$\Delta n = 26.5\ C_0$$

C_0 is the mole fraction of silver ions in bath.

Using above empirical relations between the device (d, n_0, Δn) and the process parameters (C_0, D, t), we can approximate the V parameter as

$$V = 63.85\ \sqrt{C_0 t}$$

for $\lambda = 0.6328\ \mu m$, $n_0 = 1.512$ and $D = 0.129\ \mu m^2/min$.

Using cut-off values for V parameters for various modes, the design curves are plotted in t-C_0 plane as shown in figure 2.

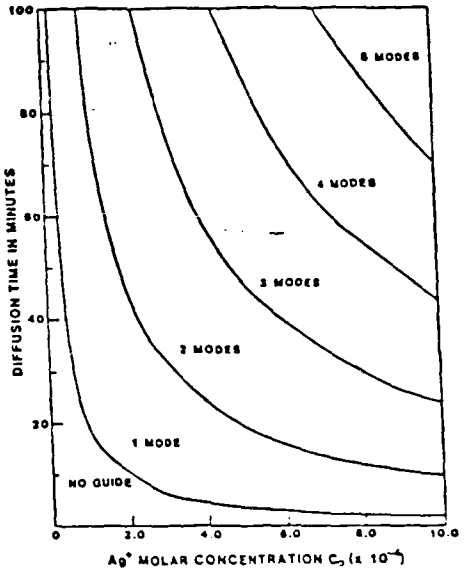

Figure 2. Design curves for various modes ($\lambda = 0.6328\ \mu m$)

3. Waveguide Characterization

The technique frequently used for measuring silver ion concentration seems to be Electron Microprobe Analysis, also referred to as Electron Microprobe [4]. The equipment needed for this technique is quite expensive and is not available at our university. We have investigated a technique using a Scanning Electron Microscope to find the silver ion concentration profile. In an SEM, the specimen is bombarded by an accelerated electron beam with an accelerating voltage in the range of 20-50 Kv. The specimen generates two types of electrons, namely, the secondary electrons and the back-scattered electrons. The back-scattered electrons which have higher energies carry the

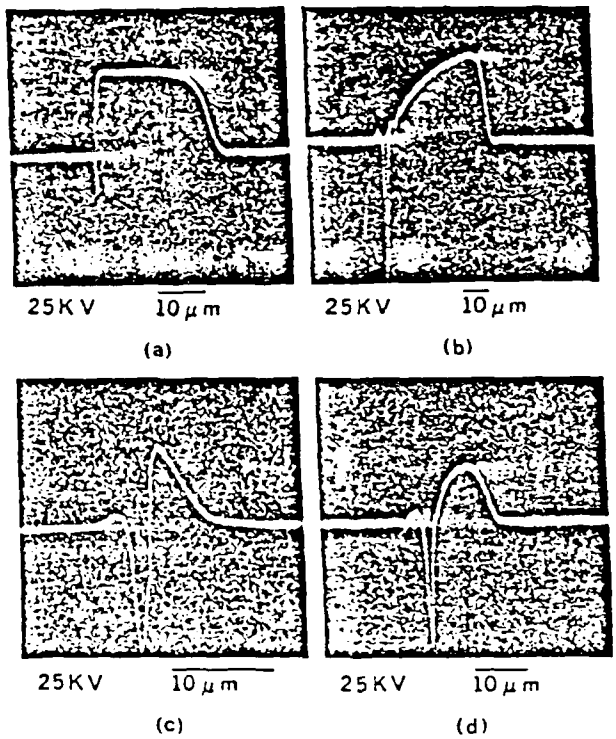

Figure 3. a) Index profile of a planar waveguide fabricated in the first step by field-assisted diffusion of silver ions. b) Second field-assisted diffusion in pure $NaNO_3$ results in a buried skewed index profile. c) Index profile of a planar waveguide fabricated in the first step by diffusion without applied electric field. d) Symmetrical index profile of a buried waveguide results of second field-assisted diffusion in pure $NaNO_3$.

information about specimen composition. Since the atomic weight of silver is much higher than that of the rest of the ions in the glass substrate, the contribution of silver ions in the guide region to the yield of back-scattered electrons is maximum. Thus, if the sample is polished across the edge of the waveguide and scanned in the SEM, the back-scattered electron intensity profile gives a good estimate of the silver ion concentration profile. Since the refractive index change is directly proportional to silver ion concentration, it also gives a good estimate of the index profile. The silver ion concentration profiles measured using this technique are shown in figures 3(a) through 3(d). It can be seen that this method has a good signal to noise ratio and high resolution. The big dip seen in the signal comes from a layer of epoxy used while polishing the waveguide. The epoxy is applied on the surface of

the guide and another glass slide is stuck to it before polishing so as to avoid the rounding at the edge of the waveguide.

4. Planar Buried Waveguide Fabrication

A two step diffusion process utilizing field-assisted diffusion is used in glass to form buried waveguides [5]. In this process, soda-lime-silicate glass slides are immersed in molten sodium nitrate where silver ions are also present. Initially, a surface waveguide is formed by a field-assisted diffusion of silver ions in glass. This is followed by a second field assisted diffusion, however in pure sodium nitrate. The diffusion time and applied field in each of the two steps are two important parameters which control the dimensions and index profile of a buried waveguide.

In the existing process, applied field in the range of 60-100 volts/mm is used. This results in a step-like waveguide (figure 3(a)), which when buried, gives a skewed index profile (figure 3(b)). These results agree with the skewed profiles of buried waveguides already reported in literature [5].

We have experimentally determined that if no field is applied in the first step, as expected, a surface waveguide with complementary error function profile is formed (figure 3(c)) which, when subjected to a field-assisted diffusion in pure sodium nitrate, results in a symmetrical structure with near parabolic index profile as shown in figure 3(d). To obtain waveguides with various widths, surface waveguides were formed without drift field for 40 minutes using the electrolytic process [2]. The time of second diffusion was varied between 20 to 80 minutes using an electric field of 30 volts/mm. The resulting waveguides were polished and analyzed using a Scanning Electron Microscope (SEM) to get the estimate of their widths. Figure 4 shows a plot of waveguide width W (measured between 95% peak values) versus the second step diffusion time indicating that symmetrical buried waveguides of arbitrary

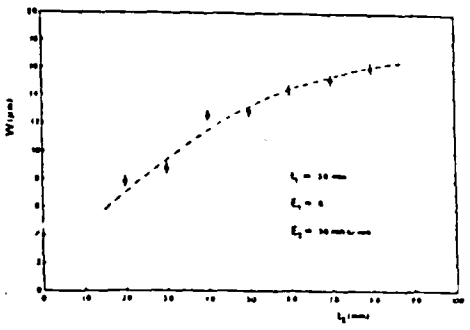

Figure 4. Relation between the waveguide width and the second step, field-assisted diffusion time

width in the range of 6-16 μms can easily be achieved and that diffusion depth exhibits the expected $\sqrt{t}$ dependence.

5. Conclusion

Design curves which can be used to determine the concentration of silver ions and the time of diffusion required for a planar waveguide of given width, number of modes, and surface index change are reported. A simple, new technique which uses the back-scattered electrons in an SEM to determine the refractive index profile and waveguide width of glass waveguides is also described. In addition, we have presented a procedure for fabricating buried glass waveguides with fiber-like index profile of varying widths.

Acknowledgments

The authors would like to thank E. J. Jenkins of the Department of Material Science and Engineering for his assistance in SEM analysis and C. Wayne Twiddy for his help in waveguide fabrication. This work was supported in part by a grant from AFOSR Contract number AFOSR 84-0369.

References

1. R. K. Lagu and R. V. Ramaswamy, "Fabrication of single mode glass waveguides by electrolytic release of silver ions," Applied Physics Letters, 45, 117-118, 1984.
2. S. I. Najafi, R. V. Ramaswamy and R. K. Lagu, "An Improved method for fabricating ion-exchanged waveguides through electrolytic release of silver ions," to be published in IEEE J. Lightwave Tech.
3. R. V. Ramaswamy and R. K. Lagu, "Numerical field solution for an arbitrary asymmetrical graded-index planar waveguide," IEEE J. Lightwave Tech. JLT-1, 408-417, 1983.
4. G. Stewart, C. A. Miller, P. J. R. Laybourn, C. D. W. Wilkinson and R. M. Delaru, "Planar optical waveguides formed by silver ion migration in glass," IEEE J. Quantum Electron., QE-13, 192-200, 1977.
5. G. Chartier, P. Collier, A. Guez, P. Jaussaud and Y. Won, "Graded index surface or buried waveguides by ion-exchange in glass," Applied Optics, 19, 1092-1095, 1980.

REFERENCE [9]

Gradient-Index Optical Imaging Systems Conference,

Palermo (Italy), Sept. (1985)

12.1

Ag^+-Diffused Graded-Index Glass Waveguides: Diffusion and Modal Characterization

S. I. Najafi and R. V. Ramaswamy

Department of Electrical Engineering
University of Florida
Gainesville, Florida 32611

Introduction

In a conventional optical system, the index of refraction of each optical component is homogeneous. To achieve desired operating characteristics, take for example a lens, usually several parameters like the curvature, the thickness, and the index of refraction are varied. In many other systems, often these parameters are used to optimize the performance of a device under consideration. However, gradient-index techniques have proven to be useful in the design of imaging systems [1] and guided wave optical components. For example, axial and radial gradients have been used to correct distortion and chromatic aberration in lenses [2]. In addition to the fabrication overlay lenses [3] for spectrum analyzer applications, gradient-index optical devices have been used in the design of multiplexers [4] for communication system applications. In addition, graded index waveguides have also found numerous applications in passive and active optical system components. In particular, passive, single mode, glass waveguides, compatible with single mode optical fibers, are expected to play a major role at the receiving end of an optical communication system.

Several techniques, e.g. chemical vapor deposition, polymerization, ion-diffusion and etc. have been employed to obtain refractive index changes both in glass and plastics. Of all the techniques, ion-exchange or ion-indiffusion is the most popular approach in fabricating gradient-index components in glass. At University of Florida our emphasis has been on gradient-index optical waveguides for passive integrated optical components.

A variety of monovalent ions e.g., Tl^+, K^+, Cs^+ and Ag^+ have been used to fabricate optical components (waveguides) by several groups around the world. Our choice of Ag^+ was dictated by the fact that not only pure (99.999%) silver electrodes are readily available for electrolytic release [5], but a heavy element like silver is easily amenable to SEM analysis for index-profile measurement [6]. Besides, the in-situ measurement of Ag^+ concentration [7] allows the replenishment of Ag^+ as needed. Although such a scheme facilitates precise control of the fabrication parameters, fundamental understanding of the diffusion process and its relationship to modal characterization is essential for the design and fabrication of both the gradient-index and passive optical components, with assured repeatability.

In this paper, we present a detailed study of diffusion of silver ions into the glass substrate for design of a planar waveguide with desired parameters, with specific emphasis on the influence of diffusion time, electric field and concentration of silver ions on the waveguide parameters.

Buried wavguides with nearly symmetric profile have been fabricated by a two-step diffusion process appropriately assisted by the application of an electric field at each step. Assuming that Ag^+ concentration profile corresponds to the index profile, calculation of modal field profiles indicate that the results are in reasonable agreement with the predicted field profile.

Diffusion Process

The fabrication of graded-index glass waveguides is accomplished by in-diffusion of Ag^+ into the glass substrate at elevated temperatures in a molten $NaNO_3$ bath that contains Ag^+ ions. The refractive index profile can be tailored to desired specifications by varying the different process parameters in a two-step process [8]. In particular, the parameters that control the buried waveguide properties in the two-step diffusion process are

t_1, E_1 = Time of diffusion and applied field in the first step ($NaNO_3$ + Ag^+),
t_2, E_2 = Time of diffusion and applied field in second step (pure $NaNO_3$),
C_0 = Silver ion concentration in the bath,
T = Fabrication temperature = 330°C.

The presence of an applied electric field during the diffusion causes the silver ions to move deeper inside the glass substrate [8-10]. Moreover, if C_0 equals zero in the second step, an out-diffusion of silver ions appears to occur from the cover-surface of the guiding film. The buried single mode waveguides thus fabricated showed the expected [8,10] skewed index profile giving rise to modal field distribution which is not necessarily optimum for maximum power coupling into a single mode fiber.

In an attempt to acquire a better control of the process parameters and understand their influence on the waveguide characteristics, we have investigated the two-step diffusion process using the electrolytic release technique [6] in detail. To begin with, we studied the first step process in detail. For small concentration of Ag^+, with $E_1 = 0$, the concentration profile is

$$C(x,t) = C_0 \operatorname{erfc}\left[\frac{x}{2\sqrt{Dt}}\right] , \qquad (1)$$

where D is the self-diffusion coefficient of Ag^+ in glass. The effective diffusion depth W_0 is specified at $x = 2\sqrt{Dt}$, at which point erfc (1) = 0.157. From the diffusion depth W_0, obtained for bath concentrations of the order of $\geq 10^{-3}$ MF or greater, we obtain a value of D = 0.28 μm^2/min for Ag^+ in-diffusion into glass substrate. For concentrations $C_0 < 10^{-3}$, D appears to decrease monotonically with C_0. This behavior is presently being investigated.

Since we are ultimately interested in comparing the diffusion depth W as a function of the parameters of the two-step diffusion process, we define W to represent the distance between the 1/e points on the SEM profile photograph. It can be easily shown that $W = 0.64\ W_0$. Fig. 1 shows the expected square-root dependence of W on diffusion time t_1 for two different values of C_0. For large values of C_0 ($> 10^{-3}$), using the above value for D, we estimate the slope of W vs. $\sqrt{t_1}$, be 0.68, which agrees well with the fitted value of 0.72 shown in Fig. 1. As stated previously, this value monotonically decreases with decreasing C_0 ($C_0 < 10^{-3}$) and for $C_0 = 2 \times 10^{-4}$, D = 0.14 μm^2/min. Although we used Labmate slides, D did not vary a great deal with different laboratory glass slide substrates. Dependence of W on C_0 indicates a similar behavior and is not expected on the basis of theoretical analysis [10].

With an applied field in the first step, the concentration profile is described by [11],

$$C(x,t) = \frac{C_0}{2}\left\{e^{\frac{Eux}{D}} \operatorname{erfc}\left[\frac{x + Eut}{2\sqrt{Dt}}\right] + \operatorname{erfc}\left[\frac{x - Eut}{2\sqrt{Dt}}\right]\right\} \qquad (2)$$

which reduces for large values of Eμt, specifically for Eμt > $5\sqrt{Dt}$, to

$$C(x,t) = \frac{C_0}{2}\,\mathrm{erfc}\left[\frac{x - E\mu t}{2\sqrt{Dt}}\right] . \qquad (3)$$

SEM experimental results confirm the above profiles and furthermore, the results indicate that for fields larger than 20 V/mm, Eq. 3 is a good approximation. When $C/C_0 = 1/2$, the effective depth of diffusion W for which erfc = 1, is given by $E\mu t + 2\sqrt{Dt}$. For large fields, $E\mu t \gg 2\sqrt{Dt}$ and therefore, W approximately equals Eμt in this case. For Ag^+ diffusion in glass during the first step, at a field of $E_1 = 30$ V/mm for $t_1 = 45$ min., μ was determined to be 15.55 μm^2/V-min. Fig. 2 shows the expected linear relationship between the measured values of W from SEM measurements and the time of diffusion t_1.

However, to obtain a buried symmetrical profile, it is necessary to utilize a two-step process where the second step diffusion is carried out in pure $NaNO_3$. The dependence of the diffusion depth on different fabrication parameters in the two-step process have been studied in detail. The buried depth of the final waveguide can be altered by judicious choice of the two-step process parameters viz t_1, E_1, t_2 and E_2. Fig. 3 shows a SEM photograph of two such profiles with the surfaces of the waveguiding films placed against each other. Diffusion was carried out with $C_0 = 2 \times 10^{-3}$ MF and T = 330°C. The index profile on the right in Fig. 3 shows the effect of a non-zero electric field in the first step keeping all other parameters the same in the two runs. The presence of E_1 causes higher peak index and larger diffusion depth. The latter effect is rather obvious since the applied electric field increases the penetration depth of Ag^+ ions. However, the large peak index is caused by the particular experimental configuration used in the first step which allows the concentration C_0 near the substrate to increase locally due to the electric field and can nearly be eliminated if required by adjusting the position of the anode.

Dependence of W on t_2 in the two-step process indicates that W increases with t, in a similar fashion, for different values of C_0 and E_2. However, for a given C_0 and t_2, increasing E_2 increases the width W linearly. These and other diffusion characteristics will be discussed in detail.

Field Profile Determination

The intensity profile of the waveguide was measured by using a video camera in conjunction with an oscilloscope. The waveguide was excited using a prism coupler and the output pattern focused on the camera. The frame and line pulses from the video signal were used to trigger the oscilloscope and to select a particular line for the display of the video signal as vertical output. The horizontal scale of the oscilloscope was carefully calibrated to give the mode intensity profile directly on the screen.

Inserts in Fig. 4 shows photographs of the fundamental and the next higher order mode of a planar glass waveguide fabricated with one-step diffusion ($E_1 = E_2 = t_2 = 0$). For this waveguide with erfc complimentary index profile, V = 7.804 and only two modes are guided. Numerical solutions for highly asymmetrical waveguides [12] were used to calculate the modal profile. The experimental results agree fairly well (Fig. 4) with the predicted profile and will be discussed in detail.

References

1. D. T. Moore, Appl. Opt., 19, 1035 (1980).
2. L. G. Atkinson, Appl. Opt., 21, 993 (1982).
3. J. Southwell, J. Opt. Soc. America, 67, 1004 (1977).
4. W. J. Tomlinson, Appl. Opt., 19, 1127 (1980).
5. S. I. Najafi, R. V. Ramaswamy and R. K. Lagu, J. Lightwave Tech., accepted for publication.
6. R. K. Lagu, R. V. Ramaswamy and S. I. Najafi, Paper B10, 3rd European Conference on Integrated Optics, ECIO'85, May 6-8, 1985, Berlin, W. Germany.
7. R. K. Lagu, S. I. Najafi and R. V. Ramaswamy, Appl. Opt. 23, 3925 (1984).
8. G. Chartier, P. Collier, A. Guez, P. Jaussand and Y. Won, Appl. Opt. 19, 1092 (1980).
9. R. K. Lagu and R. V. Ramaswamy, Appl. Phys. Lett., submitted for publication.
10. R. V. Ramaswamy, S. I. Najafi, J. Lightwave Tech., submitted for publication.
11. S. Houde-Walter, M.S. Thesis, Institute of Optics, College of Engineering, University of Rochester, New York, 1983.
12. R. V. Ramaswamy and R. K. Lagu, J. Lightwave Tech., LT-1, 408 (1983).

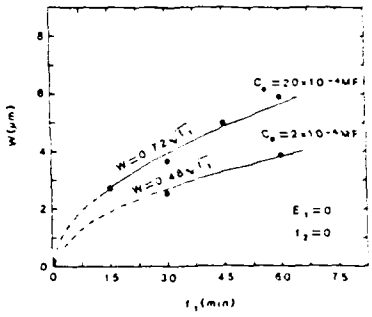

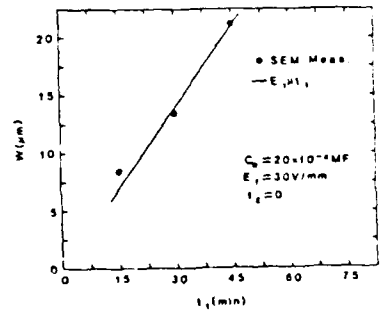

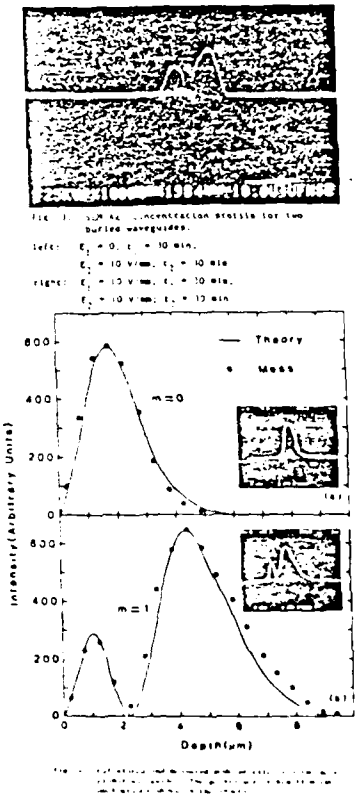

REFERENCE [10]

IEEE JOURNAL OF QUANTUM ELECTRONICS, VOL. QE-22, NO. 6, JUNE 1986

Planar, Buried, Ion-Exchanged Glass Waveguides: Diffusion Characteristics

RAMU V. RAMASWAMY, SENIOR MEMBER, IEEE, AND S. IRAJ NAJAFI

Abstract—A detailed theoretical and experimental study of Ag^+-Na^+ change in soda-lime silicate glasses in a molten bath containing a xture of $NaNO_3$ and Ag^+ is presented. With no applied field, concentration profiles $C(x, t)$ (and therefore, the index profiles for low concentrations) are given by complementary error function. The estimated value for the self-diffusion coefficient D of Ag^+ is 0.133 μm^2/min low concentrations and it monotonically increases with the surface ncentration C_0 until it saturates at about 0.3 μm^2/min for $C_0 \geq 10^{-4}$. However, square root dependence of diffusion depth with time ms to be independent of the C_0.

Presence of an external field E causes the effective depth of diffusion increase. In fact, for large E fields, the profile can accurately be scribed by $C/C_0 = \frac{1}{2}\operatorname{erfc}(x' - r)$ where $r = \mu Et/\sqrt{2Dt}$ where μ is the ic mobility of Ag^+ in glass. We define a new diffusion depth W as distance from the surface to the $1/e$ concentration point, and for ge fields, W varies linearly with E and t. Experimental results yielded alue of 15.55 $\mu m^2/V \cdot min$ for μ. As before, square root dependence W with t and the linear variation of W versus C_0 for $C_0 \leq 10^{-4}$ MF, th W saturating for $C_0 > 10^{-4}$ MF, were observed in the case of field sisted diffusion.

A two-step process, where a surface waveguide formed in the first p with either E equal to zero or some finite value, is modified by rforming a second diffusion in pure sodium nitrate to produce a bur-d, symmetrical fiber-like profile. This process is also studied in detail.

I. Introduction

RECENTLY, glass waveguides have received considerable attention because of their compatibility with single- and multimode optical fibers. They are expected to form the basis for passive integrated optical components, not only in the receiving end of an optical communication system, but also in hybrid (optical and electronic) systems as well as in other special applications. The ion-exchange technique seems to be the most common approach for fabricating graded-index waveguides in glass [1]-[8].

Recent efforts [6] in the fabrication of ion-exchanged waveguides have resulted in the improved electrolytic release technique [9]. This technique provides opportunities to control the ion concentration [10] during diffusion, thus permitting fabrication of passive glass waveguides with assured repeatability [11]. Precise control of concentration profile is quite important because glass waveguide components, unlike their counterpart in Ti-diffused $LiNbO_3$ waveguides, cannot be tuned electrooptically to compensate for fabrication errors. Typical Ti:$LiNbO_3$ single-mode waveguides are about 2 μm deep, with the peak of their refractive index located at or very near the surface. Ti:$LiNbO_3$ channel waveguides of small strip widths with such shallow diffusion depths couple rather poorly to single-mode optical fibers because of significant modal mismatch. Moreover, the coupling loss increases with decreasing guide widths [12]. On the other hand, a two-step diffusion process [13] allows the refractive index to be adjusted in the depth direction, thus permitting the realization of buried, symmetrical waveguides with fiber-like refractive index profile.

In this paper, an ion-exchanged process in glass is described involving the cation Ag^+. Section II presents a simple analysis of the single-step Ag^+-Na^+ ion-exchange process with and without the presence of an applied electric field used to enhance the diffusion. Section III presents a detailed experimental study of both the single-step and the two-step diffusion process and the associated parameters that control the refractive index profile and the dimensions of the buried waveguide. In addition, a back-scattered scanning electron microscope (SEM) technique [13] to measure the depth of diffusion and its dependence on the applied field, the time of diffusion in each step, and the concentration of silver ions in the bath is discussed in detail. Besides providing a better understanding of the Ag^+-Na^+ interdiffusion phenomenon which is applicable to similar ion exchanges, the results are useful in the design of single- and multimode waveguides using the process.

II. Theoretical Analysis

A. Interdiffusion Model

Optical waveguides in glass substrates are often fabricated by creating a layer of higher refractive index on the surface of the substrates. This can be accomplished by the diffusion of monovalent atoms of higher polarizability, e.g., cesium [1], rubidium [1], potassium [2], silver [3]-[6], and thallium [7], [8]. Although the diffusion of one of the above ionic species into an isotropic, homogeneous medium such as glass could conceivably create the requisite increase in refractive index, it is widely believed that ions of higher polarizability actually exchange [1]-[8] with those already present in the glass, thus preserving charge neutrality. Glass constituents consist of formers,

Manuscript received June 28, 1985; revised December 17, 1985. This work was supported by the U.S. Air Force Office of Scientific Research under Contract AFOSR 84-0369.

The authors are with the Department of Electrical Engineering, University of Florida, Gainesville, FL 32611.

IEEE Log Number 8608205.

0018-9197/86/0600-0883$01.00 © 1986 IEEE

intermediates, and glass modifiers; specifically, the alkali ions of the network modifier (e.g., Na^+) are believed to exchange with the external ions (e.g., Ag^+) diffusing into the glass, thus preserving the structural integrity of the glass substrates.

The ionic mobility of the indigenous species is usually different from that of the incoming species. Unequal transport properties of these ions will in turn create a localized imbalance in the charge distribution in the glass, thus giving rise to a potential difference. The induced field will assist the movement of the slower ions while impeding the progress of the faster ions. This in turn will balance the interdiffusion of the ions by making their flow rate equal and thereby maintaining the charge neutrality.

If ion exchange indeed occurs between an incoming cation A and an indigenous cation B, the process is often described by writing for each species the Fick's law [14] in one dimension, except that the self-diffusion coefficient in the equation is replaced by an interdiffusion coefficient $\tilde{D}$ [15]:

$$\tilde{D} = \frac{D_A D_B}{N_A D_A + N_B D_B} \tag{1}$$

where N_i ($i = A, B$) is the mole fraction of exchangable ions, i.e., the ratio of the concentration of species i to the total concentration and D_i is the self-diffusion coefficient of the species i.

Therefore, Fick's law in one dimension becomes the diffusion equation

$$\frac{\partial C_A}{\partial t} = \frac{\partial}{\partial x}\left(\tilde{D}\,\frac{\partial C_A}{\partial x}\right). \tag{2}$$

Solution of (2) is dictated by the nature of the diffusion coefficient $\tilde{D}$. As seen from (1), $\tilde{D}$ depends on the concentration of the diffusing species and varies as a function of position x in the glass. This implies that (2) must be solved to determine the distribution C_A of the incoming species A. For the case of a semi-infinite glass substrate containing initially none of the incoming species and in contact with a salt bath which includes the species A with its concentration C_0 constant at the interface, Crank has presented the numerical integral solutions of Fujita in normalized monograph form [14]. Crank's graphical representation of C/C_0 versus x/W_0, with D_A/D_B as the parameter where W_0 ($=2\sqrt{Dt}$) is the depth of diffusion, renders Fujita's solutions useful.

B. Self-Diffusion Equation Without External Electric Field

In special cases, however, the interdiffusion coefficient $\tilde{D}$ is essentially the same as the self-diffusion coefficient D_A of the incoming species A. One such case is when the self-diffusion coefficients are equal. Inspection of (1) reveals that when $D_A = D_B$ and since $N_A + N_B = 1$, the interdiffusion coefficient $\tilde{D}$ equals D_A. Another case arises when the molar concentration C_A of the incoming species is quite small, i.e., $N_A \approx 0$ and $N_B \to 1$. As a result, $\tilde{D}$ approaches D_A in this case as well. However, since the concentration C_A is small, the diffusion coefficient D_A of the incoming ions is unaffected by their presence inside the glass substrates. This implies that D_A is independent of the position x and the diffusion equation (2) further reduces to the simplest case

$$\frac{\partial C}{\partial t} = D\,\frac{\partial^2 C}{\partial x^2} \tag{3}$$

where we have dropped the subscript A as we are dealing with only one species.

Fabrication of planar waveguides requires the diffusion of atoms with higher electronic polarizability into a glass substrate placed in a large molten salt bath that also contains an indigenous species already present in the glass. Usually the diffusing ion concentration is small compared to that of the indigenous species. A typical example would be the presence of a small concentration of silver ions in a sodium nitrate bath and the diffusion of silver ions into a semi-infinite glass substrate. If the substrate contains no silver ions to start with, then the simple diffusion equation given by (3) applies. To solve (3), we also require the concentration C_0 of Ag^+, although small, be held constant at all times. Therefore, the initial and the boundary conditions are

$$C(x, 0) = 0 \qquad \text{at } x > 0$$

and

$$C(0, t) = C_0 \qquad \text{for all } t \geq 0. \tag{4}$$

The solution of (3) under these conditions is the well-known complementary error function [14]

$$C(x, t) = C_0 \operatorname{erfc}\left(\frac{x}{W_0}\right) \tag{5}$$

where

$$W_0 = 2\sqrt{Dt}$$

and

$$\operatorname{erfc}(z) = \frac{2}{\sqrt{\pi}} \int_z^\infty e^{-\alpha^2}\, d\alpha. \tag{6}$$

W_0 is called the effective depth of diffusion without the application of external field and corresponds to that distance from the waveguide surface where $C/C_0 = \operatorname{erfc}(1) = 0.157$. Curve (a) in Fig. 1 (dashed line) shows a normalized plot of erfc function (5).

C. Self-Diffusion with External Electric Field

The diffusion of incoming cation can be enhanced by applying an external field to the substrate. Fick's equation for the ionic current density J can be modified to include the drift of the incoming ion due to the external electric field E in the forward direction:

$$J = -D\,\frac{\partial C}{\partial x} + \mu E C \tag{7}$$

where μ is the ionic mobility of the incoming species in

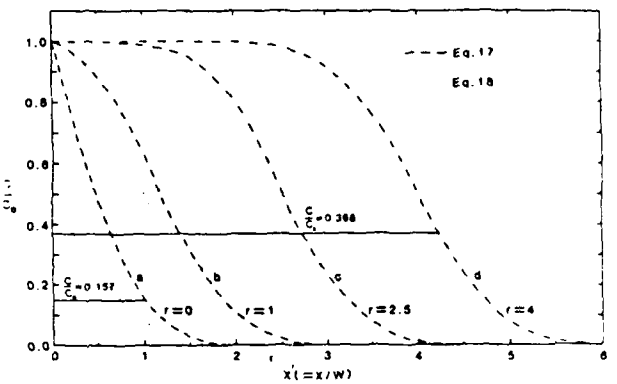

Fig. 1. Plot of concentration versus normalized depth using exact (9) and approximate (10) equations for different values of r ($=\mu Et/2\sqrt{Dt}$).

he host glass substrate. As before, if we assume that D nd μ are independent of position x in the substrate, and f we further assume that for low concentration the term $C(\partial E/\partial X)$ can be ignored, we obtain

$$\frac{\partial C}{\partial t} = D\frac{\partial^2 C}{\partial x^2} - \mu E\frac{\partial C}{\partial x}. \tag{8}$$

For diffusion into a semi-infinite glass substrate with he same initial and boundary conditions, viz. initially, the concentration inside the substrate is zero and the concentration at the surface is held constant at all times, the solution to (8) is given by [16]

$$C(x', r) = \frac{C_0}{2}\left[e^{4rx'}\,\text{erfc}\,(x' + r) + \text{erfc}\,(x' - r)\right] \tag{9}$$

where $x' = x/W_0 = x/2\sqrt{Dt}$ is the normalized effective depth of diffusion without external field and r is the ratio of the depth of diffusion due to the electric field to the effective no-field depth W_0, i.e., $r = \mu Et/W_0 = \mu Et/2\sqrt{Dt}$. For large values of μEt, since erfc approaches zero with increasing x at a faster rate than the growth of the exponential term, the contribution by the first term is negligible and the above equation can be further approximated as

$$C(x', r) \approx \frac{C_0}{2}\left[\text{erfc}\,(x' - r)\right], \qquad r \geq 2.5. \tag{10}$$

Fig. 1 shows the dependence of the diffusing ion concentration on the normalized position x'. The dashed curve (a) represents the case of zero external electric field and curves (b)–(d) correspond to the increasing electric field associated with the ratio $r = 1$, 2.5, and 4, respectively. The dashed curves show the behavior for large field approximation as given by (10). It can be seen that as μEt increases, the field-assisted diffusion dominates the process, and for $\mu Et \geq 2.5\ W_0\ (= 5\sqrt{Dt})$, (10) becomes an excellent approximation for the general solution given by (9). Furthermore, for $\mu Et \geq 2.5\ W_0$, C/C_0 always equals 0.5 at $x' = r$, i.e., at $x = \mu Et$. In fact, under the large field approximation ($r > 2.5$), the argument of the complementary error function (10) is positive only when $x' > r$. The shape of the curve in the region $x' > r$ is the well-known erfc profile. However, in the region $x' < r$, the negative argument of the complementary error function results in an antisymmetric (or inverse) profile about the point $x' = r$ since erfc $(-z) = 2 - \text{erfc}\,(z)$.

A few words about the definitions of the depth of diffusion are in order. In the case of $r = 0$, $W_0\ (\approx 2\sqrt{Dt})$ is an appropriate measure and corresponds to that position in the substrate where $C/C_0 = \text{erfc}(1) = 0.157$. However, for non-erfc profiles obtained in the presence of low external electric fields or buried symmetric profiles, achieved by using the two-step process [13] and which are described in detail later in this paper, this definition is not adequate. The problem can be best illustrated by considering the case of large field-assisted diffusion. If we define the effective depth as before as the point x at which the argument of the complementary error function equals 1, then as seen from (10), the depth of diffusion now represents the point x where $C/C_0 = 0.079$ rather than 0.157. We need, therefore, a different definition for the effective depth. There are two other choices worth considering.

1) $W_{1/2}$ = that value of x for which $C/C_0 = \frac{1}{2}$. This seems appropriate as it has the advantage in that for $r > 2.5$, the effective depth of diffusion $W_{1/2}$ represents the position of the half concentration point and equals μEt, the field-assisted contribution (actual translation, in the case of large fields) to the normal diffusion obtained for $r = 0$.

2) W = that value for which $C/C_0 = 1/e$. This definition seems convenient for defining the width of symmetric or quasi-symmetric index profile obtained in the two-step process where the width of the profile is represented by the distance between the points which have concentrations given by $C/C_0 = 1/e$ where C_0 now is the peak value.

The latter definition for the diffusion depth W for all the cases including the no-field case ($r = 0$) requires reconsideration of the two extreme cases, namely, $r = 0$ and $r \geq 2.5$, in order to relate the depth W to W_0.

1) $r = 0$. For the no-field case, setting $r = 0$ in (9) yields the same relationship as stated by (5), viz. $C/C_0 = \text{erfc}\,(x') = \text{erfc}\,(x/2\sqrt{Dt})$. At the position where $C/C_0 = 1/e = 0.368$, the argument of the complementary error function $x'\,(= x/2\sqrt{Dt})$ must equal 0.64. Thus, the effective depth of diffusion $W = 0.64\ (2\sqrt{Dt})$. In other words,

$$W = 0.64\ W_0 \tag{11}$$

and this can be easily verified from the dashed curve (a) in Fig. 1 by inspecting the position x' at which $C/C_0 = 0.368$.

2) $r \geq 2.5$. Following the above procedure, it can be shown by considering (10) that the normalized depth x' for which $C/C_0 = 0.368$ is given by $x' = r + 0.24$. Therefore,

$$W = \mu Et + 0.24\ W_0. \tag{12}$$

For extremely large values of E, $W \approx \mu Et$.

Hereafter, we will denote the depth of diffusion by W for all the cases including the no-field ($r = 0$) case.

III. Experimental Results

A. Self-Diffusion Without Applied Electric Field

Our experiments were carried out by using soda-lime silicate laboratory (Fisher Brand) glass slides, immersed in a bath of molten sodium nitrate at 330°C containing a small amount of electrolytically released silver ions [9]. The bath was stirred to assure uniform concentration of Ag^+ in the bath. Concentration C_0 of Ag^+ varied from 2×10^{-4} to 2×10^{-3} MF where 1 mmole fraction (10^{-3} MF) corresponds to ≈ 0.5 g of Ag^+, released into a molten bath of 400 g of $NaNO_3$.

First diffusion of Ag^+ ions into the glass substrate was carried out for 30 min with no external field ($E = 0$) and with $C_0 = 2 \times 10^{-4}$ MF. For such small concentrations, according to (5), we expect an error function complement profile irrespective of whether Ag^+ exchange with the constituent Na^+ or self-diffuse into vacant or interstitial sites in the glass matrix. The photograph shown in Fig. 2 shows the depth profile of silver ions in the glass substrate obtained by detecting the backscattered electrons when the sample is bombarded by high-energy (25 kV) electrons in a scanning electron microscope (SEM). On account of the higher atomic weight, contribution of silver atoms to the yield of backscattered electrons is much higher than that of other constituents [17]. Samples were prepared by epoxying a small glass pad made of the same material as the glass substrate over the waveguide surface, then polishing across the edge of the waveguide, and finally depositing about 50 Å thick carbon film over the viewing sample to avoid any charge buildup. The dip in the profile to the left of the waveguiding surface identifies the epoxy region which does not contribute to backscattered electrons. As seen from Fig. 3, the silver ion profile of Fig. 2, when replotted, by assuming the zero-crossing point to be the waveguide surface of the epoxy glass sample interface, agrees very well with the predicted erfc profile (5). By minimizing the sum of the square of the errors, the value of D that best fitted the data is 0.133 μm^2/min, which agrees very well with the value of 0.13 μm^2/min obtained from the modal characteristics of these waveguides, results of which are presented elsewhere [18]. The effective depth of diffusion W_0, specified at $x = 2\sqrt{Dt}$ (at which point the argument of erfc is 1 and $C/C_0 = 0.157$) equals 3.98 μm and agrees very well with the SEM data of samples diffused at 330°C for 30 min. In fact, the value of D for Ag^+ in glass did not vary very much between soda-lime silicate glasses from various vendors (Fisher, Schott, and Labmate).

Several planar waveguides were fabricated without any applied field by varying the time of diffusion for two concentrations $C_0 = 2 \times 10^{-4}$ and 2×10^{-3} MF. Measured values of W exhibit a square root dependence on t, as expected from (5), and this is experimentally verified as shown in Fig. 4. For relatively small concentrations ($C_0 = 2 \times 10^{-4}$ MF), the estimated constant of proportionality equals 0.48. As seen from (11), this must equal the constant of proportionalty $1.28\sqrt{D}$. This implies a value of $D = 0.14$ μm^2/min and agrees quite well with our previous result derived from Fig. 2. However, as concentration is increased above this value, D increased as well. As seen from the W versus t_1 curve for the larger concentration ($C_0 = 2 \times 10^{-3}$), $D = 0.32$ μm^2/min, which is about a factor of two larger than that for the lower concentration. We will further discuss the dependency of D on concentration C_0 in the following paragraph. The subscripts 1 and 2 of parameters E and t in Fig. 4 identify each part of the two-step diffusion process described later. For the present, with the single-step diffusion process, $E_2 = t_2 = 0$ and $t_1 \neq 0$.

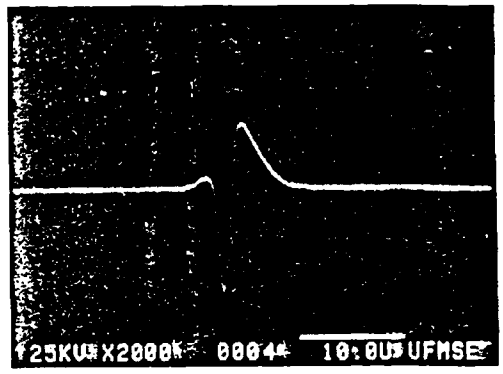

Fig. 2. Ag^+ profile of a planar waveguide fabricated by a first-step diffusion without applied electric field.

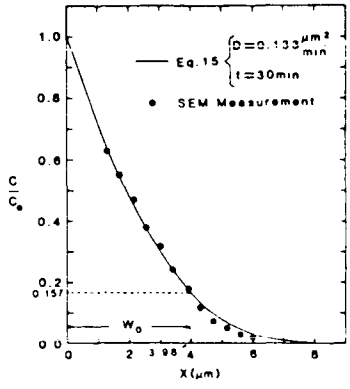

Fig. 3. Comparison of the experimentally measured index profile of Fig. 2 to the theoretical prediction.

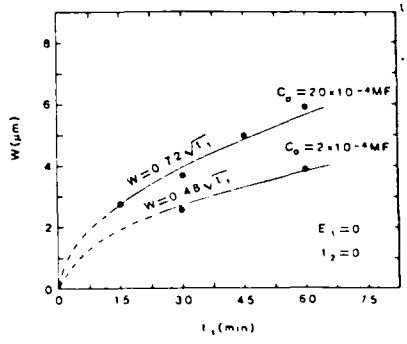

Fig. 4. Variation of diffusion depth with time in one-step, without applied electric field, diffusion process.

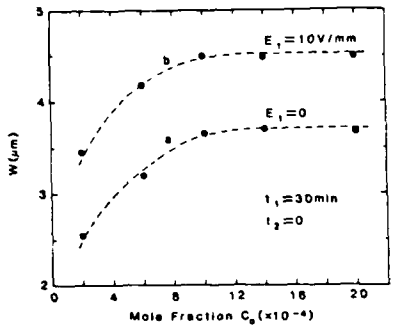

Fig. 5. Variation of diffusion depth with bath concentration in one-step diffusion process.

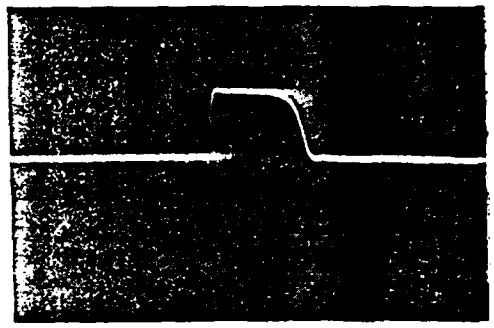

Fig. 6. Ag^+ profile of a planar waveguide fabricated by a first-step diffusion with applied electric field.

TABLE I
DIFFUSION COEFFICIENT VERSUS CONCENTRATION

C_0 (MF)	D (μm^2/min)
2×10^{-3}	0.28
1.4×10^{-3}	0.28
1×10^{-3}	0.25
6×10^{-4}	0.21
2×10^{-4}	0.14

Curve (a) in Fig. 5 shows the dependence of the depth of diffusion W on the silver ion concentration C_0 for $E_1 = 0$ and $t_1 = 30$ min. According to the simple theory for low Ag^+ concentrations, W should be independent of C_0 as D represents the self-diffusion coefficient of incoming silver ions in glass. Instead, W increases monotonically with C_0 until $C_0 \approx 10^{-3}$ MF and then begins to saturate. Table I shows the dependence of D, estimated from the diffusion depth (W), versus concentration (C_0) data.

This dependence indicates the existence of a concentration-dependent D even at such low concentration, even though for a given C_0, W varies as $\sqrt{t}$ as evidenced by Fig. 4. Saturation of W with increasing C_0 could very well mean that Ag^+–Na^+ exchange indeed occurs and that no further sites for Ag^+ indiffusion are available or that the Ag^+ in-diffusion has possibly reached the solubility limit. However, lower values of D for low concentrations are rather unexpected, and the exact diffusion mechanism that is responsible for the W versus C_0 behavior is presently under investigation. Furthermore, the question of whether a simple ion exchange through a liquid–solid interface produces a concentration-dependent diffusion needs to be resolved. It does not appear that the diffusion is restricted to a simple case of self-diffusion of silver ions. Curve (b) in Fig. 5 will be discussed in the following section under self-diffusion with applied electric field.

B. Self-Diffusion with Applied Electric Field

The SEM picture of Fig. 6 shows the Ag^+ profile for diffusion at 330°C for $C_0 = 2 \times 10^{-4}$, $E_1 = 45$ V/mm, and $t_1 = 30$ min. Again, subscript 1 identifies the first, and in this case, the only step in the diffusion process. Fig. 7 shows data points of the SEM profile of Ag^+ for

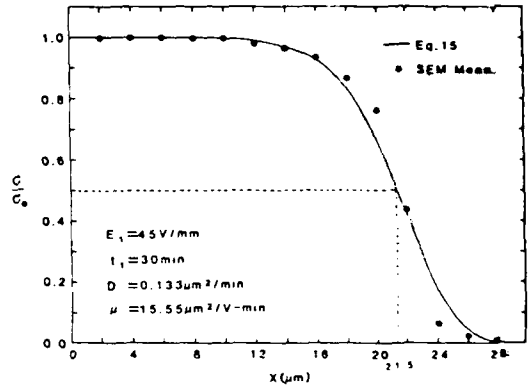

Fig. 7. Comparison of measured index profile of Fig. 6 to the theoretical prediction.

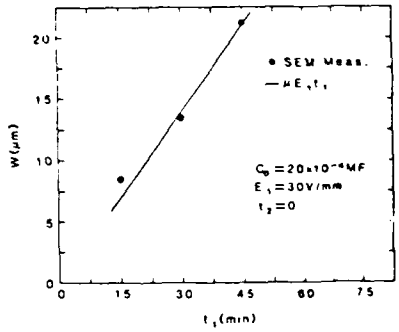

Fig. 8. Variation of diffusion depth with time in one-step, with applied electric field, diffusion process.

$E_1 = 45$ V/mm, $t_1 = 30$ min. With $D = 0.133$ μm^2/min, the best theoretical fit (19) obtained for $\mu = 15.55$ μm^2/V · min is shown as the continuous curve. As seen from Fig. 7, $\mu E_1 t_1 = 21.5$ μm at $C/C_0 = \frac{1}{2}$. Since the ratio r is clearly greater than 2.5, as described earlier, $W_{1/2} = \mu E_1 t_1$, and as seen from (12), the effective depth of diffusion $W \approx \mu E_1 t_1$, illustrating the dominance of field-assisted diffusion. This point is further illustrated in Fig. 8 where the effective diffusion depth W, in the presence of an applied electric field of 30 V/mm for $C_0 = 2 \times 10^{-4}$ MF, is plotted against t_1. For $t_1 = 15$, 30, and 45 min, $r = 1.6$, 2.3, and 2.8, respectively. The solid line represents the field-assisted diffusion depth $\mu E_1 t_1$, i.e., 0.47 t_1, and surprisingly, as seen in Fig. 8, W agrees very well

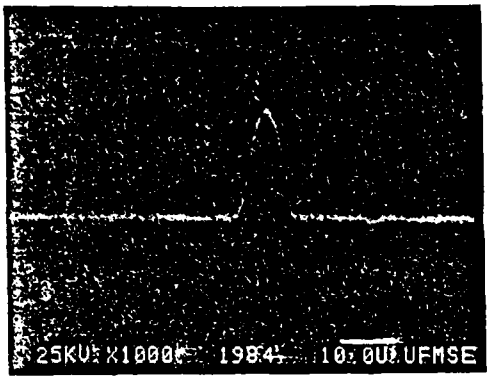

Fig. 9. Ag^+ profile of two planar waveguides (stuck face to face) fabricated by a first-step diffusion; left: without field, right: with field.

with the measured values, although r values are relatively low.

Variation of W versus C_0 with $E_1 = 10$ V/mm and $t_1 = 30$ min, shown in curve (b) in Fig. 5, discussed in the last section, exhibits a similar dependence as curve (a). W saturates as before for $C_0 \geq 10^{-3}$, and for this case, $D \approx 0.3\ \mu m^2/min$. Therefore, W_0 equals 6.0 μm and $\mu E_1 t_1 = 4.67\ \mu m$. This is an intermediate case where $r = 0.78$, and as such, there is no dominance of field-assisted diffusion yet. From Fig. 1, it is seen that $W \approx 1.2\ W_0$. However, measured values in Fig. 5(b) are about 36 percent less. In fact, W equals $\mu E_1 t_2$, and this result is in accordance with the data shown in Fig. 8. Although the data agree well with $r = 0$ and 2.5, for values of r in between, the theory does not seem to be valid. This behavior seems to indicate that the theoretical model is not quite appropriate. Comparison of the diffusion to a low field E_1 should be slightly larger than $0.64\ W_0$ and much smaller than the depth $\mu E_1 t_1 + 0.24\ W_0$ corresponding to large E_1. The measured difference should be less than the calculated value, which is about 2.3 μm. Comparison of curves (a) and (b) in Fig. 5 reveals indeed a shift of only ≈ 1 μm due to the field of 10 V/mm. Whatever the mechanism is of diffusion without the applied field, a translation of the concentration profile occurs due to the electric field. The effective depth of diffusion W equals the translation depth $\mu E_1 t_1$ for both small and large fields, although the theory predicts this behavior only when $r = \mu E_1 t_1 / 2\sqrt{D t_1} \geq 2.5$ since the self-diffusion contribution is negligible only in this region.

Another effect that was observed is illustrated in Fig. 9. Here two waveguide surfaces fabricated under the same conditions, viz. concentration in the bath $C_0 = 2 \times 10^{-3}$, $t_1 = 30$ min, and $T = 330$°C, except that the guide on the left was made with $E_1 = 0$ and the one on the right with $E_1 = 10$ V/mm. According to (9), concentration at the surface ($x' = 0$) should be the same for both waveguides, namely, C_0, regardless of the value of r. However, the SEM picture in Fig. 9 shows that the concentration on the surface in the case of diffusion with electric field is slightly higher. The explanation, we believe, lies in the fact that the finite conductivity of the molten $NaNO_3$ bath (measured to be 0.004 Ω/cm) supports an electric field between the glass surface that is in contact with the bath and the aluminum foil anode placed 10 mm directly beneath it. The field is applied between the cathode, i.e., the metal contact deposited on the other surface of the sample not in contact with the bath and the aluminum foil anode. The Ag^+ concentration increases slightly near the surface of the glass sample as these ions are driven by the electric field towards the surface until an equilibrium is reached due to the increased charge buildup near the surface. A relative potential drop across the distance (10 mm) in the solution between the glass surface and the anode indicates the presence of a field approximately 1.5 V/mm when the applied field was 10 V/mm. This local field causes the concentration to increase in the vicinity of the sample while the field across the sample decreases by a small amount. Careful analysis of Fig. 9 shows that the ratios of the surface concentrations with and without the field to be about 1.1, which is in close agreement with our rough estimation based on a field-induced increase in the concentration at the surface. It is clear that in the case of field-assisted diffusion, the actual concentrations in the presence of an applied field should be considered for diffusion as well as index profile studies. To achieve equal concentrations with and without the presence of applied field, we must reduce the potential drop between the electrode and the glass substrate. One possibility is that the gap between the electrode and the surface guide can be reduced to minimize the potential drop.

One of the problems usually encountered in field-assisted diffusion is that of electrode deterioration [19]. Under the influence of the applied electric field, sodium ions in the glass migrate towards the electrode and are converted into sodium metal at the electrode (cathode). Since sodium is highly reactive, it attacks the aluminum electrode. Thus, films of noble metals like gold or platinum, being chemically inert, serve as better electrodes. Unlike platinum which has a high melting point (1772°C), gold (melting point 1064°C) is easier to evaporate; however, a thin layer of chromium was deposited prior to the evaporation of gold to provide better adhesion to glass. An electrode made of 50 Å chromium and 1000 Å gold has worked well in our experiments.

C. Two-Step Diffusion Process and the Fabrication of Buried Waveguides

Field-assisted diffusion permits tailoring of the refractive index profile. A two-step diffusion process has been used previously to fabricate buried waveguides in glass [13]. In this process, initially, a surface waveguide is formed with field (45 V/mm)-assisted diffusion of silver ions (Fig. 6) for $t_1 = 30$ min. This was followed by a second field-assisted diffusion for 30 min under the same field conditions now in pure sodium nitrate. The silver ions move deeper inside the glass substrate under the influence of the applied electric field. In addition, the new boundary condition at the surface of the substrate, viz. that $C_0 = 0$, requires out-diffusion of silver ions as well,

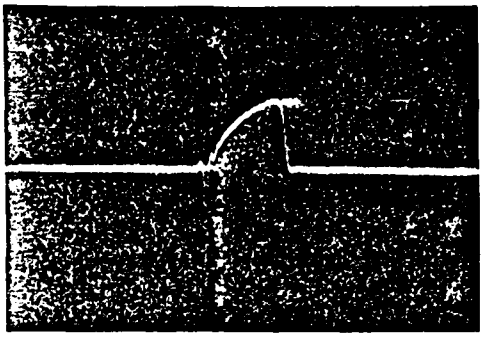

Fig. 10. Skewed index profile of a buried waveguide fabricated by a two-step diffusion process.

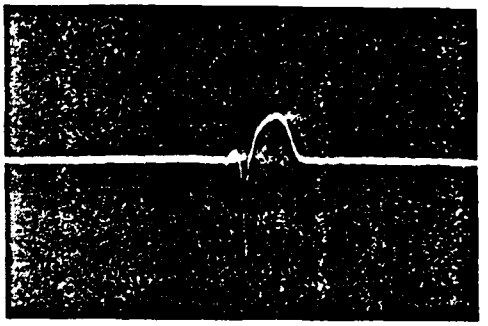

Fig. 11. Nearly symmetrical index profile of a buried waveguide fabricated by a two-step diffusion process.

d perhaps sodium diffuses into the surface. As a result, buried waveguide is formed as shown in the SEM photograph of Fig. 10. Our initial analysis of experimental data indicates a net decrease, although quite small, in the content of Ag^+ in the substrate. The buried waveguides fabricated in this fashion exhibit skewed index profiles that are not compatible with optical fibers which have symmetric index profiles.

We have investigated the two-step diffusion process in detail. We find that buried waveguides with nearly symmetric profiles can be fabricated by using either simple (no-field) or field-assisted diffusion in the first step, followed by either a no-field or an appropriate field-assisted diffusion in the second step.

The six parameters which control the dimensions and the index profile of a buried waveguides are given below.

t_1 = Time of diffusion in the first step ($NaNO_3$ + Ag^+).
E_1 = Applied field in the first step ($NaNO_3$ + Ag^+).
t_2 = Time of diffusion in the second step (pure $NaNO_3$).
E_2 = Applied field in the second step (pure $NaNO_3$).
C_0 = Silver ion concentration in the bath.
T = Fabrication temperature in °C.

Diffusion time represents the total immersion time. It is estimated that the total warm-up and cool-down period is not more than a few minutes.

In the two-step diffusion process to fabricate symmetrical, buried waveguides reported here, we have kept $E_1 = 0$ and $t_1 = 30$ min so that erfc profiles are obtained during the first step. Fig. 11 shows a SEM photograph of the nearly symmetrical profile for $E_2 = 30$ V/mm and $t_2 = 30$ min. The rest of the experiments were carried out by keeping the field during the second step at $E_2 = 10$ V/mm for each C_0 ($= 2 \times 10^{-4}$, 10^{-3} MF) and varying the duration t_2 of the second step diffusion. Fig. 12 shows the effective width W, measured between $1/e$ points from the SEM photographs. Increasing t_2 increases the width almost in proportion to $\sqrt{t_2}$ for small concentrations. As the silver ions in the glass tend to drift further into the substrate due to the field E_2, they also tend to diffuse out as well towards the surface because the new boundary condition that $C_0 = 0$ now imposes at the surface during the second step. For $C_0 = 10^{-3}$ MF and E_2 now set at 30 V/mm, similar W versus t_2 behavior (Fig. 12) is seen. However, for a given $C_0 = 10^{-3}$ MF and t_2 (30 min), increasing E_2 increases the width W linearly as illustrated in Fig. 13. For E_2 between 5 and 50 V/mm and $t_2 = 30$ min, $\mu_2 E_2 t_2$ varies between 2.3 and 23; therefore, for $E_2 > 20$ V/mm, the field is essentially large enough to translate the profile linearly deeper into the substrate. Analytical study of the depth of diffusion and the width of the buried, diffused profile for the two-step process and its correlation with the experimental result are presently being pursued.

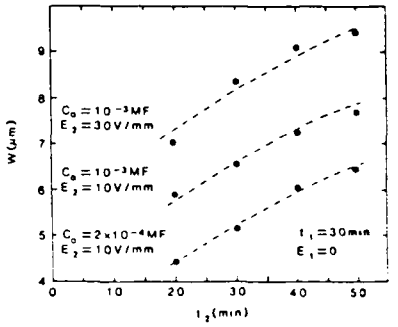

Fig. 12. Variation of diffusion depth with second step diffusion time in two-step diffusion process.

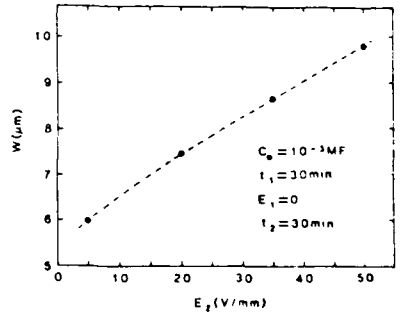

Fig. 13. Variation of diffusion depth with the applied field in second step in two-step diffusion process.

The SEM photograph in Fig. 14 illustrates two buried waveguide samples epoxied face to face. For the sample on the right, $E_1 = 10$ V/mm, and for the one on the left, $E_1 = 0$. In both cases, $t_1 = 30$ min, $E_2 = 10$ V/mm, and

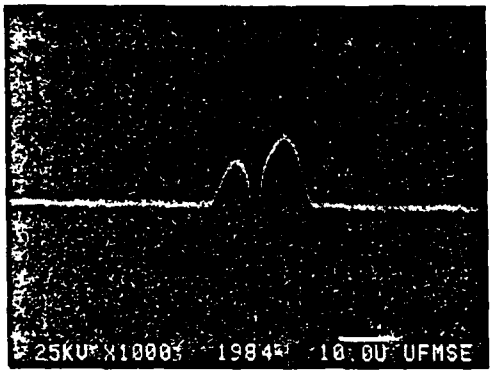

Fig. 14. Nearly symmetrical index profile of two buried waveguides fabricated without (left) and with (right) applied electric field in the first step.

t_2 = 30 min. As before, we see an increased peak index due to an increased concentration of silver ions at the surface with the presence of an electrical field during the first step. As before, an increase in concentration at the glass surface occurs due to action of the field in the bath.

VI. Conclusion

In conclusion, we have presented a detailed study of the Ag^+-Na^+ exchange in soda-lime silicate glasses in a molten bath containing a mixture of $NaNO_3$ and Ag^+. Information on the index distribution in the glass substrate, required for the design of optical waveguides, can be obtained by studying the Ag^+ concentration profile. For low Ag^+ concentrations, this is a good approximation.

Concentration profiles $C(x, t)$ obtained using backscattered electrons in a SEM indicate that for low Ag^+ concentration C_0 at the surface, the profile is given by the complementary error function. In fact, $C(x, t)/C_0$ = erfc (x') where the normalized diffusion depth $x' = x/W_0$ and $W_0 = 2\sqrt{Dt}$ is the effective diffusion depth measured at the point $x' = 1$. Our experimental results, as evidenced by erfc profiles for Ag^+ diffusion without applied field in conjunction with the theoretical analysis, confirm the fact that for low concentrations (C_0), the nature of the diffusion process—whether it is self-diffusion of Ag^+ or Ag^+-Na^+ exchange—is indistinguishable. From the experimental data, the self-diffusion coefficient D for Ag^+ in glass was determined to be 0.133 μm^2/min for low Ag^+ concentrations and increased linearly with C_0 until it saturated at about 0.3 μm^2/min, and this value did not vary much with different substrates obtained from various vendors. In addition, the effective diffusion depth W varied as the square root of diffusion time t, irrespective of the concentration C_0. However, monotonic increase of diffusion depth W with Ag^+ concentration until C_0 equals 10^{-3} MF is probably due to the glass reaching the Ag^+ solubility limit, and this behavior is presently being investigated. Further work is presently being undertaken in order to better understand the diffusion.

Application of an external field E during diffusion enhances the depth of diffusion. While for $E = 0$, we obtain an erfc profile, viz. erfc (x') for large E fields, the profile can accurately be described by $C/C_0 = \frac{1}{2}$ erfc $(x' - r)$ where r is the ratio of μEt over $2\sqrt{Dt}$. As long as $r \geq 2.5$, the translation of the profile due to the presence of the field is much larger than that due to self-diffusion. The dominance of the field-assisted diffusion is illustrated by the fact that the effective depth of diffusion W, defined as the distance from the surface to the $1/e$ concentration point, however, equals $\mu Et + 0.24\ W_0$. For large fields, effective depth of diffusion W essentially varies linearly with E and t. Although for large fields, the entire erfc profile appears to be translated by μEt from the surface due to the application of the field E, only the portion of the profile for $x' > r$ (i.e., $x \geq \mu Et$) represents a complementary error function with positive argument. Our experimental results confirm the above predictions, and from the data, the best fit yields a value of the mobility μ of Ag^+ in glass to be 15.55 $\mu m^2/V \cdot$ min. In addition, as with the case when E was zero, the square root dependence of the effective diffusion depth W on time t and the linear dependence of W versus C_0 for low concentrations ($C_0 \leq 10^{-3}$ MF) were observed. $C_0 = 10^{-3}$ MF seems to be the limit at which the diffusion coefficient of Ag^+ into glass seem to saturate. Due to the presence of a local electric field in the bath near the surface, the surface concentration of Ag^+ increases with the applied E field.

Finally, we have demonstrated a two-step diffusion process where an initial surface waveguide formed with either E equal to zero or some finite value during the first step can be modified to yield a buried, symmetrical fiber-like profile by a second diffusion in a bath of pure sodium nitrate. The effective depth of diffusion W measured between $1/e$ points of the peak value of the symmetric profiles varies as $\sqrt{t_2}$ with $E_1 = 0$ and for any given C_0, t_1, and E_2. Moreover, W, as before, varies linearly with E_2 (and probably with t_2) when the field $E_1 = 0$ for a given C_0, t_1, and t_2 (or E_2). As before, the peak of the buried concentration profile of the sample, fabricated under the same conditions except with the field $E_1 \neq 0$, showed an increase over that fabricated with $E_1 = 0$.

The theoretical analysis [16] confirms our experimental results for diffusion with either no applied or very large applied fields. For intermediate E fields, the estimated diffusion depths are much larger than the measured values. This discrepancy needs further study of the diffusion mechanism.

Acknowledgment

The authors would like to thank Prof. P. Holloway and Prof. J. Hren for suggesting the backscattered electron technique for Ag^+ concentration studies. We also acknowledge the assistance of the Major Analytical Instrumentation Center in the SEM analysis. The critical reading of the manuscript by Prof. R. Srivastava and Prof. T. J. Anderson has helped improve the clarity of the paper. We are grateful to Dr. D. Ulrich for his continued support of this work.

REFERENCES

[1] V. Neuman, O. Parriaux, and L. M. Walpita, "Double-alkali effect: influence on index profile of ion-exchanged waveguides," *Electron. Lett.*, vol. 15, pp. 704–706, 1979.

[2] T. G. Giallorenzi, E. J. West, R. Kirk, R. Ginther, and R. A. Andrews, "Optical waveguides formed by thermal migration of ions in glass," *Appl. Opt.*, vol. 12, pp. 1240–1245, 1973.

[3] G. Stewart, C. A. Miller, P. J. R. Laybourn, C. D. W. Wilkinson, and R. M. De LaRue, "Planar optical waveguides formed by silver ion migration in glass," *IEEE J. Quantum Electron.*, vol. QE-13, pp. 192–200, 1971.

G. H. Chartier, P. J. Jaussaud, A. D. DeOliveira, and O. Parriaux, "Optical waveguides fabricated by electric-field controlled ion exchange in glass," *Electron. Lett.*, vol. 14, pp. 132–134, 1978.

M. Imai, N. Haneda, and Y. Ohtsuka, "Losses in optical waveguides formed by silver-sodium ion exchange," *J. Lightwave Technol.*, vol. LT-1, pp. 611–615, 1983.

R. K. Lagu and V. Ramaswamy, "Fabrication of single-mode glass waveguides by electrolytic release of silver ions," *Appl. Phys. Lett.*, vol. 45, pp. 117–118, 1984.

T. Izawa and H. Nakagome, "Optical waveguides formed by electrically induced migration of ions in glass plates," *Appl. Phys. Lett.*, vol. 21, pp. 584–586, 1972.

T. Findakly, "Glass waveguides by ion-exchange: A review," *Opt. Eng.*, vol. 24, pp. 244–250, 1985.

S. I. Najafi, V. Ramaswamy, and R. K. Lagu, "An improved method for fabricating ion-exchanged waveguides through electrolytic release of silver ions," *J. Lightwave Technol.*, vol. LT-3, no. 4, pp. 763–766, 1985.

R. K. Lagu, S. I. Najafi, and V. Ramaswamy, "In situ measurement of ionic concentration during fabrication of ion-exchanged waveguides," *Appl. Opt.*, vol. 23, pp. 3925–3930, 1984.

R. V. Ramaswamy, R. K. Lagu, and S. I. Najafi, "Fabrication of ion-exchanged glass waveguides through electrolytic release of silver ions," in *SPIE Proc., 1st Int. Conf. Integrated Opt. Circuit Eng.*, Cambridge, MA, Oct. 21–26, 1984.

[4] R. V. Ramaswamy, R. C. Alferness, and M. Divino, "High efficiency single-mode fiber to Ti:$LiNbO_3$ waveguide coupling," *Electron. Lett.*, vol. 18, pp. 30–31, 1982.

[5] R. K. Lagu and R. V. Ramaswamy, "Silver ion-exchanged, buried, glass waveguides with symmetric index profile," submitted to *Appl. Phys. Lett.*

[6] J. Crank, *The Mathematics of Diffusion*. London: Oxford Univ. Press, 1956.

[7] R. H. Doremus, "Exchange and diffusion of ions in glass," *J. Phys. Chem.*, vol. 68, pp. 2212–2218, 1964.

[8] R. Sh. Malkovich, "Methods for calculating the mobility of impurity ions in a solid," *Sov. Phys. Solid State*, vol. 2, pp. 2479–2488, 1961; T. I. Cucher, "The problem of diffusion in an evaporating solid medium," *Sov. Phys. Solid State*, vol. 3, pp. 401–404, 1961.

[17] J. Goldstein, D. Newbury, P. Echlin, D. Joy, C. Fiori, and E. Lifshin, *Scanning Electron Microscopy and X-Ray Microanalysis*, New York: Plenum, 1981.

[18] R. K. Lagu and R. V. Ramaswamy, "Process and waveguide parameter relationships for the design of planar, silver ion-diffused glass waveguides," submitted to *J. Lightwave Technol.*

[19] T. Findakly and E. Garmire, "Reduction and control of optical waveguides losses in glass," *Appl. Phys. Lett.*, vol. 34, pp. 855–856, 1980.

Ramu V. Ramaswamy (M'62—SM'80) was born in Madras, India, in June 1938. He received the B.S. degree in physics from Madras University, Madras, India, in 1957, and the Diploma D.M.I.T. in electronics engineering from Madras Institute of Technology, Chromepet, Madras, India, in 1960. He received the M.S. and Ph.D. degrees in electrical engineering from Northwestern University, Evanston, IL, in 1962 and 1969, respectively. His doctoral work consisted of wave-propagation studies in semiconductor plasmas.

From 1962 to 1965, he served as a member of the research department of Zenith Radio Corporation, Chicago, IL, working on solid-state parametic amplifiers, and microwave components. In 1969, he joined Bell Laboratories, Crawford Hill Laboratory, Holdmel, NJ, where he was engaged in research on thin-film optical device, polarization effects in single-mode fibers and fiber-waveguide couplers. Since 1981, he has been a Professor in the Department of Electrical Engineering, University of Florida, Gainesville, where his current interests include passive integrated-optical devices, fiber-optic sensors, and optoelectronic devices. He is currently the Director of both the Photonics Research Laboratory in the Electrical Engineering Department and a university-wide interdisciplinary program known as MICROFABRITCH which will emphasize both the fundamental and engineering aspects in research and development of novel layered materials and structures for optical and high speed electronic micro circuits. Dr. Ramaswamy is a senior member of Sigma Xi.

S. Iraj Najafi was born in Tabrize, Iran, on March 2, 1953. He received the B.Sc. and M.Sc. degrees in physics from Pahlavi University of Shiraz and the Docteur-Ingenieur (Ph.D.) degree from Ecole Centrale des Arts et Manufactures of Paris, Paris, France.

He joined the optical communication group, Department of Electrical Engineering, University of Florida, Gainesville, in June 1984 as a post-doctoral research associate. His present research interests include fabrication and characterization of integrated-optical devices.

REFERENCE [11]

Ion exchange between soda–lime–silica glass and sodium nitrate – silver nitrate molten salts

P. Chludzinski
Department of Chemical Engineering

R. V. Ramaswamy
Department of Electrical Engineering

T. J. Anderson
Department of Chemical Engineering

University of Florida, Gainesville, Florida 32611, USA

Manuscript received 3 November 1986
Revision received 5 January 1987

The ion exchange process of silver in a $AgNO_3$–$NaNO_3$ melt for sodium in a soda–lime–silica glass was studied at 330°C as a function of melt mixing condition, exchange time, and melt composition. Using wet chemical etching and atomic absorption spectroscopy, silver concentration profiles in the glass were obtained for melt compositions in the range $1{\cdot}9 \times 10^{-4}$ to $1{\cdot}2 \times 10^{-2}$ silver cation fraction. From the results of studies with variable mixing conditions and exchange times, melt mass transfer and kinetic limitations were found to be negligible. The 330°C equilibrium isotherm was determined from the measured glass surface concentrations and could be described by a regular solution model in the melt and a n type model in the glass. The silver self diffusion coefficient was obtained by a Matano–Boltzmann procedure from the measured concentration profiles and a value $4{\cdot}1 \times 10^{-11}$ cm²/s is reported.

Glass waveguides have recently generated considerable interest as a possible basis for passive integrated optical devices: they are attractive because they can readily be coupled to an optical fibre and the substrate is inexpensive compared to other material candidates such as GaAs and $LiNbO_3$. Glass waveguides are commonly fabricated with a field-assisted ion exchange process between molten salt and glass.[1-8] Unlike $LiNbO_3$ waveguides, ion exchanged glass waveguides cannot be tuned electrooptically to compensate for fabrication errors[9] and consequently, strict fabrication tolerances must be met to produce useful devices. An understanding of the transport phenomena and equilibrium chemistry would benefit the development of improved process control techniques.

When a soft glass, such as soda–lime–silica glass, is introduced into a salt melt containing monovalent cations such as Ag^+, these ions can exchange with mobile cations such as sodium in the glass.[10] The Ag^+–Na^+ ion exchange process can be described by the chemical reaction

$$Ag^+ + \bar{N}a^+ \rightleftarrows \bar{A}g^+ + Na^+ \qquad (1)$$

where the bar indicates the cation in the glass phase.

In a liquid–solid exchange process, the rate of ion exchange can be limited by mass transfer of reactants to and removal of products from the reaction interface in the melt, by the kinetics of the reaction at the interface, and by diffusion and drift of cations in the glass. In the absence of melt mass transfer and kinetic limitations, the equilibrium state of Reaction (1) specifies the surface boundary condition of the glass diffusion process. The cation exchange profile may be controlled by manipulating this boundary condition, the cation transport properties in the glass, and the applied electric field.

In soda–lime–silica glass, the extent of silver–sodium ion exchange strongly changes the refractive index,[3,5,6,9,11] thus making it attractive for optical waveguides. The ion exchange kinetics[10,12-21] and equilibrium condition[21-25] of silver exchange have been investigated for a variety of glasses but the transport and thermodynamic properties depend on the specific exchange conditions and glass composition. In the present investigation the importance of melt mass transfer limitations, the equilibrium isotherm, and solid phase transport properties are investigated under processing conditions and with a glass composition that have been used to produce low loss single mode waveguides.[26]

Experimental procedure

The ion exchange of Ag^+ with Na^+ in soda-lime-silica glass was investigated as a function of time, melt stirring condition, and melt composition for $AgNO_3$–$NaNO_3$ molten salts dilute in silver. All experiments were performed at 330 ± 2°C for exchange times in the range of 1–4 h and silver cation fractions in the range of $1{\cdot}90 \times 10^{-4}$ to $1{\cdot}20 \times 10^{-2}$ (see Table 1). Fisher brand microscope slides were used in this work, and the composition and density, obtained from the manufacturer, are given in Table 2. Precleaned slides were rinsed in deionised water, allowed to dry, and placed in a sample holder prior to each experiment. The salt mixture was prepared by weighing between 400 and 600 g of $NaNO_3$ and the desired amount of $AgNO_3$. The variation of the melt composition as a result of the exchange process was never more than 2%. The bath, sample holder, and stirrers were constructed of aluminium; the thermocouple sheath was stainless steel.

After exchange the glass sample was removed from the melt and allowed to cool, and subsequently washed in deionised water to remove adsorbed salt. The glass was then etched in steps in a 0·58 wt% HF solution (a typical etch rate was 0·08 μm/min) and the resulting etch solution for each step was analysed for silver with a Perkin-Elmer model 280 atomic absorption spectrophotometer calibrated with standards of known concentration. The estimated precision of the concentration is $\pm 0{\cdot}03$ cation fraction and of the depth is $\pm 1{\cdot}6 \times 10^{-6}$ cm. In this manner concentration profiles were determined.

Table 1. *Summary of experimental conditions for ion exchange studies at 330 C*

Sample	N_{Ag}	Time (h)	Number of stirrers
A	$1{\cdot}90 \times 10^{-4}$	1	0
B	$1{\cdot}90 \times 10^{-4}$	1	0
C	$1{\cdot}90 \times 10^{-4}$	1	1
D	$1{\cdot}90 \times 10^{-4}$	1	1
E	$1{\cdot}90 \times 10^{-4}$	1	2
F	$1{\cdot}90 \times 10^{-4}$	3	1
G	$1{\cdot}90 \times 10^{-4}$	4	1
H	$9{\cdot}97 \times 10^{-4}$	4	1
I	$1{\cdot}97 \times 10^{-3}$	4	1
J	$4{\cdot}06 \times 10^{-3}$	4	1
K	$8{\cdot}03 \times 10^{-3}$	4	1
L	$1{\cdot}20 \times 10^{-2}$	4	1

Table 2. *Chemical composition (wt%) of Fisher brand glass slide: Density = 2·4667 g/cm³*

Oxide	
SiO_2	72·25
Na_2O	14·31
CaO	6·40
Al_2O_3	1·20
K_2O	1·20
MgO	4·30
Fe_2O_3	0·03
SO_3	0·30

Results and discussion

Rate limitation on the surface concentration

In order to ensure that the measured glass surface concentration corresponds to the value in equilibrium with the melt at the overall liquid composition, the influence of liquid phase mass transfer or surface kinetic effects must be negligible. If the mass transport processes in the melt and glass are purely diffusional then, for an infinite composite medium with constant diffusion coefficients, the quantity $(\bar{C}_i/C_i)(\bar{D}_i/D_i)^{1/2}$ must be much smaller than unity for the concentration gradient in the melt to be negligible.[27] Using the Ag^+ tracer diffusion coefficient in $NaNO_3$ of Inman & Bockris[28] and the Ag^+ self-diffusion coefficient in soda-lime-silica glass and the distribution coefficient determined in this study, the characteristic quantity is of the order of 0·1. Based on this estimate, diffusion limitations in the melt are not expected to dominate the exchange rate. It is noted that the glass surface concentration is independent of time in this model and decreases with increasing importance of diffusion limitations in the melt. Another possible limitation on the surface concentration is the presence of a resistance at or near the melt–glass interface (e.g. mass transfer, reaction). If the rate of this process is assumed to be first order and characterised by a proportionality constant, α, the dimensionless variable $\alpha(t/\bar{D}_i)^{1/2}$ should be large (>10) to ensure that the measured glass surface concentration corresponds to the value in equilibrium with the bulk melt concentration. In this model the surface concentration is an increasing function of time. Measurement of the surface concentration as a function of melt mixing conditions should provide evidence on the existence of diffusional or convective mass transfer (the value of α is a function of the mixing conditions) limitations. In addition, measurement of the surface concentration as a function of exchange time should indicate whether melt depletion, convective mass transfer, or surface kinetic effects are important.

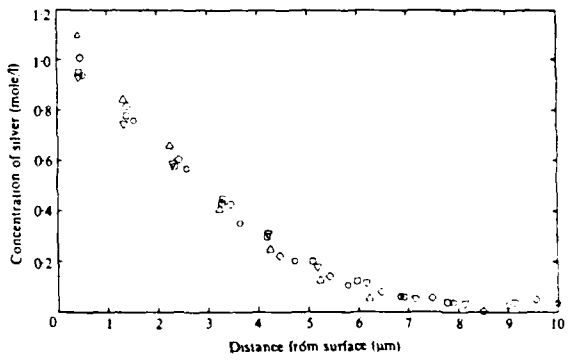

Figure 1. *Concentration profiles of silver from a silver nitrate – sodium nitrate melt into soda-lime-silica glass at 330°C for 60 min; $N_{Ag} = 1{\cdot}9 \times 10^{-4}$*
▽ sample A △ sample C ○ sample E
□ sample B ◇ sample D

The influence of stirring rate and exchange time on the Ag^+–Na^+ exchange was studied for a Ag^+ melt cation fraction of 1.90×10^{-4}. This composition is the lowest one examined and represents the composition with the largest distribution coefficient, $\bar{C}_i/C_i$, and therefore with the largest possible melt diffusional limitation. Measured Ag^+ concentration profiles are illustrated in Figure 1 under conditions of no stirring and with one or two stirrers placed in the molten salt bath for an exchange time of 1 h. It is observed that the concentration profiles do not vary significantly as the mixing conditions are changed. Concentration profiles were also measured for exchange times of 3 and 4 h with one stirrer in place. As shown in Table 3, a slight decrease in the surface concentration was observed; this was within the experimental error of the measurement and only a small portion of the decrease is attributable to melt depletion. It can be concluded from these results that the dominant resistance in the exchange process is cation transport in the glass.

Ion exchange equilibrium

The surface concentration of Ag^+ in soda-lime-silica glass was determined for each sample listed in Table 1 by extrapolation of the measured concentration profiles; this was performed by normalising the data for silver concentration in the glass, $\bar{C}_{Ag}$, against depth with an arbitrary concentration, $\bar{C}_s$. The normalised concentration was equated to the normal probability distribution

$$\frac{\bar{C}_{Ag}}{\bar{C}_s} = \text{prob}(z) = \frac{1}{\sqrt{2\pi}} \int_{-\infty}^{z} \exp(-y^2/2)\,dy, \qquad (2)$$

which is related to the error function by

$$\text{erf}(z) = 2\,\text{prob}(z\sqrt{2}) - 1. \qquad (3)$$

The extrapolation of the data for $\bar{C}_{Ag}$ against depth in probability coordinates is convenient because the transformed data are more adaptable to simple representation (i.e. because prob(z) is related to erf(z), sections of data with an approximately constant interdiffusion coefficient are linear). The extrapolated silver surface cation fractions and bulk melt cation fractions are summarised in Table 3.

The equilibrium constant for the exchange reaction

Table 3. *Extrapolated Ag^+ surface concentrations*

Sample	N_{Ag}	$\bar{N}_{Ag}$
A	1.90×10^{-4}	0.0837
B	1.90×10^{-4}	0.0793
C	1.90×10^{-4}	0.0973
D	1.90×10^{-4}	0.0918
E	1.90×10^{-4}	0.0857
F	1.90×10^{-4}	0.0797
G	1.90×10^{-4}	0.0744
H	9.97×10^{-4}	0.231
I	1.97×10^{-3}	0.339
J	4.06×10^{-3}	0.444
K	8.03×10^{-3}	0.547
L	1.20×10^{-2}	0.527

is given by

$$K = \frac{\bar{a}_{Ag}\, a_{Na}}{\bar{a}_{Na}\, a_{Ag}} = \frac{\bar{\gamma}_{Na}\, N_{Na}\, \bar{a}_{Ag}}{\bar{\gamma}_{Ag}\, N_{Ag}\, \bar{a}_{Na}} \qquad (4)$$

in which a_i is the thermodynamic activity of component i and γ_i is the liquid phase activity coefficient of i where i is the mole fraction of $NaNO_3$ or $AgNO_3$ in the melt, N_i. Taking the reference state for the melt as the pure salt, the emf measurements of Laity[29] at 330°C suggest regular solution behaviour with a value of the interaction energy, A, equal to 3515 J/mole. The standard state selected for the solid exchanger is that in which all of the exchangeable cations are of the ion of interest. A successful empirical relationship first suggested by Rothmund & Kornfield[30] for the ratio of the activities of the ions in a glass exchanger is

$$\frac{\bar{a}_{Ag}}{\bar{a}_{Na}} = \left(\frac{\bar{N}_{Ag}}{\bar{N}_{Na}}\right)^n \qquad (5)$$

where $\bar{N}_i$ is the cation mole fraction. Garrels & Christ[31] have shown that this empirical relationship is equivalent to regular solution theory for intermediate glass compositions. Substitution of the regular solution expressions for the melt component activity coefficients and the ratio of the component activities in the glass into Equation (4) gives

$$\ln\left(\frac{N_{Ag}}{1-N_{Ag}}\right) + \frac{A}{RT}(1-2N_{Ag}) = n\ln\left(\frac{\bar{N}_{Ag}}{1-\bar{N}_{Ag}}\right) - \ln K. \qquad (6)$$

If the assumption of regular solution behaviour in both solutions is valid, a plot of the left hand side of Equation (6) against $\ln[(1-\bar{N}_{Ag})/\bar{N}_{Ag}]$ should yield a straight line with slope equal to n and intercept equal to $\ln(1/K)$. This type of plot is illustrated in Figure 2 and it appears to be linear to within experimental error with a least squares value of n equal to 1.49 and K equal to 75. Thus, the partitioning of silver ions between the nitrate melt and the soda-lime-silica glass is nonlinear in the composition range studied.

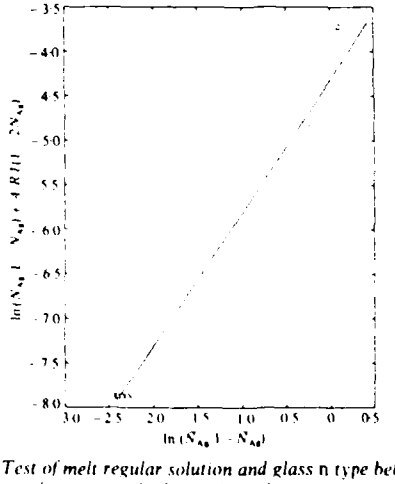

Figure 2. *Test of melt regular solution and glass n type behaviour for Ag^+–Na^+ exchange in soda-lime-silica glass*

The results of these equilibrium studies are compared in Figure 3 to the smoothed measurements of Schulze[23] in a soda–lime–silica glass of wt% composition 69SiO_2, 15·2Na_2O, 3·6K_2O, 7·4CaO, 4·4Al_2O_3, 0·4Fe_2O_3, 0·4MgO. Using the same regular solution description of the melt, the values of n and K derived from the data of Schulze are reported to be 1·08 and 120. Figure 3 also shows the 315°C equilibrium results of Stewart & Laybourn[25] determined on a type of glass similar to that studied in this work; the reported values of n and K are 1·32 and 131. The value of n determined in this study indicates larger positive deviations from ideal solution behaviour than suggested by either Schulze or Stewart & Laybourn and is close to the value of 1·4 reported by Garfinkel[22] for a sodium borosilicate glass. The reason for the difference in the values of this exponent is not clear, but is probably related to differences in either glass composition or structure. The value of the temperature dependent equilibrium constant is in fair agreement with the results of Schulze and Stewart & Laybourn as well as those of Doremus[21] for the high silica phase of two-phase Pyrex. The results of this work suggest a large value for the silver partition coefficient, similar to the values determined by silver ion tracer diffusion studies in soda–lime–silica glass ($\bar{N}_{Ag}/N_{Ag} = 200$)[10] and sodium borosilicate glass ($\bar{N}_{Ag}/N_{Ag} = 500$).[22]

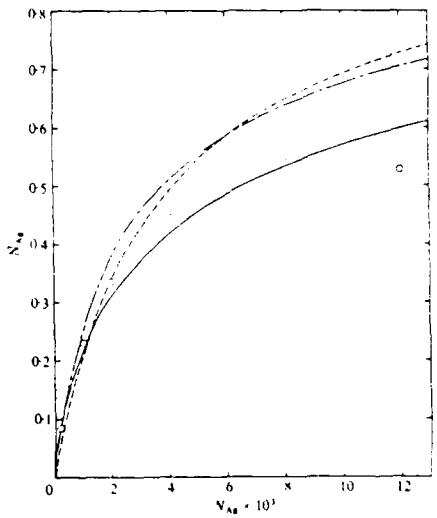

Figure 3. *Partitioning of silver between a silver nitrate – sodium nitrate melt and soda-lime-silica glass at 330°C*

——— calculated isotherm with $n = 1·49$ and $K = 75$
- - - - - calculated isotherm with $n = 1·08$ and $K = 120$ from a reduction of the measurements of Schulze[23]
— - — - calculated isotherm with $n = 1·32$ and $K = 131$ from measurements of Stewart & Laybourn[25]

Interdiffusion

Under the experimental conditions of this study the ion exchange process consists of the inward diffusion of Ag^+ and an equal flux of Na^+ in the opposite direction, the Ag^+ and Na^+ surface concentrations being constant and in equilibrium with the ion concentrations in the bulk melt. This process is characterised by a concentration dependent interdiffusion coefficient[10]

$$D_{AB} = \frac{D_A D_B}{\bar{N}_A D_A + \bar{N}_B D_B} \frac{\partial \ln \bar{a}_i}{\partial \ln \bar{C}_i} \tag{7}$$

where D_A and D_B are the cation self-diffusion coefficients and may also be a function of composition. With the solution model of Rothmund & Kornfeld[30] the thermodynamic factor, $\partial \ln \bar{a}_i / \partial \ln \bar{C}_i$, has a value equal to n.

Values of the interdiffusion coefficient were evaluated numerically from the measured silver ion concentration using the Matano–Boltzmann method.[27] All slopes were measured from data smoothed by mapping it into probability coordinates and all calculations were performed in double precision to minimise round-off error. The concentration profiles were extrapolated beyond the largest measured depth by assuming that the interdiffusion coefficient was constant in this dilute region (i.e. $D_{Ag^+\text{-}Na^+} = D_{Ag^+} = \text{constant}$).

From the definition of cation mole fraction, Equation (7) can be rearranged to give

$$\frac{n}{D_{AB}} = \frac{1}{D_A} + \bar{N}_A \left(\frac{1}{D_A} - \frac{1}{D_B} \right). \tag{8}$$

If the self-diffusion coefficients are independent of composition, a plot of $n/D_{Ag^+\text{-}Na^+}$ against $\bar{N}_{Ag^+}$ should produce a straight line with an intercept of $1/D_{Ag^+}$ and slope of $-[(1/D_{Ag^+}) - (1/D_{Na^+})]$. Shown in Figure 4 is a plot of the reciprocal interdiffusion coefficient calculated by the above procedure against the silver cation fraction for the three highest Ag ion melt concentrations studied. It is seen that a linear relationship is followed at high Ag^+ glass concentrations but deviations from a straight line are found at low Ag^+ concentrations, such that a maximum in $n/D_{Ag^+\text{-}Na^+}$ is produced. An extremum in the calculated interdiffusion coefficient against $\bar{N}_{Ag}$ was also reported by Fainaro *et al.*[12] for several concentration profiles

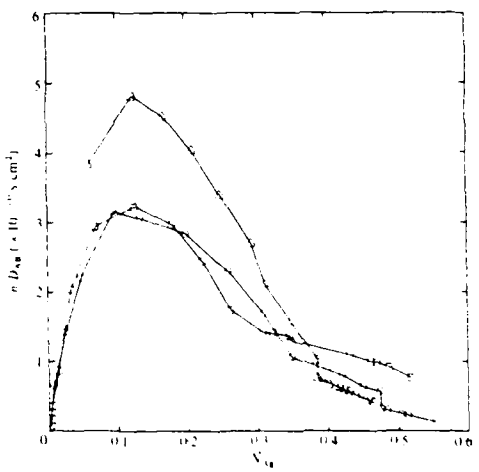

Figure 4. *Interdiffusion coefficient calculated by the Matano–Boltzmann procedure as a function of silver cation fraction at 330°C* ○ sample J □ sample K △ sample L

measured in soda–lime–silica and alkali aluminosilicate glasses. An extremum in the value of $D_{Ag^+-Na^+}$ as a function of cation fraction is consistent with the presence of a mixed alkali effect[33] which involves a dramatic change in transport properties as the alkali composition is varied in the glass. With respect to ion diffusion coefficients in binary alkali glasses, the diffusion coefficient of alkali ion A is found to decrease as the glass composition changes from pure A to pure alkali B. Furthermore, the value of the diffusion coefficient of the trace ion in a pure glass is always smaller than the value of the self-diffusion coefficient of the pure element. This behaviour gives an extremum in the value of $D_{A^+-B^+}$ at an intermediate alkali composition. In addition, the diffusing ion with the lowest mobility changes from ion A to ion B at a specific glass composition.

The experimental errors in the concentration and depth measurements and the error in the procedure for extrapolating the concentration profiles become more important in the analysis at low Ag^+ concentrations. Also, the results were found to be sensitive to the smoothing function used. For example, the discontinuity in $n'D_{AB}$ at $\bar{N}_{Ag} = 0.48$ for the analysis of sample L in Figure 4 is a result of changing the order of the smoothing function. Extrapolating the linear portion of these curves at high silver concentrations in the glass to zero Ag^+ concentration gives nearly identical values for the Ag^+ self-diffusion coefficient, 4.1×10^{-11} cm^2/s. This value is compared to the values of 2.7×10^{-11} cm^2/s determined from Ag^+ tracer diffusion coefficient studies[10] in soda–lime–silica glass (an activation energy of 83.7 kJ/mole was used to correct D_{Ag^+} from 374 to 330°C) and 1.4×10^{-11} cm^2/s determined from refractive index measurements of ion exchanged soda–lime–silica glass slides using a dilute silver nitrate melt.[25] These three values of D_{Ag^+} were measured at different Ag cation fractions, suggesting a weak dependence of D_{Ag^+} on glass composition. The value of D_{Na^+} determined from the slope of Figure 4 is 1.6×10^{-11} cm^2/s, which is considerably lower than the self-diffusion coefficient of sodium in silver free soda–lime–silica glass determined by Doremus[10] (3.3×10^{-10} cm^2/s, assuming an activation energy of 83.7 kJ/mole), suggesting a strong mixed alkali effect for Na.

In summary, concentration profiles of silver in a ion exchanged sodia–lime–silica glass were measured for various values of exchange time, molten salt mixing condition, and melt composition by atomic absorption spectroscopy. No limitations on the exchange rate due to melt mass transfer or surface reaction could be ascertained from the measured results; thus, measured surface concentrations represent values which are in equilibrium with the melt. The 330 C isotherm was described with a regular solution model applied to both phases. With the $AgNO_3$–$NaNO_3$ melt interaction energy, A, fixed at the previously measured value of 3515 kJ/mole,[29] the value of the glass cation solution model parameter, n, was determined to be 1.49; the corresponding value of the equilibrium constant for the exchange reaction, K, was 75. From an analysis of the concentration profiles, the values of the silver and sodium cation diffusion coefficients were estimated as

$$D_{Ag^+} = 4.1 \times 10^{-11} \text{ cm}^2/\text{s}$$

and

$$D_{Na^+} = 1.6 \times 10^{-11} \text{ cm}^2/\text{s}.$$

Acknowledgements

The authors are grateful to L. E. Johns and R. Srivastava for stimulating discussions. Support for this study was provided by AFOSR under grant 84-3069. In particular, we gratefully acknowledge the support of Dr. D. Ulrich.

References

1. Neuman, V., Parriaux, O. & Walpita, L. (1979). *Electron. Lett.* **15**, 704.
2. Giallorenzi, T., West, E., Kirk, R., Ginther, R. & Andrews, R. (1973). *Appl. Opt.* **12**, 1240.
3. Stewart, G., Miller, C., Laybourn, P., Wilkinson, C. & De LaRue, R. (1971). *J. Quantum Electron.* **13**, 192.
4. Chartier, G., Jaussaud, P., DeOliveira, A. & Parriaux, O. (1978). *Electron. Lett.* **14**, 132.
5. Imai, M., Haneda, N. & Ohtsuka, Y. (1983). *J. Ilohtwate Technol.* **1**, 611.
6. Lagu, R. & Ramaswamy, V. (1984). *Appl. Phys. Lett.* **45**, 117.
7. Izawa, T. & Nakagome, H. (1972). *Appl. Phys. Lett.* **21**, 584.
8. Findakly, T. (1985). *Opt. Engng* **24**, 244.
9. Lagu, R., Ramaswamy, V. & Najafi, S. (1985). *Proc. 3rd European Conf. on Integrated Optics*, Springer Verlag, Berlin. Pp. 75–80.
10. Doremus, R. (1964). *J. phys. Chem.* **68** (8), 2212.
11. Chartier, G., Collier, P., Guez, A., Jassaud, P. & Won, Y. (1980). *Appl. Opt.* **19** (7), 1092.
12. Fainaro, L., Ish Shalom, M., Ron, M. & Lipson, S. (1984). *Physics Chem. Glasses* **25** (1), 16.
13. Matousek, J. & Blazek, J. (1979). *Silikaty* **23** (3), 193.
14. Matousek, J. & Hlavacek, E. (1979). *Silikaty* **23** (3), 203.
15. Malinin, V. R., Evstrop'ev, K. K. & Tsekhomskii, V. A. (1972). *J. appl. Chem. USSR* **45** (12), 172.
16. Moiseev, V. V., Permyakova, T. V. & Plotnikova, M. N. (1970). *Glass Technol.* **11** (1), 6.
17. Meistring, R., Frischat, G. H. & Hennicke, H. W. (1974). *Proc. 10th Int. Congr. Glass, Kyoto*, Section 8, Pp. 71–8.
18. Pask, J. A. & Parmelee, C. W. (1943). *J. Am. Ceram. Soc.* **26** (8), 267.
19. Kaps, Ch. & Völksch, G. (1982). *J. Non-Cryst. Solids* **53**, 143.
20. Stern, K. H. (1968). *J. phys. Chem.* **72** (6), 2256.
21. Doremus, R. H. (1968). *Physics Chem. Glasses* **9** (4), 128.
22. Garfinkel, H. M. (1968). *J. phys. Chem.* **72**, 4175.
23. Schulze, G. (1913). *Annls Phys.* **40**, 335.
24. Stern, K. H. (1971). *J. electrochem. Soc.* **118** (7), 1111.
25. Stewart, G. & Laybourn, P. J. R. (1978). *J. Quantum Electron.* **14**, 930.
26. Ramaswamy, R. V. & Najafi, S. I. (1986). *J. Quantum Electron.* **22**, 968.
27. Crank, J. (1979). *The mathematics of diffusion*. Clarendon Press, Oxford.
28. Inman, D. & Bockris, J. O'M. (1962). *J. electroanal. Chem.* **3**, 126.
29. Laity, R. W. (1957). *J. Am. chem. Soc.* **79**, 1849.
30. Rothmund, V. & Kornfeld, G. (1918). *Z. anorg. allg. Chem.* **103**, 129.
31. Garrels, R. M. & Christ, C. L. (1965). *Solutions, minerals, and equilibria*. Harper & Row, New York. P. 272.
32. Doremus, R. H. (1966). *Ion exchange: a series of advances*. Marcel Dekker Inc., New York. P. 11.
33. Day, D. E. (1976). *J. Non-Cryst. Solids* **21**, 343.

REFERENCE [12]

Influence of Ag^+ - Na^+ ion-exchange equilibrium on the index profile of single-mode glass waveguides

R. V. Ramaswamy and R. Srivastava
Department of Electrical Engineering
University of Florida
Gainesville, FL 32611

and

P. Chludzinski
Department of Chemical Engineering
University of Florida
Gainesville, FL 32611

Abstract

The equilibrium study of the Na^+ - Ag^+ exchange process at $Ag\ NO_3$ + $Na\ NO_3$ melt-glass interface explains the strong dependence of the surface index change on the low silver concentration in the melt used for fabricating single-mode waveguides.

Influence of $Ag^+ - Na^+$ ion-exchange equilibrium on the index profile of single-mode glass waveguides

R. V. Ramaswamy and R. Srivastava
Department of Electrical Engineering
University of Florida
Gainesville, FL 32611

and

P. Chludzinski
Department of Chemical Engineering
University of Florida
Gainesville, FL 32611

The binary $Ag^+ - Na^+$ exchange has been widely used for fabrication of planar and channel waveguides generally using pure Ag NO_3 melt. The single-mode waveguides thus obtained [1] have large surface index change ($\Delta n \sim 0.1$), show large scattering losses, are incompatible with fiber-core dimensions, and their characteristics are not reproducible to desired accuracy. To circumvent these problems, low melt concentrations of silver ($N_{Ag} \sim 10^{-2} - 10^{-3}$ molar fractions where $N_{Ag} = C_{Ag}/(C_{Ag} + C_{Na})$ and C_i is the absolute concentration of the cation i) in Na NO_3 bath have been used [2-4]. However, at low concentrations, Δn is a very strong function of N_{Ag} [4] saturating at ~ 0.1 for pure Ag NO_3 melts in most soda-lime glasses. Since for fiber compatible single-mode guides, $N_{Ag} \sim 10^{-4}$ MF, this strong dependence of Δn on N_{Ag} calls for a precise control of N_{Ag} and its understanding via a detailed study of the transport phenomena and thermodynamical equilibrium between the melt and glass phases. While such a study has been reported [2,3,5] for $N_{Ag} > 10^{-2}$, the results are not applicable to the low concentrations involved in the fabrication of single-mode waveguides. Besides, the results are likely to depend on the processing temperature and the substrate glass. Moreover, since the concentration profile depends on the interdiffusion coefficient which is concentration independent only if the silver concentration in glass is very small, a knowledge of its dependence on N_{Ag} will permit the solution of the diffusion equation with concentration-dependent interdiffusion coefficient [2].

In the present investigation, the importance of melt transfer limitations and the equilibrium isotherm, are investigated under process conditions with a glass composition that have been used successfully to produce low-loss single-mode waveguides with high reproducibility. The experiments were carried out by immersing the glass substrates in molten salt mixture at 330° C and measuring the resulting silver concentration profile as a function of time, melt-stirring condition and the melt composition. The glass was etched in steps and the resulting etch solution was analyzed for silver with an atomic absorption spectrophotometer. The concentration profiles were also measured independently by analyzing the back-scattered electrons in a scanning electron microscope and the accompanying surface-index change Δn was derived by correlating the measured mode indices to those calculated theoretically for the measured concentration profile [4]. Fig. 1 shows the silver concentration at the glass surface and the measured index change Δn for various values of N_{Ag}.

The $Ag^+ - Na^+$ ion-exchange process can be described [5] by the following chemical reaction

$$Ag^+ + \bar{N}a^+ \rightleftharpoons \bar{A}g^+ + Na^+ \qquad (1)$$

where the bar indicates the cation in the glass phase. In such a liquid-solid exchange process, the rate of ion exchange can be limited by the following processes:

(i) The mass transfer of the reactants to and removal of the products from the reaction interface in the melt.

(ii) The kinetics of the reaction at the interface.

(iii) The cation transport (diffusion) in the glass.

In order to ensure that the measured glass surface concentration corresponds to the value in equilibrium with the melt, the effects of (i) and (ii) must be negligible. That this was the case in our experiments was borne out from the following considerations: Firstly, stirring the melt did not alter the index change or the profile. Secondly, the quantity $(\bar{N}_{Ag}/N_{Ag})(\bar{D}_{Ag}/D_{Ag})^{1/2}$ was sufficiently small [6] to impose any significant limitations due to the diffusion process in the melt for the values of N_{Ag} studied (2×10^{-4} - 1×10^{-2} MF). D here denotes the self-diffusion coefficient. Furthermore, for large diffusion times (3-4 hours), there is no measurable decrease in the surface concentration attributable to melt depletion. In addition, Δn is independent of time of diffusion, even for diffusion time of the order of a few minutes. These results indicate that the dominant resistance in the exchange process is the cation transport (diffusion) in the glass.

The equilibrium constant for the exchange reaction is given by $K = \gamma_{Na} N_{Na} \bar{a}_{Ag}/\gamma_{Ag} N_{Ag} \bar{a}_{Na}$ where a_i is the thermodynamic activity of component i and γ_i is its activity coefficient at mole fraction N_i in the melt. The ratio of the two activity coefficients in the melt can be described by regular solution theory and in the glass by an n-type behaviour, i.e., $(a_{Ag}/a_{Na}) = (\bar{N}_{Ag}/\bar{N}_{Na})^n$. These considerations yield a relation between $\bar{N}_{Ag}$ and N_{Ag} in the form [5]

$$\ell n \frac{N_{Ag}}{1-N_{Ag}} + \frac{A}{RT}(1-2\,N_{Ag}) = n\,\ell n \frac{\bar{N}_{Ag}}{1-\bar{N}_{Ag}} - \ell n\, K$$

The above relation is shown as the straight-line plot of Fig. 2 with A = 3515 J/mole. The slope gives n = 1.49 and the intercept gives K = 75 for the soda-lime glass used. These values are similar to those reported by other authors [2,5] for various glasses. The large value of the equilibrium constant is thus responsible for the large ratio $\bar{N}_{Ag}/N_{Ag}$. These results justify the assumption of concentration independent interdiffusion coefficient and the resulting erfc index profiles only for very small melt concentrations ($N_{Ag} \lesssim 10^{-4}$ MF). For $N_{Ag} > 10^{-3}$ MF, the interdiffusion coefficient is concentration dependent and the resulting index profiles deviate substantially from erfc.

This work was supported by contract no. 84-0369 from AFOSR.

References

1. R. G. Walker, C. D. W. Wilkinson, and J. A. H. Wilkinson, Appl. Opt. 22, 1923 (1983)
2. G. Stewart and P. J. R. Laybourn, IEEE J.Q.E., QE-14, 930 (1978).
3. G. Chartier, P. Collier, A. Guez, P. Jaussaud, and Y. Won, Appl. Opt. 19, 1092 (1980).
4. R. V. Ramaswamy and S.I. Najafi, IEEE J.Q.E., QE-22, 883 (1986).
5. H. M. Garfinkel, J. Phys. Chem. 72, 4175 (1968).
6. J. Crank, "The Mathematics of Diffusion", Clarendon Press, Oxford (1979).

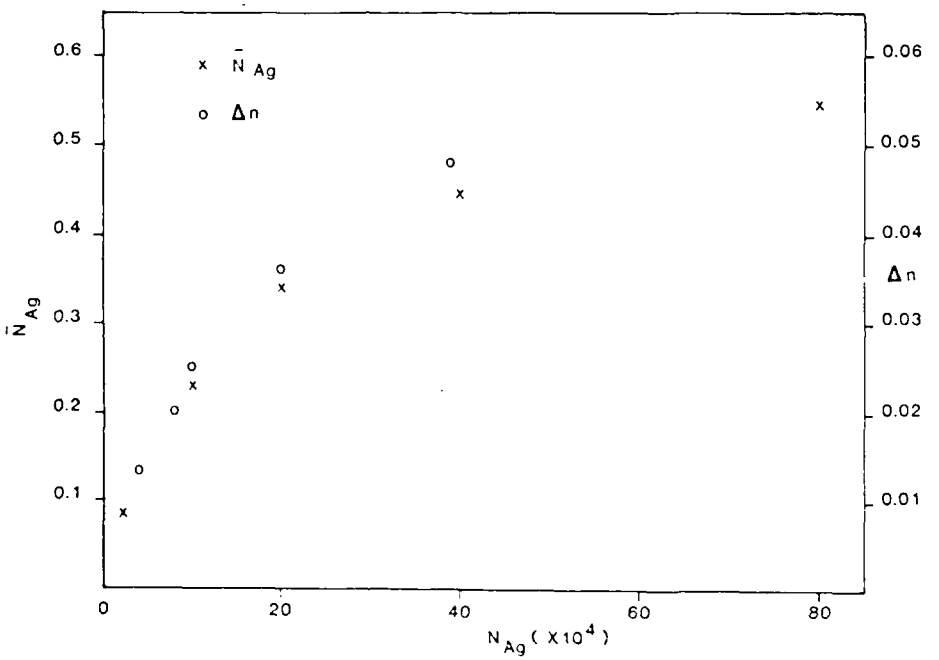

Fig.1 Variation of surface-silver concentration (MF) and the surface-index change in the glass with melt concentration.

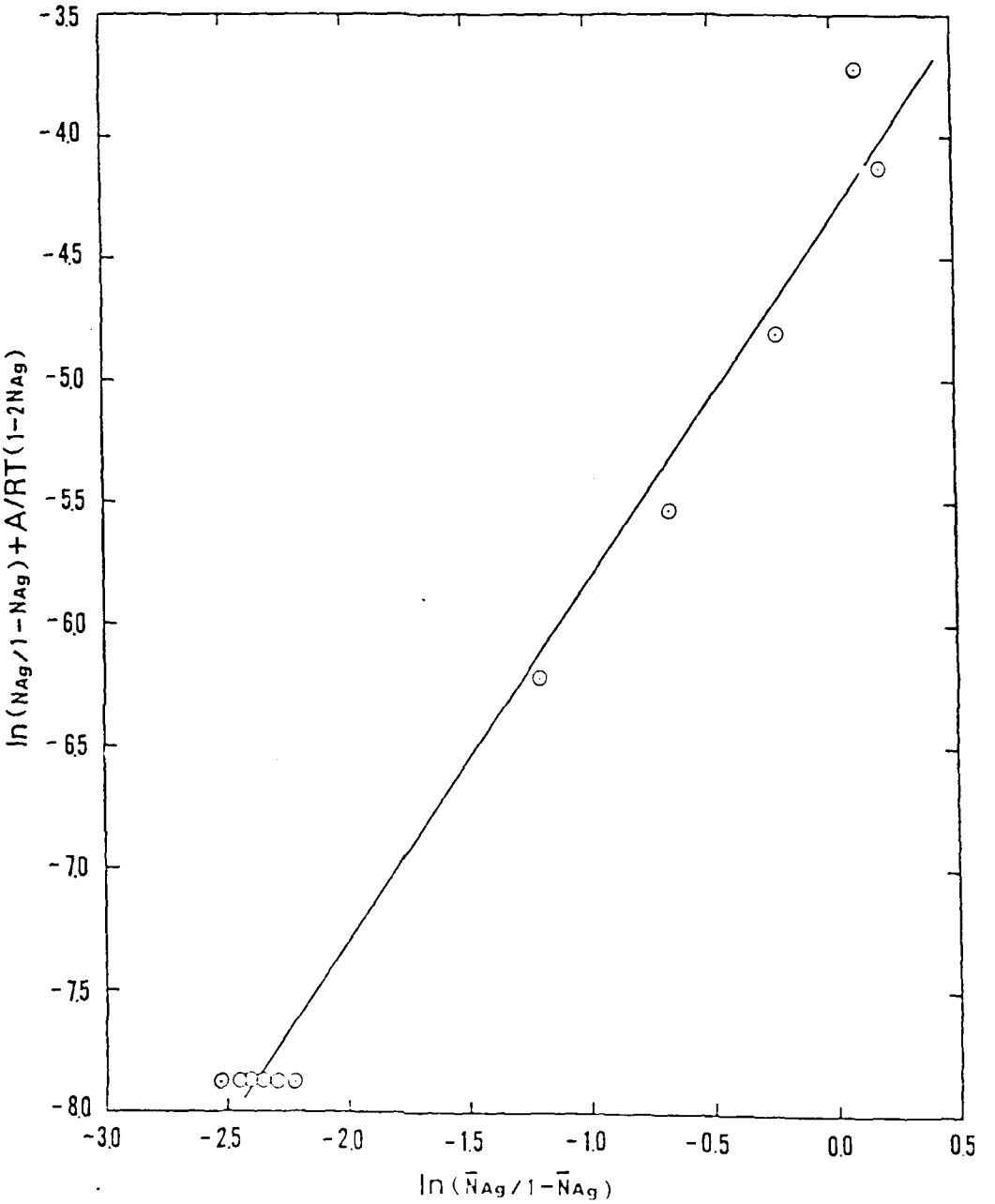

Fig. 2 The test of the n-type behaviour for Ag^+ - Na^+ exchange.

REFERENCE [13]

MICROSTRUCTURAL DEFINITION OF ION-EXCHANGED GLASS OPTICAL WAVEGUIDES

P. Chludzinski, R. V. Ramaswamy and T.J. Anderson

University of Florida
Gainesville, FL 32611

We have performed detailed studies of the ion-exchange process at the $AgNO_3$ + $NaNO_3$ melt-glass interface. The results indicate that at the processing temperature (330°C), for dilute concentration of Ag^+, variable mixing conditions, mass transfer (diffusion or convection in the melt) or the kinetics at the liquid-solid interface do not influence the exchange process significantly. As a result of the equilibrium condition at the interface, the concentration of silver at the glass surface is orders of magnitude higher than that in the melt and for low concentration ($< 10^{-4}$ mole fraction), the dopant profile (and hence the refractive index profile) is primarily determined by the diffusion of silver ions in the glass matrix. However, for large concentrations, the diffusion coefficient is concentration dependent and therefore varies as a function of positon inside the glass. It appears that the exchange process can be best described by equilibrium at the melt-glass interface with a regular solution theory in the melt and an n-type behavior of the thermodynamical activities of the ions in the glass and by the diffusion limited transport in the glass.

INTRODUCTION

The ion-exchange technique, which has been used for more than a century to produce tinted glass, has received increased attention in recent years because it has been found to improve the surface-mechanical properties of glass [1] and, more importantly, to introduce a gradient index in the glass. The technique has been successfully used in manufacturing low-loss optical fibers, gradient-index optical components for imaging applications, and, more recently, in the fabrication of planar and channel waveguides in glass susbstrates for application in integrated optics. Optical waveguides in glass substrates are fabricated by creating a layer of higher refractive index near the surface of the substrate. This is normally accomplished by diffusion of monovalent ions of higher polarizability e.g., Cs^+, Rb^+, K^+, Ag^+, or Tl^+ into the glass matrix where they exchange with Na^+ or K^+ ions. Besides the polarizability of the ions, the net index change also depends on the difference in the sizes of the two exchanging ions, the accompanying change in the polarizability of the oxygen ions, and formation of any elastic stress in the glass. Of the various monovalent ions exchanged in soda-lime glass by diffusion, the binary exchange of Ag^+ - Na^+ is by far the most researched technique [2,3,4]. When pure $AgNO_3$ melt is used for the exchange process, large surface index changes ($\Delta n \sim 0.1$) are obtained which have some disadvantages: a larger silver concentration causes coloring due to silver reduction ; secondly, the single-mode waveguides thus made are shallow and the field distribution of the guided mode is not compatible with that of the conventional optical fibers. Moreover, the time of diffusion involved is rather short, thereby causing uncertainty and lack of reproducibility in the waveguide characteristics. Dilute melts of mixtures of $AgNO_3$ and $NaNO_3$ allow achievement of lower Δn and more controllable diffusion times with fiber compatible waveguides [4]. It is known [5] that a very low ionic concentration of silver in the $NaNO_3$ melt ($N_{Ag} \sim 10^{-4}$ mole fractions) is necessary to obtain the desired single-mode waveguides. Moreover, unlike the case of K^+ - Na^+ ion exchange where the surface-index change (Δn) depends linearly on the concentration of K^+ ions in the KNO_3 + $NaNO_3$ melt [6], in the case of Ag^+ - Na^+ exchange Δn is found to be highly nonlinear function of the silver ion melt concentration even at such low concentrations [4]. Since Δn is expected to be a linear fuction of the concentration of silver ions in the glass matrix [7], it is necessary to understand how the silver ion intake

by the glass is affected by the ion-exchange parameters, namely the melt concentration , the time and other boundary conditions such as the stirring of the melt. An ion-exchange equilibrium study would thus not only provide the correlation between the measured index change and the melt concentration, but also permit determination of the boundary conditions for solution of the diffusion equation to calculate the index profile. In particular, it will demonstrate to what extent the general assumption that the interdiffusion coefficient is concentration independent, is valid.

Previous studies of ion-exchange equilibrium in glasses include the early work of Schulze [8] and later the pioneering work of Garfinkel [6] involving many different cation pairs. In both these studies, the silver cation concentration was relatively large ($N_{Ag} > 0.1$), More recently, Stewart and Laybourn [3] reported a study of Ag^+ - Na^+ exchange at very low concentrations ($N_{Ag} \sim 10^{-4}$) required for fabrication of single-mode waveguides. However, the information on the surface concentration of Ag^+ in glass was obtained indirectly by optical measurements on the waveguides. There are two drawbacks in such a method; first, the WKB method employed to determine the mode indices is subject to error in some cases and second, the assumption that in the case of pure $AgNO_3$ melt, all the surface Na^+ ions in glass are substituted for Ag^+ ions, may not necessarily be valid. In this work we measure absolute concentration of Ag^+ ions in a soda-lime glass which we have successfully used to fabricate glass waveguides of desired and reproducible characteristics [5].

THEORY

Upon immersion of the glass substrate in the salt solution, silver is driven into the glass by an interphase chemical potential gradient [9]. However, because Ag^+ is a monovalent cation, an equivalent amount of charge, i.e., a Na^+ ion, is transported in the opposite direction to preserve charge neutrality. The Ag^+ - Na^+ binary exchange process can be described [6] by the following chemical reaction:

$$Ag^+ + \overline{Na}^+ = \overline{Ag}^+ + Na^+, \qquad (1)$$

where the bar indicates the cations in the glass phase. In a liquid-solid phase exchange process, the rate of ion exchange may be limited by the

following processes:

(i) The mass transfer of reactants to and removal of products from the reaction interface in the melt.

(ii) The kinetics of the reaction at the interface.

(iii) The transport of ions in the glass phase.

The transfer of cations in the melt takes place via diffusion and convection. For diffusion to be the limiting process in the melt, Crank [10] has shown that the important parameter is

$$\frac{\bar{N}_{Ag}}{N_{Ag}} \left(\frac{\bar{D}_{Ag}}{D_{Ag}}\right)^{\frac{1}{2}} ,$$

where N_{Ag} denotes the silver concentration and D_{Ag} the self-diffusion coefficient. If this parameter is greater than about 10, the rate is not mass-transfer limited in the melt. Under the experimental conditions used in this study, this indeed was the case.

Convection in the melt can be altered via stirring the melt and its influence on the mass transfer can be minimized. The kinetics of the reaction is expected to be rather fast and the most important limiting factor thus is the transport of Ag^+ ions in the glass. This transport occurs via diffusion and the equilibrium state of reaction (1) specifies the surface boundary condition for this diffusion process. Control of the surface-index change or the cation exchange profile in glass is affected by manipulating this boundary condition and the cation transport properties in the glass.

We define the equilibrium constant for reaction (1) as

$$K = \frac{\bar{a}_{Ag}\, a_{Na}}{\bar{a}_{Na}\, a_{Ag}} \qquad (2)$$

Where the a's are the thermodynamic activities of the ions. The absolute value of K depends upon the reference functions and states chosen to define the activities. For molten salts, the reference state is normally chosen such

that the activity coefficient of the ion approaches its mole fraction N in the pure state. The reference state for the glass phase is taken as that in which all of the exchangeable cations are of the species in question. The ratio of the activity coefficients in the molten salt can be represented by the Regular Solution Theory [11]

$$\ln\left(\frac{a_{Ag}}{a_{Na}}\right) = \ln\left(\frac{N_{Ag}}{N_{Na}}\right) - \frac{A}{RT}\left(1 - 2N_{N_a}\right) \qquad (3)$$

Where A is the net interaction energy which is assumed to be independent of temperature and melt composition. The measurements of Laity [12] at 330°C suggest the value of A equal to 3515 J/mole for the $AgNO_3$ + $NaNO_3$ melt.

The ratio of the activities in glass is represented by the n-type behavior first suggested by Rothmund and Kornfeld [13],

$$\frac{\bar{a}_{Ag}}{\bar{a}_{Na}} = \left(\frac{\bar{N}_{Ag}}{\bar{N}_{Na}}\right)^n \qquad (4)$$

Garrel and Christ [14] have shown that this empirical relationship is equivalent to regular solution theory for intermediate glass compositions. Substitution of the ratios of the activities in (2) gives

$$\ln\left(\frac{N_{Ag}}{1 - N_{Ag}}\right) + \frac{A}{RT}\left(1 - 2\,N_{Ag}\right) = n\ln\left(\frac{\bar{N}_{Ag}}{1 - \bar{N}_{Ag}}\right) - \ln K \qquad (5)$$

If the models for the activity coefficients in the two phases are valid, a plot of the left hand side of (5) versus

$$\ln\left(\frac{\bar{N}_{Ag}}{1 - \bar{N}_{Ag}}\right)$$

should yield a straight line with slope equal to n and intercept equal to ln(1/K).

EXPERIMENTAL PROCEDURE

The ion exchange of Ag^+ with Na^+ in soda-lime silicate glass was carried out at 330°C as a function of time, melt composition of $AgNO_3$ + $NaNO_3$ molten salts, and melt stirring conditions.

A summary of the experimental conditions is given in Table 1. The

composition and density of the soda-lime glass used in the experiments is given in Table 2. Precleaned glass slides were rinsed in de-ionized water, allowed to dry and then placed in a sample holder prior to each experiment. The bath, sample holder and stirrers were all constructed of aluminum. The temperature was controlled to ± 2°C and monitored by a thermocouple with stainless steel sheath.

After exchange the glass sample was removed from the melt and allowed to cool. It was then washed in de-ionized water to remove absorbed salt. The glass was then etched in steps in a 0.58 wt. percent HF solution. The resulting etch solution for each step was analyzed for silver in Perkin-Elmer Model 280 atomic absorption spectrophotometer calibrated with standards of known concentration. The estimated precision of the concentration is ± 0.3 cation fraction and of the depth is ± 1.6×10^{-6} cm. In this manner concentration profiles of silver in the glass matrix were determined.

RESULTS AND DISCUSSION

Fig. 1 shows the measured concentration profiles for the samples listed in Table 1. The surface concentration of Ag^+ in glass was determined by extrapolation of the measured concentration profile. Extrapolation was performed by fitting the profile by complimentary error function, viz:

$$\bar{N}_{Ag}(x) = \bar{N}_{Ag}(x = 0)\ \mathrm{erfc}\ (x/\ 2\sqrt{Dt})$$

$$\text{where}\quad \mathrm{erfc}\ (z) = \frac{2}{\sqrt{\pi}} \int_{z}^{\infty} e^{-\alpha^2}\, d\alpha$$

Here t is the diffusion time. The assumption of the erfc profile is based on the solution of the one-dimensional diffusion equation with time-independent boundary condition at the glass-melt interface [10]. The fact that the profile for a given melt concentration does not depend on the stirring condition suggests that the ion-exchange process is not mass transfer limited in the melt. The extrapolated silver cation fractions and the corresponding melt cation fractions are summarized in Table 3. The data of Table 3 are plotted in Fig. 2 and as expected according to (5) the plot appears to be linear to within experimental error with a least squares value of n equal to 1.49 and K equal to 75. Thus, the partitioning of silver ions between the nitrate melt and soda-lime silicate glass is nonlinear in the composition

range studied.

The results of these equilibrium studies are compared in Fig. 3 to the smoothed measurements of Schulze [8] in a soda-lime silicate glass. Using the same regular solution description of the melt, the values of n and K derived from the data of Schulze [8] are reported to be 1.08 and 120. Figure 3 also shows the 315°C equilibrium results of Stewart and Laybourn [3] determined in a similar type glass as studied in this work. The reported values of n and K are 1.32 and 131. The value of n reported in this work is close to the value of 1.4 reported by Garfinkel [6] in soda-lime borosilicate glass. The reason for the differences in the values of the exponent is probably related to differences in glass composition and /or structure. The value of the temperature dependent equilibrium constant is in fair agreement with the results of Schulze [8] and Stewart and Laybourn [3], and the results of Doremus [15] in the high silica phase of two-phase pyrex. The results of our work suggest a large value of the silver partition coefficient which is similar to the values determined by silver ion tracer diffusion studies in soda-lime glass [9].

CONCLUSION

Concentration profiles of silver in an ion-exchanged soda-lime silicate glass were measured by atomic absorption spectroscopy for various values of exchange time, molten salt mixing condition and melt composition. No melt mass transfer or surface reaction limitation on the exchange rate could be ascertained from the measured results. Thus, the measured surface concentration represents values which are in equilibrium with the melt. The 330°C isotherm is described with a regular solution model applied to the activities of the cations in the melt and an n-type behavior in the glass phase. With the $AgNO_3$ + $NaNO_3$ melt interaction energy fixed at the previously measured value of 3515J/mole, the value of n was determined to be 1.49; the corresponding value of the equilibrium constant for the exchange reaction was K=75. The results explain the nonlinear dependence of the surface index change with the melt concentration of the silver ions at such low concentrations.

REFERENCES

1. A.J. Burggraaf and J. Cornelissen Phys. Chem. Glasses, 5, 123 (1964).

2. T.G. Giallorenzi, E.J. West, R. Kirk, R. Ginther, and R.A. Andrews, Appl. Opt., 12, 1240 (1973).

3. G. Stewart and P.J.R. Laybourn, IEEE J. Quantum Electron, QE-14, 930 (1978).

4. R.K. Lagu and R.V. Ramaswamy, J. Lightwave Tech, LT-4, 176 (1986).

5. R.V. Ramaswamy and S.I. Najafi, IEEE J. Quantum Electron, QE-22, 883 (1986).

6. H.M. Garfinkel, J. Phys. Chem., 72, 4175 (1968).

7. I. Fainaro, M.Ish Shalom, M. Ron, and S. Lipson, Phys. Chem. Glasses, 25, 16 (1984).

8. G. Schulze, Ann. Physik, 40, 335 (1913).

9. R.H. Doremus, J. Phys. Chem., 68, 2212 (1964).

10. J. Crank, "Mathematics of Diffusion", Clarendon Press, Oxford (1979).

11. J.G. Kirkwood, and I. Oppenheim, "Chemical Thermodynamics". McGraw-Hill , New York (1961).

12. R. W. Laity, J. Am. Chem. Soc. 79, 1849 (1957).

13. V. Rothmund and G. Kornfeld, Z. Anorg. Allg. Chem., 103, 129 (1918).

14. R.M. Garrels and C.L. Christ, "Solutions, Minerals, and Equilibria", Harper & Row, New York (1965).

15. R.H. Doremus, Phys. Chem. Glasses, 9, 128 (1968).

LIST OF FIGURES

Table 1. Summary of experimental conditions for ion-exchange studies at 330°C

Sample	N_{Ag}	Time (h)	Number of stirrers
A	1.90×10^{-4}	1	0
B	1.90×10^{-4}	1	0
C	1.90×10^{-4}	1	1
D	1.90×10^{-4}	1	1
E	1.90×10^{-4}	1	2
F	1.90×10^{-4}	3	1
G	1.90×10^{-4}	4	1
H	9.97×10^{-4}	4	1
I	1.97×10^{-3}	4	1
J	4.06×10^{-3}	4	1
K	8.03×10^{-3}	4	1
L	1.20×10^{-2}	4	1

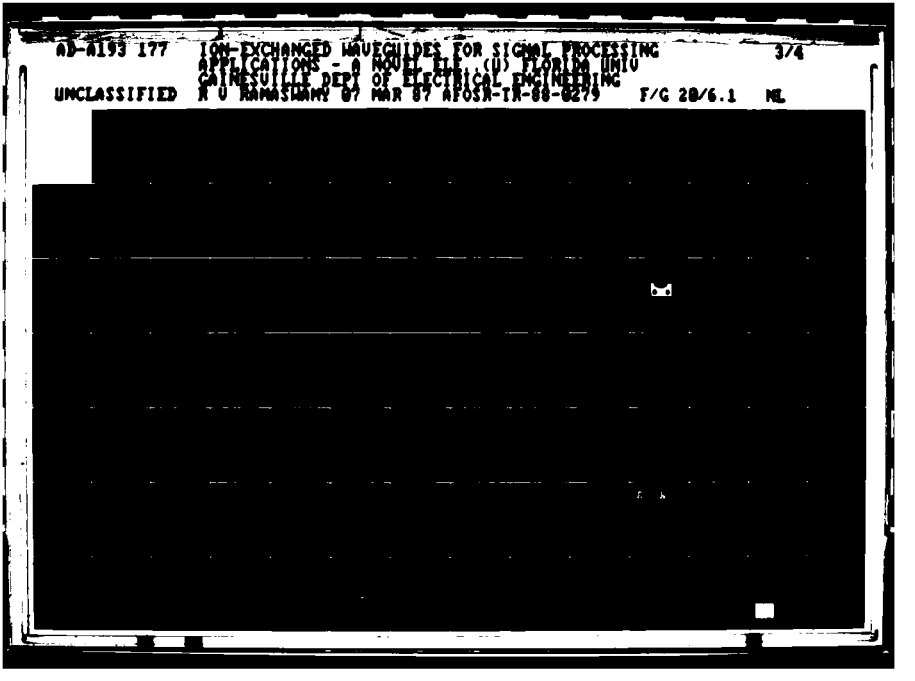
AD-A193 177 ION-EXCHANGED WAVEGUIDES FOR SIGNAL PROCESSING APPLICATIONS - A NOVEL ELE (U) FLORIDA UNIV GAINESVILLE DEPT OF ELECTRICAL ENGINEERING
3/4
UNCLASSIFIED K U RAMASWAMY 07 MAR 87 AFOSR-TR-88-0279 F/G 20/6.1 NL

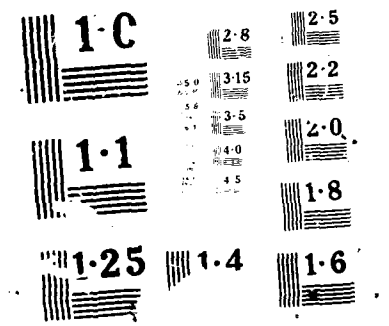
1·C
2·8
2·5
3·15
2·2
3·5
2·0
1·1
4·0
1·8
1·25
1·4
1·6

Table 2. Chemical composition of Fischer brand glass slide (mole %)

Oxide	Weight %
SiO_2	72.25
Na_2O	14.31
CaO	6.40
Al_2O_3	1.20
K_2O	1.20
MgO	4.30
Fe_2O_3	0.03
SO_3	0.30

Density = 2.46668 g/cm^3

Table 3. Extrapolated Ag^+ surface concentrations

Sample	N_{Ag}	$\bar{N}_{Ag}$
A	1.90×10^{-4}	0.0837
B	1.90×10^{-4}	0.0793
C	1.90×10^{-4}	0.0973
D	1.90×10^{-4}	0.0918
E	1.90×10^{-4}	0.0857
F	1.90×10^{-4}	0.0797
G	1.90×10^{-4}	0.0744
H	9.97×10^{-4}	0.231
I	1.97×10^{-3}	0.339
J	4.06×10^{-3}	0.444
K	8.03×10^{-3}	0.547
L	1.20×10^{-2}	0.527

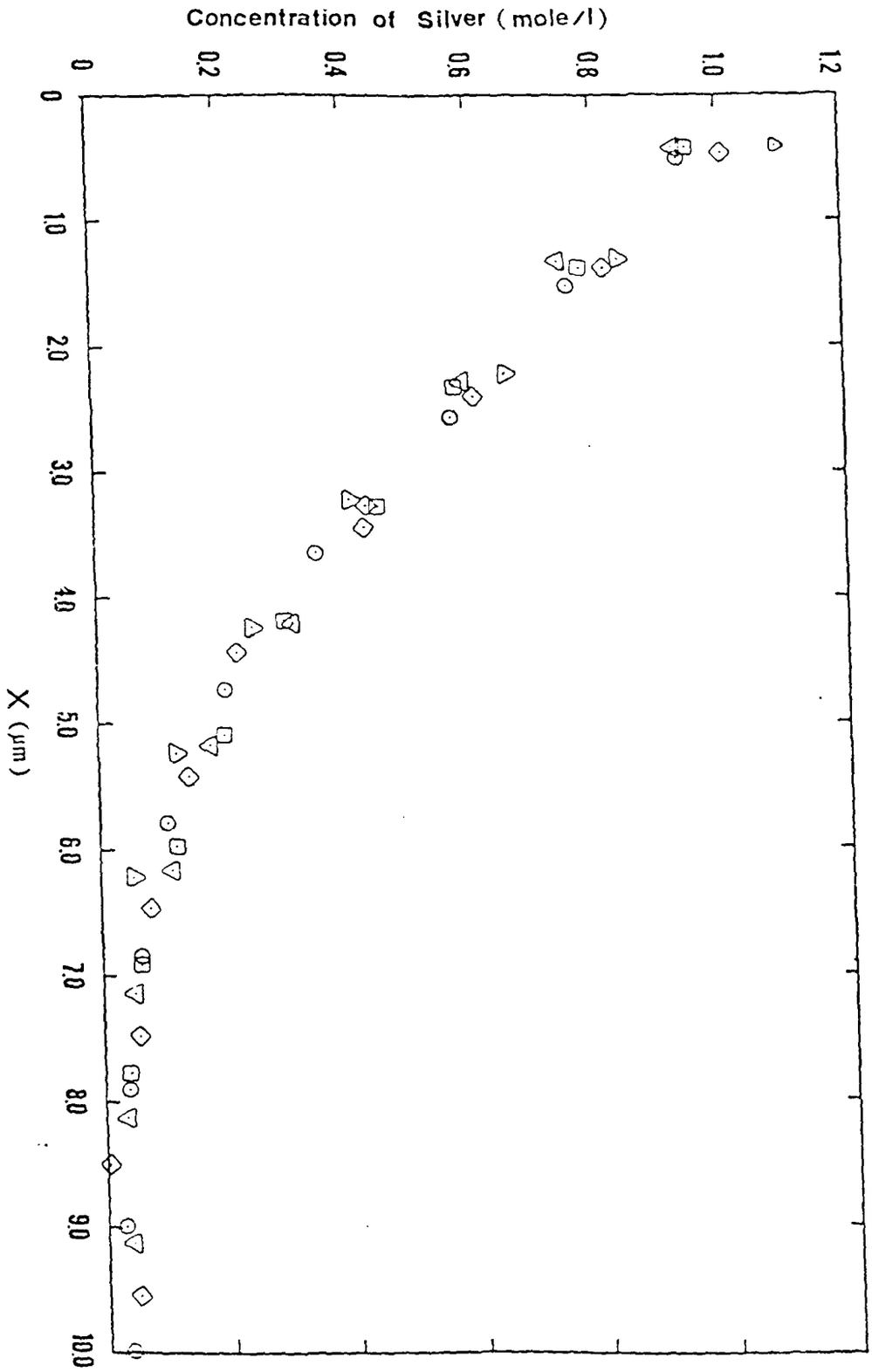
Concentration of Silver (mole/l)
0
0.2
0.4
0.6
0.8
1.0
1.2
X (μm)
0
1.0
2.0
3.0
4.0
5.0
6.0
7.0
8.0
9.0
10.0

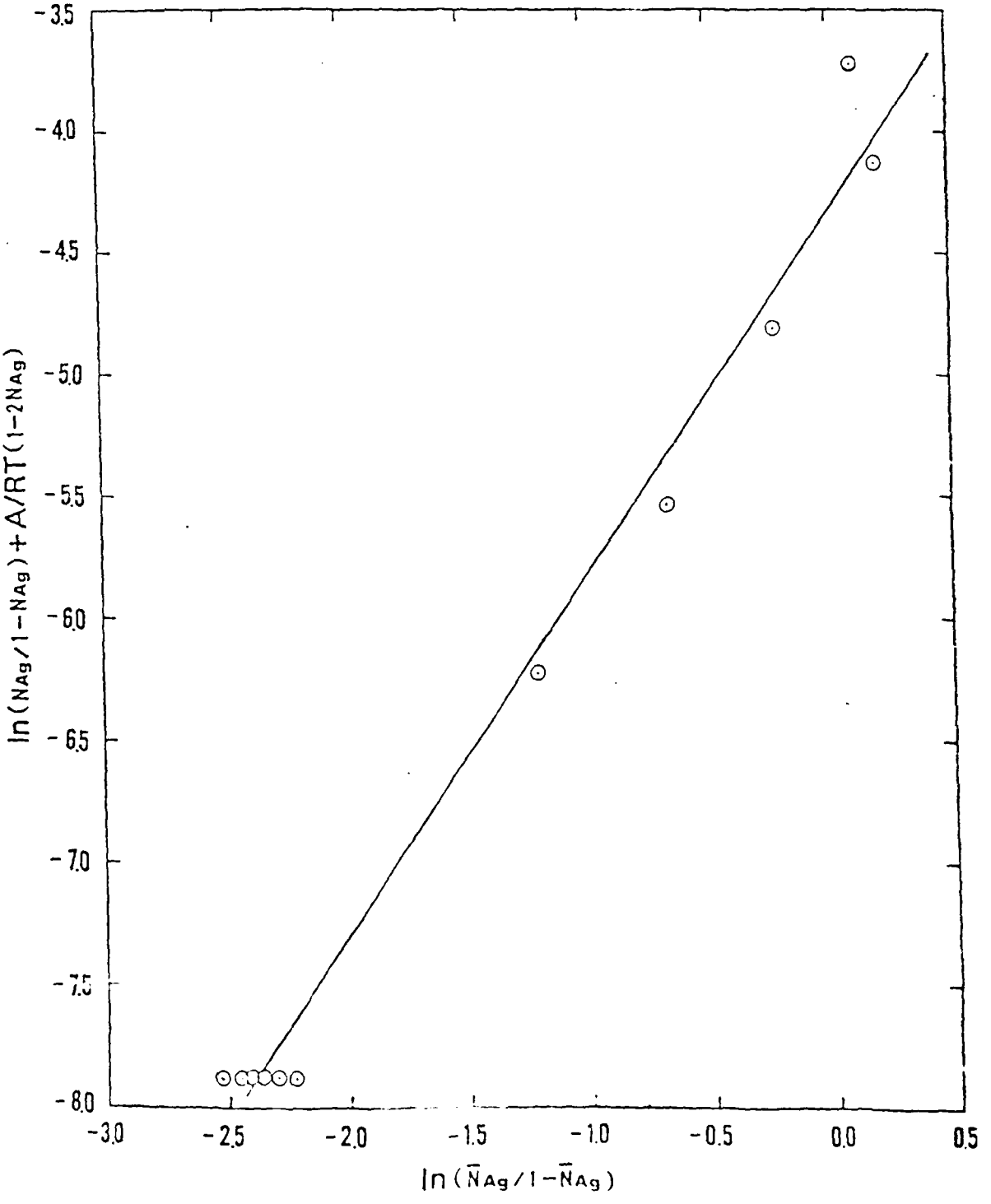
-3.5
-4.0
-4.5
-5.0
-5.5
-6.0
-6.5
-7.0
-7.5
-8.0
ln(NAg/1-NAg)+A/RT(1-2NAg)
-3.0
-2.5
-2.0
-1.5
-1.0
-0.5
0.0
0.5
ln(N̄Ag/1-N̄Ag)

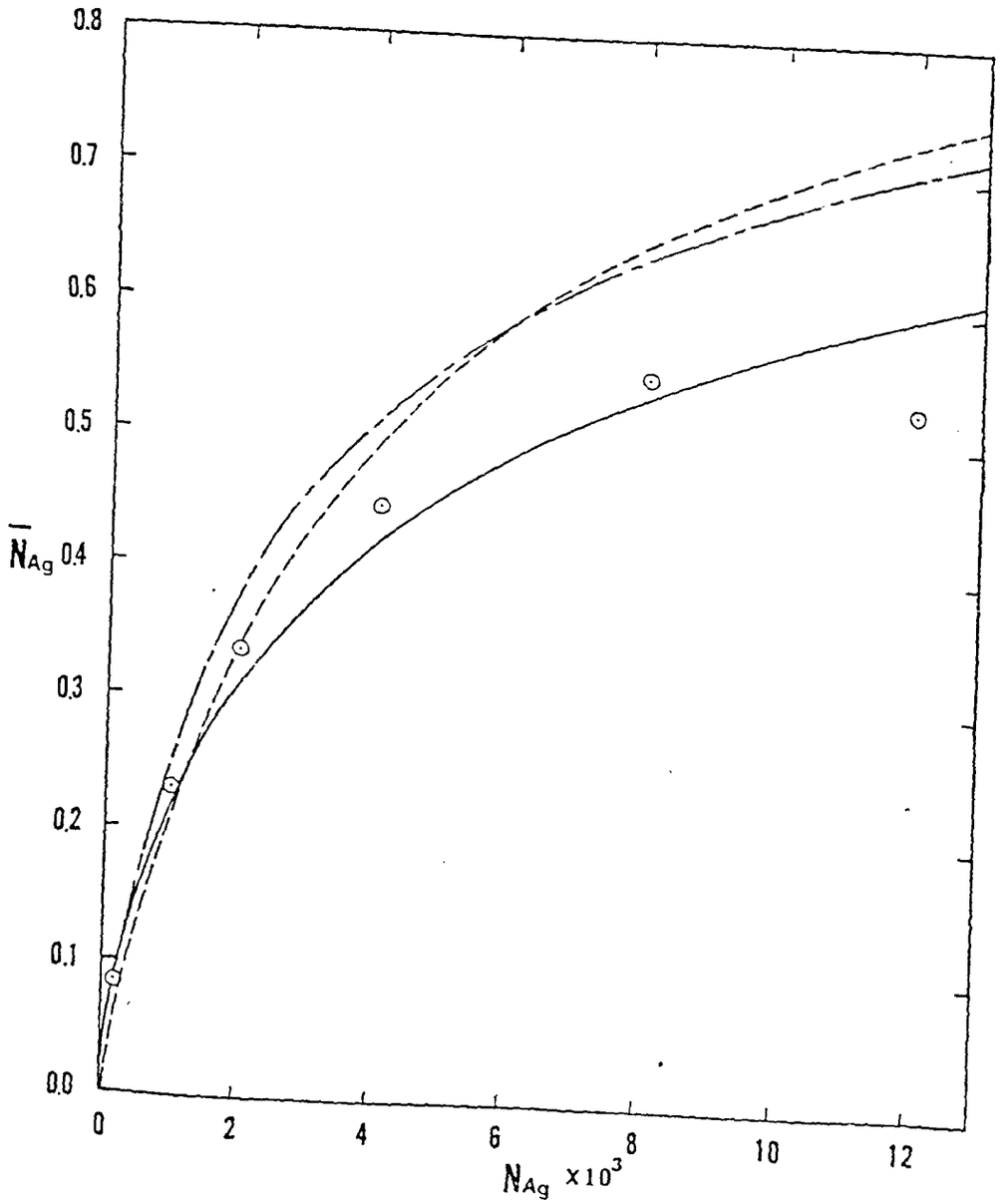
0.8
0.7
0.6
0.5
$\bar{N}_{Ag}$ 0.4
0.3
0.2
0.1
0.0
0
2
4
6
8
10
12
$N_{Ag} \times 10^3$

REFERENCE [14]

Influence of Ag^+ - Na^+ Ion-Exchange Equilibrium On Waveguide Index Profiles

R. V. Ramaswamy, R. Srivastava, P. Chludzinski**
and T. J. Anderson*

Department of Electrical Engineering
University of Florida,
Gainesville, Florida 32611

** Corning Glass Works, Wilmington, N. C.

* Department of Chemical Engineering
University of Florida, Gainesville, FL 32611

Abstract

The Ag^+-Na^+ ion-exchange process in a soda-lime silicate glass was studied at 330° as a function of composition of $AgNO_3$-$NaNO_3$ melt, mixing condition and exchange time. The concentration profile of silver in glass was measured by atomic absorption spectroscopy and SEM technique. The surface index change and the index profile were determined from mode index measurement. An excellent correlation between the index profile and diffusion profile was observed and an empirical linear relation between the surface-silver concentration and the surface-index change was obtained. Ion-exchange was modeled by an ion diffusion limited process in the glass with an equilibrium chemical reaction at the melt-glass interface. A large value of 75 for the equilibrium constant at low silver melt concentrations ($<10^{-2}$ mole fractions) shows that uptake of silver in glass varies in highly nonlinear fashion with the melt concentration. The results provide boundary conditions necessary for solution of the diffusion equation and design of single-mode waveguides.

I. Introduction

The binary exchange between Ag^+ and Na^+ ions in soda-lime glass has been successfully used by many researchers to fabricate passive waveguide components for applications in optical signal processing and sensors [1-10]. Basically, there are two approaches to waveguide formation by ion-exchange. In one method [7,8], a silver film is first deposited on a glass surface. Then ion exchange between Ag^+ and Na^+ is effected at elevated temperature by field-assisted diffusion. Experimentally it is found that an external electric field is necessary for ion-exchange to occur from a metal film. In an alternative and widely studied approach [1-6], a glass substrate is immersed in a binary molten salt bath of silver and sodium nitrate. When pure $AgNO_3$ melt is used, large surface index changes ($\Delta n \sim 0.1$) are obtained associated with the large silver concentration in the glass matrix which causes scattering and absorption. Both these mechanisms are caused by reduction of silver to the zero oxidation state [6].

Single-mode waveguides made by both processes are shallow, and the mode-field distribution is not compatible with that of conventional single-mode fibers. In addition, ion-exchange times usually are relatively short (~ few minutes), thus producing uncertainty and irreproducibility in the waveguide characteristics. In order to circumvent these problems, very dilute concentrations of Ag^+ ions in $NaNO_3$ have been used. These low concentrations are achieved either by using an initial molten salt composition dilute in $AgNO_3$ [3,4,9] or by releasing silver ions electrolytically from a pure silver cathode into an intially pure $NaNO_3$ melt [10]. The surface index change and the index profile depend strongly upon the silver concentration in the melt. A very low silver concentration, N_{Ag}, in the $NaNO_3$ melt ($\sim 10^{-4}$ mole fraction) is necessary to obtain the desired single-mode waveguides [9]. The

electrolytic release technique allows on-line control of melt Ag^+ concentration and therefore control of the index profile. As the surface-index change is expected to be a linear function of the concentration of silver ions in the glass [11], it is necessary to understand how the silver ion intake by the glass is affected by the process parameters in the ion-exchange technique (e.g., melt Ag^+ concentration, exchange time, temperature, melt mixing condition). In particular, knowledge of the Ag^+-Na^+ ion-exchange equilibrium isotherm is necessary to establish the correct boundary condition for solution of the diffusion equation. The calculated concentration profile in the glass is directly related to the index profile which can be verified by optical measurements or analysis of back-scattered electrons in a scanning electron microscope (SEM) [12]. In this way, the validity of assuming a constant interdiffusion coefficient can be checked [3,12].

Previous studies of ion-exchange equilibrium in glasses include the early work of Schulze [13] and later, the pioneering work of Garfinkel [14] involving several cation pairs. In both these studies, the silver cation concentration was relatively large ($N_{Ag} > 0.1$). More recently, Stewart and Laybourn [3] reported a study of Ag^+ - Na^+ exchange in the concentration range required for fabrication of single-mode waveguides ($N_{Ag} \sim 10^{-4}$) . The Ag^+ surface concentration in glass was obtained indirectly by optical measurements on fabricated waveguides. There are, however, two disadvantages in this method of determining surface concentration. First, the WKB method employed to determine the mode indices is subject to error under conditions where the waveguide supports only one or two modes. Also, the assumption of complete ion-exchange (all surface Na^+ ions in glass are substituted for Ag^+ ions) may not be valid. For example, in the case of K^+-Na^+ exchange from pure KNO_3 melts, only 90% of Na^+ sites at the glass surface are replaced by K^+ [15]. In

this work, the absolute concentration of Ag^+ ions in a soda-lime glass was measured by atomic absorption spectrometry (AA) for glass compositions that have been used to successfully fabricate glass waveguides of desired and reproducible characteristics [9,10,12,16]. The measured surface-silver concentration has been related to the surface index change (Δn) derived from the mode indices.

II. Theory:

A. The Diffusion Equation

The time dependent one- dimensional continuity equation for Ag^+, can be written as [17]:

$$\frac{\partial \bar{N}_{Ag}}{\partial t} = \frac{\partial}{\partial x} \left(\tilde{D} \frac{\partial \bar{N}_{Ag}}{\partial x} \right) \qquad (1)$$

where $\bar{N}_{Ag} = \dfrac{\bar{C}_{Ag}}{\bar{C}_{Na} + \bar{C}_{Ag}}$ is the mole fraction of Ag^+ in the glass phase,

$\bar{C}_i$ is the molar concentration of ion i, and $\tilde{D}$ is the interdiffusion coefficient given by [18]:

$$\tilde{D} = \frac{\bar{D}_{Ag}\,\bar{D}_{Na}}{\bar{N}_{Ag}\,\bar{D}_{Ag} + \bar{N}_{Na}\,\bar{D}_{Na}}\, n, \qquad (2)$$

In this expression, $\bar{D}_i$ is the tracer diffusion coefficient for ion i in the glass (self-diffusion coefficient) of the respective ion. The coefficient n is related to the concentration derivative of the Ag^+ activity in the glass (see Section II B).

In the case that $\bar{D}_{Ag} = \bar{D}_{Na}$ or $\bar{N}_{Ag} \ll 1$, the interdiffusion coefficient $\tilde{D}$ is directly proportional to the self-diffusion coefficient of silver, $\bar{D}_{Ag}$. Thus, under conditions of low silver concentration in the glass, $\bar{D}_{Ag}$ is expected to be approximately constant and the assumption of a

concentration independent interdiffusion coefficient is valid. As previously mentioned, one of the objectives of this study was to determine diffused Ag^+ concentration profiles produced under typical process conditions and thus identify the concentration range for which the above assumption is valid.

With the assumption that $\tilde{D}$ is independent of $\bar{N}_{Ag}$, equation (1) reduces to

$$\frac{\partial \bar{N}_{Ag}}{\partial t} = n\bar{D}_{Ag} \frac{\partial^2 \bar{N}_{Ag}}{\partial x^2} \quad . \tag{3}$$

With the initial and the boundary conditions,

$$\bar{N}_{Ag}\ (x,0) = 0 \quad \text{at } x > 0\ ,$$
$$\bar{N}_{Ag}\ (0,t) = \bar{N}^{o}_{Ag} = \text{constant}$$
$$\bar{N}_{Ag}\ (\infty,t) = 0,$$

the solution to equation (3) is [17]:

$$\bar{N}_{Ag}\ (x,t) = \bar{N}^{o}_{Ag}\ \text{erfc}\ (x/W_o), \tag{4}$$

where

$$W_o = 2\sqrt{\tilde{D}t} = 2\sqrt{n\bar{D}_{Ag}t}\ , \tag{5}$$

B. Ion-Exchange Equilibrium

Upon immersion of the glass substrate in the salt solution, Ag^+ is driven into the glass by an interphase chemical potential gradient [18]. To preserve charge neutrality, an equivalent amount of charge (i.e., Na^+) is transported in the opposite direction. The Ag^+ - Na^+ binary exchange process can be described [14] by the following chemical reaction:

$$Ag^+ + \bar{N}a^+ \quad \bar{A}g^+ + Na^+ \qquad (6)$$

where the bar indicates cations in the glass phase. In a liquid-solid phase exchange process, the rate of ion exchange may be limited by the following processes:

(i) Mass transfer of reactants to and removal of products from the reaction interface in the melt.

(ii) Kinetics of the reaction at the interface.

(iii) Transport of ions in the glass phase.

Transfer of cations in the melt can take place by diffusion and convection (natural or forced). Natural convection is driven by density variations and is not expected to be a dominant mechanism because of isothermal operation and small exchange amounts. By proper arrangement of the exchange geometry (horizonal placement of the glass at the top of the melt) solutal-driven natural convection can be eliminated. Forced convection can have a significant effect on ion transport in the bath melt. A hydrodynamic boundary layer, however, will develop near the solid surface; the extent of the boundary layer depending on the geometry. Ion diffusion is the mechanism of transport in a stagnant melt or across a stagnant boundary layer. For an infinite composite medium, Crank [17] gives the concentration in the melt as

$$N_{Ag} = \left[N_{Ag}^{o}/\left\{1+\frac{\bar{N}_{Ag}^{o}}{N_{Ag}^{o}}\left(\frac{\bar{D}_{Ag}}{D_{Ag}}\right)^{1/2}\right\}\right]\left\{1+\frac{\bar{N}_{Ag}^{o}}{N_{Ag}^{o}}\left(\frac{\bar{D}_{Ag}}{D_{Ag}}\right)^{1/2}\operatorname{erfc}\left(x/2\sqrt{D_{Ag}t}\right)\right\}$$

where N^{o}_{Ag} and D_{Ag} are the silver concentration at the melt-glass interface and diffusion coefficient in the melt and the bar signifies these quantities in the glass. When the quantity $(\bar{N}^{o}_{Ag} / N^{o}_{Ag})\ (\bar{D}_{Ag}/D_{Ag})^{1/2}$ is small compared to unity, the concentration is nearly constant in the melt and the diffusion resistance in the melt is small. The value of this quantity at conditions investigated in this study is on the order of 0.1. The values of the $\bar{D}_{Ag}$ and $(\bar{N}^{o}_{Ag} / N^{o}_{Ag})$ were taken from the results reported here and the value of D_{Ag} according to Inmann and Bockris [19]. Thus ion diffusion in the melt is not expected to be the major resistance in the exchange process.

Forced convection in the melt can be achieved by stirring the melt to increase the melt mass transfer rate. Reaction rates are generally rather fast and the limiting process is expected to be transport of Ag^{+} in the glass. This transport occurs by ion diffusion and the equilibrium state of reaction (6) specifies the surface boundary condition for this diffusion process. Control of the surface-index change and the cation exchange profile in glass is affected by manipulating this boundary condition and the cation transport properties in the glass.

The equilibrium constant for reaction (6) is defined as

$$K = \frac{\bar{a}_{Ag}\ a_{Na}}{\bar{a}_{Na}\ a_{Ag}} \quad , \tag{7}$$

where the a_i is the thermodynamic activity of Na or Ag. The value of K is a function of temperature and the composition of the glass and melt. For molten salts, the standard state is normally chosen to be the pure molten salt at the temperature of interest. The reference state for the glass phase is taken as that in which all of the exchangeable cations are of the species in

question. The ratio of the molten salt component activities for $AgNO_3$-$NaNO_3$ is well represented by regular solution theory [20]

$$\ln \left(\frac{a_{Ag}}{a_{Na}}\right) = \ln \left(\frac{N_{Ag}}{N_{Na}}\right) - \frac{A}{RT}\left(1 - 2N_{Na}\right) , \qquad (8)$$

where A is the net interaction energy which is assumed to be independent of temperature and melt composition. The measurements of Laity [21] at 330°C suggest the value of A equal to 3515 J/mole for the $AgNO_3$ + $NaNO_3$ melt.

The ratio of component activities in glass can be represented by an emperical n-type model, first suggested by Rothmund and Kornfeld [22],

$$\frac{\bar{a}_{Ag}}{\bar{a}_{Na}} = \left(\frac{\bar{N}_{Ag}}{\bar{N}_{Na}}\right)^n \qquad (9)$$

Garrel and Christ [23] have shown that this empirical relationship is equivalent to regular solution theory for intermediate glass compositions. Substitution of the activity ratios in equation (7) gives

$$\ln \left(\frac{N_{Ag}}{1 - N_{Ag}}\right) + \frac{A}{RT}\left(1 - 2\,N_{Ag}\right) = n \ln\left(\frac{\bar{N}_{Ag}}{1 - \bar{N}_{Ag}}\right) - \ln K \qquad (10)$$

If the activity models used to describe the solution behavior of both phases are valid, a plot of the left hand side of (10) versus $\ln \{ \bar{N}_{Ag} / (1 - \bar{N}_{Ag}) \}$ should yield a straight line with slope equal to n and intercept equal to ln(1/K).

III. EXPERIMENTAL PROCEDURE

The ion-exchange of Ag^+ with Na^+ in soda-lime silicate glass was carried out at 330°C as a function of time, $AgNO_3$ - $NaNO_3$ melt composition and melt stirring condition.

A summary of the experimental conditions is given in Table 1. The composition and density of the soda-lime glass used in the experiments is given in Table 2. Precleaned glass slides were rinsed in de-ionized water, allowed to dry and then placed in a sample holder prior to each experiment. The bath, sample holder and stirrers were all constructed of aluminum. The temperature was controlled to ± 2°C and monitored by a thermocouple housed in a stainless steel sheath.

After exchange, the glass sample was removed from the melt and allowed to cool. It was then washed in de-ionized water to remove adsorbed salt. The glass was then etched in steps of ~ 1μm in a 0.58 wt. percent HF solution. The resulting etch solution for each step was analyzed for silver in a Perkin-Elmer Model 280 atomic absorption spectrophotometer calibrated with standards of known concentration. The estimated precision of the measured concentration is ± 0.03 cation fraction and of the depth is ± 1.6×10^{-6} cm. In this manner concentration profiles of silver in the glass matrix were determined. It was observed that the profile data agrees very well with the erfc functionality expressed in equation (4). The best fit to the data was used to derive the value of surface concentration $\bar{N}_{Ag}^{o}$. This extrapolation procedure to derive $\bar{N}_{Ag}^{o}$ is reasonably accurate for low melt concentrations ($N_{Ag} < 10^{-3}$) since the silver concentration profile resembles erfc. At higher melt concentrations however, the profile is slightly altered and the extrapolation may cause errors on the order of 10% in $\bar{N}_{Ag}^{o}$.

Waveguides fabricated from the same batch were also analyzed by SEM to determine the silver diffusion profile. The experimental details are given in Ref. [12].

In addition, planar waveguides were characterized for the mode indices using a prism coupler. In the case of waveguides which supported one or two modes, the mode index data were correlated with the theory as follows: The one-dimensional normalized Helmholtz equation was solved for the measured profile by a finite-difference method to obtain the mode indices of the TE modes. The two parameters Δn and $W_o = 2\sqrt{\tilde{D}\,t}$ were adjusted to give the best fit to the measured mode indices. When waveguides supported many modes (>6), the inverse WKB method [24] was employed to give the index profile and the surface-index change (Δn).

IV. RESULTS AND DISCUSSION

Fig. 1 shows the measured concentration profiles for some of the samples listed in Table 1 ($N_{Ag} = 1.9\times10^{-4}$). The fact that the profile for a given melt concentration does not depend on the stirring condition suggests that the ion-exchange process is not mass transfer limited in the melt. The data of Fig. 1 can be adequately fit to the erfc index profile given by equations (4,5). This indicates that the interdiffusion coefficient, $\tilde{D}$, is indeed concentration-independent at low Ag^+ melt concentrations. The value of $\tilde{D}$, (2.2×10^{-15} m^2/s) as obtained from the data of Fig. 1, is in excellent agreement with that derived from measured optical mode indices and by the SEM technique.

A comparison of the values of $\tilde{D}$ obtained by various workers in similar glasses is shown in Table 3 where we have extrapolated their data to 330°C using an activation energy of 9.1×10^4 J/mole for $\tilde{D}$ [3,9]. Although our

results are in close agreement with the results of these authors except those of [5], close agreement is not expected a priori since the glass as well as melt compositions differ considerably and the procedures for deriving the values of $\tilde{D}$ from the measured diffusion profile also vary. For example, in the case of Ref. [28] the results were obtained by measuring the diffusion depth of the step-like profiles observed in the presence of an applied field and using the Einstein relation for the mobility and self-diffusion coefficient of silver ions. The extrapolated silver cation fractions and the corresponding melt cation fractions are plotted in Fig. 2 and, consistent with equation (10), the plot is linear within the experimental measurement error. A least-squares regression analysis of the data gives a value of n equal to 1.49 and K equal to 75. Thus, the partitioning of silver ions between the nitrate melt and soda-lime silicate glass is nonlinear in the composition studied. This non-linear behavior indicates that the assumption of concentration independent $\tilde{D}$ is valid only at very low melt concentration of silver ($\bar{N}_{Ag} \leq 0.1$ or equivalently $N_{Ag} \leq 2\times10^{-4}$). For $N_{Ag} > 10^{-3}$, almost 25% of the sodium ions in the glass are replaced by silver ions. For these compositions the first term in the denominator of equation (2) cannot be neglected and $\tilde{D}$ becomes concentration dependent. This is evidenced by a change in the concentration profile which is not consistent with equation (4) as discussed in Section II-A.

The results of these equilibrium studies are compared in Fig. 3 to the smoothed measurements of Schulze [13] in a soda-lime silicate glass. Using the same regular solution description of the melt, the values of n and K derived from the data of Schulze [13] are reported to be 1.08 and 120. Figure 3 also shows the 315° equilibrium results of Stewart and Laybourn [3] determined in a glass similar to that studied in this work. The reported

values of n and K are 1.32 and 131. The value of n reported in this work is close to the value of 1.4 reported by Garfinkel [4] in a borosilicate glass. The differences in the values of the exponent are probably related to differences in glass composition and/or structure. The value of the temperature dependent equilibrium constant is in fair agreement with the results of Schulze [13], Stewart and Laybourn [3], and of Doremus [25] in the high silica phase of two-phase pyrex. The results of our work suggest a large value of the silver partition coefficient, similar to the values determined by silver ion tracer diffusion studies in soda-lime glass [19]. Fig. 4 shows the correlation between Δn and $\bar{N}_{Ag}^{o}$ as a function of N_{Ag}. As expected, the two quantities obey a linear relationship, with $\Delta n \simeq 0.1\ \bar{N}_{Ag}$ for this glass composition. These results are in agreement with those of Fainaro et. al. [26] who used energy dispersive x-ray spectrometry for concentration measurements in a soda-lime glass of composition similiar to the one reported in this work.

The large value of equilibrium constant which is responsible for the steep slope of the $\bar{N}_{Ag}$ vs. N_{Ag} curve in Fig. 3 has important implications in batch fabrication of single mode fiber compatible waveguides using the Ag^{+}-Na^{+} ion-exchange process. Such guides are required to have diffusion depths of the order of 10 μm which translates into peak index changes of the order of $\Delta n = 3 \times 10^{-3}$. Such small changes can only be achieved at very low melt concentrations ($N_{Ag} \sim 10^{-4}$). Precise control of the melt concentration at values of $N_{Ag} \leq 10^{-4}$ is required to achieve adequate reproducibility in the waveguide characteristics. This can be achieved by using an electrolytic technique [10] for release of silver ions in the melt and insitu galvanic potential measurement to determine N_{Ag} and thus provide a feedback control loop [27].

V. Conclusion:

The Ag^+-Na^+ ion-exchange equilibrium has been studied under conditions used for fabrication of optical waveguides in soda-lime silicate glass. The concentration profile of silver in glass was measured by atomic absorption spectroscopy and analysis of back-scattered electrons in SEM. The surface-index change and the interdiffusion coefficient were determined from measurement of mode indices using a prism coupler. The ion exchange process was modeled by an ion diffusion limited process in the glass with an equilibrium chemical reaction at the melt- glass interface. The value of the equilibrium constant, K, was determined assuming a regular solution theory for the thermodynamic activity of the cations in the melt and an n-type behaviour in the glass phase. The large value of K indicates that the uptake of silver in glass varies in a highly nonlinear fashion with melt concentration. The results are in reasonable agreement with previous studies on similar glasses at higher melt concentrations. The surface-silver melt concentration N_{Ag}^{o} was correlated to the surface-index change and a linear relation, $\Delta n = 0.1\ \bar{N}_{Ag}^{o}$, was empirically determined for this glass composition. It was found that the interdiffusion coefficient is concentration independent at low melt concentration and excellent agreement was observed in the concentration values obtained by AA, SEM and optical techniques.

Acknowledgement: This work was supported by Grant No. 84-0369 from Air Force Office of Scientific Research. We thank Dr. Don Ulrich and Mr. H. C. Cheng for many helpful discussions.

REFERENCES

1. T. G. Giallorenzi, E. J. West, R. Kirk, R. Ginther, and R. A. Andrews, "Optical Waveguides formed by thermal migration of ions in glass," Appl. Opt., Vol 12 pp. 1240-1245, 1973.

2. J. G. Gallagher and R. M. de LaRue, "Single-mode stripe optical waveguides formed by silver ion exchange", Electron. Lett., Vol. 12, pp. 397-398, 1976.

3. G. Stewart and P. J. R. Laybourn, "Fabrication of ion-exchanged waveguides from dilute silver nitrate melts", IEEE J. Quantum Electron., Vol. QE-14, pp. 930-934, 1978.

4. G. Chartier, P. Collier, A. Guez, P. Jaussand, and Y. Won, "Graded-index surface or buried waveguides by ion exchange in glass", Appl. Opt., Vol. 19, pp. 1092-1095, 1980.

5. R. G. Walker and C. D. W. Wilkinson, "Integrated optical waveguiding structures made by silver ion-exchange in glass: 1: The propagation characteristics of stripe ion-exchanged waveguides; a theoretical and experimental investigation", Appl. Opt., Vol. 22, pp. 1923-1928, 1983.

6. R. G. Eguchi, E. A. Mounders and I. K. Naik, "Fabrication of low-loss waveguides in BK-7 by ion exchange", Proc. SPIE, Vol. 408, pp. 21-26, 1983.

7. T. Findakly and E. Garmire, "Reduction and control of optical waveguide losses in glass", Appl. Phys. Lett., Vol. 37, pp. 855-856, 1980.

8. S. I. Najafi, P. G. Suchoski, Jr., and R. V. Ramaswamy, "Silver film-diffused glass waveguides: diffusion process and optical properties", IEEE J. Quantum Electron,. Vol. QE-22, pp. 2213-2218, 1986.

9. R. K. Lagu and R. V. Ramaswamy, " Process and Waveguides parameter relationships for the design of planar, silver ion-exchanged glass waveguides", IEEE J. Lightwave Tech., Vol. LT-4, pp. 176-181, 1986.

10. R. K. Lagu and R. V. Ramaswamy, "Fabrication of single-mode glass waveguide by electrolytic release of silver ions", Appl. Phys. Lett., Vol. 45, pp. 117-118, 1984.

11. M. L. Huggins, "The refractive index of silicate glasses as a function of composition", J. Opt. Soc. Am., Vol. 30, pp. 495-504, 1940.

12. R. V. Ramaswamy and S. I. Najafi, "Planar, buried, ion-exchanged glass waveguide: diffusion characteristics", IEEE J. Quantum Electron. Vol. QE-22, pp. 883-893, 1986.

13. G. Schulze, "Versuche uber die diffusion von silber in glas", Ann. Physik, Vol. 40, pp. 335-367, 1913.

14. H. M. Garfinkel, "Ion-exchange equilibria between glass and molten salts", J. Phys. Chem. Vol. 72, pp. 4175-4181, 1968.

15. T. J. Cullen, C. M. Ironside, C. T. Seaton, and G. I. Stegeman, "Semiconductor-doped glass ion-exchanged waveguides", Appl. Phys. Lett., Vol. 49, pp. 1403-1405, 1986.

16. H. C. Cheng, R. V. Ramaswamy, and R. Srivastava, "Buried Na^+ - Ag^+ ion exchanged waveguides: theory and experiment", Tech. Digest, Seventh Toptical Meeting on Grandient-Index Optical Imaging Systems, Jan. 15-16, 1987, Reno, Nev. pp. 28-30.

17. J. Crank; The Mathematics of Diffusion-Oxford at the clarendon Press, 1956.

18. R. H. Doremus, "Exahange and diffusion of ions in glass", J. Phys. Chem. Vol. 68, pp. 2212-2218, 1964.

19. O. Inman, and Bockris J. O. M. Bockris, " The application of the galvanostatic potential-time technique to analysis in molten salts." J. Electroanal. Chem 3, 126 (1962).

20. J. G. Kirkwood and J. Oppenheim, Chemical Thermodynamics, McGraw-Hill, New York, 1961.

21. R. W. Laity, "Fused Salt Concentration cells with Transference. Activity Coefficients in the System Silver Nitrate -Sodium Nitrate," Am. Chem. Soc., Vol. 79, pp. 1849-1851, 1957.

22. V. Rothmund and G. Kornfeld, "Der basenaustausch im permutit. I.", Z. Anorg. Allg. Chem., Vol. 103, pp. 129, 1918.

23. R. M. Garrel and C. L. Christ; Solutions, Minerals, and Equilibria: Harper and Row, New York, 1965.

24. J. M. White and P. F. Heidrich, "Optical waveguide refractive index profiles determined from measurement of mode indices: A simple analysis", Appl. Opt., Vol. 15, pp. 151-155, 1976.

25. R. H. Doremus; Ion Exchange: A series of Advances; Marcel Dekker Inc. New York, 1966

26. I. Fainaro, M. Tsh Shalom, M. Ron, and S. Libson, "Interdifusion of silver in glasses and the related variations in electronic polarisability", Phys. Chem. Glasses, Vol. 25, pp. 16-21, 1984.

27. R. K. Lagu, S. E. Najafi and V. Ramaswamy, "Insitu measurement of ionic concentration during fabrication of ion-exchanged wageguides," Appl. Opt. Vol. 23, pp. 3925 -3920, 1984.

28. H. J. Lilienhof, E. Voges, D. Ritter, and B. Pantschew, "Field-induced index profiles of multimode ion-exchanged strip waveguides", IEEE J. Quantum Electron, Vol. QE-18, pp. 1877-1883, 1982.

LIST OF FIGURES

Table 1. Summary of experimental conditions for ion-exchange studies at 330°C.

Sample	N_{Ag}	Time (h)	Number of stirrers
A	1.90×10^{-4}	1	0
B	1.90×10^{-4}	1	0
C	1.90×10^{-4}	1	1
D	1.90×10^{-4}	1	1
E	1.90×10^{-4}	1	2
F	1.90×10^{-4}	3	1
G	1.90×10^{-4}	4	1
H	9.97×10^{-4}	4	1
I	1.97×10^{-3}	4	1
J	4.06×10^{-3}	4	1
K	8.03×10^{-3}	4	1
L	1.20×10^{-2}	4	1

Table 2. Chemical composition of Fisher brand glass slide (wt%).

Oxide	Weight %
SiO_2	72.25
Na_2O	14.31
CaO	6.40
Al_2O_3	1.20
K_2O	1.20
MgO	4.30
Fe_2O_3	0.03
SO_3	0.30

Density = 2.4667 g/cm^3

Table 3. Interdiffusion Coefficients (330°C).

Reference	$\tilde{D}$ ($10^{-15} m^2/s$)
This work	2.2
3	2.06
18	2.47
28	1.77
5	7.1

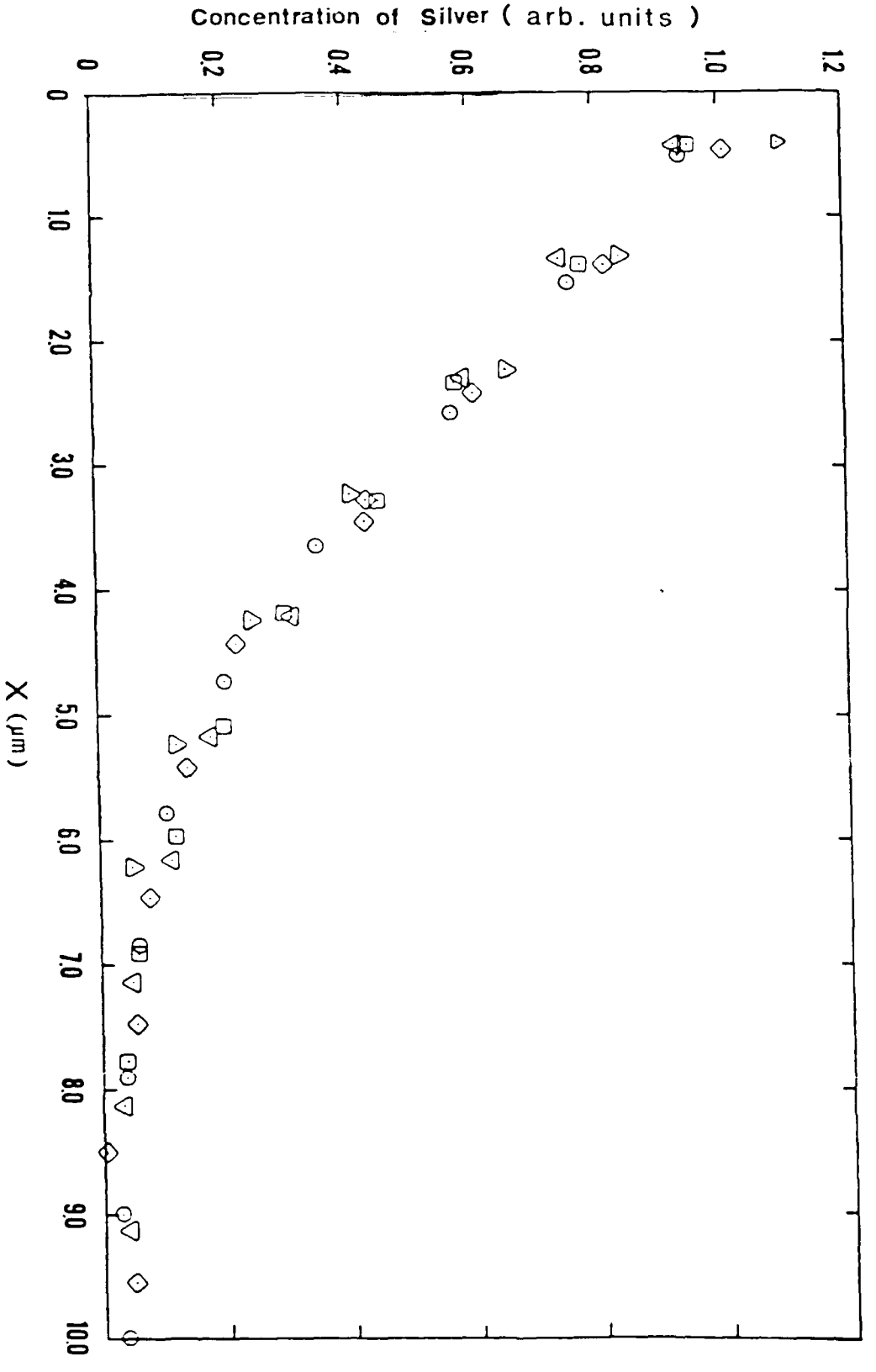
Concentration of Silver (arb. units)
0
0.2
0.4
0.6
0.8
1.0
1.2
X (μm)
0
1.0
2.0
3.0
4.0
5.0
6.0
7.0
8.0
9.0
10.0

Fig. 1

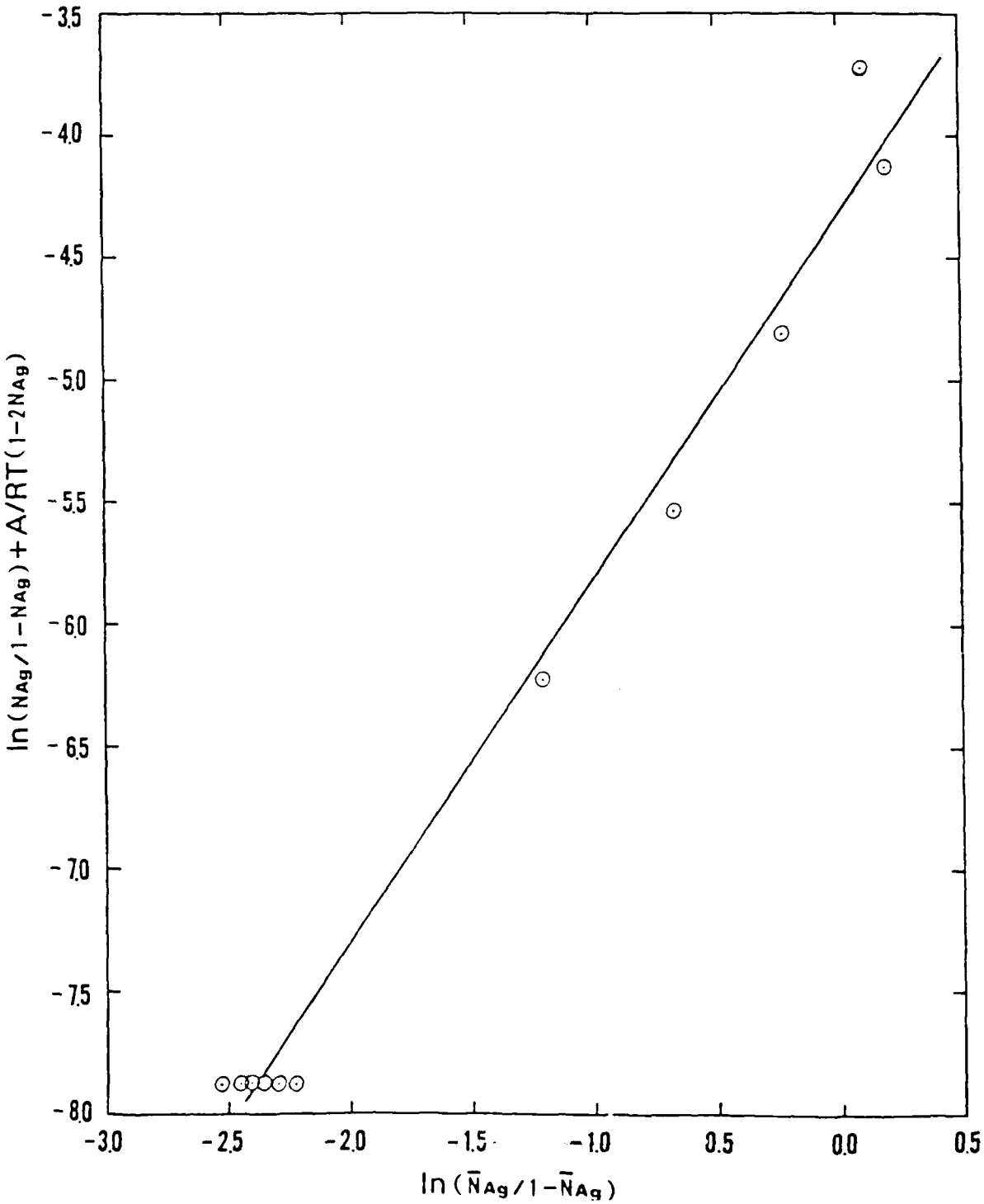
-3.5
-4.0
-4.5
-5.0
-5.5
-6.0
-6.5
-7.0
-7.5
-8.0
-3.0
-2.5
-2.0
-1.5
-1.0
0.5
0.0
0.5
ln(NAg/1-NAg)+A/RT(1-2NAg)
ln(N̄Ag/1-N̄Ag)

Fig. 2

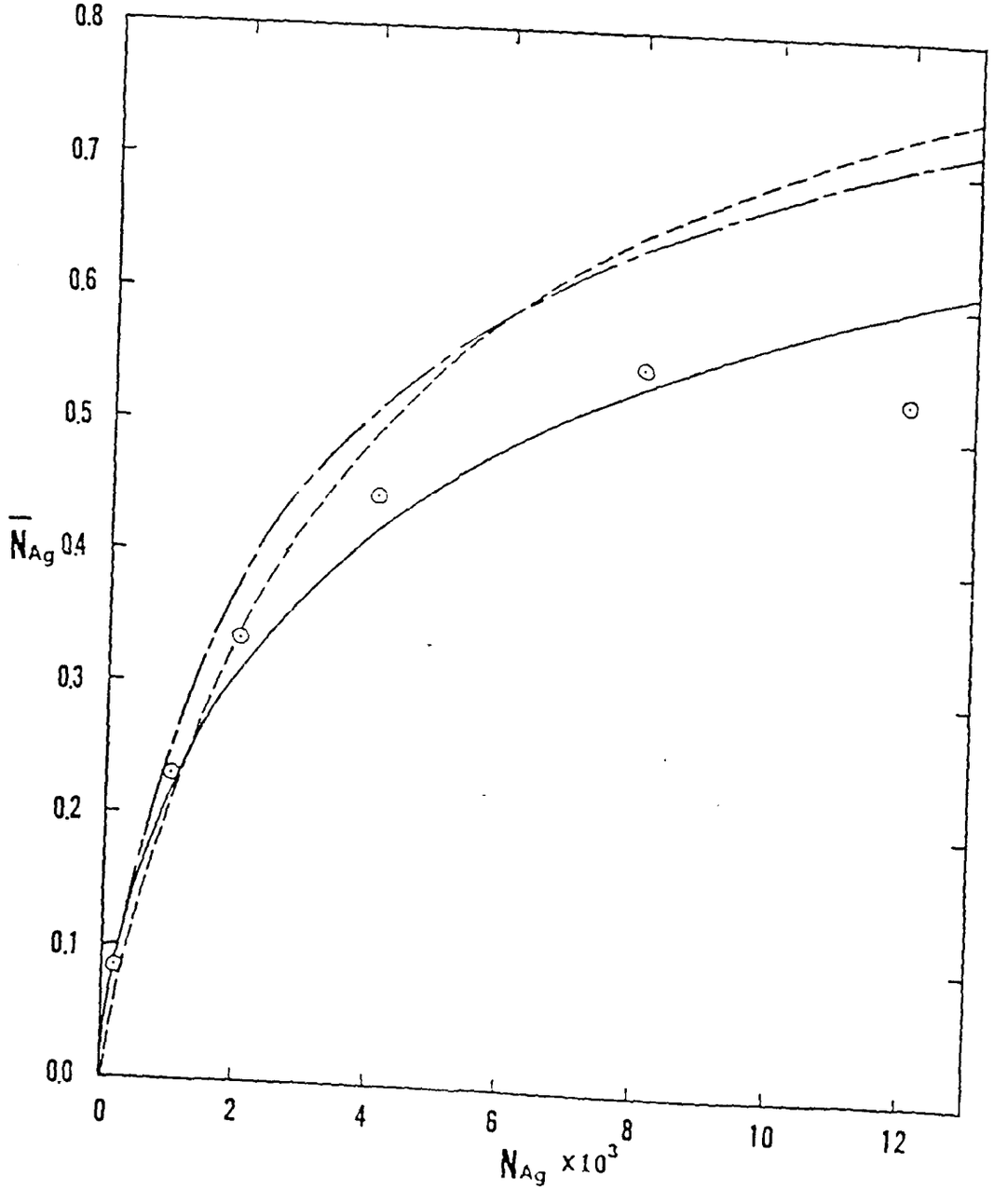

Fig. 3

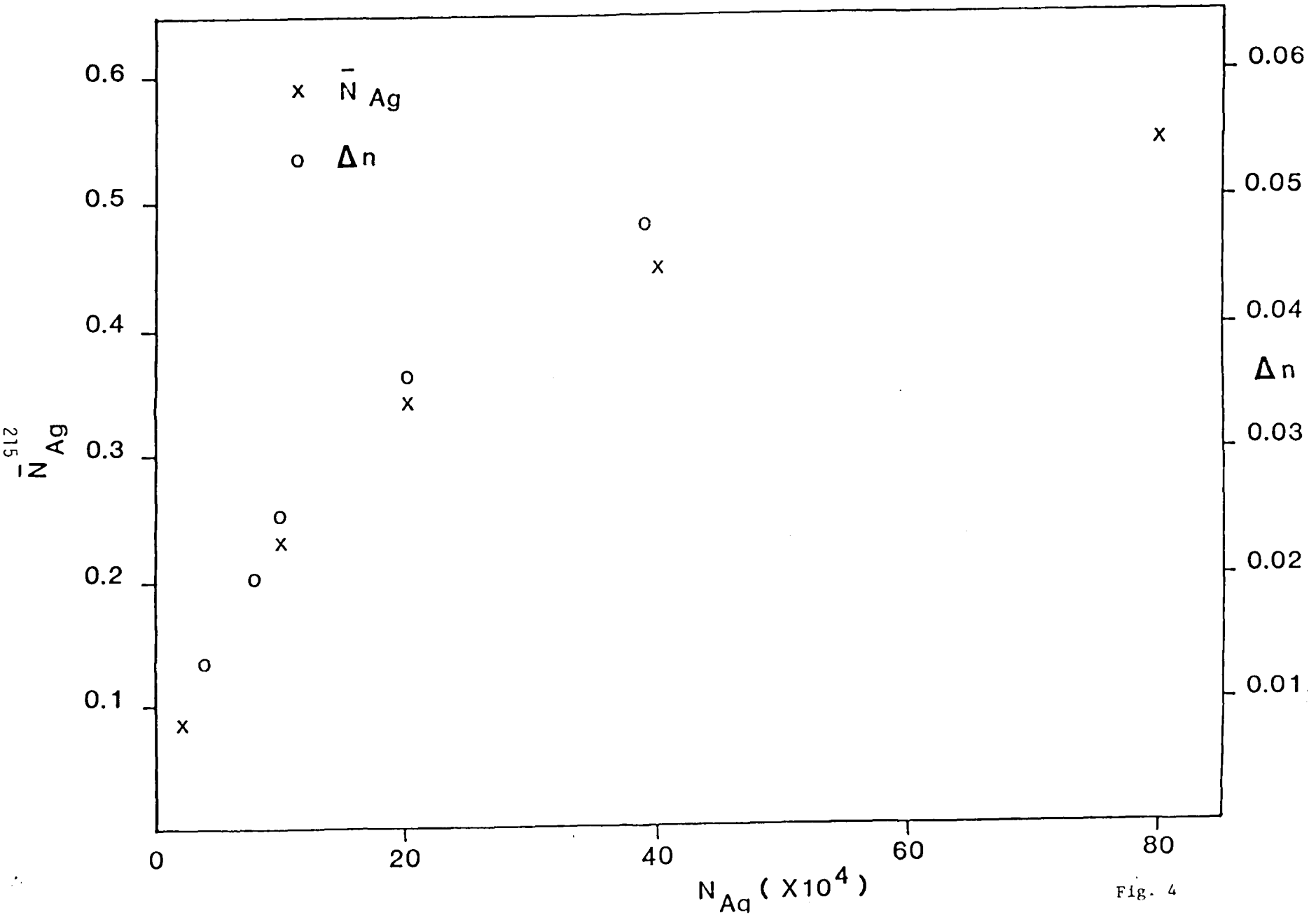
x $\bar{N}_{Ag}$
o Δn
0.6
0.5
0.4
0.3
0.2
0.1
0.06
0.05
0.04
0.03
0.02
0.01
Δn
$\bar{N}_{Ag}$
0
20
40
60
80
N_{Ag} (X10^4)

Fig. 4

REFERENCE [15]

Fabrication and Characterization of Single-Mode Glass Waveguides

R. Srivastava, R. V. Ramaswamy, H. C. Cheng and H. Zhenquang*

Department of Electrical Engineering
University of Florida, Gainesville, FL 32611
*Permanent Address: Changchun Institute of Technology
Changchun, China.

Abstract

We describe fabrication and characterization techniques for glass waveguides for integrated optical components using ion-exchange technique, with emphasis on silver-sodium exchange in soda-lime silicate glass. A systematic study of the relationship between process parameters and waveguide performance is presented with the objective of optimization of the I-O components for fiber compatibility.

I. INTRODUCTION

Passive glass waveguides made by ion-exchange technique are considered to be prime candidates for I-O device applications such as star couplers, access couplers, wavefront sensors, multiplexers, demultiplexers, and in sensors such as gyroscopes. The importance of the glass waveguide-based I-O components is borne out by their compatibility with optical fibers, potentially low cost, and low propagation losses. However, strict tolerance requirements are placed on passive components as the glass index cannot be varied by application of an external field. Fabrication of devices such as multiplexers calls for reproducibility in the propagation constant of the guided mode to an accuracy of better than 10^{-4}. In order to fabricate glass waveguide devices with such reproducible characteristics, it is necessary that the role of processing parameters on the waveguide performance be well understood.

Ion-Exchange Process

Optical waveguides in glass substrates can be fabricated by ion-exchange process[1] which creates a layer of higher effective index near the surface of the substrate. This is accomplished by diffusion of a monovalent cation of higher polarizability e.g. Cs^+, Rb^+, K^+, Ag^+, Tl^+ into the glass matrix where it exchanges with Na^+ or K^+ ions.[2-4] Of the various ions exchanged in glass by diffusion, each one has its advantages and disadvantages.[5] Most of the work published in the literature is based on K^+-Na^+ or Ag^+-Na^+ binary systems. K^+ can be easily incorporated in soda-lime,[6] borosilicate or pyrex glasses[7] from pure KNO_3 melt. The accompanying surface-index change is small (~0.01) and the diffusion process is characterized by a small diffusion coefficient ($D \sim 2\times10^{-16}$ m^2/s at 385°C). Thus large diffusion times (~ few hours) are necessary for suitable waveguiding to occur. K^+-Na^+ exchange has been used for fabrication of channel waveguides,[8] star couplers[9] and directional couplers[8] for single-mode device aplications but the structures have not been optimized either for the waveguide losses or for their compatibility with optical fibers. Moreover, the resulting waveguides are observed to be birefringent.[6]

Ag^+-Na^+ Exchange

The binary exchange of Ag^+-Na^+ is by far the most researched technique[3,10-18] and in the following we will emphasize this process particularly. When pure $AgNO_3$ melt is used, large Δn (~0.1) waveguides are obtained which have some disadvantages: A large silver concentration in glass causes coloring due to silver reduction; single-mode guides are shallow (~ 2 μm deep) and thus incompatible with optical fibers used in optical communications systems. Moreover, the diffusion time is rather short (~ minutes), thereby causing uncertainty and lack of reproducibility in waveguide characteristics. Dilute solutions of $AgNO_3$ and $NaNO_3$ are therefore used[13,14] to allow lower Δn and more controllable diffusion times (~ 60 min.). A very low ionic concentration ($N_{Ag} \sim 10^{-4}$ mole fractions) of silver is necessary to obtain single-mode waveguides with diffusion depth compatible with singe-mode fiber cores. This is attributed to a relatively large partition coefficient of silver in soda-lime glass as determined by ion-exchange equilibrium studies.[16] The results (shown in Fig. 1) show uptake of Ag^+ by glass is a highly nonlinear function of silver melt concentration and a slight variation in its value is expected to cause large changes in the surface-index change. This accentuates the requirement for a tight control of N_{Ag}. Such a control may be achieved by on-line monitoring of N_{Ag} using a concentration cell,[17] releasing silver ions into the molten $NaNO_3$ salt bath by the electrolytic release technique[17] and controlling the concentration using a feed back loop.

II. PROCESS PARAMETERS AND WAVEGUIDE CHARACTERISTICS

For I-O applications it is desirable to fabricate waveguides with low propagation loss and desired refractive index profile. The propagation losses are dominated by absorption primarily due to presence of foreign impurities in the substrate glass and the scattering contributions caused by the glass inhomogeneity and surface or geometric imperfections. By careful choice of the host glass, absorption losses as low as 0.07 dB/cm have been obtained.[18] Scattering losses, on the other hand, are generally introduced in the processing steps. Dopants introduce additional Rayleigh scattering to the background losses caused by the multicomponent nature of the glass. Reduction of the incoming ions to matallic silver in the glass matrix can give rise to additional losses. Surface irregularities invariably interact with the propagating field and contribute to losses by scattering. This can be minimized by burying the waveguide under the glass surface by carrying out a two-step ion-exchange process. In channel waveguides, the imperfect wall boundaries caused during the photolithography may introduce additional loss. This loss contribution is less serious, however, since the diffusion process smooths out such irregularities. Finally, in devices, the waveguides invariably go through bends, bifurcations or tapered transitions. These transitions have to be designed carefully to limit the radiation losses.

The refractive index profile on the other hand, depends on various parameters in an intricate manner. The composition of the host glass, the nature of the incoming ion and its concentrationn in the melt, the diffusion temperature, time and the magnitude of the externally applied field, all affect the index profile.

The modelling of the diffusion profile in glasses requires a knowledge of the boundary and initial conditions and solution of the diffusion equation which involves parameters such as surface concentration, diffusion coefficient $\tilde{D}$ and mobility μ of the incoming ion and their temperature dependence. These parameters are determined by first fabricating a planar waveguide and measuring the absolute concentration profile. The diffusion width Wo is related to the diffusion coefficient $\tilde{D}$ via $Wo = 2\sqrt{\tilde{D}t}$ where t is the diffusion time. The surface-index change Δn is linearly proportional to the surface-silver concentration $\tilde{N}_o$ in the glass and can be either derived from empirical formulas given by Huggins[19] or measured optically. The mobility μ is obtained by fabricating a planar waveguide in presence of an applied field E and fitting the resulting concentration (index) profile to an analytical solution of the diffusion equation using previously determined values of $\tilde{D}$ and Δn.[20] μ is kept as the fitting parameter as it cannot be determined from $\tilde{D}$ since the Einstein's relation does not hold in glasses.[21] Once these parameters have been determined, two-dimensional diffusion equation can be numerically solved to predict the channel waveguide diffusion profile for a given set of processing conditions. The propagation characteristics of the resulting waveguides can be calculated by solving the two-dimensional Helmholtz equation using one of the several numerical methods developed for arbitrary index profiles.[22-24] A comparison of the theoretically predicted properties with the characterization results provides the necessary correlation to optimize the processing for specific waveguide properties.

III. FABRICATION

The schematics of the Ag^+-Na^+ ion-exchange technique from molten salts is shown in Fig. 2. The melt is held in a crucible or beaker which is kept at a constant temperature by enclosing it in a furnace. The melt consists of the appropriate salt as the source for the diffusing ions. The desirable characteristics which influence the choice of the salt for a given ion are its melting point and the dissociation temperature. Nitrate salts have been used extensively as they have some of the lowest melting temperatures and exhibit reasonable stability. The diffusion temperature is adjusted to control the rate of diffusion. In some cases, melting temperatures can be lowered by using a mixture of two nitrate salts. For example, pure KNO_3 melts at 334°C and pure $NaNO_3$ at 307°C; however, a mixture of 10 wt % KNO_3 and 90wt% $NaNO_3$ melts at 290°C. In the schematics of Fig. 2, silver ions are released electrolytically[14] and their concentration measured during diffusion.[17]

For planar waveguide fabrication, polished glass substrates are immersed in the molten bath by using an aluminum sample holder. Strip waveguides are prepared by first carrying out photolithography to create masked regions of aluminum or some other material such as Al_2O_3, SiO_2, etc. First a 1500-2000 A° layer of aluminum is evaporated on the glass surface. A photoresist layer ~1μm thick is then spun over the Al layer. The glass is then baked at 80°C for about 25 min. and then the photoresist layer is exposed to ultra-violet radiation under the appropriate mask. Following this, the exposed photoresist regions are developed and the underlying aluminum layer is removed by aluminum etch. These glass samples are then immersed to bring the masked surface in contact with the molten salt, permitting ion-exchange in the open regions (channels).

In order to apply the electric field during the ion exchange process, two approaches

have been implemented. In one case, the negative electrode consists of a platinum wire pressing against a gold film evaporated on a thin chromium film on the back surface of the glass sample.[20] Chromium is helpful in making a good contact with the gold film. An alternative to the gold film is to use a molten salt mixture. This eliminates the step of evaporating gold and therefore, is the less expensive method. The melt has to be kept bubble-free to assure uniform field across the substrate. In either case, the anode consists of a platinum wire immersed in the molten salt as shown in Fig. 2. The resistivity of the melt depends on its composition and temperature and there is a potential drop across the melt which may be of the order of 10% of the total applied voltage for 1mm thick soda-lime glass substrates with 4-5 cm^2 cathode area.[20]

IV. CHARACTERIZATION

The important characterizations of passive waveguides include measurement of index (dopant) profile, propagation constants of the guided modes, attenuation and mode field pattern.

There are two different approaches for measurement of the refractive index profile in a glass waveguide fabricated by ion-exchange process. One of these involves measuring the dopant profile using analytical tools such as electron or ion microprobe,[3] analysis of back-scattered electrons in a scanning electron microscope,[20] or atomic absorption spectrophotometry.[16] The other alternative is to carry out optical measurements of parameters such as surface reflectivity or mode indices of the guided modes. The latter data are then used to derive the index profile by using inverse WKB approximation[25] which works well only for highly multimode waveguides with graded-index profiles.

Concentration Profile

Electron microprobe has been used to measure the profile of the diffusing ion.[3] In this technique, the high-energy electrons are collected and analyzed for the concentration of the ion of interest. The results have to be analyzed carefully as the presence of other ions e.g. Ca^{++}, Al^{+++}, Mg^{++} etc. in the glass may give rise to spurious effects.[3] Electron microprobe is universal in the sense that any ion can be analyzed. However, sensitivity depends strongly on the ion with the result,the data can be very noisy to draw useful or definite conclusion, particularly if the concentration of the ion is extremely low, such as the case of Ag^+-Na^+ exchanged single mode waveguides.[15] Spatial resolution of the order of 2 μm is typically achieved, making the technique suitable for multimode waveguides only.

Scanning electron microscope can be used for determination of the profile in two ways. One either analyzes the x-rays (energy dispersive spectrometry, EDS) characteristic of the ion in question[26] or, alternatively, analyze the back-scattered electrons originating from the ion.[20] Both have been successfully used to measure Ag^+ concentration in multimode soda-lime glass waveguides. The resolution is of the order of 1 μm and since the scattering efficiency is higher for ions of larger atomic numbers, only heavier ions such as Cs^+, Rb^+ and Ag^+ may be amenable for this analysis. High mobility of ions such as sodium under the beam precludes their measurement using this method.

Atomic absorption spectrophotometry is an analytical tool for concentration measurement of any element. Here a thin layer of the sample surface is etched using HF acid solution and the solution is analyzed for the ionic concentration. Subsequent etching is performed and the analysis repeatedly carried out until the concentration profile is determined.[16] Depending on the diffusion depth, and the spatial resolution desired, the number of steps may be anywhere between 10 and 20. The technique is destructive but is capable of giving absolute concentrations without a great deal of effort.

Refractive-Index Profile

Although for low concentration of the diffusing ions generally encountered in ion-exchange problems, the concentration profile gives the refractive index profile, there are cases where this is not true. In fact, it has been shown recently that Huggins relation,[16] widely used for predicting the index change upon substitution of the host ion by the diffusing ion, does not hold in certain cases such as when Ag^+-Na^+ exchange occurs from pure $AgNO_3$ melt in high-content sodium glasses.[37] Thus, it is of great importance to know the index profile directly.

There are several techniques for measurement of the index profile in waveguides. These include interferometry, reflectivity measurement and the inverse WKB method which relies on the mode indices data.

Interferometry is by far the most accurate and direct technique. Here, monochromatic light beam is split into two arms of a Mach-Zhender interferometer. One beam passes through a thin (~30μm) polished sample and the other through a reference object. The two beams are

combined at a detector and the resulting interference pattern is recorded. The fringe data is converted back into index information and two-dimensional profile can be obtained. The difficulty lies in the sample-preparation which is time consuming and laborious. Moreover, it is a destructive method. Commercial interference microscopes are not readily available and consequently one has to build his own equipment.

The two-dimensional index profile can also be determined by measuring reflectivity from polished faces with the aid of an optical multi-channel detection system.[28] The surface of the sample is first beveled to a small angle (few degrees) and then illuminated at normal incidence in an optical microscope. The two-dimensional reflectivity is measured by a vidicon tube attached to the microscope. The index distribution is calculated from Fresnel's formula. High spatial resolution can be easily achieved because of the beveling. The system can be calibrated by measuring the reflectivity of a known sample. It is necessary that the vidicon response be linear for the intensity levels involved. The system should be capable of accounting for the stray light. Requirment of absolute measurements of power levels make this technique subject to error. However, the resolution of index change measured is limited to 10^{-3}, making this method suitable only for multimode guides.

Although both the methods described above yield the index distribution in two dimensions, they require absolute measurements of illumination. Another method which yields the index profile of the waveguide relies on the measurement of mode indices. This can be easily accomplished by the prism coupler technique with accuracies approaching 1×10^{-4}. From the mode-index data, the index profile is derived using the inverse WKB method.[25] While this method gives reasonably good results in the case of ERFC and exponential profiles, there are serious problems in determining the refractive index near the glass surface[25] as well as at the profile tails (where it approaches the substrate value and mode index values are inaccurate). Thus, care should be taken when the index profile is flat (as in the case of Gaussian or step-like profiles) or if there are step-like transitions such as the case of electric-field induced ion-exchange or the Cs^+-Na^+ ion-exchange (where the double alkali effect gives sharp, step-like profile[4]). Moreover, the WKB approximation is known to be erroneous near the mode cutoffs.[29] The method may thus give reliable results for determining diffusion depths but the value of surface-index change is always subject to error. In case of surface waveguides (such that prism coupling can be employed for measurement of mode indices) with large number of guided modes, WKB method has been used extensively for characterization of waveguides.[6,7,11,13] In the Ag^+-Na^+ exchanged single-mode guides, the index profile is ERFC when low concentration of silver in the melt ($_{Ag}$~10^{-4}) is used. W_o and Δn are determined by fitting the measured mode indices to those calculated by solving the Helmholtz equation and treating W_o and Δn as adjustible parameters.[15]

Attenuation and Mode Field Profile

The techniques for measurement of attenuation and mode field profile in ion-exchanged waveguides are similar to those used in integrated optics with Ti:$LiNbO_3$ waveguides. For planar guides, attenuation can be measured by the three-prism method.[30] This method measures total attenuation, i.e., contribution from scattering as well as absorption. Alternatively, scattering contribution to attenuation can be measured independently by probing a fiber tip along the waveguide and capturing the scattered signal. The variation of this signal as a function of propagation distance along the waveguide is plotted to determine the scattering loss. If the attenuation is below 0.1 dB/cm, neither the three-prism nor the fiber probe method is adequate and one resorts to resonant structures such as Fabry-Perot ring resonator.[31] In this case light is coupled into a ring waveguide from a straight waveguide by distributed directional coupling mechanism and the output from the ring is extracted in a similar fashion. By measuring the transmission of the Fabry-Parot as a function of temperature, both the finesse and the contrast can be determined and from these parameters the loss per unit pass can be extracted.[31] Another method of estimating propagation losses in single-mode channel waveguides is described in the following section.

Mode field profile measurement is of paramount importance in waveguide characterization. Fiber-waveguide coupling, performance of the directional coupler, curvature-induced losses, all depend on the mode field. Near field method shown schematically in Fig. 3 is the most convenient and direct way to measure the field pattern.[32] In fact, beside the waveguide mode field, the method shown here allows determination of various other parameters with very little additional effort. These are: the fiber mode field, the fiber-waveguide coupling loss and the propagation loss in the waveguide. The measurement procedure is as follows:[33]

Light from either a He-Ne laser or a 1.3 μm semiconductor laser is coupled into a short piece of a single-mode fiber. The fiber is either birefringent type so that it maintains the linear polarization or in the case of conventional fiber, the fiber is kept as steady as possible to prevent polarization fluctuations and linear output polarization is achieved by adjusting the compensator at the input end. Linear polarization allows excitation of either

TE or TM like modes in the guide. The waveguide output is collected by a high-quality planar objective by imaging the waveguide end on a phodetector/amplifier with a pinhole mounted at its front end. The two-dimensional nearfield intensity pattern is measured by scanning the detector horizonally and vertically and recording the signal from the lock-in amplifier on a chart recorder or storing it in a computer. The Fabry-Perot effect caused by the Fresnel reflections at the fiber-waveguide gap is taken care of by adjusting the spacing for maximum transmission.[33] Fiber-near field can also be measured using the same procedure after removing the waveguide. The magnification of the system is determined by imaging a known mask pattern at the detector face and scanning the detector.

In order to determine the fiber-waveguide throughput efficiency, the output from the fiber is first measured. Then the waveguide is adjusted for maximum transmission and the output once again measured. Accuracies of the order of 0.01dB can be achieved using this procedure.[33]

In order to derive the propagation losses from the measurement of fiber-waveguide throughtput loss and the fiber and waveguide mode profiles, the following procedure can be used. The total throughput loss is made of three components: 1) Fresnel loss due to reflections of the optical field at the waveguide input and output interfaces, 2) the propagation loss, and 3) mode mismatch loss due to different field distributions of the single-mode fiber and channel waveguide. Since the refractive indices of the fiber and glass substrate are very nearly equal (1.46 and 1.51 respectively), the Fresnel loss is small and can be made negligible if the fiber-waveguide spacing is adjusted for maximum transmission. The mode mismatch loss is calculated by evaluating the normalized overlap integral[34]

$$\eta = \frac{\left[\int_{-\infty}^{\infty} E_f(x,y)\, E_g(x,y)\, dxdy\right]^2}{\left[\int_{-\infty}^{\infty}\int_{-\infty}^{\infty} E_f^2(x,y)\, dxdy\right]\left[\int_{-\infty}^{\infty}\int_{-\infty}^{\infty} E_g^2(x,y)\, dxdy\right]} \qquad (1)$$

where $E_f(x,y)$ and $E_g(x,y)$ are the mode field profiles of the fiber and waveguide respectively. The mode-mismatch loss is given by $-10 \log_{10} \eta$. If it is assumed that the two mode profiles are Gaussian along both the x and y axes, then

$$\eta = \frac{4}{\left(\frac{w_x}{d} + \frac{d}{w_x}\right)\left(\frac{w_y}{d} + \frac{d}{w_y}\right)} \qquad (2)$$

where w_x and w_y are the 1/e intensity full width and depth of the waveguide mode and d is the 1/e intensity diameter of the fiber mode. Although the Gaussian mode approximation may be reasonable for well-guided modes in buried channel waveguides where the field distribution tends to be symmetric, surface waveguides with not-so-well guided modes deviate from the Gaussian case and a numerical evaluation of integral (1) is necessary to determine the mode mismatch loss accurately.

Once the mode mismatch losses have been determined, the propagation loss in the waveguide is obtained by subtracting is from the overall fiber-waveguide throughtput loss.

V. OPTIMIZATION

Table I lists composition of a commercial soda-lime glass which has been used for fabrication of ion-exchanged waveguides. Fabricating planar guide in dilute concentration of $AgNO_3$ in $NaNO_3$ melt, diffusion constant, Δn and μ were measured at 330°C.[15,20,35] Using these data, surface channel waveguides were fabricated at 330°C with mask width W_c ranging from 2 μm to 10μm, and characterized for their index profile,[36] cutoff wavelengths,[36] and modefield profiles.[37] Comparison of the surface-index change Δn and diffusion depth W_o with the corresponding planar waveguides indicated that although both Δn and W_o for channel waveguides are smaller than the corresponding values for planar guides, their values increase with increasing W_c and approach the planar values for W_c approaching 6 μm.[36] Moreover, there was substantial side diffusion of silver under the metallic masks[36] (Fig. 4) which gave rise to highly elliptical mode field distribution.[37] Single-mode surface guides were obtained with diffusion times of 1 hour for $3 < W_c < 7$μm. No external electric field is necessary in the first step.

A minimum fiber-waveguide throughput loss of 1.6dB was obtained for channels 17 mm long with W_c in the range of 5-6 μm. However, when these waveguides were buried by applying an external field in the second step, the resulting field distributions were quite circular.[37] Both scattering and mode mismatch losses were reduced and a total fiber-waveguide throughput loss of 1 dB was achieved for the same channels. This relative

insensitivity of the mode field distribution to the mask width is desirable for satisfactory reproducibility. The results show that the two-step ion-exchange process is essential to get low loss symmetrical waveguides.[37] While index profile of the buried guide can be controlled by adequate choice of D, N_{Ag}, diffusion times and the applied field, the position of the index peak depends only on the product of the applied field and second-step diffusion time. It appears that the waveguides can be buried to desired depth and the index profile can be tailored fairly independently by a careful choice of parameters.[35]

What is the reproducibility of these waveguides? In planar waveguides, the index profile and the propagation constant have shown excellent reproducibility. Even when electric field is applied, the propagation constant can be reproduced to better that 2×10^{-4} accuracy. In the case of channel waveguides, as pointed out earlier, the field profile and attenuation are highly reproducible as they are relatively insensitive to the actual index profile. But in devices such as directional couplers, it is not only the overlap between the fields of the adjacent guides which should be reproducible, but also their individual propagation constants since the power transfer depends on the phase mismatch between the two modes. Experiments are in progress at present to answer these questions as the feasibility of mass production of passive waveguide components depends very critically on these issues.

Acknowledgement: This work was supported by Bell Communications Research and Air Force Office of Scientific Research.

References

1. R.H. Doremus, "Ion Exchange: A series of Advances," Ed. J.A. Marinsky, Vol. 2, Marcel Dekker Inc., New York, 1966.
2. T. Izawa and H. Nakagome, Appl. Phys. Lett. 21, 584 (1972).
3. T.G. Giallorenzi, E.J. West, R. Kirk, R. Ginther, and R.A. Andrews, Appl. Opt. 12, 1240 (1973).
4. V. Neuman, O. Parriaux, and L.M. Walpita, Electron,. Lett. 15, 704 (1979).
5. T. Findakly, Opt. Engg. 24, 244 (1985).
6. G.L. Yip and J. Albert, Opt. Lett. 10, 151 (1985).
7. J.E. Gortych and D.G. Hall, IEEE J. Quantum Electron. QE-22, 892 (1986).
8. G.L. Yip and J. Finak, Opt. Lett. 9, 423 (1984).
9. T. Findakly and B. Chen, Appl. Phys. Lett., 40, 549 (1982).
10. J.G. Gallagher and R.M. de la Rue, Electron. Lett. 12, 397 (1976).
11. G. Chartier, P. Collier, A. Guez, P. Jaussaud, and Y. Won, Appl. Opt. 19, 1092 (1980).
12. R.G. Walker, C.D.W. Wilkinson, and J.A.H. Wilkinson, Appl. Opt. 22, 1923 (1983).
13. G. Stewart and P.J.R. Laybourn, IEEE J. Quantum Electron, QE-14, 930 (1978).
14. R.K. Laqu and V. Ramaswamy, Appl. Phys. Lett. 45, 117 (1984).
15. R.K. Laqu and R.V. Ramaswamy, J. Lightwave Tech. LT-4, 176 (1986).
16. P. Chludzinski, R.V. Ramaswamy and T.J. Anderson, Phys. Chem. Glasses. To be published.
17. R.K. Laqu, S.I. Najafi and V. Ramaswamy, Appl. Opt. 23, 3925 (1984).
18. R. G. Equchi, E. A. Maunders and I.K. Naik, Proc. S.P.I.E. 408, 21 (1983).
19. M.L. Huggins, J. Opt. Soc. Am. 30, 495 (1940).
20. R. V. Ramaswamy and S.I. Najafi, IEEE J. Quantum Electron, QE-22 883 (1986).
21. R. Tarai and R. Havami, J. Non-cryst. Solids 18, 217 (1975).
22. G. B. Hocker and W.K. Burns, Appl. Opt. 16, 113 (1977).
23. H. Matsuhara, J Opt. Soc. Am. 63, 1514 (1973).
24. R.K. Laqu and R.V. Ramaswamy, IEEE J. Quantum Electron., QE-22, 968 (1986).
25. J.M. White and P.F. Heidrich, App. Opt. 15, 151 (1976).
26. I. Fainaro, M. Ish Shalom, M. Ron and S. Lipson, Phys. Chem, Glasses, 15, 16 (1984).
27. S.N. Houde-Walter and D.T. Moore, Appl. Op. 25, 3373 (1986).
28. H.J. Lilienhof, E. Voges, D. Ritter, and B. Pantchew, IEEE J. Quantum Electron,. QE-18, 1877 (1982).
29. R. Srivastava, C.K. Kao and R. V. Ramaswamy, J. Lightwave Tech. To be published.
30. Y.H. Won. P.C. Jaussaud, and G.H. Chartier, Appl. Phys. Lett. 37, 269 (1980).
31. R.G. Walker and C.D.W. Wilkinson, Appl. Opt. 22, 1029 (1983).
32. F.M. Sladen, D.N. Payne and M.J. Adams, Appl. Phys. Lett. 28, 255 (1976).
33. p.G. Suchosko, Jr. and R. V. Ramaswamy, IEEE J. Quantum Electron, 1987, To be published.
34. W.K. Burns and G.B. Hocker, Appl. Opt. 16, 2048 (1977).
35. H.C. Cheng, R.V. Ramaswamy and R. Srivastava, Tech. Digest, Conference on Gradient-Index Optical Imaging Systems, Reno, Nev., Jan. 1987, pp. 52-54.
36. S. I. Najafi and R. V. Ramaswamy, Tech. Digest, Conference on Integrated and Guided Wave Optics, Altanta, Ga., Feb. 1986, pp. 60-61.
37. H.C. Cheng, R.V. Ramaswamy and R. Srivastava, 'Fabrication, characterization and modelling of channel waveguides with fiber-like mode profiles,' Unpublished.

Table I

Composition of soda-lime glass.

Oxide	Weight %	Oxide	Weight %
SiO_2	72.25	K_2O	1.20
Na_2O	14.31	MgO	4.30
CaO	6.40	Fe_2O_3	0.03
Al_2O_3	1.20	SO_3	0.30

Density = 2.467 g/cm^3

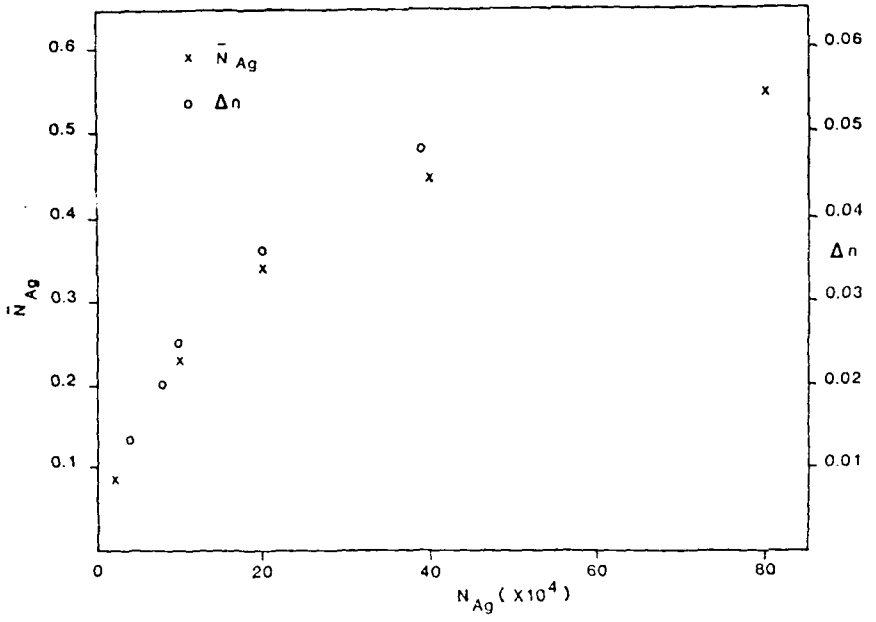

Fig. 1. Variation of surface-concentration of silver ions ($\bar{N}_{Ag}$) and surface index change (Δn) with the silver melt concentration (N_{Ag}).

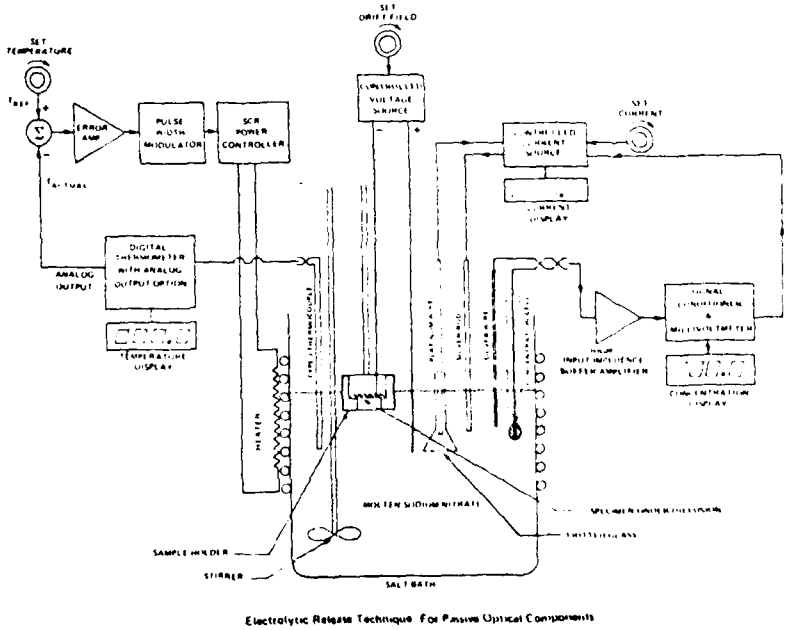

Fig. 2. Schematics of Ion-exchange technique.

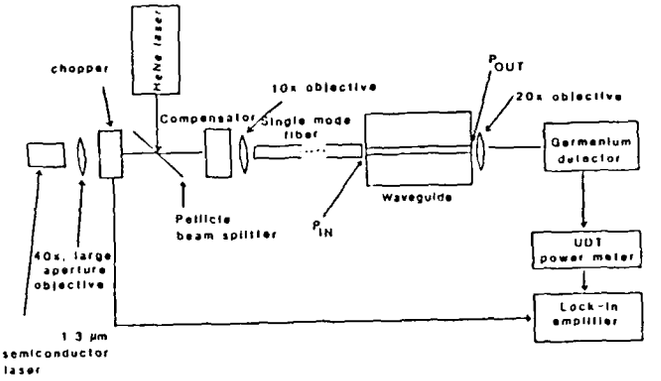

Fig. 3. Schematics for near field measurement.

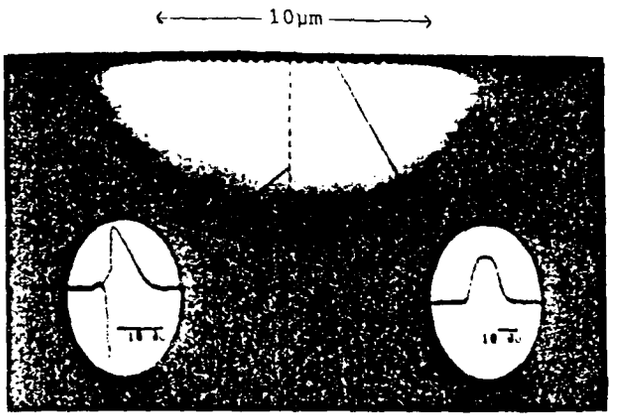

Fig. 4. Silver concentration profile of channel waveguide.

Buried Na^+-Ag^+ Ion-Exchanged Glass Waveguides: Theory and Experiment

H. C. Cheng, R. V. Ramaswamy and R. Srivastava
Department of Electrical Engineering
University of Florida
Gainesville, Fl. 32611

Glass waveguides are generally fabricated by ion-exchange process by immersing the glass substrate in a molten salt mixture. These waveguides have the maximum index change at the glass surface, and their index profile depends upon the diffusion time, the melt temperature, the compositions of the glass and the melt, and on any applied electric field. The surface waveguides can be buried by immersing them in pure salt bath and carrying out diffusion in one more step with or without external field. Burying the waveguide under the glass surface reduces the scattering losses arising from the surface irregularities. The buried profile can be tailored to give desired waveguide characteristics by changing the process parameters. Both planar and channel Na^+-Ag^+ ion-exchanged buried waveguides have been reported [1-3]. Since the silver melt concentration used in these studies was relatively large ($N_{Ag} > 0.1$ mole fraction), the resultant surface index change was also large ($\Delta n \sim 0.1$), giving rise to either multimode waveguides or very shallow single-mode guides, incompatible with single-mode fibers. Moreover, the interdiffusion coefficient under these conditions is concentration dependent, a fact that makes the solution of the diffusion equation more cumbersome.

To circumvent these problems, we have fabricated quasi-single-mode buried waveguides with very low melt concentrations ($N_{Ag} \sim 10^{-4} - 10^{-3}$ MF) and measured the silver concentration profile in the glass by analyzing the back-scattered electrons in a scanning electron microscope [4]. Under these conditions the diffusion is characterized by the self-diffusion coefficient of silver in glass. The one-dimensional diffusion equation has been solved using a very simple multiple integration technique. For the first time the resulting profiles have been correlated to the measured ones at such low-melt concentrations by varying processing paramenters in a two-step ion-exchange process in the presence of an external field.

We solve the one-dimensional diffusion equation

$$\frac{\partial C}{\partial t} = D \frac{\partial^2 C}{\partial x^2} - \mu E \frac{\partial C}{\partial x} , \qquad (1)$$

where C is the concentration, D the self-diffusion coefficient, and μ the mobility of the diffusing ion, respectively, in the glass, and E is the applied field. D, μ , and E are assumed to be position independent as well as independent of each other. This is in contrast to the previous analyses where D and μ were assumed to be related via the Einstein's relation. Since this relation does not hold for glasses [5], this assumption is likely to give erroneous results. Consider an arbitrary initial concentration $C(x,0) = C_0(x)$ in the glass which can be approximated by

$$C_0(x) = \sum_i C(x_i)\delta(x-x_i) .$$

For a linear system, the solution of (1) can be expressed as the summation of all the impulse responses,

$$C(x,t) = \sum_i \frac{C(x_i)}{\sqrt{4\pi Dt}} \exp\left[-\frac{(x-x_i-\mu Et)^2}{4Dt}\right] .$$

For the initial concentration given by the continuous function $C_0(x)$,

$$C(x,t) = \int_{-\infty}^{\infty} \frac{C_0(x')}{\sqrt{4\pi Dt}} \exp\left[-\frac{(x-x'-\mu Et)^2}{4Dt}\right] .$$

Since during diffusion $C_0(x')$ is a time dependent boundary condition, $C(x,t_i)$ is evaluated by dividing time into many small and equal steps of interval Δt. Thus $t_i = i\Delta t$ and

$$C(x,t_i) = \underbrace{\int_{-\infty}^{\infty} \cdots \int_{-\infty}^{\infty}}_{i \text{ integrals}} \frac{C_0(x')}{\sqrt{4\pi Dt}} \exp\left[-\frac{(x-x'-\mu E\Delta t)^2}{4D\Delta t}\right] (dx')^i . \qquad (2)$$

We have checked the accuracy of (2) for two cases where the solutions of (1) are obtained in analytical form: the single-step process with and without applied field. In both cases the agreement was excellent.

The one-step concentration profile is next used as the initial condition for the second step. It is assumed that there are no silver ions in the melt and the electric field is sufficiently large to block the diffusion of Ag^+ ions back into the melt. The resulting index profile for the case of no applied field in the first step for $u > -\mu E_2 t_2/2\sqrt{Dt_2}$ can be written as

$$C(u) = \int_0^{\infty} \frac{C_1(u'\sqrt{\tau})}{\sqrt{\pi}} \exp[-(u-u')^2]du' . \qquad (3)$$

where

$$u \equiv \frac{x-\mu E_2 t_2}{2\sqrt{Dt_2}} ; \quad u' = \frac{x'}{2\sqrt{Dt_2}}$$

$$\tau = t_2/t_1$$

t_i = diffusion time of the ith step, i = 1,2

E_2 = applied field of the 2nd step

and

$C_1(u'\sqrt{\tau})$ = concentration profile of the 1st step.

Eq. (3) was used to calculate index profiles and the resulting field profiles of the guided modes using previously determined values of D and μ [4] at the processing temperature of 330°C and melt silver concentrations of $\sim 10^{-4}$ - 10^{-3} MF. Under these conditions

$$C_1(u'\sqrt{\tau}) = C_0 \operatorname{erfc}(\sqrt{\tau}\, u') \quad . \tag{4}$$

Using (4) in (3) we have calculated the index profile, index peak position, the waveguide width and the peak index change in buried guides as a function of t_2 and E_2, keeping $E_1 = 0$ and t_1 fixed. The dependence of the waveguide width is shown in Fig. 1. It varies approximately as $\sqrt{t_2}$, in agreement with the experimental results [4].

However, the calculated dependence on E_2 is not linear and shows a smaller change with field E_2 than earlier reported results [4]. This discrepancy is being investigated and the results will be discussed. The peak position varies linearly with t_2 or E_2 as expected, whereas the peak index in the second step drops rapidly to 10-15% of its initial (first-step) surface value within 30 minutes; thereafter it decreases very slowly. The results give the design parameters and show that fiber-compatible single-mode buried waveguides can be fabricated from melt concentrations of the order of 10^{-3}MF. Propagation characteristics of these waveguides will also be presented.

This work was supported in part by Bell Communication Research and AFOSR contract No. 84-0369.

References

1. G. Chartier, P. Collier, A. Guez, P. Jaussaud, and Y. Won, Appl. Opt. 19, 1092 (1980).
2. H.J. Liliehhof, E. Voges, D. Ritter, and B. Pantschew, IEEE J.Q.E. QE-18, 1877 (1982).
3. R.G. Walker, C.D.W. Wilkinson, and J.A.H. Wilkinson, Appl. Opt. 22, 1923 (1983).
4. R.V. Ramaswamy and S.I. Najafi, IEEE J.Q.E. QE-22, 883 (1986).
5. R. Terai and R. Hayami, J. Noncryst. Solids 18, 217 (1975).

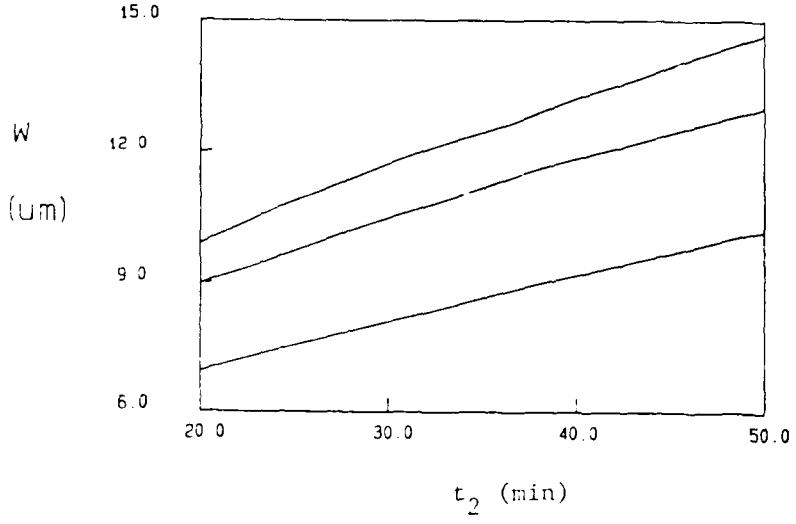

Fig. 1 Variation of the Waveguide width with second-step diffusion time.

upper curve $N_{A_g}=10^{-3}$MF, E_2=30V/mm

middle curve $N_{A_g}=10^{-3}$MF, E_2=10V/mm

lower curve $N_{A_g}=10^{-4}$MF, E_2=10V/mm

REFERENCE [17]

Process Optimization of Buried Ag^+-Na^+ Ion-Exchanged Waveguides: Theory and Experiment

R. V. Ramaswamy, H. C. Cheng and R. Srivastava

Department of Electrical Engineering
University of Florida
Gainesville, Florida 32611

Abstract

We report optimization of the processing conditions for fabrication of single-mode Ag^+-Na^+ ion-exchanged waveguides in a soda-lime glass. The surface-index change, the mobility and diffusion coefficient of Ag^+ have been measured at low melt concentrations and the results used for calculation of index profile using a new simple numerical method for solving the diffusion equation in a two-step process where the index profile is buried by applying an electric field in the second step. The calculated profile is in agreement with that measured. This correlation allows solution of the Helmholtz equation for given process parameters. Single-mode waveguides with desired mode-field distribution have been designed and fabricated with optimized performance and fiber compatibility at 1.3 μm.

Process Optimization of Buried Ag^+-Na^+ Ion-Exchanged Waveguides: Theory and Experiment

R. V. Ramaswamy, H. C. Cheng and R. Srivastava

Department of Electrical Engineering

University of Florida

Gainesville, Florida 32611

I Introduction

Glass waveguides are considered to be prime candidates for integrated optic device applications such as star couplers, access couplers, wavefront sensors, multiplexers, demultiplexers, and in sensors such as gyroscopes. The importance of the glass waveguide-based I-O components is borne out by their compatibility with optical fibers and potentially low cost. In addition, they have low propagation loss and can be fabricated and integrated into the system with relative ease. However, unlike its electro-optic and semiconducting counterpart substrate materials (e.g., $LiNbO_3$, GaAs, etc.), glass index cannot be tuned by application of an external electric field, and therefore glass devices must be fabricated with assured reproducibility within specified tolerances. Fabrication of devices such as multiplexers calls for reproducibility in the propagation constant of the guided mode to an accuracy of better than 10^{-4}. In order to fabricate glass waveguide devices of such

reproducible characteristics, we have studied the Ag^+-Na^+ exchange and diffusion process in detail to understand the role of the processing parameters [1-4].

It is known that when pure $AgNO_3$ melt is used for the exchange process, large $\Delta n(\sim 0.1)$ waveguides are obtained which have some disadvantages: a large silver concentration causes coloring due to silver reduction; secondly, single-mode waveguides are shallow and therefore, are incompatible with single mode optical fibers. Moreover, the time of diffusion involved is rather short, thereby causing uncertainty and lack of reproducibility in the waveguide characteristics. Dilute solutions of $AgNO_3$ and $NaNO_3$ allow achievement of lower Δn and more controllable diffusion times [1-6]. However, in Ag^+-Na^+ ion-exchanged waveguides, the surface-index change and the index profile depend strongly upon the melt silver concentration [2,5,6]. In fact, very low silver concentration in the melt [$N_{Ag} \sim 10^{-4}$ mole fractions] is required to obtain single-mode waveguides. As the index change is expected to be a linear function of the concentration of silver ions in the glass, it is necessary to understand how the silver ion intake by the glass in affected by the process parameters in the ion-exchange technique, viz; melt composition, diffusion time, temperature, and melt stirring. To answer some of these questions, an ion-exchange equilibrium study [3,4] was recently reported for accurate determination of the boundary conditions for the solution of the diffusion equation to calculate the index profile and correlate it with the measured profile.

In this work, using the boundary conditions determined from the earlier equilibrium study [3,4] we have calculated the index profile by solving the diffusion equation numerically using a simple impulse response technique. The numerical method allows prediction of the profile for single-step as well as

two-step process used for buried waveguides and can be used even when an external electric field is applied during the ion-exchange process. The theoretically predicted index profiles are in agreement with the results obtained experimentally. A correlation between the theory and experiment allows determination of relevant parameters such as the index profile, the electric mobility of silver ions in glass, and the interdiffusion coefficient for the given melt composition and other process parameters. The measured parameters were then used to optimize the two-step process to obtain planar waveguides with desired mode-field distribution at a given operating wavelength. It is expected that the results of this work will help in design and fabrication of channel waveguides with desired characteristics and waveguide-based I-O devices for applications cited earlier.

II Theory

A. Diffusion Equation

The diffusion equation for the diffusing ion A (silver) can be derived in the following form [7]

$$\frac{\partial \bar{C}_A}{\partial t} = \mu_A \vec{E} \cdot \nabla \bar{C}_A \left[\frac{1}{1 - \alpha \bar{C}_A} \right] + \frac{n}{1 - \alpha \bar{C}_A} \bar{D}_A \nabla^2 \bar{C}_A \qquad (1)$$

where $$\alpha = 1 - \frac{\mu_A}{\mu_B} ; \qquad (2)$$

μ_i is the mobility of ion i, $\vec{E}$ is the applied field, $\bar{C}_A$ is the absolute concentration of ion A in glass,

and $$n = \frac{\partial \ln \bar{a}_A}{\partial \ln \bar{C}_A} \qquad (3)$$

where $\bar{a}_A$ is the thermodynamic activity of the ion A.

Eq. (1) can be solved to obtain the concentration profile provided the initial condition and the boundary conditions are known. One of the boundary conditions involves knowledge of the concentration of cation A at the glass surface which is a function of the melt concentration. Determination of this boundary condition was accomplished by ion-exchange equilibrium studies reported earlier [3,4].

B. **Solution of the Diffusion Equation**

a) **Diffusion without external field**

Eq. (1) can be further simplified if there is no external field present and $\nabla \cdot \vec{E}$ is set equal to zero i.e., there is no space charge present. In this case it can be shown [8] that the two-dimensional diffusion equation becomes

$$\frac{\partial \bar{N}_A}{\partial t} = \frac{\partial}{\partial x}\left(\frac{n\bar{D}_A}{1 - \alpha \bar{N}_A}\frac{\partial \bar{N}_A}{\partial x}\right) + \frac{\partial}{\partial y}\left(\frac{n\bar{D}_A}{1 - \alpha \bar{N}_A}\frac{\partial \bar{N}_A}{\partial y}\right) \qquad (4)$$

where $\bar{N}_A$ is the concentration of silver in glass in mole fractions.
In the case of planar waveguides (4) reduces to the one dimensional diffusion equation which is normally written as

$$\frac{\partial \bar{N}_A}{\partial t} = \frac{\partial}{\partial x}\left(\tilde{D}\frac{\partial \bar{N}_A}{\partial x}\right) \qquad (5)$$

where $\tilde{D}$ is called the interdiffusion coefficient given by

$$\tilde{D} = \frac{n\bar{D}_A}{1 - \alpha \bar{N}_A} = \frac{n\bar{D}_A \bar{D}_B}{\bar{D}_A \bar{N}_A + \bar{D}_B \bar{N}_B} \qquad (6)$$

For $\bar{N}_A << 1$ as in the case of single-mode Ag^+-Na^+ waveguides, $\tilde{D} = n\bar{D}_A$. In this case the diffusion equation has the simplest form

$$\frac{\partial \bar{N}_A}{\partial t} = n\bar{D}_A \frac{\partial^2 \bar{N}_A}{\partial x^2} \tag{7}$$

the solution [9] of (7) is,

$$\bar{N}_A (x,t) = \bar{N}_o \text{ erfc } (x/W_o) \tag{8}$$

where

$$W_o = 2\sqrt{n\tilde{D}_A t} \tag{9}$$

and $\bar{N}_o$ is the surface silver concentration.

b). **Diffusion With External Electric Field**

The diffusion of incoming ion can be enhanced by applying an electric field across the substrate. In this case, one has to solve the equation (1) which is a difficult task at best in the two-dimensional case. However, in the case of one-dimensional (planar) waveguides, approximate solutions can be obtained under certain conditions. For example, in the case of low concentrations ($\bar{N}_A << 1$), space-charge effects can be neglected and for planar waveguides Eq. (1) reduces to

$$\frac{\partial \bar{N}_A}{\partial t} = n\bar{D}_A \frac{\partial^2 \bar{N}_A}{\partial x^2} - \mu E \frac{\partial \bar{N}_A}{\partial x} \tag{10}$$

and $\bar{N}_A(x,t)$ is calculated by a Laplace-transform techniques [10]

$$\bar{N}_A = \frac{1}{2}\,\bar{N}_o\,\{\mathrm{erfc}\,(x' - r) + \exp(4rx')\,\mathrm{erfc}\,(x' + r)\} \qquad (11)$$

where $x' = x/W_o = x/2\sqrt{n\bar{D}_A t}$ is the normalized effective depth of diffusion without external field and $r = \mu Et/W_o$.

It has been shown [7] that the influence of the space charge leads to steeper diffusion fronts when compared to the solution (11). For large values of r, the contribution by the second term in (11) is negligible and the diffusion profile can be approximated as:

$$\bar{N}_A(x', r) \approx \frac{\bar{N}_o}{2}\,\{\mathrm{erfc}\,(x' - r)\},\ r > 2.5 \qquad (12)$$

In the two-dimensional case, Eq. (1) has been solved [7] neglecting the concentration dependence of the interdiffusion coefficient and assuming that the diffusion term in (1) is small. While such analytical solutions are valid for very large applied fields such as involved in multimode waveguides, the case of single-mode guides does not fall in this category. In such situations equation (1) can be solved only by numerical methods [8].

c). **Two-Step Ion Exchange (Buried Waveguides)**

Surface waveguides obtained by ion-exchange are characterized by higher loss caused by surface scattering. Furthermore, the intensity profile of the guided mode is not circularly symmetric and compatible with optical fiber. These drawbacks can be overcome by burying the waveguides in a second ion exchange in a melt free of the cation A. An external field may be applied during this step to control the buried depth and the index profile. Since the initial conditions in this case are determined by the first-step diffusion

profile, analytical solutions to Eq. (1) cannot be obtained and one has to resort to numerical techniques once again. In the following, we describe a simple numerical method to solve (1) in the case of planar buried waveguides.

d). **Modeling of the Diffusion (Index) Profile for Buried Waveguides**

To solve the one dimensional diffusion equation

$$\frac{\partial \bar{C}}{\partial t} = \tilde{D} \frac{\partial^2 \bar{C}}{\partial x^2} - \mu E \frac{\partial \bar{C}}{\partial x} \qquad (13)$$

for the concentration profile $\bar{C}(x)$ of silver in glass in analytical form, a reasonable assumption about the concentration dependence of the interdiffusion coefficient $\tilde{D}$ must be made. Our ion-exchange equilibrium results [3,4] suggest that at the melt concentrations involved in our work, 10-15% of the sodium ions are replaced by silver in the first-step diffusion. Besides, the self diffusion coefficient of silver is a factor to 3-10 smaller than that of sodium in these glasses [8,11]. Under these conditions, Eq. (6) indicates that the interdiffusion coefficient is only weakly dependent on the silver concentration (provided the self-diffusion coefficients themselves do not exhibit any drastic changes with the respective ionic concentration). If it is further assumed that not only $\tilde{D}$, but the mobility μ and the electric field E all are concentration (or position) independent, the analysis is greatly simplified.

In order to solve (13), consider an arbitrary initial concentration $\bar{C}(x,0) = \bar{C}_o(x)$ in the glass. We write

$$\bar{C}_o(x) = \Sigma_i \bar{C}_i(x_i)\, \delta(x-x_i) \qquad (14)$$

For linear systems, the solution of (13) can be expressed as the summation of all the impluse responses,

$$\bar{C}(x,t) = \sum_i \frac{\bar{C}_i(x_i)}{\sqrt{4\pi Dt}} \exp\left[- \frac{(x-x_i-\mu Et)^2}{4Dt} \right] . \qquad (15)$$

For the initial concentration given by the continuous function $\bar{C}_o(x)$,

$$\bar{C}(x,t) = \int_{-\infty}^{\infty} \frac{\bar{C}_o(x')}{\sqrt{4\pi Dt}} \exp\left[- \frac{(x-x'-\mu Et)^2}{4Dt} \right] dx' . \qquad (16)$$

Since during diffusion $\bar{C}_o(x')$ is a time dependent boundary condition, $\bar{C}(x,t_i)$ is evaluated by dividing time into many small and equal steps of interval Δt. Thus $t_i = i\Delta t$ and

$$\bar{C}(x,t_i) = \underbrace{\int_{-\infty}^{\infty} \cdots \int_{-\infty}^{\infty}}_{i \text{ integrals}} \frac{\bar{C}_o(x')}{\sqrt{4\pi Dt}} \exp\left[- \frac{(x-x'-\mu E\Delta t)^2}{4D\Delta t} \right] (dx')^i . \qquad (17)$$

We have checked the accuracy of (17) for two cases where the solutions of (13) are obtained in analytical form: the single-step process with and without applied field [Eqs. (8) and (11) respectively]. In this case, $\bar{C}_o(x) = 0$ for $-\infty < x < 0$ except at the glass-melt interface (x=0) where its value is constant at all times and is determined by the ion-exchange equilibrium . In both cases the agreement between the results obtained by evaluating (17) and those given in the corresponding analytical form was excellent. These agreements are shown in Fig. 1.

The one-step concentration profile is next used as the initial condition for the second step. It is assumed that there are no silver ions in the melt and the electric field is sufficiently large to block the diffusion of Ag^+ ions back into the melt. The resulting index profile for the case of no

applied field in the first step in the case where $u > -\mu E_2 t_2 / 2\sqrt{Dt_2}$ can be written as

$$\bar{C}(u) = \int_0^\infty \frac{\bar{C}_1(u'\sqrt{\tau})}{\sqrt{\pi}} \exp\left[-(u-u')^2\right] du'. \qquad (18)$$

where

$$u \equiv \frac{x-\mu E_2 t_2}{2\sqrt{Dt_2}}; \quad u' = \frac{x'}{2\sqrt{Dt_2}}$$
$$\tau = t_2/t_1$$

and $\bar{C}_1(u'\sqrt{\tau})$ = concentration profile of the 1st step.

Eq. (18) was used to calculate index profiles and the resulting field profiles of the guided modes using determined values of $\tilde{D}$ and μ at the processing temperature of 330°C and melt silver concentrations of $\sim 10^{-4} - 10^{-3}$MF. Under these conditions, the initial condition for the second step is given by

$$\bar{C}_1(u'\sqrt{\tau}) = \bar{C}_o(0)\ \mathrm{erfc}(\sqrt{\tau u'}) \qquad (19)$$

where $\bar{C}_o(0)$ denotes the surface concentration determined by the ion-exchange equilibrium at the melt-glass interface. It is proportional to $\bar{N}_o$ present in the expressions given by (8), (11) and (12).

III. EXPERIMENTAL PROCEDURE

The ion exchange of Ag^+ with Na^+ in soda-lime silicate glass was carried out at 330°C . Schematics of the procedure is shown in Fig. 2 and the

composition and density of the soda-lime glass used in the experiments is given in Table 1.

The waveguides were analyzed for the silver diffusion profiles using an atomic absorption spectrophotometer (AAS), an electron microprobe, or a scanning electron microscope (SEM). The experimental details are given in [2,3].

Alternatively, the planar waveguides were characterized for their mode indices by using a prism coupler. In the case of waveguides which supported one or two modes, the mode index data were correlated with the theory as follows: The one-dimensional normalized Helmholtz equation was solved for the measured profile by a finite-difference method to obtain the mode indices of the TE modes. The two variable parameters were Δn and $W_o = 2\sqrt{\tilde{D}\, t}$ which were adjusted to give the best fit to the measured mode indices. In the case of waveguides which supported many modes (>6), the inverse WKB method [12] was employed to give the index profile and the surface-index change (Δn).

IV. RESULTS AND DISCUSSION

Fig. 3 shows the concentration (index) profiles measured by the various techniques for $N_{Ag} = 2\times10^{-4}$ demonstrating an excellent agreement in the results. The data can be best fit to the ERFC profile given by (8) and shown as a solid curve in Fig. 3. This indicates that the interdiffusion coefficient is indeed concentration independent at low silver-melt concentrations. Our earlier results of ion-exchange equilibrium study [3,4] show that the partitioning of silver ions between the melt and the glass is highly nonlinear and, for higher melt concentrations ($N_{Ag} \sim 10^{-3}$), almost 25% of the sodium ions in the glass are replaced by silver ions. At this composition the $\bar{D}_A \bar{N}_A$ term in the denominator of (6) cannot be neglected

and $\tilde{D}$ becomes significantly concentration dependent. This was evidenced by a change in the measured concentration profile.

The large dependence of the silver intake by the glass on the melt concentration has important implications in batch fabrication of single mode fiber compatible waveguides using the Ag^+-Na^+ ion-exchange process. Such guides are required to have diffusion depths of the order of 10 μm which translates into peak index changes of the order of $\Delta n = 3\times10^{-3}$. Such small changes can only be achieved at very low melt concentrations ($N_{Ag} \sim 10^{-4}$). Precise control of the melt concentration at $N_{Ag} \sim 10^{-4}$ is required to achieve adequate reproducibility in the waveguide characteristics. This can be achieved, for example, by using an electrolytic technique [13] for release of silver ions in the melt and insitu galvanic potential measurement to determine N_{Ag} and thus provide a feed back control loop [14].

Determination of $\tilde{D}$ and μ

Besides the boundary conditions obtained by the ion-exchange equilibrium reported earlier [3,4], complete solutions of the diffusion equation (13) also requires knowledge of the interdiffusion coefficient $\tilde{D}$ and the mobility μ. This was achieved as follows:

Single- and multimode surface waveguides were prepared in melt compositions with $N_{Ag} = 4\times10^{-4}$ and their mode indices measured by prism coupler. Based on the diffusion profile data of Fig. 3 indicating it to be erfc, the mode index data for the two lowest order modes were fitted theoretically to the solution of the Helmholtz equation obtained by a finite difference method [15]. The variable parameters were Δn and $\tilde{D}$. Whereas this procedure works best for guides with two modes, it is cumbersome and time consuming for multimode guides. In the latter case, however, inverse WKB method [12] works very well for the well-guided modes and a-prior knowledge of

the index profile is not necessary. Curve 1 in Fig. 4 shows the inverse WKB points and the best fitted erfc profile for a 5-mode waveguide for the process parameters listed. The values of Δn as well as $\tilde{D}$ obtained by finite-difference method and inverse WKB agree within 5% and the values of $\tilde{D}$ obtained by the above fitting procedure to the mode indices data are in excellent agreement with those obtained by SEM, electron microprobe, and AAS methods [Fig. 3].

In order to determine the ionic moblity μ, multimode surface waveguides were prepared by applying external electric field and the data fitted to Eqn. (11). It was assumed that Δn varies linearly with the dopant concentration and does not depend on the applied field such that the previously determined values of Δn for a given concentration (without external field) could be used in the fit. The values of the adjustable parameters $\tilde{D}$ and μ were thus obtained. Curve 2 in Fig. 4 shows such a fit. Two observations can be made regarding the results of the fit for curve 2.

(i) The fit is not as good as that for curve 1 (without field). This may primarily be due to the index profile having a steep slope in which case inverse WKB is known to give erroneous results near the sharp tail [12]. Similar results were encountered when SEM data [7] was used for fitting to Eqn. (11). Another reason for such an unsatisfactory fit may be the inadequacy of expression (11) to describe the index profile even for such low melt concentrations. Space charge effects alluded to in section II and the concentration dependence of the self-diffusion coefficients may all be responsible for this deviation.

(ii) The value of inter-diffusion coefficient determined by the best fit is much lower than that obtained without field (curve 1). This is reflected in the steepness of the index profile.

Once all the necessary parameters were determined from single-step ion-exchange, Eqns. (18) and (19), were used for predicting the index profile, the index peak position, the waveguide width and the peak index change in buried guides as a function of diffusion time t_2 and electric field E_2 used during the second-step. In all cases, E_1 (electric field in the first step) was kept at zero. This was necessary to obtain very symmetrical and single-mode index profiles.

Fig. 5 shows the evolution of the index profile with time t_2. As time evolves, the peak index decreases, the profile width increases and the peak index position moves deeper into the glass. The variation of the peak index change is plotted in Fig. 6, as a function of t_2 for two different fields. It is seen that the applied field has virtually no effect on this parameter.

Fig. 7 shows the variation of the index profile width W and the index peak position x_{peak} with t_2 for various values of E_2. It is observed that $W \sim \sqrt{t_2}$, a result in agreement with the experimental data [2] shown by the full squares in the curve 1. This square-root dependence of 1/e index width W on t_2 is a direct consequence of the diffusion model implicit in (15). The index peak position depends linearly on time as well as on the field E_2. This result is tantamount to saying that as time evolves, the whole profile is translated by the applied field and the net translation is governed by the product $\mu E_2 t_2$.

Waveguide Optimization

Once the diffusion profile was determined, a finite-difference method [15] was used to solve the Helmholtz equation to obtain the mode-index and the

mode field profile. Thus, using N_{Ag} and t_1 as the variable parameters in the first step ($E_1 = 0$) and t_2, E_2 as the ones in the second step ($N_{Ag} = 0$), the waveguide parameters were calculated. Since the mode field profile of a planar guide is not a very sensitive function of the index profile, the corresponding process parameters are not uniquely determined for a given mode profile. Therefore, it may be possible to obtain the same desired waveguide performance by a range of combination of these parameters. One such set of parameters selected to match a conventional Corning SM fiber with mode field diameter of 9.8 μm, is given in Table 2. The planar waveguide thus designed has mode field diameter W_e (defined at $\frac{1}{e}$ points in the field) of 9.8 μm at the wavelength of 1.3μm. The corresponding normalized propagation constant b is ~ 0.5 showing that the guide is single-mode and the mode is well guided.

V. Conclusion:

The concentration profile of silver in glass waveguides was measured by atomic absorption spectroscopy, electron microprobe, and analysis of back-scattered electrons in SEM. The surface-index change, the index profile and the interdiffusion coefficient were determined from measurement of mode indices using a prism coupler. The interdiffusion coefficient $\tilde{D}$ is concentration independent at low melt concentrations and excellent agreement was observed in the concentration (index) profiles obtained by the various techniques. The profile data of surface waveguides were fitted to appropriate analytical expressions for the solution of the diffusion equation to determine the ionic mobility and $\tilde{D}$ in presence of an external field.

The surface planar waveguides obtained in the first-step exchange were buried by carrying out diffusion in the second step with an applied field without any silver in the melt. The results obtained by the proposed simple

numerical solution of the diffusion equation show that the buried depth increases linearly with the applied field or the second-step diffusion time t_2 and the index profile width varies as $\sqrt{t_2}$, in agreement with the experimental results. Using these relations, the optimum process parameters for a desired waveguide can easily be determined. It is expected that these results will be helpful in designing passive single-mode channel waveguide based devices with optimum characteristics for I-O applications.

Acknowledgement: This work was supported by AFOSR Contract No. 84-0369 and by a grant from Bell Communications Research. We are grateful to Prof. D. O. Shah for use of his Perkin-Elmer Atomic Absorption Spectrometer in our AAS measurements.

References

1. R. K. Lagu and R. V. Ramaswamy, J. Lightwave Tech. LT-4, 176 (1986).
2. R. V. Ramaswamy and S. I. Najafi, IEEE J. Quantum Electron., QE - 22, 883 (1986).
3. R. V. Ramaswamy, R. Srivastava, P. Chludzinski, and T. J. Anderson, submitted to IEEE, J. Quantum Electron.
4. R. V. Ramaswamy, R. Srivastava, and P. Chludzinski, GRIN '87, Reno, Nev. Paper Th B2-1.
5. G. Stewart and P.J.R. Laybourn, IEEE J. Quantam Electron. QE- 14, 930 (1978).
6. R. G. Eguchi, E. A. Mounders and I. K. Naik, Proc. SPIE, 408, 21 (1983).
7. H. J. Lilienhof, E. Voges, D. Ritter, and B. Pantschew, IEEE J. Quantum Electron., QE-18, 1377 (1982).
8. R. G. Walker, C. D. W. Wilkinson, and J. A. H. Wilkinson, Appl. Opt. 22, 1923 (1983).
9. J. Crank, 'The Mathematics of Diffusion," Oxford Press, 1956.
10. M. Abou-el-Leil and A. R. Cooper, J. Amer, Ceram. Soc. 62, 390 (1979).
11. R. H. Doremus, J. Phys. Chem. 68, 2212 (1964).

12. J. M. White and P. F. Heidrich, Appl. Opt. 15, 151 (1976).

13. R. K. Lagu and V. Ramaswamy, Appl. Phys. Lett. 45, 117 (1984).

14. R. K. Lagu, S. I. Najafi, and V. Ramaswamy, Appl Opt. 23, 3925 (1984).

15. E. Rodriguez, R. V. Ramaswamy and R. Srivastava, unpublished.

Figure Captions

Fig. 1. Comparison of index profile as given by Eqn. (17) { dotted curve } and by Eqn.(11) { solid curve }
$T = 30$ min, $\tilde{D} = 0.15\mu m^2/min$, for each curve.
For curve 2, $\mu = 5.0\mu m^2/Vmin$, $E = 45V/mm$

Fig. 2. Schematics of the experimental and theoretical procedure.

Fig. 3. A comparison of the index profile results using various techniques. +AAS, x SEM, 0 Inv. WKB, * Electron microprobe, --fitted ERFC to the measured mode indices using finite difference method. $W_o = 2\sqrt{\tilde{D}t}$.

Fig. 4. Fitting of mode indices by inverse WKB method. x's indicate mode indices of surface guides without external field and O's indicate data with external field. Curve 1 is fitted erfc profile with $\tilde{D} = 0.15\ \mu m^2/min$ and $t_1 = 120$ min. Curve 2 represents Eqn. (11) with $\tilde{D}=0.04\mu m^2/min$, $\mu=5.0\mu m^2/min$ $E_1 = 45$ V/min and $t_1 = 30$ min. Silver melt concentration in both cases is $N_{Ag} = 4x10^{-4}$.

Fig. 5. Evolution of index profile with the second-step diffusion time.

Fig. 6. Variation of peak index change with second-step diffusion time.

Fig. 7. Variation of the index peak position x_{peak} and the 1/e index width W with the second-step parameters. Curves 1 , 2, and 3 correspond to $E_2 = 10$, 40, and 70 v/mm respectively. The data points are from Ref. [2].

Table 1. Chemical composition of Fisher brand glass slide (wt %).

Oxide	Weight %
SiO_2	72.25
Na_2O	14.31
CaO	6.40
Al_2O_3	1.20
K_2O	1.20
MgO	4.30
Fe_2O_3	0.03
SO_3	0.30

Density = 2.4667 g/cm^3

Table 2: Optimization

$T = 330$ C
$\lambda_o = 1.3\mu m$

FIRST STEP

$N_{Ag} = 3 \times 10^{-4}$ Mole Fractions

$\Delta n = 0.012$

$E_1 = 0$

$t_1 = 15$ Min.

$D = 0.14\ \mu m^2/Min.$

SECOND STEP

$E_2 = 75$ V/mm

$t_2 = 50$ Min.

$D = 0.045\ \mu m^2/Min.$

$\mu = 5\ \mu m^2/V\text{-}Min.$

WAVEGUIDE PARAMETERS

$W = 6.6\ \mu m$

$x_{peak} = 20\ \mu m$

$\Delta n = 3.2 \times 10^{-3}$

$V = 3.1$

MODE PARAMETERS

$W_e = 9.8\ \mu m$

$b = 0.5$

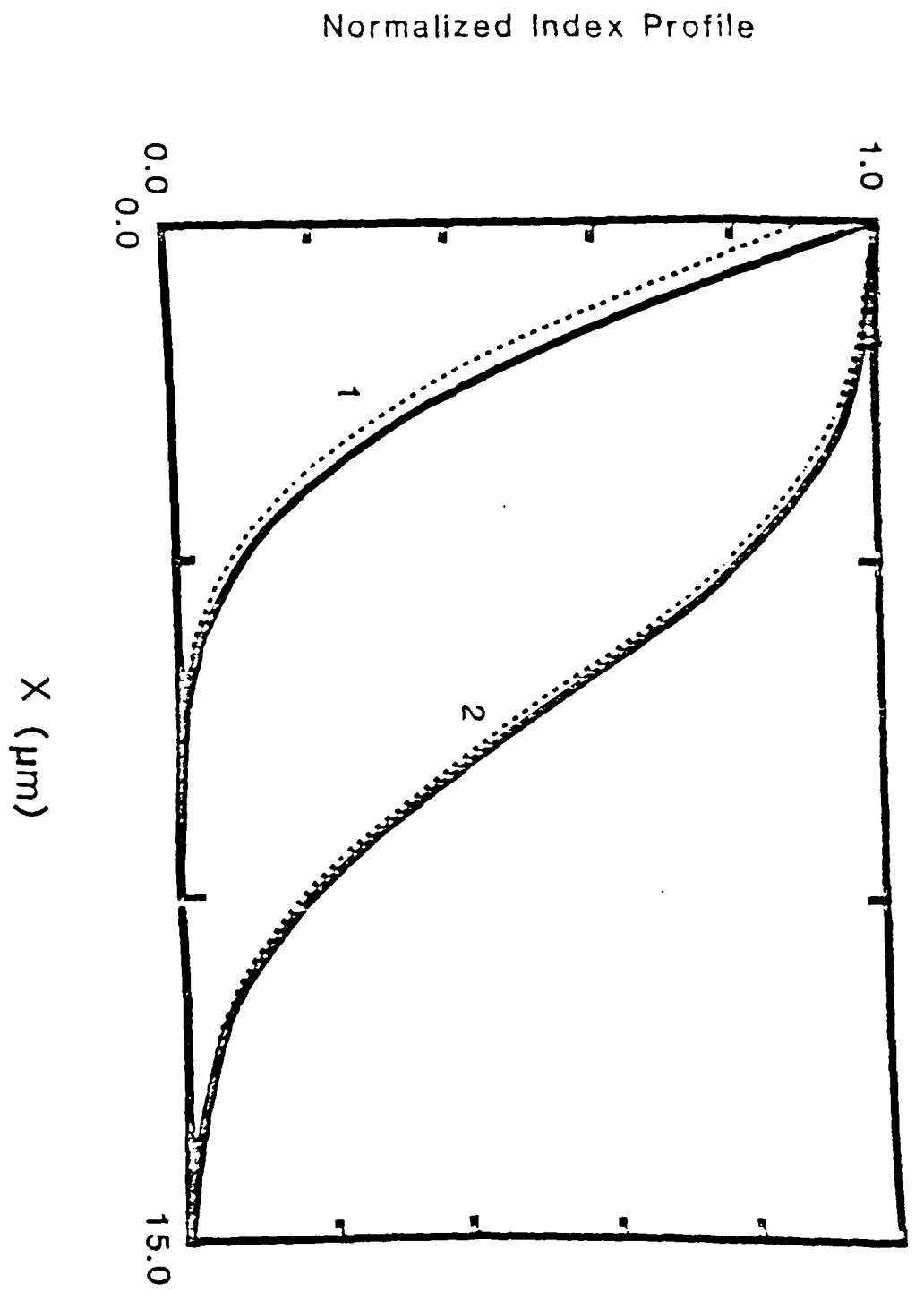

Fig. 1

Two - Step Ion - Exchange

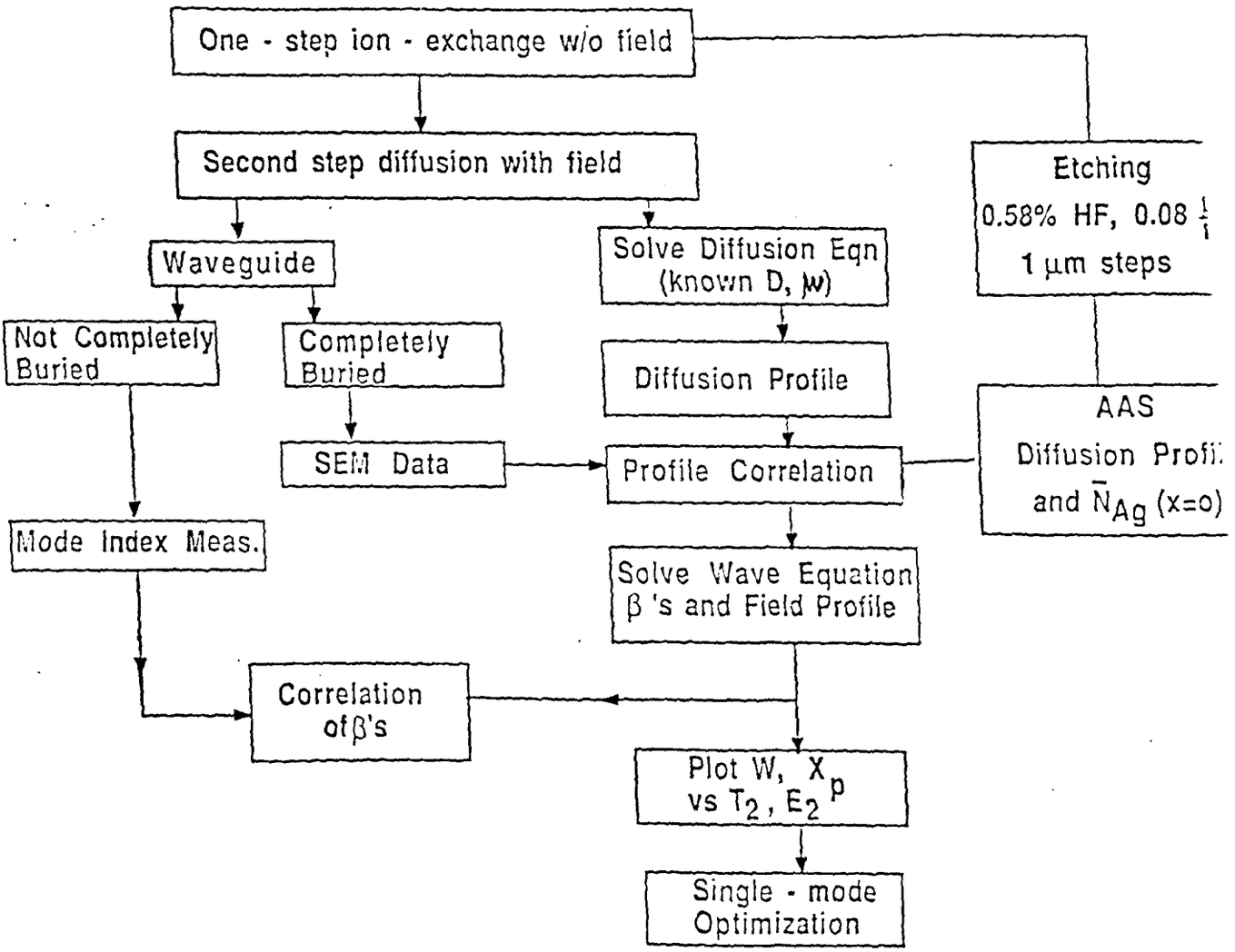

Fig. 2

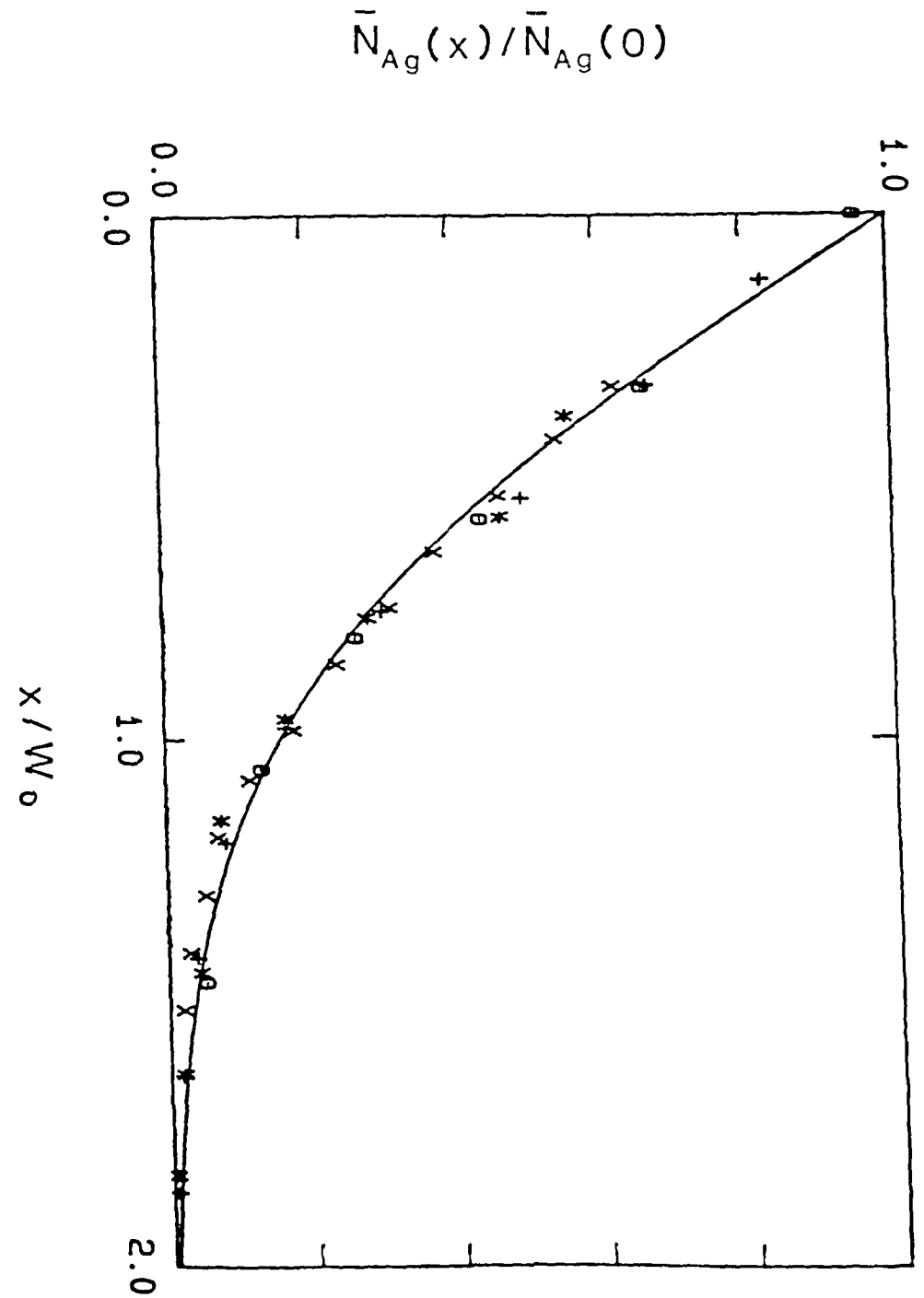

Fig. 3

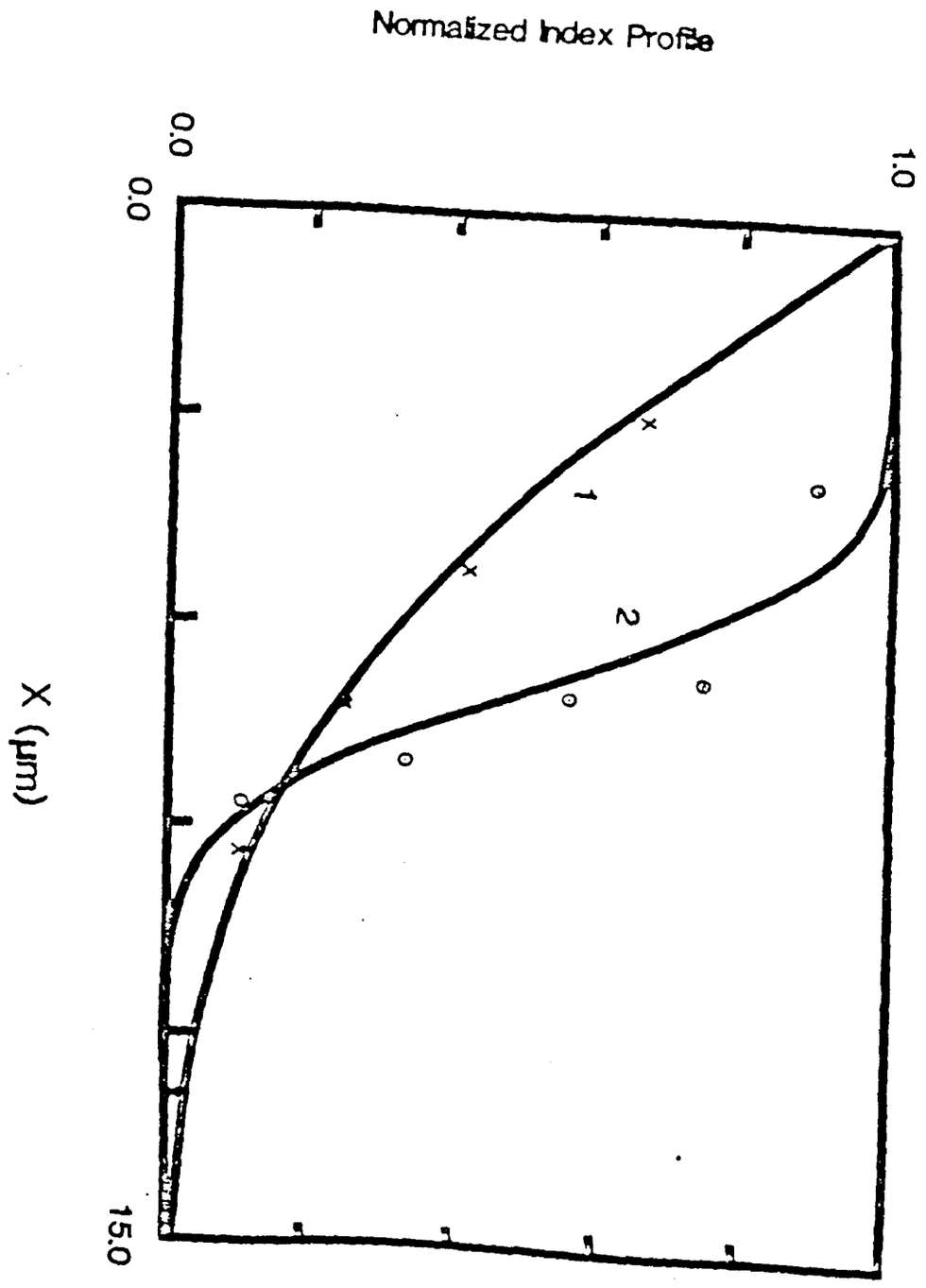

Fig. 4

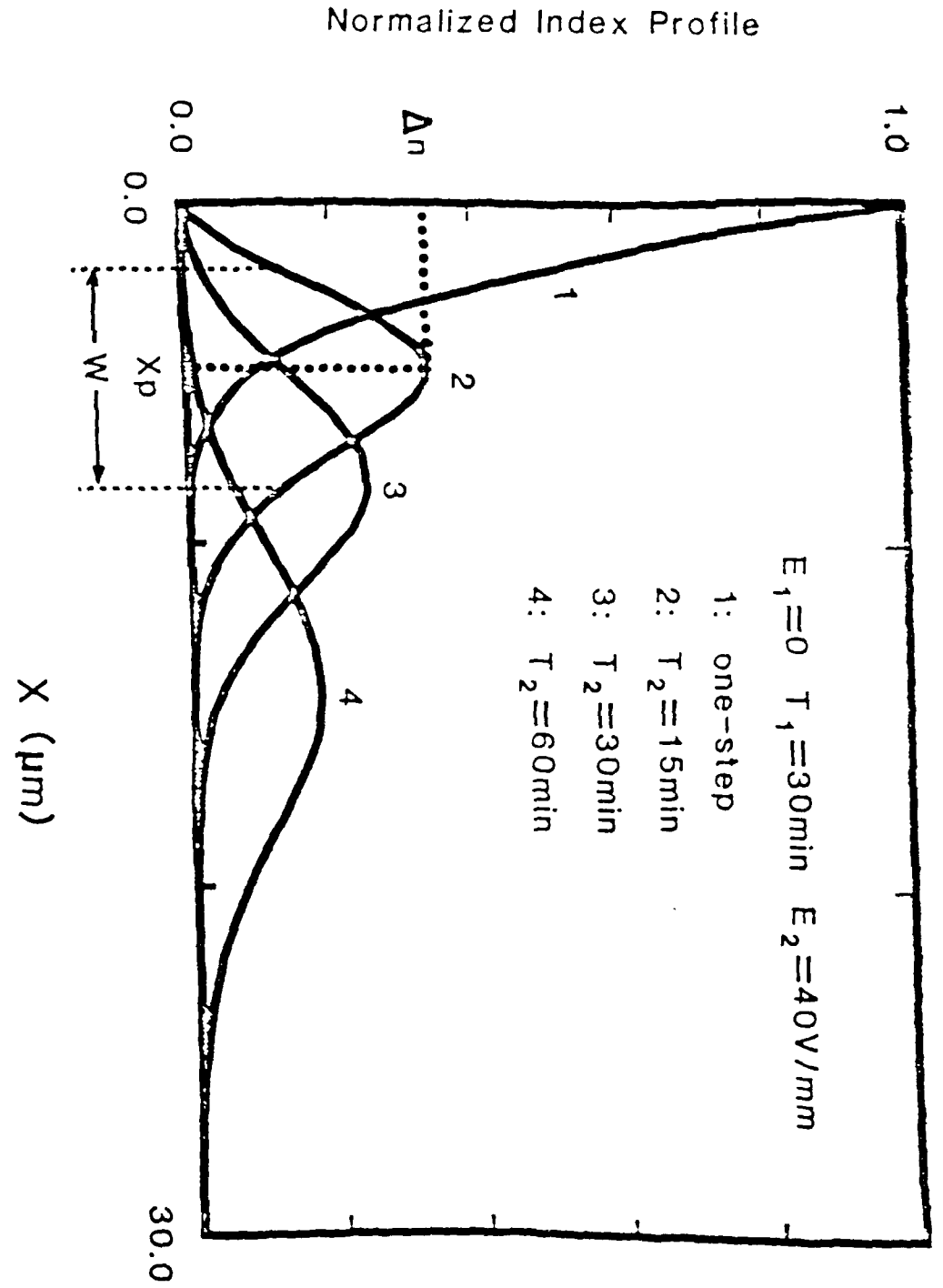
Normalized Index Profile
Δn
0.0
1.0
0.0
30.0
X (μm)
W
Xp
1
2
3
4
E1=0 T1=30min E2=40V/mm
1: one-step
2: T2=15min
3: T2=30min
4: T2=60min

Fig. 5

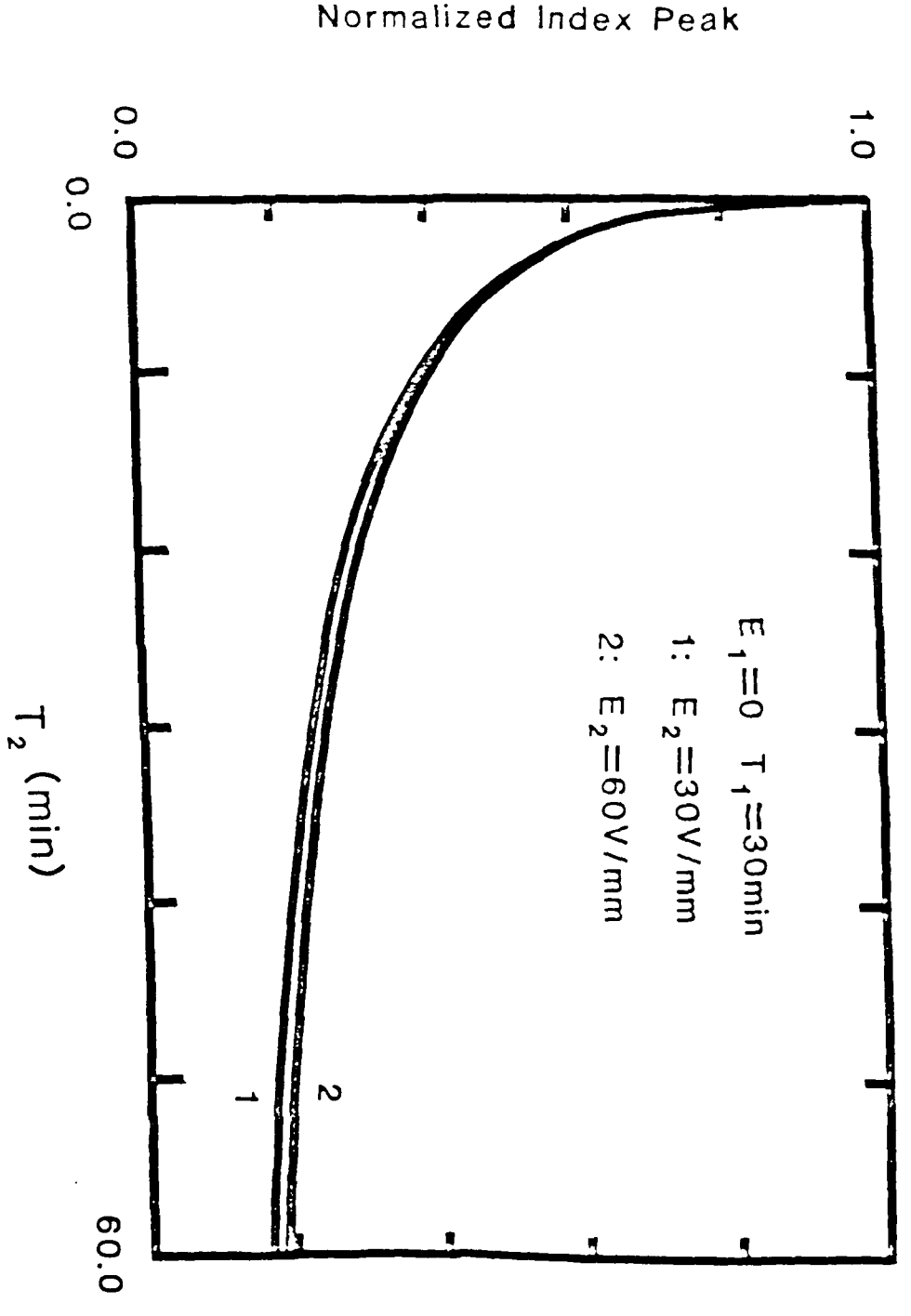
Normalized Index Peak
0.0
1.0
0.0
60.0
T_2 (min)
E_1=0 T_1=30min
1: E_2=30V/mm
2: E_2=60V/mm
1
2

Fig. 6

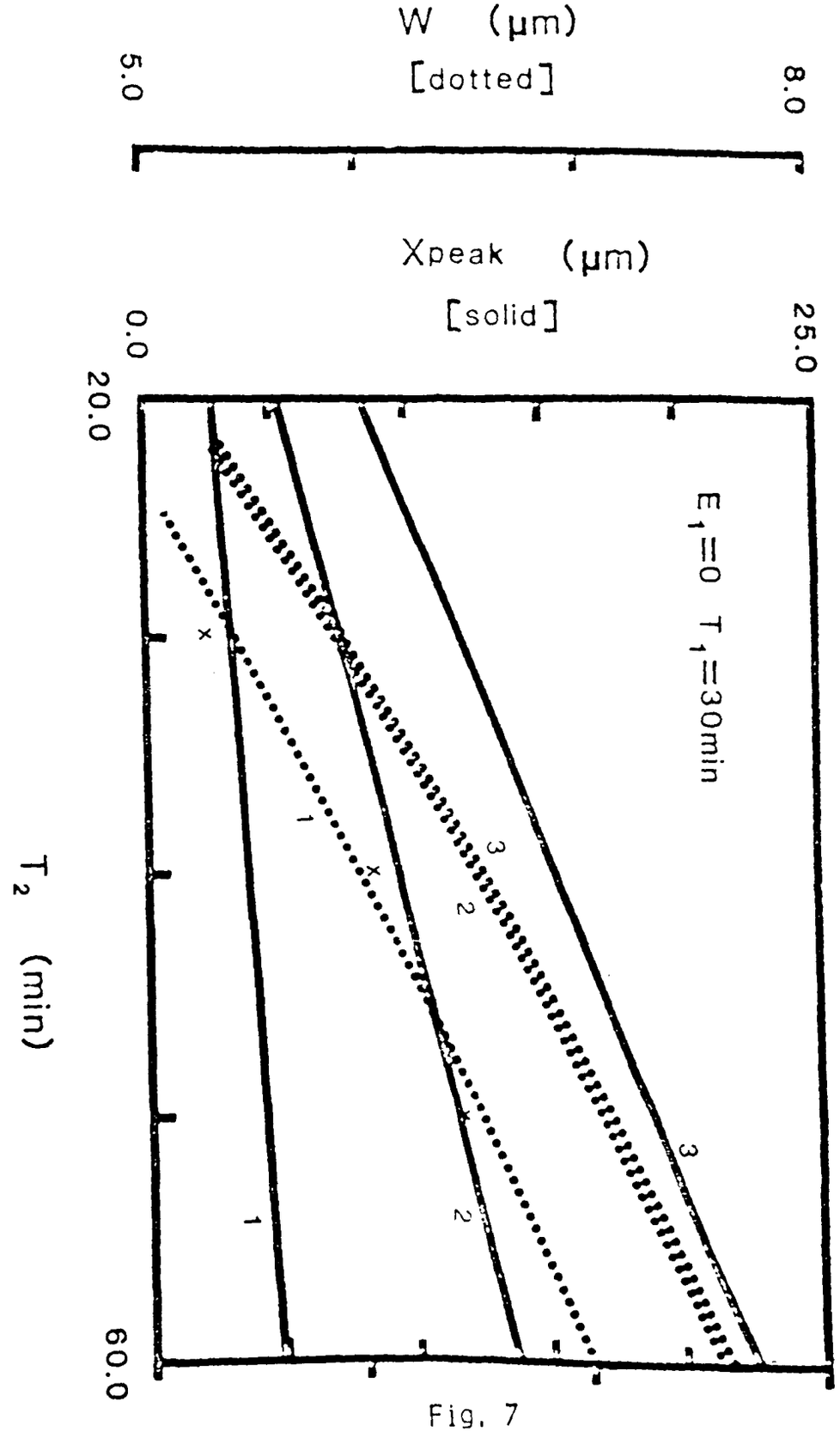
W (μm)
[dotted]
5.0
8.0
Xpeak (μm)
[solid]
0.0
25.0
20.0
60.0
T_2 (min)
$E_1=0$ $T_1=30$min
1
2
3
1
2
3
x
x

Fig. 7

REFERENCE [18]

Buried Low-Loss Fiber Compatible Single-Mode Ion-Exchanged Channel Waveguides

H.C. Cheng, H. Zhenguang, A. Miliou,
R. Srivastava and R.V. Ramaswamy

Department of Electrical Engineering
University of Florida
Gainesville, Florida 32611

Abstract

Buried single-mode channel waveguides have been designed and fabricated by optimizing the two-step Ag^+-Na^+ and K^+-Na^+ ion-exchange processes. Relatively low fiber waveguide throughput loss (<1dB) in 20 mm. long waveguides was achieved.

Category: Passive Guided-Wave Devices

Buried Low-Loss Fiber-Compatible Single-Mode Ion-Exchanged Channel Waveguides

H.C. Cheng, H. Zhenguang[+], A. Miliou,
R. Srivastava and R.V. Ramaswamy

Department of Electrical Engineering
University of Florida
Gainesville, Florida 32611

[+]Permanent Address: Changchun Institute of Physics,Changchun, China

Glass waveguides made by ion-exchange technique are potential candidates for integrated optic applications such as power dividers, star couplers and multiplexers. Although recent reports [1] have demonstrated significant progress in understanding of the basic ion-exchange process, and in the fabrication of low-loss waveguides and I-O components, the structures have not been optimized for a given application such as 1.3μm operation of single-mode fiber communication systems. Most of the work reported to date has been on surface channel waveguides which are shallow, lossy and incompatible with the fibers.

In this work, we report for the first time a systematic study of the two-step ion-exchange process for fabrication of symmetric low-loss single-mode channel guides optimized for 1.3 μm. Both Ag^+-Na^+ as well as K^+-Na^+ systems are considered. The 2-D diffusion process is modeled and the results show an excellent agreement with the measured index and modal profiles. Side diffusion, space charge effects and presence of external field are considered in the analysis.

Ag^+-Na^+ Channel Waveguides

Previously determined values of the surface-index change (Δn), interdiffusion coefficient ($\tilde{D}$) and silver ionic mobility (μ) in planar guides made in a soda-lime glass [2] were used to design channel waveguides of the desired index profile. First-step ion exchange was performed at 260°C for 24 hours in a molten mixture of 70% $NaNO_3$ + 30% KNO_3 + 1 x 10^{-4}MF $AgNO_3$. With channel opening widths of 2-10 μm, this yielded 4-14 μm wide and ~4 μm deep guides with asymmetric profiles caused by the side diffusion and the index discontinuity at the air-glass interface. A second-step ion exchange from pure $NaNO_3$ with an applied field of 25.0 V/mm for 20 minutes was subsequently performed at 330°C to bury the guides below the surface, increase the waveguide depth, and obtain a nearly circular profile. The resulting waveguides were characterized for the mode-field profile and attenuation. The results are shown in Fig. 1. An extensive modeling of the diffusion and modal profiles by solving the pertinent non-linear 2-D diffusion equation with appropriate initial and boundary conditions has been performed and the results

are correlated with the experimental data. The relatively small fiber-waveguide coupling loss (<0.1 dB) is attributed to the high degree of mode compatibility achieved.

K^+-Na^+ Waveguides

In this case, three different glasses were used. Planar surface guides were first fabricated to determine the index profile and the temperature dependence of $\tilde{D}$ in each case. The measured index profiles in the three glasses were fitted to the solutions of the 1-D diffusion equation in order to explain the differences in the profiles as well as analyze the discrepancies existing in the literature regarding their origin [3,4]. Next, planar surface guides were prepared in the presence of an external field (100V/mm). Due to the presence of the space charge, a drop in the ionic current was observed as the ion-exchange proceeded. The data points in Fig. 2 show this behavior which was modeled for the first time by taking into account the difference between the mobilities of the two alkali ions. The theoretical prediction is given by the continuous curve in Fig. 2, indicating an excellent agreement with the experimental data. Since the diffusion effects were found to be negligible, the depth ($W = \mu Et$) of index profile (Fig. 3(a)) was used to calculate the mobility of the K^+ ions in the glass.

The index profiles of the surface and buried channel waveguides are shown in Fig. 3(b). To the best of our knowledge, this is the first time the K^+-Na^+ process has been used to produce buried symmetric channel waveguides. Our results are in contradiction to the published reports [5] indicating that K^+-Na^+ waveguides cannot be buried by a second step ion exchange. Mode field profiles and attenuation were measured at 1.3 μm. The loss figures are given in Table I. The resulting mode field profiles are almost circular although the degree of circularity is not comparable to that in the Ag^+-Na^+ case. An improvement of 0.65 dB in total throughput loss in ~2 cm long waveguides was achieved as a result of the second step ion-exchange with applied field. The distinct differences in the index profiles obtained using the two cations as well as the details of the modeling and correlation between the theory and the experimental data will be presented at the meeting.

This work was supported by AFOSR contract No. 84-0369.

References

1. R.V. Ramaswamy and R. Srivastava, International Conference on Micro-optics, Tokyo, Japan, 1987.

2. H.C. Cheng, R.V. Ramaswamy and R. Srivastava, GRIN, Reno, Nev., 1987.

3. G.L. Yip and J. Albert, Opt. Lett. 10, 151 (1985).

4. J.E. Gortych and D.G. Hall, IEEE J. Quantum Electron. QE-22, 892 (1986).

5. M. McCourt, R. Rimet and C. Nissim, European FOCLAN '87, Basel, Switzerland.

Table I. Loss in K^+-Na^+ Channel Waveguide. BK-7 glass. λ = 1.3 μm.

	Surface Waveguide (17.4 mm)	Buried Waveguide (20 mm)
Fiber-waveguide Total throughput loss	1.60 dB	0.96 dB
Reflection at the output end	0.18 dB	0.18 dB
Fiber-waveguide mode mismatch	0.34 dB	0.28 dB
Propagation	0.62 dB/cm	0.25 dB/cm

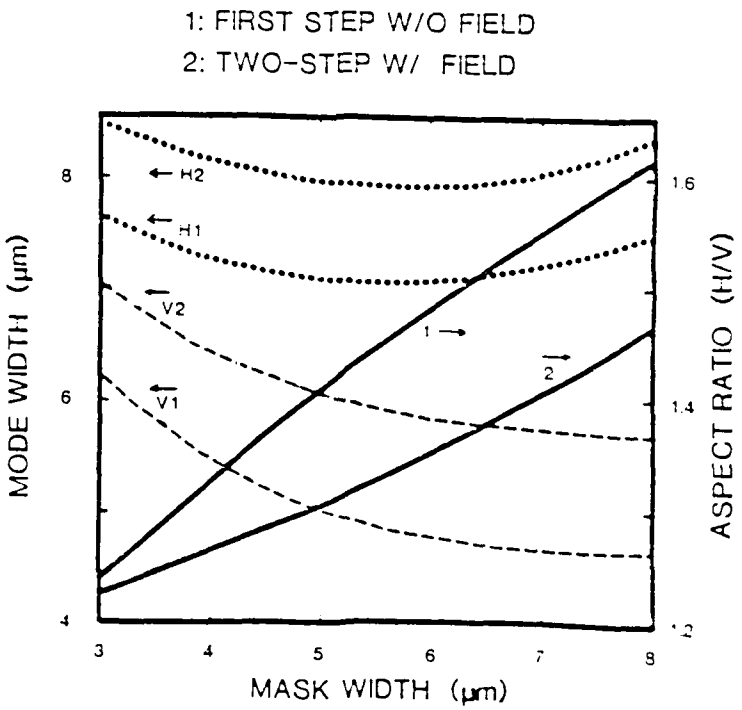

Fig. 1. Variation of 1/e mode intensity width with mask width. H - horizontal scan (along the guide width). V - vertical scan (along the guide depth).

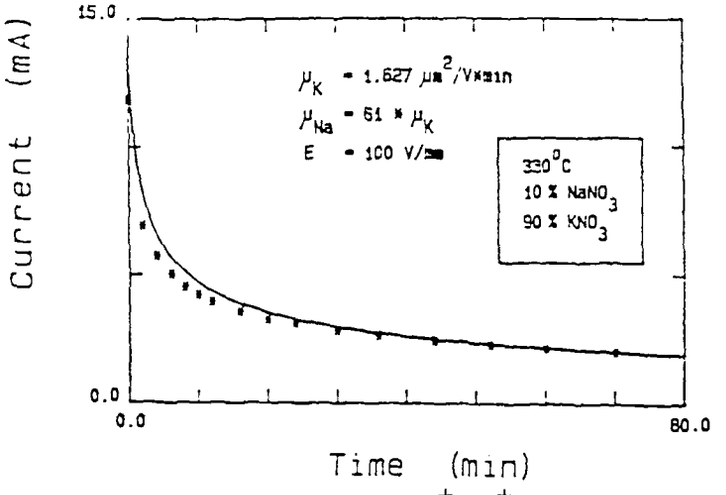

Fig. 2. Variation of ionic current in K^+-Na^+ ion exchange with applied field. * data points. ——— fitted curve.

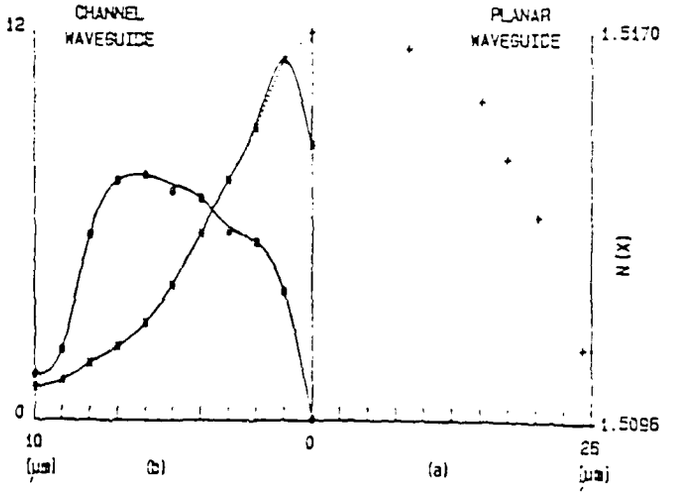

Fig. 3(a). Inverse WKB index profile of planar surface guide (330°C, 82 min., E = 100 V/mm).

Fig. 3(b). K^+ concentration profile as measured by electron microprobe.
* surface guide, 380°C & 345 min.
o buried guide, 330°C, 82 min. & E = 100 V/mm.

JOURNAL OF LIGHTWAVE TECHNOLOGY, VOL. LT-4, NO. 2, FEBRUARY 1986

Process and Waveguide Parameter Relationships for the Design of Planar Silver Ion-Exchanged Glass Waveguides

RAJENDRA K. LAGU AND RAMU V. RAMASWAMY, SENIOR MEMBER, IEEE

Abstract—**In this paper the experimental results of diffusion studies and modal characterization of Ag^+-Na^+ exchanged glass waveguides are presented. Empirical relations between the process and the device parameters are derived and subsequently used to formulate a systematic procedure for fabricating single- and multimode waveguides.**

I. Introduction

ION-EXCHANGED waveguides have received considerable attention recently and they are expected to form the basis for passive integrated optical devices. Several monovalent ions such as Tl^+ [1], K^+ [2], Ag^+ [3]-[6], have been used to form a high-index layer on the surface of glass slides. A recent electrolytic technique [7], [8] provides opportunities for precise control of Ag^+ concentration in the salt bath [9], leading to fabrication of devices with reproducible characteristics. This is quite important because glass waveguides, being passive, cannot be tuned electrooptically to compensate for fabrication errors.

The guiding characteristics of a planar waveguide depend upon the device parameters such as the maximum index change, index profile, and the waveguide depth. The device parameters, in turn, depend upon the process parameters such as the diffusion temperature, diffusion time, and Ag^+ concentration in the salt bath. To design a waveguide supporting a specific number of modes, it is necessary to determine the relation between the process and the waveguide parameters. Such relations, empirically derived and reported in this paper, are useful in the design of single and multimode planar Ag^+ diffused glass waveguides.

II. Diffusion Equation

The process of interdiffusion of sodium and silver ions in glass has already been examined in some detail. It has been shown that the silver ion diffusion can be described theoretically by a concentration-dependent one-dimensional modified Fick's diffusion equation [10], [11]

$$\frac{\partial C}{\partial t} = \frac{\partial}{\partial x}\left(\tilde{D}\frac{\partial C}{\partial x}\right) \tag{1}$$

where C is the concentration of the diffusing ion and $\tilde{D}$ is the interdiffusion coefficient defined by

$$\tilde{D} = \frac{D_A D_B}{N_A D_A + N_B D_B} \tag{2}$$

and

$$N_A \quad \text{mole fraction of silver ion} = \frac{C_A}{C_A + C_B},$$

$$N_B \quad \text{mole fraction of sodium ion} = \frac{C_B}{C_A + C_B}$$

where D_A, D_B are the self-diffusion coefficients of silver and sodium ions, and C_A, C_B are the silver and sodium ion concentrations, respectively.

In the fabrication of ion-exchanged glass waveguides, the silver ion concentration is very small, i.e., $C_A \ll C_B$. Therefore, $N_A \approx 0$ and N_B approaches unity.

Under these conditions, the interdiffusion coefficient $\tilde{D}$ in (2) becomes the self-diffusion coefficient of the incoming Ag^+, namely D_A. In addition, as C_A is quite small, it is reasonable to assume the diffusion of silver ions into the substrate remains unaffected by the presence of already diffused silver ions. In other words, D_A is independent of the position x in the substrate. As a result, (1) now simplifies to the well-known diffusion equation

$$\frac{\partial C}{\partial t} = D\frac{\partial^2 C}{\partial x^2} \tag{3}$$

where we have omitted the subscript A in the diffusion coefficient for the sake of simplicity.

The diffusion was carried out in a molten $NaNO_3$ bath, containing the electrolytically released silver ions [7], [8]. The diffusion can be considered as an infinite source diffusion since the number of silver ions diffusing into the semi-infinite glass substrate is very small compared to that present in the bath. We can therefore assume that the con-

Manuscript received May 10, 1985; revised August 19, 1985. This work was supported in part by the Air Force Office of Scientific Research under grant AFOSR 84-0369.

R. K. Lagu was with the Department of Electrical Engineering, University of Florida, Gainesville, FL 32611. He is now with the Department of Electrical and Computer Engineering, University of Iowa, Iowa City, IA 52242.

R. V. Ramaswamy is with the Department of Electrical Engineering, University of Florida, Gainesville, FL 32611.

IEEE Log Number 8406207.

centration of Ag^+ at the liquid-solid interface is constant at all times. Initially, the Ag^+ concentration is assumed to be zero in the entire substrate. Under these conditions, the diffusion equation has an analytical solution [11], given by

$$C(x, t) = C_0 \operatorname{erfc}(x/2\sqrt{Dt}) \tag{4}$$

where

C_0 concentration of silver ions in the bath,
D self-diffusion coefficient of the silver ions.

Planar waveguides fabricated in this manner exhibit a complementary error function index profile. The propagation characteristics for this highly asymmetric profile have been determined by the numerical integration of the normalized mode dispersion equation [12], [13]. We have used these analytical results to fit our experimental data in order to link the process and the device parameters.

III. Waveguide Characterization

Several sets of single-mode and multimode waveguides were fabricated using Labmate microscope slides for different values of the process parameters C_0 (Ag^+ concentration in bath) and t (diffusion time). For a particular batch, a known value of C_0 was generated using the improved electrolytic technique [8] and waveguides were fabricated for times ranging from 20 to 120 min. Prism coupling technique was used to excite the modes in order to determine the mode indices. An iterative computer program was written to estimate the diffusion coefficient D and the maximum index change Δn. The procedure is described as follows.

Assuming small index change between the substrate and the peak surface refractive index, the V parameter is defined as [14]

$$V = kd\sqrt{2n_b\Delta n} \tag{5}$$

where

k $2\pi/\lambda$, free-space propagation constant,
λ wavelength of operation,
d effective waveguide depth,
n_b bulk refractive index of the substrate,
Δn maximum change in the refractive index.

As described previously, the interdiffusion of Ag^+-Na^+, for low concentrations of Ag^+, reduces to the simple case of self-diffusion of silver ions into the glass substrate and therefore, the interdiffusion coefficient $\tilde{D}$ approaches the self-diffusion coefficient D. This fact has been experimentally determined by independent diffusion studies and the results are presented elsewhere [15].

For complementary error function, the depth of diffusion equals the waveguide width d and is given by

$$d = 2\sqrt{Dt}. \tag{6}$$

Thus

$$V = \frac{4\pi}{\lambda}\sqrt{2n_bDt\Delta n}. \tag{7}$$

A He-Ne laser ($\lambda = 0.6328\ \mu m$) was used for the mode index measurements. The bulk refractive index n_b was measured using an Abbe' refractometer and for Labmate glass $n_b = 1.5125$. Thus at $\lambda = 0.6328\ \mu m$

$$V = (3.454 \times 10^7)\sqrt{Dt\Delta n}. \tag{8}$$

The normalized propagation constant b_m for a guided mode in an asymmetrical graded index waveguide [14] is defined as

$$b_m = \frac{N_m^2 - n_b^2}{n_s^2 - n_b^2} \tag{9}$$

where

N_m β_m/k, mode index for the mode of order m,
b_m propagation constant of the mode of order m,
n_s surface index $= n_b + \Delta n$.

For small index approximation (which is valid for our glass waveguides), $\Delta n \ll n_b$ so that

$$b_m \approx \frac{N_m - n_b}{\Delta n}. \tag{10}$$

From (8) and (10), it is seen that for a given glass substrate and a given wavelength of operation, V is a function of D, Δn, and t, whereas b_m depends upon Δn and the mode index N_m. Of these parameters, N_m and n_b are determined experimentally and t is also known. Δn depends upon C_0, the concentration of Ag^+ in bath. Thus, a set of waveguides fabricated with the same C_0 but with different t have the same Δn but different depths, hence different V numbers. The computer program reads as its input data the mode order m, the mode index N_m, and the diffusion time t for each of the mode in a set of waveguides with the same Δn. The diffusion profile for these waveguides as evidenced by the backscattered electron SEM analysis Ag^+ profile [15], [16] is the theoretically anticipated complementary error function and contrasts the exponential function profile determined by the measurement of mode excitation angles and the use of inverse WKB method by Imai *et al.* [17]. A min-max error algorithm is used for fitting experimental data to the theoretically derived b-V characteristics [12], [13], for the complementary error function index profile [15] of these waveguides. To start with, for each sample, values of Δn and D were initially guessed and V was calculated from (8). For this value of V, using the theoretical analysis [12], [13], b_m was estimated numerically for each of the allowable modes. On the other hand, for the same Δn, the normalized propagation constant b_m was also calculated using (10). The error is defined as the largest difference between the value of b_m calculated from the b-V characteristics and that calculated from (10). The values of Δn and D were then varied over a prespecified range and the error calculations were repeated. The error contours were then plotted in the Δn-D plane. Fig. 1 shows a typical error contour plot corresponding to a mole fraction concentration C_0 of 1.6×10^{-4} and diffusion of Ag^+ at 338°C for three modes. The contours show that the error has a min-

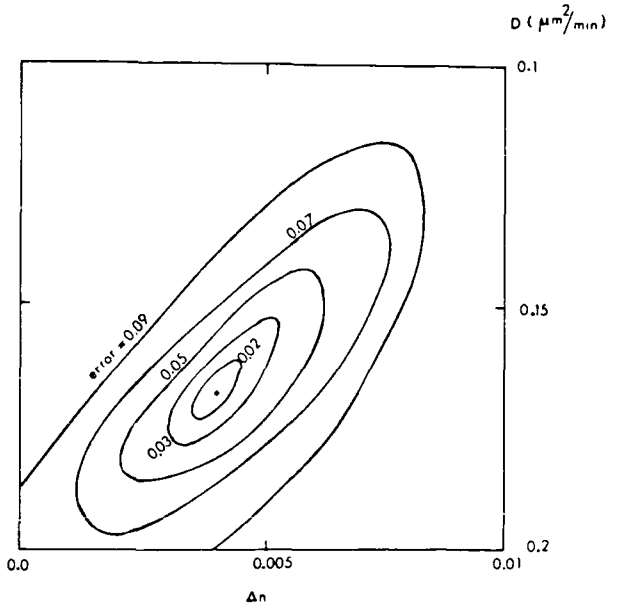

Fig. 1. Error contours in the Δn-D plane with the error in the normalized propagation constant b_m between the theoretical and experimental values for three modes.

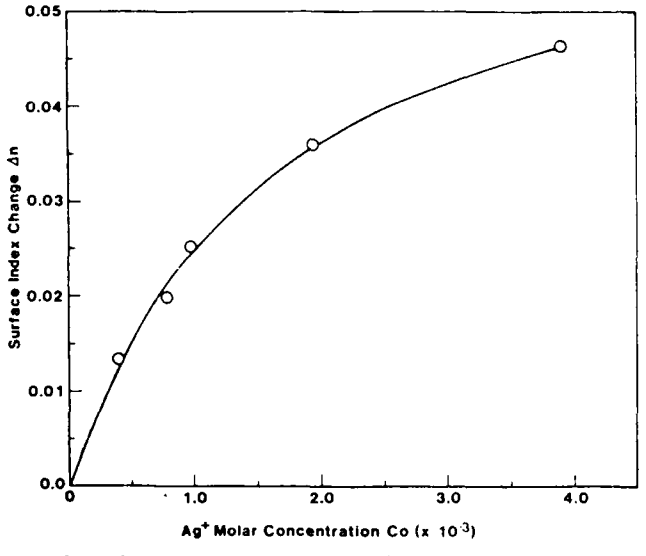

Fig. 2. Surface index change Δn versus Ag^+ concentration C_0 for Labmate glass.

imum and the values of Δn and D corresponding to this minimum are the best estimates. This procedure gives same set of values of Δn and D for each mode.

Several waveguides were fabricated with different concentration values and using the above procedure, Δn was estimated for each Ag^+ concentration. The relationship between Δn and C_0 is shown in Fig. 2. The curve in the region where the value of C_0 is small is essentially linear. For guides with small number of modes (less than six modes), the relationship between Δn and C_0 can be approximated as

$$\Delta n \approx 26.5 C_0 \tag{11}$$

where C_0 is expressed as the mole fraction of silver ions in bath.

Equation (11) provides an important link between the device parameter Δn and the process parameter C_0. This empirical relation is valid for Labmate slides used as substrates in our experiments. If we were to assume that indeed Ag^+-Na^+ exchange is taking place, any change in weight fraction of Na_2O in our different substrate would require redetermination of the linear relationship between Δn and C_0. In addition, other cations, e.g., Ca^{++}, may alter this behavior as well. However, for the weight fraction of Na_2O, in the neighborhood of 10–15 percent, the estimate of $\Delta n/C_0$, established by (11) is valid [16].

IV. Diffusion Coefficient

To estimate the variation of the diffusion coefficient D with temperature T, using the improved electrolytic release technique, three batches of waveguides were fabricated at 338, 354, and 360°C. The diffusion coefficient at these temperatures is estimated by the computer program mentioned above. The variation of D with T is given by an Arhenius type relation [10]

$$D(T) = D_0 e^{-\Delta H/RT} \tag{12}$$

where

ΔH activation energy,
R gas constant (8.314 J/K° · mole).

Taking logarithm of (11), we have

$$\ln D = \ln D_0 - (\Delta H)/RT. \tag{13}$$

Thus the slope of the curve ln D versus $(1/T)$ gives the value of $\Delta H/R$. As shown in Fig. 3, ΔH is estimated to be 8.933×10^4 J and the diffusion coefficient

$$D_0 \approx 1.1906 \times 10^{-7} \quad (m^2/sec).$$

Since for the glass waveguide fabrication, the diffusion time is of the order of tens of minutes and the diffusion depth is of the order of a few micrometers, D is expressed in square micrometers per minute. The temperature range is rather restricted, as $NaNO_3$ melts at 307°C and decomposes at 380°C. Using the above value of D_0 and ΔH in the Arhenius relation (equation (12)), D versus T is plotted over the relevant temperature range and is shown in Fig. 4. It is seen that the curve can be approximated by two linear segments with a transition around 353°C. Beyond 353°C, D changes rapidly with T so that in this region, the temperature fluctuations during fabrication will cause significant changes in D resulting in a large variation in the guide depth d. This indicates that the diffusion temperature should be chosen between 307°C and 353°C. During the experiments it was observed that a temperature gradient of as much as 20°C can exist in the bath [9], and hence, it is recommended to choose 330°C as the diffusion temperature, which is sufficiently higher than the melting point of $NaNO_3$, viz., 307°C.

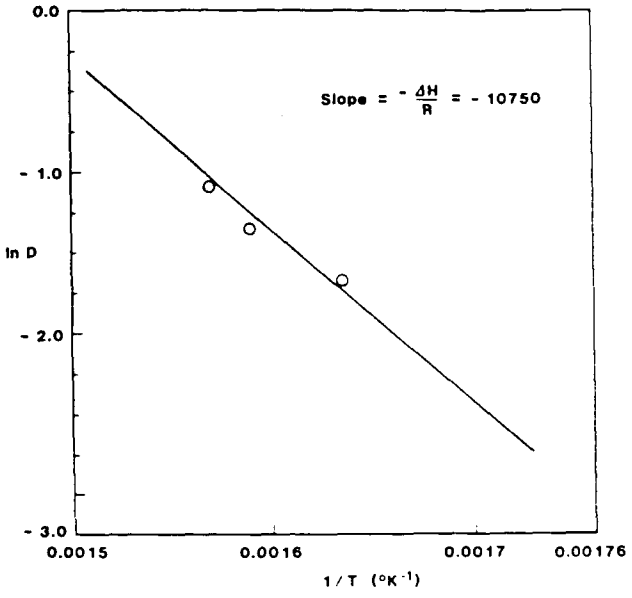

Fig. 3. Estimation of activation energy ΔH from $\ln D$ versus $1/T$ plot (Labmate glass).

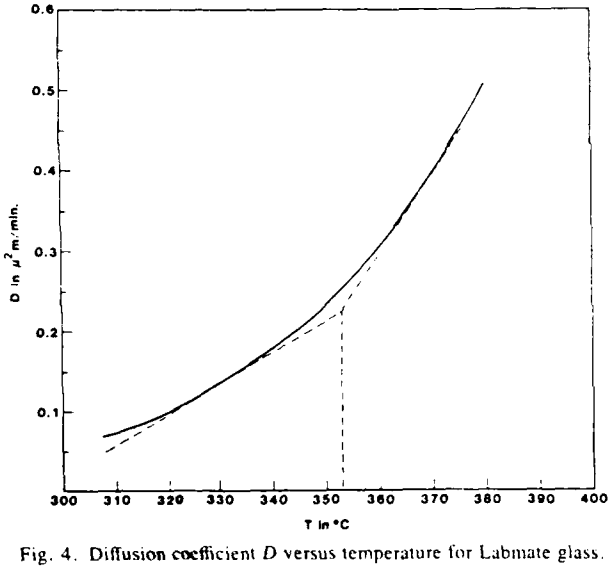

Fig. 4. Diffusion coefficient D versus temperature for Labmate glass.

At 330°C, the diffusion coefficient $D = 0.129\ \mu m^2/min$. Substituting this value in (6):

$$d = 0.718\sqrt{t}. \tag{14}$$

Equation (14) provides the second important link between the device parameter d and the process parameter t. This value, derived from modal characterization, agrees with that estimated from the diffusion studies, presented elsewhere [15].

V. Design Procedure

Using the relations given by (11) and (14), a systematic design procedure is formulated as described below.

The normalized dispersion equation for an asymmetrical graded-index planar waveguide is given by [12], [13]

$$V \int_0^{x_t'} [f(x') - b]^{1/2}\, dx' = (m + \tfrac{3}{4})\pi \tag{15}$$

where x_t' is the normalized turning point. At cutoff, $x_t' \to \infty$ and $b = 0$. For a complementary error function profile $f(x') = \text{erfc}\,(x')$. Therefore, V_{cm}, the value of V number at cutoff of the mth mode can be written as

$$V_{cm} \int_0^{\infty} \sqrt{\text{erfc}\,(x')}\, dx' = \frac{(4m + 3)\pi}{4}. \tag{16}$$

Since erfc (x') is a monotonically decreasing function with increasing x', and erfc $(2) = 0.0005$, to reduce the computation time, we can limit the integration range by using the approximation

$$\int_0^{\infty} \sqrt{\text{erfc}\,(x')}\, dx' \simeq \int_0^{2} \sqrt{\text{erfc}\,(x')}\, dx'. \tag{17}$$

The integral on the right-hand side of (17) is evaluated numerically and its value is found to be 0.89. Thus

$$(0.89)\ V_{cm} = \frac{(4m + 3)\pi}{4}. \tag{18}$$

From (6), (7), (11), and (14), for $\lambda = 0.6328\ \mu m$, $n_b = 1.5125$ and $D = 0.129\ \mu m^2/min$

$$V = 63.85\sqrt{tC_0}. \tag{19}$$

From (18) and (19), the cutoff value V_{cm} can be eliminated

$$V_{cm} = \frac{(4m + 3)\pi}{4(0.89)} = (63.85)\ (\sqrt{tC_0})_{\text{cutoff}}. \tag{20}$$

C_0 and t in the above equations correspond to those values of diffusion depth and Δn which give the respective mode cutoff. Thus, the cutoff condition for mode m dictated by the process parameters t and C_0 is

$$(tC_0)_{\text{cutoff}} = (1.91 \times 10^{-4})\ (4m + 3)^2. \tag{21}$$

For various values of m, the relations between t and C_0 as given by (21) are plotted in Fig. 5. Since these curves distinguish the regions of various modes, the design can be done entirely using the process parameters, making the device parameters invisible in the design procedure. For example, for a given time of diffusion (as decided by the required waveguide depth), one can find the value of C_0 which keeps the waveguide single mode. Generation of this value of C_0 can be done precisely using the electrolytic process [7], [8]. The inherent capability of this process to generate arbitrary values of C_0 can likewise be used together with these curves to fabricate waveguides supporting a specific number of modes. Neglecting the material dispersion effects, the relation between Δn and C_0 given by (11) is essentially valid for other wavelengths as well. Thus, similar design curves can be plotted for any other wavelength, e.g., for $\lambda = 1.32\ \mu m$ as shown in Fig.

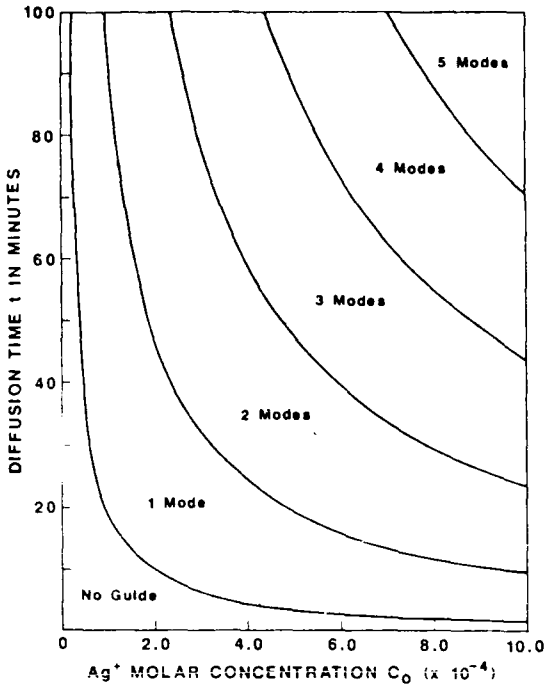

Fig. 5. Diffusion time t versus Ag^+ mole concentration—design curves at cutoff for $\lambda = 0.6328$ μm.

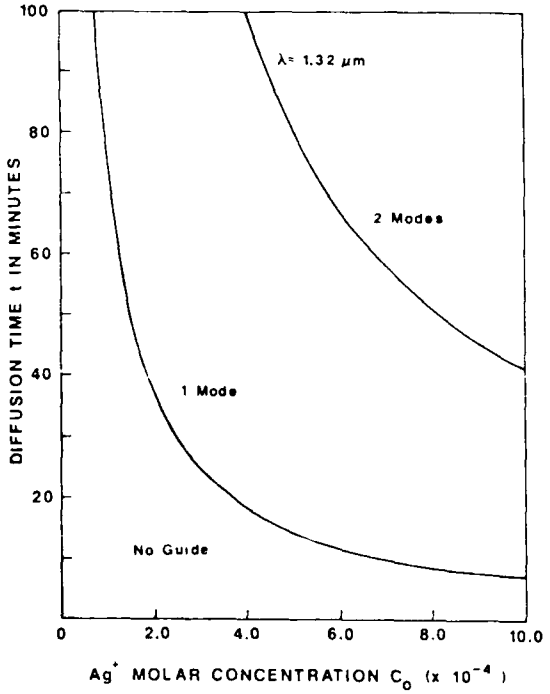

Fig. 6. Diffusion time t versus Ag^+ mole concentration—design curves at cutoff for $\lambda = 1.32$ μm.

6. We have experimentally confirmed the validity of the curves for $\lambda = 0.6328$ μm by fabricating various graded index (erfc) waveguides by electrolytic release technique and evaluating them using the prism coupler.

VI. Conclusions

We have presented the results of an experimental study of modal characterization of planar waveguides fabricated using Ag^+ diffusion into glass substrate. With the help of a numerical solution for a graded index (erfc) waveguide, the guiding characteristics were used to estimate the device parameters, viz., the maximum index change and the effective guide width. Using an appropriate diffusion model, the dependence of the diffusion coefficient of Ag^+ in glass and the diffusion depth on process parameters, viz., diffusion temperature and time were estimated. The resulting empirical data were used to establish the links between the process and the device parameters and to formulate a systematic procedure for fabricating glass waveguides supporting a specified number of modes.

References

[1] T. Izawa and H. Nakagome, "Optical waveguides formed by electrically induced migration of ions in glass plates," *Appl. Phys. Lett.*, vol. 21, pp. 584-586, 1972.

[2] T. G. Giallorenzi, E. J. West, R. Kirk, R. Ginther, and R. A. Andrews, "Optical waveguides formed by thermal migration of ions in glass," *Appl. Opt.*, vol. 12, pp. 1240-1245, 1973.

[3] G. Stewart, C. A. Miller, P. J. R. Leybourn, C. D. W. Wilkinson, and R. M. DeLarue, "Planar optical waveguides formed by silver ion migration in glass," *IEEE J. Quantum Electron.*, vol. QE-13, pp. 192-202, 1977.

[4] G. Chartier, P. Collier, A. Guez, P. Jaussaud, and Y. Won, "Graded index surface or buried waveguides by ion-exchange in glass," *Appl. Opt.*, vol. 19, pp. 1092-1095, 1980.

[5] H. J. Lilienhof, E. Voges, D. Ritter, and P. Pantschew, "Field induced index profiles of multimode ion-exchanged strip waveguides," *IEEE J. Quantum Electron.*, vol. QE-18, pp. 1877-1883, 1982.

[6] T. Findakly and E. Gamire, "Reduction and control of optical waveguide losses in glass," *Appl. Phys. Lett.*, vol. 37, pp. 855-856, 1980.

[7] R. K. Lagu and R. V. Ramaswamy, "Fabrication of single mode glass waveguides by electrolytic release of silver ions," *Appl. Phys. Lett.*, vol. 45, pp. 117-118, 1984.

[8] S. I. Najafi, R. V. Ramaswamy, and R. K. Lagu, "An improved method for fabricating ion-exchanged waveguides through electrolytic release of silver ions," *J. Lightwave Technol.*, vol. LT-3, no. 4, pp. 763-766, Aug. 1985.

[9] R. K. Lagu, S. I. Najafi, and R. V. Ramaswamy, "*In situ* measurement of ionic concentration during fabrication of ion-exchanged waveguides," *Appl. Opt.*, vol. 23, p. 3925, 1984.

[10] R. H. Doremus, "Exchange and diffusion of ions in glass," *J. Phys. Chem.*, vol. 68, pp. 2212-2218, 1964.

[11] J. Crank, *Mathematics of Diffusion*. London: England: Oxford, 1956.

[12] G. B. Hocker and W. K. Burns, "Modes in diffused optical waveguides of arbitrary index profiles," *IEEE J. Quantum Electron.*, vol. QE-11, pp. 270-276, 1975.

[13] R. V. Ramaswamy and R. K. Lagu, "Numerical field solution for an arbitrary, asymmetrical, graded index planar waveguides," *J. Lightwave Technol.*, vol. LT-1, pp. 408, 1983.

[14] H. Kogelnik and R. V. Ramaswamy, "Scaling rules for thin film optical waveguides," *Appl. Opt.*, p. 1857, 1974.

[15] R. V. Ramaswamy and S. I. Najafi, "Planar, buried, ion-exchange glass waveguides: Diffusion characteristics," *IEEE J. Quantum Electron.*, accepted for publication.

[16] R. K. Lagu, R. V. Ramaswamy, and S. I. Najafi, presented at 3rd Eur. Conf. Integrated Optics (ECIO'85), Berlin, W. Germany, May 6-8, 1985, pap. B10.

[17] M. Imai, N. Haneda, and Y. Ohtsuka, "Losses in optical waveguides formed by silver-sodium ion exchange," *J. Lightwave Technol.*, vol. LT-1, pp. 611-615, 1983.

Rajendra K. Lagu was born in Poona, India, on June 7, 1956. He received the B.Tech. and M.Tech. degrees in electrical engineering from the Indian Institute of Technology, Bombay, India, in 1978 and 1981, respectively. He received the Ph.D. degree in electrical engineering from the University of Florida, Gainesville, in 1985.

He worked as a Development Engineer in Peico Electronics and Electricals Limited, India, from June 1978 to May 1979. He was a Research Fellow in the Department of Electrical Engineering, I.I.T., Bombay, from June 1979 to December 1981. He worked as a Graduate Research Assistant in the Department of Electrical Engineering, University of Florida, Gainesville, from January 1982 to December 1984. Currently he is working as an Assistant Professor in the Department of Electrical Engineering, University of Iowa, Iowa City. His current research interests include fiber and integrated optics.

Dr. Lagu is a member of Eta Kappa Nu, Tau Beta Pi, and Phi Kappa Phi.

*

Ramu V. Ramaswamy (M'62–SM'80) was born in Madras, India, in June 1938. He received the B.S. degree in physics from Madras University, Madras, India, in 1957, and the Diploma D.M.I.T. in electronics engineering from Madras Institute of Technology, Chromepet, Madras, India, in 1960. He received the M.S. and Ph.D. degrees in electrical engineering from Northwestern University, Evanston, IL, in 1962 and 1969, respectively. His doctoral work consisted of wave-propagation studies in semiconductor plasmas.

From 1962 to 1965, he served as a member of the research department of Zenith Radio Corporation, Chicago, IL, working on solid-state parametric amplifiers, and microwave components. In 1969, he joined Bell Laboratories, Crawford Hill Laboratory, Holmdel, NJ, where he was engaged in research on thin-film optical device, polarization effects in single-mode fibers and fiber-waveguide couplers. Since 1981, he has been a Professor in the Department of Electrical Engineering, University of Florida, Gainesville, where his current interests include passive integrated-optical devices, fiber-optic sensors, and optoelectronic devices.

Dr. Ramaswamy is currently the Director of a university-wide interdisciplinary program known as MICROFABRITECH which will emphasize both the fundamental and engineering aspects in the research and development of novel layered materials and structures for optical and high speed electronic micro circuits. He is a member of Sigma Xi.

REFERENCE [20]

IEEE JOURNAL OF QUANTUM ELECTRONICS, VOL. QE-22, NO. 6, JUNE 1986

A Variational Finite-Difference Method for Analyzing Channel Waveguides with Arbitrary Index Profiles.

RAJENDRA K. LAGU AND RAMU V. RAMASWAMY, SENIOR MEMBER, IEEE

Abstract—A variational, finite-difference method for computing the normalized propagation constants and the normalized field profiles of channel waveguides with arbitrary index profiles as well as aspect ratios is presented. Mode dispersion curves and the field profiles of the fundamental mode of channel waveguides having profiles of practical interest are included.

I. Introduction

THE analysis of channel waveguides plays a significant role in the design of integrated optical devices since channel waveguides form the basic building blocks of many devices, e.g., directional couplers, electrooptic modulators, switches, etc. The channel waveguide mode dispersion is crucial to the device design because reproducible fabrication of these devices needs a prior knowledge of the waveguide modal behavior. A number of methods for analyzing both step and graded index waveguides are already available in the literature. Goell [1] has used circular harmonic analysis for a step index channel immersed in an infinite medium of lower index. Marcatili [2] has analyzed the step index channel by ignoring the fields in the corner regions. This approximate analytical solution gives accurate results for waveguides far away from cutoff because the field in the corner region of such waveguides can indeed be ignored. Neither approach mentioned above, however, is applicable to graded index waveguides. Schweig and Bridges [3] have reported a finite-difference method for computing mode dispersion of step index waveguides. Hocker and Burns [4] have extended the effective index method [5] to graded index waveguides; other approaches to graded index waveguides include Yeh's finite element analysis [6], Pichot's method based on vector integral equations [7], and the variational method reported by Matsuhara [8] and Taylor [9]. None of the above methods, regardless of the approach being analytical or numerical, provides normalized solutions for channel waveguides of arbitrary index profiles and aspect ratios.

Manuscript received November 5, 1985; revised March 3, 1986. This work was supported by a grant from AFOSR Contract 84-0369.

R. K. Lagu was with the Department of Electrical Engineering, University of Florida, Gainesville, FL 32611. He is now with the Department of Electrical Engineering, University of Iowa, Iowa City, IA 52242.

R. V. Ramaswamy is with the Department of Electrical Engineering, University of Florida, Gainesville, FL 32611.

The waveguides used in practice are often made by diffusion which results in channels with index profiles (typically Gaussian and complementary error function) which are not amenable to analytical treatment. Numerical methods, on the other hand, give solutions which are applicable to specific waveguides, and recomputation is necessary if the waveguides' parameters are changed. If the associated Helmholtz equation can be normalized prior to the numerical solution, the results will turn out to be fairly general and applicable to any graded index profile. We have used this approach to calculate the normalized field profiles of a highly asymmetrical, planar graded index waveguide [11]. In this paper, we extend it to channel waveguides with arbitrary index profiles. The reported method has the following advantages.

1) It accepts any index profile, even if it is available at discrete points. The method, therefore, can directly use the results of diffusion simulation, in which case the index profile as obtained from the numerical solution of the two-dimensional diffusion equation is available only at discrete points.

2) It solves the *normalized Helmholtz equation* so that the results are applicable to all waveguides of a given index profile.

3) Most importantly, unlike other numerical techniques, it accepts various waveguide aspect ratios without any additional reformulation. This feature is important because the aspect ratio of a practical waveguide depends on both the diffusion depth and the waveguide width, which in turn depends on the lateral diffusion. Thus, the aspect ratio usually has a value other than unity.

Therefore, the approach is applicable in the evaluation of channel waveguides with a given depth, and any aspect ratio, e.g., two-dimensional tapered waveguide transitions, without extensive recompilation.

The numerical approach presented here involves a combination of both variational and finite-difference techniques. The straightforward finite-difference approach to solve the normalized Helmholtz equation requires a large number of subintervals since for that method, the field is discontinuous at the subinterval boundaries. For a reasonably accurate solution, it is estimated that at least 50 intervals will be needed along the x and y directions. This will result in matrices of size (2500 × 2500) and the numerical computations such as matrix inversion will be vir-

0018-9197/86/0600-0968$01.00

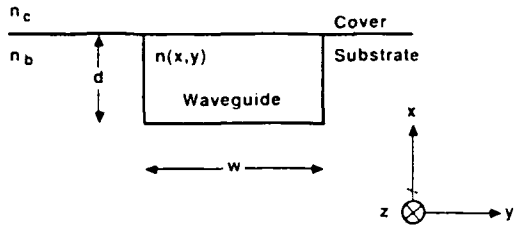

Fig. 1. A step index channel waveguide for graded index channel waveguides; the boundaries are nonexistent.

ually impossible. In the variational approach with bilinear interpolation, the field is continuous at the subinterval boundaries, and with as low as 14 subintervals in the x and y directions, quite an accurate solution is achieved.

II. Theory

A. Normalization

The step index dielectric channel waveguide under consideration is shown in Fig. 1. Obviously, for diffused channel waveguides, there are no sharp boundaries between the waveguide and the substrate as shown in the figure. In that case, the width w and the depth d should be taken as the diffusion width and the diffusion depth, respectively.

The index profile can be expressed as

$$n(x, y) = n_b + \Delta n f(x, y) \tag{1}$$

where $f(x, y)$ is the normalized index profile function which takes values between 0 and 1. For the substrate region, $n(x, y) = n_b$; therefore, $f(x, y) = 0$. The peak of the index profile occurs when $f(x, y) = 1$ and the peak index is given by $n_p = n_b + \Delta n$.

Assuming a small index difference, i.e., $\Delta n << n_b$, the modes supported by this waveguide can be divided into two groups:

1) quasi-TE modes in which the primary field components are E_y, H_x, and H_z.

2) quasi-TM modes in which the primary field components are E_x, H_y, and E_z.

For quasi-TE modes, the field E_y can be expressed as

$$E_y = E(x, y)\, e^{-j\beta z}. \tag{2}$$

The field amplitude $E(x, y)$ satisfies the two-dimensional scalar Helmholtz equation

$$\frac{\partial^2 E}{\partial x^2} + \frac{\partial^2 E}{\partial y^2} + [k_0^2 n^2(x, y) - \beta^2]E = 0. \tag{3}$$

The following normalized space variables are defined:

$$x' = x/d$$
$$y' = y/w$$
$$r = w/d \tag{4}$$

where x', y', and r represent the normalized depth, width, and the aspect ratio, respectively.

The V and b parameters are defined in the usual way as [12]

$$b = \frac{N^2 - n_b^2}{n_p^2 - n_b^2} \tag{5}$$

and

$$V = \frac{2\pi}{\lambda_0} d(n_p^2 - n_b^2)^{1/2} \tag{6}$$

where

N = mode index and

λ_0 = wavelength of operation.

These normalized variables can be used to convert (3) into a normalized partial differential equation:

$$\frac{1}{r^2}\frac{\partial^2 E}{\partial y'^2} + \frac{\partial^2 E}{\partial x'^2} + V^2[f(x', y') - b]E = 0. \tag{7}$$

B. Variational Formulation

The variational formulation converts the problem of solving a partial differential equation into that of finding the maximum of a functional involving integrals. In addition, the variational approach typically converges more quickly than the direct finite-difference method. Since numerical integration is inherently stable, the variational formulation eliminates the problems of instability associated with the numerical solution of partial differential equations. Matsuhara [8], Taylor [9], and Korotky *et al.* [10] have used this approach to solve the Helmholtz equation (3). We apply this method to the normalized Helmholtz equation (7) in order to obtain the normalized solution directly. The method is described briefly below.

We define a scalar functional

$$\phi = \iint_D F\left(E, \frac{\partial E}{\partial x'}, \frac{\partial E}{\partial y'}, x', y'\right) dx'\, dy' \tag{8}$$

where x', y' are the independent variables and E is the dependent variable. The integration is carried out over domain D in the (x', y') plane and the boundary of the domain D is considered fixed for all variations. The surface $E(x', y')$ which extremizes the functional ϕ can be shown to be the solution of the Euler–Lagrange equation [13]

$$\frac{\partial F}{\partial E} - \frac{\partial}{\partial y'}\left(\frac{\partial F}{\partial p}\right) - \frac{\partial}{\partial x'}\left(\frac{\partial F}{\partial q}\right) = 0 \tag{9}$$

where $p = \partial E/\partial y'$ and $q = \partial E/\partial x'$.
If we choose

$$F = V^2 f(x', y')\, E^2 - \frac{1}{r^2}\left(\frac{\partial E}{\partial y'}\right)^2 - \left(\frac{\partial E}{\partial x'}\right)^2 - V^2 b E^2 \tag{10}$$

then the Euler–Lagrange equation for this choice of F becomes the normalized Helmholtz equation (7).

Thus, any $E(x', y')$ which extremizes ϕ is the solution of (7), and hence is the normalized field profile of the channel waveguide. The variational formulation thus converts the problem of solving the partial differential equa-

tion (7) to the problem of extremizing the functional ϕ given by

$$\phi = \iint_D \left\{ V^2 f(x', y') E^2 - \frac{1}{r^2} \left(\frac{\partial E}{\partial y'}\right)^2 - \left(\frac{\partial E}{\partial x'}\right)^2 - V^2 b E^2 \right\} dx' dy'. \quad (11)$$

From physical considerations, the fields in an optical waveguide vanish at infinity. This provides a boundary for this variational problem. In other words, the required boundary of domain D which is fixed for all variations is contained in the fact that E should be identically zero on this boundary.

Since the field decays exponentially in the substrate and the cover, it is reasonable to assume that the field vanishes at some finite point. This assumption is necessary to economize on the numerical calculations, and hence the computer time.

We now describe the steps involved in the extremization of ϕ given by (8). We define the functionals I and J as

$$I = \iint_D \left\{ V^2 f(x', y') E^2 - \frac{1}{r^2} \cdot \left(\frac{\partial E}{\partial y'}\right)^2 - \left(\frac{\partial E}{\partial x'}\right)^2 \right\} dx' dy' \quad (12)$$

$$J = \iint_D E^2 \, dx' \, dy'. \quad (13)$$

Substitution of (12) and (13) in (11) gives the following equation for ϕ:

$$\phi = I - (V^2 b) J. \quad (14)$$

At the extremum, $\delta\phi = 0$, so that

$$\delta I - (V^2 b)\, \delta J = 0. \quad (15)$$

We define a scalar function λ (not to be confused with the wavelength λ_0) given by

$$\lambda = I/J. \quad (16)$$

This function attains a stationary value λ^* when

$$\delta\lambda|_{\lambda^*} = 0. \quad (17)$$

Taking differentials in (16), we get

$$\delta\lambda = \frac{J\delta I - I\delta J}{J^2}. \quad (18)$$

Comparing (17) and (18), we obtain the following condition at the extremum of λ:

$$J\delta I - I\delta J = 0 \quad (19)$$

which can be rewritten as

$$\delta I - (I/J)\, \delta J = 0 \quad (20)$$

or

$$\delta I - (\lambda^*)\, \delta J = 0. \quad (21)$$

Comparison of (15) and (21) yields

$$\lambda^* = V^2 b. \quad (22)$$

For a given V, we have thus found the normalized propagation constant b in terms of the parameter λ^* which can be shown to be the extremum value of I/J. In other words, we have converted the problem of solving the partial differential equation (7) into that of extremizing I/J where I and J are given by (12) and (13), respectively.

To proceed with the extremization of I/J, it is necessary to make an approximation for the functional form of the normalized field distribution $E(x', y')$. As seen from (12) and (13), J depends on $E(x', y')$, while I depends on both $E(x', y')$ and the index profile function $f(x', y')$.

Matsuhara [7] and Taylor [8] have expressed the field profile $E(x, y)$ as a linear combination of a finite number of parabolic cylinder functions. Since they did not normalize the Helmholtz equation, they deal with the field profile $E(x, y)$ rather than the normalized field profile $E(x', y')$. The finite series is given by

$$E(x, y) = \sum_{i,j} a_{ij} (2\pi\xi\eta i! j!)^{-1/2} D_i(x'\xi)\, D_j(y - y_0)\eta \quad (23)$$

where D_i and D_j are the parabolic cylinder functions of order i and j, respectively. The factor $(2\pi\xi\eta i! j!)$ is used to normalize the modal functions. a_{ij}, ξ, and η are determined by stationary conditions. To account for the fact that the peak of the field occurs within the waveguide at some finite depth rather than at the surface, Taylor has introduced the term x_0 in the arguments of D_i.

Schweig and Bridges [3] have reported a computer analysis using a variational approach where they have defined a mesh that covers the region of integration and express the field using a four-point Laplace operator, with the assumption that the index is constant inside each cell of the mesh. They have applied their method to a step index waveguide and have shown that their solution compares quite well to that of Marcatili [2].

To make the task of numerical computation easier and to allow index variation in the region of integration, we choose to represent the field using bivariate interpolation. As shown in Fig. 2, the waveguide *ABCD* is surrounded by a boundary *PQRS* where the modal field is assumed to vanish. For well-guided modes, the fact that the field decreases rapidly in the substrate and the cover (although more rapidly in the cover for the highly asymmetrical case) justifies this assumption. For modes closer to cutoff, obviously, the boundary *PQRS* needs to be extended much farther from the waveguide. To illustrate the method, consider a square grid drawn inside the box with 14 rows and 14 columns. The field is defined at the grid points as shown in Fig. 2. Thus, we have the field specified by vector $[E(1), E(2) \cdots E(196)]$. Inside the grid, the field is expressed as a bilinear interpolation of the four grid point

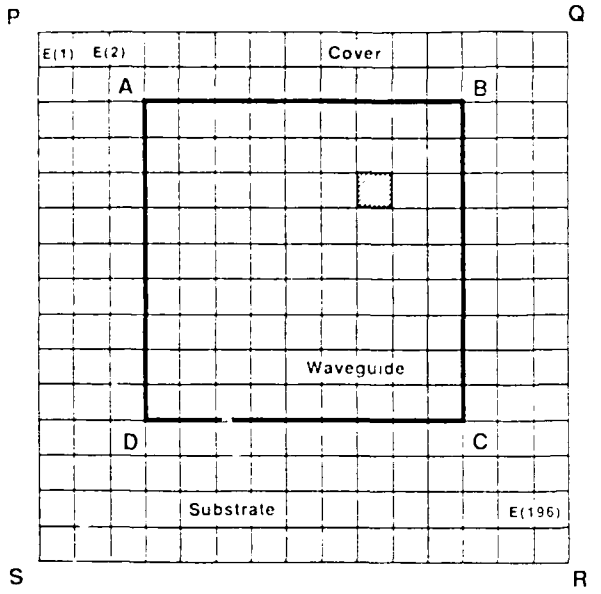

Fig. 2. Channel waveguide $ABCD$ surrounded by the boundary $PQRS$ where the field vanishes. The grid points corresponding to a 14×14 square grid represent the 196 E field values as shown.

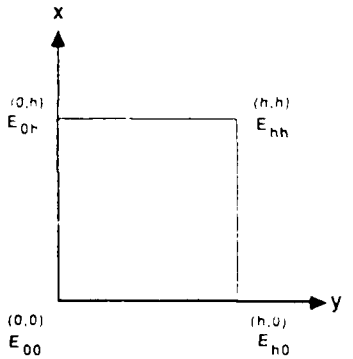

Fig. 3. Expanded square cell (shaded box in Fig. 2) used in the bivariate interpolation.

values [14]. A typical square cell (shown in Fig. 2 as a shaded box) is expanded in Fig. 3. The field distribution for points inside this cell is written as

$$E(x', y') = \frac{1}{h^2}\,[E_{hh}x'y' + E_{oo}(h - x')(h - y') + E_{ho}y'(h - x') + E_{oh}(h - y')x']. \quad (24)$$

Since this form of interpolation is linear on each link of the net, it provides $E(x', y')$ which is continuous on the whole region. We select $E(x', y')$ to vanish at the nodes on the boundary $PQRS$, so that it automatically satisfies the boundary condition.

C. Numerical Solution

With the definition of the square grid and the field at the grid points, it is possible to express the integral functions I and J as summations of their values on a single square cell.

Since we have assumed the field to vanish on the boundary $PQRS$ (and beyond) we get

$$J = \int_{-\infty}^{+\infty}\int E^2(x', y')\,dx'\,dy' = \iint_{\substack{\text{Rectangle}\\ PQRS}} E^2(x', y')\,dx'\,dy'. \quad (25)$$

The integration over the rectangle $PQRS$ can be expressed as a summation, giving the following relation:

$$\iint_{\substack{\text{Rectangle}\\ PQRS}} E^2(x', y')\,dx'\,dy' = \sum \iint_{S_h} E^2(x', y')\,dx'\,dy' \quad (26)$$

where S_h is a single square cell with side h (as shown in Fig. 3).

The above integral (26) can be evaluated in terms of the values of the E field at the corner points of a single cell and then summed over all cells. Thus, we can write

$$\begin{aligned}\iint_{S_h} E^2(x', y')\,dx'\,dy' = \iint_{S_h} \frac{1}{h^4}\,[&E_{hh}x'y' \\ &+ E_{ho}y'(h - x') \\ &+ E_{oo}(h - x')(h - y') \\ &+ E_{oh}x'(h - y')]^2\,dx'\,dy' \\ = \frac{h^2}{9}\,&(E_{oo}^2 + E_{ho}^2 + E_{oh}^2 + E_{hh}^2) \\ &+ \frac{h^2}{18}\,(E_{oo}E_{ho} + E_{oo}E_{oh} \\ &+ E_{ho}E_{hh} + E_{hh}E_{oh}) \\ &+ \frac{h^2}{36}\,(E_{oo}E_{hh} + E_{ho}E_{oh}).\end{aligned} \quad (27)$$

The expression for I is more involved because it has complex terms such as $V^2 f(x', y')\,E^2$, $(\partial E/\partial x')^2$ and $(\partial E/\partial x')^2$ [as indicated in (12)]. The partial derivative $(\partial E/\partial x')$ is expressed as [14]:

$$\frac{\partial E}{\partial x'} = \frac{1}{h^2}\,[E_{ho}y' - E_{oo}(h - y') + E_{hh}y' + E_{oh}(h - y')]. \quad (28)$$

A similar expression is written for $(\partial E/\partial y')$.

The term $V^2 f(x', y')\,E^2$ is written as

$$\frac{V^2}{h^2}\,[f_{oo}(h - x')(h - y') + f_{ho}x'y' + f_{oh}(h - y')x' + f_{hh}y'(h - x')]\,[E_{oo}(h - x')(h - y') + E_{ho}x'y' + E_{oh}(h - y')x' + E_{hh}y'(h - x')]^2$$

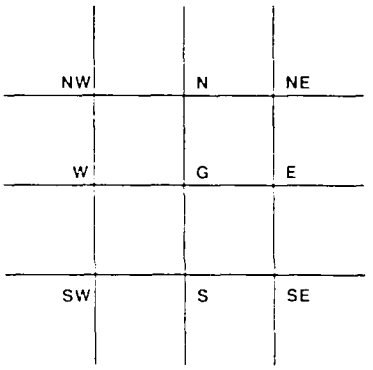

Fig. 4. Grid point and corresponding eight nearest neighbors and their notations used to simplify the summation over the four square cells in terms of the field values at the nearest neighbors that involve $E(G)$.

The above expression is integrated over a unit square cell to obtain the result in terms of the values of the field at the corners (i.e., E_{oo}, E_{oh}, E_{ho}, and E_{hh}) and the values of the index at the corner (i.e., f_{oo}, f_{oh}, f_{ho}, and f_{hh}). The expressions are too long and have been omitted for the sake of brevity.

Thus, the integrals of functions I (12) and J (13) over a single cell are summations involving the square terms E_{oo}^2, E_{oh}^2, E_{hh}^2, E_{ho}^2, and the cross-product terms $E_{oo}E_{oh}$, $E_{hh}E_{ho}$, etc.

To calculate the integrals over the entire region bounded by $PQRS$, these summations are added over all the cells in $PQRS$. The housekeeping involved in the summation process is very complex, and the following scheme is used to simplify the same. As shown in Fig. 4, corresponding to a grid point G, eight nearest neighbors are defined and denoted by their directions. In terms of the field values at the nearest neighbors, the summation over all four cells involving the field $E(G)$ at point G [from (27)] is expressed as

$$\sum_{\substack{\text{squares}\\ \text{containing}\\ \text{point } G}} \iint_{S_0} E^2\,dx'\,dy'$$

$$= \frac{h^2}{18} E(G)\Big[8E(G) + 2E(E) + 2E(N) + 2E(W) + 2E(S) + \frac{1}{2}E(NE) + \frac{1}{2}E(NW) + \frac{1}{2}E(SW) + \frac{1}{2}E(SE)\Big]. \tag{29}$$

Equation (29) indicates that the expressions for I and J only have square terms $E(G)^2$ and cross-product terms $E(G)\,E(N)$, $E(G)\,E(NW)$, etc. Therefore, I and J can be expressed in quadratic forms given by

$$I = U^T A U \tag{30}$$

and

$$J = U^T B U \tag{31}$$

where A and B are real symmetric matrices and U is a vector containing the values of the field at the grid points, i.e.,

$$U = [E(1), E(2), \cdots, E(196)]^T.$$

Now λ is expressed from (16) as

$$\lambda = I/J = (U^T A U)/(U^T B U). \tag{32}$$

For given matrices A and B, λ is a function of the vector U and its stationary value λ^* is given by the condition

$$\frac{\partial \lambda}{\partial U} = 0. \tag{33}$$

Differentiating (32) and substituting in (33), we get

$$AU = \lambda^* BU. \tag{34}$$

Premultiplying both sides of (34) by B^{-1}, we get a matrix-eigenvalue equation

$$(B^{-1}A)U = \lambda^* U. \tag{35}$$

For a given set of waveguide parameters, namely, the index profile $f(x', y')$ and the V number, the matrices A and B are found by evaluating the summations for the functions I and J as outlined before. Then λ^* is found by calculating the eigenvalues of the matrix $(B^{-1}A)$ and (22) is used to calculate b from λ^*.

$(B^{-1}A)$ is a (196 × 196) matrix, and therefore has 196 eigenvalues. We are interested in finding only those eigenvalues which correspond to the mode propagation constants. Since $0 \le b \le 1$, from (22) we see that the only values of λ^* that lie between 0 and V^2 correspond to the modes of the waveguide.

For numerical computation of the eigenvalues of a matrix, simple algorithms are available to find the largest eigenvalue, such as the power method. This method can be modified to find the eigenvalues between the range 0-V^2 as follows.

In general, for any matrix A, if $\mu_1, \mu_2, \mu_3, \cdots, \mu_N$ are its eigenvalues with eigenvectors $U_1, U_2, U_3, \cdots, U_N$, then the matrix $(A - mI)^{-1}$ has the same eigenvectors corresponding to the eigenvalues $(\mu_i - m)^{-1}$, and hence the power method, applied to $(A - mI)^{-1}$, converges to the eigenvalue $(\mu_k - m)^{-1}$.

From the physical considerations, a reasonable estimate of the value of b is available for a given waveguide. For example, the fundamental TE mode has its b closest to 1 compared to any other mode.

Thus, the eigenvalue λ^* can be estimated as

$$\lambda_{est}^* = V^2 b_{est} \tag{36}$$

and this estimated value of λ^* is used in the modified power method. The algorithm can handle arbitrary aspect ratios as follows.

Consider the integral I as given by (12). It can be re-

written as the sum of three integrals so that

$$I = \iint_D V^2 f(x', y')\, E^2\, dx', dy' - \frac{1}{r^2} \cdot \iint_D \left(\frac{\partial E}{\partial y'}\right)^2 dx'\, dy' - \iint_D \left(\frac{\partial E}{\partial x'}\right)^2 dx'\, dy'. \quad (37)$$

Now each of these integrals is expressed in a quadratic form, so that the matrix A in (30) can be expressed as the sum of three matrices:

$$A = A_1 - \frac{1}{r^2} A_2 - A_3 \quad (38)$$

where A_1, A_2, A_3 correspond to integrals on the right-hand side of the equation.

Note that $(1/r^2)$ appears as a scalar which multiplies A_2, and as a result, no reformulation of matrices A_1, A_2, A_3 is needed when the aspect ratio r is changed. This permits the method to consider arbitrary changes in aspect ratios without any additional reformulation. As a result, the aspect ratio can be read as an input datum by the algorithm.

The steps involved in the algorithm are given as follows.

1) Read the values of the V number, aspect ratio r, and an estimate of b.

2) Read the index profile $f(x', y')$ at grid points.

3) Set up matrices A and B.

4) Calculate $B^{-1}A$.

5) Apply the power method to find λ, the eigenvalue and U, the eigenvector of $B^{-1}A$.

6) Calculate b.

7) Print the values of $E(x', y')$ at the grid points (the field profile) and the value of b (the normalized propagation constant).

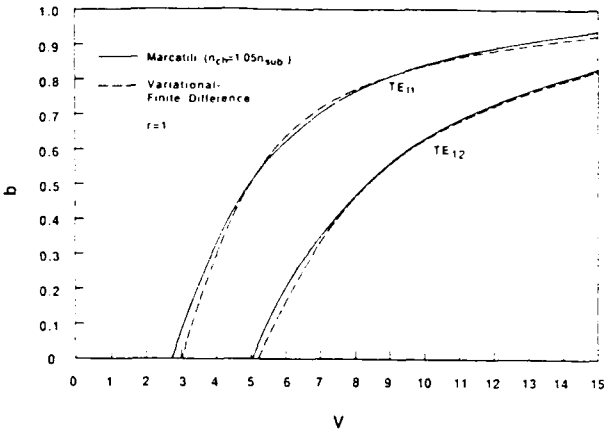

Fig. 5. b-V characteristics comparison between variational-difference method and Marcatili's method for an asymmetrical, step index channel waveguide with the aspect ratio $r = 1$.

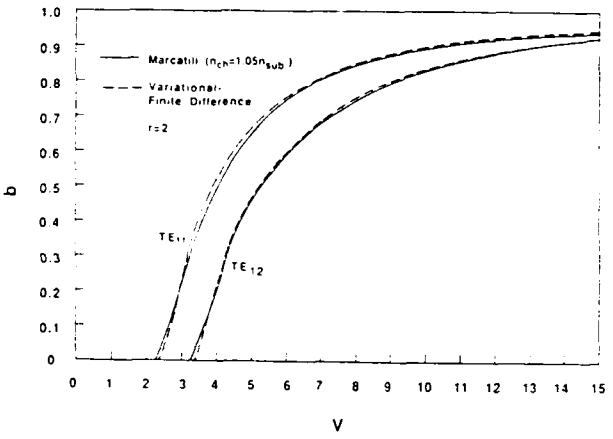

Fig. 6. b-V characteristics comparison between variational-difference method and Marcatili's method for an asymmetrical, step index channel waveguide with the aspect ratio $r = 2$.

III. Verification and Case Studies

The algorithm is coded in Fortran. The main program reads the index, sets up the A and B matrices, and calls separate subroutines for matrix inversion and eigenvalue estimation. We illustrate our results for the quasi-TE modes only. This is convenient because the first eigenvalue determined always corresponds to that of the TE mode since the b value for the quasi-TE mode is always larger than that of the quasi-TM mode for a given V value. Double precision arithmetic is used to keep the numerical errors in the matrix inversion as small as possible.

To verify the accuracy of our variational-finite difference method, a specific asymmetrical step index channel waveguide ($n_{\text{channel}} = 1.05 \times n_{\text{substrate}}$) is considered. For this wavelength, the b-V characteristics have already been presented by Marcatili [2]. Figs. 5 and 6 show the results for aspect ratios $r = 1$ and 2, respectively. It is seen that the results are in excellent agreement, establishing the validity of the variational-finite difference method. The results of the variational-finite difference method, however, are useful for any arbitrary aspect ratio and index profile.

The algorithm is executed on Harris 800 minicomputer. Due to the limited computer time and memory capacity, a 14 × 14 grid is chosen (as shown in Fig. 2). Execution on a mainframe computer will make it possible to choose a larger grid size and thus improve the results near cutoff. There are no inherent limitations to the accuracy of this method.

As an additional verification, the method is applied to channel waveguides with a very large aspect ratio ($r = 100$) to simulate planar waveguides of two index profiles, namely, the Gaussian-Gaussian and the erfc-Gaussian profiles. The b-V characteristics of these large aspect ratio channel waveguides should approach those of planar waveguides with the corresponding index profiles in the depth direction. The b-V characteristics for the planar waveguides are calculated by the numerical integration of the normalized mode dispersion equation [15]. Fig. 7 shows the comparison between the b-V characteristics of the TE_{11} mode for the channel waveguides and the fundamental mode ($m = 0$) for the planar waveguides. The excellent agreement as seen from Fig. 7 gives an addi-

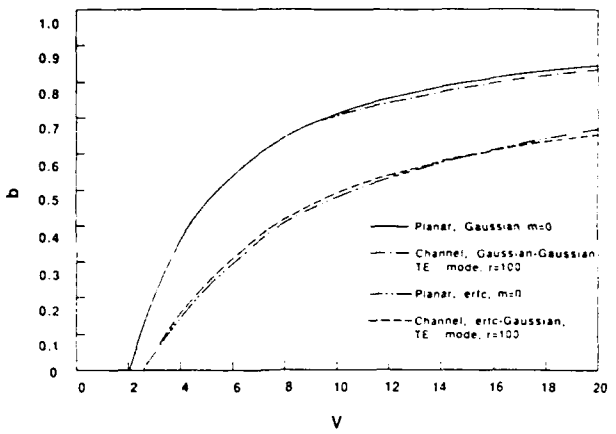

Fig. 7. Comparison between the b-V characteristics of the fundamental (quasi TE_{11}) mode of the channel waveguide and the fundamental mode (TE_0) of the planar waveguides for large aspect ratios. The curves are plotted for $r = 100$.

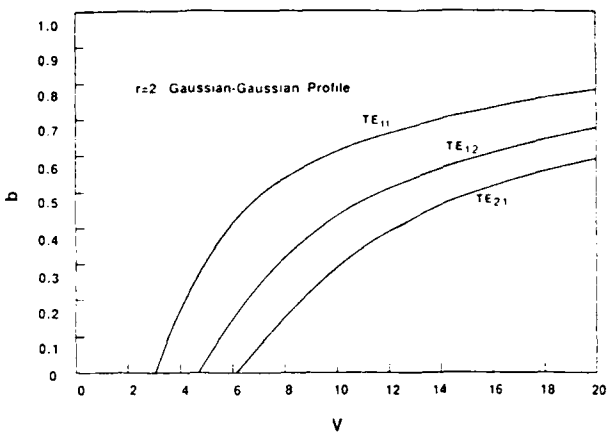

Fig. 9. b-V characteristics for the first three (TE_{11}, TE_{12}, and TE_{21}) modes for the Gaussian-Gaussian profile and $r = 2$.

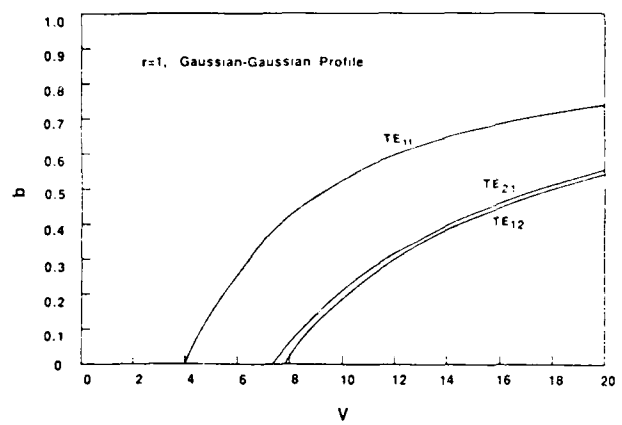

Fig. 8. b-V characteristics for the first three (TE_{11}, TE_{12}, and TE_{21}) modes for the Gaussian-Gaussian profile and $r = 1$.

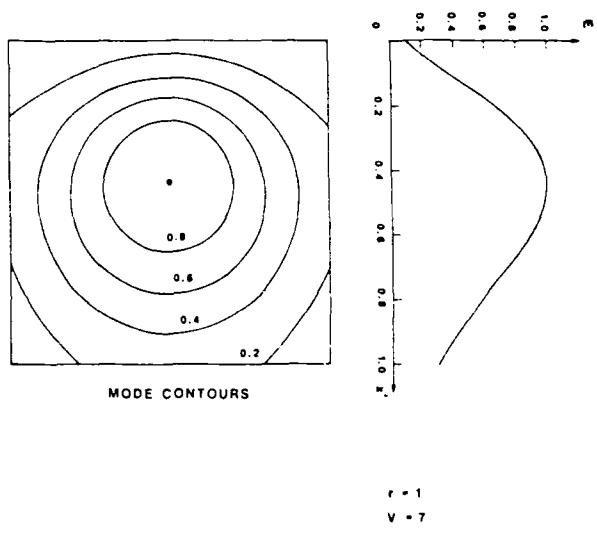

Fig. 10. Normalized modal field profile for the fundamental mode for the Gaussian-Gaussian profile, $r = 1$ and $V = 7$.

tional confirmation for the validity of the variational-finite difference method.

We present the normalized propagation characteristics of diffused channel waveguides of practical interest, viz. the Gaussian-Gaussian and the erfc-Gaussian profile. These profiles are realistic in the case of titanium diffusion [16] in $LiNbO_3$ and Ag^+-Na^+ (or any other set of species) ion-exchanged glass waveguides [17]. For the Gaussian-Gaussian function, the profile can be approximated by

$$f(x', y') = e^{-x'^2} e^{-y'^2}. \tag{39}$$

For ion exchange in glass, the profile can be approximated by the erfc Gaussian function given by

$$f(x', y') = e^{-y'^2} \operatorname{erfc}(x'). \tag{40}$$

The variational-finite difference method is applied to these profiles for calculating the b-V characteristics of the first three modes (i.e., TE_{11}, TE_{12}, and TE_{21} modes). Figs. 8 and 9 show the results for the Gaussian-Gaussian profile for the aspect ratios of 1 and 2, respectively. As seen in Fig. 8, the TE_{21} and TE_{12} modes for the Gaussian-Gaussian profile are almost degenerate when the aspect ratio is 1.

We now describe the calculation of the normalized field profiles in graded index channel waveguides. We have calculated the eigenvalues of matrix $(B^{-1}A)$ to find b. Since the elements of vector U are the field amplitudes at the grid points [i.e., $E(1)$, $E(2)$ $\cdots$ $E(196)$], the eigenvector of $(B^{-1}A)$ associated with the λ^* corresponding to a mode gives the values of the modal field distribution $E(x', y')$ at the grid points. In our calculations, we present contours for two different aspect ratios, viz. $r = 1$ and 2. These contour plots can find applications in the design of wave-

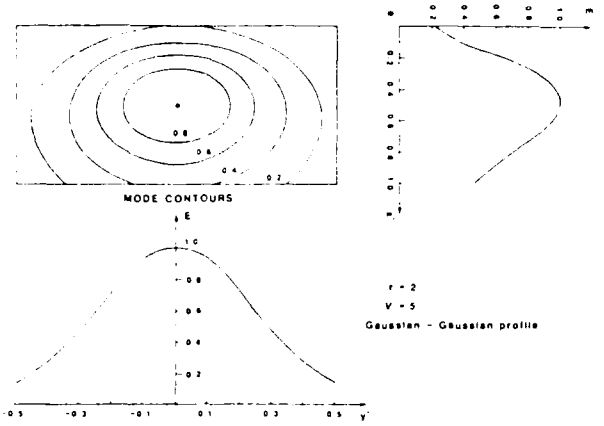

Fig. 11. Normalized modal field profile for the fundamental mode for the Gaussian-Gaussian profile, $r = 2$ and $V = 5$.

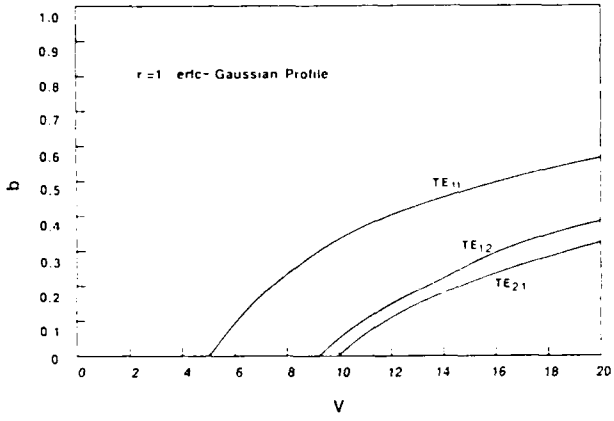

Fig. 12. b-V characteristics of the first three modes for the erfc-Gaussian profile and $r = 1$.

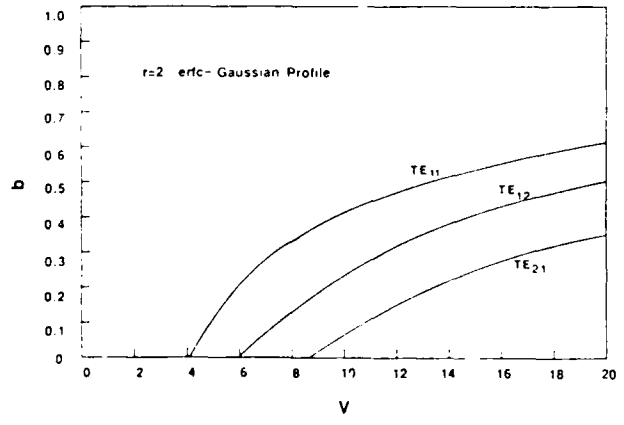

Fig. 13. b-V characteristics of the first three modes for the erfc-Gaussian profile and $r = 2$.

guide-waveguide and waveguide-fiber couplers since the coupling coefficient (in butt coupling) depends upon the overlap of modal fields of the individual channel or fiber waveguides.

Fig. 10 shows the normalized model field profile and contours of such a channel waveguide with $r = 1$ for the fundamental mode when the first-order hybrid mode TE_{12}

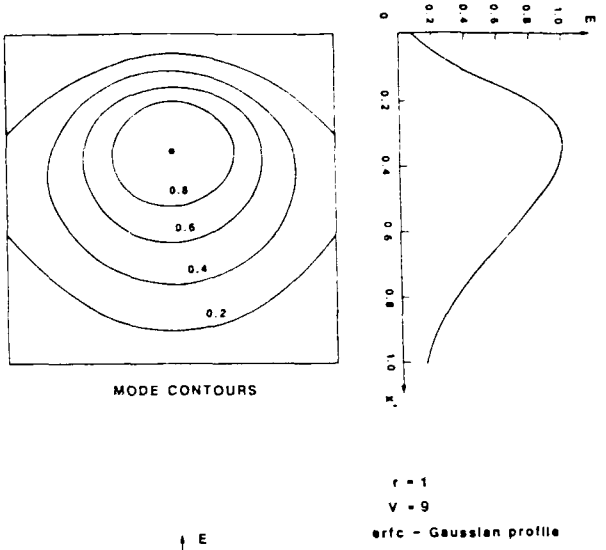

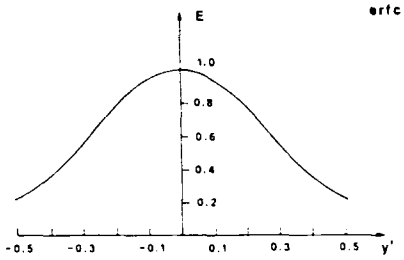

Fig. 14. Normalized modal field contours for the fundamental mode for the erfc-Gaussian profile, $r = 1$ and $V = 9$.

is just at cutoff corresponding to a V value of 7. Similarly, Fig. 11 shows the fundamental mode profile for $r = 2$ and $V = 5$ with TE_{12} barely propagating.

When the aspect ratio is increased to 2, as expected, the TE_{12} mode propagates with a higher propagation constant compared to that of the TE_{21} mode. Similar results for b-V characteristics of the erfc-Gaussian profile for $r = 1$ and 2 are plotted in Figs. 12 and 13, respectively. The cutoff V numbers for the modes of an erfc-Gaussian profile are higher than those of the corresponding modes of the Gaussian-Gaussian profile (with the same aspect ratio). This behavior is also observed in asymmetric planar graded index waveguides [11], [15].

As before, normalized modal field contours and the profiles as a function of x' and y' are also presented for the fundamental modes in Figs. 14 and 15 for the case $r = 1$, $V = 9$ and $r = 2$, $V = 6$, respectively, which corresponds again to the case when the next higher order mode TE_{12} just begins to propagate.

These b-V curves and modal field distributions are useful in the design of directional couplers, Mach-Zehnder interferometers, sensors, and switches as well as scores of other components which require diffused channel waveguides. Although these curves are not quite accurate near cutoff, they give an accurate estimate of the range of V over which the waveguides are single mode. The accuracy near cutoff can be increased by increasing the matrix size and computation time. The knowledge of propagation characteristics far away from cutoff, however, is

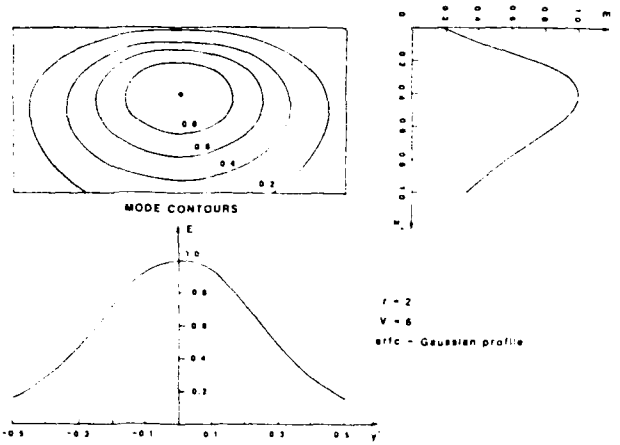

Fig. 15. Normalized modal field contours for the fundamental mode for the erfc-Gaussian profile, $r = 2$ and $V = 6$.

essential in the fabrication of certain devices (especially planar Mach–Zehender interferometer sensors) which require well-guided waveguides with only one propagating mode.

IV. Conclusion

In conclusion, we have reported a variational-finite difference method for analyzing graded index channel waveguides with arbitrary index profiles and aspect ratios. The index profiles of practical interest are analyzed using this method, and the resulting b-V characteristics and the normalized field profiles are presented as case studies.

Acknowledgment

The authors appreciate the critical reading of the manuscript by Prof. R. Srivastava and P. Suchoski, Jr.

References

[1] J. G. Goell, "A circular-harmonic computer analysis of rectangular dielectric waveguides," *Bell Syst. Tech. J.*, vol. 48, pp. 2132–2160, 1969.

[2] E. A. J. Marcatili, "Dielectric rectangular waveguides and directional couplers for integrated optics," *Bell Syst. Tech. J.*, vol. 48, pp. 2071–2101, 1969.

[3] E. Schweig and W. B. Bridges, "Computer analysis of dielectric waveguides: A finite-difference method," *IEEE Trans. Microwave Theory Tech.*, vol. MTT-32, pp. 531–541, 1984.

[4] G. B. Hocker and W. K. Burns, "Mode dispersion in diffused channel waveguides by effective index method," *Appl. Opt.*, vol. 16, pp. 113–118, 1977.

[5] V. Ramaswamy, "Strip loaded film waveguide," *Bell Syst. Tech. J.*, pp. 697–704, 1974.

[6] C. Yeh, S. B. Dong, and W. Oliver, "Arbitrarily shaped inhomogeneous optical fiber or integrated optical waveguides," *J. Appl. Phys.*, vol. 46, pp. 2125–2129, 1975.

[7] Ch. Pichot, "Exact numerical solution for the diffused channel waveguides, *Opt. Commun.*, vol. 47, pp. 169–173, 1982.

[8] M. Matsuhara, "Analysis of TEM modes in dielectric waveguides by a variational method," *J. Opt. Soc. Amer.*, vol. 63, pp. 1514–1517, 1973.

[9] H. F. Taylor, "Dispersion characteristics of diffused channel waveguides," *IEEE J. Quantum Electron.*, vol. QE-12, pp. 748–752, 1976.

[10] S. Korotky, W. Minford, L. Buhl, M. Divino, and R. Alferness, "Mode size and method for estimating the propagation constant of single-mode Ti:$LiNbO_3$ strip waveguides," *IEEE Trans. Microwave Theory Tech.*, vol. MTT-30, pp. 1784–1789, 1982.

[11] V. Ramaswamy and R. K. Lagu, "Numerical field solution for an arbitrary asymmetrical graded-index planar waveguide," *J. Lightwave Technol.*, vol. LT-1, pp. 408–417, 1983.

[12] H. Kogelnik and V. Ramaswamy, "Scaling rules for thin film waveguides," *Appl. Opt.*, vol. 13, pp. 1857–1867, 1974.

[13] J. Irving and N. Mullineux, *Mathematics in Physics and Engineering*. New York: Academic, 1959.

[14] G. E. Forsythe and W. R. Wasow, *Finite-Difference Methods for Partial Differential Equations*. New York: Wiley, 1960.

[15] G. B. Hocker and W. K. Burns, "Modes in diffused optical waveguides of arbitrary index profiles," *IEEE J. Quantum Electron.*, vol. QE-11, pp. 270–276, 1975.

[16] M. Fukuma and J. Noda, "Optical properties of Ti-diffused $LiNbO_3$ strip waveguides and their fiber coupling characteristics," *Appl. Opt.*, vol. 19, pp. 591–597, 1980.

[17] S. I. Najafi and R. V. Ramaswamy, "Diffusion and modal characterization of Ag^+-Na^+ exchanged channel waveguides," submitted to Integrated Guided Wave Opt. Conf., Atlanta, GA, Feb. 1986.

Rajendra K. Lagu was born in Poona, India, on June 7, 1956. He received the B.Tech. and M.Tech. degrees in electrical engineering from the Indian Institute of Technology, Bombay, India, in 1978 and 1981, respectively. He received the Ph.D. degree in electrical engineering from the University of Florida, Gainesville, in 1985.

He worked as a Developmental Engineer with Peico Electronics and Electricals Limited, India, from June 1978 to May 1979. He was a Research Fellow with the Department of Electrical Engineering, I.I.T., Bombay, from June 1979 to December 1981. He worked as a Graduate Research Assistant in the Department of Electrical Engineering, University of Florida, Gainesville, from January 1982 to December 1984. Currently, he is working as an Assistant Professor with the Department of Electrical and Computer Engineering, University of Iowa, Iowa City. His current research interests include fiber and integrated optics.

Dr. Lagu is a member of Eta Kappa Nu, Tau Beta Pi, and Phi Kappa Phi.

Ramu V. Ramaswamy (M'62–SM'80), for a photograph and biography, see this issue, p. 891

REFERENCE [21]

JOURNAL OF LIGHTWAVE TECHNOLOGY, VOL. LT-5, NO. 11, NOVEMBER 1987

WKB Analysis of Planar Surface Waveguides with Truncated Index Profiles

RAMAKANT SRIVASTAVA, C. K. KAO, AND RAMU V. RAMASWAMY, SENIOR MEMBER, IEEE

Abstract—We present a WKB analysis of planar surface waveguides with truncated arbitrary refractive index profiles. It is shown that the phase change at the turning point on the substrate side approaches zero near the cutoff. The validity of the conventional assumption of constant phase change of $\pi/2$ at the turning point is investigated, and the consequent errors near the mode cutoffs are analyzed for index profiles of practical interest.

THE WKB method has been extensively used for the calculation of propagation constants of guided modes in optical waveguides [1]-[7]. In the limit of slow index variations across the guiding cross section, with the transverse waveguide dimensions much larger than the wavelength, this method predicts the propagation characteristics of multimode optical fibers [1] with reasonable accuracy. In the case of a step-index planar waveguide, the method gives exact results independent of the waveguide dimensions (represented by the V parameter), and the derived propagation constant values ($b - V$ curves) are the same as those obtained by solving the wave equation with appropriate boundary conditions [2]. This is attributed to the fact that in the case of the step-index planar waveguide, exact expressions for the phase change for the total internal reflection at the cover and substrate interfaces are available which are valid regardless of the propagation constant of the guided mode [3]. Motivated by the success of the WKB theory in step-index planar waveguides, researchers have applied it to the graded-index waveguides [4]-[7]. In this approach, it is generally assumed that the phase change $2\phi_t$ at the turning point on the substrate side is $\pi/2$. Moreover, since most surface waveguides have air as the surrounding cover medium, the mode cutoff condition is determined by the substrate refractive index. In this limit, the phase change upon total internal reflection at the cover surface is very nearly π. With these assumptions, $b - V$ curves and modal fields have been calculated [7] for graded-index waveguides and shown to be in agreement with exact analytical solutions for parabolic and exponential index profiles in the case of large V. The error caused by assuming a constant phase shift of π at the cover surface has also been examined [7]. When a mode is buried and one of the turning points lies near the film–cover interface, the phase change upon reflection at this turning point becomes dependent on the propagation constant. In this case, WKB approximation has been shown [5] to give accurate results for well-guided modes provided the above dependence is included in the analysis.

In this paper we show that although the approximation of the $\pi/2$ phase shift at the turning point on the substrate side is acceptable for well-guided modes (large V), errors are caused in the calculated propagation constant at lower V-values, particularly near the cutoff. This problem is of paramount importance when the $b - V$ curves are used for calculation of the field profile of guided modes, especially in the case of single-mode waveguides. Furthermore, since the $b - V$ curves are often used to characterize the planar waveguides for the diffusion profile [8], [9] and the Δn value from mode index measurements [8]–[10], any error in these curves is likely to give erroneous results for the waveguide parameters. The quantitative evaluation of the error introduced by the assumption of $\phi_t = \pi/4$ for modes near cutoff was first alluded to in [5] for surface waveguides with parabolic profile. It was suggested that the correction to ϕ_t depends on the first derivative of the index at the film–substrate boundary and decreases as the mode effective index approaches the substrate index, i.e., as the mode approaches the cutoff. However, no analysis was presented to understand the behavior of ϕ_t near cutoff. Recognizing that in truncated profiles the phase shift $2\phi_t$ has to approach zero near the mode cutoff, we have obtained curves for ϕ_t as a function of the propagation constant by using the WKB theory and comparing it with $b - V$ curves as obtained by the numerical solution of the wave equation using the finite difference method [12]. The variation of ϕ_t is shown to be directly related to the change of the slope of the refractive index profile near the substrate interface, and the quantitative results are in agreement with those of [5]. To the best of our knowledge, this is the first report which considers quantitative variation of ϕ_t in the cutoff region using the WKB approximation.

Consider the truncated graded-index profile $n(x)$ of the waveguide as shown in Fig. 1. The curved ray trajectories make an angle $\theta(x)$ with the x-axis. The propagation constant β and the transverse propagation constant $\kappa(x)$ are

Manuscript received August 25, 1986; revised November 20, 1986. This work was supported by AFOSR Contract 84-0369

R. Srivastava is with the Department of Electrical Engineering University of Florida, Gainesville, FL 32611, on leave from Unicamp, Campinas, Brazil

C. K. Kao and R. V. Ramaswamy are with the Department of Electrical Engineering, University of Florida, Gainesville, FL 32611.

IEEE Log Number 8714966

0733-8724/87/1100-1605$01.00

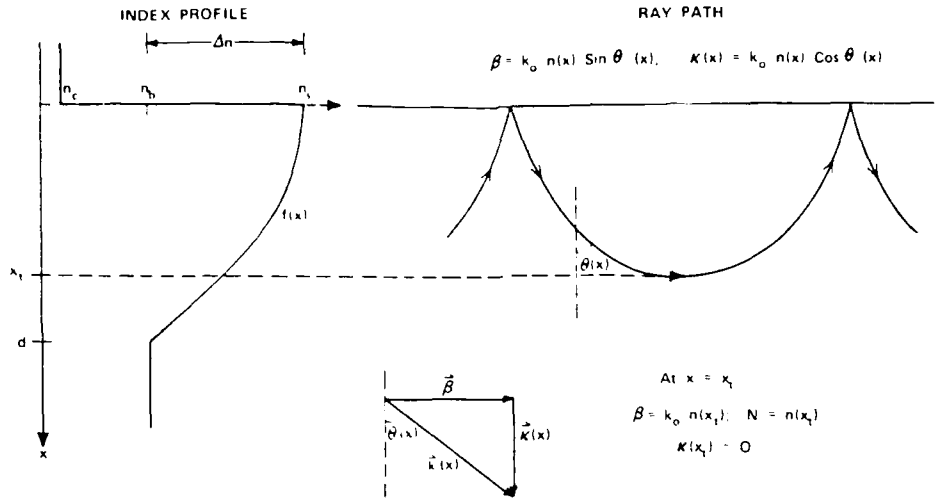

Fig. 1. Index profile and the ray trajectories showing the parameters used in the text.

given by:

$$\beta = k_0 n(x) \sin\theta(x) \tag{1}$$

$$\kappa(x) = k_0 n(x) \cos\theta(x) = \sqrt{k_0^2 n^2(x) - \beta^2}. \tag{2}$$

Using the WKB approach, the condition for the TE_m mode propagation is given by the characteristic equation [2]

$$\int_0^{x_t} \kappa(x)\, dx = m\pi + \phi_c + \phi_f \tag{3}$$

where ϕ_c is one-half the phase change at the cover surface. The expressions for ϕ_c and ϕ_f are given by [3], [6]

$$\phi_c = \tan^{-1}\left[\frac{\beta^2 - k_0^2 n_c^2}{k_0^2 n_s^2 - \beta^2}\right]^{1/2} \tag{4}$$

and

$$\phi_f = \lim_{\delta \to 0} \tan^{-2}\left[\frac{\beta^2 - k_0^2 n^2(x_t + \delta)}{k_0^2 n^2(x_t - \delta) - \beta^2}\right]^{1/2}$$

Upon binomial expansion of the RHS, the above equation becomes

$$\phi_f = \lim_{\delta \to 0} \tan^{-1} \sqrt{\left(\frac{dn}{dx}\bigg|_{(x_t+\delta)} \Big/ \frac{dn}{dx}\bigg|_{(x_t-\delta)}\right)}. \tag{5}$$

At the turning point

$$\theta(x_t) = \frac{\pi}{2}$$

and

$$\beta = k_0 n(x_t).$$

If the turning point x_t is "far" from the substrate interface, the wave does not "see" the discontinuity in the slope of the index profile at the interface. In this limit, it has been shown [6] that $\phi_f = \pi/4$ with the total phase change $2\phi_f = \pi/2$ at the turning point. This corresponds to the case of a well-guided mode ($\beta \to k_0 n_s$), or to any mode of an untruncated profile such as Gaussian or exponential. However, in truncated profiles, as the mode approaches its cutoff, $\beta \to k_0 n_b$ and $x_t \to$ film–substrate interface. At the cutoff, therefore, the slope discontinuity forces the numerator in (5) to be zero. Thus we obtain $\phi_f = 0$ for $b = 0$ and $\phi_f = \pi/4$ for $b \to 1$.

The fact that ϕ_f is zero at the cutoff is not surprising. In the case of an asymmetric step-index waveguide, the phase change at the substrate interface is given by

$$\phi_s = \tan^{-1}\left[\frac{\beta^2 - k_0^2 n_b^2}{k_0^2 n_s^2 - \beta^2}\right]^{1/2}$$

which approaches zero at the cutoff. Interpreted differently, it reflects the fact that as the ray approaches the critical angle of incidence at the interface, the phase change drops to zero. We return to this point later when we discuss the case of a buried waveguide with a symmetric profile. For the sake of completeness, we also write the expression for ϕ_c at the cutoff point for the asymmetric surface waveguide of the type shown in Fig. 1:

$$(\phi_c)_{\text{cutoff}} = \tan^{-1}\sqrt{a_E} \tag{6}$$

where a_E is the asymmetry parameter defined by [2]:

$$a_E = \left(\frac{n_b^2 - n_c^2}{n_s^2 - n_b^2}\right). \tag{7}$$

For an ion-exchanged glass waveguide, $n_c = 1$, $n_b = 1.5$ and $n_s \sim 1.52$ and (8) gives $\phi_c = \tan^{-1}\sqrt{20.7} = 0.43\,\pi$. In $LiNbO_3$ and GaAs based waveguides, ϕ_c is larger due to the higher asymmetry and is therefore close to $\pi/2$.

In dealing with waveguides, it is convenient to write the dispersion relations in terms of the normalized frequency V and the normalized propagation constant b given by [2]

$$V = k_0 d\sqrt{n_s^2 - n_b^2} \tag{8}$$

and

$$b = \frac{\left(\frac{\beta^2}{k_0^2} - n_b^2\right)}{(n_s^2 - n_b^2)}. \tag{9}$$

Here d is some measure of the diffusion depth depending on the profile.

Now let us write the characteristic equation (3) in terms of the normalized parameters [7]. We write

$$x' = \frac{x}{d} \tag{10}$$

and

$$f(x') = (n(x') - n_b)/\Delta n. \tag{11}$$

Thus (3) for the case $\Delta n \ll n_b$ becomes

$$\int_0^{x_t} V\sqrt{f(x') - b}\, dx' = m\pi + \phi_c + \phi_f. \tag{12}$$

Let us consider the following index profiles:

$$\begin{aligned} f(x') &= 1 && \text{(step-index)} \\ &= e^{-x'} && \text{(exponential)} \\ &= e^{-x'^2} && \text{(Gaussian)} \\ &= 1 - x'^2 && \text{(parabolic)} \\ &= 1 - x' && \text{(linear)}. \end{aligned} \tag{13}$$

From (12), assuming $\phi_c = \pi/2$ and $\phi_f = \pi/4$ [4]-[7], we get the cutoff condition

$$V_c \int_0^{x_t} \sqrt{f(x')}\, dx' = m\pi + \tfrac{3}{4}\pi. \tag{14a}$$

On the other hand, using the expression for ϕ_c as given by (4) and using $\phi_f = 0$ at the cutoff, we get

$$V_c \int_0^{x_t} \sqrt{f(x')}\, dx' = m\pi + \tan^{-1}\left(\frac{n_b^2 - n_c^2}{n_s^2 - n_b^2}\right)^{1/2} \tag{14b}$$

showing that the error in the cutoff normalized frequency V_c of any mode is given by $(\frac{3}{4}\pi - 0.43\pi)/(\int_0^{x_t} \sqrt{f(x')}\, dx')$ for the ion exchange case described previously. The value of the integral in the denominator is 2, $\sqrt{\pi/2}$, $\pi/4$, and $2/3$ for untruncated exponential, untruncated Gaussian, parabolic, and linear profiles, respectively. Thus the error in V_c amounts to 0.44, 0.70, 1.12, and 1.32 for the four profiles, respectively. The waveguides of practical interest have a Gaussian or an ERFC profile or a combination of the two. Therefore, theoretically $\phi_f = \pi/4$, independent of b, due to the infinite width of these functions ($x_t' = \infty$). However, in practice the diffused waveguides have truncated profiles and the function $f(x')$ does go to zero at a finite distance. Nevertheless, the errors cited above will not change significantly due to the truncation of these profiles as the contribution to the integral on the LHS of (14) is negligible beyond $x' = 5$.

The conclusion that the phase shift at the turning point near the cutoff goes to zero can also be reached by analyzing the case of a buried waveguide with a symmetric profile with x_t' and x_t' as turning points. The characteristic equation in this case becomes

$$\int_{x_t}^{x_t} V\sqrt{f(x') - b}\, dx' = m\pi + 2\phi_f. \tag{15}$$

In the limit $b \to 0$, it is required that for the fundamental mode, the cutoff V value be zero. This is achieved only if $\phi_f \to 0$.

So far we have discussed only the two extreme cases, $b = 0$ and $b \to 1$. The picture in the intermediate range (of practical interest) is not so clear and exact analytical expressions for ϕ_f are difficult to obtain. In order to overcome this problem, we have numerically calculated the $b - V$ curves for the step-index and all the four graded-index profiles, using the finite difference method [11]. The high accuracy of the finite difference method was checked by comparing the calculated $b - V$ curves and the mode field profiles with those obtained by the exact analytical solution of the characteristic equation derived from the field continuity conditions in the case of step-index and exponential profiles. We have observed that the discontinuity in the index profile does not appear to affect the numerical field solutions to any detectable extent. A detailed study of the finite difference method will be reported elsewhere [12]. In order to calculate the b-dependence of ϕ_f, ϕ_f was used as a parameter and for a given b its value was chosen to be that which gave agreement with the $b - V$ curves obtained by the finite difference method. Fig. 2 shows the results for the two lowest order modes in the case of linear and parabolic profiles. It is observed that for b values down to 0.5, ϕ_f remains constant and equals $\pi/4$. It then starts decreasing, reaching a very large slope near $b \sim 0.1$, and approaching zero as $b \to 0$. It is this steepness of the curve for lower b-values which is responsible for the flatness of the $b - V$ curves near the cutoff. In this region, therefore, the conventional WKB gives large errors. No calculations were made for $b < 0.01$ as a very large number of grid points is necessary to give accurate results in the finite difference method. In practice, the mode becomes highly attenuated for $b < 0.1$ and the cutoff is measured at higher V-values than those predicted theoretically. This behavior also suggests that the $b - V$ curves should be used with caution to estimate the theoretical cutoff values.

A few words regarding the shape of the curves in Fig. 2 are in order at this point. In particular, (5) predicts an abrupt drop in ϕ_f from $\pi/4$ to zero at $b = 0$, whereas Fig. 2 shows a gradual decrease in ϕ_f. The explanation of this behavior lies in the proximity of the turning points to the film-substrate interface given by $x' = 1$ for these profiles. The positions of these turning points for linear and parabolic profiles are given by $x_t' = (1 - b)$ and $x_t' = \sqrt{1 - b}$, respectively. The corresponding normalized distances from the film-substrate interface are b and $1 -$

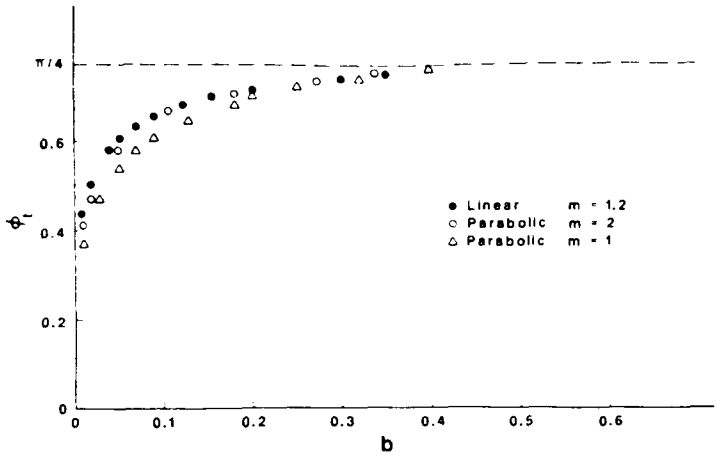

Fig. 2. Phase shift dependence on the propagation constant.

$\sqrt{1-b}$, respectively. Thus for $b \sim 0.1$, these distances are of the order of wavelength of the radiation, and the profile slope discontinuity at $x' = 1$ therefore is likely to influence the phase shift. As b decreases further, the effect of the slope discontinuity is larger, causing a steep decline in the $\phi_t(b)$ curve shown in Fig. 2. This also explains the fact that for a given b value, ϕ_t for the linear profile is larger than that for the parabolic profile, and the exact form of the ϕ_t versus b curve depends on the index profile. The larger discrepancy at lower b-values between the conventional WKB ($\phi_t = \pi/4$) and the analysis presented here is in contrast with the results of [5] where the error was found to decrease for higher order modes in the case of the exponential profile. This is related to the fact that in [5] ϕ_t was assumed to be constant ($= \pi/4$), which is a perfectly valid assumption for untruncated profiles. For the case of an unburied parabolic profile, however, the WKB results for the TE_3 mode in [5] show an error similar to that discussed here.

Although the results for truncated Gaussian and ERFC profiles are not presented here, similar behavior ws observed in these cases. For untruncated profiles, on the other hand, $f(x')$ never goes to zero at a finite value of x' and therefore x_t for any mode theoretically occurs well within the guiding region. Therefore ϕ_t remains constant at a value of $\pi/4$. This was shown quantitatively for the exponential profile even for the cutoff of the fundamental mode [13]. This is consistent with the requirement that ϕ_t go to zero at cutoff only when the turning point is at the discontinuity of the slope of the refractive index, where dn/dx becomes zero beyond the turning point as required by (5).

In conclusion, we have analyzed the error in the conventional WKB theory caused by the assumption of a constant phase shift of $\pi/2$ at the turning point on the substrate side of a planar graded-index surface waveguide. It is shown that in untruncated profiles the phase shift at the turning point on the substrate side depends on the propagation constant and approaches zero at the cutoff. The exact variation of the phase change depends on the index profile.

REFERENCES

[1] D. Gloge and E. A. J. Marcatili, "Multimode theory of graded-core-fibers," *Bell Syst. Tech. J.*, vol. 52, p. 1563, 1973.
[2] H. Kogelnik and V. Ramaswamy, "Scaling rules for thin film optical waveguides," *Appl. Opt.*, vol. 13, p. 1857, 1974.
[3] P. K. Tien, "Light waves in thin films and integrated optics," *Appl. Opt.*, vol. 10, p. 2395, 1971.
[4] A. Gedeon, "Comparison between rigorous theory and WKB analysis of modes in graded-index waveguides," *Opt. Commun.*, vol. 12, p. 329, 1974.
[5] J. Janta and J. Ctyroky, "On the accuracy of WKB analysis of TE and TM modes in planar-graded-index waveguides," *Opt. Commun.*, vol. 25, p. 49, 1978.
[6] G. B. Hocker and W. K. Burns, "Modes in diffused optical waveguides of arbitrary index profiles," *IEEE J. Quantum Electron.*, vol. QE-11, p. 270, 1975.
[7] R. V. Ramaswamy and R. K. Lagu, "Numerical field solution for an arbitrary asymmetrical graded-index planar waveguide," *J. Lightwave Tech.*, vol. LT-1, p. 408, 1985.
[8] R. K. Lagu and R. V. Ramaswamy, "Process and waveguide parameter relationships for the design of planar silver ion-diffused glass waveguides," *J. Lightwave Technol.*, vol. LT-4, p. 176, 1986.
[9] S. I. Najafi and R. V. Ramaswamy, "Ag^+-diffused graded-index glass waveguides. Diffusion and modal characterization," presented at Gradient-Index Optical Imaging Systems Conf., Palermo, Italy, Sept. 1985.
[10] G. C. Yip and J. Albert, "Characterization of planar optical waveguides by K^+-ion exchange in glass," *Opt. Lett.*, vol. 10, p. 151, 1985.
[11] E. Schweig and W. B. Bridges, "Computer analysis of dielectric waveguides: A finite-difference method," *IEEE Trans. Microwave Theory Tech.*, vol. MTT-32, p. 531, 1984.
[12] R. V. Ramaswamy, E. Rodrigues, and R. Srivastava, "Normalized finite-difference solutions to symmetrical and asymmetrical arbitrary graded-index slab waveguides," unpublished.
[13] E. M. Conwell, "WKB approximation for optical guide modes in a medium with exponentially varying index," *J. Appl. Phys.*, vol. 46, p. 1407, 1975.

*

Ramakant Srivastava was born in Hardoi, Uttar Pradesh, India, on January 12, 1943. He received the B.Sc. degree from Agra University in 1961 and the M.S. and Ph.D. degrees in physics from Indiana University, Bloomington, IN, in 1969 and 1973, respectively. His doctorial thesis was related to Raman study of phase transitions in transition-metal oxides.

In 1974 he joined the State University of Campinas (UNICAMP), Brazil, as an Assistant Professor where he has taught and conducted research

in Raman and infrared spectroscopy of solids, optical fibers, and nonlinear optics. From 1978 to 1984 he was Manager of the Optical Fiber Project at UNICAMP. In 1985 he became Associate Professor. He visited the National Bureau of Standards, Boulder, CO, from June 1984 to March 1985 and presently he is a visiting Associate Professor at the University of Florida. His research interests include optical fibers, integrated optics, lasers, and nonlinear guided wave optics.

Dr. Srivastava is a member of the Optical Society of America and SPIE.

*

C. K. Kao, photograph and biography not available at time of publication

*

Ramu V. Ramaswamy (M'62–SM'80) was born in Madras, India, in June 1938. He received the B.S. degree in physics from Madras University, Madras, India in 1957, and the diploma D.M.I.T. in electronics engineering from Madras Institute of Technology, Chromepet, Madras, India, in 1960. He received the M.S. and Ph.D. degrees in electrical engineering from Northwestern University, Evanston, IL, in 1962 and 1969, respectively. His doctoral work consisted of wave-propagation studies in semiconductor plasmas.

From 1962 to 1965, he served as a Member of the Research Department of Zenith Radio Corporation, Chicago, IL, working on solid state parametric amplifiers and microwave components. In 1969, he joined Bell Laboratories, Crawford Hill Laboratory, Holdmel, NJ, where he was engaged in research in thin-film optical devices, polarization effects in single-mode fibers, and fiber-waveguide couplers. Since 1981, he has been a Professor in the Department of Electrical Engineering, University of Florida, Gainesville, where his current interests include passive integrated-optical devices, fiber-optic sensors, and optoelectronic devices.

Dr. Ramaswamy is currently the Director of a University-wide interdisciplinary program known as MICROFABRITCH which will emphasize both the fundamental and engineering aspects in the research and development of novel layered materials and structures for optical and high-speed electronic microcircuits. He is a member of Sigma Xi.

REFERENCE [22]

Wavelength-dependent propagation characteristics of Ag^+–Na^+ exchanged planar glass waveguides

S. I. Najafi, R. Srivastava, and R. V. Ramaswamy

Planar glass waveguides fabricated by diffusion of silver ions in soda-lime-silicate glass substrates have been characterized by measuring the wavelength dependence of propagation constants of the guided modes. The results are in good agreement with theoretical prediction obtained by an accurate WKB analysis using a complementary error function for the index profile. Cutoff wavelengths of higher-order modes are larger than were predicted by the analysis and are a result of higher attenuation encountered close to the cutoff.

I. Introduction

Glass waveguides fabricated by ion exchange in soda-lime glass have assumed an important role in many applications such as optical communicaton, sensors, and more recently as potential candidates for use in optical signal processing. Different ions, e.g., Tl^+, Ag^+, K^+, have been diffused in glass to obtain an adequate graded-index profile to achieve guidance.[1] Each of these ions has its advantages and drawbacks. For example, Tl^+ is known to be relatively toxic, Ag^+ is susceptible to reduction and K^+ provides very low index changes. Of these, we have extensively studied incorporation of Ag^+ by ion exchange using a highly controlled electrolytic process[2] for release of Ag^+ in a molten bath of $NaNO_3$. Unlike the conventional methods where glass substrates are immersed in molten $AgNO_3$, giving rise to large values of index change at the surface ($\Delta n \sim 0.08$), this technique allows very low concentrations of Ag^+ in the bath. Since Δn depends on Ag^+ concentration, the lower value of Δn obtained is helpful in controlling the V-number of the guide because the diffusion depth can then be increased considerably which can be controlled precisely by diffusion time and bath temperature. Single-mode guides with reproducible characteristics have produced in the laboratory using this process. We found Ag^+ attractive for fabrication of planar waveguides due to two important features: it is possible to detect Ag^+ using the backscattered SEM (scanning electron microscopy) analysis which is helpful in index profile studies, and silver rods of high purity are commercially available for the release technique. In fact, planar and buried slab and channel waveguides have also been fabricated and analyzed.[3,4]

In previous work[5,6] we reported detailed studies of Ag^+–Na^+ exchange waveguides. It is shown that the diffusion profile as measured by the SEM technique closely resembles a complementary error function. This conclusion was confirmed by the fit of the index data (index profile assumed to be that of the Ag^+ diffusion) to the measured values of the mode index for all the guided modes. This was performed using two fitting parameters—the diffusion coefficient D and Δn. Empirical linear relations were thus obtained between the low Ag^+ concentration and the corresponding index change Δn.[5]

In this paper we report the results of the measurement of the mode index as a function of wavelength. The data are then fitted to the b–V curves as predicted by a more accurate WKB analysis in which the b-dependent phase change at the turning points and the cover surface are included.[7] The only fitting parameter used is Δn. It is observed that for all the guided modes, the data give a much better fit to the calculated b–V curves for the erfc index profile compared with the Gaussian or exponential profile. This result, confirmed by our previous work,[3-6] supports the postulation that the index profile is a complementary error function when diffusion takes place from an infinite source and is in sharp contrast to the reports where the mode index data were found to be consistent with Gaussian or a polynomial[8] profile. It is also observed that cutoff wavelengths of the higher-order modes are larger than those predicted by theory, a fact consistent with the higher attenuation suffered by the higher-order modes near the cutoff.

The authors are with University of Florida, Department of Electrical Engineering, Gainesville, Florida 32611.

Received 6 February 1986.
0003-6935/86/111840-04$02.00/0.

II. Diffusion and Propagation Characteristics

The diffusion equation in the case studied here may be written as[6]

$$\frac{\partial C}{\partial t} = D\frac{\partial^2 C}{\partial x^2}. \tag{1}$$

where C is the concentration of the silver ion, D is its self-diffusion coefficient, and t is the time of diffusion.

The solution of Eq. (1), subject to boundary conditions $C(x,0) = 0$ and $C(0,t) = C_0$, is given by

$$C(x,t) = C_0 \operatorname{erfc}\left(\frac{x}{W_0}\right), \tag{2}$$

where

$$W_0 = 2\sqrt{Dt}, \tag{3}$$

$$\operatorname{erfc}(z) = \frac{2}{\sqrt{\pi}}\int_z^\infty \exp(-\alpha^2)d\alpha. \tag{4}$$

W_0 is called the effective depth of diffusion and corresponds to[6]

$$C(W_0,t) = 0.157C_0. \tag{5}$$

Note that the condition $C(0,t) = C_0$ assumes an inexhaustible source of diffusing ions. W_0 depends on the self-diffusion coefficient D which in turn depends on the structure and composition of the glass, the concentration C_0 and the diffusion temperature. For small values of C_0, Eq. (2) represents the refractive-index profile

$$n(x) = \Delta n \operatorname{erfc}\left(\frac{x}{W_0}\right) + n_b, \tag{6}$$

where Δn is the refractive-index change at the surface and n_b is the substrate index. Since direct-index profile measurement using optical methods in planar waveguides is not an easy task, the backscattered SEM analysis of Ag^+ concentration in glass has been performed[6] to obtain this information, at least for low concentrations. For low values [$\sim 10^{-4}$ MF (mole fraction)] of C_0, D was observed to increase linearly with C_0. For given values of temperature T and C_0, the value of D may not vary much from one glass to another. This is shown in Fig. 1 which is a SEM photograph of two waveguides made in identical conditions (same T, C_0, and t) with Schott 8011 glass (left) and a Fisher microscope slide (right). Although the difusion depth ratio

$$\frac{W_{0\,\text{Schott}}}{W_{0\,\text{Fisher}}} \simeq 1.1 \tag{7}$$

gives $D_{\text{Schott}}/D_{\text{Fisher}} \simeq 1.1$ in these conditions, the refractive-index change for the two glasses is very different,

$$\frac{\Delta n_{\text{Schott}}}{\Delta n_{\text{Fisher}}} \simeq 4.2. \tag{8}$$

This is believed to be due to the compositional variation, especially different Na^+ concentrations in the glass. Once the index profile is determined, the propagation characteristics and the modal field profiles $E_y(x)$ for the TE modes can be calculated by solving the wave equation

$$\frac{d^2E_y}{dx^2} + [k_0^2 n^2(x) - \beta^2]E_y = 0 \tag{9}$$

for each mode. In this work we are interested in the wavelength dependence of the propagation constant β for each mode. This can be calculated by the WKB theory which involves solving Eq. (9):

$$V\int_0^{x_r} [f(x') - b]^{1/2}dx' = \left(m + \frac{3}{4}\right)\pi, \tag{10}$$

where the normalized frequency

$$V = k_0 d\sqrt{2n_b\Delta n} \tag{11}$$

and the normalized propagation constant

$$b = (N^2 - n_b^2)/(2n_b\Delta n) \simeq \frac{N - n_b}{\Delta n}. \tag{12}$$

Here $N = \beta/K_0$, $x' = x/d$, and x_r' is the turning point on the substrate side for the rays representing mode m. $f(x')$ is the normalized index profile given by

$$f(x') = \frac{n(x') - n_b}{\Delta n}. \tag{13}$$

For a complementary error function profile, $f(x') = \operatorname{erfc}(x')$ and $d = W_0$. For Gaussian exponential profiles $f(x')$ is $\exp(-x'^2)$ and $\exp(-x')$, respectively, and $f(d) = 1/e$.

Equation (10) assumes that the phase shift is $-\pi$ at the cover interface and $-\pi/2$ at the turning point. When the cover material is air and the mode is well guided ($b \to 1$), these approximations do not introduce large errors in the b–V curves.[9] However, it is expected that the phase shifts on the cover as well as on the substrate side be b dependent. If these considerations are incorporated in the WKB equation, the exact b–V curves can be obtained. We have verified their accuracy for homogeneous slab waveguides as well as for

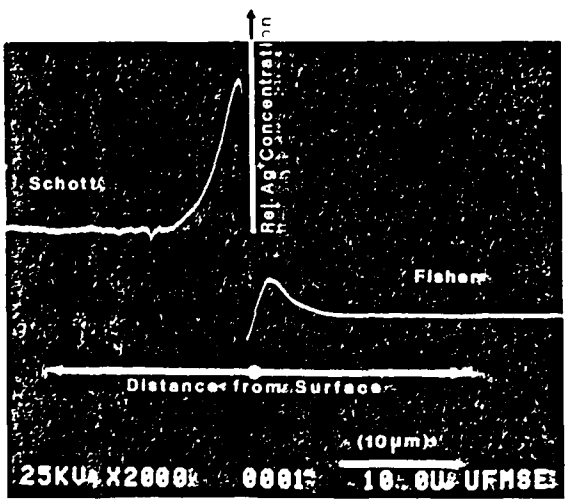

Fig. 1. SEM photograph of two waveguides epoxied face to face. The dip between the two waveguides is due to the epoxy.

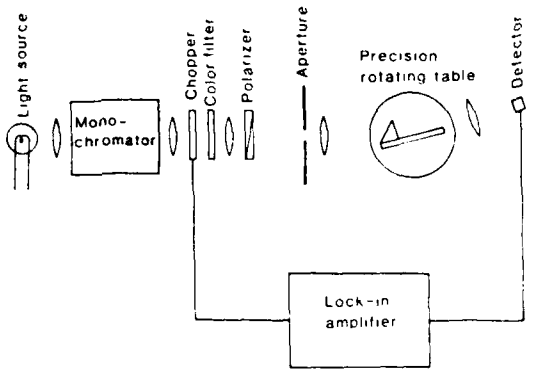

Fig. 2. Schematics for measurement of wavelength dependence of the mode index.

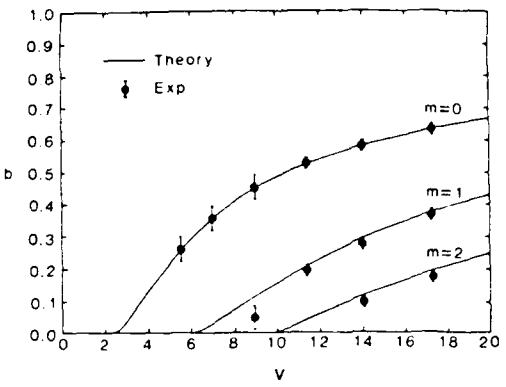

Fig. 3. b–V characteristics for the complementary error function profile. The points are the experimental values giving the closest agreement to theory.

the three profiles considered here, namely, erfc, Gaussian, and exponential, by solving Eq. (9) using the finite difference method.[7] Therefore, to analyze our data, we have used these more accurate b–V curves. These are shown in Figs. 3–5 and will be discussed later.

III. Experimental

The fabrication procedure is the same as described earlier.[2] The results reported here are for the waveguide made in the following conditions:

Ag^+ concentration, $C_0 = 4 \times 10^{-4}$MF;

Fabrication temperature, $T = 330$°C; and

Diffusion time, $t = 45$ min.

For optical characterization, the waveguide was polished at one end and the collimated radiation from a monochromator was prism coupled as shown in the schematics in Fig. 2. It was possible to collimate the beam by using a 2-mm diam aperture and by focusing the beam on the prism using a 40-cm focal length lens. The incident beam and the prism coupled output visible radiation could be seen on a white card when the room lights were off. The angle of incidence i which the incident beam makes with the prism normal is related to mode index N by the well-known relation

$$N = n_p \sin\left[A + \sin^{-1}\left(\frac{\sin i}{n_p}\right)\right], \tag{14}$$

where n_p is the prism refractive index and A is the prism angle.

The angle i for each guided mode was measured by rotating the prism table until maximum power was detected in that mode at the waveguide exit and indicating maximum coupling. The output power was collimated by an objective lens, detected by a photodetector, and monitored by a lock-in amplifier. Measurements were repeated five times for each mode and at each wavelength and the average value of i was chosen for calculation of N using Eq. (14). The mode indices were measured at discrete wavelengths in the 500–1000-nm region. The wavelength dependence of n_p was calculated by using the Sellmeier coefficients provided by the manufacturer (Schott SF-18 glass).

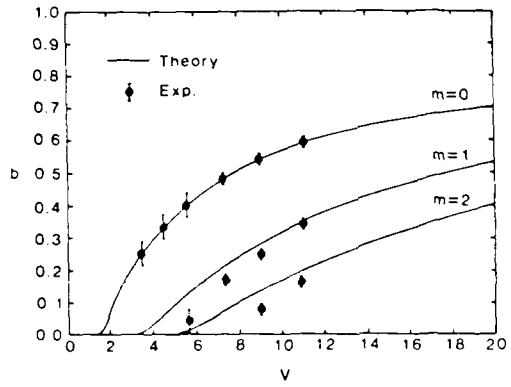

Fig. 4. b–V curves for the exponential profile and the experimental data.

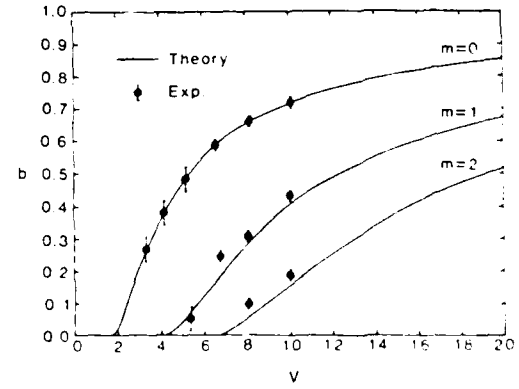

Fig. 5. b–V curves for the Gaussian profile. Points show the experimental data.

AD-A193 177 ION-EXCHANGED WAVEGUIDES FOR SIGNAL PROCESSING APPLICATIONS - A NOVEL ELE..(U) FLORIDA UNIV GAINESVILLE DEPT OF ELECTRICAL ENGINEERING 4/4

UNCLASSIFIED R V RAMASWAMY 07 MAR 87 AFOSR-TR-88-0279 F/G 20/6.1 NL

END
DATE FILMED
7 88

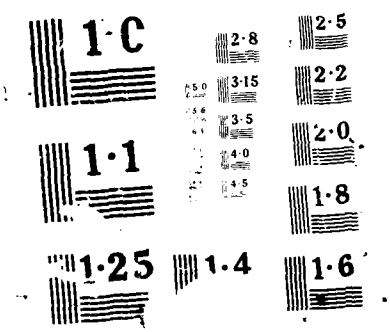
1·C
2·8
2·5
3·15
2·2
3·5
2·0
4·0
1·8
4·5
1·1
1·25
1·4
1·6

As will be seen in the following section, a complete analysis of our data requires knowledge of the wavelength dependence of the refractive index n_b of the glass substrate. The measurements of n_b were carried out at the wavelengths of interest by using the monochromator and an Abbe refractometer whose prism refractive index was calculated by using the Sellmeier coefficients furnished by the manufacturer of the instrument (Bellingham & Stanley, Ltd., England). The accuracy of these measurements was $\pm 1 \times 10^{-4}$ in the visible and $\pm 5 \times 10^{-4}$ in the infrared, because of the faint illumination at each wavelength. The monochromator slits were set to give a spectral linewidth of the order of 3 nm in each case.

IV. Results

Once the index N is determined using Eq. (14), the b parameter can be obtained from Eq. (12) provided Δn is known. On the other hand, the corresponding V value for the respective mode also requires knowledge of d, which was obtained from the SEM data for the Schott glass in Fig. 1 and equals 5.7 μm. Δn was thus the only parameter which was varied to fit the mode index data to the calculated b–V curves for each index profile.[5] For each wavelength, the measured mode index of the zero-order mode was fitted to the calculated b–V curve and the calculated value of Δn was used to determine the values of b and V for the next two higher-order modes. The points in Figs. 3–5 correspond to the b values for this value of Δn. This procedure was repeated at other wavelengths. It can be seen that the complementary error function profile matches best with the measured data for all the guided modes. The agreement between the theoretical curves and the experimental values is poorer in the case of exponential and Gaussian profiles. The same conclusion was derived by fitting the SEM data and is consistent with the diffusion equation solution for the case where the supply of Ag^+ is inexhaustible, as is the case here. This result which agrees very well with our previous work,[3–6] however, is in sharp contrast with the K^+ diffusion where the data have been shown to fit well to the Gaussian profile.[8] A few comments about the experimental points near the cutoff are in order. In this region, the data points in Fig. 3 lie below the theoretical curve for the TE_1 and TE_2 modes whereas in Figs. 4 and 5 there is no such trend. The behavior of the experimental points near the cutoff in Fig. 3 can be reasonably expected on the basis of premature leakage of the mode from the guiding region due to presence of defects in the waveguide, especially at the cover surface. Similar effects have been observed in single-mode optical fibers[10] where microbending or curvature of the fiber shifts the higher-order mode cutoff to shorter wavelengths. In fibers, however, this effect is highly accentuated due to the much larger propagation lengths involved. It must be noted, however, that the cutoff values thus measured depend on the criterion used for defining the cutoff point, whereas in optical fibers standard procedures[11] have been agreed on for defining the cutoff wavelength, no such criteria are available for planar or channel waveguides. Finally, we recently became aware of a similar measurement of the cutoff wavelength[12] in $LiNbO_3$ waveguides.

We gratefully acknowledge the support of Don Ulrich and AFOSR contract AFOSR 84-3069.

R. Srivastava is on leave of absence from Instituto de Fisica, Unicamp, Campiras, Brazil.

References

1. T. Findakly, "Glass Waveguides by Ion Exchange: A Review," Opt. Eng. **24**, 244 (1985).
2. S. I. Najafi, R. V. Ramaswamy, and R. K. Lagu, "An Improved Method for Fabricating Ion-Exchange Waveguides Through Electrolytic Release of Silver Ions," IEEE/OSA J. Lightwave Technol. **LT-3**, 763 (1985).
3. S. I. Najafi and R. V. Ramaswamy, "Ag^+-Exchanged Graded-Index Glass Waveguides: Diffusion and Modal Characterization," paper presented at the Gradient-Index Optical Imaging Systems Conference, Palermo, Italy (Sept. 1985).
4. S. I. Najafi and R. V. Ramaswamy, "Diffusion and Modal Characterization of Ag^+-Na^+ Exchanged Channel Waveguides," paper presented at the Integrated and Guided Wave Optics Conference, Atlanta (Feb. 1986).
5. R. K. Lagu and R. V. Ramaswamy, "Process and Waveguide Parameter Relationships for the Design of Planar Silver Ion-Diffused Glass Waveguides," IEEE/OSA J. Lightwave Technol. **LT-4**, 176 (1986).
6. R. V. Ramaswamy and S. I. Najafi, "Planar, Buried, Ion-Exchanged Glass Waveguides: Diffusion Characteristics," IEEE J. Quantum Electron., to be published in special issue on Integrated Optics, June 1986.
7. R. Srivastava, C. K. Kao, and R. V. Ramaswamy, "An Accurate WKB Analysis of Planar Optical Waveguides," IEEE/OSA J. Lightwave Technology, in press.
8. G. L. Yip and J. Albert, "Characterization of Planar Optical Waveguides by K^+-Ion Exchange in Glass," Opt. Lett. **10**, 151 (1985).
9. R. V. Ramaswamy and R. K. Lagu, "Numerical Field Solution for an Arbitrary Asymmetrical Grade-Index Planar Waveguide," IEEE/OSA J. Lightwave Technol. **LT-1**, 408 (1983).
10. W. T. Anderson and T. A. Lenahan, "Length Dependence of the Effective Cutoff Wavelength in Single-Mode Fibers," IEEE/OSA J. Lightwave Technol. **LT-2**, 238 (1984).
11. D. L. Franzen, "Determining the Effective Cutoff Wavelength of Single-Mode Fiber: an Interlaboratory Comparison," IEEE/OSA J. Lightwave Technol. **LT-3**, 128 (1985).
12. K. Thyagarajan, A. Enard, P. Kayoun, D. Papillon, and M. Popuchon, "Measurement of Guided Mode Cutoff Wavelengths in Ti:$LiNbO_3$ Channel Waveguides," in *Proceedings, Third European Conference, ECIO '85, Berlin*, H. P. Nolting and R. Ulrich, Eds. (Springer-Verlag, New York, 1985), pp. 236–239.

REFERENCE [23]

Silver ion-exchanged, buried, glass optical waveguides with symmetric index profile

R. K. Lagu[a)] and R. V. Ramaswamy
Department of Electrical Engineering, University of Florida, Gainesville, Florida 32611

(Received 15 April 1985; accepted for publication 22 October 1985)

Symmetrical buried waveguides with fiberlike refractive index profiles using Ag^{+}-Na^{+} exchange have been realized in soda-lime-silicate glass substrates. A simple scanning electron microscope technique to determine the silver ion (refractive index) profile is also reported.

Optical waveguiding layers on planar substrates are useful for making a variety of integrated optical devices. Most of the work so far has been carried out by using titanium indiffusion in lithium niobate leading to the successful fabrication of directional couplers, modulators, and switches.[1] One of the problems with diffusion of Ti into $LiNbO_3$ is that the electric field cannot be applied to enhance the diffusion process. As a result, Ti:$LiNbO_3$ waveguides are shallow ($\simeq 2\mu$m deep) and channel waveguides of narrow widths couple poorly to single mode fibers due to significant modal mismatch.[2] Glass waveguides, on the other hand, are compatible with optical fibers and are useful in the fabrication of passive devices needed for systems applications.

Recently, an ion-exchange technique has been used to fabricate graded index surface and buried waveguides in glass[3] utilizing a two-step field-assisted diffusion process. In this process, soda-lime-silicate glass slides are immersed in a salt bath containing a mixture of molten sodium nitrate and silver nitrate. Initially, a surface waveguide is formed by a field-assisted diffusion of silver ions into the glass substrate. This is followed by a second field-assisted diffusion with the sample immersed in pure sodium nitrate. The index profile of buried waveguides produced in this manner is skewed[3] and is significantly different from that of single mode fibers which have nearly parabolic index profiles. In this letter we present a procedure for fabricating symmetrical buried waveguides which are comparable in shape and size to the core of single mode fibers. In addition, a simple but precise scanning electron microscope (SEM) technique to characterize the silver ion distribution and hence the refractive index profile is reported. In the two-step diffusion procedure, the diffusion time and the applied field in each of the two steps are two of the important parameters that control the dimensions and the index profile of a buried waveguide. In the previously reported process[3] an applied field in the range of 30–100 V/mm was used. In our experiments, initial field-assisted diffusion of silver ions was carried out for 30 min at 330 °C under a field of 45 V/mm with the concentration of silver ions equal to 0.1 wt. % of $NaNO_3$. It was then followed by a second field-assisted diffusion in pure sodium nitrate for 30 min under the same field, viz., 45 V/mm. This results in a steplike waveguide, Fig. 1(a), which when buried gives a skewed index profile, Fig. 1(b). These results agree with profiles of buried waveguides aleady reported in literature.[3]

The technique frequently used for measuring silver ion concentration in glass waveguides is either sputter-etched SEM[3] or electron microprobe analysis,[4] which are quite expensive and are not available at our university. We have investigated an alternative technique that uses backscattered electrons in a scanning electron microscope to determine the silver ion concentration profile. The sample is bombarded by an accelerated electron beam in a SEM with an accelerating voltage in the range of 20–50 kV. The sample generates two types of electrons, namely, secondary electrons and backscattered electrons. The secondary electrons are low-energy electrons (< 50 eV) usually coming from the surface layer of the sample (< 500 Å for the insulators), which contain the information about the surface topography. The backscattered electrons, which have higher energies (> 100 eV), provide the information about sample composition. The yield of the backscattered electrons increases monotonically with the atomic number of the specimen,[5] while that of the secondary electron is relatively insensitive to the sample composition.

In ion-exchanged glass waveguides, the substrate material usually contains ions such as Na^{+}, Si^{4+}, O^{--}, Ca^{++}, etc., while the waveguiding region contains silver ions in addition to the above. Since the atomic weight of silver is much higher than that of the rest of the ions, the contribution of silver ions to the yield of backscattered electrons is maximum. Thus, if we scan the end face of an ion-exchanged waveguide using the SEM, it is possible to obtain a good estimate of the silver ion concentration and hence the index profile by looking at the backscattered electron intensity profile.

The yield of the backscattered electrons is somewhat dependent on the microscopic variations on the surface of the sample relative to the incident electron beam and therefore, it is important to have a smooth surface to avoid backward contribution due to surface roughness.[5] Thus, it is necessary to cut the sample perpendicular to the waveguide surface and polish the end face carefully. To avoid rounding the edge of the waveguide while polishing, it is necessary to cement a glass pad (made of the same material as the substrate) to the surface of the guide using an epoxy. After the polishing has been completed, the sample is coated with 50 A of carbon to avoid charging of the sample. In making the SEM measurements, it is necessary for the electron beam to be incident perpendicular to the sample. If this is not the

a) Present address: Department of Electrical and Computer Engineering, University of Iowa, Iowa City, IA 52242

 0003-6951/86/010019-02$01.00

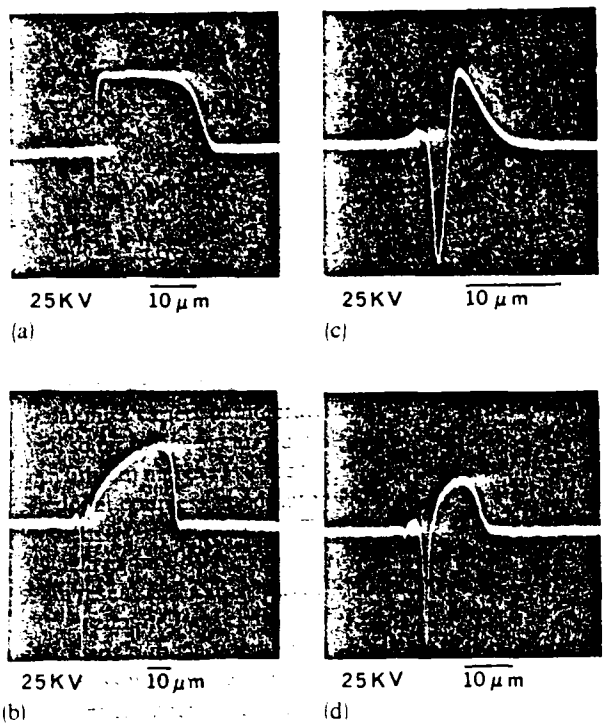

FIG. 1. (a) Index profile of a planar waveguide fabricated by field-assisted diffusion of silver ions in the first step. (b) Skewed index profile of a buried waveguide due to a second field-assisted diffusion of the sample shown in 1(a), now in pure $NaNO_3$. (c) erfc index profile of a planar waveguide fabricated by a first step diffusion process without applied electric field. (d) Symmetrical index profile of a buried waveguide with a second step field-assisted diffusion of the sample shown in 1(c), now in pure $NaNO_3$.

case, a distorted profile is obtained due to the fact that backscattered electrons have a relatively large interaction volume.[5] The silver ion concentration profiles obtained using this technique are shown in Figs. 1(a)–1(d). The dip in the signal in the middle indicates the epoxy layer which has a lower index than that of the glass slides on both sides. The backscattered electron contribution due the epoxy, which is an organic compound, is quite negligible. The silver ion profile at the surface to the right of the epoxy layer indicates the effective change in the index of the glass substrate due to Ag^+ diffusion. We are presently working on characterizing these waveguides.

Using an improved technique[6] that utilizes a novel electrolytic release process[7] in which silver ions are released electrolytically into molten sodium nitrate, we fabricated several single and multimode waveguides at $\lambda = 0.633\ \mu m$. It was experimentally determined that if no field is applied during the first diffusion step, a surface waveguide with complementary error function profile (as expected for a constant source diffusion) is formed. Figure 1(c) shows such an erfc concentration profile obtained for the case when the diffusion time was 30 min. When this waveguide is subjected to a second diffusion, now with an applied field and in pure sodium nitrate, we obtain a symmetrical structure with near parabolic index profile as shown in Fig. 1(d). The duration of the first diffusion, the strength of the electric field, and the diffusion time during the second step need to be controlled in order to achieve the desired symmetrical, buried index profile. For example, for the waveguide profile shown in Fig. 1(d), the first diffusion without drift field was carried out for 30 min at a temperature of 330 °C. The time of the second diffusion was 30 min with an applied electric field of 30 V/mm. The resulting waveguides were polished and analyzed using SEM to obtain an estimate of their widths and refractive index profiles.

In conclusion, we have presented a procedure for fabricating buried glass waveguides with fiberlike index profile using Ag^+–Na^+ exchange in glass. A simple technique which uses backscattered electrons in a SEM to determine both the refractive index profile and the effective waveguide width of Ag^+–Na^+ exchanged glass waveguides is also presented.

The authors would like to thank E. J. Jenkins of the Department of Materials Science and Engineering for his assistance in SEM analysis and C. Wayne Twiddy for polishing the waveguides. They would also like to thank S. Iraj Najafi and Paul Suchoski, Jr. for critical reading of the manuscript. This work was supported in part by a grant from Air Force Office of Scientific Research, contract No. AFOSR 84-0369.

[1] For example, see R. C. Alferness, IEEE J. Quantum Electron. **QE-17**, 946 (1981).
[2] R. V. Ramaswamy, R. C. Alferness, and M. Divino, Electron. Lett. **18**, 30 (1982).
[3] G. Chartier, P. Collier, A. Guez, P. Jaussaud, and Y. Won, Appl. Opt. **19**, 1092 (1980).
[4] G. Stewart, C. A. Miller, P. J. R. Laybourn, C. D. W. Wilkinson, and R. M. DeLaRue, IEEE J. Quantum Electron. **QE-13**, 192 (1977).
[5] J. Goldstein, D. Newbury, P. Echlin, D. Joy, C. Fiori, and E. Lifshin, *Scanning Electron Microscopy and X-ray Microanalysis*, 1st ed. (Plenum, New York, 1981).
[6] S. I. Najafi, R. V. Ramaswamy, and R. K. Lagu, J. Lightwave Technol. **LT-3**, 763 (1985).
[7] R. K. Lagu and R. V. Ramaswamy, Appl. Phys. Lett. **45**, 117 (1984).

FDD2 Diffusion and modal characterization of Ag^+–Na^+ exchanged channel waveguides

S. I. NAJAFI and R. V. RAMASWAMY, U. Florida, Department of Electrical Engineering, Gainesville, FL 32611.

Ion-exchanged glass waveguides are expected to form the basis for the potentially inexpensive passive integrated optical components compatible with single-mode optical fibers. Recently, an improved electrolytic release technique,[1] where silver ions were introduced into a bath of molten $NaNO_3$ containing the glass substrate with the Ag^+ concentration controlled to better than ± 1 μg, was used to fabricate low-loss (≈0.1-dB/cm) optical waveguides by using Ag^+–Na^+ exchange at elevated temperatures.

Although such a scheme facilitates precise electronic control of all the process parameters, namely, concentration, temperature, and time, fundamental understanding of the diffusion process and its relationship to the device characteristics is essential for the design of passive optical components with assured repeatability. The diffusion process has already been studied in detail[2] by using the SEM backscattered electron yield as a function of waveguide depth. For a small concentration of Ag^+ with no applied field, the Ag^+ concentration (and hence the refractive-index) profile is given by

$$C(x,t) = C_0 \operatorname{erfc}\left(\frac{x}{2\sqrt{Dt}}\right).$$

For $C_0 \geq 10^{-3}$ MF, $D = 0.28$ μm²/min for Ag^+–Na^+ exchange in glass substrates. However, this value of D decreases monotonically with decreasing concentration. This behavior is not fully understood and is presently under investigation. For large applied fields, specifically for $E\mu t > 5\sqrt{Dt}$, the profile given by

$$C(x,t) = \frac{C_0}{2} \operatorname{erfc}\left(\frac{x - E\mu t}{2\sqrt{Dt}}\right)$$

is confirmed by SEM experimental results. A detailed study of the two-step process to achieve buried symmetrical profiles where the second step diffusion is carried out in pure $NaNO_3$ and the extension of the study to Ag^+–Na^+ exchanged channel waveguides in particular will be presented. Absolute values of Δn for the channel waveguides are obtained by measuring the ratio of the peak indices for the channel and planar waveguides using SEM data and comparing the values of Δn for the planar waveguides.[3]

Channel waveguides were formed by the Ag^+–Na^+ exchange through a window of varying (2–10-μm) widths with the pattern replicated in an aluminum mask over the glass substrate using the standard photolithographic techniques. The diffusion profile of the channel waveguide is determined by measuring the backscattered electrons as a function of both waveguide depth and width using a SEM.[2] Figure 1 shows a typical 2-D backscattered electron profile for a channel waveguide, 10 μm wide, fabricated at $T = 330$°C with $C_0 = 2 \times 10^{-3}$ MF and $t = 60$ min. We did not observe, however, any deposition of silver under the edges of the aluminum mask opening as reported in the literature.[4]

The channel waveguide was epoxied against a planar waveguide fabricated in identical conditions and analyzed using a SEM. Figure 2 shows the variation of diffusion depth (measured at the $1/e$ point from the surface) for the channel waveguide compared with that of the planar waveguide, as a function of mask width. As before, decreasing C_0 decreases diffusion depth, and the increasing guide width increases the depth of diffusion approaching that of the planar waveguide. However, for lower concentrations, planar values are achieved at lower guide widths. The absolute value of Δn of the channel waveguides can be determined by using the corresponding value in planar waveguides.[3] For low silver concentration, the peak value of Δn varies between 0.005 and 0.02 depending on the Ag^+ concentration and operating wavelength. These experimental results and index profile measurement will be compared to the theoretical predictions.

Light was coupled to channel waveguides using a microscope objective at He–Ne (0.6328-μm) and Nd:YAG (1.32-μm) laser wavelengths. The number of modes measured at each wavelength is summarized in Table I. Using a similar setup reported elsewhere,[5] the cutoff wavelength for the lowest-order mode was measured. The cutoff wavelength for the smallest waveguide (2 μm) is $\lambda_c = 1.43$ μm. The variation of the cutoff wavelength with waveguide dimensions, estimation of Δn, and a comparison with the theoretical analysis will also be discussed. **(12 min)**

1. S. I. Najafi, R. V. Ramaswamy, and R. K. Lagu, IEEE/OSA J. Lightwave Technol. **LT-3**, 763 (1985).
2. R. V. Ramaswamy and S. I. Najafi, IEEE J. Quantum Electron., submitted for publication.
3. R. K. Lagu and R. V. Ramaswamy, IEEE/OSA J. Lightwave Technol., accepted for publication; S. I. Najafi, R. Srivastava, and R. V. Ramaswamy, Appl. Opt., submitted for publication.
4. R. G. Walker, C. D. W. Wilkinson, and J. A. H. Wilkinson, Appl. Opt. **22**, 1923 (1983).
5. K. Thyagarajan, A. Enard, P. Kajoun, D. Papillon, and M. Papuchon, at Third European Conferences ECIO 85, Berlin, 6–8 May 1985.

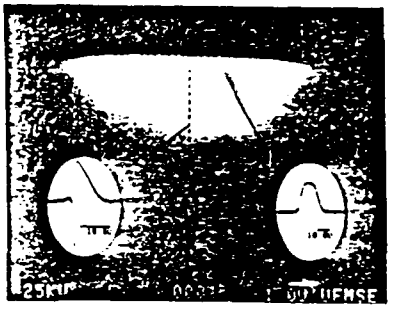

FDD2 Fig. 1. Diffusion profile of 10-μm wide Ag^+–Na^+ exchanged channel waveguide. Two-dimensional scan; insets represent the 1-D scan along the dotted lines.

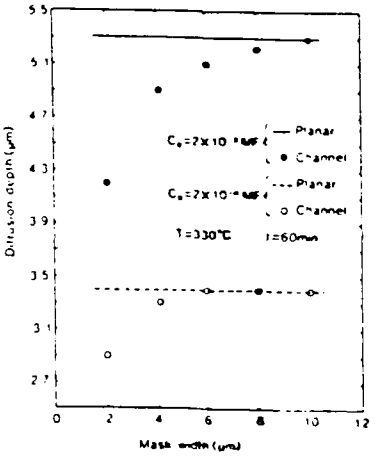

FDD2 Fig. 2. Variation of diffusion depth as a function of mask width is compared with that of the planar waveguide. C_0 is the molar concentration of silver in the bath.

FDD2 Table I. Number of TE or TM Modes in Silver Ion-Exchanged Glass Waveguides; Concentration = 2×10^{-4} MF, $T = 330$°C, $t = 90$ min

Mask width	0.6328 μm	1.32 μm
10.0	5	2
8.5	3	2
6.5	3	1
4.0	2	1
2.5	2	1

REFERENCE [25]

Guided Waves in Graded-Index Planar Waveguides with Nonlinear Cover Medium

R. K. Varshney†, M. A. Nehme, R. Srivastava and R. V. Ramaswamy
Department of Electrical Engineering
University of Florida, Gainesville, Florida 32611

Abstract

Dispersion relations for TE modes in planar, exponentially graded-index waveguide with self-focussing nonlinear cover material have been solved numerically. It is shown that the threshold power required to pull the field maximum out of the film region into the cover, is lower compared to that for the step-index waveguide. Empirical relations to calculate the corresponding minimum film thickness and the minimum threshold power are given for the lowest order mode.

Introduction

Intensity-dependent phenomena in optical guided-waves have attracted a great deal of interest [1-6] in the past few years because of their potential use in all-optical signal processing. The main advantage lies in lower threshold powers caused by large interaction lengths involved and power confinement over smaller cross-sections. At moderate power levels when the modal fields do not exhibit significant changes, the coupled mode approach [2] is adequate to describe the intensity-dependent propagation constant. Using this formalism, non-linear directional coupler [7] and bistability in channel waveguides [8] have been analyzed. However, at larger power densities, the modal field undergoes drastic changes and the coupled mode approach can not be used. Detailed studies of the intensity dependent behavior of the guided modes in waveguides with homogeneous film and nonlinear surrounding media have recently been reported by several research workers [1-6] showing existence of

†Permanent Address: Physics Department, Indian Institute of Technology
New Delhi 10016, India

multi-valued propagation constant above some threshold power levels, arousing interest in possible bistable behavior of waveguides. Experimental observation of nonlinear guided waves has also been reported in at least two cases [9, 10].

In this letter, we solve the problem of TE modes in an exponentially graded planar waveguide with nonlinear self-focussing material as the cover. In any graded-index waveguide the threshold power needed to shift the field maximum into the nonlinear cover medium is expected to be lower as the peak of the modal field is closer to the cover surface. Our interest in exponential grading is two fold: it is not only amenable to analytical solutions for the TE modes [11], its propagation characteristics closely approximate the Gaussian and complementary error function (ERFC) profiles of practical interest which do not subject themselves to such an exact analysis. In fact, it is known [12] that in graded-index waveguides, the fundamental mode profile is not very sensitive to the exact form of the index profile. Our results show that a minimum film thickness d_{min} (diffusion depth) is necessary to observe multi-valued β (above a threshold power) in the lowest order mode. As expected, the threshold power requirements are considerably relaxed by the index grading. As the film thickness is increased from the minimum value, the threshold power increases almost linearly. In the case of the fundamental mode in a symmetric waveguide with minimum thickness, the field cross-over to the cover region occurs at approximately the same value of the normalized propagation constant and the normalized frequency, independent of the film-cover index difference. This allows us to compute the design curves from which one can predict, with reasonable accuracy, the minimum thickness and the corresponding threshold power required for this crossover in a given waveguide. In comparison, in the case of the next higher order mode, no minimum thickness is necessary as long as the waveguide supports this mode.

Analysis

We consider the following index profile:

$$n^2(x) = n_c^2 + \alpha|E|^2 \quad \text{for } x < 0$$
$$= n_b^2 \{1 + 2\Delta \exp(-x/d)\} \quad x > 0 \tag{1}$$

where $\Delta = \dfrac{n_s^2 - n_b^2}{2n_b^2}$

E, n_c, n_b, n_s, d, α are local field, cover index at very low power, refractive index of the bulk (substrate) material, surface film index, diffusion depth and nonlinear coefficient of the cover material, respectively. For self-focussing nonlinear media $\alpha > 0$.

The field distribution $E(x, z, t) = E_y(x) \exp\{i(\omega t - \beta z)\}$ of the TE modes of the waveguide is obtained by solving the wave equation in two different regions (i.e. $x > 0$ and $x < 0$), and can be expressed as [1, 11]:

$$E_y(x) = \sqrt{\frac{2}{\alpha}}\, q \,\mathrm{sech}\{k_o q (x_1 - x)\} \quad \text{for } x < 0$$
$$= A\, J_{2\rho}\{2V \exp(-x/2d)\} \quad x > 0 \tag{2}$$

where $q = \{(\beta/k_o)^2 - n_c^2\}^{1/2}$, $\rho = k_o d\{(\beta/k_o)^2 - n_b^2\}^{1/2}$

and $V = k_o d\, n_b \sqrt{2\Delta}$.

Here A is a constant; k_o, and β are free-space wave number and propagation constant of the mode respectively. x_1 is a power-dependent constant and has a finite value (while for the linear case it is infinite). $x_1 = 0$ corresponds to the field maximum at $x = 0$, as seen from Eq. (2). The value of A and the power dependent dispersion relation obtained by ensuring the continuity of E_y and H_z (i.e. $\dfrac{\partial E_y}{\partial x}$), respectively, are written as:

$$A = \sqrt{\frac{2}{\alpha}} \frac{q}{J_{2\rho}(2V)} \,\mathrm{sech}\,(k_o q x_1) \tag{3}$$

and

$$\gamma T = \frac{J_{2\rho}(2V)}{J_{2\rho}(2V)} V - \rho \tag{4}$$

where $\gamma = k_o qd$, $T = \tanh(k_o q x_1)$

The guided wave power per unit length along the y-axis is obtained as

$$P_g = \tfrac{1}{2}\int_{-\infty}^{\infty} (\vec{E} \times \vec{H}^*)_z \, dx = P_c + P_f \tag{5}$$

where $P_c = \frac{B}{2\gamma}(1 - T)$

$P_f = BD(1 - T^2)$

$$B = \frac{2d\beta q^2}{k_o n_c^2 n_{2c}}$$

$$D = \frac{1}{J_{2p}^2(2V)} \int_o^{2V} \frac{1}{y'} J_{2p}^2(y')dy' \tag{6}$$

$$n_{2c} = \frac{\alpha}{n_c^2}\sqrt{\frac{\mu_o}{\varepsilon_o}}$$

After some mathematical manipulation, Eq. (5) can be written as

$$T = \left[\left\{\left(1 + \frac{1}{4\gamma D}\right)^2 - \frac{P_g}{BD}\right\}^{1/2} - \frac{1}{4\gamma D}\right] \tag{7}$$

Here, ε_o and μ_o are free-space permittivity and permeability, respectively. Minimum threshold power P_g (min) is the power corresponding to $T = 0$ and this corresponds to the minimum thickness (in the case of the lowest order mode).

Thus by using Eqs. (2) through (7), we obtain the threshold power, power dependence of the modal field and the propagation constant etc. of the TE modes. If the nonlinear medium is self-defocussing (i.e. $n_{2c} < o$); same expressions can be used except that tanh(t), sech(t), n_{2c} and α are replaced by coth(t), cosech(t), $|n_{2c}|$ and $|\alpha|$, respectively in the entire analysis.

Results and Discussion

The analytical relations given above were solved numerically to obtain detailed information about the power dependence of the guided waves and to

compare our results with those obtained in the case of the homogeneous step index waveguide with nonlinear cover. Due to the nonlinearity, the self consistent solution was obtained by assuming that only one mode was guided. Unless otherwise stated, all cases assume symmetrical waveguides i.e., $n_b = n_c$, $\lambda = 0.515$, $n_s = 1.57$, λ 0.515 μm and $n_{2c} = 10^{-9}$ m^2/W. These values are chosen to compare our results with those of Ref. [6].

TE_o mode

Figure 1 shows the effective index (β/k_o) of the fundamental mode vs. the total guided power (P_g) for two different thicknesses. Initially for low guided powers, the propagation constant increases almost linearly. The increase is predicted by the coupled-mode theory and can alternatively be viewed as arising from the fact that the creation of a higher refractive index in the cover medium adjacent to the cover-film interface causes an increase in the effective width of the guide. However, the rate of increase of β with the guided power is larger for smaller film thickness. This can be explained as follows. For a given power, as the film thickness decreases, the peak of the fundamental mode shifts closer to the surface and the field amplitude at the cover-film interface increases. For smaller thickness therefore, as the power is increased, the nonlinearity in the cover medium has the stronger effect in shifting the peak toward the interface and increasing the effecive index. In fact if the thickness is below certain critical value, the rapid shift allows the peak to reach the interface at power levels well below the minimum power required to obtain sufficiently large β/k_o characteristic of the surface polariton. Multivalued behavior in the propagaton constant is not observed in

such cases. In our case, the minimum film thickness to observe multi-valued β is $d_{min} = 1.42$ μm. The curves in Fig. 1 have the same characteristics as in the case of the homogeneous film, including the presence of a surface-polariton like mode for $\beta/k_o > n_s$. Although the occurance of multi-valued propagation constant is reminiscent of a possible bistable behavior, there are some doubts [13] whether the various branches shown in Fig. 1 are stable. Stability analysis of the branch where $dP_g/d\beta > 0$ indicates that the corresponding field configuration is stable where as the region with $dP_g/d\beta < 0$ is likely to be unstable [14]. Although the threshold power required to obtain multiple-valued β increases linearly with the thickness, the threshold occurs at a relatively constant value of the field amplitude at the cover-film interface. This is consistent with the requirement (and our observation) that the peak of the field shift to the cover layer when the cover index at the interface be slightly larger than the film-index. The field profiles corresponding to the three power levels indicated in Fig. 1 are shown in Fig. 2. At sufficiently large powers, most of the power flows in the cover. In the steady-state case analyzed here, the peak of the field stays very close to the surface at all the power levels studied.

To compare our results for the minimum threshold power, we have calculated its value as a function of Δ under the same conditions as in Ref. [6]. Namely, for each Δ, the thickness d was gradually increased until a maximum in the P_g vs. β/k_o curve first appeared. The two curves in Fig. 3 represented by solid lines A and B show the behavior for $n_b = 1.55$ and 3.0 respectively. As can be seen the minimum threshold power is lower as compared to the homogeneous film [6], does not depend significantly on the index of the surrounding medium and can be obtained for any given value of n_c, and d by

interpolatin. linearly between the curves. Moreover, in each case the minimum threshold power occurs at T = 0 and at a thickness for which the normalized frequency V = 4.4 ± 0.4. This happens at a (surprisingly) constant value of the normalized propagation constant $\left(b = \left(\frac{(\frac{\beta}{k_o})^2 - n_b^2}{n_s^2 - n_b^2}\right)\right) = 0.66 \pm 0.007$. This fact can be used to readily obtain an estimate, within ± 10%, of the minimum thickness and the corresponding threshold power required for the given waveguide parameters and the wavelength. These estimates are not likely to differ substantially for the Gaussian or ERCF profiles. Furthermore, the asymmetric graded profiles ($n_c > n_b$) will have even smaller threshold powers as the peak of the modal field is closer to the surface at a given power level.

TE_1 mode

Figure 4 shows variation of the effective index (β/k_o) of the TE_1 mode mode with the guided mode power (P_g). It is found that the peak in the P_g vs. β/k_o curve for this mode can be obtained at any thickness greater than the minimum thickness required for guiding this mode. One significant result of the film index grading is that the threshold power for obtaining this peak in the case of the TE_1 mode is reduced by almost a factor of two from the corresponding value for homogeneous film [6]. This conclusion was arrived at by comparing the two values for a waveguide thickness anywhere between 25 and 100% larger than the cutoff thickness at $\lambda = 0.515\ \lambda m$ for the TE_1 mode.

Figure 5 shows the field profile at the guided power levels corresponding to the points A, B, and C in Fig. 4. A comparison with the TE_o mode shows that the field peaks in the cover farther away from the surface in the case of TE_1 mode. However, a substantial part of the power always stays inside the film.

In conclusion, we have analyzed the intensity dependent modes in graded-index planar waveguide with self focussing nonlinear cover medium. The results show that the threshold power requirements are considerably relaxed by grading. Empirical relations are presented from which threshold power and minimum film thickness required for the multivalued behavior in the propagation constant of the lowest order mode can be calculated for a given waveguide within 10% error.

Acknowledgements:

One of the authors, R. K. Varshney acknowledges support of the council for International Exchange of Scholars via an 'Indo-American Fellowship' Award. This work was supported by a contract from AFOSR #124505196 and by the Microfabritech program of the University of Florida.

Figure Captions

Fig.1: Variation of TE_0 guided wave power with effective index for d = 1.5μm (dashed curve) and d = 3.0 μm (solid curve). The points A, B and C represent the power level corresponding to the field profile of TE_0 mode shown in Fig. 2.

Fig. 2: Field profile of TE_0 mode corresponding to three different power levels (identified by the points A, B and C in Fig. 1) for d = 3.0 μm.

Fig. 3: Minimum TE_0 guided wave power as a function of $(n_s - n_c)$ for n_b = 1.55 (curve A), and = 3.0 (curve B). Circles correspond to Ref. [6] with the homogeneous film for n_b = 1.55.

Fig. 4: The variation of TE_1 guided wave power with effective index for d = 1.5 μm (dashed curve) and d = 3.0 μm (solid curve). The points A, B and C correspond to the power levels for field profile of TE_1 mode shown in Fig. 5.

Fig. 5: Field profile of TE_1 mode for three different power levels marked by points A, B and C in Fig. 4 for d = 1.5 μm.

References

1). N. N. Akhmediev, Sov. Phys. JETP, 56, 299 (1982).

2). G. I. Stegeman, IEEE J. Quant. Electron., QE-18, 1610 (1982).

3). C. T. Seaton, Xu Mai, G. I. Stegeman and H. G. Winful, Opt. Eng., 24, 593 (1985).

4). U. Langbein, F. Lederer and H. E. Ponath, Opt. Commun., 52, 417 (1985).

5). A. D. Boardman and P. Egan, IEEE J. Quant. Electron., QE-21, 1701 (1985).

6). C. T. Seaton, J. D. Valera, R. L. Shoemaker, G. I. Stegeman, J. T. Chilwell and S. D. Smith, IEEE J. Quant. Electron., QE-21, 774 (1985).

7). S. M. Jensen, IEEE J. Quant. Electron., QE-18, 1580 (1982).

8). D. Sarid, Opt. Lett., 6, 552 (1981).

9). H. Vach, G. I. Stegeman, C. T. Seaton and I. C. Khoo, Opt. Lett., 9, 238 (1984).

10). I. Bennion, M. J. Goodwin and W. J. Stewart, Elect. Lett., 21, 41 (1985).

11). E. M. Conwell, Appl. Phys. Lett., 23, 328 (1973).

12). R. V. Ramaswamy and R. K. Lagu, J. Lightwave Tech., LT-1, 408 (1983).

13). C. K. R. T. Jones and J. V. Moloney, Tech. Digest Toptical Meet. on Optical Bistability Tucson (Arizona), paper WD5, Dec., 1985.

14). J. V. Moloney, J. Ariyasu, C. T. Seaton, and G. I. Stegeman, Appl. Phys. Lett., 48, 826 (1986).

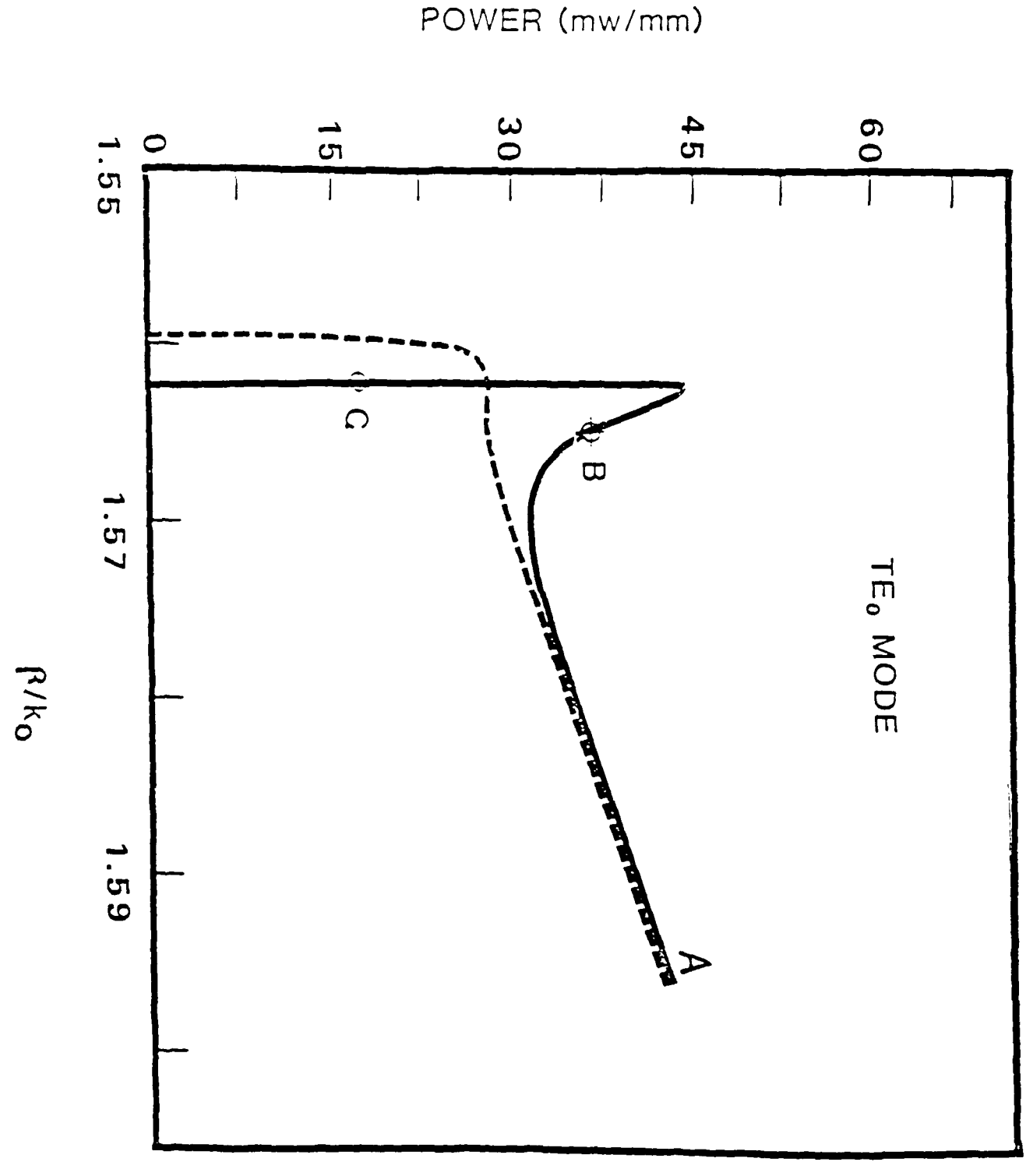
POWER (mw/mm)
0
15
30
45
60
1.55
1.57
1.59
R/k_o
A
B
C
TE_o MODE

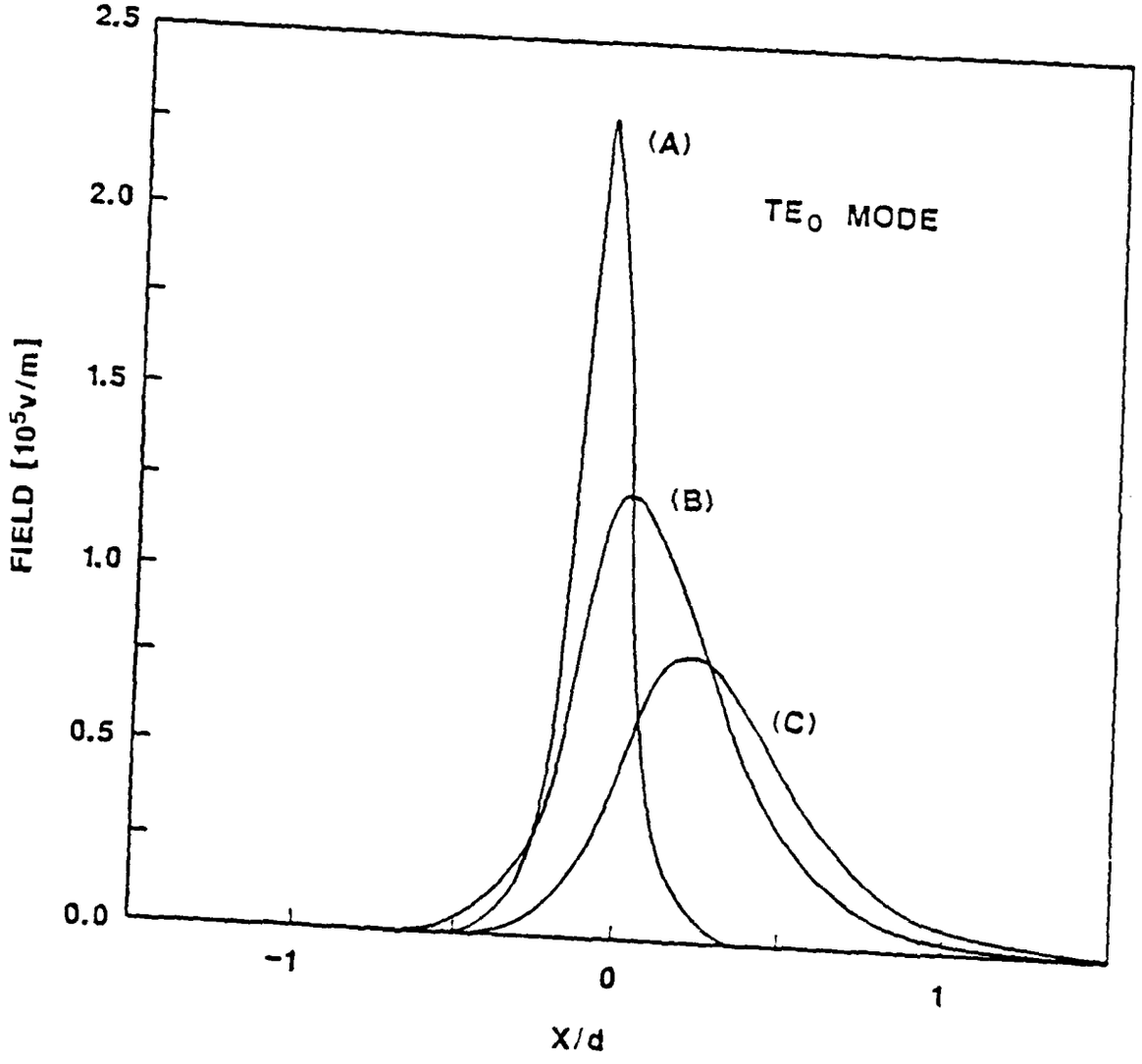
2.5
2.0
1.5
1.0
0.5
0.0
FIELD [10^5v/m]
(A)
TE_0 MODE
(B)
(C)
−1
0
1
X/d

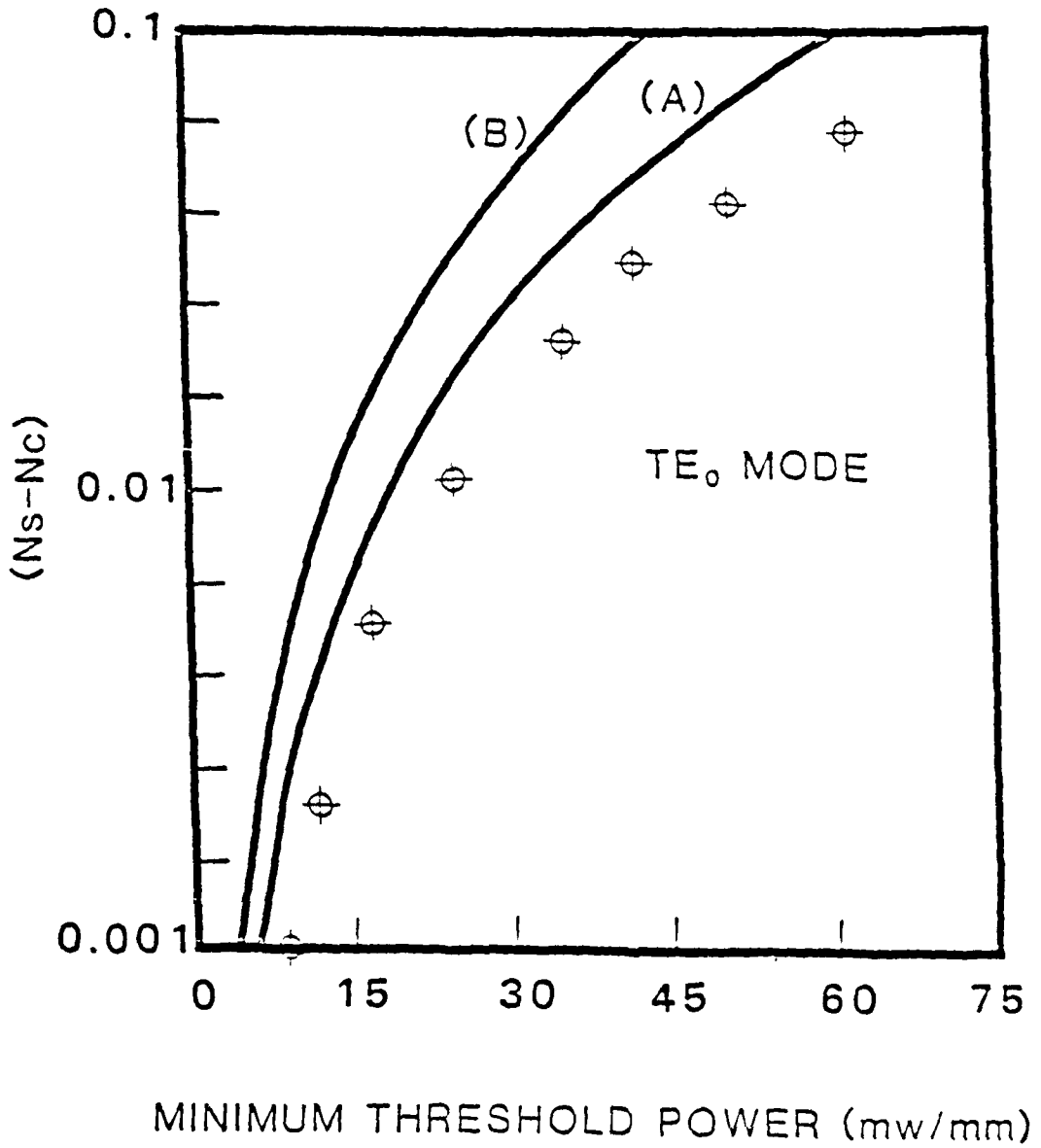
0.1
0.01
0.001
(Ns-Nc)
(B)
(A)
TE₀ MODE
0
15
30
45
60
75
MINIMUM THRESHOLD POWER (mw/mm)

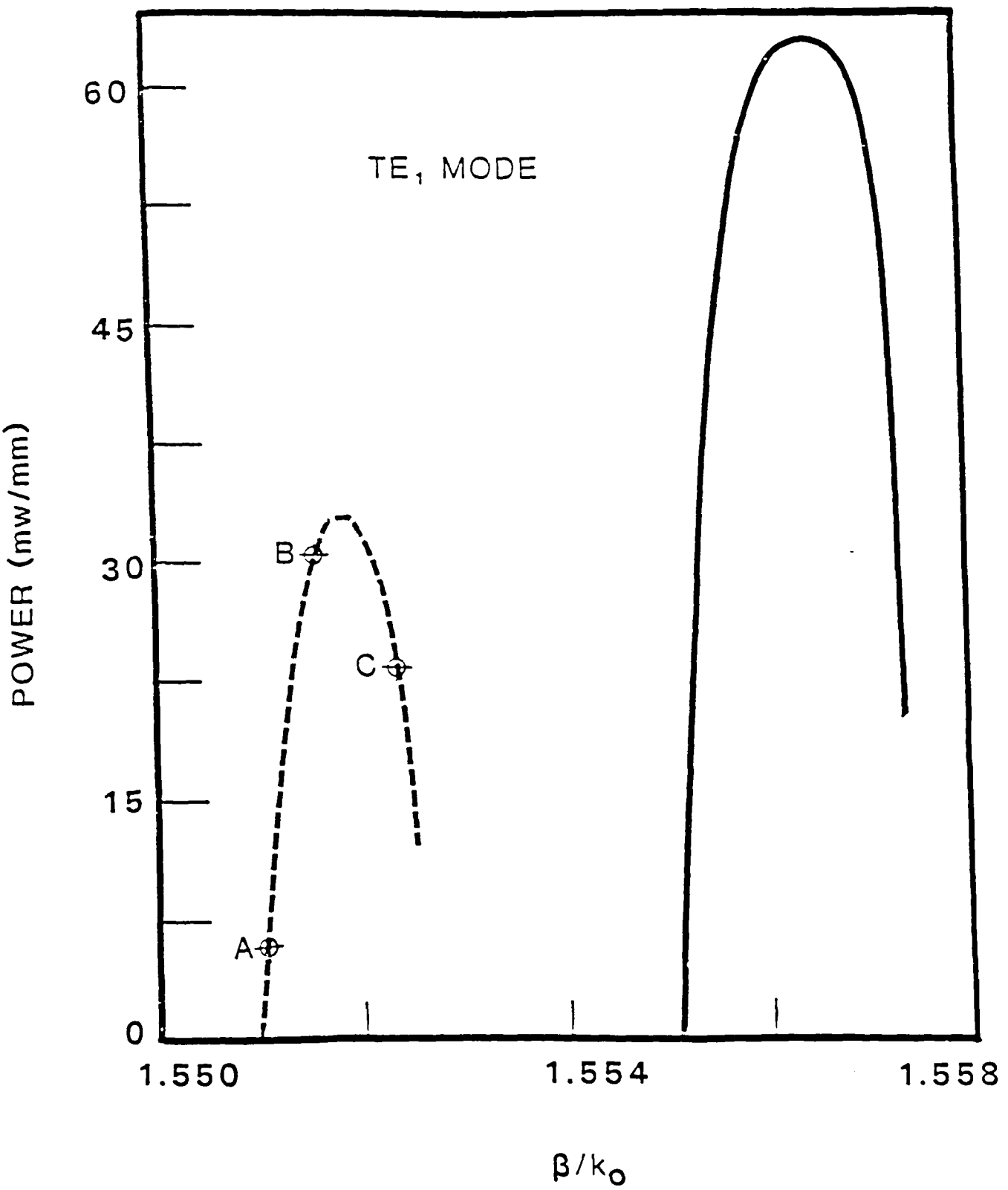
60
45
30
15
0
TE, MODE
B
C
A
POWER (mw/mm)
1.550
1.554
1.558
β/k₀

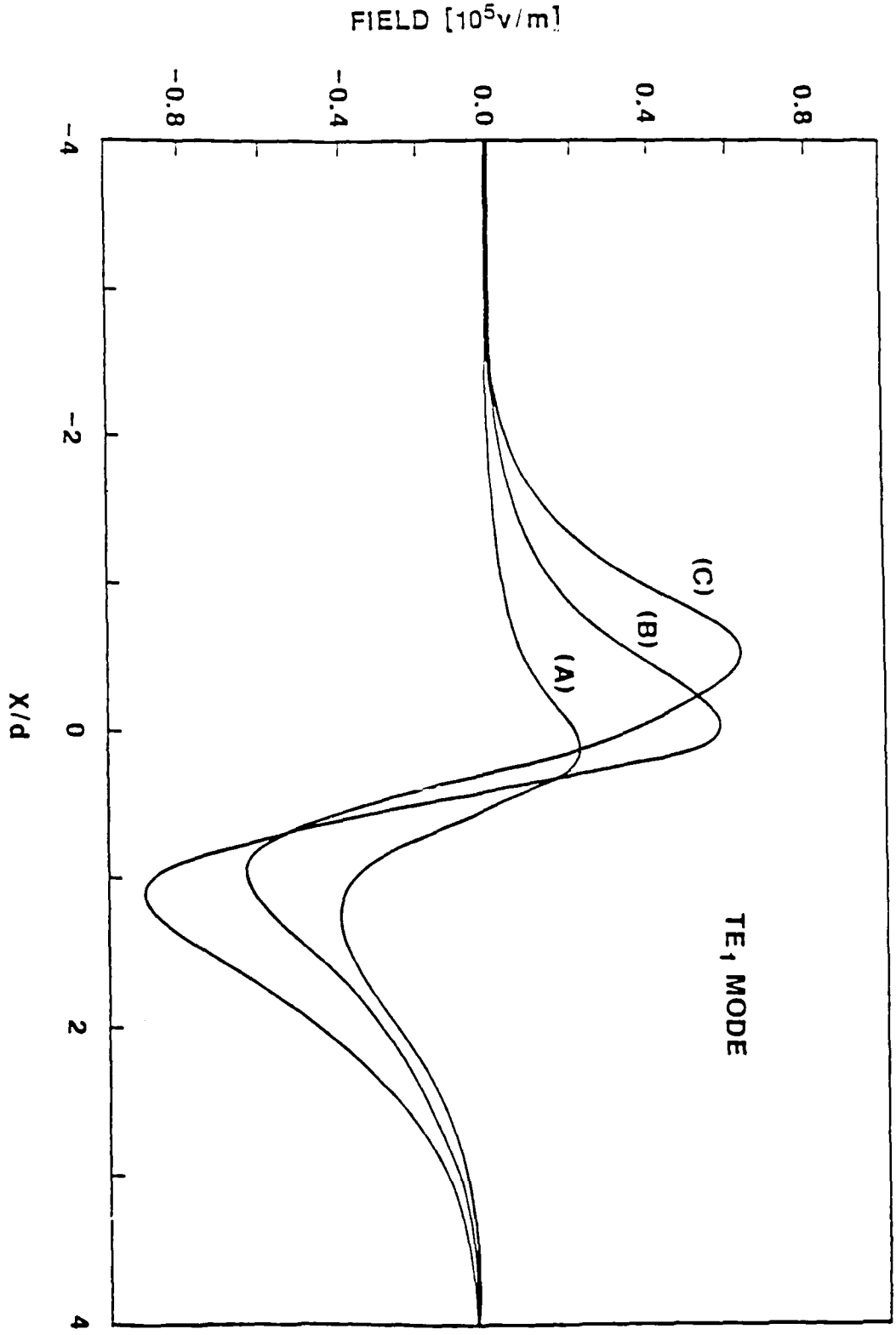
FIELD [10^5v/m]
-0.8
-0.4
0.0
0.4
0.8
-4
-2
0
2
4
X/d
(C)
(B)
(A)
TE1 MODE

REFERENCE [26]

Guided waves in graded-index planar waveguides with nonlinear cover medium

R. K. Varshney, M. A. Nehme, R. Srivastava, and R. V. Ramaswamy

Dispersion relations for TE modes in a planar exponentially graded-index waveguide with self-focusing nonlinear cover material have been solved numerically. It is shown that the threshold power required to pull the field maximum out of the film region into the cover is lower compared with that for the step-index waveguide and agrees well with the experimental results. Empirical relations to calculate the corresponding minimum film thickness and the minimum threshold power are given for the lowest-order mode.

I. Introduction

Intensity-dependent phenomena in optical guided waves have attracted a great deal of interest[1-6] in the last few years because of their potential use in all-optical signal processing. The main advantage lies in lower threshold powers caused by large interaction lengths involved and power confinement over smaller cross sections. At moderate power levels when the modal fields do not exhibit significant changes, the coupled mode approach[2] is adequate to describe the intensity-dependent propagation constant. Using this formalism, the nonlinear directional coupler[7] and bistability in channel waveguides[8] have been analyzed. However, at larger power densities, the modal field undergoes drastic changes, and the coupled mode approach cannot be used. Detailed studies of the intensity-dependent behavior of the guided modes in waveguides with homogeneous film and nonlinear surrounding media have recently been reported by several research workers[1-6] showing the existence of multivalued propagation constant above some threshold power levels, arousing interest in possible bistable behavior of waveguides. Experimental observation of nonlinear guided waves has also been reported in at least two cases.[9,10] In Ref. 9, the hysterisis was observed in the TE_1 mode when the nonlinear medium was liquid crystal MBBA, which acted as the cover for a step-index planar glass waveguide, whereas in Ref. 10, CS_2 was used as the nonlinear cover medium on an ion-exchanged glass waveguide, and an intensity-dependent hysterisis was observed in the TE_0 mode.

In this paper, we solve the problem of TE modes in an exponentially graded planar waveguide with nonlinear self-focusing material as the cover. In any graded-index waveguide the threshold power needed to shift the field maximum into the nonlinear cover medium is expected to be lower as the peak of the modal field is closer to the cover surface. Our interest in exponential grading is twofold: it is not only amenable to analytical solutions for the TE modes,[11] its propagation characteristics closely approximate the Gaussian and complementary error function (ERFC) profiles of practical interest, which do not subject themselves to such an exact analysis. In fact, it is known[12] that in graded-index waveguides the fundamental mode profile is not very sensitive to the exact form of the index profile. Our results show that in the case of the lowest-order mode a minimum film thickness d_{min} (diffusion depth) is necessary to observe multivalued β (above a threshold power). As expected, the threshold power requirements are considerably relaxed by the index grading, and the predicted values agree well with the experimental results of Ref. 10. As the film thickness is increased from the minimum value, the threshold power increases almost linearly. In the case of the fundamental mode in a symmetric waveguide with minimum thickness, the field crossover to the cover region occurs at approximately the same value of the normalized propagation constant and the normalized frequency, independent of the film-cover index difference. This allows us to compute the design curves from which one can predict, with reasonable accuracy, the minimum thickness and corresponding threshold power required for this crossover in a given waveguide. In comparison, in the case of the next higher order mode, no minimum thickness is necessary as long as the waveguide supports this mode.

II. Analysis

We consider the following index profile:

The authors are with University of Florida, Department of Electrical Engineering, Gainesville, Florida 32611.

Received 27 June 1986.
0003-6935/86/213899-04$02.00/0.

$$n^2(x) = n_c^2 + \alpha|E|^2 \qquad \text{for } x < 0$$
$$= n_s^2[1 + 2\Delta \exp(-x/d)] \qquad x > 0, \tag{1}$$

where

$$\Delta = \frac{n_s^2 - n_b^2}{2n_b^2}.$$

E, n_c, n_b, n_s, d, α are local field, cover index at very low power, refractive index of the bulk (substrate) material, surface film index, diffusion depth, and nonlinear coefficient of the cover material, respectively. For self-focusing nonlinear media $\alpha > 0$.

The field distribution $E(x, z, t) = E_y(x) \exp[i(\omega t - \beta z)]$ of the TE modes of the waveguide is obtained by solving the wave equation in two different regions (i.e., $x > 0$ and $x < 0$) and can be expressed as[1,11]

$$E_y(x) = \sqrt{\frac{2}{\alpha}}\, q\, \mathrm{sech}[k_0 q(x_1 - x)] \text{ for } x < 0,$$
$$= AJ_{2\rho}[2V \exp(-x/2d)] \qquad x > 0, \tag{2}$$

where

$$q = [(\beta/k_0)^2 - n_c^2]^{1/2},\ \rho = k_0 d[(\beta/k_0)^2 - n_b^2]^{1/2},$$
$$V = k_0 d n_b \sqrt{2\Delta}.$$

Here A is a constant; k_0 and β are the free-space wavenumber and propagation constant of the mode, respectively. x_1 is a power-dependent constant and has a finite value (while for the linear case it is infinite). $x_1 = 0$ corresponds to the field maximum at $x = 0$, as seen from Eq. (2). The value of A and the power-dependent dispersion relation obtained by ensuring the continuity of E_y and H_z [i.e., $(\partial E_y)/\partial x$], respectively, are written as

$$A = \sqrt{\frac{2}{\alpha}}\, \frac{q}{J_{2\rho}(2V)}\, \mathrm{sech}(k_0 q x_1), \tag{3}$$

$$\gamma T = \frac{J_{2\rho+1}(2V)}{J_{2\rho}(2V)}\, V - \rho, \tag{4}$$

where $\gamma = k_0 q d$, $T = \tanh(k_0 q x_0)$.

The guided wave power per unit length along the y axis is obtained as

$$P_g = \tfrac{1}{2}\int_{-\infty}^{\infty} (\mathbf{E} \times \mathbf{H})_z^* dx = P_c + P_f, \tag{5}$$

where

$$\left.\begin{aligned} P_c &= \frac{B}{2\gamma}(1 - T), \\ P_f &= BD(1 - T^2), \\ B &= \frac{2d\beta q^2}{k_0 n_c^2 n_{2c}}, \\ D &= \frac{1}{J_{2\rho}^2(2V)} \int_0^{2V} \frac{1}{v^2} J_{2\rho}^2(v)\, dv, \\ n_{2c} &= \frac{\alpha}{n_c^2}\sqrt{\frac{\mu_0}{\epsilon_0}}. \end{aligned}\right\} \tag{6}$$

After some mathematical manipulation, Eq. (5) can be written as

$$T = \left\{\left[\left(1 + \frac{1}{4\gamma D}\right)^2 - \frac{P_g}{BD}\right]^{1/2} - \frac{1}{4\gamma D}\right\}. \tag{7}$$

Here ϵ_0 and μ_0 are free-space permittivity and permeability, respectively. Minimum threshold power $P_g(\min)$ is the power corresponding to $T = 0$, and this corresponds to the minimum thickness (in the case of the lowest-order mode).

Thus, by using Eqs. (2)–(7), we obtain the threshold power, power dependence of the modal field, propagation constant, etc. of the TE modes. If the nonlinear medium is self-defocusing (i.e., $n_{2c} < 0$), the same expressions can be used except that $\tanh(t)$, $\mathrm{sech}(t)$, n_{2c}, and α are replaced by $\coth(t)$, $\mathrm{cosech}(t)$, $|n_{2c}|$, and $|\alpha|$, respectively, in the entire analysis.

III. Results and Discussion

The analytical relations given above were solved numerically to obtain detailed information about the power dependence of the guided waves and to compare our results with those obtained in the case of the homogeneous step-index waveguide with nonlinear cover. Due to the nonlinearity, the self-consistent solution was obtained by assuming that only one mode was guided. Unless otherwise stated, all cases assume symmetrical waveguides, i.e., $n_b = n_c$, $n_s = 1.57$, $\lambda_0 = 0.515$ μm, and $n_{2c} = 10^{-9}$ m^2/W. These values are chosen to compare our results with those of Ref. 6.

A. TE_0 Mode

Figure 1 shows the effective index (β/k_0) of the fundamental mode vs the total guided power P_g for two different thicknesses. Initially, for low guided powers, the propagation constant increases almost linearly. The increase is predicted by the coupled-mode theory and can alternatively be viewed as arising from the fact that creation of a higher refractive index in the cover

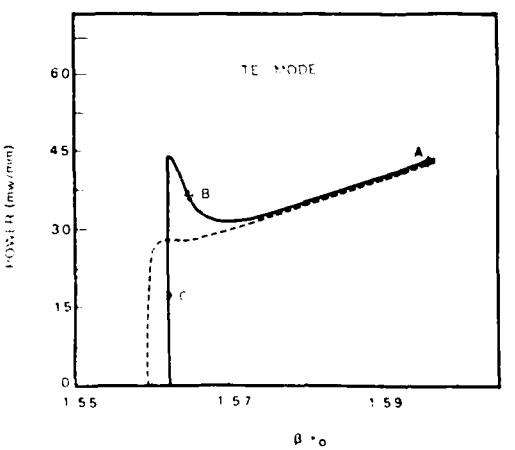

Fig. 1. Variation of TE_0 guided wave power with the effective index for $d = 1.5$ μm (dashed curve) and $d = 3.0$ μm (solid curve). Points A, B, and C represent the power level corresponding to the field profile of the TE_0 mode shown in Fig. 2.

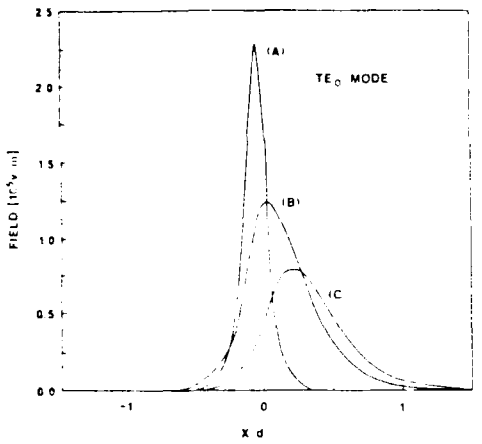

Fig. 2. Field profile of the TE_0 mode corresponding to three different power levels (identified by the points A, B, and C in Fig. 1) for d = 3.0 μm.

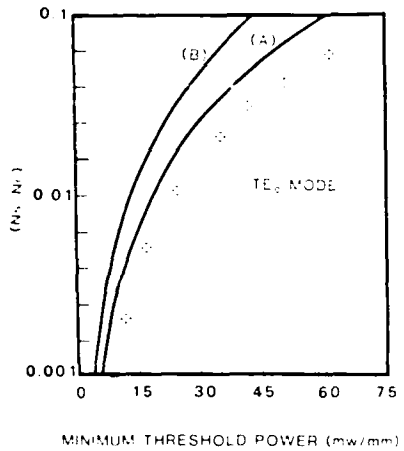

Fig. 3. Minimum TE_0 guided wave power as a function of $(n_c - n_s)$ for n_b = 1.55 (curve A) and = 3.0 (curve B). Circles correspond to Ref. 6 with the homogeneous film for n_b = 1.55.

medium adjacent to the cover–film interface causes an increase in the effective width of the guide. However, the rate of increase of β with the guided power is larger for smaller film thickness. This can be explained as follows. For a given power, as the film thickness decreases, the peak of the fundamental mode shifts closer to the surface, and the field amplitude at the cover–film interface increases. For smaller thickness, therefore, as the power is increased, the nonlinearity in the cover medium has the stronger effect in shifting the peak toward the interface and increasing the effective index. In fact, if the thickness is below a certain critical value, the rapid shift allows the peak to reach the interface at power levels well below the minimum power required to obtain sufficiently large β/k_0 characteristic of the surface polariton. Multivalued behavior in the propagation constant is not observed in such cases. In our case, the minimum film thickness to observe multivalues β is $d_{min} \approx 1.42\ \mu$m. The curves in Fig. 1 have the same characteristics as in the case of the homogeneous film, including the presence of a surface-polaritonlike mode for $\beta/k_0 > n_c$. Although the occurrence of multivalued propagation constant is reminiscent of a possible bistable behavior, there are some doubts[13] whether the various branches shown in Fig. 1 are stable. Stability analysis of the branch where $dP_g/d\beta > 0$ indicates that the corresponding field configuration is stable whereas the region with $dP_g/d\beta < 0$ is likely to be unstable.[14] Although the threshold power required to obtain multiple-valued β increases linearly with the thickness, the threshold occurs at a relatively constant value of the field amplitude at the cover–film interface. This is consistent with the requirement (and our observation) that the peak of the field shift to the cover layer when the cover index at the interface be slightly larger than the film-index. The field profiles corresponding to the three power levels indicated in Fig. 1 are shown in Fig. 2. At sufficiently large powers, most of the power flows in the cover. In the steady-state case analyzed here, the peak of the field stays very close to the surface at all the power levels studied.

To compare our results for the minimum threshold power, we have calculated its value as a function of Δ in the same conditions as in Ref. 6. Namely, for each Δ, the thickness d was gradually increased until a maximum in the P_g vs β/k_0 curve first appeared. The two curves in Fig. 3 represented by solid lines A and B show the behavior for n_b = 1.55 and 3.0, respectively. As can be seen the minimum threshold power is lower compared to the homogeneous film,[6] does not depend significantly on the index of the surrounding medium, and can be obtained for any given value of n_c and d by interpolating linearly between the curves. Moreover, in each case the minimum threshold power occurs at T = 0 and at a thickness for which the normalized frequency $V \approx 4.4 \pm 0.4$. This happens at a (surprisingly) constant value of the normalized propagation constant

$$\left\{ b = \left[\frac{(\beta/k_0)^2 - n_s^2}{n_c^2 - n_s^2} \right] \right\} \approx 0.66 \pm 0.007.$$

This fact can be used to readily obtain an estimate within $\pm 10\%$ of the minimum thickness and the corresponding threshold power required for the given waveguide parameters and wavelength. These estimates are not likely to differ substantially for the Gaussian or ERCF profiles. Furthermore, the asymmetric graded profiles ($n_c > n_b$) will have even smaller threshold powers as the peak of the modal field is closer to the surface at a given power level. For example, in the experiment of Ref. 10, $(n_c - n_b) \approx 10^{-3}$ and $n_2 c = 3 \times 10^{-5}$ cm^2/MW. Figure 3 predicts a threshold of 2 MW/mm. Assuming a typical beam size of 1-mm diameter for the unfocused YAG laser, the measured value of 2 MW/mm^2 is in reasonable agreement with our prediction.

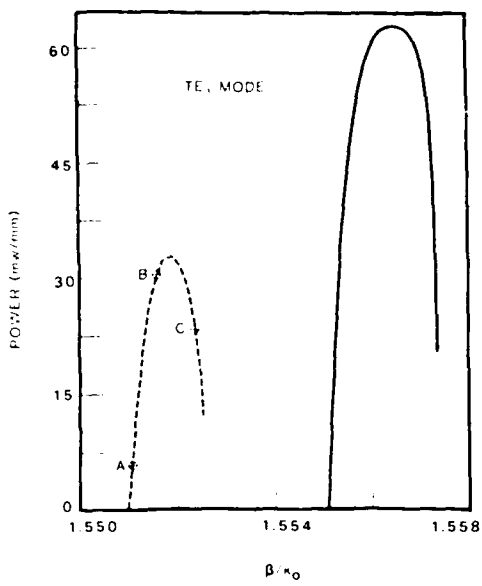

Fig. 4. Variation of TE_1 guided wave power with effective index for $d = 1.5\ \mu m$ (dashed curve) and $d = 3.0\ \mu m$ (solid curve). Points A, B, and C correspond to the power levels for the field profile of the TE_1 mode shown in Fig. 5.

B. TE_1 mode

Figure 4 shows a variation of the effective index (β/k_0) of the TE_1 mode mode with the guided mode power P_g. It is found that the peak in the P_g vs β/k_0 curve for this mode can be obtained at any thickness greater than the minimum thickness required for guiding this mode. One significant result of the film index grading is that the threshold power for obtaining this peak in the case of the TE_1 mode is reduced by almost a factor of 2 from the corresponding value for homogeneous film.[6] This conclusion was arrived at by comparing the two values for a waveguide thickness anywhere between 25 and 100% larger than the cutoff thickness at $\lambda = 0.515\ \mu m$ for the TE_1 mode.

Figure 5 shows the field profile at the guided power levels corresponding to points A, B, and C in Fig. 4. A comparison with the TE_0 mode shows that the field peaks in the cover farther away from the surface in the case of the TE_1 mode. However, a substantial part of the power always stays inside the film.

In conclusion: we have analyzed the intensity-dependent modes in a graded-index planar waveguide with a self-focusing nonlinear cover medium. The results show that the threshold power requirements are considerably relaxed by grading, and the predicted values agree well with the experimental results reported. Empirical relations are presented from which threshold power and minimum film thickness required for the multivalued behavior in the propagation constant of the lowest order mode can be calculated for a given waveguide within 10% error.

One of the authors, R. K. Varshney, acknowledges support of the Council for International Exchange of Scholars via an Indo-American Fellowship Award. He

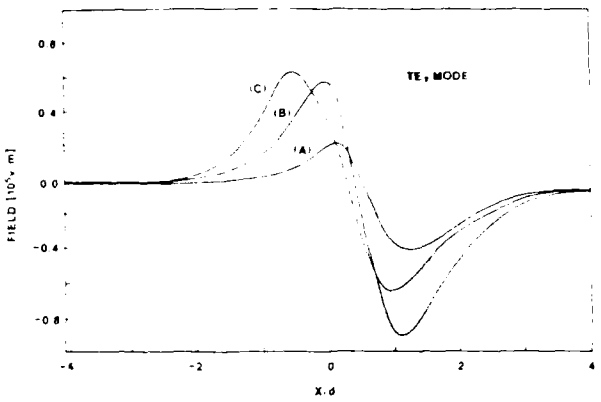

Fig. 5. Field profiles of the TE_1 mode for three different power levels marked by points A, B, and C in Fig. 4 for $d = 1.5\ \mu m$.

is on leave from the Physics Department of the Indian Institute of Technology, New Delhi. This work was supported by a contract from AFOSR 124505196 and by the Microfabritech program of the University of Florida.

References

1. N. N. Akhmediev, "Novel Class of Nonlinear Surface Waves: Asymmetric Modes in a Symmetric Layered Structure," Sov. Phys. JETP **56**, 299 (1982).
2. G. I. Stegeman, "Guided Wave Approaches to Optical Bistability," IEEE J. Quantum Electron. **QE-18**, 1610 (1982).
3. C. T. Seaton, Xu Mai, G. I. Stegeman, and H. G. Winful, "Nonlinear Guided Wave Applications," Opt. Eng. **24**, 593 (1985).
4. U. Langbein, F. Lederer, and H. E. Ponath, "Generalized Dispersion Relations for Nonlinear Slab Guided Waves," Opt. Commun. **52**, 417 (1985).
5. A. D. Boardman and P. Egan, "S-Polarized Waves in a Thin Dielectric Film asymmetrically bounded by Optically Nonlinear Media," IEEE J. Quantum Electron. **QE-21**, 1701 (1985).
6. C. T. Seaton, J. D. Valera, R. L. Shoemaker, G. I. Stegeman, J. T. Chilwell, and S. D. Smith, "Calculations of Nonlinear TE Waves guided by Thin Dielectric Films Bounded by Nonlinear Media," IEEE J. Quantum Electron. **QE-21**, 774 (1985).
7. S. M. Jensen, "The Nonlinear Coherent Coupler," IEEE J. Quantum Electron. **QE-18**, 1580 (1982).
8. D. Sarid, "Analysis of Bistability in a Ring-Channel Waveguide," Opt. Lett. **6**, 552 (1981).
9. H. Vach, C. T. Seaton, G. I. Stegeman, and I. C. Khoo, "Observation of Intensity-Dependent Guided Waves," Opt. Lett. **9**, 238 (1984).
10. I. Bennion, M. J. Goodwin, and W. J. Stewart, "Experimental Nonlinear Optical Waveguide Device," Electron. Lett. **21**, 41 (1985).
11. E. M. Conwell, "Modes in Optical Waveguides formed by Diffusion," Appl. Phys. Lett. **23**, 328 (1973).
12. R. V. Ramaswamy and R. K. Lagu, "Numerical Field Solution for an Arbitrary Asymmetrical Graded-Index Planar Waveguide," IEEE/OSA J. Lightwave Technol. **LT-1**, 408 (1983).
13. C. K. R. T. Jones and J. V. Moloney, "Stability and Instability of Nonlinear Waveguide Modes," in *Technical Digest, Topical Meeting on Optical Bistability (OB3)* (Optical Society of America, Washington, DC, 1985), paper WD5.
14. J. V. Moloney, J. Ariyasu, C. T. Seaton, and G. I. Stegeman, "Stability of Nonlinear Stationary Waves guided by a Thin Film bounded by Nonlinear Media," Appl. Phys. Lett. **43**, 826 (1986).

REFERENCE [27]

Nonlinear Prism Coupling and Power Limiting in Ion-Exchanged Waveguides

H. Zhenguang*, R. Srivastava, and R. V. Ramaswamy

Department of Electrical Engineering

University of Florida, Gainesville, Florida 32611

* Permanent Address: Changchun Institute of Physics, Chinese Academy of Sciences, Changchun, China

Abstract

Nonlinear prism coupling, power limiting and mode field variations were observed at record low powers in planar ion-exchanged semiconductor-doped waveguides. For the first time, power limiting in channels was also observed. Thermal origin of the effects is corroborated.

Nonlinear Prism Coupling and Power Limiting in Ion-Exchanged Waveguides

H. Zhenguang*, R. Srivastava, and R.V. Ramaswamy

Department of Electrical Engineering
University of Florida, Gainesville, Florida 32611

*Permanent Address: Changchun Institute of Physics, Chinese Academy of Sciences, Changchun, China

Introduction Glasses doped with Cd S_{1-x} Se_x semiconductors form an important class of nonlinear materials in that they exhibit large third order nonlinearity with fast relaxation times, making them attractive for signal processing applications[1]. Nonlinear prism coupling in a sputtered glass waveguide in color glass substrates with a cw threshold of the order of 200mW has been reported[2]. K^+-Na^+ ion-exchanged waveguides in sodium rich Cd $S_{1-x}Se_x$ doped glass have been fabricated[3], and thermal nonlinear prism coupling under pulsed regime has been reported in ion-exchanged as well as sputtered glass waveguides [4,5].

We report results of nonlinear prism coupling, power limiting, and for the first time, observation of the mode field variation in ion-exchanged waveguides in a Cd $S_{1-x}Se_x$ doped glass. In the prism coupler, the threshold power for the onset of nonlinearity is ~ 20mW and limiting occurs at 60mW input power. This is the lowest value reported thus far. We present for the first time power limiting in butt-coupled channel waveguides and convincing evidence that the effect is dominated by thermal contribution.

Experiment K^+-Na^+ ion-exchange was carried out at 345°C by immersing clean glass substrates in molten KNO_3 bath for 40 min. The low-power effective index of the TE_0 and TM_0 modes at 515nm was measured to be 1.5273 and 1.5292 respectively. The material absorption coefficient at the operating wavelength of the 515nm Ar^+ laser line was $6cm^{-1}$. Figure 1 shows the experimental set up. The beam was focused by a 450 mm focal length lens into a ~100 μm diameter spot at the prism base. Low-power coupling efficiency was ~ 30%. The output end of the guide was polished to allow measurement of the mode field at various input power levels.

Results Fig. 2 shows the variation of the output power from the prism coupled waveguide as the input power is increased while the low-power coupling condition is maintained. The extrapolated straight lines correspond to the coupling efficiency in the low-power regime. Open circles represent the output measured within a second after the input is incident on the prism. Closed circles and crosses represent the steady-state output power obtained after a few seconds. The significant features of our results can be summarized as follows: (a) The nonlinear threshold power for the TE_0 mode (~ 20mW) is an order of magnitude lower than previously reported[2]; (b) We observe a saturation (limiting) in the output power beginning at input power level of ~ 60mW and a subsequent decrease at higher input power; (c) There is significant dependence of the nonlinear behavior on the distance of propagation d between the coupling region and waveguide exit end face; (d) We observe a relaxation effect caused by heating due to absorption similar to the

one observed in the case of liquid crystal[6]. When the low power synchronism is maintained and the input power is suddenly increased, the output decreases from an initial value (open circles in Fig. 1) which is smaller than that expected from the extrapolation of the linear behavior, to a steady state value (lower curves). Once the steady-state was reached (lower curves) and the prism-waveguide assembly was then rotated or translated to optimize the output, no significant increase was observed unlike the case of Refs. 2 and 6 where an increase was reported. The thermal effect also explains the observations cited above in item (c). As the distance d increases, more absorption occurs which causes a larger thermal effect and hence larger temperature rise. This in turn shifts the absorption edge to higher wavelengths resulting in further increase in absorption until thermal equilibrium is reached. This nonlinear absorption is therefore of opposite sign compared to the relatively fast effect arising from the band filling[7] in which the absorption decreases with increasing input power. At low input powers (linear regime), the shape of the coupling curve (measured by angular scanning of the prism-waveguide assembly) is identical for scans in both the directions. However, as the power is increased the two curves are unidentical if sufficient time is not allowed for the waveguide to cool down to the ambient. Moreover, the maximum change in the coupling angle (corresponding to the peak output signal) is less that 1 m rad as the input power P_{in} is increased from 5 mW to 1 W for d = 10 mm case and immeasurable for d = 2mm, indicating a very small decrease in the mode effective index ($\Delta n_e \sim 3\times10^{-4}$ for $P_{in} > 30$mW). Similar changes were reported in Ref. 2 from which the sign and magnitude of n_2 were derived. In our case, the film has graded-index and both the film and the substrate are nonlinear and a solution of the wave equation is very difficult. In fact, it is the temperature profile of the absorbed energy as well as the local intensity profile which will determine the steady state index distribution of the waveguide. Moreover, this distribution is likely to vary along the direction of propagation as the propagating power is reduced by absorption, reducing the local heating of the waveguide. However, the small decrease in the measured mode index with increasing input power indicates that the nonlinearity is self-defocussing. If we take 30 mW as the input power for the nonlinear threshold behavior (Fig. 2), then under the linear regime, the coupled power P_c=10 mW and $n_2 \sim \Delta n_e A/P_c$. In our case, cross section area A = 100 μm x 2μm, yielding $n_2 \sim -6 \times 10^{-12}$ m^2/W which is an order of magnitude smaller than that reported in Ref. 2. Our measurements of the temperature dependence of the substrate glass index show a qualitative agreement with these results.

While we did not observe many of the effects predicted theoretically for the nonlinear prism coupler[3], the hysteresis observed is similar to that reported in other experiments[2,9] and is caused by the thermal effect. Another consequence of the heating is a shift in the intensity pattern of the output power as obtained by imaging the near field of the output using a microscope objective and scanning the distribution by a detector with a pin-hole. While the shape of the field profile does not change at high power, the peak position shifts to the substrate side by approximately half the width of the mode. The shift decreases as d decreases. No such shifts or output nonlinearity were observed when the experiment was repeated with soda-lime K^+-Na^+ exchanged waveguides. While the direction of the peak shift is consistent with the decrease in the waveguide index due to the nonlinearity, the invariance of the shape of the field distribution indicates that the shape of index profile remains relatively unaffected by the waveguide heating.

Power was also coupled to channel waveguides fabricated in the glass. Fiber-waveguide butt coupling was used and the waveguide output was measured as a function of input power. A nonlinearity was observed starting ~15 mW of input power and power limiting occurs > 40 mW corresponding to a coupled input intensity of ~200 KW/cm^2, well above the expected saturation intensity for the fast Kerr type electronic contribution to the nonlinearity in these glasses. More results on the channel waveguides including the damage threshold and nonlinear directional coupler studies will be presented at the meeting.

This work was supported by Air Force Office of Scientific Research, Contract No. 84-3069. We thank H. C. Cheng for assistance in waveguide fabrication.

References

1. R.K. Jain and R.C. Lind, J.Opt. Soc. Am., 73, 647 (1983).

2. S. Patela, H. Jerominek, C. Delisle and R. Tremblay, Electron. Lett., 22, 411 (1986).

3. T.J. Cullen, C.N. Ironside, C.T. Seaton and G.I. Stegeman, Appl., Phys. Lett., 49, 1403 (1986).

4. G. Assanto, A. Gabel, C.T. Seaton, G.I. Stegeman, C.N. Ironside and T.J. Cullen, Electron Lett., 23, 484 (1987).

5. H. Jerominek, S. Patela, C. Delisle and R. Tremblay, Proc. SPIE, 667, 115 (1986).

6. J.D. Valera, C.T. Seaton, G.I. Stegeman, R.L. Shoemaker, Mai Xu and C. Liao, Appl. Phys. Lett., 45 1013 (1984).

7. N. Peyghambarian, G.R. Olbright, B. Fluegel and S.W. Kock, NSF Workshop on Nonlinearities, Fast Phenomena and Signal Processing, Tuscon, Az., May, 1986, pp. 281-291.

8. C. Liao, G.I. Stegeman, C.T. Seaton, R.L. Shoemaker and J.D. Valera, J. Opt. Soc. Am. A2, 590 (1985).

9. G. Assanto, B. Svensson, D. Kuchibhatla, U.J. Gibson, C.T. Seaton and G.I. Stegeman, Opt. Lett., 11, 644 (1986).

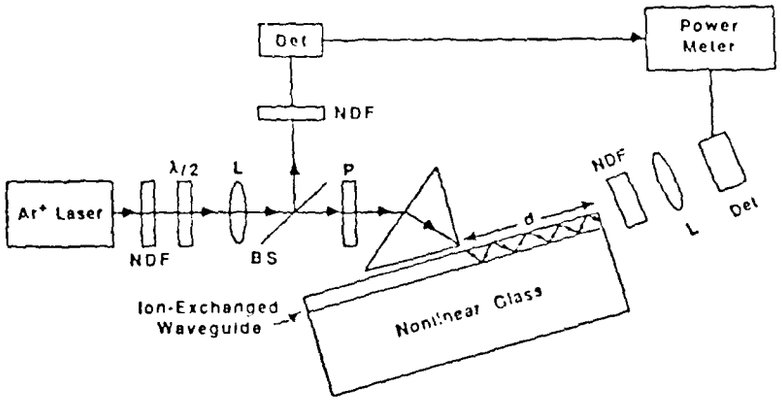

Fig. 1 Schematics of characterization set up. NDF is neutral density filter.

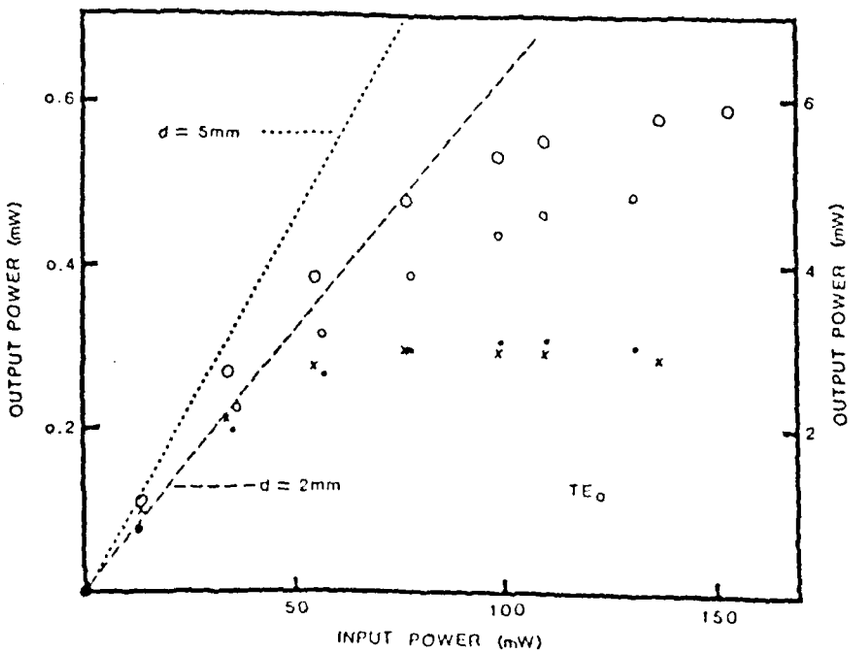

Fig. 2 Variation of output power with input power for d = 5 mm (left-side scale) and d = 2 mm (right-side scale). O (o) and X (•) represent initial and final output for d = 5(2) mm.

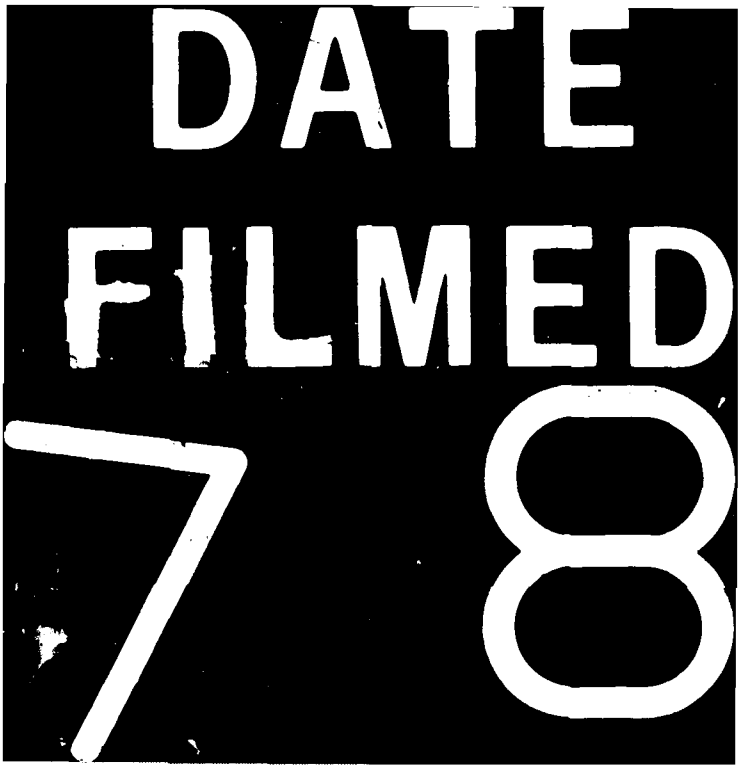
DATE
FILMED
7 8